MICHIGAN OHIO UNIVERSITY TRANSPORTATION CENTER

Alternate energy and system mobility to stimulate economic development.

Report No: MIOH UTC AF3p2 2007-Final
MDOT Report No: RC-1545

PRODUCTION OF FUEL ETHANOL FROM CELLULOSIC PEAT FOR FUTURE TRANSPORTATION SYSTEMS

First Year, Annual Report

May 1, 2007 to December 31, 2007

Principal Investigator
Mark Benvenuto, University of Detroit Mercy

Co-Principal Investigators
Charles W. Winter, Wayne State University
John Shewchun, Wayne State University
Detroit, MI 48202

Report No: MIOH UTC AF3p2 2007-Final

AF 3, Series, Project 2, November 2007
FINAL REPORT

Developed By: **Mark Benvenuto**
Principal Investigator, UDM
benvenma@udmercy.edu
313-993-1184

SPONSORS

This is a Michigan Ohio University Transportation Center project supported by the U.S. Department of Transportation, the Michigan Department of Transportation, University of Detroit Mercy, and Wayne State University.

DISCLAIMERS

Technical Report Documentation Page

1. Report No. RC-1545	**2. Government Accession No.**	**3. MDOT Project Manager** Niles Annelin	
4. Title and Subtitle Michigan Ohio University Transportation Center Subtitle: "Production of Fuel Ethanol from Cellulosic Peat for Future Transportation Systems"		**5. Report Date** December 2007 **6. Performing Organization Code**	
7. Author(s) Dr. Mark Benvenuto, University of Detroit Mercy Dr. Charles W. Winter, Wayne State University Dr. John Sewchun, Wayne State University		**8. Performing Org. Report No.** MIOH UTC AF3 p2 2007-Final	
9. Performing Organization Name and Address Michigan Ohio University Transportation Center University of Detroit Mercy, Detroit, MI 48221 Wayne State University, Detroit MI 48202		**10. Work Unit No. (TRAIS)** **11. Contract No.** 2007-0538 **11(a). Authorization No.**	
12. Sponsoring Agency Name and Address Michigan Department of Transportation Van Wagoner Building, 425 West Ottawa P. O. Box 30050, Lansing, Michigan 48909		**13. Type of Report & Period Covered** Research, May 2007 - December 2007 **14. Sponsoring Agency Code**	
15. Supplementary Notes Additional Sponsors: US DOT Research & Innovative Technology Administration, the University of Detroit Mercy and Wayne State University.			
16. Abstract MIOH UTC AF3 p2 2007-Final The production of bioethanol from peat is proposed. A search of the available literature yields no prior information on the use of peat as a carbon source for bioethanol. This proposal addresses the production in the most cost-effective manner possible, utilizing special enzymes, and using materials native to Michigan. The bioethanol proposed will either be utilized as fuel or in fuel blends.			
17. Key Words Ethanol, Methanol fuels, Production methods, Peat, Cost effectiveness, Michigan, Fuels, Hydrogen, Fuel cell vehicles, Research projects		**18. Distribution Statement** No restrictions. This document is available to the public through the Michigan Department of Transportation.	
19. Security Classification - report	**20. Security Classification - page**	**21. No. of Pages** 5	**22. Price**

PRODUCTION OF FUEL ETHANOL FROM CELLULOSIC PEAT FOR FUTURE TRANSPORTATION SYSTEMS

Abstract

The production of bioethanol from peat is proposed. A search of the available literature yields no prior information on the use of peat as a carbon source for bioethanol. This proposal addresses the production in the most cost-effective manner possible, utilizing special enzymes, and using materials native to Michigan. The bioethanol proposed will either be utilized as fuel or in fuel blends.

First Year, Annual Report

May 1, 2007 to December 31, 2007

Thus far, the Winter and Benvenuto labs have completed the following in producing ethanol from cellulosic biomass:

Production of peat ethanol:

- This has been accomplished on a small scale in Dr. Winter's lab. Reaction batches are generally 1 liter in volume, or slightly less, and contain 15% - 17% ethanol.
- In Dr. Benvenuto's lab, peat was used as a biomass source along with common yeasts as fermentors. Specifically, baker's yeast and brewer's yeast. The results were negative. Although this was expected, the reactions were run to be sure of the negative result.

Ethanol production from other sources:

- Basic fermentations were performed, using common sugars, plus common yeasts, in Dr. Benvenuto's lab. The aim of these experiments was to determine if the simple chemistry of fermentation can be performed in a teaching lab setting in a secondary or middle school. This is in accordance with the MI-OH UTC education component, which encourages dissemination of results to other educators.

- Refined cellulose fermentation using common yeasts was examined in Dr. Benvenuto's lab. The results were negative, but the use of cellulose represents an important middle step, between the fermentation of simple and complex sugars, and the fermentation of unrefined complex biomass, such as peat. Refined cellulose was provided by Fisher Science Education (formula $(C_6H_{10}O_5)_n$, product number S75083).
- Fermentation trials of common sugars and cellulose using cellulase trichoderma reesei (ATCC 26921) were begun. Cellulase purchased from Sigma (product C8546-10KU). Results are pending.

At the current point in this project, both labs have done enough examination of existing background literature to arrive at the conclusion that peat, while a renewable resource, is not renewable on the time scale that would be called for should a sharp rise in the need for biomass feedstocks for ethanol production occur. Because of this, a switch is being made, from the idea of examining a wide variety of yeasts and enzymes combined with peat, to that same variety of yeasts and enzymes in combination with cellulose, guar gum, and other weedy, biomass materials that may be digestible to the yeasts and enzymes.

Note: In light of reported findings, funding for this series of projects was not continued by the MIOH UTC Operating Committee after review November 2007.

MICHIGAN OHIO UNIVERSITY TRANSPORTATION CENTER
Alternate energy and system mobility to stimulate economic development.

Report No: MIOH UTC AF4p2-5 2011-Final
MDOT Report No: RC1545

IMPROVED OXIDATIVE STABILITY OF BIODIESEL FUELS:

ANTIOXIDANT RESEARCH AND DEVELOPMENT

FINAL REPORT

PROJECT TEAM

Dr. Haiying Tang
Dr. K.Y. Simon Ng
Dr. Steven O. Salley
Chemical Engineering
Wayne State University
5050 Anthony Wayne Drive
Detroit, MI 48202,USA

Report No: MIOH UTC AF4p2-5 2011-Final

AF4, Series, Projects 2, 3, 4 and 5 January 2011
FINAL REPORT

Developed By:

Haiying Tang
Assistant Professor (research), Chemical Engineering, WSU
ak3268@wayne.edu

K.Y. Simon Ng
Interim Associate Dean for Research
Director, Electric-drive Vehicle Engineering
Director, Alternative Energy Technology
Professor of Chemical Engineering, WSU
sng@wayne.edu

Steven O. Salley
Principal Investigator
Assoc. Professor, Chemical Engineering, WSU
ssalley@wayne.edu

SPONSORS

This is a Michigan Ohio University Transportation Center project supported by the U.S. Department of Transportation, the Michigan Department of Transportation, Wayne State University and NextEnergy.

ACKNOWLEDGEMENT

The Project Team would like to acknowledge support from the National Biofuel Energy Laboratory and NextEnergy during the course of this research.

DISCLAMER

Technical Report Documentation Page

1. Report No. RC-1545	2. Government Accession No.	3. MDOT Project Manager Niles Annelin
4. Title and Subtitle Michigan Ohio University Transportation Center Subtitle: "Improved Oxidative Stability of Biodiesel Fuels: Antioxidant Research and Development"		5. Report Date January 2011 6. Performing Organization Code
7. Author(s) Dr. Haiying Tang, Wayne State University Dr. Steven O. Salley, Wayne State University Dr. K.Y. Simon Ng, Wayne State University		8. Performing Org. Report No. MIOH UTC AF4p2-5 2011-Final
9. Performing Organization Name and Address Michigan Ohio University Transportation Center University of Detroit Mercy, Detroit, MI 48221 and Wayne State University, Detroit, MI 48202		10. Work Unit No. (TRAIS) 11. Contract No. 2007-0538 11(a). Authorization No.
12. Sponsoring Agency Name and Address Michigan Department of Transportation Van Wagoner Building, 425 West Ottawa P. O. Box 30050, Lansing, Michigan 48909		13. Type of Report & Period Covered Research, November 2006–January 2011 14. Sponsoring Agency Code

15. Supplementary Notes
Additional Sponsors: US DOT Research & Innovative Technology Administration and Wayne State University. Additional Support: the National Biofuel Energy Laboratory and NexEnergy.

16. Abstract
MIOH UTC AF4p2-5 2011-Final
Biodiesel is a domestic, renewable fuel that is gaining wide acceptance, especially in Europe. When blended with conventional petroleum diesel, biodiesel reduces hydrocarbon, particulate and carbon monoxide emissions, while having minimal to no effect on NOx. It also improves lubricity, lowers sulfur, and has a high cetane number. The promise of biodiesel is tremendous, but some significant obstacles remain to its complete acceptance by diesel engine manufacturers, most significantly with respect to oxidative stability. This proposed project will investigate the factors associated with biodiesel oxidative stability, including natural and synthetic antioxidants, storage and processing conditions. Results of this project will provide much needed guidelines to industry with regards to storage conditions and antioxidant additive levels. Additionally, biodiesel production changes will be recommended which will optimize the preservation of natural antioxidant levels in the fuel. Finally, factors required for the development of a user-level sensor for biodiesel oxidative stability will be quantified.

17. Key Words	18. Distribution Statement
Biodiesel fuels, Antioxidants, Petroleum, Diesel fuels, Carbon monoxide, Diesel engine exhaust gases, Sulfur, Exhaust gases, and Research projects.	No restrictions. This document is available to the public through the Michigan Department of Transportation.

19. Security Classification - report	20. Security Classification - page	21. No. of Pages	22. Price
		46	

ABSTRACT

Biodiesel is a domestic, renewable fuel that is gaining wide acceptance, especially in Europe. When blended with conventional petroleum diesel, biodiesel reduces hydrocarbon, particulate and carbon monoxide emissions, while having minimal to no effect on NOx. It also improves lubricity, lowers sulfur, and has a high cetane number. The promise of biodiesel is tremendous, but some significant obstacles remain to its complete acceptance by diesel engine manufacturers, most significantly with respect to oxidative stability. This proposed project will investigate the factors associated with biodiesel oxidative stability, including natural and synthetic antioxidants, storage and processing conditions. Results of this project will provide much needed guidelines to industry with regards to storage conditions and antioxidant additive levels. Additionally, biodiesel production changes will be recommended which will optimize the preservation of natural antioxidant levels in the fuel. Finally, factors required for the development of a user-level sensor for biodiesel oxidative stability will be quantified.

Table of Contents

LIST OF FIGURES

LIST OF TABLES

1. EXECUTIVE SUMMARY

The effectiveness of one natural antioxidant (α-tocopherol (α-T)), six synthetic antioxidants (butylated hydroxyanisole (BHA), butyl-4-hydroxytoluene (BHT), *t*-butylhydroquinone (TBHQ), 2,5-di-*tert*-butyl-hydroquinone (DTBHQ), propylgallate (PG), and pyrogallol (PY)), and one commercial antioxidant (ionol BF200 (IB)) on the oxidative stability (as measured by the induction period (IP)) of biodiesel was investigated [1]. Results indicate that different types of biodiesel have different natural levels of oxidative stability, indicating that natural antioxidants and FAME composition play a significant role in determining oxidative stability. Moreover, PG, PY, TBHQ, BHA, BHT, DTBHQ, and IB can enhance the oxidative stability for these different types of biodiesel. Antioxidant activity increased with increasing concentration. The induction period of SBO-, CSO-, YG-, and distilled SBO-based biodiesel could be improved significantly with PY, PG and TBHQ, while PY, BHA, and BHT show the best results for PF-based biodiesel. This indicates that the effect of each antioxidant on biodiesel differs depending on different feedstock. Moreover, the effect of antioxidants on B20 and B100 was similar; suggesting that improving the oxidative stability of biodiesel can effectively increase that of biodiesel blends.

The effectiveness of blends of primary antioxidants from combinations of butylated hydroxyanisole (BHA), propyl gallate (PG), pyrogallol (PY) and *tert*-butyl hydroquinone (TBHQ) to increase oxidative stability was examined [2]. Results indicate that binary antioxidant formulations: TBHQ:BHA, TBHQ:PG and TBHQ:PY were most effective at 2:1, 1:1, 2:1 weight ratio, respectively in both distilled soybean oil- (DSBO) and distilled poultry fat- (DPF) based biodiesel. Antioxidant activity increased as the loadings were increased. The synergisms of the antioxidant pairs were different with different biodiesel types, suggesting a dependence on the fatty acid methyl ester (FAME) composition. The best synergistic effect was observed with the TBHQ:BHA blends while the best stabilization factors (SF) were achieved by using the TBHQ:PY blends. Quantification of antioxidant content in stored biodiesel with TBHQ:PY blend demonstrates that the main factor of synergy is the regeneration of PY by TBHQ.

The effectiveness of various individual and binary antioxidants ((α-tocopherol (α-T), butylated hydroxyanisole (BHA), butyl-4-methylphenol (BHT), t-butylhydroquinone (TBHQ), 2, 5- Di-tert-butyl-hydroquinone (DTBHQ), ionol BF200 (IB), propylgallate (PG), and pyrogallol (PY)) on induction period (IP), acid number, and viscosity of SBO-based biodiesel during long-term storage, as well as the efficacy of binary antioxidants on distilled SBO-based biodiesel under long-term storage were evaluated [3]. Moreover, the FAME content, FAME composition, and antioxidant content after long-term storage were investigated. Results indicate that the induction period (IP) of untreated SBO-based biodiesel significantly decreased with the increasing storage time, while the IP values with adding TBHQ to SBO-based biodiesel remained constant for up to 42 months. Moreover, the binary antioxidant formulations of THBQ: BHA maintained the IP of distilled SBO-based biodiesel stable over a six-month period. TBHQ is the most effective antioxidant to improve the storage stability of SBO-based biodiesel.

The catalytic activity of Al, Cu, Fe and Zn in their nitrate form in reducing the oxidative stability was investigated, as measured by the induction period (IP)) of soybean oil (SBO) based biodiesel blends with and without the antioxidant (AOx) tert-Butylhydroquinone (TBHQ). Results indicate that the catalytic effects of the metals follow the hierarchy: Cu >> Fe > Al ≈ Zn. The IP drops resulted mostly from the metals degrading TBHQ followed by the direct attack on the lipid producing radicals and metal transition states that further speed up the chain reaction. In B20, ultra low sulfur diesel (ULSD) proved to be invaluable in maintaining the oxidative stability by minimizing the metal attack on both the SBO component and its AOx.

2. ACTION PLAN FOR RESEARCH

Eight antioxidants (namely α-tocopherol (α-T), BHA, BHT, TBHQ, 2, 5- Di-tert-butyl-hydroquinone (DTBHQ), ional BF200 (IB), PG, and PY) were evaluated for their potential to reduce the degree of oxidation of various biodiesels under various storage conditions. Each antioxidant was added at concentrations from 250 to 1000 ppm to biodiesel derived from soybean oil (SBO), cottonseed oil (CSO), poultry fat (PF), and yellow grease (YG) . Moreover, the effect of antioxidants on distilled SBO (DSBO)-based biodiesel, and 20% SBO-based biodiesel blends (B20) were investigated, in comparison to unblended B100.

The synergy of synthetic antioxidants in biodiesel was fully elucidated, including (i) the synergistic effects of synthetic antioxidants: BHA, TBHQ, PG and PY in binary formulations on biodiesel were investigated; (ii) the degree of unsaturation to the antioxidant activity was correlated; and (iii) a mechanistic understanding of the synergistic effect was developed.

The long-term stability of soy-based biodiesel with or without synthetic/natural antioxidants was investigated up to 42 months. The different individual antioxidant additives on induction period (IP), acid number, and viscosity of SBO-based biodiesel during long-term storage, as well as the efficacy of binary antioxidants on distilled SBO-based biodiesel under long-term storage were also evaluated. Moreover, the FAME content, FAME composition, and antioxidant content after long-term storage were investigated.

3. INTRODUCTION

Biodiesel is a renewable fuel for diesel engines that is derived from natural oils and fats (e.g., vegetable oils, recycled cooking greases or oils and animal fats) and that specifically meets the specifications of the American Society for Testing and Materials (ASTM) D 6751. It is composed of monoalkyl esters of long-chain fatty acids, produced by the transesterification with alcohol of the above natural oils. Biodiesel is a U.S. Department of Energy (DOE) designated alternative fuel and is registered as a fuel and fuel additive with the U.S. Environmental Protection Agency (EPA). Research on the use of alternative fuels such as biodiesel is mentioned as one many elements of the DOT Strategic Plan.

Biodiesel offers many benefits over conventional petroleum diesel. It burns cleaner, with net emissions reductions in particulates, hydrocarbons, and carbon monoxide (and with zero to slight increases in NOx). Biodiesel also possesses a high cetane number (averaging over 50) and improves petroleum diesel cetane performance when blended. Since it is naturally low in sulfur content, it also lowers sulfur emissions when blended with petroleum diesel. Biodiesel blending also imparts improved lubricity to petroleum diesel.

Since it is domestically produced, biodiesel shows great potential for reducing U.S. dependence on foreign energy supplies. It provides a "closed economic loop" in that the feedstock can be grown locally, the biodiesel can be produced locally, and the fuel can be used locally. Furthermore, it is evident that very minimal to no infrastructure change is necessary to implement widespread biodiesel use. Biodiesel blends can be used in any diesel engine and can be transported and stored using existing infrastructure.

Pure biodiesel is environmentally non-toxic and biodegradable. With its high energy balance of 3.2 to 1, biodiesel provides a beneficial 78% life cycle CO_2 reduction. While biodiesel shows such tremendous potential, there are still unresolved challenges to its complete acceptance. In the list of Research Priorities from the Biodiesel Technical Workshop in Denver, Colorado, in November 2005, the top two items identified by this group of experts were: 1) Fuel Quality and Quality Standards, and 2) Fuel Stability. A distant third priority was cold flow properties. The fuel quality and standards issues are being addressed in the ASTM Fuel Standards subcommittee. Thus, the single most critical acceptance issue requiring research and development is that of biodiesel stability; in particular, oxidative stability.

Oxidative Stability. All fuels (whether petroleum or biofuels) are subject to degradation over time during storage. Currently, best practice involves limiting the storing of biodiesel or biodiesel blends to six months or fewer.

This degradation of the diesel fuels is generally due to oxidation, which is indicated by increased acid number and viscosity, as well as the formation of gums and sediments. The oxidation process starts with the formation of hydroperoxides by the addition of an oxygen molecule to a carbon atom adjacent to a C=C double bond. As oxidation proceeds, the peroxides break away to form aldehydes and short-chain acids. Alternatively, peroxides may generate free radicals, which promote polymerization and crosslinking among the olefinic (C=C containing) molecules. Therefore, oxidation reactivity is related to the degree of C=C bonds in the fuel. Increased content of the C=C bonds correlates to decreased oxidative stability of the fuel. The increase in instability of a given diesel fuel molecule is generally directly proportional to the number of C=C bonds in the molecule (i.e., a molecule containing two C=C bonds has half the stability of a molecule containing one C=C bond). The oxidative stability of a diesel fuel is estimated using the iodine number (ASTM D 1510), and the longer-term stability of a diesel fuel can be evaluated using an accelerated stability test (ASTM D 2274). The iodine value is defined as the amount of iodine (in grams) absorbed by 100 mL fuel, and it is a very crude but commonly used indicator of the level of saturation of oil.

Biodiesel usually has a significantly higher content of unsaturated fatty acid derived esters, therefore their iodine values are noticeable higher than that of petroleum diesel. Some metals act as catalysts for the oxidation process, notably brass, bronze, copper, lead, tin, and zinc. Steel and aluminum equipment are recommended for the manufacture, processing and storing of biodiesel. However, some feedstock for biodiesel production possibly contains some metals at very low concentration. For instance, 0.03-0.05 ppm and 0.02-0.06 ppm copper are present in the crude and refined soybean oil, respectively and could possibly be retained in biodiesel.

Oxidation of oils can be reduced or slowed by means of antioxidants (AO). Soybean oil and other vegetable oils possess natural AOs, which provide some degree of protection against oxidation. These are generally lost or reduced as a result of the biodiesel production process, however.

4. OBJECTIVE

The overall objective of this proposed research is to improve the acceptability of biodiesel as a commercial fuel 1) by developing new AOs in order to enhance stability and 2) by exploring alternative processing strategies that will retain natural AOs in biodiesel. This project supports the Alternative Fuels focal area in fulfilling the mission of the MIOH.

5. LITERATURE SURVEY

Augmenting petroleum-derived fuels with renewable fuels has gained widespread attention in the past few years. One such renewable fuel is biodiesel, which is defined as the mono-alkyl esters of long-chain fatty acids derived from vegetable oils or animal fats, according to ASTM D 6751-07 [4]. Biodiesel offers numerous environmental, economic and energy security benefits, and production capacity has grown considerably in the past two to three years, especially in Europe and the USA. Annual biodiesel production in the USA was only two million gallons in 2000, increasing to 25, 75 and 250 million gallons in 2004, 2005 and 2006, respectively [5]. Currently, methanol is predominantly used in the transesterification process for biodiesel production [6]. The presence of high levels of unsaturated fatty acid methyl esters (FAME) makes biodiesel very susceptible to oxidation as compared to petroleum diesel [7]. Oxidative processes bring about increased viscosity as a result of condensation reactions involving double bonds, also leading to the formation of insolubles, which can potentially plug fuel filters and injection systems [8]. The increased acidity and increased peroxide value as a result of oxidation reactions can also cause the corrosion of fuel system components, hardening of rubber components, and fusion of moving components[8-9]. ASTM D6751-07 includes an oxidation stability standard of a three-hour minimum induction period (IP) as measured using the Rancimat test (EN14112)[4]. The European Committee for standardization adopted a six-hour minimum IP as the specification [10]. A survey of retail biodiesel samples performed in 2004 indicated that only four out of 27 B100 samples met the oxidative stability standard of three-hour and over 85% had an IP less than two hours [11].

In a 2006 survey report, the range of induction periods in 10 samples was 0.43 to 4.26 hours, and only three out of 10 B100 samples met the standard [12]. Our survey [13] of B20, B10, and B5 samples from retail stations also found that over 50% had an IP less than 6 hours, the proposed ASTM oxidative stability for B6- B20.

5.1. Effect of Antioxidants on the Oxidative Stability of Biodiesel

Factors which influence the oxidative stability of biodiesel include fatty acid composition, natural antioxidant content, the level of total glycerin, and the conditions of fuel storage such as temperature, exposure to light and air, and tank material of construction [11, 14-15]. Previous studies have found that antioxidants can be effective in increasing the stability of biodiesel [7, 14, 16-17]. However, these effects have not been fully elucidated and results have been inconclusive or conflicting. Sendzikiene *et al*. [14] found that butylated hydroxyanisole (BHA) and butyl-4-hydroxytoluene (BHT) have nearly the same effect on the oxidative stability of rapeseed oil-, and tallow-based biodiesel, and the optimal level of synthetic antioxidants was determined to be 400 ppm. Mittelbach *et al*. [18] reported that pyrogallol (PY), propylgallate (PG), and t-butylhydroquinone (TBHQ) could significantly improve the stability of biodiesel obtained from rapeseed oil, used frying oil, and beef tallow, whereas BHT was not very effective. Moreover, Domingos *et al*. [7] found that BHT had the highest effectiveness for refined soybean oil-based biodiesel, while BHA displayed little effectiveness.

5.2. Synergistic Effects of Antioxidants on the Oxidative Stability of Biodiesel

Lipid autoxidation reactions have been investigated extensively [8-11]. Through the resultant transesterification of lipid materials, biodiesel exhibits the same fatty acid profile as the source oil or fat. Since many vegetable oils and animal fats possess significant amounts of unsaturated fatty acids (UFA), oxidative stability is of concern, especially under long periods in storage conditions above ambient temperatures, with exposure to air and/or light, and/or in the presence of some contaminants [12]. The main fatty acid methyl esters (FAMEs) in biodiesel are saturated C16, and saturated and unsaturated C18; C18 contain one double bond for oleic acid (C18:1), two for linoleic acid (C18:2), and three for linolenic acid (C18:3). Relative oxidation rates were found to increase as the degree of saturation increased [13]. The polyunsaturated fatty acid chains contain a higher total number of reactive bis-allylic sites than the monounsaturated ones, and hence are more prone to oxidation. Also, dimerization and oligomerization can occur from peroxides, formed from the reactions of radicals through oxidation, reacting with other fatty acids. Fang and McCormick [14] reported that dimerization of the peroxides is not the sole mechanism for molecular weight growth and formation of deposits in biodiesel, but all possible mechanisms involve peroxide formation at the initiation reaction of oxidation. This stresses the importance of minimizing peroxide formation in biodiesel manufacturing and handling, hence the need for antioxidants.

Inhibition of oxidation through the use of antioxidants has been observed to increase the induction period (IP) of biodiesel to varying degrees [15-17]. Cooperative effects (synergy) of antioxidants in fats and oils are documented in several studies [19-24].

Miranova et al.[19] reported that mixtures of α-T and myricetin produced a synergistic effect during the autoxidation of triglycerols of sunflower oil, where the best interaction was achieved using equal molar ratios of the antioxidants at concentrations lower than 0.001 M. Kinetic analysis demonstrated that α-T regenerates myricetin during autoxidation. A study conducted by Becker et al. [20] showed that binary combinations of four antioxidants (α-T, astaxanthin, quercetin and rutin) revealed factors that may affect the synergism and antagonism of antioxidant blends: structural organization of the lipid; solubility, polarity and the hydrophilic nature of the antioxidants. A transfer of hydrogen from BHT-regenerated BHA resulting in higher antioxidant activity than the components used singly in soybean oil, lard and methyl oleate [21]. Niki et al. [22] demonstrated synergism between α-T and ascorbic acid in methyl linoleate; it was observed that ascorbic acid donates hydrogen to regenerate α-T. Antioxidants (BHT, alkylated phenol/dithiophosphoric acid ester/diphenylamine and zinc diamyl dithiocarbamate) and anti-wear additives combinations were also reported to have synergistic effects in vegetable oil-based lubricants based on the FA profile (especially on the polyunsaturation) and the effectiveness of the inhibitors [23, 24].

5.3. Effect of Antioxidants on the Storage Stability of Biodiesel

Biodiesel degradation is caused by an auto-oxidation chain mechanism [19]. The location and number of double bonds in UFAME affect the susceptibility of the fatty acids chain to oxygen attack [20]. The relative rates of oxidation of methyl oleate (C18:1), methyl linoleate (C18:2), and methyl linolenate (C18:3) are 1, 41, and 98, respectively [20]. Moreover, environmental factors affect the stability of biodiesel. Leung *et al.* [21] reported that high temperature, together with air exposure greatly increased the biodiesel degradation rate, but high temperature or air exposure alone had little effect. Lin *et al.* [22] found that higher storage temperature and a longer storage time significantly accelerated the oxidative reaction in palm-oil biodiesel. While the oxidative stability of biodiesel may be improved by modification of the fatty acid methyl ester (FAME) composition [23-25]; this generally adversely affects low-temperature operability [26]. Instead, antioxidant additives (between 200 to 1000 ppm) are commonly employed to improve the oxidative stability of biodiesel. Many studies have demonstrated that antioxidants can improve the oxidative stability of biodiesel [7, 14, 16-17]. The addition of 400 ppm of PY can significantly improve the oxidative stability of rapeseed oil, sunflower oil, and used frying oil-based biodiesel [27]. Our previous study [1-2] also showed that different antioxidants (butylated hydroxyanisole (BHA), butyl-4-methylphenol (BHT), t-butylhydroquinone (TBHQ), 2, 5- Di-tert-butyl-hydroquinone (DTBHQ), ionol BF200 (IB), propylgallate (PG), and pyrogallol (PY)) can enhance the oxidative stability of soybean oil (SBO-), cottonseed oil (CSO-), poultry fat (PF-), and yellow grease (YG-) based biodiesel at the varying concentrations between 250 and 1000 ppm. The effect of each antioxidant on biodiesel differs depending on different feedstock. However, few studies investigated the effect of antioxidant on long term storage stability.

One study of the addition of BHT to palm oil biodiesel demonstrated significantly oxidation over a 3,000-hour period [22].

6. METHODOLOGY

6.1. Materials

Fresh SBO-, CSO-, PF-, and YG-based biodiesel, were obtained directly from Biodiesel Industries (Denton, Texas). Certification #2 ultra low sulfur diesel (ULSD) was obtained from Haltermann Products (Channelview, Texas). Distilled SBO (DSBO)-based biodiesel was obtained by vacuum distillation at 132-138 °C from SBO-based biodiesel. The blends were made on a volume basis and stored in glass bottles at room temperature. Biodiesel was used as B100 or in a blend with petroleum diesel. A blend of 20 % biodiesel with 80 % ULSD, by volume, is termed: "B20" [28].

The α-tocopherol (α-T), butylated hydroxyanisole (BHA, 98.5%), butyl-4-methylphenol (BHT), 2, 5- Di-tert-butyl-hydroquinone (DTBHQ, 99%), propylgallate (PG), t-butylhydroquinone (TBHQ, 97%), and pyrogallol (PY, 99%) were purchased from Sigma-Aldrich Inc. (St. Louis, MO). Ionol BF200 (IB) was obtained from Degussa Sant Celoni (Barcelona, Spain). Up to 1000 ppm of antioxidants was found to dissolve in the biodiesel samples. The chemical structures of antioxidants are shown in Figure 1.

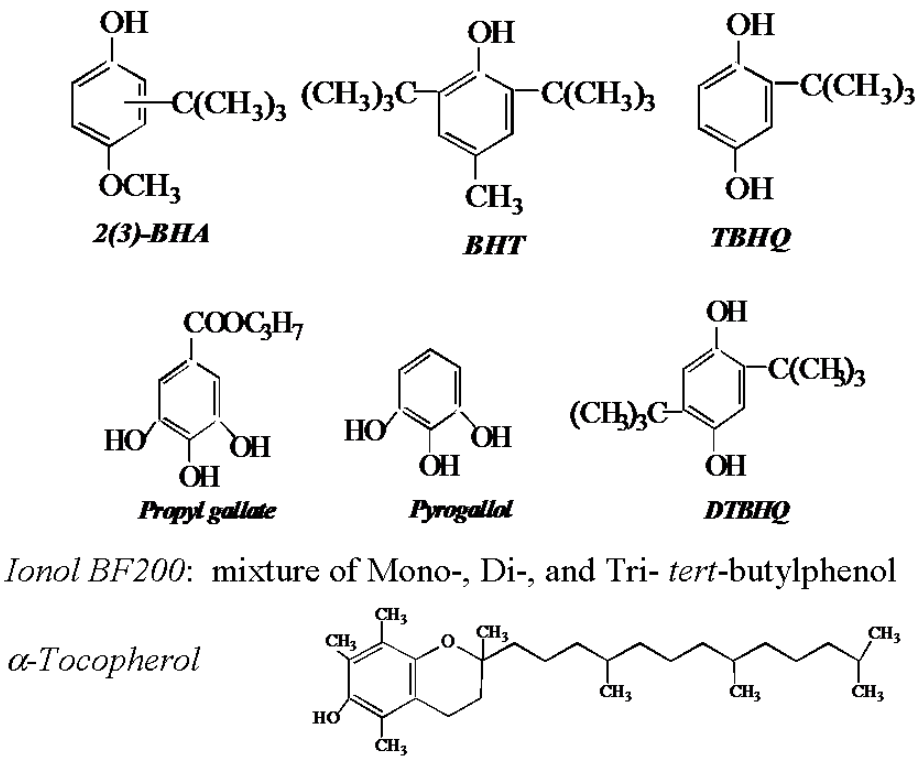

Figure 1. Chemical Structures of Antioxidants

6.2. Binary Sample Preparation

Soybean oil (SBO) based-biodiesel was obtained from NextDiesel (Adrian, MI, USA) and poultry fat (PF) based-biodiesel was obtained from Biodiesel Industries (Denton, TX, USA). Distilled soybean oil (DSBO) and distilled poultry fat (DPF) biodiesels were produced at 185 °C and 4.7 mbar using a Koehler (Bohemia, NY, USA) K80200 vacuum distillation apparatus to minimize the effects of minor components, naturally occurring antioxidant, as well as other volatile contaminants on the oxidative stability of the biodiesel. The different binary blends were prepared by mixing different solid phase antioxidants at weight ratios of 1:0, 0:1, 1:1, 2:1, 1:2, 3:1 and 1:3. The antioxidant blends, with a total loading of 1000 ppm, were added to DSBO-B100 and DPF-B100 and mixed thoroughly. The effects of loading (1000, 500, 250, 200, 150, 100, and 50 ppm) for selected blends were also investigated. Extra care was taken to avoid contamination and degradation of the antioxidants used. Freshly distilled samples without any additives were used as the control for DSBO and DPF.

6.3. Long-Term Storage Stability

6.3.1. Individual Antioxidants

SBO-I-based biodiesel both without and with different antioxidants at a concentration of 1000 ppm were stored in three-gallon carbon-steel containers. The containers were not purged with nitrogen and were not airtight to allow sample contact with air. One set of samples was stored indoors (at room temperature, 23 ºC); the others were stored outdoors (at Michigan ambient temperature from December 2006 to September 2007). The recorded ambient temperature value ranged between -13.1 ºC and 27.4 ºC (Table 1) according to national climatic data center. Samples of 100 mL were periodically taken for determination of acid number, kinematic viscosity, IP, and the concentration of antioxidant and biodiesel.

6.3.2. Binary Antioxidants

DSBO-II-based biodiesel with 500ppm of TBHQ: BHA (2:1), TBHQ: PG (1:1) and TBHQ: PY (1:1) antioxidant mixtures were stored in three-gallon carbon-steel containers. The containers were not purged with nitrogen and were not airtight to allow sample contact with air. One set of samples was stored indoors (at room temperature, 23 ºC); the others were stored outdoors (at Michigan ambient temperature from February 2009 to September 2009). The recorded ambient temperature value ranged between -12 ºC and 27 ºC (Table 2).

Table 1. Detroit Average Temperature (ºF) from December 2006 to September 2007

Month	Dec, 2006	Jan, 2007	Feb, 2007	Mar, 2007	Apr, 2007	May, 2007	Jun, 2007	Jul, 2007	Aug, 2007	Sep, 2007
Max ºC	4.7	0.2	-4.3	8.4	12.4	21.6	26.7	27.4	26.9	23.9
Min ºC	-2.2	-7.4	-13.1	-2.5	1.2	8.1	12.2	12.7	15.2	11
Ave ºC	1.2	-3.7	-8.7	2.9	6.8	14.8	19.4	20.1	21	17.4

Table 2. Detroit Average Temperature (ºC) from February 2009 to September 2009

	Feb-09	Mar-09	Apr-09	May-09	Jun-09	Jul-09	Aug-09	Sep-09
Max ºC	10	15	23	23	27	27	27	23
Min ºC	-12	-10	0	11	13	17	14	16
Ave ºC	-2	3	9	16	19	21	22	19

6.4. Analysis

6.4.1. FAME Composition

The fatty acid composition of each biodiesel was determined using a Perkin-Elmer Clarus 500 GC-MS with a split automatic injector, and a Rtx-WAX (Restek, Bellefonte, PA) column (length: 60 meters; ID: 0.25 mm, coating: 0.25 μm). Details of the procedure have been described elsewhere[29].

6.4.2. Oxidative Stability

Oxidative stability of biodiesel with and without the addition of antioxidant was determined according to the Rancimat method using a Metrohm 743 Rancimat instrument (Herisau, Switzerland). The Rancimat test is the specified standard method for oxidative stability testing for biodiesel in accordance with EN14112 [10]. The IP was determined by the measurement of a sudden increase of conductivity upon the formation of volatile acids. Samples of 3 g (B100) or 7.5 g (B20) were analyzed at a heating block temperature of 110 ºC and constant air flow of 10L/h. To evaluate the reliability of the method employed, one group of the tests was carried out in triplicate (Fig 1), the absolute difference between two independent single test results did not exceed the repeatability limit of EN14112 method.

Tests results are reported as the mean of triplicate runs (the Rancimat results are repeatable within ± five percent) within the repeatability limits of their respective standard method.

6.4.3. Kinematic Viscosity and Acid Number

The viscosity of biodiesel at 40 ºC was determined following ASTM D 445 using a Rheotek AKV8000 automated kinematic viscometer (Poulten Selfe & Lee Ltd., Essex, England). Acid number of biodiesel was determined according to ASTM D 664 using a Brinkman/Metrohm 809 Titrando (Westbury, NY). The acid number is the quantity of base, expressed as milligrams of potassium hydroxide per gram of sample, required to titrate a sample to a specified end point.

6.4.4. Free Glycerin and Total Glycerin

Free glycerin and total glycerin were determined according to ASTM D 6584 [30] with a PerkinElmer Clarus 500 GC equipped with a flame ionization detector (GC-FID). A PE-5HT column (15 m in length, with a 0.32 mm internal diameter, and a 0.1 μm film thickness) was used. The column was held at 50 ºC for one minute and then ramped to 180 ºC at 15 ºC/min, 230 ºC at 7 ºC/min, and 380 ºC at 30 ºC/min, respectively. Finally, it was held at 380 ºC for 10 minutes. Hydrogen (99.9999%, Cryogenic Gases, Detroit, MI) was used as the carrier gas with a flow rate of 3 mL/min.

6.4.5. Cloud Point, Pour Point, and Cloud Filter Plugging Point

The CP, PP, and CFPP measurements were done as per ASTM standards, D 2500-25 for CP [31], D 97-96a for PP [32], and D 6371-05 for CFPP [33]. A Lawler model DR-34H automated cold properties analyzer (Lawler Manufacturing Corporation, Edison, NJ) was used to measure the cold flow properties.

6.4.6. Antioxidant Content by GC-FID

The content of TBHQ and PY were analyzed with a PerkinElmer Clarus 500 GC-FID. The sample (~100 mg) was mixed with 100 μL of ISTD1, and 100 μL of MSTFA in a vial, and allowed to sit for 30 min at room temperature. Finally, 2 mL of heptane was added to the vial. A PE-5HT column (15 m in length, with a 0.32 mm internal diameter, and a 0.1 μm film thickness) obtained from PerkinElmer, Shelton, CT) was held at 50 ºC for 1 minute and then ramped to 180 ºC at 15 ºC/min, 230 ºC at 7 ºC/min, and 380 ºC at 30 ºC/min. Finally, it was held at 380 ºC for 10 minutes. Hydrogen (99.9999%, Cryogenic Gases, Detroit, MI) was used as carrier gas with a flow rate of 3 mL/min.

7. DISCUSSION OF RESULTS

7.1. Effect of Individual Antioxidants on Oxidative Stability of Biodiesel

7.1.1. Analysis of Biodiesel Samples

Physical property data on the five types of biodiesel samples are given in Table 3. On the whole, most of the values were within the limits given by ASTM D6751-07. Attention should be paid to the high acid number in YG-based biodiesel. SBO- and CSO-based biodiesel met the limit of a three-hour induction period; however, PF-, YG-, and DSBO-based biodiesel did not meet the oxidative stability specification. The IP of CSO-based biodiesel was the highest without added antioxidant among the five types of biodiesel.

Table 3. Physical Properties of SBO-, DSBO-, CSO-, PF-, YG-Based Biodiesel, and ULSD

	ASTM method	ASTM specification [a]	SBO	DSBO	CSO	PF	YG	ULSD
Viscosity, 40 ºC (mm^2/s)	D 445	1.9-6.0	4.336	4.050	4.221	4.386	4.552	2.154
Acid number (mg KOH/g)	D 664	0.5 max	0.215	0.179	0.262	0.298	0.515	0.005
Free glycerin (mass %)	D 6584	0.020	0.006	0	0.001	0.001	0.000	-
Total glycerin (mass %)	D 6584	0.24	0.177	0	0.186	0.143	0.016	-
Cloud point (ºC)	D 2500	Report	3	4	6	7	13	-25
Pour point (ºC)	D 97		-3	0	0	3	0	-36
Cold filter plugging point (ºC)	D 6371		-3	0	3	2	-3	-26
Oxidative stability Induction Period (hr)	EN 14112	3 minimum	3.52	0.77	6.57	0.67	2.25	-

[a] Specification as given in Reference [34]

The FAME compositions for the different biodiesel samples are shown in Table 4. For SBO-based biodiesel, methyl linoleate (C18:2) is the predominant FAME (48.7%); followed by methyl oleate (C18:1, 25.3%), and methyl palmitate (C16:0, 14.1%). As expected, the FAME compositions of DSBO-based biodiesel and SBO-based biodiesel are nearly identical. Similarly, for YG- based biodiesel, methyl linoleate is the predominant FAME (46.2%), followed by methyl oleate (31.43%), and methyl palmitate (16.1%). CSO-based biodiesel also was predominantly methyl linoleate (53%), but with methyl palmitate having the second greatest abundance (24.7%), followed by methyl oleate (18.5%). The FAME composition of PF–based biodiesel differed greatly from the vegetable oil-based biodiesel, where methyl oleate (36.6%) was the predominant FAME, followed by methyl linoleate (27%), and methyl palmitate (21.8%). For SBO-based biodiesel, total saturated FAME (19.2%) was lower than the values of CSO (28.2%) and PF (30.9%). These results are in good agreement with other reports [35-36].

Table 4. Fatty Acid Methyl Esters (FAME) Composition of SBO-, DSBO-, CSO-, PF-, and YG-Based Biodiesel.

	FAME composition (wt) %				
FA	SBO	Distilled SBO	CSO	PF	YG
C14:0	0	0	0.76	1.04	0.14
C16:0	14.1	16.02	24.74	21.82	16.12
C16:1	0.7	0.56	0.37	3.71	0.02
C18:0	5.15	5.37	2.68	7.61	3.96
C18:1	25.29	26.51	18.45	36.59	31.43
C18:2	48.7	46.31	52.99	27.02	46.05
C18:3	6.08	5.23	0	1.78	2.28
∑SFA (%)	19.2	21.39	28.2	30.9	20.22
∑UFA (%)	80.8	78.61	71.8	69.1	79.78

The oxidative stability of biodiesel in general depends on the FAME compositions as well as the presence of natural antioxidants in the feedstock. High levels of unsaturated fatty acids make the biodiesel more susceptible to oxidation and resultant shorter induction times [20, 37]. The CSO-based biodiesel has less unsaturated FAME than SBO-based biodiesel, and the IP is indeed higher for CSO-based biodiesel. Moreover, the natural antioxidants appear to remain in the distillation residue following distillation, which results in a lower IP in DSBO-based biodiesel than SBO-based biodiesel while having the same FAME composition [11, 38].

Previous studies have also shown that un-distilled biodiesel is more stable when compared with distilled biodiesel [38-39]. It is interesting to note that PF-based biodiesel has a lower unsaturated FAME content; however it exhibits poor oxidative stability, as compared to SBO-based biodiesel. This can be attributed to lower concentrations of naturally occurring antioxidants in PF-based biodiesel [14]. Similar results have shown that the vegetable oil-based biodiesel is more stable than animal fat-based biodiesel [14].

7.1.2. Effect of Antioxidants on Oxidative Stability of SBO-, CSO-, PF-, and YG-Based Biodiesel

Figure 2 shows the IP of SBO-based biodiesel as a function of the concentration of added antioxidant. The antioxidants were added to the SBO-based biodiesel in a concentration range between 250 and 1000 ppm. Generally, the IP of samples were observed to increasing with the increasing antioxidant concentration. PY was found to be the most effective antioxidant in terms of increasing IP over the range of 250 -1000 ppm, while α-T shows the smallest increase. PG was the second most effective antioxidant in the range of concentrations between 250 and 500 ppm, followed by TBHQ, however, TBHQ was more effective than PG at 1000 ppm. The addition of BHA, BHT, DTBHQ, and IB was found to increase IP, and their effects are very close to each other with BHA exhibiting the highest IP increase at concentrations near 1000 ppm.

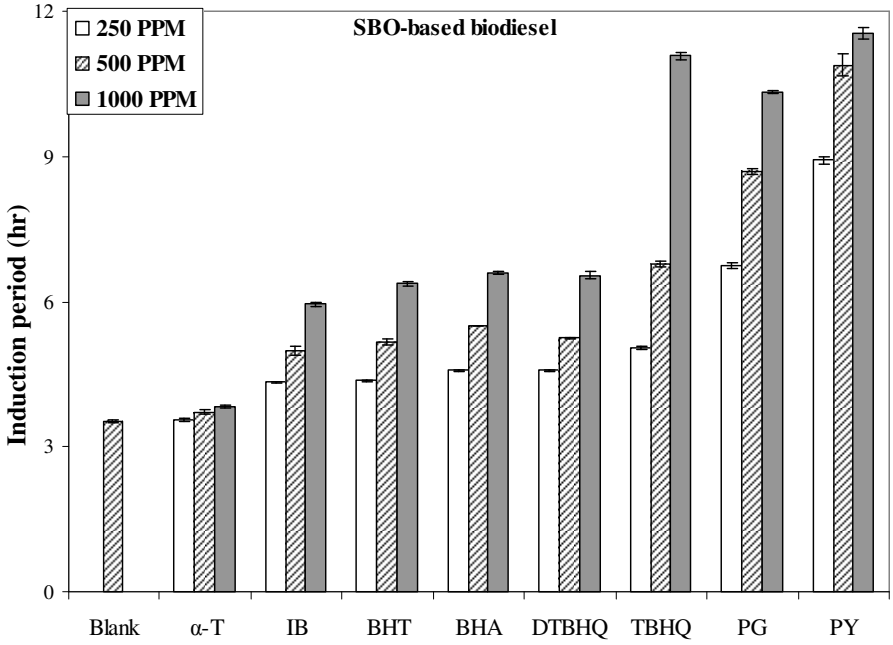

Figure 2. Effects of Concentration of α-T, IB, BHT, BHA, DTBHQ, TBHQ, PG, and PY on the Induction Period of Soybean Oil (SBO-) Based Biodiesel

Dunn [40] reported that PG, BHT, and BHA were most effective and α-T least effective in increasing oxidation onset temperature (OT) of soybean oil. In this study, PG, and PY were the most effective antioxidants with an IP > 6 hr at 250 ppm and TBHQ improved the IP > 6 hr at 500 ppm, while DTBHQ, BHT, and BHA increased IP > 6 hr at 1000 ppm. However, Ruger *et al*. [41] showed that TBHQ was the most effective for soy based biodiesel as measured by viscosity, while PG increased slightly and BHT and BHA show no improvement. Domingos *et al*. [7] showed that BHT displayed the highest effectiveness in the concentration range from 200 to 7000 ppm in refined soybean oil based biodiesel, TBHQ displayed a greater stabilizing potential at 8000 ppm, while BHA showed no noticeable increase from 2000 to 8000 ppm. It should be noted in their study, the original biodiesel had a very low IP (0.16 hr), and different range of additive concentrations were utilized [7]. Therefore, different results on antioxidant may be due to differences in the feedstocks of biodiesel, and experimental protocols.

The effects of the concentration of eight antioxidants on the oxidative stability of CSO-, YG-, and PF-based biodiesel are shown in Figures 3, 4, and 5, respectively. All antioxidants were found to increase the IP with increasing concentration.

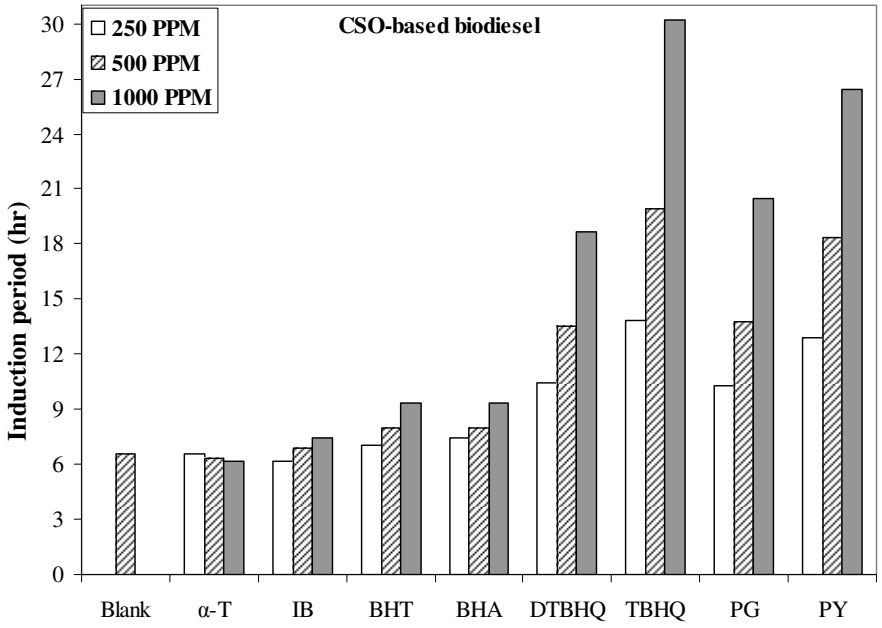

Figure 3. Effects of Concentration of α-T, IB, BHT, BHA, DTBHQ, TBHQ, PG, and PY on the Induction Period of Cottonseed Oil (CSO-) Based Biodiesel

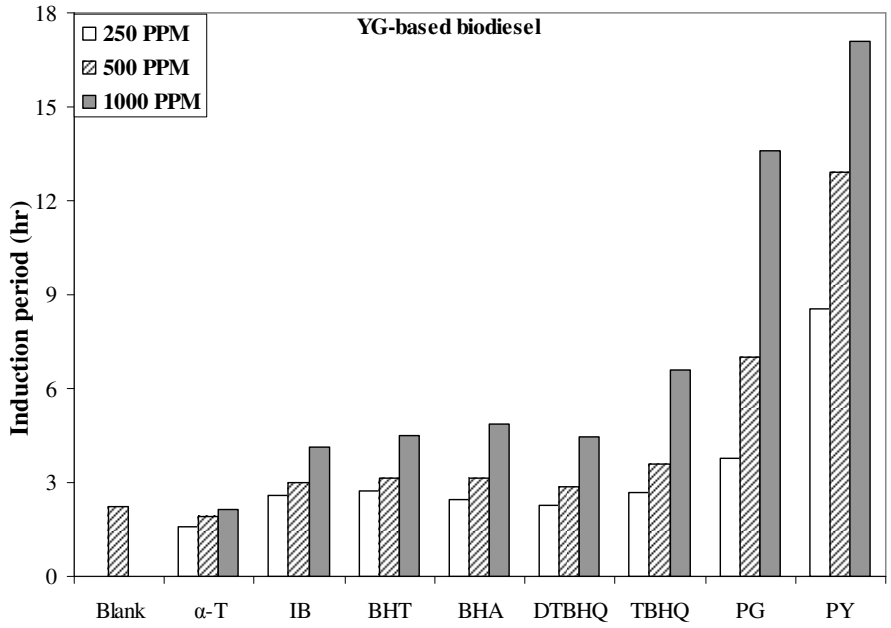

Figure 4. Effects of Concentration of α-T, IB, BHT, BHA, DTBHQ, TBHQ, PG, and PY on the Induction Period of Yellow Grease (YG-) Based Biodiesel

For CSO-based biodiesel, TBHQ gave the highest IP increase at 250-1000 ppm, followed by PY, PG, and DTBHQ (Figure 3). It was noted that BHA and BHT had almost the same effectiveness with the CSO-based biodiesel. However, the addition of IB displayed no noticeable increase in oxidative stability at 250 ppm and 500 ppm, and only a slight increase at 1000 ppm. Compared to the SBO-based biodiesel, the effectiveness of antioxidants for CSO-based biodiesel was somewhat different, with TBHQ having the greatest effect on oxidative stability, reaching to 30.2 hr at 1000 ppm.

For the YG-based biodiesel (Figure 4), the untreated sample did not reach the ASTM specification for B100 (2.25 hr vs. 3 hr). The effectiveness of antioxidants on the IP of YG-based biodiesel is very similar to SBO-based biodiesel: PY produced the best improvement. PG was the second most effective antioxidant followed by TBHQ, BHA, BHT, DTBHQ, and IB. However, the addition of α-T had no or even negative effects. It was noted that only PY at 250 ppm can improve the IP > 6 hr, as well as PG at 500 ppm and TBHQ at 1000 ppm. The effect of PY, PG, TBHA, BHA, and BHT are consistent with a previous study with frying oil based biodiesel [18]. Schober *et al.* [15] also showed that DTBHQ is a good additive for recycled cooking oil methyl ester stability.

For PF-based biodiesel (Figure 5), the IP of untreated biodiesel was very low (0.67 hr). PY was found to provide the greatest improvement, followed by BHA. BHT was the third most effective antioxidant, where the IP can meet the ASTM specification (> 3 hr) at 500 ppm while PG, TBHQ, and IB are effective only at 1000 ppm. The addition of DTBHQ even at 1000 ppm was ineffective in meeting ASTM specs.

No noticeable increase in oxidative stability was observed by the addition of α-T. Raemy *et al*. [42] reported that PG can improve the oxidative stability of chicken fat. In this study, only PY and BHA at 500 ppm could improve the IP > 6 hr.

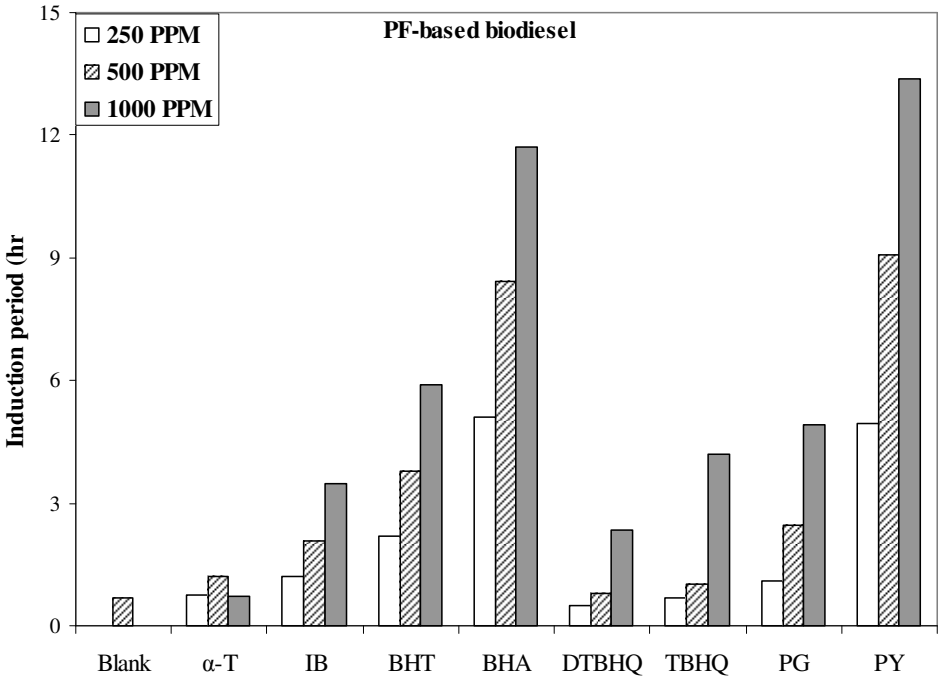

Figure 5. Effects of Concentration of α-T, IB, BHT, BHA, DTBHQ, TBHQ, PG, and PY on the Induction Period of Poultry Fat (PF-) Based Biodiesel

Many antioxidants have been studied for their effects on biodiesel oxidative stability [4; 15; 31; 34], including PG, TBHQ, BHT, BHA, IB, and α-T. In this study, all of the test antioxidants except the natural antioxidant α-T had a measurable positive impact on the oxidative stability of all different types of biodiesel. The pattern of effectiveness for antioxidants on SBO-, CSO-and YG-based biodiesel is BHA ~ BHT < DTBHQ ~ TBHQ < PG ~ PY, with the exception of TBHQ having the most effect on the oxidative stability for CSO-based biodiesel. The different effects of antioxidants can be attributed to their molecular structures. These types of antioxidants have an aromatic ring with different functional groups at different position of the ring. The active hydroxyl group can provide protons that combine with oxidized free radicals, thus delaying the initiation of or slowing the rate of oxidation [16, 43]. Based on their electro-negativities (which is defined as the tendency of the hydroxyl group to attract a bonding pair of electrons), the antioxidants having an active hydroxyl groups (-OH) can be ranked as: BHA ~ BHT < DTBHQ ~ TBHQ < PG ~ PY. For vegetable oil based biodiesel, they were almost in accordance with the rank. However, the antioxidant action on PF-based biodiesel was different: the rank is TBHQ < BHT << PY~BHA. These suggest that the effect of antioxidants on biodiesel depend on the oil feedstock (Table 2).

Mittelbach and Schober [18] showed that TBHQ produced the best results at 1000 ppm for rapeseed oil based biodiesel; while PG and PY are the most effective followed by TBHQ, BHA, and BHT for used frying oil, and sunflower seed oil based biodiesel; and PY is the best for beef tallow oil based biodiesel. Surprisingly, α-T displayed no noticeable effectiveness in this study. Similar results were also observed elsewhere [43].

7.1.3. Effect of Antioxidant on Distilled Biodiesel

Our study has investigated the effectiveness of one natural antioxidant (α-tocopherol (α-T)), six synthetic antioxidants (butylated hydroxyanisole (BHA), butyl-4-hydroxytoluene (BHT), *t*-butylhydroquinone (TBHQ), 2,5-di-*tert*-butyl-hydroquinone (DTBHQ), propylgallate (PG), and pyrogallol (PY)), and one commercial antioxidant (ionol BF200 (IB)) on the oxidative stability of biodiesel [1]. We found that all of synthetic antioxidants enhanced the oxidative stability of different types of biodiesel, while adding α-T had no noticeable effect. The IP increased as a function of the antioxidant concentration over the range of 250 -1000 ppm. Moreover, the effect of each antioxidant on biodiesel stability was different depending on the feedstock: PY, PG, and TBHQ were the most effective antioxidants for SBO-, CSO- and YG-based biodiesel, while PY, BHA, and PG were most effective for PF-based biodiesel.

Distillation of biodiesel can remove the minor components such as the glycerides, sterols, and natural antioxidants, while the FAME composition remains relatively constant. To eliminate the effect of age, oxidative history, and minor components, we studied the effect of eight antioxidants (1000 ppm) on distilled SBO- (DSBO-), and PF- (DPF-) based biodiesel (Figure 6). The IP of distilled SBO-based biodiesel significantly decreases, compared to undistilled, which can be attributed to a decrease in the content of natural antioxidant. The effect of different antioxidants on distilled biodiesel is similar to the original biodiesel: PY, PG, and TBHQ gave the best result, followed by BHA, BHT, DTBHQ, IB, and α-tocopherol. Interestingly, the activity of PY and PG on DSBO-1-based biodiesel appears more efficient than on untreated ones, while the effectiveness of TBHQ on DSBO-2-based biodiesel significantly increases. For PF-based biodiesel, TBHQ, PY, and PG are the best antioxidants on the distilled fuels, while BHA, PY, and PG are the best ones on untreated ones. Moreover, the antioxidants in DPF-based biodiesel are much more effective than in untreated PF-based biodiesel. This may be attributed to the fact that PF-based biodiesel does not contain natural antioxidants, and is easily oxidized.

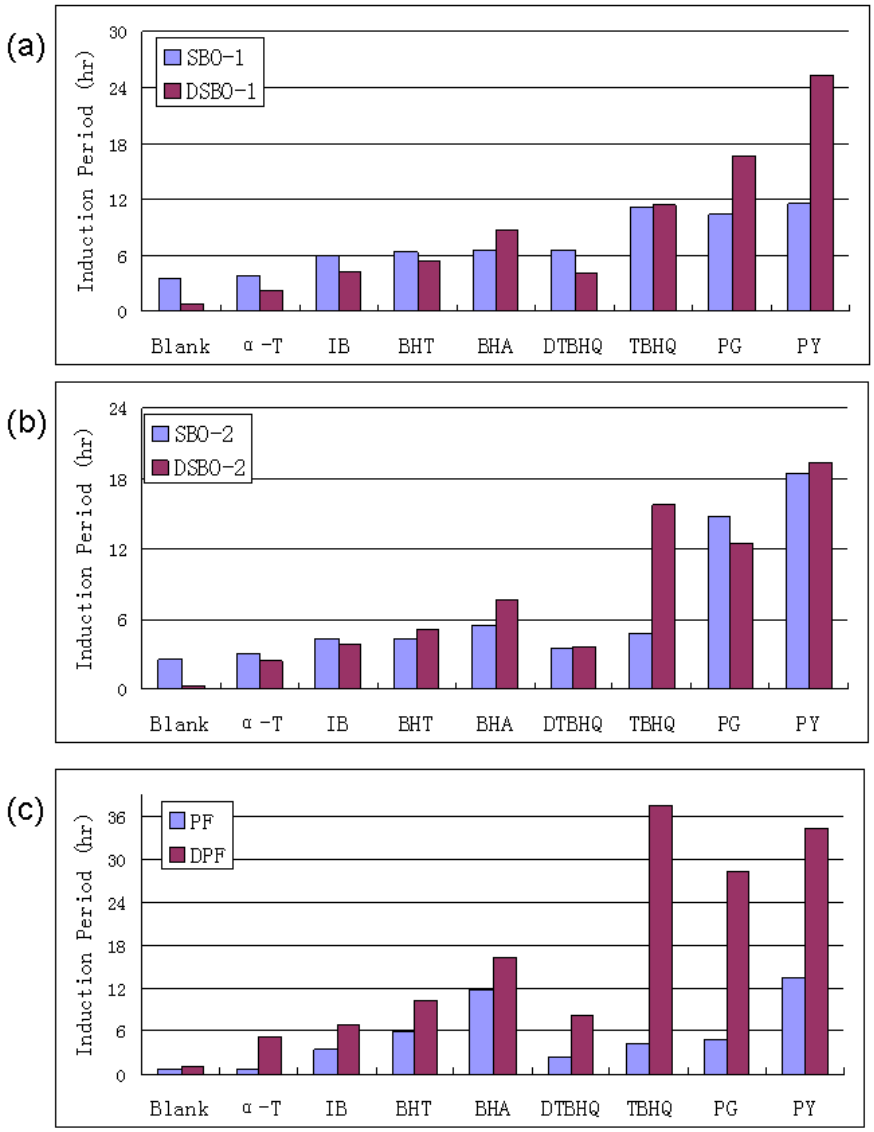

Figure 6. Effects of Concentration of α-T, IB, BHT, BHA, DTBHQ, TBHQ, PG, and PY on the Induction Period of: (a) SBO-1; (b) SBO-2; and (c) PF-Based Un-Distilled and Distilled Biodiesel

7.1.4. Effect of Antioxidant on Oxidative Stability of SBO-Based B100 and B20

In Figure 7, the effect of eight types of antioxidants on the IP of both B20 and B100 soy-based biodiesel is shown. Antioxidant was added at a concentration of 200 ppm for the B20 and 1000 ppm for the B100. The IP of untreated B20 is significantly higher than that of the B100. For B20 samples, the addition of PY resulted in the highest IP (34.49 hr), followed by PG and TBHQ. BHA, BHT, DTBHQ, and IB had similar effects; whereas α-T was not effective. For B100, there is a similar observation on the effect of antioxidant. Moreover, the ratios of IP between B20 and B100 for different antioxidants were observed to be relatively constant (2.4 ~ 3.2). These results suggested that the effect of antioxidants on B20 and B100 was similar.

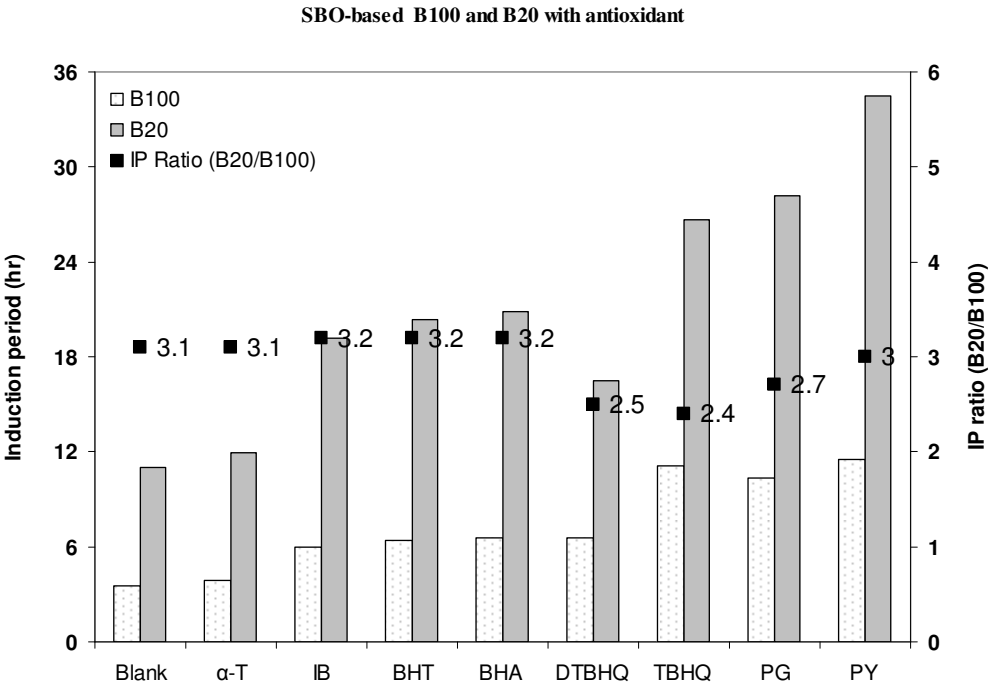

Figure 7. Effects of Antioxidants on the Induction Period of SBO-based B100 and B20

7.2. Effect of FAME in Feedstocks on Oxidizability

FAME compositions, α-tocopherol content, oxidizability (OX), and the IP for eight types of biodiesel are shown in Table 4. These include biodiesel based on soybean oil (SBO), cottonseed oil (CSO), palm oil (PO), yellow grease (YG), poultry fat (PF), and choice white grease (CWG). The oxidizability measures the relative oxidation rate [20],as determined by the equation:

$$\text{Oxidizability (OX)} = [0.02\ (\%\ 18{:}1) + (\%\ 18{:}2) + 2\ (\%\ 18{:}\ 3)]/100$$

based on 18-carbon chains containing one double bond for oleic acid (18:1), two for linoleic acid (18:2), and three for linolenic (18:3).

Table 5. Fatty Acid Methyl Esters (FAME) Composition, Oxidizability (OX), Tocopherol Content, and Induction Period (IP) of Biodiesel Based on SBO, CSO, PO, YG, PF, and CWG

	FAME Composition (wt%)							
FA	SBO-1	SBO-2	SBO-3	CSO	PO	YG	PF	CWG
14:0	0.0	0.0	0.0	0.8	0.6	0.1	1.0	1.9
16:0	14.1	10.2	11.0	24.7	47.2	16.1	21.8	22.6
16:1	0.7	0.0	0.0	0.4	0.0	0.0	3.7	3.0
18:0	5.2	4.3	4.2	2.7	3.0	4.0	7.6	12.8
18:1	25.3	22.6	22.6	18.5	40.8	31.4	36.6	41.2
18:2	48.7	55.4	55.0	53.0	8.2	46.1	27.0	16.9
18:3	6.1	7.5	7.2	0.0	0.2	2.3	1.8	1.7
∑SFA (%)	19.2	14.5	15.2	28.2	50.9	20.2	30.9	37.2
∑UFA (%)	80.8	85.5	84.8	71.8	49.1	79.8	69.1	62.8
Oxidizability	0.61	0.71	0.70	0.53	0.09	0.51	0.31	0.21
Amount of natural antioxidant (ppm)	733	167	69	970	281	-	-	-
Oxidative stability induction period (h)	3.5	2.8	7.2	6.6	11.1	2.3	0.8	8.1

FAME compositions are significantly different for the different types of biodiesel: Methyl linoleate (18:2) is the principal ester in SBO, CSO, and YG, while methyl oleate (18:1) predominates in PF- and CWG-based biodiesel. However, methyl palmitate (16:0) is the major FAME in PO. There are clear inconsistencies between the computed OX and the measured IP. As to be expected, PO-based biodiesel, with the lowest OX has the highest IP. On the other hand, PF-based biodiesel displayed the lowest IP while having only a moderately high OX. The three of SBO-based biodiesel samples, with relatively similar FAME compositions and almost the same OX, have significantly different IP. This indicates that the OX of biodiesel alone is not sufficient for discriminating the oxidative stability. Rather, the natural antioxidant content should be also considered. Tocopherols are the most common natural antioxidants in vegetable oils. In this study, SBO-, CSO, and PO-based biodiesel contained 69-970 ppm of tocopherols, while no tocopherols were detected in YG-, PF-, and CWG-based biodiesel. Even for the same feedstock (soybean oil), the level of tocopherol varied: SBO-1-based biodiesel (733 ppm) had more tocopherol than SBO-2-based biodiesel (167 ppm), with a corresponding increase in IP. On the other hand, SBO-3-based biodiesel had the lowest tocopherol content (69 ppm), but it has the highest IP, suggesting the likely presence of a synthetic antioxidant.

7.3. Synergistic Effects of Antioxidants on the Oxidative Stability of Biodiesel

7.3.1. Oxidation and Analysis of Biodiesel

The biodiesel was vacuum distilled to eliminate effects on the oxidative stability by impurities such as trace metals. The trace Cu and Fe levels within the distilled biodiesel were determined using a Perkin-Elmer Optima 2100 DV optical emission spectrometer (Restek, Bellefonte, PA, USA) and were found to be in the range of 0.0001 ppm and 0.001 ppm, respectively. Oxidation of the samples using the Rancimat at 110 °C with the addition of 0.01% and 0.02% citric acid metal chelator indicated negligible effect of metals in the oxidation.

Table 6 summarizes the IP, TAN and viscosity results for the distilled and undistilled biodiesel along with the limit values in the biodiesel standard. FAME compositions, total SFA and UFA, and natural AO content of the biodiesel are shown in Table 7. FAME compositions of SBO and DSBO had no significant differences and the SBO FAME profile is in agreement with other studies [28, 29]. On the other hand, distillation of PF to DPF resulted in a decrease in the total UFA profile from 71.6% to 66.4% which is mainly due to C18:1 and C18:2. Consequently, the total SFA composition rose because of C16:0. This instance may be attributed to mild oxidation during the distillation process causing the unsaturated component of DPF to drop.

Table 6. Specifications Related to the Quality in Biodiesel Standards

Specification	Methods	Unit	ASTM D6751	EN 14214	Biodiesel Samples			
					SBO	DSBO	PF	DPF
Oxidative Stability (IP)	EN 14112	hr	3 min	6 min	2.68	0.17	0.52	0.93
FAME content ≥ 4 double bonds	EN 14103	% m/m	-	1 max	-	-	-	-
Linolenic acid content (C18:3)		% m/m	-	12 max	7.5	7.2	1.4	1.4
Total Acid Number (TAN)	ASTM D664, EN 14104	mg KOH/g	0.500 max	0.500 max	0.525	0.309	0.550	0.360
Kinematic viscosity (ν)	ASTM D445, ISO 3104/3105	mm^2/s	1.9 - 6.0	3.5 - 5.0	4.14	3.99	4.32	4.29

A study of the kinetics of lipid autoxidation reported that relative oxidation rates of UFA are as follows: C18:3 > C18:2 >> C18:1 [13]. In general, the higher the degree of unsaturation, especially the polyunsaturation, the higher the rate of oxidation with the total amount of C18:3 and C18:2 for SBO (63%) much higher than PF (28.4%), the IP for SBO should be expected to be much lower than the IP of PF. However, in this case it is the opposite, with the IP of SBO (2.68 hours) being much higher than that of PF (0.52 hr). This is likely due to the amount of natural antioxidants present in the biodiesel, as indicated by previous studies [12, 19] which have concluded that the oxidative stability of biodiesel depends on the FAME compositions as well as other factors such as natural antioxidant content. SBO was found to contain 167 ppm of natural antioxidant while none could be detected in PF. This finding confirms the higher oxidative stability observed for vegetable oil-based biodiesel than animal fat-based biodiesel [16]. In addition, this finding suggests that the amount of natural antioxidant plays a major role in determining the oxidative stability of biodiesel.

Upon distillation, the biodiesel minor components (sterols, glycerides and natural antioxidant) were greatly reduced. The natural antioxidant content in SBO dropped from 167 ppm to 40 ppm, while the IP decreased from 2.68 hours to 0.17 hours, on the other hand, the IP of DPF (0.93 hr) was higher than the IP of PF (0.52). Even though there is a concern on the validity of an IP below one hour, this reproducible observation may be a result of the decrease of the total UFA, removal of the some oxidation products, volatile impurities and polymeric materials in the vacuum distillation. Likewise, the reduction of TAN, conforming to ASTM D6751 and EN 14214, and viscosity values support this conclusion.

The IP for all the biodiesel samples and the TAN value for the undistilled biodiesel samples did not meet the ASTM D6751-07 and EN 14214 specifications suggesting that the biodiesel samples under study were already significantly oxidized. The results also suggest that the viscosity is not greatly affected by the level of oxidation; consequently, it is not a good indicator of the level of oxidation.

Table 7. Fatty Acid Methyl Ester (FAME) Composition and the Physical Properties of SBO-, DSBO-, PF- and DPF-Based Biodiesel Samples

FAME composition (wt) %										natural AO (ppm)
FA	C14:0	C16:0	C16:1	C18:0	C18:1	C18:2	C18:3	∑SFA	∑UFA	
SBO	0	10.2	0	4.3	22.6	55.5	7.5	14.5	85.5	167
DSBO	0	12.4	0	4.1	22.1	54.2	7.2	16.5	83.5	40
PF	1	20.1	3.1	7.3	40.1	27	1.4	28.4	71.6	-
DPF	1.6	25.9	4.1	6.1	36	25	1.4	33.6	66.4	-

7.3.2. Antioxidant Blending

The effects of blending ratios of TBHQ: BHA, PG and PY on the IP of B100 are shown in Figure 8. The highest IP (32.79 hrs) was achieved by using a 2:1 weight ratio (667 ppm TBHQ, 333 ppm PY) in DSBO. Similarly, the highest IP (43.49 hours) was obtained by using this same antioxidant binary formulation in DPF. As a general observation, using any blend ratio of TBHQ:BHA, TBHQ:PG and TBHQ:PY in DSBO and DPF resulted in an improved IP greater than when using the individual antioxidants by themselves at the same loading, regardless of type of biodiesel.

The effects of the different antioxidant blends on the pertinent parameters relating to oxidative stability (IP, TAN, viscosity and stabilization factor (SF) which expresses the antioxidant effectiveness by the IP ratio of inhibited and uninhibited oxidation [19]) are presented in Table 3. The most effective antioxidant is PY, followed by PG, TBHQ and finally BHA during oxidation of DSBO and DPF at 110 $^{\circ}$C is in good agreement with previous studies [18, 30]. The antioxidant effectiveness (based on SF) in both DSBO and DPF is highest with PY (individual or in binary formulation).

The SF is expressed as:

$$SF = {}^{IP_1}/_{IP_0} \qquad (1)$$

where IP_1 is the IP with inhibitor while IP_0 is the IP of the control sample without antioxidant.

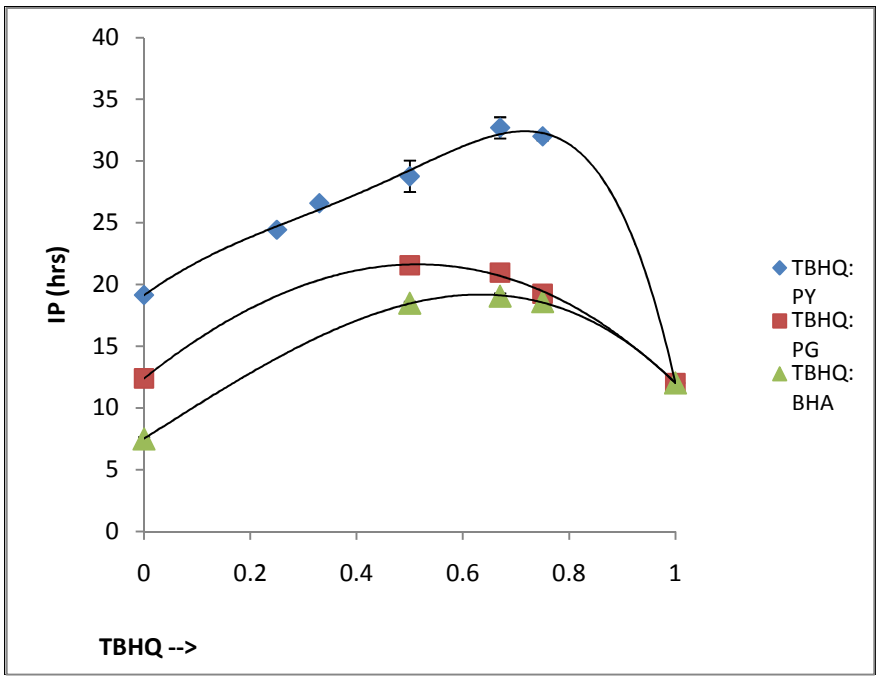

(a)

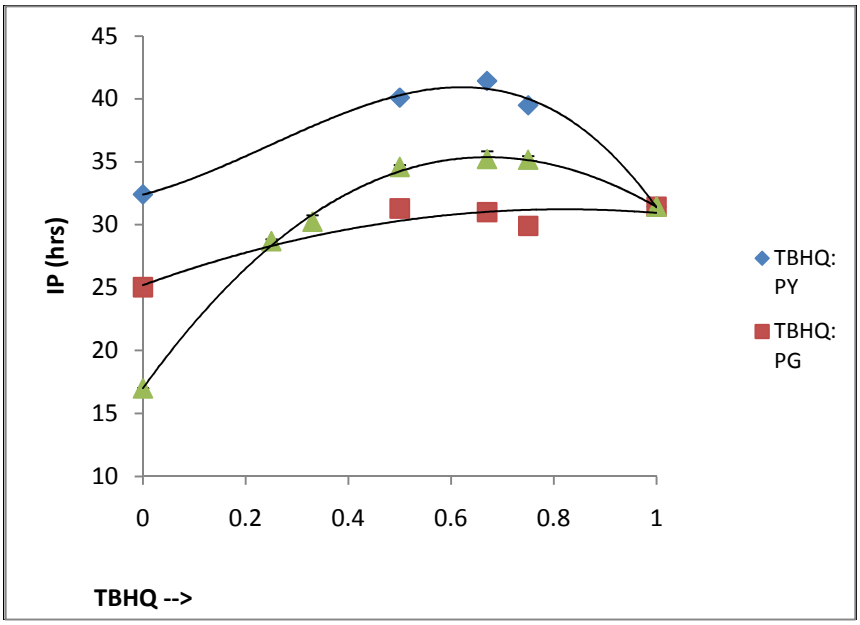

(b)

Figure 8. The Resultant IP Values of using Binary Antioxidant Blends at 1000 ppm Loading: (a) in DSBO, and (b) in DPF

Similar to the previous study [18], biodiesel with PG or PY loading produced increased TAN values (Table 8). The highest TAN values 0.521 and 0.433 mgKOH/g with 1:1 TBHQ: PG in DSBO and DPF, respectively, were observed. On the other hand, there was very little difference in viscosity, as the increase in viscosity is linked more to secondary degradation products.

According to Miranova et al [19], inhibition of oxidation can be expressed using two kinetic characteristics: the effectiveness and the strength of the inhibitor. The effectiveness of the inhibitor represents the possibility of blocking the propagation phase through interaction with the peroxyl radicals, which is responsible for the duration to reach the IP. The strength gives the possibility of antioxidant moieties participating in other side reactions which may change the oxidation rate during the course of IP. For our study, we focus on the effectiveness of the inhibitor systems, expressed as equation (1) above.

The resulting improvement in IP (considering the stability reported in our previous study [18]) and the SF are in the order of PY>PG>TBHQ>BHA in DSBO and DPF (Table 8). In DPF, the SF for TBHQ and PG are similar and close to the SF for PY. This is quite different from the SFs in DSBO. In general PY (individual or in blends) have highest SF in both DSBO and DPF.

Table 8. Inhibited Oxidation Parameters of DSBO- and DPF-Based Biodiesel Samples

Biodiesel	Antioxidant	Concentration		Ratio		IP (hr)	TAN(mg KOH/g)	Viscosity, 40 °C (mm^2/s)	SF	% SYN
		ppm	M x 10^{-4}	Weight	Molar					
DSBO	TBHQ	500	3.5			6.85			40.29	
	TBHQ	667	4.6			8.73			51.35	
	BHA	333	2.1			4.00			23.53	
	PG	500	2.7			10.46			61.53	
	PY	333	3			15.82			93.06	
	TBHQ:BHA	1000	6.7	2:1	2:1	19.51	0.342	4.03	114.77	56.09
	TBHQ:PG	1000	6.2	1:1	1:1	21.55	0.521	4.02	126.76	25.99
	TBHQ:PY	1000	7.6	2:1	1:1	32.69	0.431	4.02	192.29	34.32
DPF	TBHQ	500	3.5			17.43			19.28	
	TBHQ	667	4.6			21.05			22.63	
	BHA	333	2.1			11.05			11.88	
	PG	500	2.7			19.52			20.99	
	PY	333	3			25.11			27	
	TBHQ:BHA	1000	6.7	2:1	2:1	35.21	0.406	4.33	37.86	(13.36)
	TBHQ:PG	1000	6.2	1:1	1:1	31.19	0.433	4.31	33.54	(-13.76)
	TBHQ:PY	1000	7.6	2:1	1:1	43.49	0.371	4.30	46.76	(-3.93)

7.3.3. Antioxidant Synergy

Inhibitors sometimes can reinforce each other synergistically. The percent synergism (% SYN) is calculated on the basis of the IPs observed as follows [8]:

$$\%SYN = \frac{(IP_{mix} - IP_0) - [(IP_1 - IP_0) + (IP_2 - IP_0)]}{[(IP_1 - IP_0) + (IP_2 - IP_0)]}\ x\ 100\% \qquad (2)$$

where IP_{mix}, IP_0, IP_1 and IP_2 are the induction periods of the samples containing the mixture of inhibitors, of the control sample, and of the samples containing the individual antioxidants. A positive value defines a synergistic effect between the implicated antioxidants, while a negative value corresponds to an antagonistic effect.

The IP using the same antioxidants is much higher in DPF than in DSBO. Sharma et al. [23] concluded that antioxidants increased their response in oils with less amount of polyunsaturation which was the case for the degree of polyunsaturation of DPF versus DSBO. Similarly, all IP improvement using antioxidant blends in DPF were greater than in DSBO. In our study, all binary blending of the different antioxidants produced higher IP compared to the sum of IPs of each antioxidant component in DSBO (Table 3), hence a positive % SYN value. However, in DPF only the 2:1 TBHQ:BHA weight ratio produced a positive synergy (13.36%), while 1:1 TBHQ:PG and 2:1 TBHQ:PY resulted in antagonism (-13.76% and -3.93%, respectively), this contradicts the significant IP results above. Although there was observed negative synergy, the huge IP increase in DPF is still noteworthy. Details of this phenomenon may be linked to the high level of oxidation of the parent PF-based biodiesel. On the other hand, it was reported that the effectiveness of antioxidants depends on the nature biodiesel feedstock [18], thus, for this study we note the synergy of antioxidants is also feedstock dependent.

Based on the previous studies [19-24] on antioxidant synergy and this investigation, we propose two schemes of interaction: (i) hydrogen donation of the more active antioxidant to regenerate the other antioxidant and (ii) formation of heterodimer from the moieties of the antioxidant during autoxidation. Figures 3(a) and 3(b) show the two proposed schemes that are assumed to work simultaneously within the system to arrive at total synergistic effect.

7.3.4. Antioxidant Regeneration

Primary antioxidants act as radical scavengers to inhibit oxidation [15-18, 23]. Hydrogen is abstracted from the active hydroxyl (-OH) groups and then donated to the free radical to inhibit the rate of oxidation. The resulting antioxidant is a stable radical that can react with other fatty acid free radicals and further contribute to oxidation inhibition. In the same manner, when antioxidants are present in combinations, one antioxidant can become a hydrogen donor for the other, thus regeneration takes place, as in BHA and BHT [21]. Through this mechanism, the donor is consumed while the hydrogen acceptor antioxidant propagates its oxidation inhibition.

In Figure 9(a), the proposed mechanism is the regeneration of PY in the TBHQ: PY blends. PY, being the more effective antioxidant, readily donates its hydrogen from its hydroxyl group to fatty acid free radicals creating an antioxidant radical in the process. TBHQ then transfers hydrogen to the antioxidant radical to regenerate it back to PY. In the process, TBHQ was converted to a radical that can form stable products with other free radicals; this together with the interaction and regeneration of PY represents an effective synergistic effect between the two antioxidants. Antioxidant quantification using GC-FID from a three-month storage study of DSBO with 2:1 TBHQ: PY indicated that the consumption of TBHQ is greater than the consumption of PY, with the total amount of PY close to its original value (values not shown here). The results support the assumption for the regeneration of PY by TBHQ.

(a)

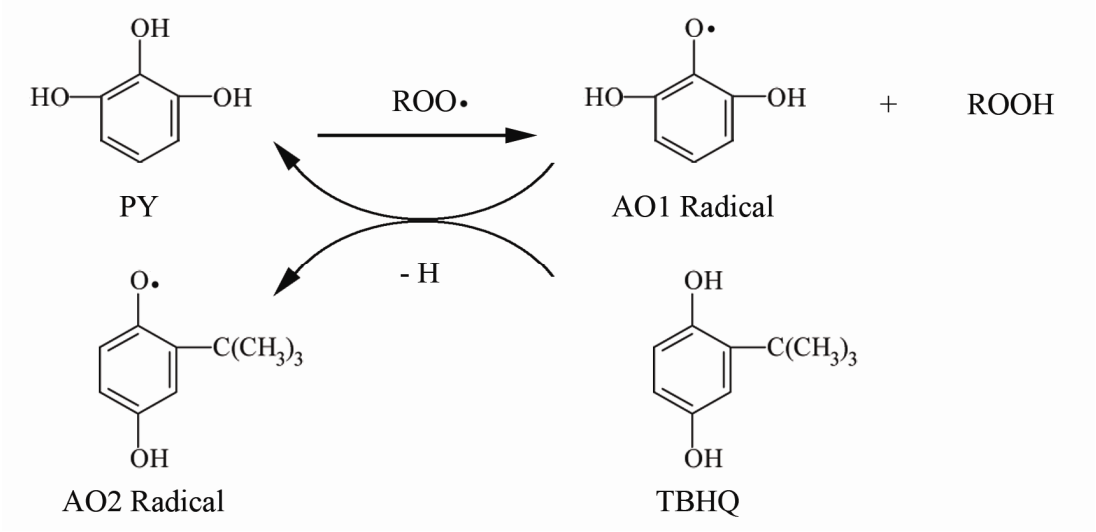

(b)

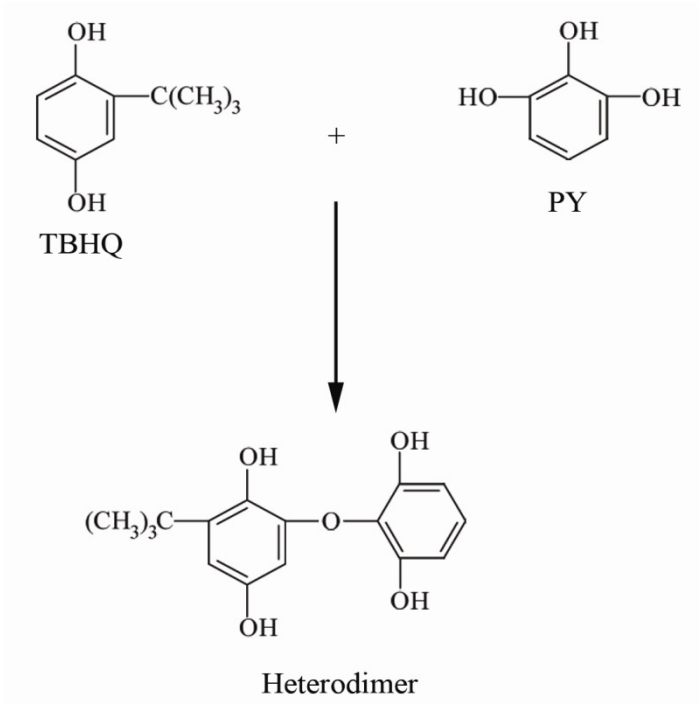

Figure 9. Proposed Mechanisms for the Synergistic Interaction Between TBHQ and PY: (a) Antioxidant Regeneration and (b) Antioxidant Heterodimer Formation

7.3.5. Heterodimer Antioxidant

Primary antioxidants degrade to form different species/moieties that participate in the reaction during the autoxidation of fats and oils. Kikugawa et al. [31] reviewed the study of degradation effects in the mechanism of action of primary antioxidants, properties of degradation products and the role of synergists (antioxidant class) in regenerating primary antioxidants. Degradation under autoxidation of fats and oils in thermal oxidation, active oxygen method and UV/Vis irradiation were carried out, formations of moieties and antioxidant dimers were observed in primary antioxidants. TBHQ yielded derivative products that retain antioxidant properties, some even have higher activity than TBHQ based on different substrates [32]. Degradation of PG resulted in the formation of species that retained antioxidant properties, a similar analogy can be used in the case of PY.

Antioxidant mixtures initiated the formation of heterodimers from the degradation products of the primary antioxidants. Based on previous studies [33, 34], mixtures of BHA and BHT produced heterodimers of comparable activity to that of BHT. Likewise, BHT and PG produced two heterodimers composed of two phenols each, the products were found to be better antioxidants in SBO. Cuvelier et al. [35] established the relationship between structure and the activity of these phenolic antioxidants. Combinations of two phenols were found to increase efficiency as compared to lone phenols. From our results of antioxidant blending, the best combination was achieved by using TBHQ: PY and it can be inferred that the degradation product moieties of both the primary antioxidants are effective antioxidants as well. In Figure 9 (b), the dimerization of these moieties produced new antioxidant species that contain two phenols which in effect are better antioxidants than the parent antioxidants. The synergism is a result of the effect of increase in activity of these resultant heterodimers coupled with the effectiveness of the original antioxidants. Proper detection/quantification of such antioxidant moieties/heterodimers within the biodiesel sample system is still under study.

7.3.6. Effect of Antioxidant Blends Concentration

An increase in the IP was observed as antioxidant loading was increased in both DSBO and DPF. In Figure 10 (a), a nearly linear increase in IP was observed up to 500 ppm, and leveling off from 500 to 1000 ppm. The leveling observation may be attributed to the possible saturation of biodiesel with the antioxidant blend. Another possibility may be related to the dissolution of the solid-phase antioxidants, as reported by Dunn [36] for both PY and PG. Interestingly, for DPF a more linear concentration effect and greater magnitude were observed (Figure 10 (b), this shows the increased effect of the antioxidants at lower polyunsaturation to a point of maximized efficiency without saturation.

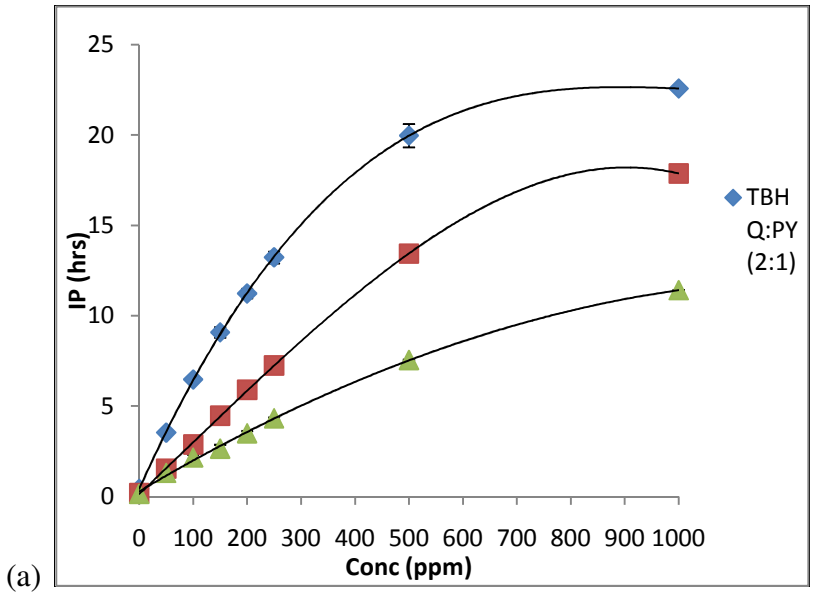

(a)

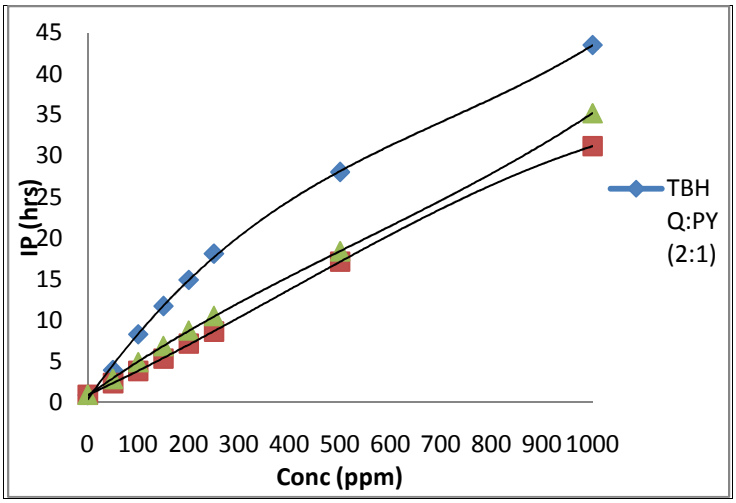

(b)

Figure 10. The IP values at varying antioxidant blend loadings of 1:1 TBHQ: BHA, 1:1 TBHQ: PG and 2:1 TBHQ: PY in (a) DSBO and (b) DPF

Compared with the four commercial antioxidants (A, B, C and D) at equal loading of 200 ppm (active ingredient content), the IP with a 2:1 TBHQ: PY formulation in both DSBO and DPF was much higher (Figure 5). Similarly, all binary formulation in Table 9 produced better IP values as compared to the commercial antioxidants.

Table 9. Inhibited Oxidation Parameters of DSBO- and DPF-Based Biodiesel Samples

Biodiesel	Antioxidant	Concentration		Ratio		IP (hr)	TAN(mg KOH/g)	Viscosity, 40 °C (mm^2/s)	SF	% SYN
		ppm	M x 10^{-4}	Weight	Molar					
DSBO	TBHQ	500	3.5			6.85			40.29	
	TBHQ	667	4.6			8.73			51.35	
	BHA	333	2.1			4.00			23.53	
	PG	500	2.7			10.46			61.53	
	PY	333	3			15.82			93.06	
	TBHQ:BHA	1000	6.7	2:1	2:1	19.51	0.342	4.03	114.77	56.09
	TBHQ:PG	1000	6.2	1:1	1:1	21.55	0.521	4.02	126.76	25.99
	TBHQ:PY	1000	7.6	2:1	1:1	32.69	0.431	4.02	192.29	34.32
DPF	TBHQ	500	3.5			17.43			19.28	
	TBHQ	667	4.6			21.05			22.63	
	BHA	333	2.1			11.05			11.88	
	PG	500	2.7			19.52			20.99	
	PY	333	3			25.11			27	
	TBHQ:BHA	1000	6.7	2:1	2:1	35.21	0.406	4.33	37.86	(13.36)
	TBHQ:PG	1000	6.2	1:1	1:1	31.19	0.433	4.31	33.54	(-13.76)
	TBHQ:PY	1000	7.6	2:1	1:1	43.49	0.371	4.30	46.76	(-3.93)

7.4. Long-Term Storage Stability of Biodiesel

7.4.1. Analysis of Biodiesel Samples

Physical property data on the SBO-I- and DSBO-II-based biodiesel are given in Table 10. On the whole, most of the values were within the limits given by ASTM D 6751-08 [44]. SBO-I-based biodiesel met the limit of a three-hour induction period; however, DSBO-II-based biodiesel did not meet the oxidative stability specification, which was caused by significantly removing the natural antioxidant during distillation process [45].

Table 10. Physical Property Data on the SBO-I- and DSBO-II-Based Biodiesel

	ASTM method	ASTM specification	SBO-I	DSBO-II
Viscosity, 40 ºC (mm^2/s)	D 445	1.9-6.0	4.34	3.99
Acid number (mg KOH/g)	D 664	0.5 max	0.22	0.31
Free glycerin (mass %)	D 6584	0.020	0.006	0
Total glycerin (mass %)	D 6584	0.24	0.177	0
Cloud point (ºC)	D 2500	Report	3	-1
Pour point (ºC)	D 97		-3	0
Cold filter plugging point (ºC)	D 6371		-3	-2
Oxidative stability Induction Period (hr)	EN 14112	3 minimum	3.52	0.17

7.4.2. Effect of Individual Antioxidants: Indoor Storage

Figure 11 shows the IP of SBO-I-based biodiesel with or without different antioxidant over a period of 30 months. The IP of untreated SBO-I-based biodiesel gradually and decreased from 3.5 hours to 0.3 hours over the 30 months, while the biodiesel with TBHQ was found to be very stable. The IP of biodiesel with α-T decreased from 3.84 hours to less than three hours after two months of storage; while biodiesel with PY failed the oxidative stability specification after four months. The value of IP of SBO-I-based biodiesel with PY, PG, DTBHQ, BHA, BHT, and IB are significantly increased to 11.5 hours, 10.3 hours, 6.5 hours, 6.6 hours, 6.4 hours, and 5.9 hours at the initial time, respectively; but significantly decreased over the 30-month period. The addition of BHA and BHT could retain the IP above 3 hours for 12 months, while IB and DTBHQ reached 18 months, following by PG for 24 months. The rank of antioxidants on improving storage stability during 30-month period is TBHQ >> PG > IB~DTBHQ > BHA~BHT > PY > α-T. TBHQ can maintain storage stability of biodiesel for a long term. The antioxidant (α-T) was less effective on oxidative and storage stability than the synthetic antioxidants. This result agrees with a similar study, which showed that TBHQ in SBO-based biodiesel was more effective than α-T for three months [46].

Figure 12 shows the acid number of SBO-I-based biodiesel with different antioxidants as a function of storage time. The acid number for untreated SBO-I-based biodiesel increased with time, and reached 0.52 mg KOH /g after 18 months. Samples with antioxidants α-T, BHT, BHA, and DTBHQ had a slight increase in acid number during the first nine-month period, then significantly increased, exceeding the ASTM D 6751-08 specification after 24 months. IB and TBHQ had a very slow increase in acid number during the first 18-month period, and exceeded the ASTM D 6751-08 specification after 30 months.

The viscosity of SBO-I-based biodiesel with different antioxidants as function of storage time was also measured (Figure 13). The viscosity for untreated SBO-I-based biodiesel increased from 4.3 to 5mm^2/s over the 30-month period. On the other hand, adding TBHQ resulted in a stable viscosity (4.3mm^2/s) over the entire 30-month period. For biodiesel with added α-T, BHA, DTBHQ, and PY there was observed a slow increase in viscosity during the first 12-month period, then a rapid increase after that. The viscosity of biodiesel with IB, BHT, and PG only had a slight increase during the 30-month period. It should be noted that the ASTM D 6751-08 specification (1.9 - 6.0 mm^2/s) at 40 ºC was not exceeded in any cases. This result is in agreement with a previous study that recommended that viscosity cannot be used as a sole parameter to estimate fuel quality [46].

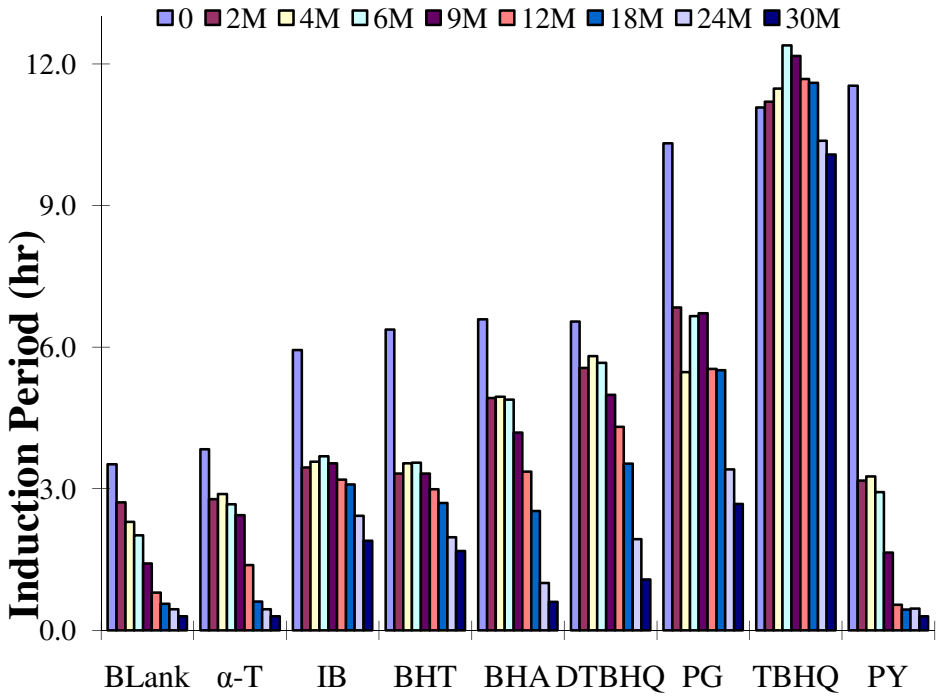

Figure 11. Effects of 1000 ppm of α-T, IB, BHT, BHA, DTBHQ, TBHQ, PG, and PY on the Induction Period of Soybean Oil-I (SBO-I-) Based Biodiesel as a Function of Indoor Stored Time

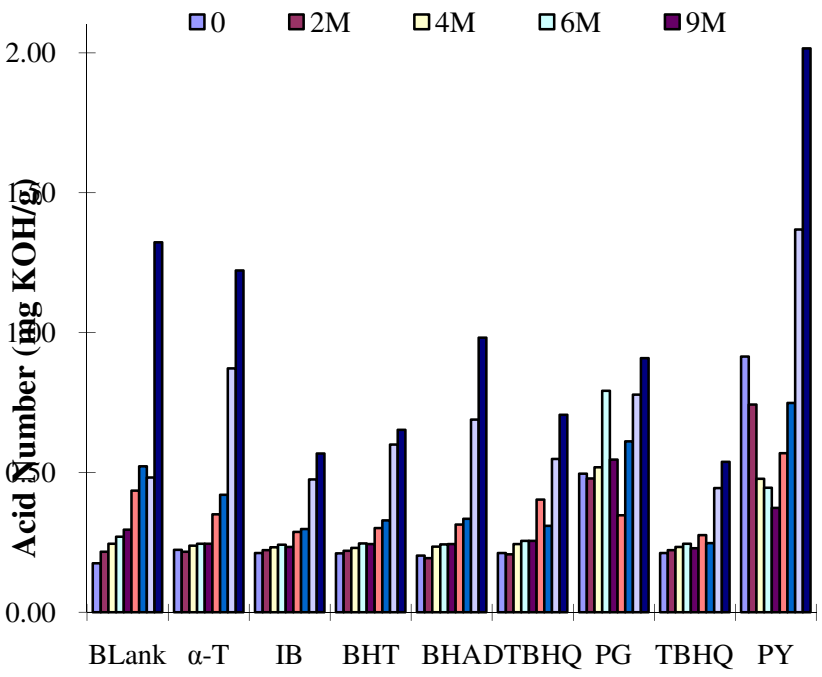

Figure 12. Acid Number of SBO-I-Based Biodiesel with Antioxidants as a Function of Indoor Storage Time

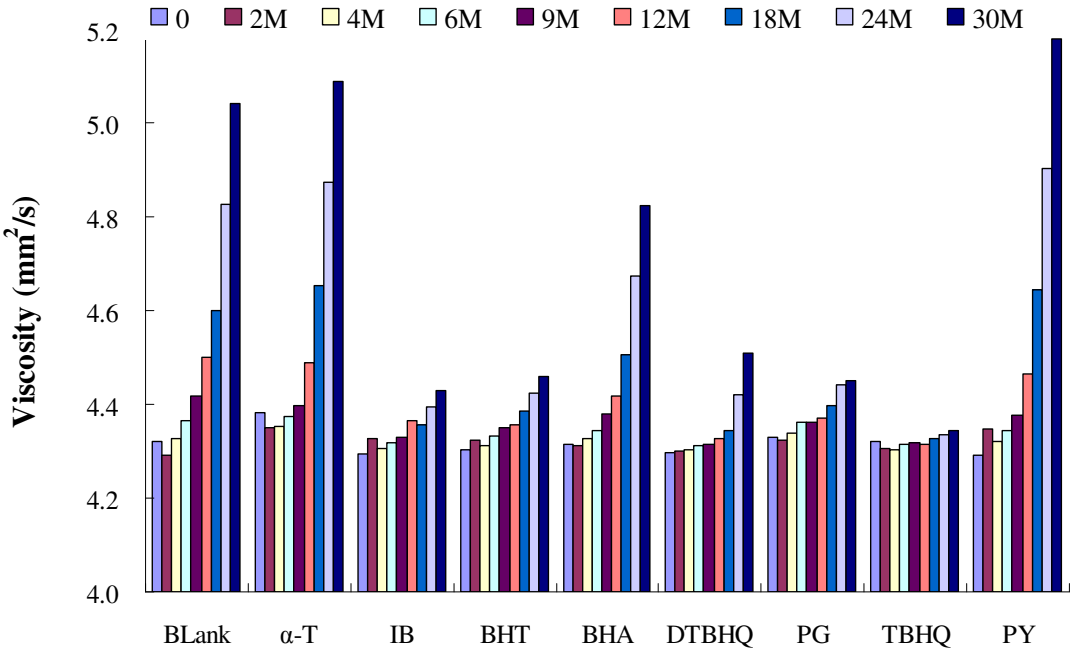

Figure 13. Kinematic Viscosity of SBO-I-Based Biodiesel with Antioxidants at 40 ºC as a Function of Indoor Storage Time

Table 11 shows the FAME content of untreated and treated SBO-I-based biodiesel after 18-, 24-, and 30-month storage. For the untreated sample, the FAME content significantly decreased from 100 to 87.5% after 30 months. However, the biodiesel with adding TBHQ remained relatively unchanged (about 98%) for up to 30 months. FAME levels for biodiesel with other antioxidants significantly decreased to levels ranging from 97.1% to as low as 86.8% over the 30-month storage. The more effective antioxidants on storage stability of biodiesel (such as TBHQ, BHA, DTBHQ, BHT, PG, and IB) can maintain relatively higher FAME content as compared to the less effective antioxidants (α-T and PY).

Table 11. Effect of Antioxidants on FAME Content of SBO-I-Based Biodiesel after 18-, 24-, and 30-month Indoor Storage

	FAME Content by GC-MS								
Time	Control	TBHQ	PG	PY	IB	BHA	α-T	BHT	DTBHQ
0	100%	100%	100%	100%	100%	100%	100%	100%	100%
18M	93.1%	97.2%	96.4%	93.7%	96.9%	94.1%	92.3%	96.5%	97.0%
24M	90.9%	98.2%	96.4%	91.9%	95.2%	92.1%	90.6%	96.0%	94.2%
30M	87.5%	98.9%	96.4%	88.2%	97.1%	90.0%	86.8%	96.0%	95.1%

The FAME compositions after 18, 24, and 30 months for the untreated SBO-I-based biodiesel and of the biodiesel treated with TBHQ and PY are shown in Figure 14. For all of SBO-I-based biodiesel samples, methyl linoleate (C18:2) is the predominant FAME; followed by methyl oleate (C18:1), and methyl palmitate (C16:0). Over the 30-month period, the methyl linolenate (C18:3), and the methyl linoleate of untreated biodiesel gradually decreased by 32.8% and 20.3%, respectively; while methyl palmitate and methyl oleate underwent no significantly change. The total UFAME of untreated biodiesel was decreased by 14.9%. The long chain and polyunsaturated FAME was more readily oxidized than the monounsaturated and saturated ones. Similar results have shown that UFAME in palm oil-based biodiesel was also decreased over a period of 3000 hrs [22]. The biodiesel treated with PY underwent a similar change in FAME composition as the untreated fuel. The methyl linolenate and methyl linoleate were significantly decreased over 30-month period and the total UFAME was decreased by 12.1%. However, there was no significant change in the total UFAME of the biodiesel treated with TBHQ over 30-month storage. These results are consistent with the oxidative stability observations.

The TBHQ and PY content in biodiesel after 18-, 24-, and 30-month storage are shown in Table 12. The added PY in biodiesel declined from 1000 ppm to less than 100 ppm after 18 months, while TBHQ content only gradually decreased to 575 ppm after 30 months. This indicates that the PY was consumed within a short time period. Conversely, the TBHQ content in biodiesel degraded slowly, maintaining the oxidative and storage stability of biodiesel.

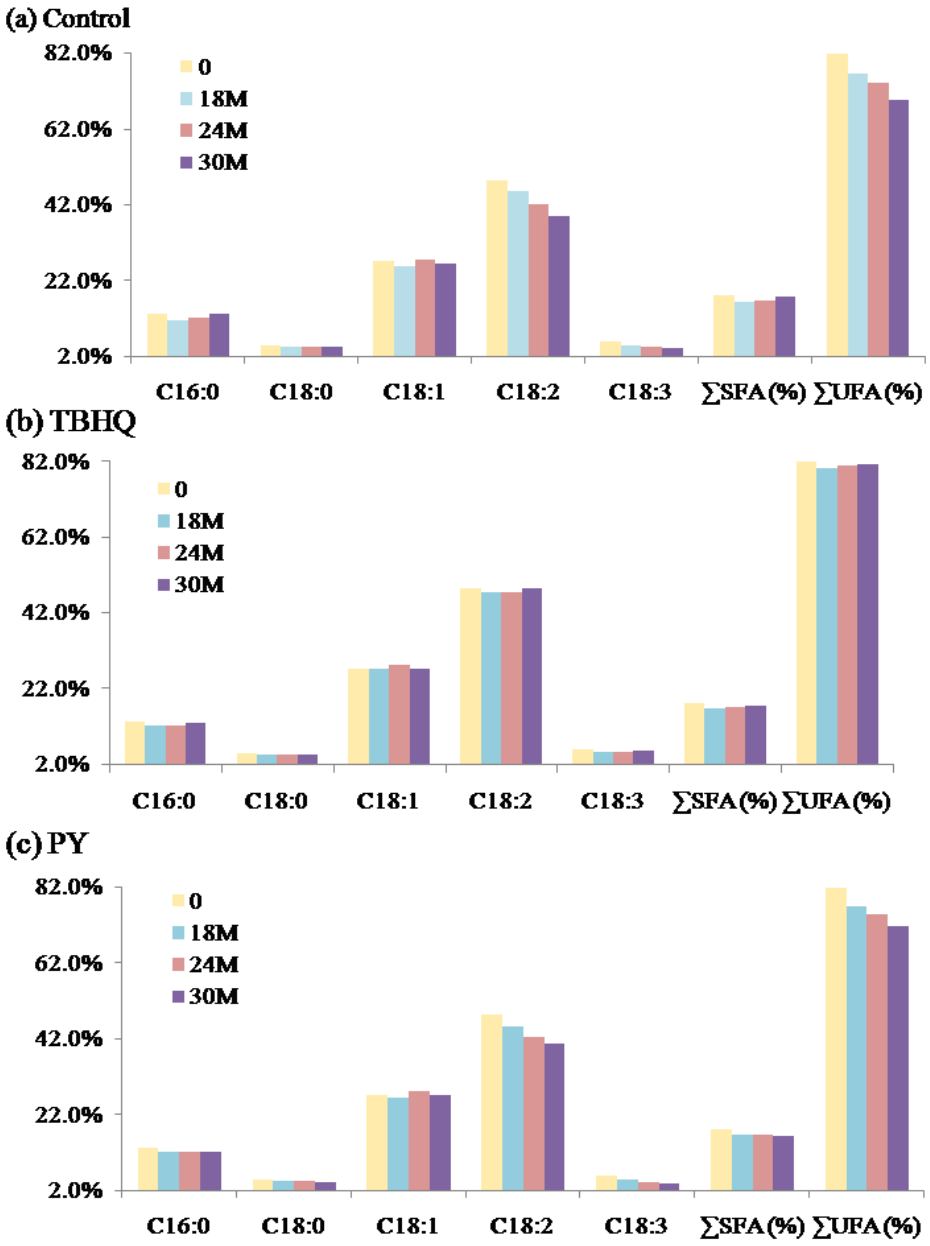

Figure 14. Effect of Fatty Acid Methyl Esters (FAME) Composition of (a) SBO-I-Based Biodiesel; (b) SBO-I-Based Biodiesel with TBHQ; and (c) SBO-I-Based Biodiesel with PY as a Function of Indoor Storage Time

Table 12. Effect of Antioxidants Concentration as a Function of Indoor Storage Time

Antioxidant Concentration (ppm)		
Time	TBHQ	PY
Control	1000	1000
18M	764	<100
24M	677	<100
30M	575	<100

7.4.3. Effect of Individual Antioxidants: Outdoor Storage

For outdoor storage, conditions of the Michigan ambient temperature from December 2006 to September 2007 prevailed (Table 1). Under outside storage conditions, samples were exposed to a range of low and high temperature during the 9-month period. The oxidative stability of untreated SBO-based biodiesel decreased gradually by 38.8% (Figure 15 b). At the same time, adding TBHQ resulted in a stable IP for up to 9 months. The effect of BHT (decrease by 47.1%) and IB (decrease by 40.1%) under outdoor storage was very similar to indoors. However, the stability of biodiesel with DTBHQ, BHA, PY, PG, and α-T during the outdoor storage period is different with indoors: with a slow decrease in oxidative stability during the first four-month period (winter time), and then rapid decrease after that (summer time). Those samples with added PY had a significant decrease from 9.89 hours to 0.4 hours during the six to nine-month period. Clearly, the Michigan ambient temperature during the summer period significantly affected the effectiveness of antioxidants PY, PG, DTBHQ, and BHA. Notably, TBHQ and PG were able to maintain an IP of 6 hr for up to 9-months outdoor storage. Bondilli *et al*. [47] reported that TBHQ decreased by approximately 8% of its initial value, whereas PY did not show any significant variation under commercial storage conditions over one year.

Table 14 shows the acid number of SBO-based biodiesel with different antioxidants as function of storage time. It is an indicator for the stability of the fuel because the acid value may increase as the fuel is oxidized. The value of the acid number for untreated SBO-based biodiesel increased with time under both indoor and outdoor storage. Samples with antioxidants α-T, IB, BHT, BHA, DTBHQ, and TBHQ have slight increases in acid number. However, these values are within the specification (0.5KOH mg/g). Interestingly, the initial values of acid number by adding of both PY and PG were observed to reach to 0.91 and 0.496 KOH mg/ g, respectively, and they were not very stable during storage. Similar results were also observed in the European BIOSTAB project [48]. This can be attributed to poor solubility of PY and PG in biodiesel [40].

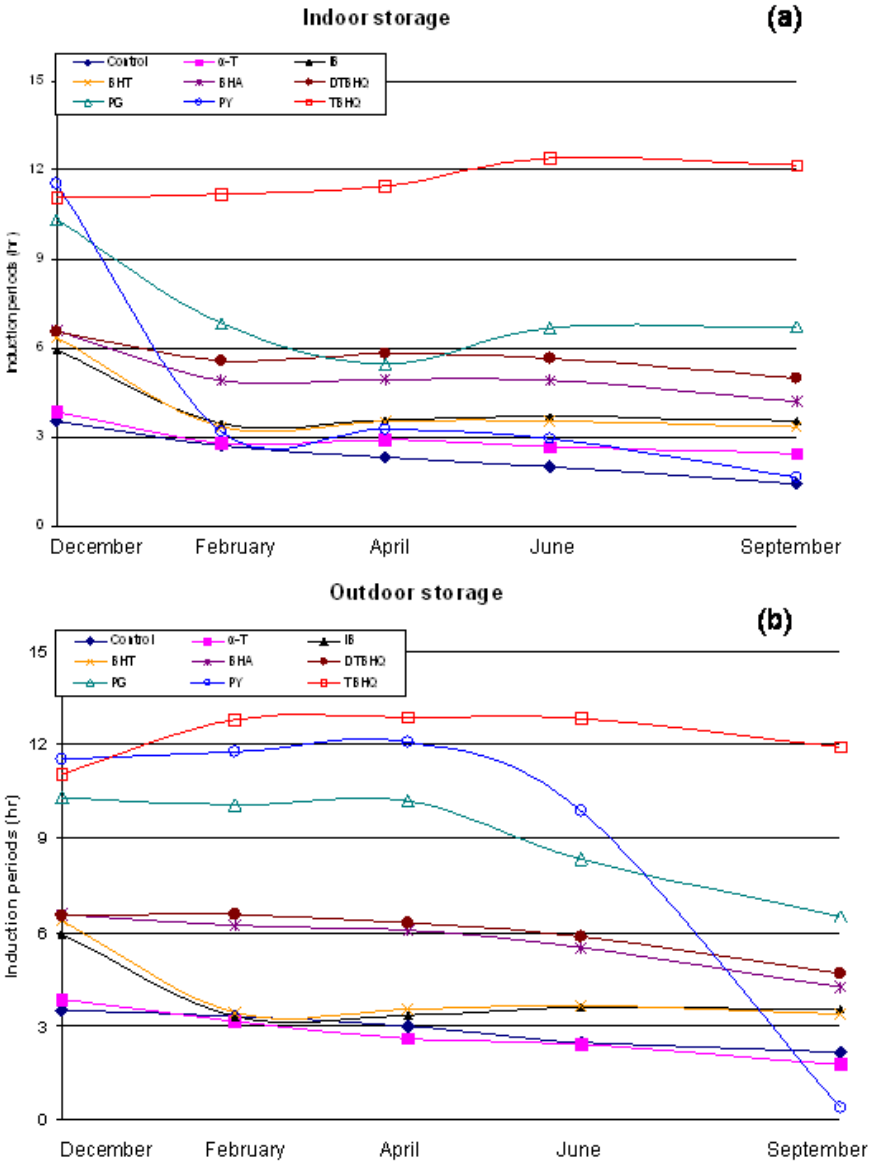

Figure 15. Effects of Antioxidants on the Induction Period of SBO-Based Biodiesel as a Function of Stored Time: (a) Indoor, and (b) Outdoor

The viscosity of SBO-based biodiesel with different antioxidants as function of storage time was also measured (Table 15). Viscosity of biodiesel increases when the sample is oxidized to form the polymeric compounds. The values of viscosity for all of samples were found to slightly increase for up to nine months. However, the limit value (6.0mm^2/s) at 40 ℃ was not reached in any cases. These results suggested that the changes in acid number and viscosity may not correlate closely with the changes in oxidation stability of biodiesel [48].

Table 13. Acid Number of SBO-Based Biodiesel with Antioxidant as a Function of Storage Time

	Acid Number (mg KOH/g)								
		Indoor				Outdoor			
Antioxidant	Control	2-mon	4-mon	6-mon	9-mon	2-mon	4-mon	6-mon	9-mon
blank	0.176	0.217	0.245	0.27	0.296	0.214	0.233	0.242	0.282
α-T	0.224	0.217	0.238	0.245	0.245	0.205	0.225	0.239	0.263
IB	0.212	0.223	0.233	0.242	0.234	0.209	0.229	0.233	0.237
BHT	0.211	0.22	0.23	0.246	0.244	0.209	0.229	0.232	0.243
BHA	0.203	0.194	0.235	0.243	0.244	0.204	0.216	0.228	0.242
DTBHQ	0.212	0.208	0.244	0.256	0.256	0.212	0.23	0.247	0.29
TBHQ	0.212	0.222	0.234	0.245	0.229	0.212	0.222	0.231	0.227
PG	0.496	0.479	0.519	0.792	0.546	0.485	0.508	0.78	0.3
PY	0.914	0.743	0.478	0.445	0.373	0.988	0.797	0.373	0.511

Table 14. Kinematic Viscosity of SBO-Based Biodiesel with Antioxidant at 40 ºC as a Function of Storage Time

	Kinematic viscosity (mm^2/s)								
		Indoor				Outdoor			
Antioxidant	Control	2-mon	4-mon	6-mon	9-mon	2-mon	4-mon	6-mon	9-mon
blank	4.321	4.291	4.326	4.364	4.419	4.292	4.299	4.319	4.329
α-T	4.381	4.35	4.353	4.373	4.396	4.339	4.352	4.384	4.423
IB	4.295	4.325	4.307	4.319	4.329	4.288	4.292	4.306	4.322
BHT	4.302	4.323	4.313	4.331	4.35	4.312	4.293	4.317	4.334
BHA	4.315	4.312	4.325	4.344	4.379	4.291	4.297	4.33	4.394
DTBHQ	4.298	4.3	4.304	4.311	4.314	4.303	4.3	4.307	4.309
TBHQ	4.321	4.306	4.303	4.316	4.318	4.288	4.299	4.315	4.317
PG	4.329	4.324	4.338	4.363	4.361	4.346	4.323	4.337	4.369
PY	4.292	4.348	4.32	4.344	4.377	4.332	4.295	4.301	4.337

7.4.4. Effect of Binary Antioxidants

The IP for DSBO-II biodiesel with 500 ppm binary antioxidants and stored indoors (23 °C) and outdoors for six months was measured (Figure 16). The IP of DSBO-II biodiesel without antioxidant was less than one hour, while addition of binary antioxidants of TBHQ:PY, TBHQ:PG, and TBHQ:BHA significantly improved the initial IP of biodiesel up to 16.6 hours, 5.9 hours, and 8.6 hours, respectively. However, our

previously published results showed that PY and PG alone at 250 ppm could increase the IP of DSBO-B100 to 3.8 hours and 2.2 hours, respectively, and TBHQ and BHA alone at 500 ppm could improve the IP to 6.5 hours, and 6.6 hours respectively [1]. For indoor samples, the IP of biodiesel with TBHQ: BHA remained at 8 hr for up to six months, while the IP of biodiesel with TBHQ: PY had a significant decrease from 16.6 hours to less than one hour after six months; the IP of the biodiesel with TBHQ: PG slowly decreased from 5.9 hours to 4.7 hours after three months, and rapidly reduced to 1.9 hours after six months. Under outside storage conditions, samples were exposed to a range of low and high temperature over the six-month period. The IP of distilled biodiesel with TBHQ: BHA remained relatively stable for up to six months. On the other hand, fuel with TBHQ: PG or TBHQ: PY displayed the similar effect on oxidative and storage stability with indoor samples over six-month period. These results suggested that TBHQ: BHA had the antioxidant synergism for up to six months; however, TBHQ: PY or TBHQ: PG cannot improve storage stability of biodiesel. PY and PG had a negative effect on the efficacy of TBHQ for storage stability improvement of biodiesel.

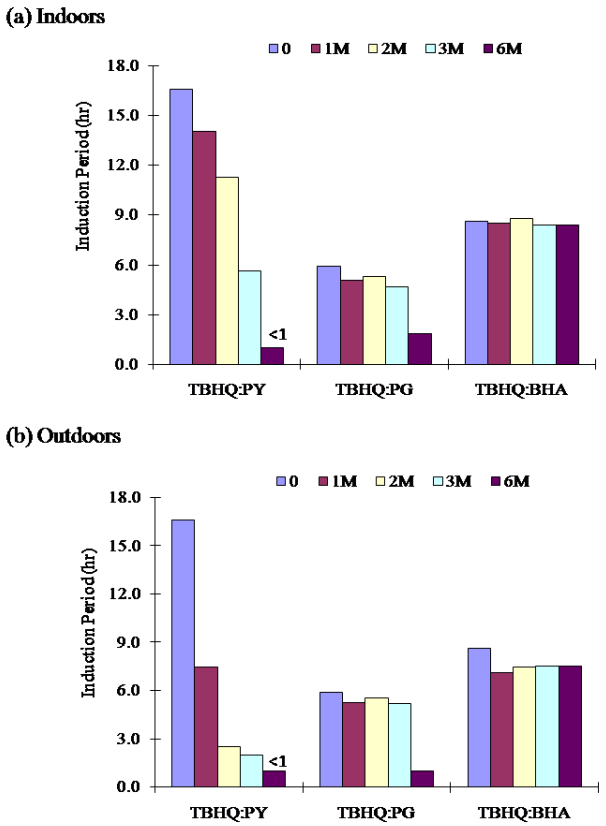

Figure 16. Effects of 500 ppm of Binary Antioxidants: TBHQ: PY, TBHQ: PG and TBHQ: BHA on the Induction Period of DSBO-II- Based Biodiesel as a Function of (a) Indoor; (b) Outdoor Stored Time

Figure 17 shows the acid number of DSBO-II-based biodiesel with and without antioxidants over a six-month period. The value of the acid number for untreated DSBO-II-based biodiesel significantly increased over time under both indoor and outdoor storage conditions. The acid number of the indoor untreated sample did not meet the ASTM specification after two months, while the outdoor untreated sample failed the specification after six months. The initial acid number of biodiesel with TBHA: PY, TBHQ: PG and TBHQ: BHA has an increase as compared to untreated one, but they were within the ASTM specification. After one month, the acid number of biodiesel with TBHA: PY did not satisfy the ASTM specification under both indoor and outdoor conditions while the sample with TBHA: PG failed the specification after two-month outdoor storage. The sample with TBHQ: BHA had a slow increase in acid number as a function of time under indoors and outdoors. The acid number after six-month indoor storage was a little higher than the ASTM specification; even though the IP was within the ASTM requirement (more than 7 hours).

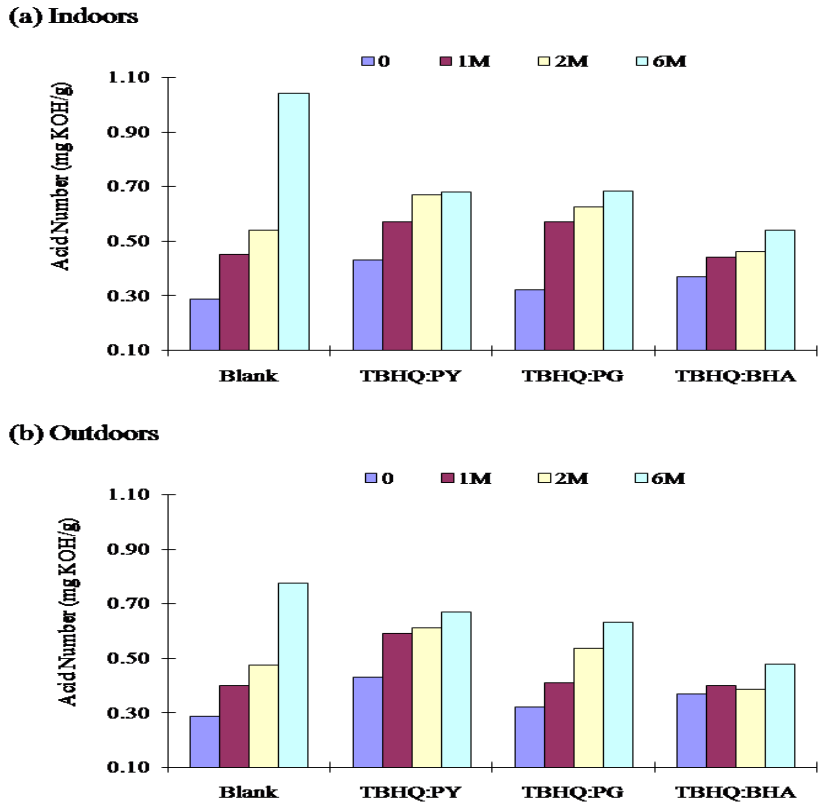

Figure 17. Acid Number of DSBO-II-Based Biodiesel with Antioxidant as a Function of (a) Indoor; (b) Outdoor Storage Time

The values of viscosity for untreated and treated DSBO-II-based biodiesel over the 6-month period are shown in Figure 18. The untreated sample had a significant increase in viscosity after six months, but this value is still within the ASTM specification. The viscosity of samples with all of the binary antioxidants was stable (~ 4.0 mm^2/s) for up to

six months. This shows that while the viscosity stayed within the ASTM specification, both the IP and acid number were not always within the ASTM specification. These results confirm the observation that neither viscosity nor acid number can be reliably used to evaluate fuel quality [1, 46].

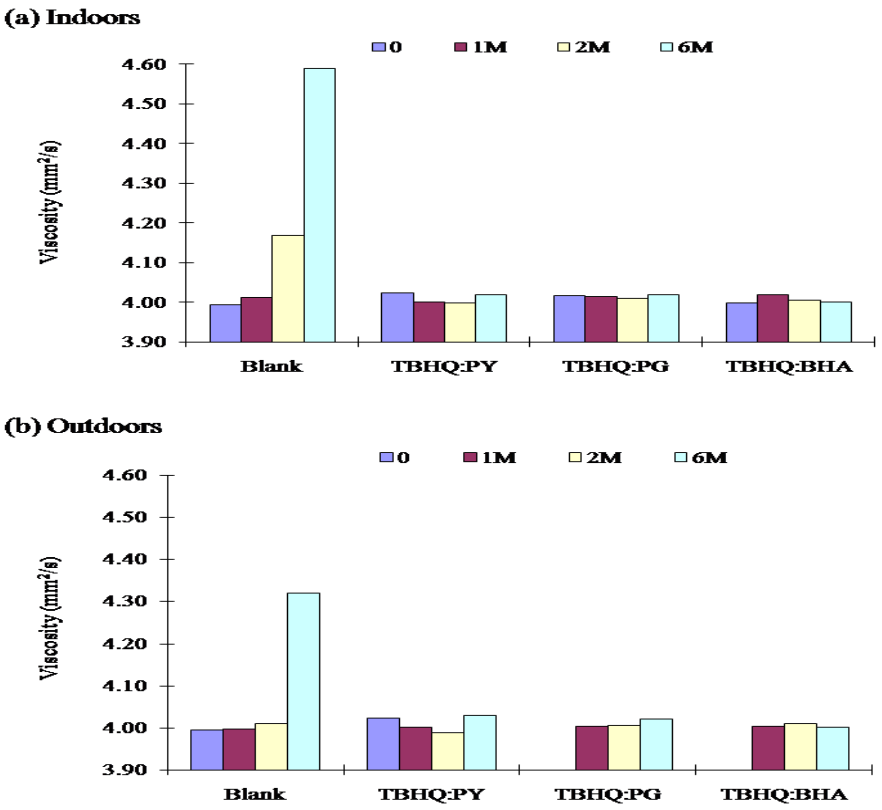

Figure 18. Kinematic Viscosity of DSBO-II-Based Biodiesel with Antioxidant at 40 °C as a Function of (a) Indoor; (b) Outdoor Storage Time

8. CONCLUSIONS

This report investigates the effectiveness of various natural and synthetic antioxidants (α-tocopherol (α-T), butylated hydroxyanisole (BHA), butyl-4-methylphenol (BHT), t-butylhydroquinone (TBHQ), 2, 5- Di-tert-butyl-hydroquinone (DTBHQ), ionol BF200 (IB), propylgallate (PG), and pyrogallol (PY)) to improve the oxidative stability of soybean oil (SBO-), cottonseed oil (CSO-), poultry fat (PF-), and yellow grease (YG-) based biodiesel at the varying concentrations between 250 and 1000 ppm. Results indicate that Different types of biodiesel have different natural levels of oxidative stability, even when derived from the same basic feedstock, due to variations in both natural antioxidant level and FAME composition. Moreover, PG, PY, TBHQ, BHA, BHT, DTBHQ, and IB can enhance the oxidative stability for these different types of biodiesel. Antioxidant activity increased with increasing concentration. The induction period of SBO-, CSO-, YG-, and distilled SBO-based biodiesel could be improved significantly with PY, PG and TBHQ, while PY, BHA, and BHT show the best results for PF-based biodiesel. This indicates that the effect of each antioxidant on biodiesel differs depending on different feedstock. Moreover, the effect of antioxidants on B20 and B100 was similar; suggesting that improving the oxidative stability of biodiesel can effectively increase that of biodiesel blends. Some binary mixtures of antioxidants are more effective in improving oxidative stability of biodiesel than individual ones, suggesting a synergistic interaction which may be important in the development of suitable blends. The best synergy was produced by the 2:1 TBHQ: BHA blend while the best improvement in IP was achieved by using the 2:1 TBHQ: PY blend. Considering %SYN and SF, these two formulations are good choices for long-term storage. The effectiveness of individual antioxidants in SBO-based biodiesel oxidative and storage stability over a 30-month period of indoor storage and binary antioxidants in distilled SBO-based biodiesel under indoor and outdoor conditions over a six-month period were studied. Results indicate that the oxidative and storage stability of both untreated SBO-based and untreated DSBO-based biodiesel decreases with time. The addition of the antioxidant TBHQ can improve and maintain oxidative and storage stability of the biodiesel over a 30-month period. The binary combination TBHQ: BHA also showed better performance than either individual antioxidant or can improve oxidative and storage stability of DSBO-based biodiesel for up to six months.

9. RECOMMENDATIONS FOR FURTHER RESEARCH

Further research will develop a user-level sensor for oxidative stability of biodiesel. While standards and tests for biodiesel fuel quality and oxidative stability have been developed, they currently require specialized equipment and training in order to be utilized. There is a need for a simple screening device that can be used at the point of delivery of biodiesel fuel in order to analyze for the degree of oxidative stability of the fuel. The correlations between key marker parameters and standard tests of oxidative stability will be developed. These correlations will form the basis for a screening sensor that can measure these marker parameters. While such a sensor may not be as exact as the definitive analytical tests, it can be used to determine if more extensive testing is needed before dispensing of the stored fuel.

10. BIBLOGRAPHY

[1] Tang HY, Wang AF, Salley SO, Ng KYS. The effect of natural and synthetic antioxidants on the oxidative stability of biodiesel. Journal of the American Oil Chemists Society. 2008;85:373-82.

[2] de Guzman R, Tang HY, Salley S, Ng KYS. Synergistic Effects of Antioxidants on the Oxidative Stability of Soybean Oil- and Poultry Fat-Based Biodiesel. Journal of the American Oil Chemists Society. 2009;86:459-67.

[3] Tang HY, De Guzman RC, Ng KYS, Salley SO. Effect of Antioxidants on the Storage Stability of Soybean-Oil-Based Biodiesel. Energy & Fuels. 2010;24:2028-33.

[4] ASTM D 6751 - 07, Standard Specification for Biodiesel Fuel Blend Stock (B100) for Middle Distillate Fuels. Philadelphia; 2007.

[5] National Biodiesel Board Web site, Estimated US biodiesel sales, http://www.biodiesel.org/pdf_files/fuelfactsheets/Biodiesel_Sales_Graph.pdf. 2007.

[6] Van Gerpen J, Shanks B, Pruszko R, Clements D, Knothe G. Biodiesel production technology. National Renewable Energy Laboratory, NREL/SR-510-36244. July 2004.

[7] Domingos AK, Saad EB, Vechiatto WWD, Wilhelm HM, Ramos LP. The influence of BHA, BHT and TBHQ on the oxidation stability of soybean oil ethyl esters (biodiesel). Journal of the Brazilian Chemical Society. 2007;18:416-23.

[8] Monyem A, Van Gerpen JH. The effect of biodiesel oxidation on engine performance and emissions. Biomass & Bioenergy. 2001;20:317-25.

[9] Tao Y. Operation of a cummins N14 diesel on biodiesel: performance, emissions and durability. National Biodiesel Board, Ortech Report No. 95-E11-B004524. 1995.

[10] EN 14112, Determination of oxidation stability (accelerated oxidation test). 2003.

[11] McCormick RL, Alleman TL, Ratcliff M, Moens L, Lawrence R. Survey of the quality and stability of biodiesel and biodiesel blends in the United States in 2004. National Renewable Energy Laboratory, NREL/TP-540-38836. October 2005.

[12] Alleman TL, McCormick RL, Deutch S. 2006 B100 quality survey results, National Renewable Energy Laboratory, NREL/TP-540-41549. May 2007.

[13] Tang HY, Abunasser N, Wang A, Clark BR, Wadumesthrige K, Zeng SD, et al. Quality survey of biodiesel blends sold at retail stations. Fuel. 2008;87:2951-5.

[14] Sendzikiene E, Makareviciene V, Janulis P. Oxidation stability of biodiesel fuel produced from fatty wastes. Polish Journal of Environmental Studies. 2005;14:335-9.

[15] Schober S, Mittellbach M. The impact of antioxidants on biodiesel oxidation stability. European Journal of Lipid Science and Technology. 2004;106:382-9.

[16] Liang YC, May CY, Foon CS, Ngan MA, Hock CC, Basiron Y. The effect of natural and synthetic antioxidants on the oxidative stability of palm diesel. Fuel. 2006;85:867-70.

[17] Liang C, Schwarzer K. Comparison of four accelerated stability methods for lard and tallow with and without antioxidants. Journal of the American Oil Chemists Society. 1998;75:1441-3.

[18] Mittelbach M, Schober S. The influence of antioxidants on the oxidation stability of biodiesel. Journal of the American Oil Chemists Society. 2003;80:817-23.

[19] Waynick JA. Characterization of biodiesel oxidation and oxidation products. National Renewable Energy Laboratory, NREL/TP-540-39096. November 2005.

[20] Neff WE, Selke E, Mounts TL, Rinsch W, Frankel EN, Zeitoun MAM. Effect of Triacylglycerol Composition and Structures on Oxidative Stability of Oils from Selected Soybean Germplasm. Journal of the American Oil Chemists Society. 1992;69:111-8.
[21] Leung DYC, Koo BCP, Guo Y. Degradation of biodiesel under different storage conditions. Bioresource Technology. 2006;97:250-6.
[22] Lin CY, Chiu CC. Effects of Oxidation during Long-term Storage on the Fuel Properties of Palm Oil-based Biodiesel. Energy & Fuels. 2009;23:3285-9.
[23] Falk O, Meyer-Pittroff R. The effect of fatty acid composition on biodiesel oxidative stability. European Journal of Lipid Science and Technology. 2004;106:837-43.
[24] Knothe G. Improving biodiesel fuel properties by modifying fatty ester composition. Energy & Environmental Science. 2009;2:759-66.
[25] Knothe G. "Designer" biodiesel: Optimizing fatty ester (composition to improve fuel properties. Energy & Fuels. 2008;22:1358-64.
[26] Moser BR. Biodiesel production, properties, and feedstocks. In Vitro Cellular & Developmental Biology-Plant. 2009;45:229-66.
[27] Pahgova J, Jorikova L, Cvengros J. Study of FAME stability. Energy & Fuels. 2008;22:1991-6.
[28] ASTM D 6751 - 03, Standard Specification for Biodiesel Fuel Blend Stock (B100) for Middle Distillate Fuels. Philadelphia; 2003.
[29] Tang HY, Salley SO, Ng KYS. Fuel properties and precipitate formation at low temperature in soy-, cottonseed-, and poultry fat-based biodiesel blends. Fuel. 2008;87:3006-17.
[30] ASTM D 6584-00, Determination of Free and Total Glycerin in B-100 Biodiesel Methyl Esters by Gas Chromatography. Philadelphia; 2000.
[31] ASTM D 2500 - 05, Standard Test Method for Cloud Point of Petroleum Products. Philadelphia2005.
[32] ASTM D 97-96a, Standard Test Method for Pour Point of Petroleum Products. Philadelphia; 1996.
[33] ASTM D 6371 - 05, Standard Test Method for Cold Filter Plugging Point of Diesel and Heating Fuels. Philadelphia; 2005.
[34] ASTM D 6751 - 08, Standard Specification for Biodiesel Fuel Blend Stock (B100) for Middle Distillate Fuels. Philadelphia: In: Annual Book of ASTM Standards, ASTM Press: West Conshohocken, 2008.; 2008.
[35] Kinast JA. Production of biodiesels from multiple feedstock's and properties of biodiesels and biodiesel/diesel blend. National Renewable Energy Laboratory, NREL/SR-510-31460. March 2003.
[36] Tyson KS. Biodiesel Handling and Use Guidelines, National Renewable Energy laboratory NREL/TP-580-30004. September 2001.
[37] McCormick RL, Ratcliff MA, Moens L, Lawrence R. Several factors affecting the stability of biodiesel in standard accelerated tests. Fuel Processing Technology. 2007;88:651-7.
[38] Mittelbach M, Gangl S. Long storage stability of biodiesel made from rapeseed and used frying oil. Journal of the American Oil Chemists Society. 2001;78:573-7.

[39] Dunn RO. Effect of oxidation under accelerated conditions on fuel properties of methyl soyate (biodiesel). Journal of the American Oil Chemists Society. 2002;79:915-20.
[40] Dunn RO. Effect of antioxidants on the oxidative stability of methyl soyate (biodiesel). Fuel Processing Technology. 2005;86:1071-85.
[41] Ruger CW, Klinker EJ, Hammond EG. Abilities of some antioxidants to stabilize soybean oil in industrial use conditions. Journal of the American Oil Chemists Society. 2002;79:733-6.
[42] Raemy A, Froelicher I, Loeliger J. Oxidation of Lipids Studied by Isothermal Heat-Flux Calorimetry. Thermochimica Acta. 1987;114:159-64.
[43] Loh SK, Chew SM, Choo YM. Oxidative stability and storage behavior of fatty acid methyl esters derived from used palm oil. Journal of the American Oil Chemists Society. 2006;83:947-52.
[44] ASTM D 6751 - 08 Annex A.1, Standard Specification for Biodiesel Fuel Blend Stock (B100) for Middle Distillate Fuels. . In: Annual Book of ASTM Standards. West Conshohocken: ASTM Press; 2008.
[45] Tang HY, De Guzman R, Salley S, Ng KYS. Comparing Process Efficiency in Reducing Steryl Glucosides in Biodiesel. Journal of the American Oil Chemists Society. 2010;87:337-45.
[46] Moser BR. Efficacy of myricetin as an antioxidant in methyl esters of soybean oil. European Journal of Lipid Science and Technology. 2008;110:1167-74.
[47] Bondioli P, Gasparoli A, Della Bella L, Tagliabue S, Toso G. Biodiesel stability under commercial storage conditions over one year. European Journal of Lipid Science and Technology. 2003;105:735-41.
[48] Prankl H, Lacoste F, MIttelbach M, Blassnegger J, Brehmer T, Frohlich A, et al. Stability of Biodiesel – Used as a fuel for diesel engines and heating systems. BIOSTAB Project Results,contract number: QLK5-CT-2000-00533. August, 2003.

11. LIST OF ACRONYMS

BHA	butylated hydroxyanisole
α-T	α-tocopherol
BHT	utyl-4-hydroxytoluene
TBHQ	*t*-butylhydroquinone
DTBHQ	2,5-di-*tert*-butyl-hydroquinone
PG	propylgallate
PY	pyrogallol
IB	ionol BF200
IP	induction period
FAME	fatty acid methyl ester
AOx	antioxidants
ULSD	ultra low sulfur diesel
SBO	soybean oil
CSO	cottonseed oil
PF	poultry fat
YG	yellow grease
DSBO	distilled soybean oil
B20	soybean oil-based biodiesel blends
DOE	U.S. Department of Energy
EPA	U.S. Environmental Protection Agency
DOT	Department of Transportation
NOx	nitrogen oxides
ASTM	American Society for Testing and Materials
AO	antioxidants
MIOH UTC	Michigan Ohio University Transportation Center
ppm	parts per million
OT	onset temperature
OX	oxidizability
DPF	distilled poultry fat
TAN	Total Acid Number

MICHIGAN OHIO UNIVERSITY TRANSPORTATION CENTER
Alternate energy and system mobility to stimulate economic development.

Report No: MIOH UTC AF12p1-2 2010-Final
MDOT No. RC1545

IMPROVING THE ENERGY DENSITY OF HYDRAULIC HYBRID VEHICLES (HHVS) AND EVALUATING PLUG-IN HHVS

Final Report

Project Team

Dr. Mark Schumack
Sujay Bodke
Department of Mechanical Engineering
University of Detroit Mercy
4001 W. McNichols Road
Detroit, MI 48221

Undertaken in conjunction with a project led by
Dr. Mohammad Elahinia, Dr. Walter Olson, and Dr. Mark Vonderembse
The University of Toledo

Report No: MIOH UTC AF12p1-2 2010-Final

AF 12, Series, Projects 1 & 2, May, 2010
FINAL REPORT

Developed by: **Dr. Mark Schumack**
Principal Investigator, UDM
schumackmr@udmercy.edu
313-993-3370

In conjunction with: **Dr. Mohammad Elahinia**
Principal Investigator, UT
mohammad.elahinia@utoledo.edu
419-530-8224

SPONSORS

This is a Michigan Ohio University Transportation Center project supported by the U.S. Department of Transportation, the Michigan Department of Transportation and the University of Detroit Mercy.

ACKNOWLEDGEMENT

The Project Team would like to acknowledge collaboration with researchers from The University of Toledo, Dynamic and Smart Systems Laboratory, MIME Department.

DISCLAIMER

Technical Report Documentation Page

1. Report No. RC-1545	**2. Government Accession No.**	**3. MDOT Project Manager** Niles Annelin
4. Title and Subtitle Michigan Ohio University Transportation Center Subtitle: "Improving the Energy Density of Hydraulic Hybrid Vehicles (HHVs) and Evaluating Plug-In HHVs"		**5. Report Date** May 2010 **6. Performing Organization Code**
7. Author(s) Dr. MarkSchumack, University of Detroit Mercy		**8. Performing Org. Report No.** MIOH UTC AF12p1-2 2010-Final
9. Performing Organization Name and Address Michigan Ohio University Transportation Center University of Detroit Mercy, Detroit, MI 48221 and University of Detroit Mercy, Detroit, MI 48221		**10. Work Unit No. (TRAIS)** **11. Contract No.** 2007-0538 **11(a). Authorization No.**
12. Sponsoring Agency Name and Address Michigan Department of Transportation Van Wagoner Building, 425 West Ottawa P. O. Box 30050, Lansing, Michigan 48909		**13. Type of Report & Period Covered** Research, October 2007- December 2009 **14. Sponsoring Agency Code**
15. Supplementary Notes Additional Sponsors: US DOT Research & Innovative Technology Administration, University of Detroit Mercy		
16. Abstract MIOH UTC AF12p1-2 2010-Final This report describes analyses performed by researchers at the University of Detroit Mercy to augment the project "Improving the Energy Density of Hydraulic Hybrid Vehicles (HHVs) and Evaluating Plug-In HHVs" led by the University of Toledo. UT researchers proposed a way to increase the energy density of standard hydraulic hybrid vehicles through an air tank/switching design. Their analysis showed that the design was impractical because too much energy was lost in the accumulator switching process and too much power from the engine was required to recharge the air tank. Their conclusions were based on a MATLAB/Simulink model of a Class VI delivery truck powered by a 7.3 liter diesel engine and a hydraulic pump/motor unit. The scope of the UDM analysis included two tasks: verification of UT's results through some relatively simple thermodynamic calculations, and evaluation of the "plug-in" feature of a modified air system. The calculations confirmed UT's conclusions about the infeasibility of the original design, and a Simulink model developed to evaluate the plug-in feature demonstrated that even with some design improvements, the air system still results in significant energy loss through the venting that must occur as part of the accumulator switching process. Simulations of a truck and two passenger vehicles were performed.		
17. Key Words Hybrid vehicles, Hybrid automobiles, Hydraulic fluids, Sport utility vehicles, Fuel consumption, Electric vehicles, Plug in hybrid electric vehicles	**18. Distribution Statement** No restrictions. This document is available to the public through the Michigan Department of Transportation.	

19. Security Classification - report	**20. Security Classification - page**	**21. No. of Pages**	**22. Price**
		14	

Abstract

This report describes analyses performed by researchers at the University of Detroit Mercy to augment the project "Improving the Energy Density of Hydraulic Hybrid Vehicles (HHVs) and Evaluating Plug-In HHVs" led by the University of Toledo. UT researchers proposed a way to increase the energy density of standard hydraulic hybrid vehicles through an air tank/switching design. Their analysis showed that the design was impractical because too much energy was lost in the accumulator switching process and too much power from the engine was required to recharge the air tank. Their conclusions were based on a MATLAB/Simulink model of a Class VI delivery truck powered by a 7.3 liter diesel engine and a hydraulic pump/motor unit. The scope of the UDM analysis included two tasks: verification of UT's results through some relatively simple thermodynamic calculations, and evaluation of the "plug-in" feature of a modified air system. The calculations confirmed UT's conclusions about the infeasibility of the original design, and a Simulink model developed to evaluate the plug-in feature demonstrated that even with some design improvements, the air system still results in significant energy loss through the venting that must occur as part of the accumulator switching process. Simulations of a truck and two passenger vehicles were performed.

Table of Contents

List of Tables

List of Figures

1. Introduction

Hydraulic hybrid vehicles can provide significant power but typically suffer from relatively low energy density due to limitations on accumulator size[1,2]. In an effort to improve the energy density, the University of Toledo proposed a system utilizing a large air storage tank to provide additional energy capacity to the accumulator[3]. By incorporating an arrangement of valves and associated controls, the system reverses the roles of the high and low-pressure accumulators in a series of switches until the tank air pressure decreases to a prescribed lower limit. At the low-pressure limit, an onboard compressor powered by the vehicle's internal combustion engine turns on and repressurizes the tank using atmospheric air.

A MATLAB/Simulink model was developed to simulate the system. The results of the simulation were not encouraging. A large amount of energy is wasted in the venting that must occur in the switching of roles of the high and low-pressure accumulators, and the compressor power to replenish the air tank was significantly higher than the IC engine capability.

In this report we describe some calculations performed to confirm UT's conclusion that the proposed system is not feasible. We then propose an alternative design that significantly decreases the amount of wasted energy in the venting process. The alternative design is modeled as a stand-alone propulsion system (i.e., as a non-hybrid system) in order to gauge its effectiveness. The new design is essentially an "air car," powered by a hydraulic system whose pressure source is compressed air. We compare our results with the claims of another advertised air car (not yet in production). Finally, we evaluate the "plug-in" capability of the alternative system assuming that the air storage tank can be recharged overnight from a stationary electric source.

2. Description of the UT System

The proposed UT system is shown in Figure 1. The system deviates from a conventional hydraulic system in that two "pressure exchangers," an air tank, control valve, a control system, and a compressor driven by the IC engine have been added.

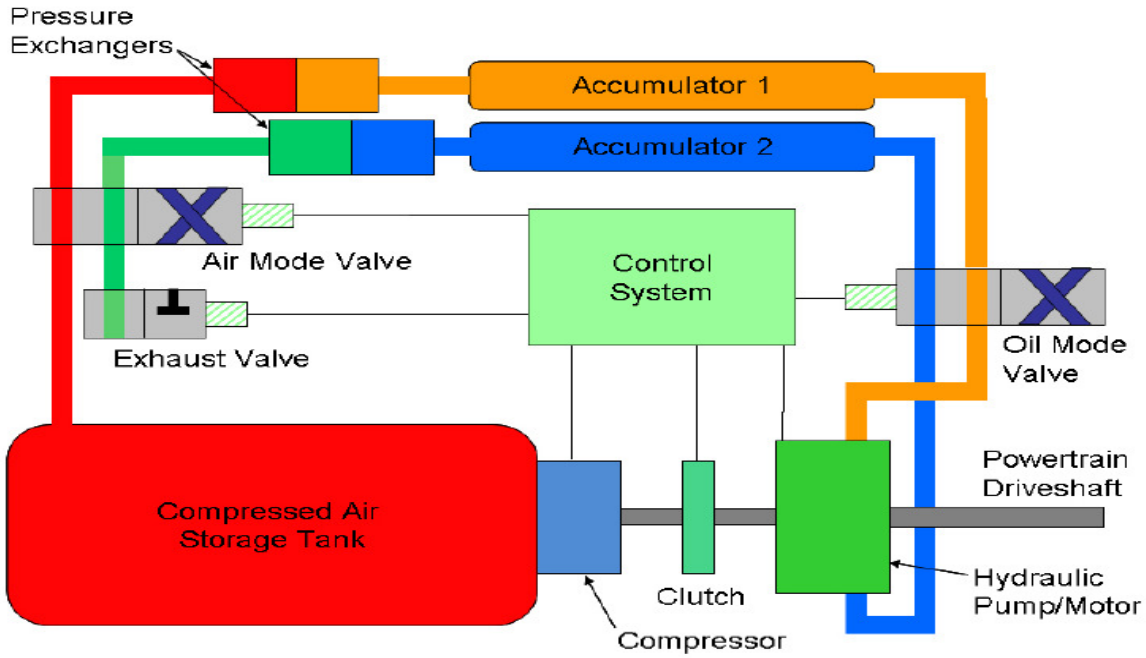

Figure 1. University of Toledo's Proposed Concept Hydraulic Hybrid System[3]

In the figure, accumulator 1 is connected to the air tank and is thus serving as the high-pressure accumulator for the hydraulic motor. The motor is discharging hydraulic fluid to accumulator 2, which is vented through a pressure exchanger to the atmosphere and thus serves as the low-pressure accumulator. When all the oil has been depleted from accumulator 1, the air mode and oil mode valves switch positions, causing accumulator 1 to be vented through its associated pressure exchanger, accumulator 2 to be pressurized by the air tank through its pressure exchanger, and the motor to now receive oil from accumulator 2 and reject oil to accumulator 1. The switching occurs until the air tank pressure is below that which is necessary to provide high-pressure to the high-pressure accumulator. When the pressure limit is reached, the compressor - driven by the IC engine - activates to recharge the air tank. A class VI delivery truck is used for all of UT's simulations, details of which can be found in reference 3.

The pressure exchangers deserve some explanation. Their sole purpose is to separate the oil in the accumulators from the pressurized air, thereby preventing a potentially explosive air/oil mixture. It is not shown in Figure 1, but the oil in the accumulators is pressurized by nitrogen, which serves as a buffer between the air and oil. Either pistons or bladders could be used to separate the fluids. Figure 2 conceptually shows how the air, nitrogen, and oil could be separated by zero-clearance pistons.

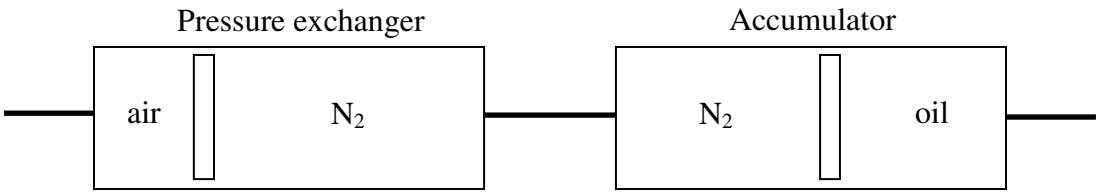

Figure 2. Conceptual Separation of Air, Nitrogen, and Oil by Pistons

The relative sizes of the pressure exchangers and accumulators in Figures 1 and 2 are misleading. The pressure exchanger is actually four times the size of the accumulator, and the relatively large exchanger volume is part of what makes the proposed air system so wasteful of energy.

3. Analysis of the UT System

The source of the pressured energy is the air tank. The maximum energy available from the tank can be determined by

$$E = m_{air} RT ln \frac{P_{tank}}{P_o} \qquad (1)$$

where E is the available stored energy, P_{tank} is the air pressure in the tank, P_o is atmospheric air pressure and m_{air} is the mass of air in the tank. This equation assumes an isothermal process. Equation (1) represents the maximum possible work available from the pressurized air source, assuming it is depressurized to atmospheric pressure. In actuality, the tank is not depressurized to atmospheric pressure, but rather to a threshold pressure below which the tank cannot maintain the pressure necessary for operation of the high-pressure accumulator.

The UT model assumes that the pressure of the nitrogen when the accumulator is fully charged is 35 MPa (about 5000 psi). Since the air tank must provide enough pressure to ensure 35 MPa in the high-pressure accumulator after each switch for multiple switches, the pressure of the air in the tank must be significantly higher than 35 MPa. Consequently, UT used 50 MPa as the initial air tank pressure. A pressure-regulating valve between the tank and pressure exchanger ensures a pressure of 35 MPa in the pressure exchanger at the beginning of every switch. The final air tank pressure (P_{min}) is 35 MPa (below this pressure, the tank would not be able to pressure the accumulator sufficiently). The maximum possible work that could be done by the air in the tank as it depressurizes is

$$\frac{W_{max} = m_{air} RT \ln P_{tank}}{P_{min}} = \frac{P_{tank} V_t \ln P_{tank}}{P_{min}} \qquad (2)$$

With P_{tank} = 50 MPa, V_t = 2 m^3, and P_{min} = 35 MPa, the maximum work is determined to be 35.7 MJ. The mass of air removed from the tank, m_{exp}, as its pressure decreases from 50 to 35 MPa can be determined from

$$m_{exp} = \frac{V_t(P_{tank} - P_{min})}{RT}$$

This comes out to 348 kg for a temperature of 300 K.

The volume of the pressure exchanger is determined by the pressure desired in the low-pressure accumulator. UT chose a low-pressure accumulator pressure of 1.75 MPa (the pressure of the accumulator as it begins to receive oil from the motor just after a switch). This pressure occurs when the pressure exchanger is vented and nitrogen fills both the pressure exchanger and the low-pressure accumulator (i.e., when the exchanger piston is all the way to the left and the accumulator piston is all the way to the right in Figure 2). Using the Ideal Gas Law and assuming an isothermal process, the product of pressure and volume must remain constant:

$$P'_{N_2\,\min}\left(V_e + V_a\right) = P_{N_2\,\max} V_{N_2\,\min}$$

where P'_{N2min} is the minimum nitrogen pressure in the low-pressure accumulator (1.75 MPa), V_e is the pressure exchanger volume, V_a is the accumulator volume (0.08 m^3), P_{N2max} is the maximum nitrogen pressure in the high-pressure accumulator (35 MPa) and V_{N2min} is the minimum nitrogen volume (0.02 m^3). Solving for V_e gives a pressure exchanger volume of 0.32 m^3.

The mass of air lost each time a pressure exchanger vents is determined from

$$m_{loss} = \frac{[(P]_e - P_0)V_e}{RT}$$

where P_e is the air pressure in the pressure exchanger (35 MPa) and P_0 is atmospheric air pressure (101.3 kPa). For a temperature of 300 K, this equation gives 130 kg as the lost air mass. The number of switches, n, after which the air tank must be replenished, can now be determined by the following equation:

$$n = \frac{m_{exp}}{m_{loss}}$$

which, for m_{exp} = 348 kg and m_{loss} = 130 kg, gives 2.7 switches. Discounting the fractional switch, and assuming the vehicle starts with a fully charged accumulator and air tank, a total of 3 accumulator transients can be accomplished before the air tank pressure must be restored.

The energy lost, W_{lost}, in the air vented from the pressure exchangers can be determined assuming an isothermal process as follows:

$$W_{lost} = m_{loss} RT \ln \frac{P_a}{P_0} \qquad (3)$$

Using values determined above, this is calculated as 65.4 MJ. It is instructive to compare this value with the maximum useful energy obtained from the high-pressure accumulator as it depressurizes from P_{N2max} (35 MPa) to P_{N2min} (=P_{N2max} * V_{N2min}/V_a = 8.75 MPa), again assuming an isothermal process:

$$W_{acc} = P_{N2max} V_{N2min} \ln\left(\frac{P_{N2max}}{P_{N2min}}\right) \qquad (4)$$

With V_{N2min} = 0.02 m^3, this becomes 0.97 MJ. Multiplying this result by the number of switches (2.7) gives an energy of 2.6 MJ, which is vastly less than that exhausted through the venting of the pressure exchangers (65.4 MJ), and also significantly less than that delivered by the air tank (35.7 MJ).

In University of Toledo's configuration, an onboard compressor recharges the air tank when the pressure drops below the threshold of 35 MPa. The compressor is powered by the IC engine and also is configured to capture energy during regenerative braking. The compressor is a three-stage positive displacement compressor whose work is calculated from[4]

$$W_c = \frac{\frac{3k}{k-1} m RT \left[\left(\frac{P_{tank}}{P_0}\right)^{\frac{k-1}{3k}} - 1\right]}{\eta_c} \qquad (5)$$

Here k is the specific heat ration for air and η_c is the compressor efficiency. For P_{tank} = 50 MPa, k = 1.4, and η_c = 0.8, the compressor work is 317 MJ. This is an enormous amount of energy, particularly for an onboard compressor designed to refill the air tank within a short period of time, and explains why UT calculated inordinately high values of compressor power during the Federal Urban Drive Schedule (FUDS). For comparison, the energy required for the truck to travel the FUDS is 44 MJ.

Table 1 summarizes the specifications for key components in the UT air/hydraulic system. Table 2 summarizes the key results from the energy calculations described above.

Table 1. Key Specifications used in Calculating Energy Quantities for the Air/Hydraulic System

Maximum nitrogen pressure in high-pressure accumulator (P_{N2max})	35 MPa
Minimum nitrogen pressure in high-pressure accumulator (P_{N2min})	8.75 MPa
Minimum nitrogen pressure in low-pressure accumulator (P'_{N2min})	1.75 MPa
Maximum air pressure in the air tank (P_{tank})	50 MPa
Minimum air pressure in the air tank (P_{min})	35 MPa
Pressure exchanger pressure (P_e)	35 MPa
Minimum nitrogen volume (V_{N2min})	0.02 m^3
Accumulator volume (V_{acc}) – equal to maximum nitrogen volume	0.08 m^3
Air tank volume (V_t)	2 m^3

Table 2. Calculated Ideal Energies*

Work that could be done by air in tank as it depressurizes from P_{tank} to P_{min} (W_{max}, equation 2)	35.7 MJ
Lost work due to pressure exchanger venting (W_{lost}, equation 3)	65.4 MJ
Work delivered by high-pressure accumulator (W_{acc}, equation 4)	0.97 MJ
Compressor work to repressurize air tank to P_{tank} (W_c, equation 5)	317 MJ

***All results are for isothermal operation (which leads to maximum energy values) except for the compressor, which is assumed adiabatic. Note the insignificance of the work delivered by the high-pressure accumulator compared to lost work through venting and the required compressor work to repressurize the air tank.**

Another result of interest is the calculation of how far the truck could travel on one air tank charge without the IC engine. A rough, upper limit estimation can be obtained by equating the ideal energy delivered by the system for *n* switches to the energy expended for road loads at a constant speed. The road load for constant speed, *V*, on a horizontal surface is given as

$$R_L = f_r W + \frac{1}{2}\rho V^2 C_d A$$

where f_r is the rolling resistance of the tires, A is the frontal area of the truck, C_d is the drag coefficient, ρ is the air density, *V* is the truck speed, and W is the weight of the truck. The energy required to propel the vehicle a distance *d* is thus $R_L d$. Equating this road load energy to the energy delivered by the accumulators for *n* switches gives:

$$d = \frac{nW_{acc}}{R_L}$$

Using a vehicle mass (see reference 3) of 10,340 kg, $f_r = 0.015$, $C_d = 0.5$, $A = 6.767$ m^2, $n = 2.7$, $V = 11$ m/s (the average FUDS speed), and ρ = 1.23 kg/m3, this equation gives *d* = 1.5 km, or about 1 mile. Clearly, as a stand-alone power system, the air/hydraulic design will not provide any appreciable range.

There are several lessons to be learned from these results. First, there is an enormous loss of energy through the venting of high-pressure air from the pressure exchangers during a switch. Second, the pressure range over which the air tank operates is relatively low, as the tank must contain enough pressure to repeatedly recharge the high-pressure accumulator. This means that much of the energy in the air tank remains unutilized. Third, since the compressor must recharge the air tank to high-pressure using air at ambient conditions, the compressor power and energy is extremely high, making onboard recompression unrealistic.

Although onboard compression is not feasible, a "plug-in" feature whereby the air is recharged from an external source over a longer period of time is worth considering. The energy of compression calculated in the previous section, 317 MJ, is equivalent to 88 kWh, which at $0.10 per kWh would result in an overnight charge costing $8.80, not an unreasonable price to pay provided the range is sufficient. In the next section we discuss a design modification that eliminates the pressure exchangers and the associated losses, thereby extending the vehicle's range and also reducing weight and cost. A "pure air/hydraulic" vehicle (i.e., the vehicle has no IC engine onboard) is simulated to gauge the feasibility of such a design.

4. The Alternate Design

As mentioned earlier, the purpose of the pressure exchanger is to keep hydraulic oil separated from high-pressure air that might otherwise form a combustible mixture should leaks occur. Hydraulic accumulators typically operate with nitrogen to avoid the issue of spontaneous combustion. Since the two accumulators in the system alternate roles from high to low-pressure, the pressure exchangers must be sized to allow the nitrogen to depressurize to a low-pressure when it serves as the low-pressure reservoir. This is what requires the pressure exchanger volume to be so large.

If, however, the danger of an explosive oil/air mixture could be eliminated, the accumulators could operate using air rather than nitrogen as the pressure source, and the pressure exchangers could be removed from the design.

Our proposed design is shown in Figure 3. A flexible bellows attached to the piston separates pressurized air from atmospheric air in the gas side of the accumulator. Now, should leakage of oil from the hydraulic fluid side occur past the piston, the bellows would prevent contact with high-pressure air from the tank. The bellows provides a second barrier. This design also enables the low-pressure accumulator to operate at essentially atmospheric pressure, meaning that the pressure difference across the hydraulic motor is higher, resulting in more power.

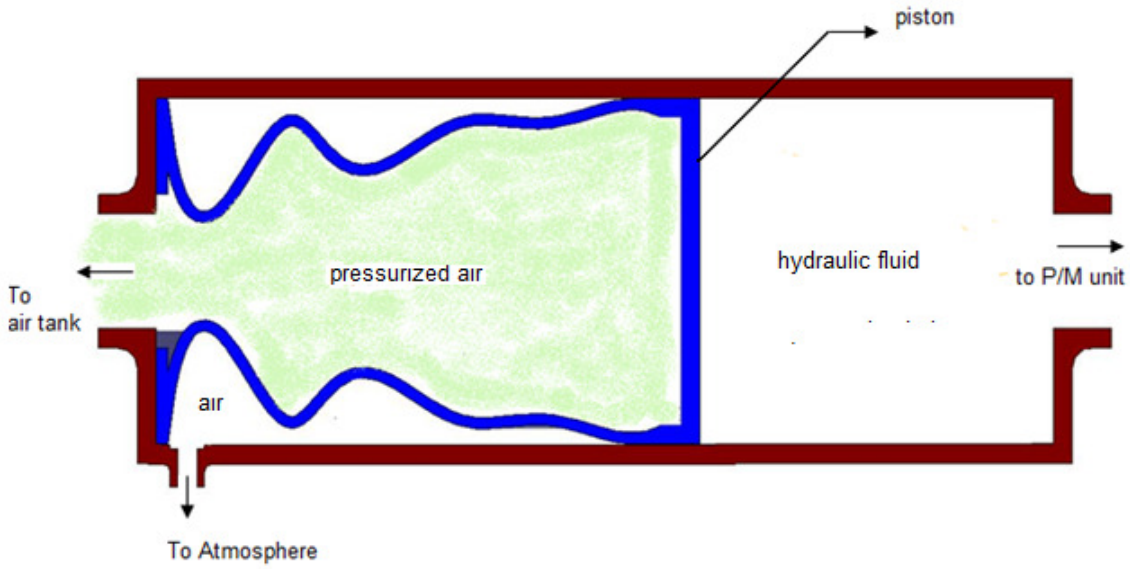

Figure 3. Accumulator with Bellows Arrangement

Figure 4 shows the arrangement of the new design. The hydraulic pump/motor unit is connected to the driveshaft using a four-speed transmission to provide reasonable energy transfer during acceleration and braking transients. The model also includes an air compressor which can operate to repressurize the air tank during braking, but its main purpose is to recharge the air tank from an external power supply while the vehicle is parked. Since the recharging takes place over an extended period of time, the size of the air compressor is much smaller than that used in UT's study.

The governing equations for the vehicle dynamic simulation were modeled using MATLAB/Simulink. Details of the model can be found in references 2 and 3. Braking regeneration occurs using either the compressor or the pump/motor unit. Figure 5 shows the Simulink block diagram. Comparisons were made by running the vehicles through the Federal Urban Drive Schedule, repeating as necessary until the available energy in the air tank is depleted.

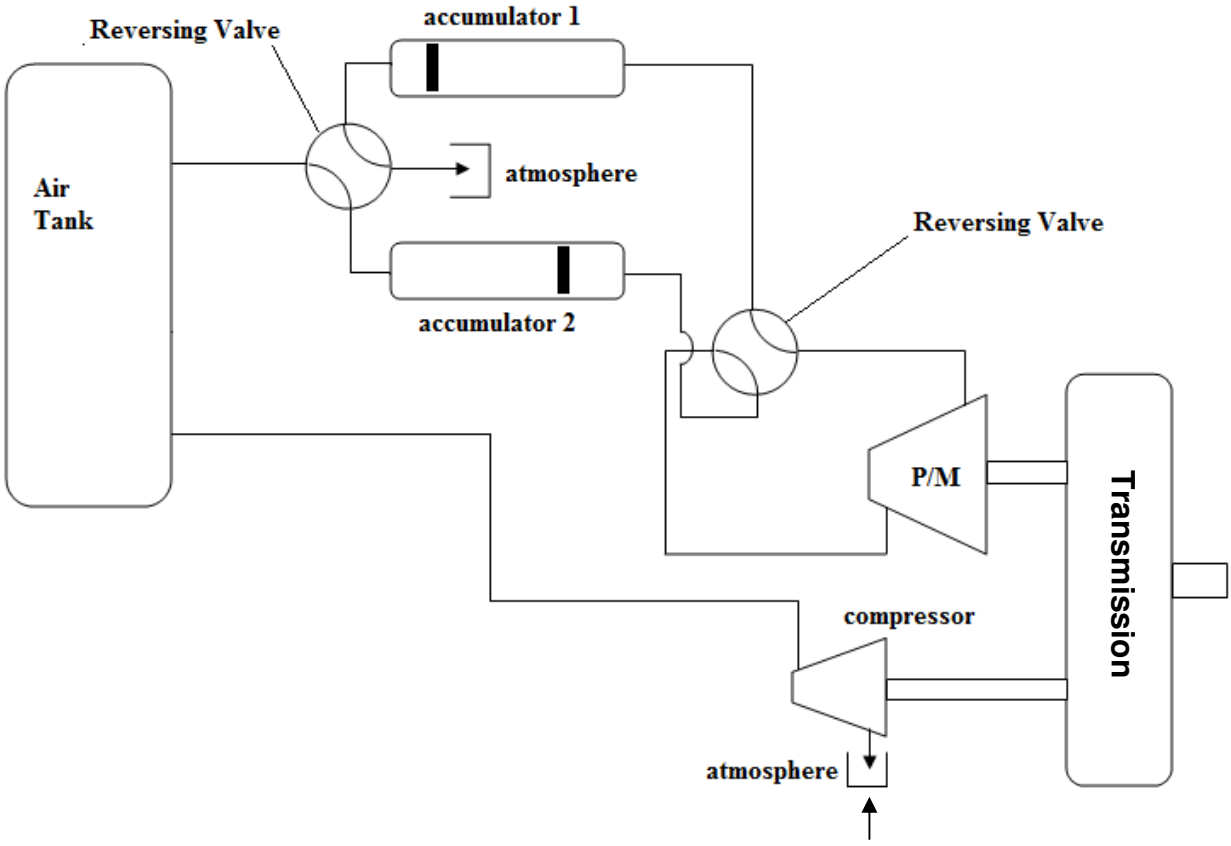

Figure 4. Schematic for the Proposed System

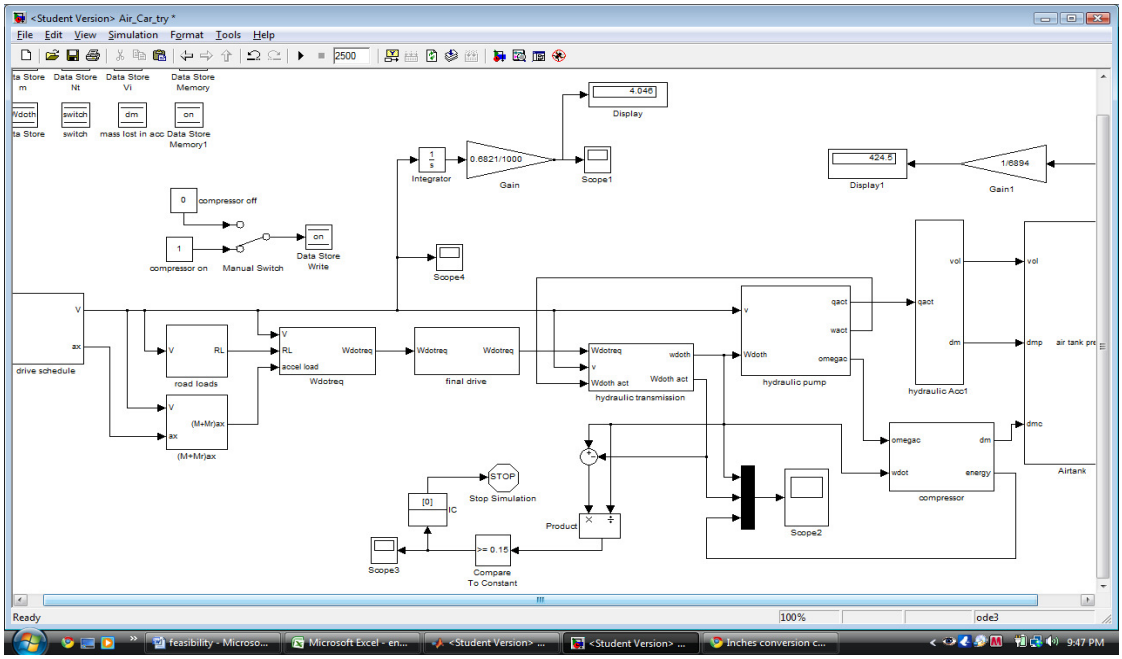

Figure 5. The Simulink Model

5. Results

After developing the new model, calculations done previously for UT's configuration are performed on our design with all the same specifications. Comparisons can be seen in Table 3. Not surprisingly, the results differ by a factor of 4, which is the ratio of the pressure exchanger volume (0.32 m^3) to the accumulator volume (0.08 m^3).

Table 3. Comparison between UT and UDM Designs for Calculated Ideal Energies and Range at Constant Speed

Quantity	UDM	UT	unit
Air mass lost in a switch	32.5	130	kg
Lost work due pressure exchanger venting per switch	16.3	65.4	MJ
Number of switches	10.8	2.7	
Constant speed distance traveled	6	1.5	km

In order to more thoroughly gauge the effectiveness of our design, we made comparisons using parameters for a truck and for two small passenger cars traveling on the Federal Urban Drive Schedule, shown in Figure 6. The truck is the same class VI vehicle analyzed by UT. The first car's (Car1) specifications are based on those of the MID AirPod[5], a French-made small urban transport vehicle that was scheduled to begin production in 2009 (there is no indication that mass production has occurred, although several videos of running prototypes can be found online; see reference 5, for example). The second car's (Car2) specifications are based on those of the Chevy Volt[6], scheduled for production release in late 2010.

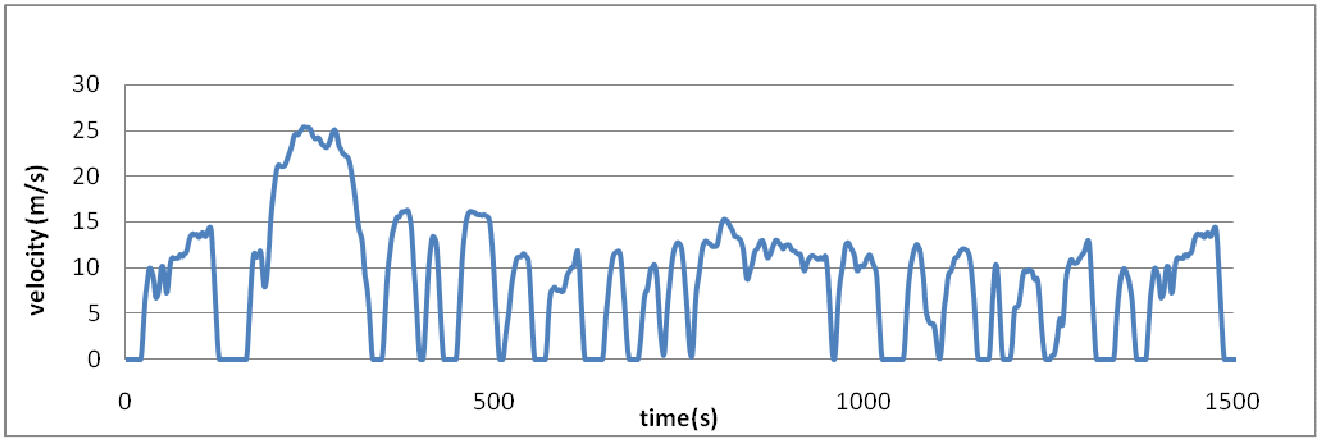

Figure 6: Velocity vs. Time Curve from FUDS

In order to increase range we changed some parameters as follows. The minimum air tank pressure P_{min} is lowered to 3.45 MPa (500 psi) from the value of 35 MPa used in the UT model. This allows a more complete utilization of the energy contained in the pressurized air tank. The accumulator volume was increased from 0.08 to 0.10 m^3.

We also used an initial air tank pressure P_{tank} of 35 MPa instead of 50 MPa to more closely reflect current upper limits on accumulator design. Key specifications for the truck and car are shown in Table 4. Simulation results are shown in Table 5.

Table 4: Specifications of the Truck and the Cars

Quantity	Truck	Car 1	Car2	units
Drag coefficient	0.5	0.29	0.35	
Frontal area	6.767	2.0	2.5	m^2
Air tank volume	2	1	1	m^3
Air mass	769.6	384	384	kg
Accumulator volume	0.1	0.1	0.1	m^3
Hydraulic pump/motor maximum displacement	0.00004	0.0000075	0.000015	m^3
Tire radius	0.4131	0.35	0.35	m
Mass of hardware only	7000	300	1500	kg

Table 5: Car and Truck Results for FUDS Simulation

Quantity	Truck	Car1	Car2	units
Energy lost in the exhaust air	267.08	152.19	152.19	MJ
Number of switches	47	24	24	
Distance traveled using regenerative energy from p/m unit	31.68	153.2	60.38	km
Distance traveled using regenerative compressor	16.57	80.98	28.29	km
Energy required to drive the car	78.73	32.7	35.28	MJ
Energy available in braking	32.69	10.28	14.69	MJ

These results show that range has significantly improved with the elimination of the pressure exchangers and greater utilization of air tank pressure. Using regenerative energy from the pump/motor unit is more effective than regenerating using the onboard air compressor because the compressor must repressurize the air tank using atmospheric air. The truck range is still probably too low for practical applications. For Car1, the range is more significant, but somewhat lower than the advertised range for the AirPod. MDI claims that the AirPod has a range of 220 km with an air tank size of 0.175 m^3 pressurized to 35 MPa[5].

Our air tank is much larger, 1 m^3, and still the range is significantly lower. The AirPod motor is a piston-type engine that runs on compressed air, meaning that it does not suffer from the energy loss that occurs each time a switch occurs in our design. The range of Car2 is comparable to the expected range for the Volt driving exclusively on battery energy. In all three vehicles, the energy lost in venting air still is significantly greater than the energy required to propel the vehicle, meaning that our design still suffers from gross inefficiencies.

6. Evaluation of Plug-In Feature

Our final task is to analyze the plug-in feature of the system. It is assumed that the onboard compressor can be driven by an electric motor plugged into a wall outlet and allowed to run overnight, with electrical energy costing $0.10/kWh. Table 6 summarizes the results.

Table 6: Plug in Results for Truck and Car*

Components	Truck	Car	Units
Compressor displacement	6.18E-5	6.18E-5	m^3
Compressor constant speed	500	500	rad/s
Time taken to refill tank from 3.45 to 35 MPa	13.34	8.03	hrs
Energy required to refill	104.56	52.28	kWh
Refill cost	10.46	5.23	dollars

***The figures above apply to both cars since they have identical air tank volumes and changes in pressure.**

For comparison, the Tesla Roadster (a high-performance electric car) has a range of 236 miles and costs approximately $5 to recharge[7]. GM claims that the Chevy Volt will recharge for less than a dollar[8].

7. Conclusions

In spite of the improved performance that we have been able to achieve through design changes and application to a lighter vehicle, it still appears that the original UT strategy – extending the energy density of a hydraulic system by adding a switching air tank design – is impractical. There is too much wasted energy in the air vented from the accumulators each time a switch occurs. If a way could be found to recover this lost energy – perhaps by venting to a reservoir rather than to the atmosphere – the air-augmented hydraulic system could possibly be made more feasible.

8. References

1. B. Wu, C. Lin, Z. Fillip, H. Peng and D. Assanis; "Optimal Power Management for a Hydraulic Hybrid Delivery Truck", *Vehicle System Dynamics*, vol. 42, nos. 1-2, pp. 23-40 (2004).
2. M. Schumack, C. Schroeder, M. Elahinia, and W. Olson; "A Hydraulic Hybrid Vehicle Simulation Program to Enhance Understanding of Engineering Fundamentals," *2008 ASEE Annual Conference Proceedings* (2008).
3. Xianwu Zeng, master's thesis "Improving the Energy Density of Hydraulic Hybrid Vehicle (HHVs) and Evaluating Plug-In HHVs," University of Toledo, February 2009.
4. M. David Burghardt; *Engineering Thermodynamics with Applications*, 2nd edition, Harper & Row (1982).
5. http://www.mdi.lu/english/airpod.php
6. http://www.chevy-volt.net/chevrolet-volt-weight-details.htm
7. http://www.teslamotors.com/electric/charging_demo.php
8. http://www.chevrolet.com/pages/open/default/future/volt.do

MICHIGAN OHIO UNIVERSITY TRANSPORTATION CENTER
Alternate energy and system mobility to stimulate economic development.

Report No: MIOH UTC SC2 p2-4 2010-Final
MDOT Report No: RC-1545

ENABLING CONGESTION AVOIDANCE AND REDUCTION IN THE MICHIGAN-OHIO TRANSPORTATION NETWORK TO IMPROVE SUPPLY CHAIN EFFICIENCY: FREIGHT ATIS

FINAL REPORT

PROJECT TEAM

Dr. Ratna Babu Chinnam
Dr. Alper Murat
Industrial & Systems Engineering
Wayne State University
4815 Fourth Street
Detroit, Michigan 48202, USA

Dr. Gregory Ulferts
School of Business Administration
University of Detroit Mercy
4001 W. McNichols Rd
Detroit, Michigan 48221, USA

Report No: MIOH UTC SC2p2-4 2010-Final
SC2, Series, Projects 2, 3 and 4 October 2010
FINAL REPORT

Developed By: **Ratna Babu Chinnam, Assoc. Professor**
Principal Investigator, WSU
r_chinnam@wayne.edu
313-577-4846

Alper Murat, Asst. Professor
Investigator, WSU
amurat@wayne.edu
313-577-3872

With Contributions By: **Gregory Ulferts, Professor**
Co-Principal Investigator, UDM
ulfertgw@udmercy.edu
313-993-1219

SPONSORS

This is a Michigan Ohio University Transportation Center project supported by the U.S. Department of Transportation, the Michigan Department of Transportation, Wayne State University and the University of Detroit Mercy.

ACKNOWLEDGEMENT

The Project Team would like to acknowledge support from the Michigan Department of Transportation (MDOT), Ford MP&L, UPS and C.H. Robinson during the course of this research.

DISCLAIMER

Technical Report Documentation Page

1. Report No.	2. Government Accession No.	3. MDOT Project Manager
RC-1545		Niles Annelin

4. Title and Subtitle	5. Report Date
Michigan Ohio University Transportation Center Subtitle: "Enabling Congestion Avoidance and Reduction in the Michigan-Ohio Transportation Network to Improve Supply Chain Efficiency: Freight Atis"	October 2010
	6. Performing Organization Code

7. Author(s)	8. Performing Org. Report No.
Dr. Ratna Babu Chinnam, Wayne State University Dr. Alper Murat, Wayne State University Dr. Gregory Ulferts, University of Detroit Mercy	MIOH UTC SC2p2-4 2010-Final

9. Performing Organization Name and Address	10. Work Unit No. (TRAIS)
Michigan Ohio University Transportation Center University of Detroit Mercy, Detroit, MI 48221 and Wayne State University, Detroit, MI 48202	11. Contract No. 2007-0538
	11(a). Authorization No.

12. Sponsoring Agency Name and Address	13. Type of Report & Period Covered
Michigan Department of Transportation Van Wagoner Building, 425 West Ottawa P. O. Box 30050, Lansing, Michigan 48909	Research, May 2007 – October 2010
	14. Sponsoring Agency Code

15. Supplementary Notes

Additional Sponsors: US DOT Research & Innovative Technology Administration, Michigan Department of Transportation (MDOT), Ford MP&L, UPS and C.H. Robinson.

16. Abstract

MIOH UTC SC2p2-4 2010-Final

In just-in-time (JIT) manufacturing environments, on-time delivery is a key performance measure for dispatching and routing freight vehicles. Growing travel time delays and variability, attributable to increasing congestion in transportation networks, are greatly impacting the efficiency of JIT logistics operations. Recurrent and non-recurrent congestion are the two primary reasons for delivery delay and variability. Over 50 percent of all travel time delays are attributable to non-recurrent congestion sources such as incidents. Despite its importance, state-of-the-art dynamic routing algorithms assume away the effect of these incidents on travel time. In this study, we propose a stochastic dynamic programming formulation for dynamic routing of vehicles in non-stationary stochastic networks subject to both recurrent and non-recurrent congestion. We also propose alternative models to estimate incident induced delays that can be integrated with dynamic routing algorithms.

Proposed dynamic routing models exploit real-time traffic information regarding speeds and incidents from Intelligent Transportation System (ITS) sources to improve delivery performance. Results are very promising when the algorithms are tested in a simulated network of southeast Michigan freeways using historical data from the MITS Center and Traffic.com.

17. Key Words	18. Distribution Statement
Incident management, Traffic congestion, Freight traffic, Efficiency factors, Delivery services, Intelligent transportation systems, Supply chain management, Research projects, Michigan and Ohio	No restrictions. This document is available to the public through the Michigan Department of Transportation.

19. Security Classification - report	20. Security Classification - page	21. No. of Pages	22. Price
		34	

ABSTRACT

In just-in-time (JIT) manufacturing environments, on-time delivery is a key performance measure for dispatching and routing freight vehicles. Growing travel time delays and variability, attributable to increasing congestion in transportation networks, are greatly impacting the efficiency of JIT logistics operations. Recurrent and non-recurrent congestion are the two primary reasons for delivery delay and variability. Over 50 percent of all travel time delays are attributable to non-recurrent congestion sources such as incidents. Despite its importance, state-of-the-art dynamic routing algorithms assume away the effect of these incidents on travel time. In this study, we propose a stochastic dynamic programming formulation for dynamic routing of vehicles in non-stationary stochastic networks subject to both recurrent and non-recurrent congestion. We also propose alternative models to estimate incident induced delays that can be integrated with dynamic routing algorithms.

Proposed dynamic routing models exploit real-time traffic information regarding speeds and incidents from Intelligent Transportation System (ITS) sources to improve delivery performance. Results are very promising when the algorithms are tested in a simulated network of southeast Michigan freeways using historical data from the MITS Center and Traffic.com.

TABLE OF CONTENTS

LIST OF TABLES

LIST OF FIGURES

1. EXECUTIVE SUMMARY

The overall goal of this project is to develop effective static and dynamic routing algorithms for congestion avoidance and reduction for commercial cargo carriers given real-time information regarding recurring and non-recurring congestion by Advanced Traveler Information Systems (ATIS).

Just-in-time supply chains require reliable deliveries. However, travel times on road networks are unfortunately stochastic in nature. This randomness might stem from multiple sources. One of the most significant sources is the high volume of traffic due to commuting. This kind of traffic congestion is called *recurrent congestion* for it usually occurs at similar hours and days on a given network. The most used approach to deal with recurrent congestion is building 'buffer time' into the trip, e. starting the trip earlier to end the trip on time. However, these buffers significantly increase driver and equipment idle time (i.e., reduce utilization).

Intelligent Transportation Systems (ITS) that collect and provide real-time traffic data are now available in most urban areas and traffic monitoring systems are beginning to provide real-time information regarding incidents. In-vehicle communication technologies, both GPS and non-GPS based, are also enabling drivers' access to this information, facilitating vehicle routing and re-routing for congestion avoidance. We are proposed dynamic vehicle routing models that use ITS traffic information to avoid both recurrent and non-recurrent congestion in stochastic transportation networks.

We developed a dynamic vehicle routing model based on Markov decision process (MDP) formulation for the non-stationary stochastic shortest path problem. The state set of the MDP is based on the position of the vehicle, the time of the day, and the traffic congestion states of the roads. ITS data from southeast Michigan road network, collected in collaboration with M-DOT's Michigan Intelligent Transportation System Center (MITS) and Traffic.com, is used to illustrate the performance of the proposed models. Recurrent congestion states of the roads and their transition patterns are determined using historic and real-time traffic data from MITS Center. In particular, states are determined using Gaussian mixture model (GMM) based clustering. To address issues of 'curse of dimensionality' common to MDPs and the recognition that information from distant arcs are unreliable and less likely to influence 'optimal' path selection, we formulated the MDP state space such that only the roads/arcs that are in proximity to the vehicle affect local decisions.

Our dynamic routing models also account for non-recurring congestion stemming from incidents. Our incident models attempt to address two questions: 1) Estimate the affect of incident on travel time (incident-induced travel time delay) and 2) Estimate the incident clearance time (incident clearance time). We estimate incident-induced arc travel time delay using a decay function based on incident severity and duration parameters. Time required to clear the incident and restore the traffic is usually defined as incident clearance time and most of the delay due to incident is experienced during this period. We model the incident-clearance process using a Markov chain with an eventual absorbing state of incident clearance. Given that a road network may encounter both types of congestion concurrently, our dynamic routing models integrally account for both types of congestion and their interactions.

Our experiments clearly illustrate the superior performance of the SDP-derived dynamic routing policies over traditional static-path-based routing. The savings however depend on the network states as well as the time of day. The savings are higher during peak times and lower when traffic tends to be static (especially at nights). Experiments also show that explicit treatment of non-recurrent congestion stemming from incidents can yield significant savings.

2. ACTION PLAN FOR RESEARCH

We start with the data collection from multiple directions. On the *network structure* (network topology, design parameters, arc characteristics) side, we developed a network represents freeway and highways of the southeast Michigan. We test our dynamic routing decisions as well as incident (i.e. accidents, breakdowns) delay models on this network.

For southeast Michigan corridor ***arc velocity data***, we have collaborated with the MITS Center and signed a data-sharing agreement with Traffic.com. We have had multiple meetings with MITS Center to develop a better understanding for their traffic monitoring system (for southeast Michigan highways) and have also received data representing several months of traffic flow (such as velocity, occupancy) for the southeast Michigan highways. We have analyzed this data to improve the quality of the models being developed for dynamic vehicle routing decision support when operating with access to Advanced Traveler Information Systems (ATIS) information. For instance, through our analyses, we identified the need for representing each arc's congestion with a different number of states (and not force all arcs to be modeled with two states – i.e., congested and uncongested). Accordingly, we have refined the recurrent congestion state modeling by employing the Gaussian Mixture Model clustering method for automated detection of number of states and state velocity thresholds. In addition to MITS Center data, we now have access to Traffic.com's sensor database covering majority of highways in the southeast Michigan corridor. These datasets (and the networks resulting from them) are playing a critical role for evaluating and refining our dynamic routing algorithms. For ***incident data*** collection, we collaborated with the MITS Center. We received several months of incident data from Monroe Pendelton and Mark Burrows of MITS Center. This data set allowed us to initiate modeling of non-recurring congestion (incidents and special events) in routing applications. In addition to MITS Center data, Traffic.com also has an extensive archive of incident data which we are currently using to develop parametric incident delay models, models of particular interest to SEMCOG.

We have initially constructed a simple hypothetical road network simulator to build, test, and validate our algorithms in Matlab. This simulator allowed us to experiment with various network, velocity and incident scenarios. In the second year, we developed a southeast Michigan road network model that covers the sensors from both MITS Center and Traffic.com. We constructed these networks using archived historical traffic ITS data provided by our research partners, MITS Center and Traffic.com. One instance from this network encompasses main freeways and arterials extending from the intersection of I-94 and I-275 to the intersection of I-696 and I-75. In addition to network construction, we developed a data extraction and network configuration tool that allowed us to automate the loop sensor velocity and incident data extraction from the ITS databases. This tool takes in the origin-destination coordinates as inputs to identify and locate loop sensors.

Subsequently, this tool first extracts sensor velocity data and incident data and then configures routing models by determining such model inputs as arc travel time distributions by departure time of day. This tool encompasses data extraction, filtering, and cleaning procedures and is based on a Microsoft Access database with Matlab interface for efficient network configuration and algorithmic implementation.

We developed compact yet effective parametric incident duration and incident delay models. We extend and refine these models by calibrating according to the incident data obtained from the MITS Center and Traffic.com. In addition, we have also extended the algorithmic framework by incorporating more realistic "non-recurring congestion" modeling and exploitation logic into the algorithms.

Extensive evaluations of our SDP algorithms on hypothetical networks revealed significant reductions in trip completion times in comparison with deterministic algorithms and static stochastic algorithms that do not account for non-recurring congestion information. We first developed a parametric multiplicative incident model for the incident delay. This model accounts for the real-time traffic congestion, incident duration, incident severity, incident response. In the second year, we have further extended previous incident model by coupling the parametric delay model with an incident clearance Markov model. The incident clearance model is a non-stationary Markov chain model in which the incident clearance probability increases with the duration of the incident. Our incident model is integrated within the recurring congestion modeling and algorithmic framework.

We have developed the road-network model for the southeast Michigan region and identified some set of origin-destination pairs for major freight routes. On these routes, we have extracted the road-network recurring and non-recurring congestion data sets and calibrated these arcs accordingly. We implemented our static and dynamic models and algorithms in these major freight routes and compared the performance differences between typical baseline routing algorithms and our stochastic dynamic routing algorithms.

3. INTRODUCTION

Supply chains that rely on just-in-time (JIT) production and distribution require timely and reliable freight pickups and deliveries from the freight carriers in all stages of the supply chain. The requirements have even spread to the supply chains' service sectors with the adoption of cross docking, merge-in-transit, and e-fulfillment, especially in developed countries with keen concern in process improvement[1]. For example, in Osaka and Kobe, Japan, as early as 1997, 52 percent (by weight) of cargo deliveries and 45 percent of cargo pickups had designated time windows or specified arrival times [2]. These requirements have now become the norm in the U.S. as well. For example, many automotive final assembly plants in Southeast Michigan receive nearly 80 percent of all assembly parts on a JIT basis (involving five to six deliveries/day for each part with no more than three hours of inventory at the plant). However, road transportation networks are experiencing ever growing congestion, which greatly hinders all travel and certainly the freight delivery performance. The cost of this congestion is growing rapidly, reaching $78 billion by 2005 (from $20 billion in 1985) just in the U.S. large metropolitan areas alone [3]. This congestion is forcing logistics solution providers to add significant travel time buffers to improve on-time delivery performance, causing idle vehicles due to early arrivals.

Figure 1, for example, illustrates the magnitude of these buffers for 2003 in the automotive industry heavy Detroit Metro area, reaching over 70 percent during peak congestion periods of the day to achieve 95 percent on-time delivery performance [4]. Given that automotive plants are heavily relying on JIT deliveries, this is increasingly forcing the automotive original equipment manufacturers (OEMs) and others to carry increased levels of safety inventory to cope with the risk of late deliveries.

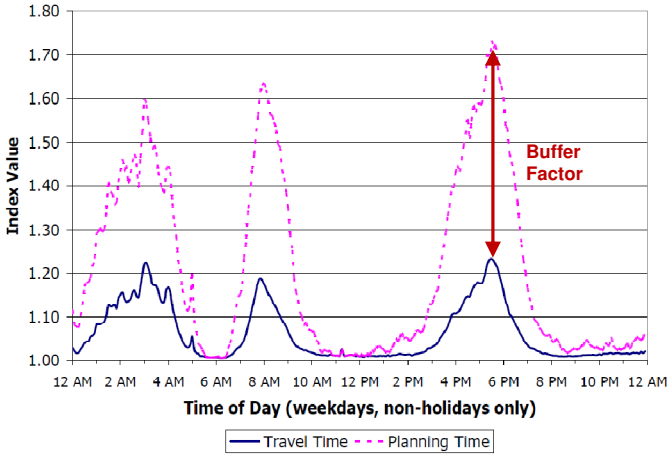

Figure 1. Extra Buffer Time Needed for On-Time Delivery with 95 Percent Confidence in Detroit [4]

The average trip travel time varies by the time of day. Travel time delays are mostly attributable to the so called 'recurrent' congestion that, for example, develops due to high volume of traffic seen during peak commuting hours. Incidents, such as accidents, vehicle breakdowns, bad weather, work zones, lane closures, special events, etc. are other important sources of traffic congestion. This type of congestion is labeled 'non-recurrent' congestion in that its location and severity is unpredictable. The Texas Transportation Institute [5] reports that over 50 percent of all travel time delays are attributable to the non-recurrent congestion. Despite its importance, current state-of-the-art dynamic routing algorithms assume away the effect of these incidents on travel time.

The standard approach to deal with congestion is to build additional 'buffer time' into the trip (i.e., starting the trip earlier so as to end the trip on time), as illustrated in Figure 1. Intelligent Traffic Systems (ITS), run by state agencies (e.g., the Michigan Intelligent Transportation Systems (MITS) Center in southeast Michigan) and/or the private sector (e.g., Traffic.com operating in many states), are providing real-time traffic data (e.g., lane speeds and volumes) in many urban areas. These traffic monitoring systems are also beginning to provide real-time information regarding traffic incidents and their severity. In-vehicle communication technologies, such as satellite navigation systems, are also enabling drivers access to this information en-route.

4. OBJECTIVE

The objective of our study is to develop methods for routing vehicles in stochastic road network environments representative of real-world conditions. In the literature, some aspects of this problem have been studied at some level but there does not exist any study that takes into account all aspects of our dynamic routing problem.

Specifically, our objectives are:

1) Methods for accurate and efficient representation of recurrent congestion, in particular, identification of multiple congestion states and their transition patterns.
2) Integrated modeling and treatment of recurrent and non-recurrent congestion for vehicle routing and demonstrating the need and value of such integration.

5. SCOPE

In this paper, we precisely consider JIT pickup/delivery service, and propose a dynamic vehicle routing model that exploits real-time ITS information to avoid both recurrent and non-recurrent congestion. We limit the scope to routing a vehicle from an origin point (say depot or warehouse) to a destination point.

Our problem setting is the non-stationary stochastic shortest path problem with both recurrent and non-recurrent congestion. We propose a dynamic vehicle routing model based on a Markov decision process (MDP) formulation. Stochastic dynamic programming is employed to derive the routing 'policy', as the static 'paths' are provably suboptimal for this problem. The MDP 'states' cover vehicle location, time of day, and network congestion state(s). Recurrent network congestion states and their transitions are estimated from the ITS historical data. The proposed framework employs Gaussian mixture model based clustering to identify the number of states and their transition rates, by time of day, for each arc of the traffic network. To prevent exponential growth of the state space, we also recommend limiting the network monitoring to a reasonable vicinity of the vehicle. As for non-recurrent congestion attributable to incidents, we estimate the incident-induced arc travel time delay using a stochastic queuing model.

6. LITERATURE SURVEY

In the classical deterministic shortest path (SP) problem, the cost of traversing an arc is deterministic and independent on the arrival time to the arc. The stochastic SP problem (S-SP) is a direct extension of this deterministic counterpart where the arc costs follow a known probability distribution. In S-SP, there are multiple potential objectives, and the two most common ones are the minimization of the total expected cost and maximization of the probability of being lowest cost [6]. To find the path with minimum total expected cost, Frank [7] suggested replacing arc costs with their expected values and subsequently solving as a deterministic SP. Loui [8] showed that this approach could lead to sub-optimal paths and proposed using utility functions instead of the expected arc costs. Eiger et al. [9] showed that Dijkstra's algorithm [10] can be used when the utility functions are linear or exponential.

Stochastic SP problems are referred as stochastic time-dependent shortest path problems (STD-SP) when arc costs are time-dependent. Hall [11] first studied the STD-SP problems and showed that the optimal solution has to be an 'adaptive decision policy' (ADP) rather than a single path.

In an ADP, the node to visit next depends on both the node and the time of arrival at that node, and therefore the standard SP algorithms cannot be used. Hall [11] employed the dynamic programming (DP) approach to derive the optimal policy. Bertsekas and Tsitsiklis [12] proved the existence of optimal policies for STD-SP. Later, Fu and Rilett [13] modified the method of Hall [11] for problems where arc costs as continuous random variables. They showed the computational intractability of the problem based on the mean-variance relationship between the travel time of a given path and the dynamic and stochastic travel times of the individual arcs.

They also proposed a heuristic in recognition of this intractability. Bander and White [14] modeled a heuristic search algorithm AO* for the problem and demonstrated significant computational advantages over DP, when there exists known strong lower bounds on the total expected travel cost between any node and the destination node. Fu [15] discussed real-time vehicle routing based on the estimation of immediate arc travel times and proposed a label-correcting algorithm as a treatment to the recursive relations in DP. Waller and Ziliaskopoulos [16] suggested polynomial algorithms to find optimal policies for stochastic shortest path problems with one-step arc and limited temporal dependencies. Gao and Chabini [17] designed an ADP algorithm and proposed efficient approximations to time and arc dependent stochastic networks. An alternative routing solution to the ADP is a single path satisfying an optimality criterion. For identifying paths with the least expected travel (LET) time, Miller-Hooks and Mahmassani [18] proposed a modified label-correcting algorithm. Miller-Hooks and Mahmassani [19] extends [18] by proposing algorithms that find the expected lower bound of LET paths and exact solutions by using hyperpaths.

All of the studies on STD-SP assume deterministic temporal dependence of arc costs, with the exception of Waller and Ziliaskopoulos [16] and Gao and Chabini [17]. In most urban transportation networks, however, the change in the cost of traversing an arc over-time is stochastic and there are very few studies addressing this issue. Most of these studies model this stochastic temporal dependence through Markov chain modeling and propose using the real-time information available through ITS systems for observing Markov states. In addition, all of these studies assume that recourse actions are possible such that the vehicle's path can be re-adjusted based on newly acquired congestion information. Accordingly, they identify optimal ADPs. Polychronopoulos and Tsitsiklis [20] is the first study to consider stochastic temporal dependence of arc costs and to suggest using online information en route. They considered an acyclic network where the cost of outgoing arcs of a node is a function of the environment state of that node and the state changes according to a Markovian process. They assumed that the arc's state is learned only when the vehicle arrives at the source node and the state of nodes are independent. They also proposed a DP procedure to solve the problem. Polychronopoulos and Tsitsiklis [21] consider a problem when recourse is possible in a network with dependent undirected arcs and the arc costs are time independent. They proposed a DP algorithm to solve the problem and discussed some non-optimal but easily computable heuristics. Azaron and Kianfar [22] extended [20] by evolving the states of current node as well as its forward nodes with independent continuous-time semi-Markov processes for ship routing problem in a stochastic but time invariant network. Kim et al. [23] studied a similar problem as in [20] except that the information of all arcs are available real-time. They proposed a DP formulation where the state space includes states of all arcs, time, and the current node. They stated that the state space of the proposed formulation becomes quite large making the problem intractable.

They reported substantial cost savings from a computational study based on the southeast Michigan road network. To address the intractable state-space issue, Kim et al. [24] proposed state space reduction methods. A limitation of Kim et al. [24], is the modeling and partitioning of travel speeds for the determination of arc congestion states. They assume that the joint distribution of velocities from any two consecutive periods follows a single unimodal Gaussian distribution, which cannot adequately represent arc travel velocities for arcs that routinely experience multiple congestion states.

Moreover, they also employ a fixed velocity threshold *(50 mph)* for all arcs and for all times in partitioning the Gaussian distribution for estimation of state-transition probabilities (i.e., transitions between congested and uncongested states). As a result, the value of real-time information is compromised rendering the loss of performance of the dynamic routing policy. Our proposed approach addresses all of these limitations.

6.1. Non-recurrent Incidents and Incident Clearance

All of the shortest-path studies reviewed above consider stochastic arc costs that are mostly attributable to recurrent congestion. However, as stated earlier, over 50 percent of all traffic congestion is attributable to non-recurrent incidents and has to be accounted for dynamic routing. Incident-induced delay time estimation models are widely studied in the transportation literature. These models can be categorized into three groups based on their approaches: shockwave theory [25-27], queuing theory [28-33], and statistical (regression) models [34-36]. All of these modeling approaches have certain requirements such as loop-sensor data or assumptions regarding traffic/vehicle behavior. For instance, the shockwave theory based models require extensive loop sensor data for accurate positioning and progression of the shockwave. Both the queuing and shockwave theory based models require assumptions about the vehicle arrival process. Regression models, as empirical methods, cannot handle missing data without compromising on accuracy.

In all these three modeling methods, the delay due to incident is a function of incident duration. Thus, the correct estimation of incident duration is fundamental and there are various distributions suggested. Gaver [37] derived probability distributions of delay under flow stopping. Truck-involved incident duration is studied by Golob et al. [38] and employs lognormal distribution. Analysis of variance is examined by Giuliano [39] and a truncated regression model to estimate incident duration is proposed by Khattak et al. [40] for incident durations in Chicago area. Gamma and exponential distributions are also suggested as good representations of incident duration distribution [41]. Since the likelihood of ending an incident is related to how long it has lasted, hazard-based models are also suggested extensively. An overview of duration models applications is presented by Hensher and Mannering [42]. Nam and Mannering [43] applied hazard-based duration models to model distribution of detect/report, respond and clear durations of incidents. Using the empirical data of two years from the state of Washington, they showed that detect/report and respond times are Weibull distributed and the clearance duration is log-logistic distributed. Modeling incident delay in conjunction with vehicle routing is in its nascence. Ferris and Ruszczynski [44] present a problem in which arcs with incidents fail and become permanently unavailable. They model the problem as an infinite-horizon Markov decision process. Thomas and White [45] consider the incident clearance process and adopt the models in Kim et al. [23] for routing under non-recurrent congestion.

They model the incident delay using a multiplicative model and the incident clearance time as a non-stationary Markov chain, with transition probabilities following a Weibull distribution with an increasing instantaneous clearance rate. To model incident-induced delay, they multiply the incident arc's cost by a constant and time-invariant scalar. However, they do not account for recurrent congestion and assume arc costs are time-invariant and deterministic. In our approach, we address these limitations by joint consideration of recurrent and non-recurrent congestion as well as more appropriate representation of incident-induced delay and clearance.

7. METHODOLOGY: MODELING RECURRENT AND NON-RECURRENT CONGESTION

7.1. Recurrent Congestion Modeling

Let the graph $G=(N,A)$ denote the road network where N is the set of nodes (intersections) and $A \subseteq N \times N$ is the set of directed arcs between nodes. For every node pair, $n', n \in N$, there exists an arc $a \equiv (n,n') \in A$, if and only if, there is a road that permits traffic flow from node n to n'. Given an origin-destination (OD) node pair, the trip planner's problem is to decide which arc to choose at each decision node such that the expected total trip travel time is minimized. We denote the origin and destination nodes with n_0 and n_d, respectively. We formulate this problem as a finite horizon Markov decision process (MDP), where the travel time on each arc follows a non-stationary stochastic process.

An arc, $a \equiv (n,n') \in A$ is labeled as observed if its real-time traffic data (e.g., velocity) is available through the traffic information system. An observed arc's traffic congestion can be in $r+1 \in Z^+$ different states at time *t*. These states represent arc's congestion level and are associated with the real-time traffic velocity on the arc. We begin with discussing how to determine an arc's congestion state given the real-time velocity information and defer the discussion on estimation of the congestion state parameters to Section 5. Let $c_a^{i-1}(t)$ and $c_a^i(t)$ for $i=1,2,...,r+1$ denote the cutoff velocities used to determine the state of arc a given the velocity at time t on arc a, $v_a(t)$. We further define $s_a^i(t)$ as the i^{th} traffic congestion state of arc a at time *t*, i.e. $s_a^1(t)=\{1\}$ and $s_a^r(t)=\{\text{Congested at level r}\}=\{r\}$. For instance, if there are two congestion levels (e.g., $r+1=2$), then there will be one congested state and the other will be uncongested state, i.e., $s_a^0(t)=\{\text{Uncongested}\}=\{0\}$ and $s_a^1(t)=\{\text{Congested}\}=\{1\}$. Congestion state, $s_a^i(t)$ of the arc a at time *t* can then be determined as:

$$s_a(t)=\left\{i, \text{if } c_a^{i-1}(t) \le v_a(t) < c_a^i(t)\right\} \quad (1)$$

We assume the congestion state of an arc evolves according to a non-stationary Markov chain and the travel time is normally distributed at each state. In a network with all arcs observed, $S(t)$ denotes the traffic congestion state vector for the entire network, i.e., $S(t)=\{s_1(t), s_2(t), ..., s_{|A|}(t)\}$ at time t. For presentation clarity, we will suppress (t) in the notation whenever time reference is obvious from the expression. Let the state realization of $S(t)$ be denoted by $s(t)$.

It is assumed that arc traffic congestion states are independent from each other and have the single-stage Markovian property. In order to estimate the state transitions for each arc, two consecutive periods' velocities are modeled jointly. Accordingly, the time-dependent single-period state transition probability from state $i=s_a(t)$ to state $j=s_a(t+1)$ is denoted with $P\{s_a(t+1)=j \mid s_a(t)=i\}=\alpha_a^{ij}(t)$. The transition probability for arc a, $\alpha_a^{ij}(t)$, is estimated from the joint velocity distribution as follows:

$$\alpha_a^{ij}(t)=\frac{\left|c_a^{i-1}(t)\le V_a(t)<c_a^{i}(t)\cap c_a^{j-1}(t+1)<V_a(t+1)<c_a^{j}(t+1)\right|}{\left|c_a^{i-1}(t)\le V_a(t)<c_a^{i}(t)\right|} \tag{2}$$

Let $T_a(t,t+1)$ denote the matrix of state transition probabilities from time t to time $t+1$, then we have $T_a(t,t+1)=\left[\alpha_a^{ij}(t)\right]_{ij}$. We further assume that arc a's congestion state is independent of other arcs' states, i.e. $P\{s_a(t+1) \mid s_{a'}(t+1), s_a(t)\}=P\{s_a(t+1) \mid s_a(t)\}=\alpha_a^{ij}(t)$ for $\forall a' \in A$. Note that the single-stage Markovian assumption is not restrictive for our approach as we could extend our methods to the multi-stage case by expanding the state space [46]. Let network be in state $S(t)$ at time t and we want to find the probability of the network state $S(t+\delta)$, where δ is a positive integer number. Given the independence assumption of arcs' congestion states, this can be formulated as follows:

$$P\left(S(t+\delta) \mid S(t)\right)=\prod_{a=1}^{|A|}P\left(s_a(t+\delta) \mid s_a(t)\right) \tag{3}$$

Then the congestion state transition probability matrix for each arc in δ periods can be found by the Kolmogorov's equation [47]:

$$T_a(t,t+\delta)=\left[\alpha_a^{ij}(t)\right]_{ij}\times\left[\alpha_a^{ij}(t+1)\right]_{ij}\times ...\times\left[\alpha_a^{ij}(t+\delta)\right]_{ij} \tag{4}$$

With the normal distribution assumption of velocities, the time to travel on an arc can be modeled as a non-stationary normal distribution. We further assume that the arc's travel time depends on the congestion state of the arc at the time of departure (equivalent to the arrival time whenever there is no waiting). It can be determined according to the corresponding normal distribution:

$$\delta(t,a,s_a)\sim N\left(\mu(t,a,s_a),\sigma^2(t,a,s_a)\right) \tag{5}$$

where $\delta(t,a,s_a)$ is the travel time on arc a at time t with congestion state $s_a(t)$; $\mu(t,a,s_a)$ and $\sigma(t,a,s_a)$ are the mean and standard deviation of the travel time on arc a at time t with congestion state $s_a(t)$. For the clarity of notation, we hereafter suppress the arc label from the parameter space wherever it is obvious, i.e. $\delta(t,a,s_a)$ will be referred as $\delta_a(t,s)$.

We assume that objective of dynamic routing is to minimize the expected travel time based on the real-time information. The nodes (intersections) of the network represent decision points where a routing decision can be made. Since our algorithm is also applicable for a network with incidents, in the next section we present our incident modeling approach, and then integrate the recurrent congestion and incident models.

7.2. Incident Modeling

In this section, we develop incident models which measure the incident clearance time and the delay experienced as a result of incident. In section 4, we integrate recurrent congestion and incident models with the dynamic routing model.

7.2.1 Estimating Incident Duration

The incident duration is defined as the total of detection/reporting, response, and clearance times. Due to the nature of most incident response mechanisms, the longer the incident has not been cleared, the more likely that it will be cleared in the next period. For example, the probability of an incident being cleared in the 15th minute, given that it has lasted 14 minutes, is greater than the probability of it being cleared in the 14th minute given that it has lasted 13 minutes. This is because it is more likely that someone has already reported the incident and an incident response team is either on the way or has already responded. Let t be the time to clear the incident. Then, we have the increasing hazard rate property, e.g., $\lambda(t+1) > \lambda(t)$, where $\lambda(t)=f(t)/(1-F(t))$ is the hazard rate of incident clearance in duration t, and $f(t)$ and $F(t)$ are the density and cumulative density functions of the clearance duration, respectively. We choose the Weibull distribution with increasing hazard rate to model the incident clearance duration.

Whenever there is an incident on an arc in the network, we assume that its starting time (t_{inc}^0), current status (i.e. cleared/not cleared), expected duration (μ), and standard deviation (σ) are available through ITS incident management and incident database systems. Hence, we can estimate the parameters of the Weibull distribution ($\varphi(a,b)$) of the incident clearance duration [47]. Furthermore, if an incident occurs en route, we may simply re-optimize the routing policy by assuming that the new origin node is the node that the driver is at or arrives next.

7.2.2 Estimating Incident-Induced Delay

Our incident delay model is based on [29]. Here incident-induced delay function, $\Theta(\cdot)$, is based on the incident duration φ, road nonincident capacity denoted with c (vehicle per hour, or *vph* in short), road capacity during the incident denoted with ρ(*vph*) and arrival rate of vehicles to the incident arc denoted with q(*vph*). Given these parameters for an incident started at t_{inc}^0, the vehicle arriving to the incident arc at time (t) experiences the following expected incident-induced delay:

$$E\left(\Theta(.)\right)=\left(\frac{c-\rho}{c}\right)\left(D_{12}-D_1P_3\right)+P_2d_m \tag{6}$$

where $D_{12}=\int_{D_1}^{D_2} x.\varphi(x)\,dx$, $D_1=\left(\frac{c-\rho}{c-q}\right)\left(t-t_{inc}^0\right)$, $D_2=\left(\frac{q}{\rho}\right)\left(t-t_{inc}^0\right)$, $d_m=\left(\frac{q-\rho}{\rho}\right)\left(t-t_{inc}^0\right)$, $P_1=\int_0^{D_2} x.\varphi(x)\,dx$, $P_2=\int_{D_2}^{\infty} x.\varphi(x)\,dx$, and $P_3=1-\left(P_1+P_2\right)$.

In order to track the amount of time that each arc has spent in the incident state, we define an incident duration vector defined over all the arcs, $I(t)$, i.e. $I(t)=\left\{i_1(t),i_2(t),...,i_{|A|}(t)\right\}$. Note that if an arc a is not an incident arc, then $i_a(t)=0$, otherwise $i_a(t)=t-t_{inc}^0(a)$ and $0<i_a(t)<\infty$, where $t_{inc}^0(a)$ is the incident onset time on arc a. For presentation clarity, we will hereafter omit the arc reference from the incident onset time, i.e. $t_{inc}^0=t_{inc}^0(a)$, whenever incident arc reference is obvious.

The incident delay model is an additive model, in that, $\Theta(\cdot)$ represents the delay time by which the arc travel time under same conditions (congestion state and the time) will be increased by a duration amounting to the incident induced delay. Specifically, given the arc travel time without the incident, $\delta_a(t,s,i=0)$, and the incident parameters, (φ,c,ρ,q,i), we can express the arc travel time with incident as:

$$\delta_a(t,s,i)=\delta_a(t,s,i=0)+\Theta_a\left(\varphi,c,\rho,q,i=t-t_{inc}^0\right) \tag{7}$$

We make the following assumptions for the incident delay function:

Assumption 1: Incident delay is only experienced on the incident arc (no propagation of the incident delay effect in the remainder of the network).

Assumption 2: Incident delay function is additive which amplifies the incumbent arc travel time.

Assumption 3: Incident delay function, $\Theta(\cdot)$, is such that the total delay associated by deciding to wait at a node (e.g., waiting time plus the incident delay), is not less than the case without waiting.

In practice, the incident effect propagates in the network in the form of a shockwave after a certain duration following the incident. Since our goal is to investigate the impact of incidents on the travel time, we choose to focus on the most important ingredient, namely the incident-induced delay on the incident arc. Hence, *Assumption 1* is acceptable under certain scenarios. One scenario is where the incident duration is not long enough that vehicles divert to alternative arcs or the capacity of alternative arcs is sufficiently large to accommodate the diversion without any change in their congestion state. The additive model assumption (*Assumption 2*) is appropriate since the travel time delay of a particular incident depends on both the incident characteristics and the incumbent travel time on the arc. *Assumption 3* is consistent with our network and travel time assumptions where we assume that waiting at a node (or on an arc) is not permitted and/or does not provide travel time savings (first-in-first-out property). The following lemma provides a requirement for the incident model parameters such that the *Assumption 3* holds.

Lemma 1. The incident-induced delay parameters (*c,q*), satisfying the following condition for the minimal waiting time of Δ (smallest discrete time interval), ensures that waiting at the incident node does not reduce the expected travel time.

$$\mu_a\left(t_k+\Delta,s\right)-\mu_a\left(t_k,s\right)\geq-\frac{q}{c}\Delta$$

Proof. Let $a\in A$ denote the incident arc with origin and destination nodes $\left(n_k,n_{k+1}\right)$. Further, let $t_{k+1}=t_k+\delta_a\left(t_k,s,t_k-t_{inc}^0\right)$ represent the arrival time to the node n_{k+1} after departing from n_k at time t_k. Then the expected travel time from node n_k to the trip destination node (n_d) under an optimal policy is $E\left\{\delta_a\left(t_k,s,i=\left(t_k-t_{inc}^0\right)\right)+F^*\left(n_{k+1},t_k+\delta_a\left(t_k,s,t_k-t_{inc}^0\right),w\right)\right\}$, where the second term is the cost-to-go from node n_{k+1} at time t_{k+1} with congestion state vector w for future arcs at t_{k+1}. Let's denote the expected travel time from node n_k to the trip destination node (n_d) at time t_k and $t_k+\Delta$ with $D\left(t_k\right)$ and $D\left(t_k+\Delta\right)$, respectively.

$$D\left(t_k\right)=\delta_a\left(t_k,s,t_k-t_{inc}^0\right)+F^*\left(n_{k+1},t_k+\delta_a\left(t_k,s,t_k-t_{inc}^0\right),w\right)$$
$$D\left(t_k+\Delta\right)=\delta_a\left(t_k+\Delta,s,t_k+\Delta-t_{inc}^0\right)+F^*\left(n_{k+1},t_k+\delta_a\left(t_k+\Delta,s,t_k+\Delta-t_{inc}^0\right),w\right)$$

Assumption 3 states that at any node arrival time $\left(t_k\right)$, waiting at the node does not lead to lower destination arrival time than without waiting. We write this condition for the minimal waiting time of Δ unit time (smallest discrete time interval),

$$E\left\{D\left(t+\Delta\right)\right\}-E\left\{D\left(t\right)\right\}\geq-\Delta$$

We assume that cost-to-go functions alone satisfy this relationship as we assumed that link travel times (in both congestion states) and state transitions are such that waiting at a node does not provide travel time savings in the recurrent congestion (e.g., first-in-first-out property). For Δ waiting time this leads to the following relation for every t_k:

$$F^*\left(n_{k+1},t_k+\Delta+\delta_a\left(t_k+\Delta,s,t_k+\Delta-t_{inc}^0\right),w\right)-F^*\left(n_{k+1},t_k+\delta_a\left(t_k,s,t_k-t_{inc}^0\right),w\right)\geq-\Delta.$$

Hence, we have the following relation:

$$E\left\{\delta_a\left(t_k+\Delta,s,t_k+\Delta-t_{inc}^0\right)\right\}-E\left\{\delta_a\left(t_k,s,t_k-t_{inc}^0\right)\right\}\geq-\Delta,$$

where,

$$\begin{aligned}E\left\{\delta_a\left(t_k,s,t_k-t_{inc}^0\right)\right\}&=E\left\{\delta_a\left(t_k,s,i=0\right)+\Theta_a\left(\varphi,c,\rho,q,i=t_k-t_{inc}^0\right)\right\}\\&=\mu_a\left(t_k,s\right)+E\left\{\Theta_a\left(\varphi,c,\rho,q,i=t_k-t_{inc}^0\right)\right\},\end{aligned}$$

and, $\mu_a\left(t_k,s\right)$ is the mean travel time on arc *a* at time t_k with congestion state *s*. The expression $E\left\{\Theta_a\left(\varphi,c,\rho,q,i=t_k-t_{inc}^0\right)\right\}$ can be expressed in two alternative closed-form expressions. In the first case, we assume that the vehicle experiences the maximum delay (i.e. fixed-delay regime in Fu and Rilett [29]),

$$E\left\{\Theta_a\left(\varphi,c,\rho,q,i=t_k-t_{inc}^0\right)\right\}=\frac{q-\rho}{\rho}\left(t_k-t_{inc}^0\right).$$

The other alternative is the variable-delay regime in which the vehicle experiences a delay somewhere between the no-delay and the maximum delay [29].

$$E\left\{\Theta_a\left(\varphi,c,\rho,q,i=t_k-t_{inc}^0\right)\right\}=\frac{c-\rho}{c}\mu_{inc}-\frac{c-q}{c}\left(t_k-t_{inc}^0\right).$$

Note that the waiting decision at the incident node is reasonable only in the case of incident queue dissipation, i.e. either the incident is cleared but the queue is not fully dissipated or the incident is not cleared but the vehicle will exit the link before the clearance. This corresponds to the variable-delay regime and we will show that this holds true by comparing the conditions derived for each case. We first express the no node waiting condition under incident for variable-delay regime as:

$$E\left\{\delta_a\left(t_k+\Delta,s,t_k+\Delta-t_{inc}^0\right)\right\}-E\left\{\delta_a\left(t_k,s,t_k-t_{inc}^0\right)\right\}\geq-\Delta$$

$$\mu_a\left(t_k+\Delta,s\right)+E\left\{\Theta_a\left(\varphi,c,\rho,q,t_k+\Delta-t_{inc}^0\right)\right\}-\mu_a\left(t_k,s\right)-E\left\{\Theta_a\left(\varphi,c,\rho,q,t_k-t_{inc}^0\right)\right\}\geq-\Delta$$

$$\mu_a\left(t_k+\Delta,s\right)-\mu_a\left(t_k,s\right)-\frac{c-q}{c}\left(t_k+\Delta-t_{inc}^0\right)+\frac{c-q}{c}\left(t_k-t_{inc}^0\right)\geq-\Delta$$

$$\mu_a\left(t_k+\Delta,s\right)-\mu_a\left(t_k,s\right)\geq-\frac{q}{c}\Delta.$$

When we take the limit $\Delta\to0$, we have,

$$\frac{d\mu_a\left(t,s\right)}{dt}\Big|_{t=t_k}\geq-\frac{q}{c}.$$

In the maximum delay case, the no node waiting condition can be expressed as:

$$E\left\{\delta_a\left(t_k+\Delta,s,t_k+\Delta-t_{inc}^0\right)\right\}-E\left\{\delta_a\left(t_k,s,t_k-t_{inc}^0\right)\right\}\geq-\Delta$$

$$\mu_a\left(t_k+\Delta,s\right)+E\left\{\Theta_a\left(\varphi,c,\rho,q,t_k+\Delta-t_{inc}^0\right)\right\}-\mu_a\left(t_k,s\right)-E\left\{\Theta_a\left(\varphi,c,\rho,q,t_k-t_{inc}^0\right)\right\}\geq-\Delta$$

$$\mu_a\left(t_k+\Delta,s\right)-\mu_a\left(t_k,s\right)+\frac{q-\rho}{\rho}\left(t_k+\Delta-t_{inc}^0\right)-\frac{q-\rho}{\rho}\left(t_k-t_{inc}^0\right)\geq-\Delta$$

$$\mu_a\left(t_k+\Delta,s\right)-\mu_a\left(t_k,s\right)\geq-\frac{q}{\rho}\Delta\,.$$

When we take the limit $\Delta\to 0$, we have,

$$\frac{d\mu_a\left(t,s\right)}{dt}\Big|_{t=t_k}\geq-\frac{q}{\rho}.$$

Note that since the capacity under incident is less than regular capacity, i.e. $c>\rho$, we have the condition for variable-delay regime more strict than the fixed-delay regime, i.e., $-q/c>q/\rho$. Hence, for arbitrary waiting time Δ, no node waiting condition under incident is:

$$\mu_a\left(t_k+\Delta,s\right)-\mu_a\left(t_k,s\right)\geq-\frac{q}{c}\Delta\,.$$

□

8. METHODOLOGY: DYNAMIC ROUTING MODEL WITH RECURRENT AND NON-RECURRENT CONGESTION

We assume that the objective of our dynamic routing model is to minimize the expected travel time based on real-time information where the trip originates at node n_0 and concludes at node n_d. Let's assume that there is a feasible path between $\left(n_0,n_d\right)$ where a path $p=\left(n_0,..,n_k,..,n_{K-1}\right)$ is defined as sequence of nodes such that $a_k\equiv(n_k,n_{k+1})\in A$, $k=0,..,K-1$ and K is the number of nodes on the path. We define set $a_k\equiv(n_k,n_{k+1})\in A$ as the *current arcs* set of node n_k, and denoted with $CrAS\left(n_k\right)$. That is, $CrAS\left(n_k\right)\equiv\left\{a_k:a_k\equiv(n_k,n_{k+1})\in A\right\}$ is the set of arcs emanating from node n_k.

Each node on a path is a decision stage (or epoch) at which a routing decision (which node to select next) is to be made. Let $n_k\in N$ be the location of k^{th} decision stage, t_k is the time at k^{th} decision stage where $t_k\in\{1,...,T\}$, $T>t_{K-1}$. Note that we are discrediting the planning horizon.

We next define our look ahead policy for projecting the congestion states in the network. While optimal dynamic routing policy requires real-time consideration and projection of the traffic states of the complete network, this approach makes the state space prohibitively large. In fact, there is little value in projecting the congestion states well ahead of the current location. This is because the projected information is not different than the long run average steady state probabilities of the arc congestion states. Hence, an efficient but practical approach would tradeoff the degree of look ahead (e.g., number of arcs to monitor) with the resulting projection accuracy and routing performance. This has been very well illustrated in Kim et al. [24]. Thus we limit our look ahead to finite number of arcs that can vary by the vehicle location on the network. The selection of the arcs to monitor would depend on factors such as arc lengths, value of real-time information, and the arcs' congestion state transition characteristics. For ease of presentation and without loss of generality, we choose to monitor only two arcs ahead of the vehicle location and model the rest of the arcs' congestion states through their steady state probabilities. Accordingly, we define the following two sets for all arcs in the network. $ScAS(a_k)$, the successor arc set of arc a_k, $ScAS(a_k) \equiv \{a_{k+1} : a_{k+1} \equiv (n_{k+1}, n_{k+2}) \in A\}$, i.e., the set of outgoing arcs from the destination node (n_{k+1}) of arc a_k. $PScAS(a_k)$, the post-successor arc set of arc a_k, $PScAS(a_k) \equiv \{a_{k+2} : a_{k+2} \equiv (n_{k+2}, n_{k+3}) \in A\}$ i.e., the set of outgoing arcs from the destination node (n_{k+2}) of arc a_{k+1}.

Since the total trip travel time is an additive function of the individual arc travel times on the path plus a penalty function measuring earliness/tardiness of arrival time to the final destination, the dynamic route selection problem can be modeled as a dynamic programming model. The state of the system at k th decision stage is denoted by $\Omega(n_k, t_k, s_{a_{k+1} \cup a_{k+2}, k}, I_k)$. This state vector is composed of the state of the vehicle and network and thus characterized by the current node (n_k), the current node arrival time (t_k), and $s_{a_{k+1} \cup a_{k+2}, k}$ the congestion state of arcs $a_{k+1} \cup a_{k+2}$ where $\{a_{k+1} : a_{k+1} \in ScAS(a_k)\}$ and $\{a_{k+2} : a_{k+2} \in PScAS(a_k)\}$, and incident durations (I_k) of the network at stage k, i.e. $I_k \equiv I(t_k)$. The action space for the state $\Omega(n_k, t_k, s_{a_{k+1} \cup a_{k+2}, k}, I_k)$ is the set of current arcs of node n_k, denoted with $CrAS(n_k)$.

At every decision stage, the trip planner evaluates the alternative arcs from $CrAS(n_k)$ based on the remaining expected travel time. The expected travel time at a given node with the selection of an outgoing arc is the expected arc travel time on the arc chosen and the expected travel time of the next node. Let $\pi = \{\pi_0, \pi_1, ..., \pi_{K-1}\}$ be the policy of the trip and is composed of policies for each of the *K-1* decision stages. For a given state $\Omega_k(n, t, S, I)$, the policy $\pi_k(\Omega_k)$ is a deterministic Markov policy which chooses the outgoing arc from node n_k, i.e., $\pi_k(\Omega_k) = a \in CrAS(n_k)$. Therefore the expected travel cost for a given policy vector $\pi = \{\pi_0, \pi_1, ..., \pi_{K-1}\}$ is as follows:

$$F_0(n,t,S,I) = \underset{\delta_k}{E}\left\{ g_{K-1}(\Omega_{K-1}) + \sum_{k=0}^{K-2} g_k\left(\Omega_k, \pi_k(\Omega_k), \delta_k\right) \right\} \tag{8}$$

where (n_0, t_0, S_0, I_0) is the starting state of the system. δ_k is the random travel time at decision stage *k*, i.e., $\delta_k \equiv \delta\left(t_k, \pi_k(\Omega_k), s_a(t_k), i_a(t_k)\right) + \Theta(\varphi, c, \rho, q, i)$ and $\Theta(\varphi, c, \rho, q, i=0) = 0$, i.e. the incident delay of an arc without incident. $g_a(\Omega_k, \delta_k)$ is cost of travel on arc $a = \pi_k(\Omega_k) \in CrAS(n_k)$ at stage k, i.e., if travel cost is a function (ϕ) of the travel time, then $g(\Omega_k, \pi_k(\Omega_k), \delta_k) \equiv \phi(\delta_k)$. Then the minimum expected travel time can be found by minimizing $F_0(n,t,S,I)$ over the policy vector $\pi = \{\pi_0, \pi_1, ..., \pi_{K-1}\}$ as follows:

$$F_0^*(n,t,S,I) = \min_{\pi=\{\pi_0,\pi_1,...,\pi_{K-1}\}} F_0(n,t,S,I) \tag{9}$$

The corresponding optimal policy is then $\pi^* = \underset{\pi=\{\pi_0,\pi_1,...,\pi_{K-1}\}}{\arg\min} F_0(n,t,S,I)$. Hence, the Bellman's cost-to-go equation for the dynamic programming model can be expressed as follows [46]:

$$F_k^*(\Omega) = \min_{\pi_k} \underset{\delta_k}{E}\left\{ g_k(\Omega, \pi(\Omega), \delta) + F_{k+1}^*(\Omega) \right\} \tag{10}$$

For a given policy $\pi_k(\Omega_k) = a_k \in CrAS(n_k)$, we can re-express the cost-to-go function by writing the expectation in the following explicit form:

$$\begin{aligned} F_k(n,t,S,I \mid a) = \sum_{\delta_k} P_k(\delta \mid n,t,S,I,a)\Big[g_k(\Omega, a, \delta) + \\ \sum_{s_{a_{k+1}}} P\left(s_{a_{k+1}}(t_k) \mid s_{a_{k+1}}(t_k + \delta_k)\right) \sum_{s_{a_{k+2}}} P\left(s_{a_{k+2}}(t)\right) \sum_{I_{k+1}} P\left(I(t_k) \mid I(t_k + \delta_k)\right) F_{k+1}\left(n, (t_k + \delta_k), S, I\right) \Big] \end{aligned} \tag{11}$$

where $P_k(\delta \mid n,t,S,I,a)$ is the probability of travelling arc a_k in δ_k periods. $P\left(s_{a_{k+2}}(t_{k+1})\right)$ is the long run probability of arc $a_{k+2} : a_{k+2} \in PScAS(a_k)$ being in state $s_{a_{k+2},k+1}$ in stage $k+1$. This probability can be calculated from the historical frequency of a state for a given arc and time.

We use backward dynamic programming algorithm to solve for $F_k^*(\Omega)$, $k = K-1, K-2, .., 0$. In the backward induction, we initialize the final decision epoch such that, $\Omega_{K-1} = \Omega(n_{K-1}, t_{K-1})$, n_{K-1} is destination node, and $F_{K-1}(\Omega) = 0$ if $t_{K-1} \le T$. Accordingly, a penalty cost is accrued whenever there is delivery tardiness, e.g., $t_{K-1} > T$.

9. DISCUSSION OF RESULTS: EXPERIMENTAL STUDY

This section demonstrates the performance of the proposed algorithm on a network from southeast Michigan with real-time traffic data from the Michigan Intelligent Transportation Systems (MITS) Center. MITS center is the hub of ITS technology applications at the Michigan Department of Transportation (MDOT) and oversees a traffic monitoring system composed of 180 freeway miles instrumented with 180 Closed Circuit TV Cameras, Dynamic Message Signs, and 2260 Inductive Loops. The methods also utilize real-time and archived data from Traffic.com, a private company that provides traffic information services in several states and also operates additional sensors and traffic monitoring devices in Michigan. Traffic.com also provides information regarding incidents causing non-recurrent congestion (e.g., incident location, type, severity, and times of incident occurrence and clearance). We implemented all our algorithms and methods in Matlab 7 and executed on a Pentium IV machine (with 1.6 GHz speed processor and 1024 MB RAM) running Microsoft Windows XP operating system.

Our experimental study is outlined as follows: Section 5.1 introduces two road networks from southeast Michigan used for demonstrating the performance of the proposed algorithms along with a description of their general traffic conditions. Section 5.2 describes the process and the results from modeling of recurrent congestion for the networks. Section 5.3 reports savings from employing the proposed dynamic routing model under recurrent congestion for a network with multiple OD pairs. Section 5.4 presents the experimental setup that involves an incident and reports results and savings from employing the proposed dynamic routing model under both recurrent and non-recurrent congestion.

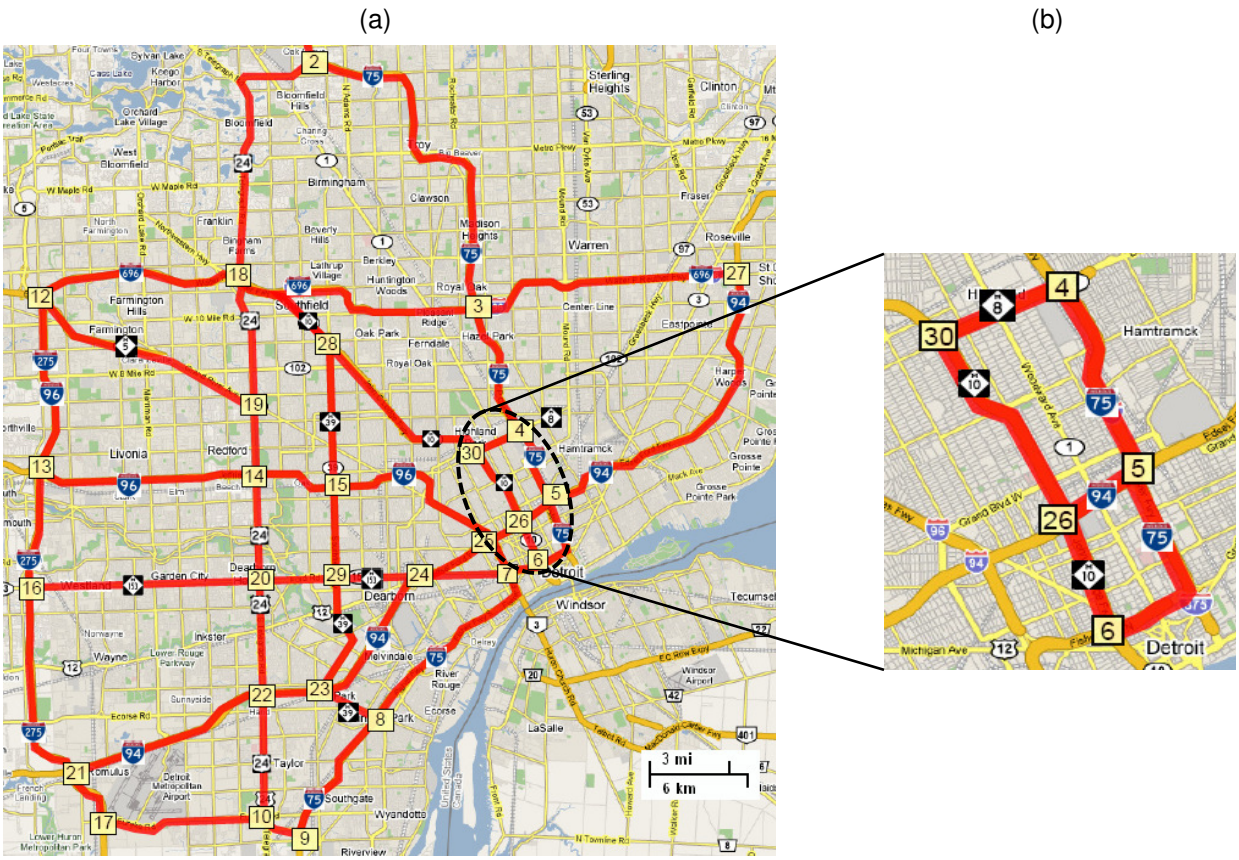

Figure 2. (a) South-East Michigan Road Network Considered for Experimental Study. (b) Sub-Network from Southeast Wayne County

9.1. Sample Networks and Traffic Data

This section introduces the road networks from southeast Michigan used for demonstrating the performance of the proposed algorithms along with a description of their general traffic conditions. As illustrated in Figure 2, the sample network covers southeast Michigan freeways and highways in and around the Detroit metropolitan area.

The network has 30 nodes and a total of 98 arcs with 43 observed arcs (with real-time ITS information from MITS Center) and 55 unobserved arcs. Real-time traffic data for the observed arcs is collected from MDOT Center for 23 weekdays from January 21, 2008 to February 20, 2008 for the full 24 hours of each day at a resolution of an observation every minute. The raw traffic speed data from the MITS Center is cleaned with a series of procedures from Texas Transportation Institute and Cambridge Systematics [4] to improve quality and reduce data errors.

A small part of our full network, labeled *sub-network*, is used here to better illustrate the methods and results (Figure 2b). The sub-network has five nodes and six observed arcs, with more details provided in Table 1.

Table 1. Information Regarding Sub-Network Nodes and Arcs

			FROM		TO	
Arc ID	Freeway	Length (miles)	Node #	Description (Exit #)	Node #	Description (Exit #)
1	I-94	1.32	5	216	26	215
2	M-8	1.75	4	56A (I-75)	30	7C (M-10)
3	I-75	3.13	4	56A	5	53B
4	I-75	2.81	5	53B	6	50
5	M-10	3.26	30	7C	26	4B
6	M-10	1.42	26	4B	6	2A

In the experiments based on the sub-network, node 4 is considered as the origin node and node six as the destination node of the trip. Given the OD pair, we present the speed data for the six different arcs of the sub-network in Figure 3. It can be seen clearly that the traffic speeds follow a stochastic non-stationary distribution that vary with the time of the day. The mean speeds and standard deviations for these same arcs are shown in Figure 4, clearly revealing the non-stationary nature of traffic.

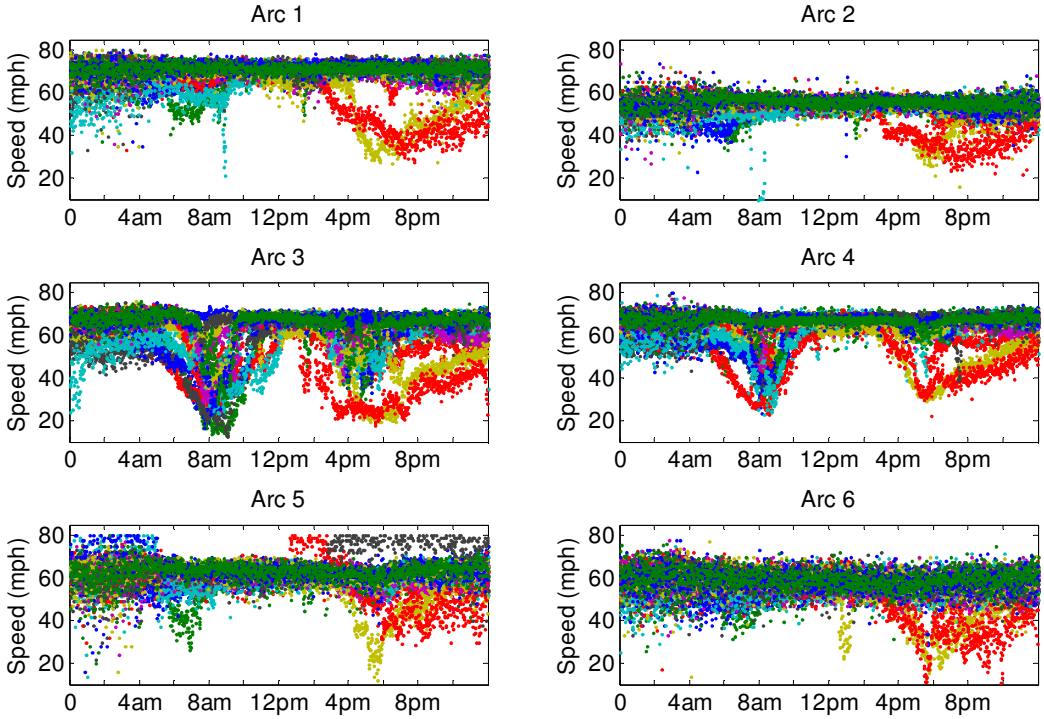

Figure 3. Raw Traffic Speeds for Arcs on Sub-Network (mph) at Different Times of the Day

(Data: Weekday traffic from January 21 to February 20. Each color represents a distinct day of 23 days)

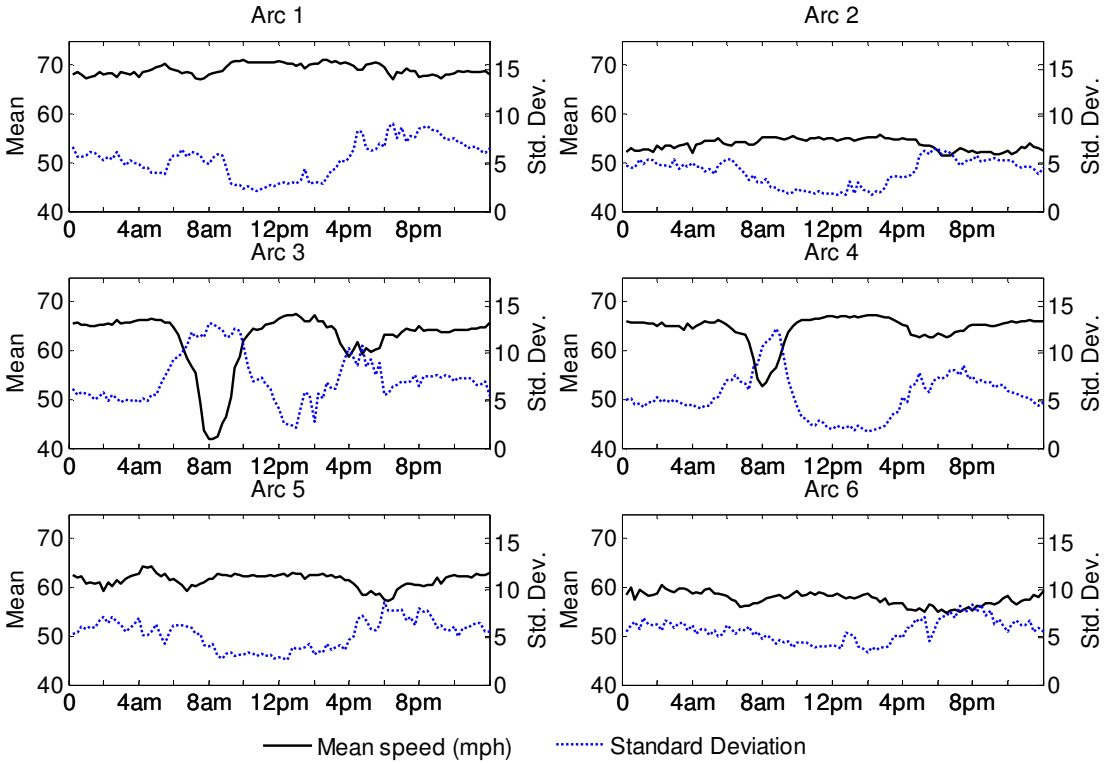

Figure 4. Traffic Mean Speeds (mph) and Standard Deviations by Time of the Day for Arcs on Sub-Network. (15 minute time interval resolution)

9.2 Recurrent Congestion Modeling

The proposed dynamic routing algorithm calls for identification of different congestion states and estimation of their state transition rates as well as arc traverse times by time of day. Given the traffic speed data from the MITS Center, we employed the Gaussian Mixture Model (GMM) clustering technique to determine the number of recurrent-congestion states for each arc by time of day. In particular, we employed the greedy learning GMM clustering method of Verbeek [48] for its computational efficiency and performance. To estimate the number of congestion states, traffic speed data from every pair of two consecutive time periods, t and t+1, are clustered and modeled using a bi-variate joint Gaussian distribution ($\boldsymbol{\mu}^{i}_{t,t+1};\boldsymbol{\Sigma}^{i}_{t,t+1}$), where i denotes the i^{th} cluster. The Gaussian distribution assumption has been employed by others in the literature (see Kim et al. [23]). The clusters are ordered by their means and the densities of their projections onto the two axes are employed to identify the congestion state speed intervals, as illustrated in Figure 5. Formally, the cut-off speed between congestion state-pair $(i,i+1)$ for arc a at time t is denoted by $c^{i}_{a}(t)$ and is calculated as follows: $c^{i}_{a}(t)=x, x: f_{i_t}(x)=f_{(i+1)_t}(x)$ where $f(\cdot)$ is the projected probability density function for state i. Unlike most clustering methods, the GMM clustering procedure employed does not call for specification of number of clusters (i.e., congestion states) in advance and can determine the optimal number of clusters based on the maximum likelihood and model complexity measures.

However, we did limit the number of clusters to two, considered quite adequate for modeling recurrent-congestion, and to limit estimation errors attributable to data scarcity. As expected, the GMM procedure generally yielded mostly two states, even without the constraint, as in Figure 5 (resulting in states denoted 'congested' and 'uncongested' states with $c_1^1(8{:}30)$= 64.9 mph), and rarely a single state during periods of low traffic (as in Figure 6). Following these observations, we have adopted two congestion states in representing arc congestion dynamics. Note that this does not compromise from the accuracy of congestion modeling, rather provides uniformity in the algorithmic data structures across all arcs in the network.

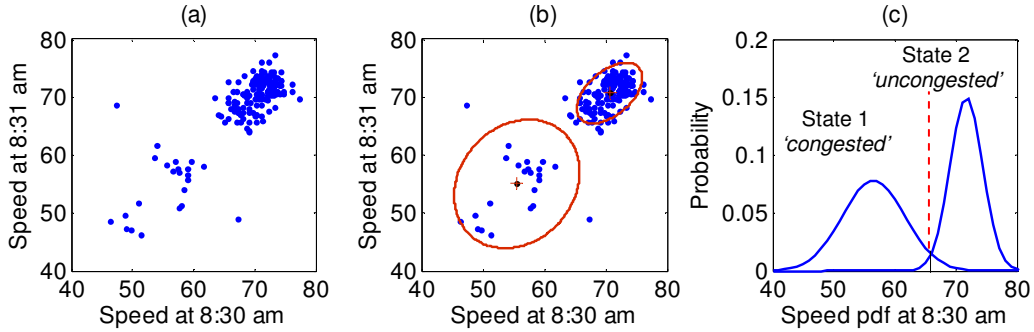

Figure 5. (a) Joint Plots of Traffic Speeds in Consecutive Periods for Modeling State-Transitions at 8:30 am, for Arc 1; (b) Cluster Joint Distributions of Speed at 8:30 am Generated by GMM; (c) Partitioned Traffic States Based on Projections

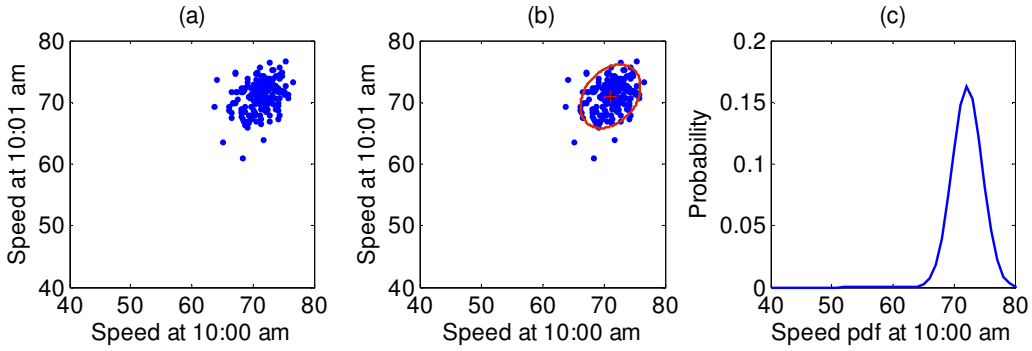

Figure 6. (a) Joint Plots of Traffic Speeds in Consecutive Periods for Modeling State-Transitions at 10:00 am, for Arc 1; (b) Single Cluster Joint Distribution of Speed at 10:00 am Generated by GMM; (c) Partitioned Traffic States Based on Projections

The parameters of the traffic state joint Gaussian distributions (i.e., $\boldsymbol{\mu}_{t,t+1}^{i};\boldsymbol{\Sigma}_{t,t+1}^{i}$) along with the computed cut-off speeds (if GMM yields more than one state) are employed to calculate travel time distribution parameters and the transition matrix elements as explained in section 3. In the event that two states are identified by GMM, α_t denotes the probability of state transition from congested state to congested state where as β_t denotes the probability of state transition from uncongested state to uncongested state.

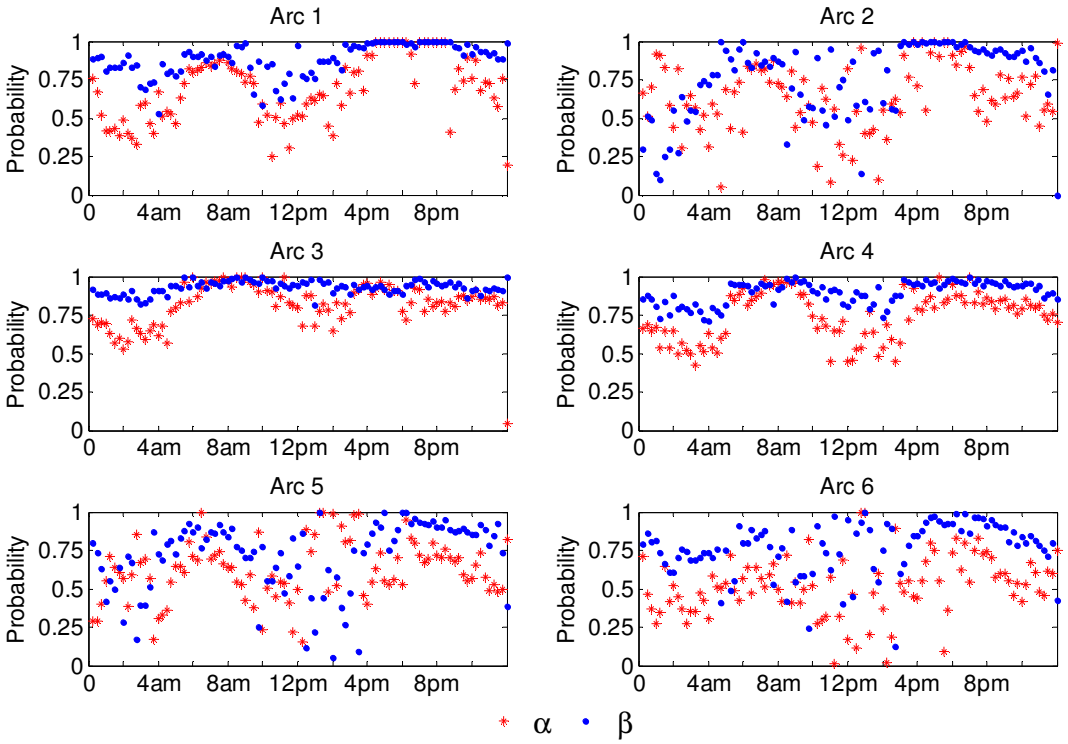

Figure 7. Recurrent Congestion State-Transition Probabilities for Arcs on Sub-Network. α: Congested to Congested Transition; β: Uncongested to Uncongested Transition Probability (Plotted with 15-minute time interval resolution)

Figure 7 plots these transition rates for the different arcs of the sub-network. Note that the state transitions to same states (i.e., congested to congested or uncongested to uncongested) are more likely during peak demand time periods, which increase the value of the congestion state information, and is the case in practice. For the sub-network, the mean and standard deviation of arc travel times are illustrated in Figure 8 and Figure 9, respectively, by traffic state and time of day.

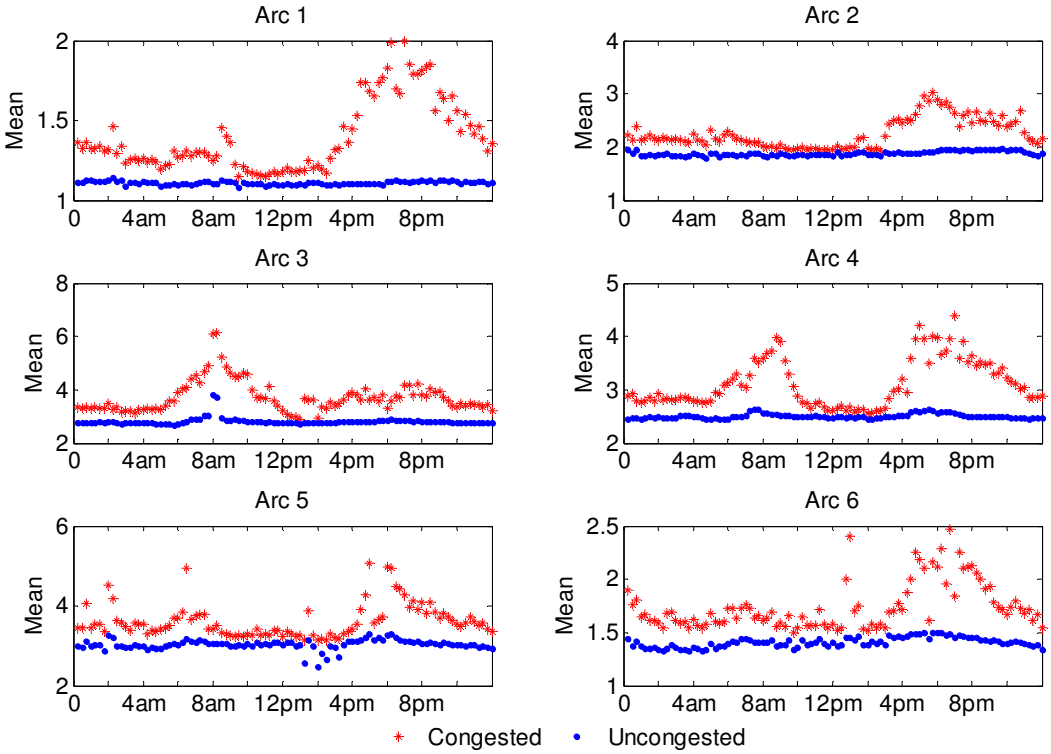

Figure 8. Sub-Network Arc Travel Time Means in Minutes (Plotted with 15-minute time interval resolution)

9.3 Results from Modeling Recurrent Congestion

This section highlights the potential savings from explicit modeling of recurrent congestion during dynamic vehicle routing. First, we discuss the results for routing on the *sub-network*. As stated earlier, we consider *node 4* as the origin node and *node 6* as the destination node of the trip. Three different path options exist (*path 1: 4-5-6; path 2: 4-5-26-6;* and *path 3: 4-30-26-6*). Note that our aim is not to identify an optimal path, rather, to identify the best policy based on the time of the day, location of the vehicle, and the traffic state of the network (for paths can be sub-optimal under non-stationary networks). However, in practice, almost all commercial logistics software aim to identify a robust (static) path that is best on the average. In this context, given the traffic flow histories for the arcs of the sub-network, *path1: 4-5-6* would be most robust, for it dominates other paths most of the day under all network states. Hence, we identify *path 1* as the *baseline path* and show the savings from using the proposed dynamic routing algorithm with regard to baseline path. Since we limit the traffic state look ahead to only successor and post-successor arcs, there are five arc states to be considered at the starting node of the trip. This implies that there are 2^5=32 starting network traffic state combinations.

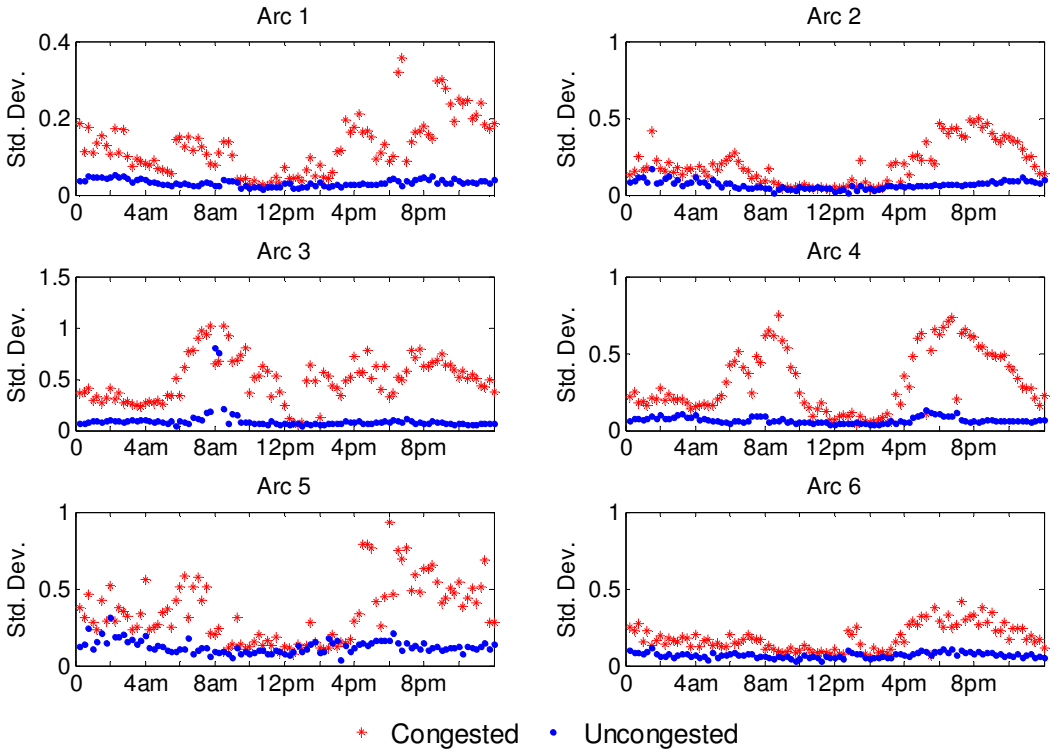

Figure 9. Sub-Network Arc Travel Time Standard Deviations in Minutes (Plotted with 15-minute time interval resolution)

We simulated the trip 10,000 times for each of these starting network traffic state combinations throughout the day for 15-minute interval starting times (yielding (24×60)/15=96 trip start times). Figure 10a plots the mean baseline path travel times over 10,000 simulation runs for every combination of the sub-network traffic state (all 32 of them) and Figure 10b plots the mean travel times for the dynamic policy.

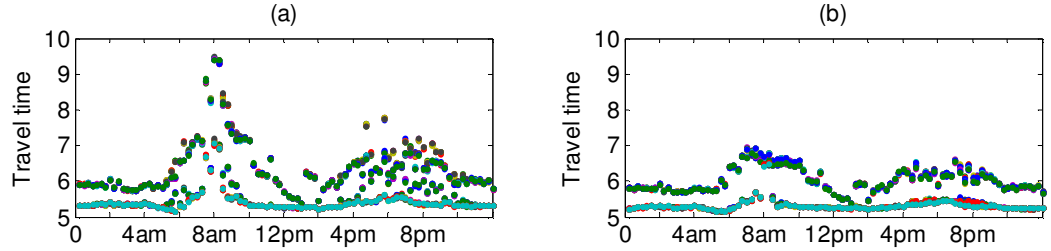

Figure 10. Mean travel times for all state combinations of the sub-network (each color represents a different state combination): (a) Baseline path. (b) Dynamic vehicle routing policy

Figure 11(a) plots the corresponding percentage savings from employing the dynamic vehicle routing policy over the baseline path for each network traffic state combination and Figure 11b shows the average savings (averaged across all network traffic states, treating them equally likely). It is clear that savings are higher and rather significant during peak traffic times and lower when there is not much congestion, as can be expected.

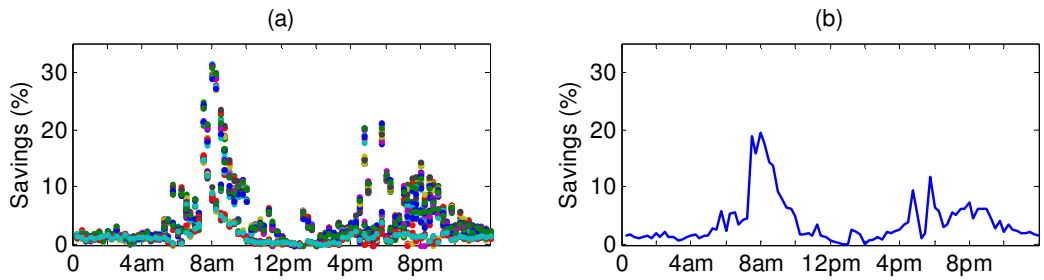

Figure 11. Savings from employing dynamic vehicle routing policy over baseline path: (a) Savings for each of the 32 network state combinations (b) Average savings across all state combinations

Besides the sub-network (Figure 2b), as listed in Table 2, we have also identified 5 other origin and destination (OD) pairs in the southeast Michigan road network (Figure 2a) to investigate the potential savings from using real-time traffic information under a dynamic routing policy. Unlike the *sub-network*, these OD pairs have both observed and unobserved arcs and each OD pair has several alternative paths from origin node to destination node.

Table 2 : Origin-Destination Pairs Selected from Southeast Michigan Road Network

	ORIGIN		DESTINATION	
OD Pair	Node #	Description (Intersection of)	Node #	Description (Intersection of)
1	2	I-75 & US-24	21	I-275 & I-94
2	12	I-96 & I-696	25	I-96 & I-94
3	19	M-5 & US-24	27	I-696 & I-94
4	23	I-94 & M-39	13	I-96 & I-275
5	3	I-75 & I-696	15	I-96 & M-39

Once again, we identify the *baseline path* for each OD pair (as explained for the case of routing on the *sub-network*) and show percentage savings in mean travel times (over 10,000 runs) over the baseline paths from using the dynamic routing policy. Figure 12 plots the percentage savings for each network traffic state combination and Figure 13 shows the average savings (averaged across all network traffic states, treating them equally likely). The savings are consistent with results from the *sub-network*, somewhat validating the sub-network results, with higher savings once again during peak traffic times.

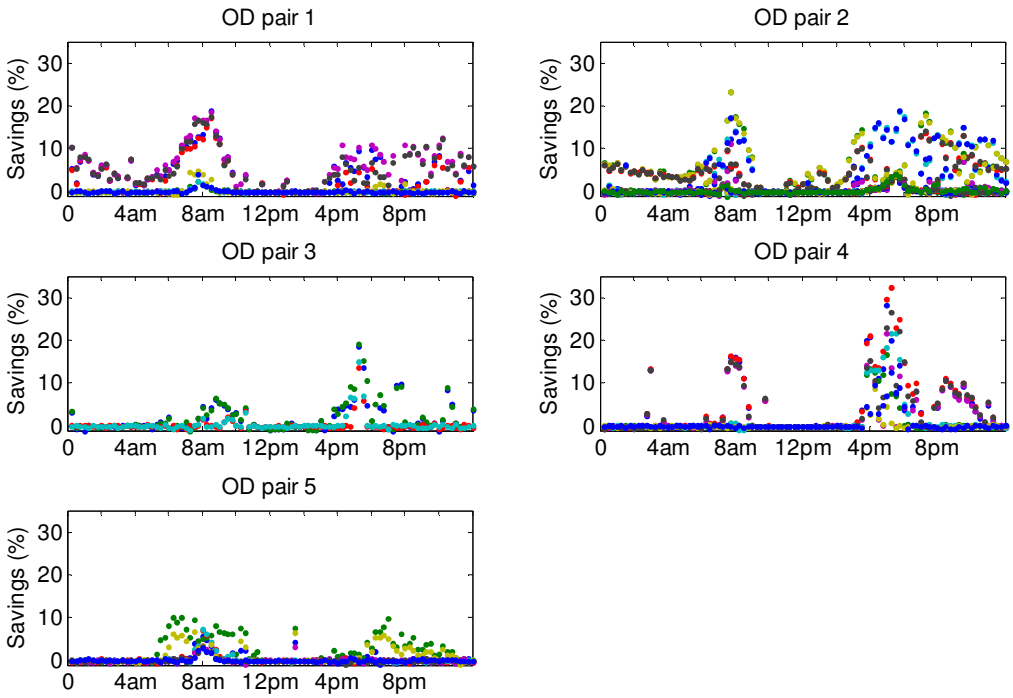

Figure 12. Savings of Dynamic Policy Over Baseline Path During the Day for All Starting States of Given OD Pairs (with 15-minute time interval resolution)

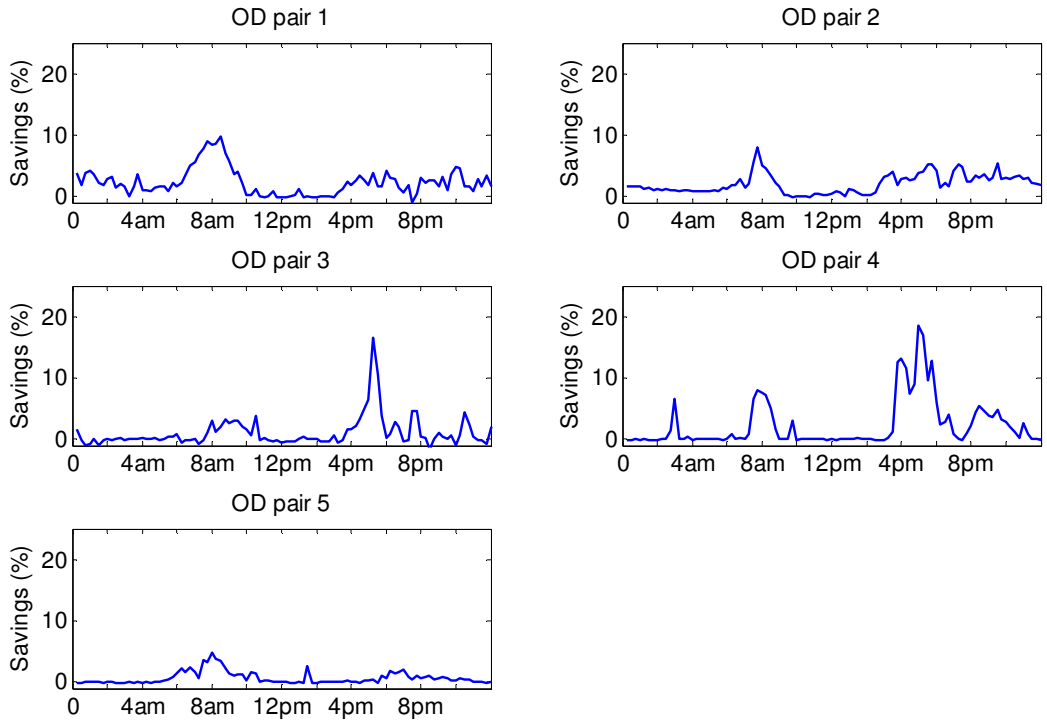

Figure 13. Average Savings of Dynamic Policy Over Baseline Path During the Day for All starting states of given OD pairs (with 15-minute time interval resolution)

9.4. Impact of Modeling Incidents

This section highlights the potential savings from explicit modeling of non-recurrent congestion along with modeling of recurrent congestion during dynamic vehicle routing. As for the setting, we focus on the sub-network (Figure 2b). We derive the dynamic routing policies in two ways. Initially, the dynamic policy does not account for non-recurrent congestion even though there is an incident in the network. Later, we allow the dynamic policy to explicitly account for non-recurrent congestion information to generate the optimal policy. We show the results for 6 starting times during the day (to study the impact of non-stationary traffic on savings): 6:30 am, 9:00 am, 10:30 am, 4:00 pm, 5:30 pm and 7:00 pm. To achieve a good comparison, we set all parameters of the incident to be the same for all starting times. We create an incident on either arc 3, or 4, or 6 with duration mean of 10 minutes and standard deviation of 5 minutes, following a Weibull distribution (scale parameter of 11 and a shape parameter of 2). We assume that all the arcs of the sub-network have a capacity of 1800 vehicles per hour (vph) under normal conditions and that the incident reduces their capacity to 1080 vph. Also, we assume in-flow traffic arrival rate for each arc to be 1500 vph during these operation times. We have also validated the assumption of no node waiting for incident arcs using the condition derived in Lemma 1.

The percentage savings from the explicit modeling of non-recurrent congesting along with recurrent congestion during dynamic vehicle routing are illustrated in Figure 14. The results are very compelling and pertain to three different scenarios. In the first scenario, the incident occurs 10 minutes before vehicle's departure from the starting node. In the second and third scenarios, the incident occurs 20 minutes and 30 minutes before vehicle's departure from the starting node, respectively. For example, if the vehicle departs the origin node at 6:30 am, incident is simulated to occur at 6:20 am or 6:10 am or 6:00 am, and incident has not yet been cleared in all three cases.

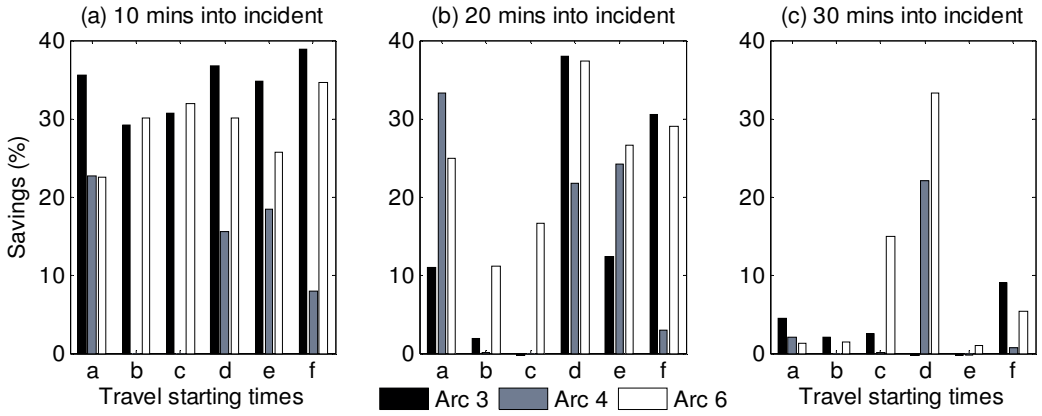

Figure 14. Savings realized by dynamic routing based on modeling both recurrent and non-recurrent congestion compared to the dynamic routing with only recurrent congestion modeling: a: 6:00, b: 7:30, c: 9:00, d: 16:00, e: 17:30, and f: 19:00. Incident is either on arc 3, or 4, or 6. Trip starts (a) 10 minutes (b) 20 minutes (c) 30 minutes after incident has occurred

The savings for the first scenario are presented in Figure 14a. Since arc 3 is close to the origin node, the effect of incident is generally high which leads to greater savings. Arc 4 is a downstream arc (i.e., it is not connected to the origin node), thus the incident is partially cleared by the time the vehicle reaches there. Subsequently, the impact of the incident on arc travel time and the savings are lesser. Arc 6 is also a downstream arc but the dynamic policy (without taking into account the non-recurrent congestion) sometimes chooses this arc, thus there are savings associated with explicit modeling of non-recurrent congestion. Due to space constraints, we are not presenting results from incidents on other arcs. The results for other arcs vary for similar reasons. The results for the second scenario (e.g., 20 minutes into the incident) are presented in Figure 14b. The savings for this scenario are less than the first scenario since the incident has partially or fully cleared by the time the vehicle reaches the incident arcs. Otherwise, we generally see consistency in savings with the first scenario. Figure 14c presents the results for the third scenario and savings for this scenario are mostly less than the other scenarios since the incident is more likely to be fully cleared by the time the vehicle reaches the incident arcs. To illustrate the results better, we also report the path distributions for the case where incident took place on arc 4 (because of space limits, we are not showing the other results). Figure 15a reports the path distribution of the dynamic policy in the absence of explicit modeling of non-recurrent congestion due to the incident that took place 10 minutes before trip start time. Figure 15b, c, and d report path distributions under explicit modeling of incidents and the resulting non-recurrent congestion, with trip start times of 10, 20, and 30 minutes into the incident, respectively. Since the incident is on path 1, there is no routing on path 1 for the case when trip starts just 10 minutes after the incident occurred (Figure 15b). As time passes, since the probability of incident clearance and no delay regime increases, dynamic routing policy starts to select this path as well (Figure 15d and d).

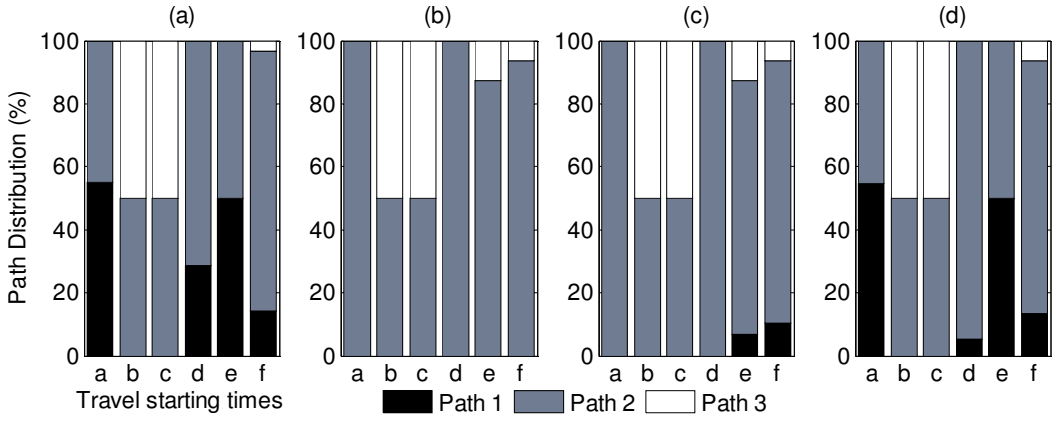

Figure 15. Path distribution from dynamic routing under an incident on arc 4 for different trip start times: a: 6:00, b: 7:30, c: 9:00, d: 16:00, e: 17:30, f: 19:00. (a) Results without modeling incident and trip starts 10 minutes into incident. (b), (c), and (d) report path distributions under explicit modeling of incidents, with trip start times of 10, 20, and 30 minutes into the incident, respectively

10. CONCLUSIONS

The paper proposes practical dynamic routing models that can effectively exploit real-time traffic information from Intelligent Transportation Systems (ITS) regarding recurrent congestion, and particularly, non-recurrent congestion stemming from incidents (e.g., accidents) in transportation networks. With the aid of this information and technologies, our models can help drivers avoid or mitigate trip delays by dynamically routing the vehicle from an origin to a destination in road networks. While non-recurrent congestion is known to be responsible for a major part of network congestion, extant literature mostly ignores this in proposing dynamic routing algorithms. We model the problem as a non-stationary stochastic shortest path problem with both recurrent and non-recurrent congestion. We propose effective data driven methods for accurate modeling and estimation of recurrent congestion states and their state transitions. A Markov decision process (MDP) formulation that generates a routing "policy" to select the best node to go next based on a "state" (vehicle location, time of day, and network congestion state) is proposed to solve the problem. While optimality is only guaranteed if we employ the full state of the transportation network to derive the policy, we recommend a limited look ahead approach to prevent exponential growth of the state space. The proposed model also estimates incident-induced arc travel time delay using a stochastic queuing model and uses that information for dynamic re-routing (rather than anticipate these low probability incidents).

ITS data from southeast Michigan road network, collected in collaboration with Michigan Intelligent Transportation System Center and Traffic.com, is used to illustrate the performance of the proposed models. Our experiments clearly illustrate the superior performance of the SDP derived dynamic routing policies when they accurately account for recurrent congestion (i.e., they differentiate between congested and uncongested traffic states) and non-recurrent congestion attributed to incidents. Experiments show that as the uncertainty (standard deviation) in the travel time information increases, the dynamic routing policy that takes real-time traffic information into account becomes increasingly superior to static path planning methods. The savings however depend on the network states as well as the time of day. The savings are higher during peak times and lower when traffic tends to be static (especially at night). Experiments also show that explicit treatment of non-recurrent congestion stemming from incidents can yield significant savings.

11. RECOMMENDATIONS FOR FURTHER RESEARCH

Further research will focus on developing dynamic routing algorithms for supporting 'milk-runs' where a vehicle departs from an origin to serve several destinations in a network with one or more of the following settings: 1) stochastic time-dependent network where vehicles may encounter recurrent and/or non-recurrent congestion during the trip, 2) vehicle must pickup/deliver within specific time-windows at customer locations, 3) stochastic dependencies and interactions between arcs' congestion states, and 4) anticipate and respond to the behavior of the rest of the traffic to the real-time ITS information.

12. RECOMMENDATIONS FOR IMPLEMENTATION

The research identified a number of recommendations for implementation to help leverage the full potential of dynamic routing of freight vehicles using real-time ITS information.

- Implementation mechanisms for ensuring data quality. Recommendations include collecting and sharing up-to-date sensor maintenance and placement information in the implementation network. This allows the users of the models and algorithms developed to revise their estimates of the travel times as well as traffic behavior under incident conditions. While the majority of the arteries do not have sensors, we found that some of the sensors in major highways are inactive. The absence of these sensors on the large segments of highways creates quality problems associated with distribution estimations for travel times as well as state transitions. In addition, the data collected from the some of the sensors are found to be inaccurate, e.g. inconsistent speed data, which may be attributable to weather, sensor's health state, and communication network inefficiencies. Recommendations for the missing sensor information or inaccurate data captures include benchmarking the traffic condition on the network segments devoid of sensors with those having sensors and reconciling and using a linear regression estimation of the speed data at any given time between adjacent sensors on a highway segment.

- The routing policies derived in this research are for point-to-point routing of the freight carrying vehicle. In most JIT systems this routing is performed in the form of milk run pickups and deliveries. Implementation recommendation for milk runs is to enumerate the potential order of customer visits and then using the historical congestion state probabilities for links emanating from each customer node visited.

- The off-line routing policy generation is impractical given the large number of links and incident state possibilities. Recommendation for implementation is to communicate the route actions (which road network link to select next) to the driver through a wireless connection (e.g., satellite) in real time. The identification of the real-time routing decisions is achieved through a centralized dynamic routing decision support system implementing the models and algorithms developed in this research. The decision support system is recommended to extract the real-time traffic congestion information from the ITS server. When the server is down or there are communication problems, the default operating mode for the decision support system is to assume the long-term congestion state probabilities. Figure 16 illustrates the recommended framework for data communication and decision support integration.

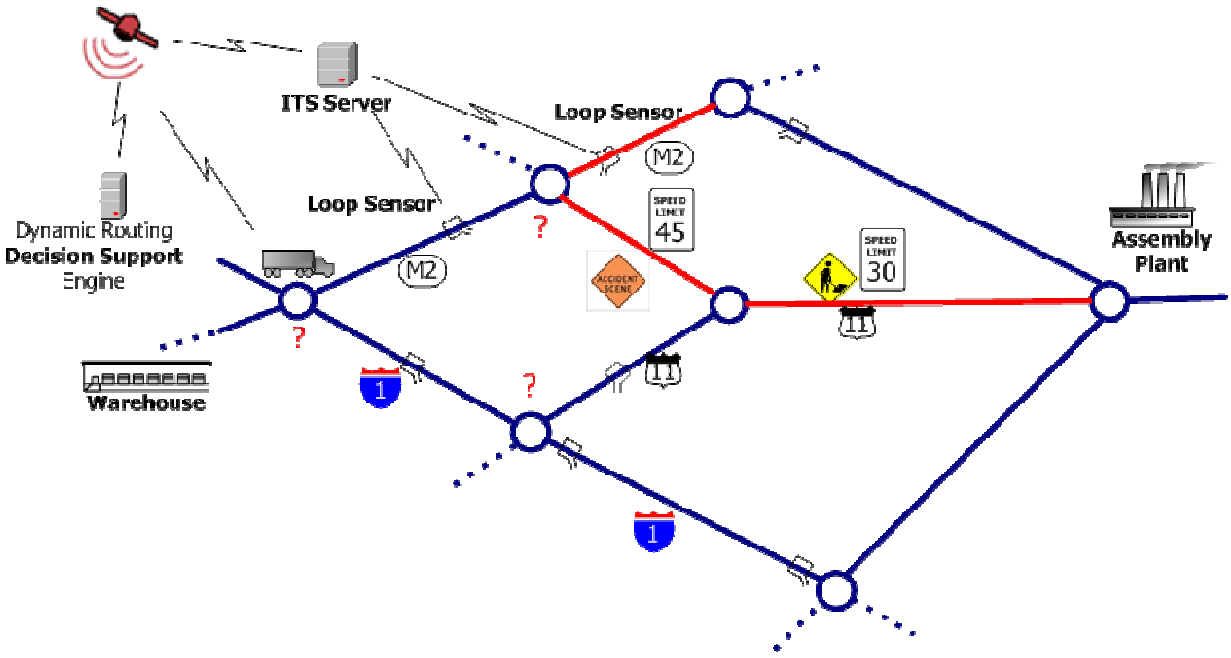

Figure 16. Recommended Framework for Data Communication and Decision Support Integration

13. BIBLIOGRAPHY

[1] Chang T-S, Wan Y-W, OOI WT. A stochastic dynamic traveling salesman problem with hard time windows. European Journal of Operational Research 2009;198(3):748-59.

[2] Taniguchi E, Thompson RG, Yamada T, Duin JHR. City logistics: Network modelling and Intelligent Transportation Systems. Pergamon: Elsevier Science; 2001.

[3] Schrank D, Lomax T. The 2007 annual urban mobility report. Urban Mobility Information: Texas Transportation Institute; 2007.

[4] Texas Transportation Institute, Cambridge Systematics Inc. Monitoring Urban Freeways in 2003: Current conditions and trends from archived operations data. Washington, DC: US FHWA Office of Operations; 2004.

[5] Cambridge Systematics Inc., Texas Transportation Institute. Traffic congestion and reliability: Linking solutions to problems. Washington, D.C: US FHWA Office of Operations; 2004.

[6] Sigal CE, Pritsker AAB, Solberg JJ. The stochastic shortest route problem. Operations Research 1980;28:1122-9.

[7] Frank H. Shortest paths in probabilistic graphs. Journal of Operational Research 1969;17:583-99.

[8] Loui RP. Optimal paths in graphs with stochastic or multidimensional weights. Communications of the ACM 1983;26(9):670-6.

[9] Eiger AP, Mirchandani P, Soroush H. Path preferences and optimal paths in probabilistic networks. Transportation Science 1985;19:75–84.

[10] Dijkstra E. A note on two problems in connection with graphs. Numerical Mathematics 1959;1:269-71.

[11] Hall R. The fastest path through a network with random time-dependent travel time. Transportation Science 1986;20(3):182-8.

[12] Bertsekas DP, Tsitsiklis J. An analysis of stochastic shortest path problems. Mathematics of Operations Research 1991;16:580-95.

[13] Fu L, Rilett LR. Expected shortest paths in dynamic and stochastic traffic networks. Transportation Research Part B 1998;32B(7):499-516.

[14] Bander JL, White III CC. A heuristic search approach for a nonstationary shortest path problem with terminal costs. Transportation Science 2002;36:218-30.

[15] Fu L. An adaptive routing algorithm for in vehicle route guidance systems with real-time information. Transportation Research Part B 2001;35B(8):749-65.

[16] Waller ST, Ziliaskopoulos AK. On the online shortest path problem with limited arc cost dependencies. Networks 2002;40 (4):216-27.

[17] Gao S, Chabini I. Optimal routing policy problems in stochastic time-dependent networks. Transportation Research Part B 2006;40B:93-122.

[18] Miller-Hooks ED, Mahmassani HS. Least possible time paths in stochastic, time-varying networks. Computers & Operations Research 1998;12:1107-25.

[19] Miller-Hooks ED, Mahmassani HS. Least expected time paths in stochastic, time-varying transportation networks. Transportation Science 2000;34 198-215.

[20] Psaraftis HN, Tsitsiklis JN. Dynamic shortest paths in acyclic networks with Markovian arc costs. Operations Research 1993;41:91-101.

[21] Polychronopoulos GH, Tsitsiklis JN. Stochastic shortest path problems with recourse. Networks 1996;27(2):133-43.

[22] Azaron A, Kianfar F. Dynamic shortest path in stochastic dynamic networks: Ship routing problem. European Journal of Operational Research 2003;144:138-56.
[23] Kim S, Lewis ME, White III CC. Optimal vehicle routing with real-time traffic information. IEEE Transactions on Intelligent Transportation Systems 2005;6(2):178-88.
[24] Kim S, Lewis ME, White III CC. State space reduction for non-stationary stochastic shortest path problems with real-time traffic congestion information. IEEE Transactions on Intelligent Transportation Systems 2005;6(3):273-84.
[25] Wirasinghe SC. Determination of traffic delays from shock-wave analysis. Transportation Research 1978;12:343-8.
[26] Al-Deek H, Garib A, Radwan AE. New method for estimating freeway incident congestion. Transportation Research Record 1995;1494:30-9.
[27] Mongeot H, Lesort JB. Analytical expressions of incident-induced flow dynamics perturbations. Transportation Research Record 2000;1710:58-68.
[28] Morales J. Analytical procedures for estimating freeway traffic congestion. Public Roads 1986;50(2):55-61.
[29] Fu L, Rilett LR. Real-time estimation of incident delay in dynamic and stochastic networks. Transportation Research Record 1997;1603:99-105.
[30] Cohen H, Southworth F. On the measurement and valuation of travel time variability due to incidents on freeways. Journal of Transportation And Statistics 1999;2(2):123-31.
[31] HCM. Highway Capacity Manual. Washington, D.C.: Transportation Research Board; 2000.
[32] Li J, Lan C-J, Gu X. Estimation of incident delay and its uncertainty on freeway networks. Transportation Research Record 2006;1959:37-45.
[33] Baykal-Gürsoy M, Xiao W, Ozbay K. Modeling traffic flow interrupted by incidents. European Journal of Operational Research 2008, In Press.
[34] Lindley JA. Urban freeway congestion: quantification of the problem and effectiveness of potential solutions. Institute of Transportation Engineers Journal 1987;57(1):27-32.
[35] Garib A, Radwan AE, Al-Deek H. Estimating magnitude and duration of incident delays. ASCE Journal of Transportation Engineering 1997;123(6):459-66.
[36] Sullivan EC. New model for predicting incidents and incident delay. ASCE Journal of Transportation Engineering 1997;123(5):267-75.
[37] Gaver DP. Highway delays resulting from flow stopping conditions. Journal of Applied Probability 1969;6:137-53.
[38] Golob TF, Recker WW, Leonard JD. An analysis of the severity and incident duration of truck-involved freeway accidents. Accident Analysis & Prevention 1987;19(4):375-95.
[39] Giuliano G. Incident characteristics, frequency, and duration on a high volume urban freeway. Transportation Research Part A 1989;23A(5):387-96.
[40] Khattak AJ, Schofer JL, Wang M-H. A simple time sequential procedure for predicting freeway incident duration. IVHS Journal 1995;2(2):113-38.
[41] Noland RB, Polak JW. Travel time variability: A review of theoretical and empirical issues. Transport Reviews 2002;22(1):39-54.
[42] Hensher D, Mannering F. Hazard-based duration models and their application to transport analysis. Transport Reviews 1994;14:63-82.
[43] Nam D, Mannering F. An exploratory hazard-based analysis of highway incident duration. Transportation Research Part A 2000;34A(2):85-102.

[44] Ferris MC, Ruszczynski A. Robust path choice in networks with failures. Networks 2000;35:181-94.
[45] Thomas BW, White III CC. The dynamic shortest path problem with anticipation. European Journal of Operational Research 2007;176:836-54.
[46] Bertsekas DP. Dynamic programming and optimal control. Athena Scientific; 2001.
[47] Ross SM. Introduction to Probability Models. Academic Press, Inc.; 2006.
[48] Verbeek JJ, Vlassis N, Kröse B. Efficient greedy learning of Gaussian Mixture Models. Neural Computation 2003;5(2):469-85.

14. LIST OF ACRONYMS

ADP	Adaptive Decision Policy
ATIS	Advanced Traveler Information Systems
DP	Dynamic Programming
GMM	Gaussian mixture model
GPS	Global Positioning System
ITS	Intelligent Transportation Systems
JIT	Just-in-Time
LET	Least Expected Travel
MDOT	Michigan Department of Transportation
MDP	Markov decision process
MITS	Michigan Intelligent Transportation System Center
MITS	Michigan Intelligent Transportations Systems
OD	Origin and Destination
OEM	Original equipment manufacturers
SDP	Stochastic Dynamic Programming
SP	Shortest Path
STD-SP	Stochastic Time-Dependent Shortest Path
vph	Vehicle per hour

MICHIGAN OHIO UNIVERSITY TRANSPORTATION CENTER
Alternate energy and system mobility to stimulate economic development.

Report No: MIOH UTC TS1p2-3 2008-Final
MDOT Report No: RC1545

CONGESTION RELIEF BY TRAVEL TIME MINIMIZATION IN NEAR REAL TIME

—----

DETROIT AREA I-75 CORRIDOR STUDY

FINAL REPORT

PROJECT TEAM

Dr. Charles Standridge
Dr. Shabbir Choudhuri
Andrew Even
Jason Gallivan
Ashfaq Rahman
Vishnu Yada
School of Engineering

Dr. David Zeitler
Andrew Van Garderen
Allison Wehr
Department of Statistics
Grand Valley State University
301 West Fulton
Grand Rapids, MI 49504

With Contributions By
Dr. Snehamay Khasnabis
S. Mishra
A. Manori
S. Swain
College of Engineering
Wayne State University
2168 Engineering Building
Detroit, MI 48202

Report No: MIOH UTC TS1p2-3 2008-Final

TS 1, Series, Projects 2 & 3, December, 2008
FINAL REPORT

Developed By:

Charles R. Standridge
Principal Investigator, GVSU
standric@gvsu.edu
616-331-6759

Shabbir Choudhuri
Investigator, GVSU
choudhus@gvsu.edu
616-331-6845

With Contributions By:

Snehamay Khasnabis
WSU
skhas@wayne.edu
313-577-3915

SPONSORS

This is a Michigan Ohio University Transportation Center project supported by the U.S. Department of Transportation, the Michigan Department of Transportation, Grand Valley State University, and Wayne State University.

ACKNOWLEDGEMENT

The Project Team would like to acknowledge support from the Michigan Department of Transportation (MDOT), the Michigan Intelligent Transportation System Center (MITSC), and the Southeastern Michigan Council of Governments (SEMCOG) during the course of this research.

DISCLAIMERS

Technical Report Documentation Page

1. Report No. RC-1545	2. Government Accession No.	3. MDOT Project Manager Niles Annelin
4. Title and Subtitle Michigan Ohio University Transportation Center Subtitle: "Congestion Relief by Travel Time Minimization in Near Real Time – Detroit Area I-75 Corridor Study"		5. Report Date December 2008 6. Performing Organization Code
7. Author(s) Dr. Charles R. Standridge, Grand Valley State University Dr. Shabbir Choudhuri, Grand Valley State University Dr. David Zeitler, Grand Valley State University Dr. Snehamay Khasnabis, Wayne State University		8. Performing Org. Report No. MIOH UTC TS1p2-3 2008-Final
9. Performing Organization Name and Address Michigan Ohio University Transportation Center University of Detroit Mercy, Detroit, MI 48221 and Grand Valley State University, Grand Rapids, MI 49504 and Wayne State University, Detroit, MI 48202		10. Work Unit No. (TRAIS) 11. Contract No. 2007-0538 11(a). Authorization No.
12. Sponsoring Agency Name and Address Michigan Department of Transportation Van Wagoner Building, 425 West Ottawa P. O. Box 30050, Lansing, Michigan 48909		13. Type of Report & Period Covered Research, May 2007 – December 2008 14. Sponsoring Agency Code
15. Supplementary Notes Additional Sponsors: US DOT Research & Innovative Technology Administration, Grand Valley State University, and Wayne State University.		
16. Abstract MIOH UTC TS1p2-3 2008-Final This project was motivated by the premise that congestion due to traffic accidents and other incidents can be avoided by using computer re-routing models combined with the analysis of voluminous data collected by intelligent transportation systems (ITS). Congestion avoidance reduces travel time and fuel consumption as well as the need for additional roadways and infrastructure, making the transportation system more efficient. The results of this project are targeted at ITS that seek to reduce congestion by better routing large volumes of traffic at a small time interval as opposed to personal travel assistants (PTAs) that route one vehicle at a time. One potential downside of rerouting large volumes of traffic in a small time interval is to simply move the congestion to a different place in the traffic corridor. This requirement is addressed.		
17. Key Words Intelligent transportation systems, Traffic flow, Time, Traffic data, Data collection, Transportation infrastructure, Traffic volume, Detroit (Michigan), Research projects.	18. Distribution Statement No restrictions. This document is available to the public through the Michigan Department of Transportation.	
19. Security Classification - report	20. Security Classification - page	21. No. of Pages 23 / 22. Price

Table of Contents

List of Figures

List of Tables

I. Overview

This document summarizes the activities concerning the project: Congestion Relief by Travel Time Minimization in Near Real Time -- Detroit Area I-75 Corridor Study since the inception of the project (Nov. 22, 2006 through September 30, 2008).

This project was motivated by the premise that congestion due to traffic accidents and other incidents can be avoided by using computer re-routing models combined with the analysis of voluminous data collected by intelligent transportation systems (ITS). Congestion avoidance reduces travel time and fuel consumption as well as the need for additional roadways and infrastructure, making the transportation system more efficient.

During the same time period as this project, personal travel assistants (PTAs) have become more and more common. This trend should continue until PTAs are ubiquitous. These devices are able to both access current commercial traffic data provided by companies such as traffic.com as well as to determine routes based on this data. Thus, the problem of routing individual vehicles appears to be solved and commercialized.

Several issues remain to be addressed:

1. How to route voluminous traffic around an incident that closes or reduces the capacity of a segment of a traffic corridor.
2. How to use the traffic data collected by an ITS to describe the flow of traffic.
3. How to forecast the speed of traffic on a traffic segment a short time from the current time.

Thus, the major and primary contribution of our project was established:

> *To describe, explain, and predict the flow of traffic in a corridor with respect to time and space as well as to apply these results in the routing of traffic.*

The results of this project are targeted at ITS that seek to reduce congestion by better routing large volumes of traffic at a small time interval as opposed to PTAs that route one vehicle at a time. One potential downside of rerouting large volumes of traffic in a small time interval is to simply move the congestion to a different place in the traffic corridor. This requirement is addressed.

The project was organized around three subprojects:

1. Statistical analysis of traffic data from the Michigan Intelligent Transportation Systems Center (MITSC) in Detroit for the purpose of describing, explaining and predicting the flow of traffic.
2. Computer-based models for re-routing large volumes of traffic around an incident with both software- and hardware-based solvers. These models can include statistical analysis results for predicting traffic flow.
3. Traffic simulation models for validating the results produced by the re-routing models.

Project highlights are summarized. The organization of the project is given. Technical progress is summarized for each of the three subprojects. The vision for the third year of the project, September 2008 through August 2009, is described.

II. Highlights

The major accomplishments of each subproject are summarized.

1. Collection and management of traffic data.
    a. Acquired archival data from MITSC center for the years 2000-2006 as well as establishing and implementing procedures for continuing to obtain data starting with January 2007. Currently, data is obtained via FTP transfer from MITSC to Grand Valley State University (GVSU) twice a month.
    b. Implemented a database management system (DBMS) in MySQL to properly organize and control the data.
        i. The volume of data is such that the initial database was limited to the I-75 corridor data for one year. This conclusion was reached after much trial and error.
        ii. Designed and implemented a user interface that supports data retrieval through SQL queries.
        iii. Traffic data: sensor occupancy, volume, and speed as well as sensor location data are stored in the database.
    c. Conducted, and are continuing to conduct, a descriptive statistics study of the MITSC data showing traffic patterns in time and space.
        i. The graphs show when and to what degree rush hour traffic volumes reduce speed for each I-75 southbound sensor for 30 days.
        ii. The graphs identify "non-routine" periods of volume increases and speed reductions perhaps correlated in time with a traffic incident or adverse weather conditions.
        iii. The graphs show that speed remains constant until volume reaches a particular threshold level.
        iv. The graph shows how traffic volumes dissipate in time and space, including how far-reaching the effect of a traffic incident is.
        v. The graphs provide the basis for proposing and testing formal explanatory and predictive statistical models.

2. Designed and implemented a traffic routing algorithm and alternative solvers for re-routing voluminous traffic around an incident in a corridor.
    a. We believe this algorithm to be unique, since existing routing algorithms are designed for routing a single vehicle and do not consider the consequences of re-routing a large number of vehicles in a relatively short span of time.
    b. The algorithm includes the idea that the selected route may change because of the volume of previously rerouted traffic. Thus, the route selected for current traffic may be different from the route selected for prior traffic. Thus, this is a dynamic routing algorithm.

c. The algorithm can consider multiple types of vehicles separately, such as cars and trucks.
d. The corridor is modeled in the usual way as a set of nodes and arcs. Each arc represents a segment of a highway, an arterial road, or a street. The metric associated with each arc is computed each time it is needed and may be a function of any variable: time, volume of traffic, arc capacity, type of vehicle and the like.
e. The M-131 / I-196 junction in downtown Grand Rapids was modeled and data available from the Grand Valley Metropolitan Council (GVMC) was employed. Routing effectiveness was evaluated by simulating traffic incidents on M-131 and I -96.
f. The traffic corridor surrounding southbound I-75 in Detroit was modeled and data available from Michigan Department of Transportation (MDOT) was employed. The model includes a traffic simulator to predict the volume increase in any arc due to re-routing. Analyses based on the model are ongoing.
g. Extension of the algorithm to include multiple simultaneous traffic incidents is ongoing.
h. Concepts for an analog, hardware-based solver for the dynamic traffic routing problem were developed and demonstrated using an eight-arc, seven-node traffic network. The solver instantaneously identifies the optimal route.
i. The development of a hardware solver for the model of the traffic corridor surrounding southbound I-75 in Detroit has been designed. Its implementation is ongoing.

3. An analytic framework for the calibration and application of a micro-simulation model, Advanced Interactive Microscopic Model for Urban and Non-urban Networks (AIMSUN), for validating the effectiveness of alternate incident management strategies (IMS) on an urban transportation network was developed.
    a. A conceptual framework was developed and demonstrated through the modeling of the I-75 corridor in Detroit area.
    b. This model was calibrated and its application demonstrated.
    c. Initial results are positive. Full-scale validation and testing with larger networks are ongoing.

4. Effective relationships with external constituents at MDOT, MITSC, Southeast Michigan Council of Governments (SEMCOG), the Grand Valley Metropolitan Council (GVMC), and Traffic.com have been made.

III. Project Organization

The project organization is shown in Table 1, with the three primary subprojects displayed. Current project staffing is indicated along with our external constituents.

Table 1: Project Organization

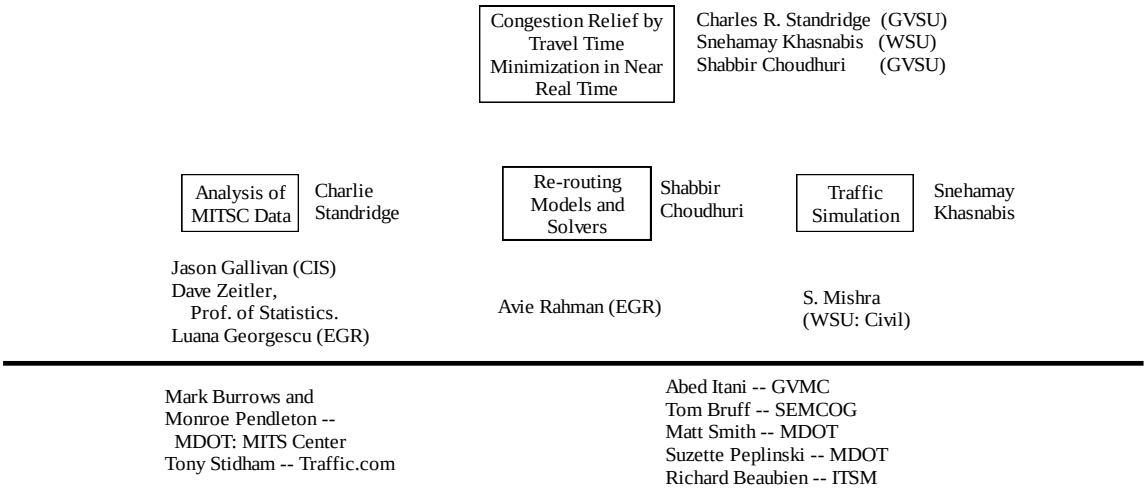

We have made contact and met with our external constituents representing the following organizations as shown in Table 1.

1. Grand Valley Metropolitan Council – Abed Itani, Transportation Director, and staff
2. Southeast Michigan Council of Governments – Tom Bruff and staff
3. Michigan Department of Transportation
    a. Michigan Intelligent Transportation Center Detroit – Monroe Pendleton
    b. Michigan Intelligent Transportation Center Grand Rapids – Suzette Peplinski and staff
    c. MDOT, Southfield Office – Matt Smith
4. Traffic.com – Tony Stidham
5. Intelligent Transportation Society of Michigan (ITS MI) – Richard Beaubien

Project activities have been supported by graduate assistants and undergraduate students as shown in Table 2. All students who have participated in the projects since their inception are shown.

Table 2: Student Participation

Student	Faculty Mentor	Department	Degree Program	Status on Project	When on Project
Vishnu Yada	Shabbir Choudhuri	GVSU, Computer Information Systems	Master of Science	20 hours weekly, Graduate Assistant	January – December 2007
Ashfaq Rahman	Shabbir Chouduri	GVSU, Engineering	Master of Science	20 hours weekly, Graduate Assistant	August 2007 – present
Andrew Even	Shabbir Chouduri	GVSU, Engineering	Master of Science	Capstone project, unpaid	January – December 2007
S. Mishra A. Manori S. Swain	Snehamay Khasnabis	WSU, Civil Engineering	Ph.D.	Hourly, Graduate Assistant	January 2007 – present September 2007-December 2007 February 2008-Present
Jason Gallivan	Charlie Standridge	GVSU, Computer Information Systems	Master of Science	20 hours weekly, Graduate Assistant	January 2007 – present
Andrew Van Garderen	Dave Zeitler	GVSU, Statistics Department	Bachelor of Science	Semester stipend	August 2007 – May 2008
Allison Wehr	Dave Zeitler	GVSU, Statistics Department	Bachelor of Science	Semester stipend	January – May 2008

IV. Technical Progress toward Objectives and Deliverables

IV.1. Analysis of MITSC Data

Objective: Developing and applying statistical methods for the analysis of ITS data, with application to the Detroit area I-75 corridor.

Deliverables: Methods and procedures for the statistical analysis of the MITSC data with application to the Detroit area I-75 corridor.

Analysis of the MITSC data requires its acquisition and management as well as the application of statistical analysis techniques.

Arrangements for acquiring the MITSC data were made with Monroe Pendleton and Mark Burrows of the MITSC staff. Data from 2000-2006 were obtained on CD-ROM. Starting in January 2007, data have been transferred from MITSC to GVSU twice monthly via FTP.

The MITSC data required significant preparation before use in statistical analysis. The data is organized in tabular form with each row representing one time for one sensor and columns containing occupancy, speed, and volume data. However, the data is recorded as a string that must be parsed to extract the data for subsequent use. Missing values must be taken into account. Invalid rows, identified by a year of 1969, are ignored. Data were grouped into minute intervals based on the hour-minute-second time stamp.

A custom pivot operation on the data was programmed in JAVA to create a table with each row representing a one-minute time interval and a set of occupancy-volume-speed columns for each sensor of interest. This was done to facilitate time-oriented statistical analysis of the data.

The database management system was implemented using MySQL, freeware that is commonly used both in academics and industry. One table was created for the traffic data and a second table for the list of sensor devices. A web based query system is found at: utc.egr.gvsu.edu. The query system supports any SQL query and has an interface for queries by sensor device and data range. Query results are placed in a .csv file.

Descriptive statistical modeling was done by generating graphs of the occupancy, volume and speed for each sensor using the R statistical programming environment. R is freeware. For southbound I-75, graphs showed patterns in the flow of traffic.

1. Speed seems to be function of volume. When the volume is below a threshold, speed is constant and slightly above the posted speed limit. When the volume is above the threshold, speed decreases as volume increases, potentially in a non-linear fashion.
2. Speed does not appear to be a function of sensor occupancy. Sensor occupancy can be seen to increase at times while speed remains constant.

3. Monday through Friday, morning rush hour is shown by large volume increases between 7:30 and 10:00 a.m. that result in a significant drop in speed. Evening rush hour is shown by a small change in volume that exceeds the threshold resulting in a small drop in speed.
4. Saturday and Sunday, volume and speed are approximately constant throughout the day.
5. Significant changes in volume at non-rush hour times indicated planned or unplanned disruptions such as traffic incidents or inclement whether.
6. There is significant sensor noise in the data, as seen by values that appear to be excessive compared to most values.
7. Throughput is not affected until a drop in speed is seen. Then throughput goes down.

Figure 1 is a graph showing data from Wednesday, Nov. 9, 2005 for one sensor.[1] This graph illustrates points 1, 2, 3, and 6 above.

Figure 2 is a graph showing data from Wednesday, Nov. 23, 2005, the day before Thanksgiving, for the same sensor as in Figure 2. This graph illustrates point 5. Note the smaller volume of traffic during the morning rush hour as well as the spike in traffic from about 4-6 p.m. that day. This could be explained by weather data showing about 2 inches of snow or perhaps many people were leaving work at the same time to prepare for the Thanksgiving holiday.

Graphs can be used to see how congestion changes in time and space. This is illustrated in Figures 3 and 4 that show occupancy, volume, and speed data from Wednesday, Nov. 23, 2005 for the sensor north of the one shown in Figure 2 (Figure 3) as well as the sensor south of the one shown in Figure 2 (Figure 4). Note the following:

1. The volume increase and speed decrease shown in Figure 2 occurs slightly later in Figure 3, indicating that time lag for traffic to backup to the north.
2. This volume increase is not seen in Figure 3, showing that traffic flow has returned to normal at this location.
3. The speed decrease shown in Figure 4 at about 12:00 p.m. is also seen in Figures 2 and 3.

For northbound I-75, graphs indicated that the sensors were not generating usable information. Note the occupancy graphs in Figure 5 where data from 12 sensors is displayed. Only two of the 12 sensors generate usable data.

[1] Our analysis shows that the date labels are determined as follows: Data is collected from 4:00 a.m. one day to 4:00 a.m. the next day for each file obtained from MITSC. The date label on the file is the date associated with the last item collected. Since the majority of data, including rush hours, are from the preceding day, the date labels appear to be off by one day.

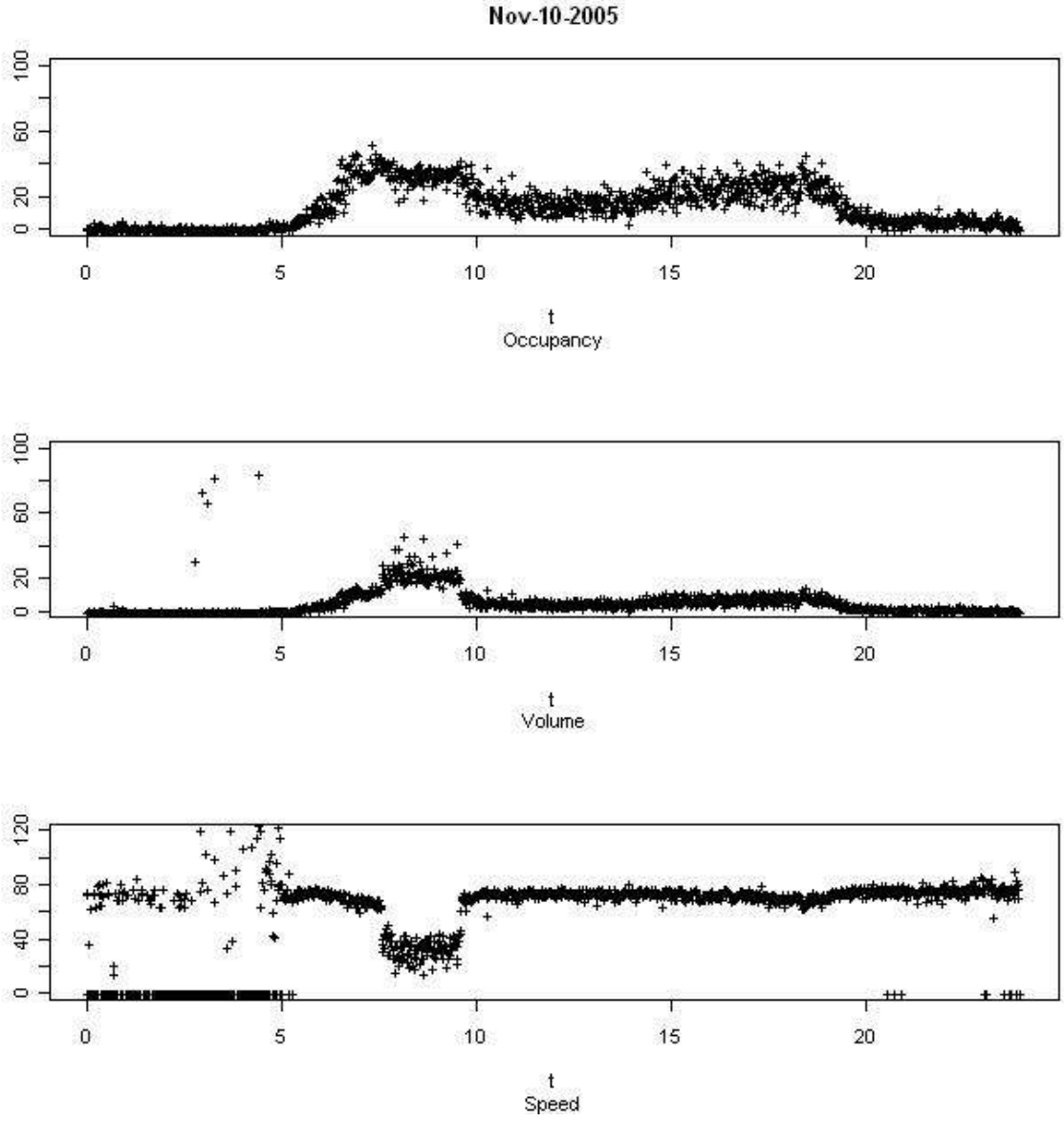

Figure 1. Occupancy, Volume, and Speed Data for Nov. 9, 2005

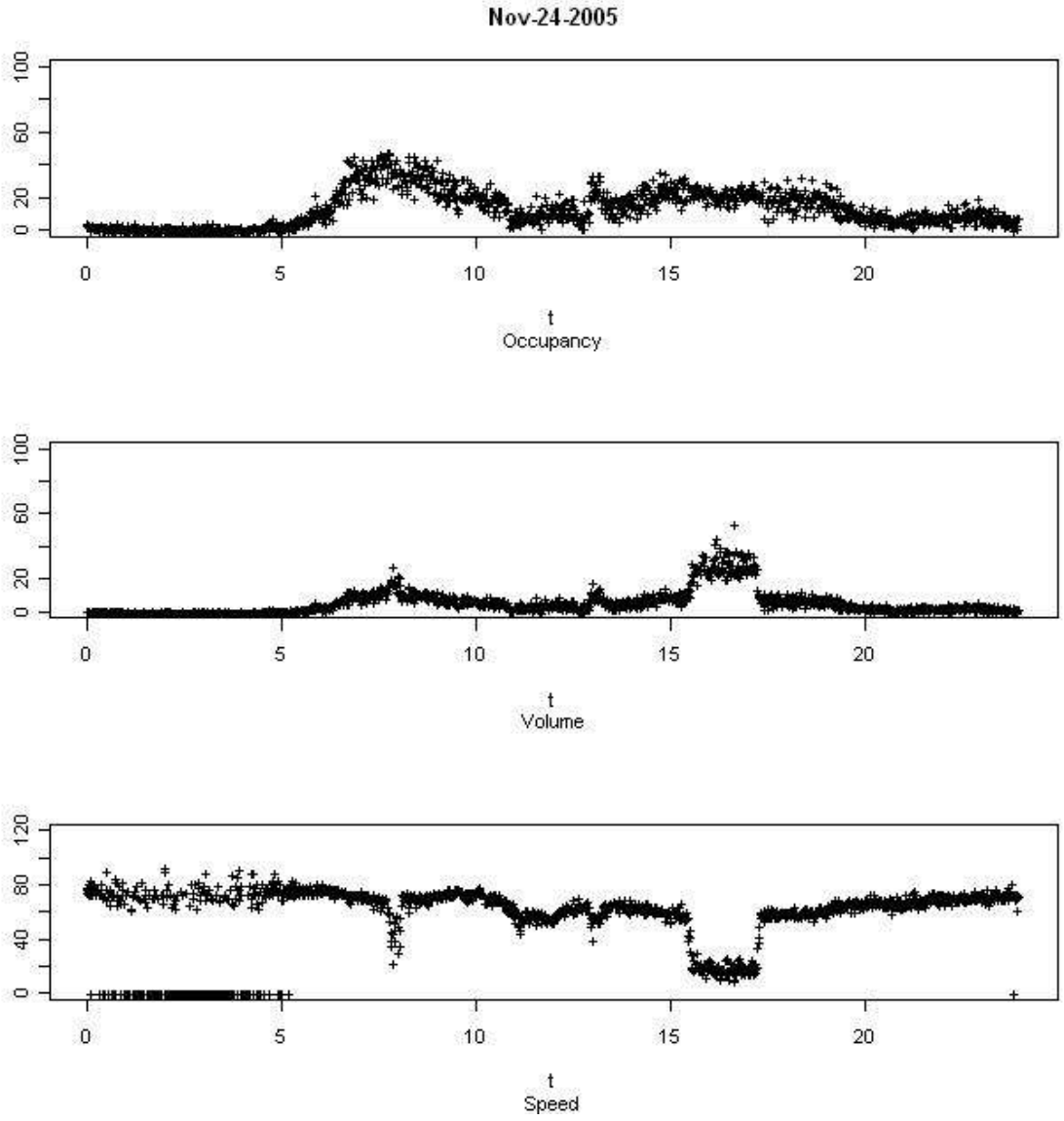

Figure 2. Occupancy, Volume, and Speed Data for Nov. 23, 2005

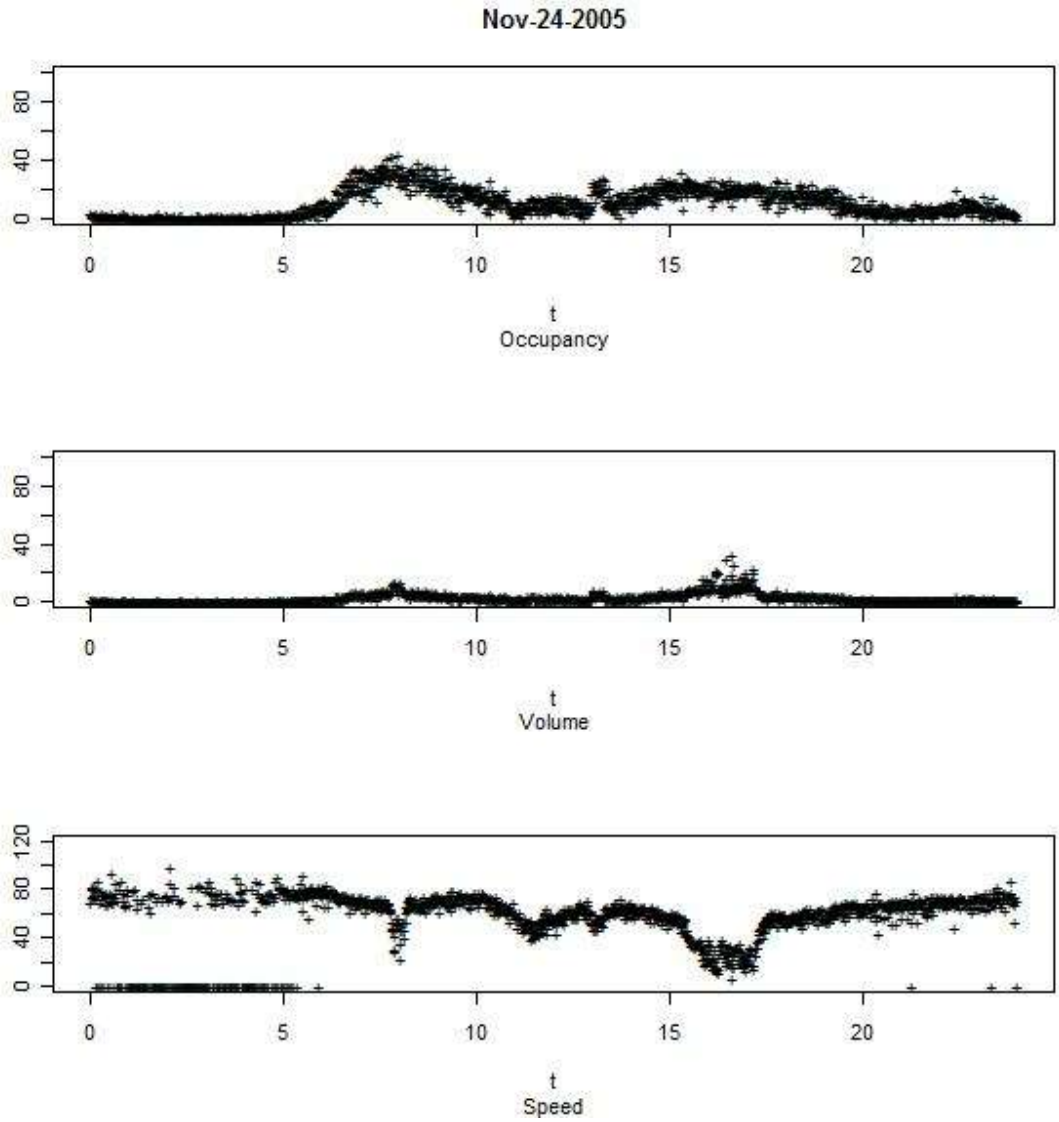

Figure 3. Occupancy, Volume, and Speed Data for Nov. 23, 2005 for the Sensor Northbound from the One in Figure 2.

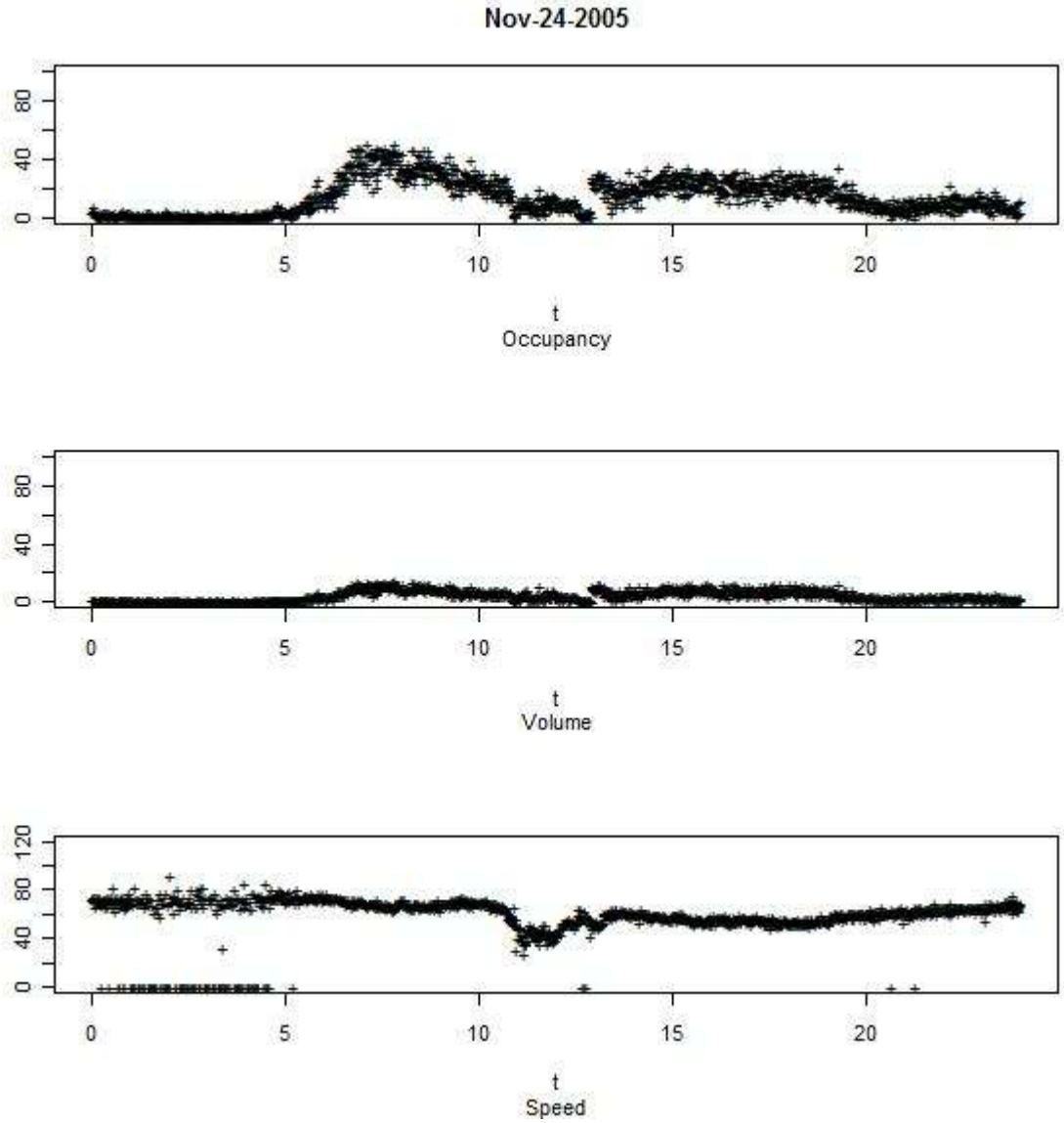

Figure 4. Occupancy, Volume, and Speed Data for Nov. 23, 2005 for the Sensor Southbound from the One in Figure 2.

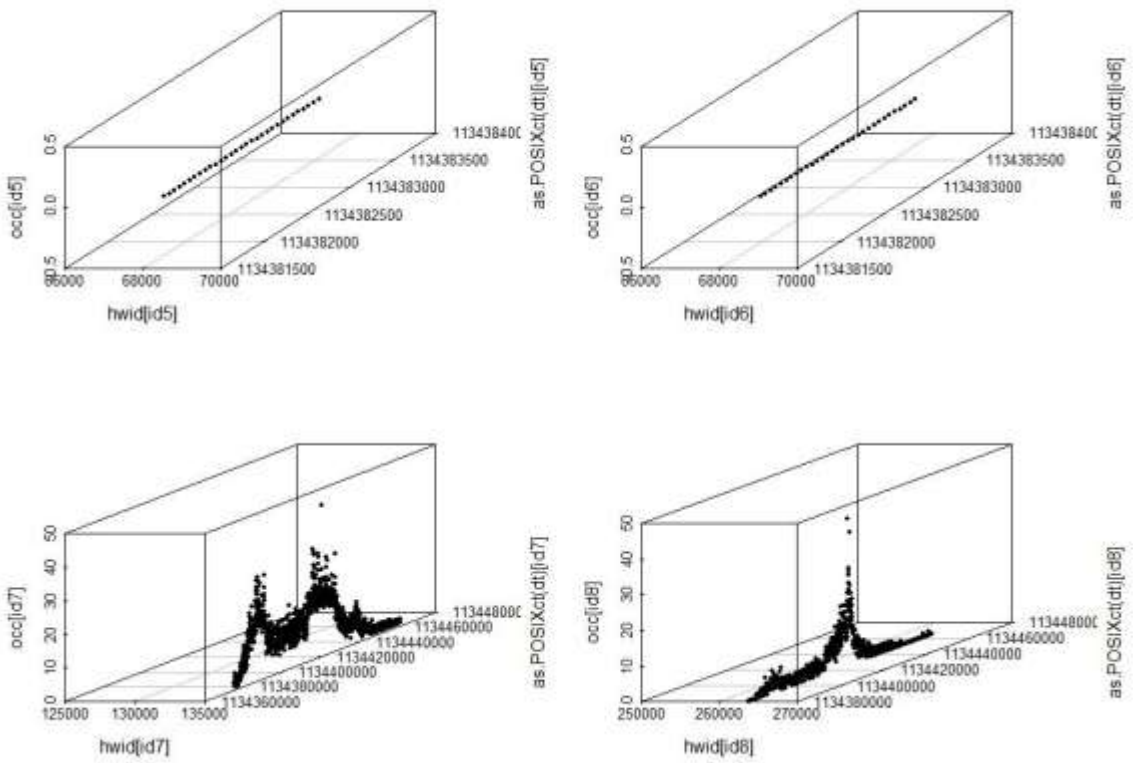

Figure 5. Occupancy Data for Northbound I-75 Graphs

IV.2. Rerouting Models and Solvers

Objective: Extension of the previously developed routing algorithm with application to the Detroit area I-75 corridor.

Deliverables: The improved algorithm with both a software- and a hardware-based solver, including a model of the Detroit area I-75 corridor.

During the first project year, a dynamic traffic rerouting algorithm around a disturbance in a freeway was developed. Based on the algorithm, test software was developed to model the M-131/I-196 junction in downtown Grand Rapids. The system was populated with the data available from GVMC. The dynamic routing capacity was evaluated by simulating interruptions on M-131 and I-96. (Even 2007; Even, Choudhuri, and Standridge 2007). The results revealed that for the similar incidences, the detour rout from M–131 changes more rapidly than that of I–196 to keep traffic moving in the surrounding network.

The algorithm takes into account that the same route may not be optimal for all routed vehicles. Vehicles may belong to different classes, such as cars and trucks. Not all classes may be allowed to use all routes. Over time, the previous rerouting of vehicles may cause the performance of a selected route to change. Thus, another route may be better. Thus, the algorithm must be dynamic.

The algorithm models a traffic corridor as a set of nodes and arcs. The metric associated with each arc may depend on a number of variables that can change in time: capacity that could be reduced due to a traffic incident, traffic volume, traffic speed and the like. The metric could depend on projections of such quantities at the time the vehicle is expected to arrive to the arc. Our algorithm allows this metric to be computed arbitrarily and for this computation to change over time.

In the current year, the traffic network shown in Figure 6, surrounding I-75 S in the Detroit metro area, was modeled. This is the same network considered in the traffic simulation discussed in the next section. The implementation also includes a simple traffic simulator to predict the volume increase in any arc of the traffic network due to rerouting.

Additional work on this model is currently ongoing including:

1. Obtaining the required input data from MDOT.
2. Analyzing I-75 south.
3. Investigating the effect of multiple simultaneous traffic incidents.

Figure 6. Map of the Detroit Area I-75 Corridor – Software Solver.

Results from the software-based rerouting algorithm showed that the best detour path, with respect to avoiding congestion, changes frequently. The computational cost of finding the optimal path for numerous evaluations may become prohibitive.

An analog solver for the dynamic traffic routing algorithm was developed. The concept was demonstrated through a small prototype traffic network (Figure 7).

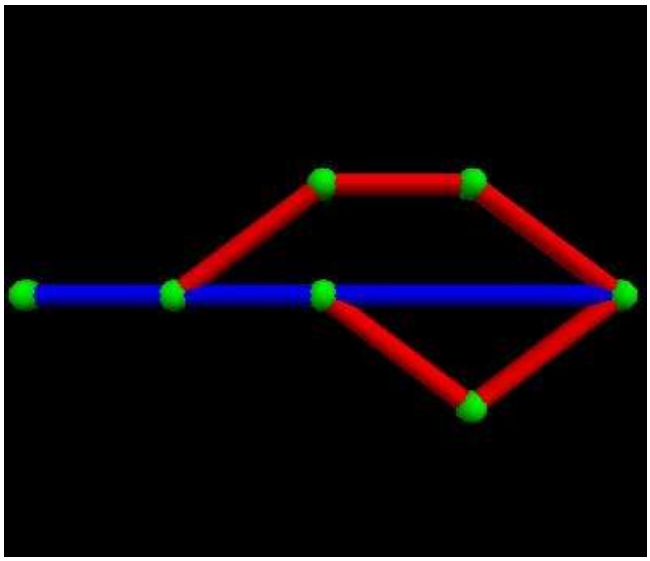

Figure 7. Prototype Traffic Network for the Hardware Solver.

The traffic network is implemented as an electric circuit. The resistance on each arc of the electric circuit corresponds to the "resistance" to traffic flow in the traffic network. The best detour path is the path of "least resistance" in the circuit. This is found by inducing a current into the circuit and monitoring which path the current takes, which occurs almost instantaneously.

A Graphical User Interface was developed to control the system as shown in Figure 8. This interface provides the hardware solver with the parameters of the network describing the current situation. The solver determines the most optimal reroute in the time it takes electricity to flow through the circuit, virtually instantaneously.

Ongoing work includes building an analog solver for a traffic network surrounding Detroit. The map of the planned area is shown in Figure 9. The same section of traffic network will be simulated using the AIMSUM software as discussed in the next section.

An equivalent electric circuit is shown in Figure 10.

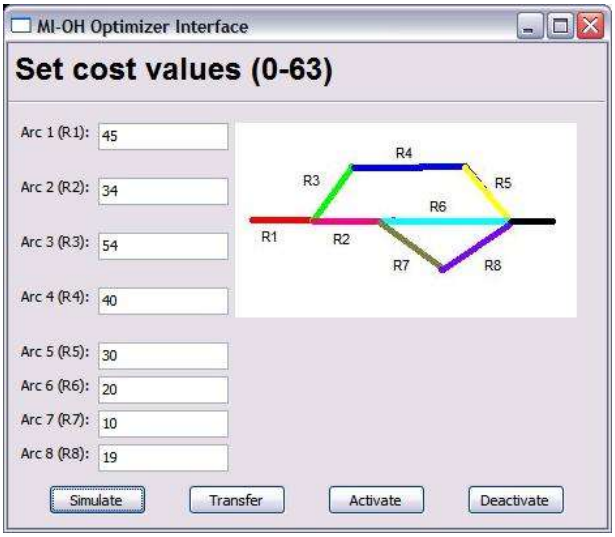

Figure 8. Hardware Solver Interface.

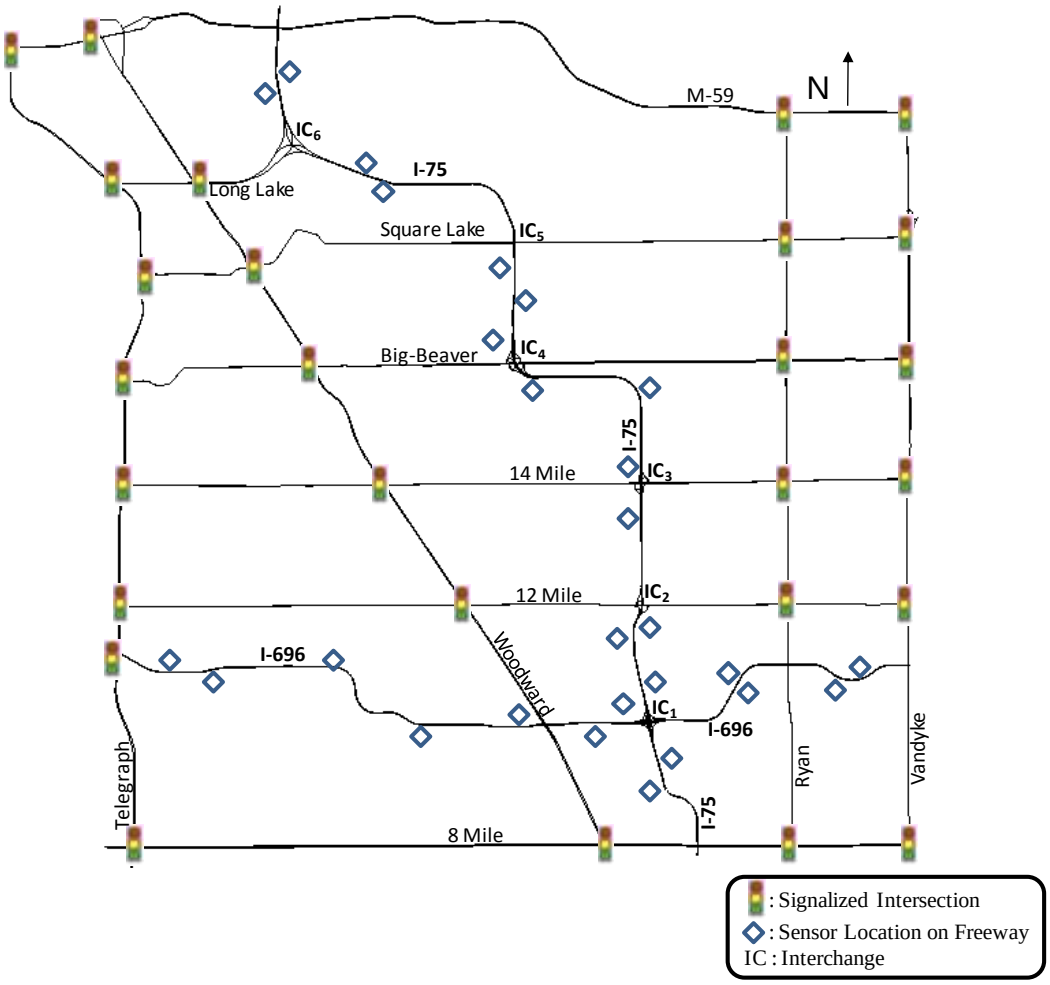

Figure 9. Map of the Detroit Area I-75 Corridor - Analog Solver

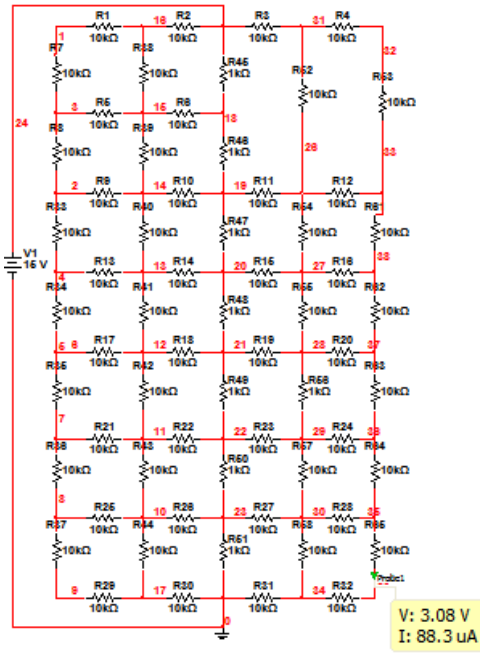

Figure 10. Electrical Schematic Representation of the Figure 9 Map.

The circuit shown in Figure 10 was modeled in SPICE and then MATLAB to iteratively decide the parameters for the hardware components. The 63 traffic arcs require 63 potentiometers and the 38 nodes require 38 amplifiers and corresponding microcontrollers. The following parameters were considered:

O-D Voltage Range:	0-30V (starting from maximum)
Gain:	5 to very high depending on the requirement (Starting with 5 to avoid the need for a gain resistor)
Offset serial resistor:	Starting with 1K
Highway Arc Resistors:	100K Max
Detour Resistors:	100K Max

From the iterative evaluation, the following parameter values were selected:

O-D Voltage: 30V
R_Highway: 4K
R_Detour: 20K

The maximum current is ~1mA. The offset voltage and amplifier gain were reevaluated using the selected parameter values. The ADC voltage is within range. Based on this evaluation, the 100 MCP41100-I/P-ND digital potentiometer has been selected for use in the analog solver.

IV. 3. Traffic Simulation

Objective: Extension of traffic simulation modeling capabilities, with application to the Detroit area I-75 corridor.

Deliverables: An AIMSUN-based traffic simulation model for the Detroit area I-75 corridor.

An analytic framework for the calibration and application of micro-simulation techniques was developed and applied to test the impact of alternate IMS on the Detroit area I-75 corridor. A thorough review of the pertinent literature was conducted in four specific areas: (1) IMS and alternate route diversion on freeways and arterials, (2) various types of path and route choice models applied in IMS, (3) measures of effectiveness (MOE) used to evaluate IMS, and (4) the application of micro-simulation models to analyze IMS. Much of the data used in the calibration and application of the model was extracted from archived records of MITSC.

The analytic framework can be summarized as follows;

1. Network creation and assembling different databases.
2. Identification of policies and development of algorithm that comprise the IMS.
3. Calibration of micro-simulation model.
4. Conducting micro-simulation-based experiments, by creating incidents on the network, and by using the databases, algorithm and policies identified in the earlier steps.
5. Analysis of results.

The micro-simulator available in the AIMSUN software is used to test the methodology. AIMSUN is developed by Transportation Simulation Systems (TSS), Barcelona, Spain, and is capable of incorporating various types of incidents in a network consisting of detectors, traffic signals, variable message signs and other attributes. The input data requirement for AIMSUN is a set of scenarios (network description, traffic control plan and traffic demand data) and parameters (simulation time, statistical intervals, reaction time, etc.) which define the experiment. MOE used in assessing the performance of the model are: travel time, delay and queue length.

The methodology is applied to test a heavily traveled portion of urban network in the Detroit metropolitan area. The network consists of two freeways and 11 arterials (Figure 9 above). The freewaysI-75 and I-696 provide major mobility needs in the region in the North-South and East-West directions respectively. The arterials serve a combination of mobility and access function in the region.

The network consists of 47 nodes and 108 links. There are 3,152 sections in the network, where a section is defined as a group of contiguous lanes where vehicles move in the same direction. The partition of the traffic network into sections is usually governed by the physical boundaries of the area and the existence of turning movements. There are 26 centroids representing 26 zones that comprise 676 origin destination (O-D) pairs.

Variable message signs (VMS) can be placed before freeway exits to inform drivers of regulations that are applicable only during certain periods of the day or under certain traffic conditions. Freeway ramps, merging points and exit points are coded according to their lengths and curvatures. Traffic volume and signal timing data were collected from SEMCOG, Macomb County Road Commission (MCRC), and Traffic.com.

The model calibration process was accomplished following the steps described earlier. Key features of calibration are as follows:

- First, a set of volume data was collected from sensors on I-75 and I-696 on a given Tuesday, June 2008, for three hours between 7 a.m. and 10 a.m. Turning movements and traffic signal data collected for the same period are also given as input to the network.

- These volume data, when input to AIMSUN, were instrumental in creating a 26 x 26 O-D matrix for the exact time period between 7 a.m. and 10 a.m.

- This trip table, when assigned to the network, produced a set of volume data on the freeway and arterials in five minute intervals for a total of 36 intervals for the three hour period.

- For assessing the goodness-of-fit of the assigned volume data, a second set of traffic volume data on the freeways was collected on another Tuesday, in June 2008, between 7 a.m. and 10 a.m. from archived records.

Results of the statistical tests of calibration are presented in Table 3. For all the tests conducted, the goodness-of-fit measures are acceptable, either by error or by degree of correlation.

Table 3: Summary of Goodness-of-fit Measures

Location	Root Mean Square Error (RMSE) % Error	Correlation Coefficient (*r*)	Theil's Weight of Large Errors (*Ui*)	Theil's Variance Proportion (*Us*)	Theil's Covariance Proportion (*Uc*)	Theil's Bias Proportion (*Um*)
I-75 at I-696	0.036	0.988	0.015	0.053	0.928	0.045
I-75 at 14 Mile	0.054	0.988	0.018	0.002	0.873	0.014
I-696 at Telegraph	0.053	0.975	0.024	0.046	0.922	0.058
I-696 at Telegraph	0.044	0.970	0.020	0.089	0.915	0.013
I-75 Corridor	0.001	0.995	0.013	0.000	0.987	0.014

A composite Root Mean Square Error (RMSE) test was also conducted for the goodness-of-fit between the two sets of volume data in the network for I-75. The simulated volume and actual volume are plotted in Figure 2 showing 612 data points being the result of multiplying 17 locations with 36 five minute counts at each location. The RMSE value computed as 0.001. Other goodness-of-fit statistics for I-75 corridor are presented in the

last row of Table 3. Further, the two sets of values, when plotted on a graph, formed a linear representation at 45^0 (Figure 11).

The model was used to analyze the effects of IMS on three types of incidents: lane closures, section incidents, and forced turnings. In the absence of archived data, a comparison of MOE can only be made between "guided" and "unguided" conditions, assuming that "unguided" conditions represent actual actions of drivers. For each IMS tested, two types of performance data are obtained: unit travel time and unit delay, both measured in seconds/mile/vehicle over one hour of simulated time.

The model output is sensitive to the operational changes associated with the strategies tested and that the trends observed in the model output appear to be logical and reasonable. A more detailed description of this work is found in Khasnabis, et al. (2008).

Conclusions of this effort are;

- The framework is conceptually sound and robust, and it incorporates five critical steps that lend themselves testing of various policy options, as well as operational changes reflecting different IMS.

- Model calibration demonstrated with two sets of independent data sources collected from sensors in the freeway system appears to reflect a reasonable correspondence between the model output and observed data.

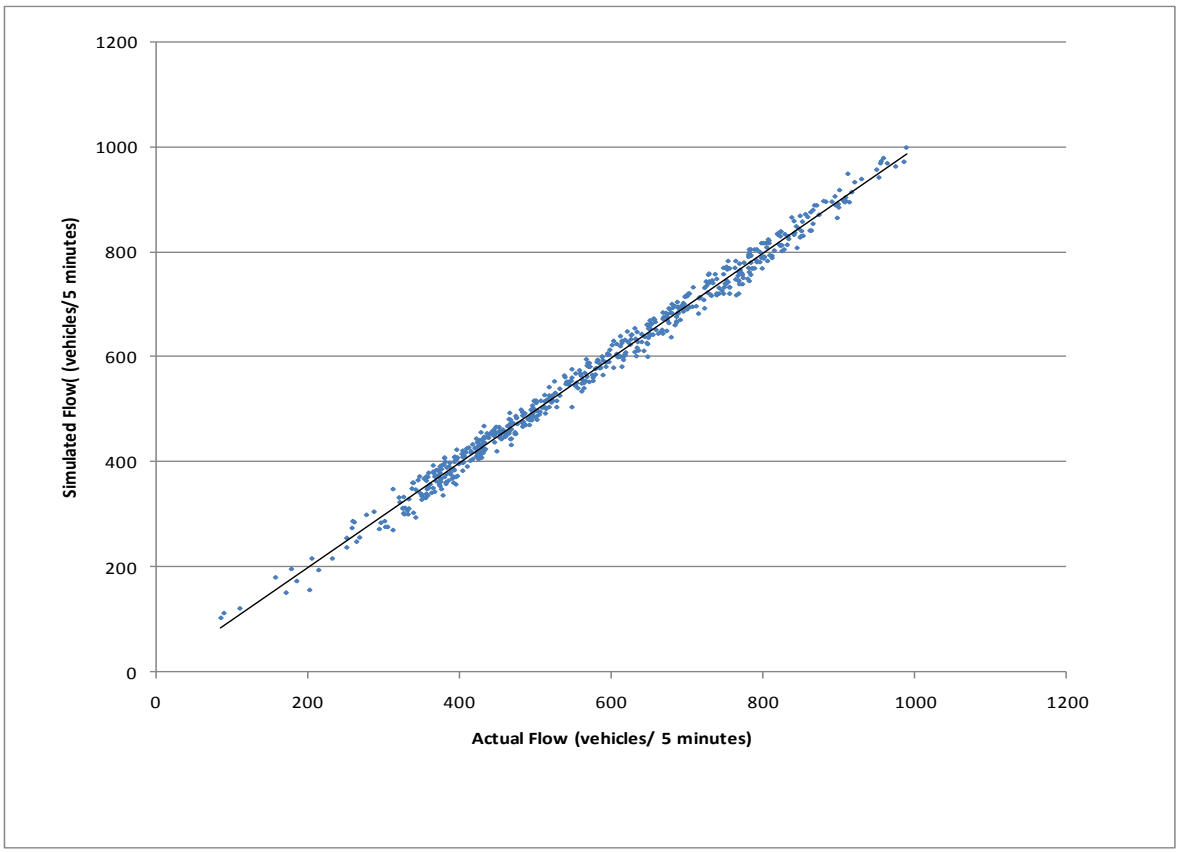

Figure 11. Actual and Simulated flow on I-75 (7 a.m. -10 a.m.)

V. Research Vision for September 2008 – August 2010

To meets its fundamental goals of understanding traffic flow in time and space, as well as to apply this understanding in routing voluminous traffic, the research team intends to transform the speed, volume, and occupancy data collected by MITSC concerning the interstate system in the Detroit metropolitan area into a highly usable public resource. Meeting this objective will involve the following, which can be addressed over a two year period:

1. Systematically acquire the MITSC data. This has been accomplished.
2. Design and implement a database management system for this voluminous data, about 50 gigabytes per year within a MySQL database. Database design and implementation has been demonstrated for a small, less than 10%, subset of the data concerning the Detroit area I-75 corridor.
3. Evaluate the quality of the data and "clean" the data as necessary. This includes determining missing data values and replacing them using proper statistical techniques as well as evaluating the effectiveness of the traffic sensors in consistently collecting data.
4. Develop and implement procedures descriptive, explanatory, and predictive statistical model building to represent the movement of traffic in time and space.
5. Apply these results to voluminous traffic rerouting in the Detroit area I-75 corridor, thus demonstrating their utility.
    a. Continue refining routing models that take into account time and space.
    b. Continue refining both software- and hardware based solvers for these models.
    c. Validate these models using traffic simulation.
    d. Develop a procedure to assist an ITS in finding alternate routes in an efficient manner in response to traffic incidents.
    e. Develop a procedure to use the validated model(s) to assess the impact of traffic incidents on the network, in partnership with an ITS.
6. Make the MITSC data, as improved by the activities in 2 above, as well as the statistical modeling procedures, openly available via the World Wide Web.

VI. Bibliography

Even, Andrew. 2007. Multi-Commodity Dynamic Vehicle Routing Subject to Capacity Constraints With Real Time Transportation Information. Unpublished Masters Project. School of Engineering, Padnos College of Engineering and Computing, Grand Valley State University.

Even, Andrew, Shabbir Choudhuri, and Charles Standridge. 2007. Dynamic Traffic Rerouting with Feedback from Infrastructure, INFORMS Annual Meeting, Seattle.

Khasnabis, Snehamay, Sabyasachee Mishra, Subrat Swain, and Anshuman Manori. 2008. Traffic Simulation: Congestion Relief By Travel Time Minimization In Near Real Time. Department of Civil Engineering, College of Engineering, Wayne State University.

Misra, Sabyasachee and Snehamay Khasnabis. 2007. Survey of Literature Review: Congestion Relief By Travel Time Minimization In Near Real Time. Department of Civil Engineering, College of Engineering, Wayne State University.

Misra, Sabyasachee. 2008. A Micro Simulation Model Application for Incident Management Strategies. Institute of Transportation Engineers (ITE) Great Lakes District.

Tusch, Guenter. 2007. ITS Data Analysis Preliminary Results. School of Computing and Information Systems, Padnos College of Engineering and Computing, Grand Valley State University.

Yada, Vishnu, Shabbir Choudhuri, and Charles Standridge. 2007. Web Based Data Repository for Collaboration among ITS Researchers, INFORMS Annual Meeting, Seattle.

VII. List of Acronyms

AIMSUN	Advanced Interactive Microscopic Model for Urban and Non-urban Networks
DBMS	Database management system
FTP	File transfer protocol
GVMC	Grand Valley Metropolitan Council
GVSU	Grand Valley State University
IMS	Incident management strategies
ITS	Intelligent transportation systems
ITS MI	Intelligent Transportation Society of Michigan
MCRC	Macomb County Road Commission
MDOT	Department of Transportation
MITSC	Michigan Intelligent Transportation Systems Center
MOE	Measures of effectiveness
PTA	Personal travel assistant
RMSE	Root Mean Square Error
SEMCOG	Southeast Michigan Council of Governments
TSS	Transportation Simulation Systems, Barcelona, Spain
WSU	Wayne State University

MICHIGAN OHIO UNIVERSITY TRANSPORTATION CENTER
Alternate energy and system mobility to stimulate economic development.

Report No: MIOH UTC TS4p2 2008-Final
RC1545

EVALUATION OF THE SCATS CONTROL SYSTEM

FINAL REPORT

PROJECT TEAM

Dr. Utpal Dutta P.E
Dr. Deb McAvoy P.E.
Dr. Jim Lynch P.E
Laurel Vandeputte

Department of Civil & Environmental Engineering
University of Detroit Mercy
4001 W. McNichols Road
Detroit, Michigan 48221

EVALUATION OF THE SCATS CONTROL SYSTEM

FINAL REPORT

Report No: MIOH UTC TS4p2 2008-Final
TS 4, Project 2, December, 2008

SPONSORS

This is a Michigan Ohio University Transportation Center project supported by the U.S. Department of Transportation, the Michigan Department of Transportation and the University of Detroit Mercy.

ACKNOWLEDGEMENT

The Project Team would like to acknowledge support from the Michigan Department of Transportation (MDOT), the Road Commission for Oakland County (RCOC), and the Southeastern Michigan Council of Governments (SEMCOG) during the course of this research.

DISCLAIMER

Technical Report Documentation Page

1. Report No. RC-1545	**2. Government Accession No.**	**3. MDOT Project Manager** Niles Annelin
4. Title and Subtitle Michigan Ohio University Transportation Center Subtitle: "Evaluation of the SCATS Control System"		**5. Report Date** December 2008 **6. Performing Organization Code**
7. Author(s) Dr. Utpal Dutta,P.E, University of Detroit Mercy Dr. Deb McAvoy, P.E. Dr. James Lynch, P.E., University of Detroit Mercy Laurel Vandeputte, University of Detroit Mercy		**8. Performing Org. Report No.** MIOH UTC TS4p2 2008-Final
9. Performing Organization Name and Address Michigan Ohio University Transportation Center University of Detroit Mercy, Detroit, MI 48221 and University of Detroit Mercy, Detroit, MI 48221		**10. Work Unit No. (TRAIS)** **11. Contract No.** 2007-0538 **11(a). Authorization No.**
12. Sponsoring Agency Name and Address Michigan Department of Transportation Van Wagoner Building, 425 West Ottawa P. O. Box 30050, Lansing, Michigan 48909		**13. Type of Report & Period Covered** Research, May 2007 – December 2008 **14. Sponsoring Agency Code**

15. Supplementary Notes
Additional Sponsors: US DOT Research & Innovative Technology Administration, University of Detroit Mercy. Additional Support: the Road Commission for Oakland County (RCOC), and the Southeastern Michigan Council of Governments (SEMCOG).

16. Abstract
MIOH UTC TS4p2 2008-Final
This research study was designed to evaluate the performance of the SCATS system at traffic signals on a selected segment of road in Oakland County, Michigan by determining the statistical significance of the effectiveness of the SCATS system in terms of traffic flow, delay, queue length, and other selected characteristics as compared to a pre-timed signal system. The primary purpose of the SCATS system is to maximize the throughput of a roadway by controlling queue formation. The SCATS system has the ability to change the signal phasing, timing strategies, and the signal coordination within a network to alleviate congestion by automatically adjusting the signal parameters according to the real time traffic demand. This study was undertaken to quantify the long-term effectiveness of the SCATS system on traffic congestion.

17. Key Words Intelligent transportation systems, Traffic flow, Time, Traffic data, Data collection, Transportation infrastructure, Traffic volume, Detroit (Michigan), Research projects.	**18. Distribution Statement** No restrictions. This document is available to the public through the Michigan Department of Transportation.

19. Security Classification - report	**20. Security Classification - page**	**21. No. of Pages** 109	**22. Price**

TABLE OF CONTENTS

LIST OF FIGURES

LIST OF TABLES

INTRODUCTION

Increasing travel demand and lack of sufficient highway capacity are serious problems in most major metropolitan areas in the United States. Large metropolitan areas have been experiencing increased traffic congestion problems over the past several years. The total delay that drivers experienced has increased from 0.7 billion hours in 1982 to 3.7 billion hours in 2003 [1]. Combining the 3.7 billion hours of delay and 2.3 billion gallons of fuel consumed due to congestion, leads to a total congestion cost of $63 billion dollars for drivers in 85 of the largest metropolitan areas of the nation [1].

In spite of the implementation of many demand management measures, the congestion in most urban areas is still increasing. In many areas congestion is no longer limited to two peak hours in a day; however, it is extended to two to three hours in the morning, afternoon and evening. Thus, the congestion experienced on urban and suburban freeways and arterial streets results in delays to the motorist, excess fuel consumption and a high level of pollutant emission not only during the peak hours in a day, but also for several hours throughout the day.

Traffic congestion has a significant impact on our nation's economy and to minimize this impact, the United States Department of Transportation (USDOT) has identified congestion mitigation as their top priority. Congestion on arterial roads can be attributable to heavy traffic volumes and poor traffic signal coordination. Recently, the NTOC 2005 National Report Card awarded the nation a "D-" grade for traffic signal operation stating that future efforts should be focused on "Mitigating bottlenecks on arterials resulting from signal timing" [2].

As with many urban areas across the nation, Oakland County, one of the largest counties in the State of Michigan has been experiencing congestion for the past two decades. During the 1990's, Oakland County experienced a surge of population growth and economic development. Associated growth in traffic required an excess of a billion dollars in road improvement needs. At the current level of funding, it will take 70 years to meet the capacity needs of the Oakland County roadways [3]. Looking for innovative and cost effective ways to improve road user mobility and safety, the Road Commission for Oakland County (RCOC) began investigating innovative traffic control strategies associated with Intelligent Transportation Systems (ITS). Subsequently, the County Board of Commissioners approved $2 million for the development of

an advanced traffic management system in southeast Oakland County. This commitment by Oakland County toward congestion mitigation, prompted the United States Congress to financially support this effort as a Federal demonstration project with $10 million in funding. The innovative traffic control system created in Oakland County with the Federal and County funds is called "FAST-TRAC", an acronym which stands for Faster and Safer Travel through Traffic Routing and Advanced Controls.

As a part of a field demonstration project, traffic signals at 28 intersections in the city of Troy within Oakland County were converted from a pre-timed coordinated traffic signal system to SCATS (Sydney Coordinated Adaptive Traffic System) control in 1992. SCATS is a computer controlled traffic signal system, developed in Australia and used widely in the Pacific Rim. SCATS uses anticipatory and adaptive techniques to increase the efficiency of the road network by minimizing the overall number of vehicular stops and delay experienced by motorists. The primary purpose of the SCATS system is to maximize the throughput of a roadway by controlling queue formation.

As a part of the SCATS system, vehicle presence at an intersection is detected by a video imaging processing system called 'Autoscope'. The Autoscope system analyzes an intersection through a video imaging camera mounted above the intersection by detecting vehicles queued at the traffic signal along with other traffic flow parameters. The traffic flow parameters are then transmitted to a SCATS control box located at each intersection and coordinated with a central computer located at the Traffic Operation Center (TOC). The SCATS system has the ability to change the signal phasing, timing strategies, and the signal coordination within a network to alleviate congestion by automatically adjusting the signal parameters according to the real time traffic demand.

Since 1992, traffic signals in Oakland County and a portion of Macomb and Wayne Counties have been converted to the SCATS signal system. County traffic engineers have been adjusting various SCATS parameters to improve the roadway network's effectiveness in terms of delay, traffic flow, queue length and crash or severity occurrences.

However, there have not been any comprehensive studies conducted that evaluated the performance of the SCATS systems in terms of delay, flow, queue length and other characteristics in the past several years. In order to quantify the long-term effectiveness of the SCATS systems on traffic congestion, a comprehensive study is needed. This research study was designed to evaluate the performance of the SCATS system by determining the statistical significance of the effectiveness of the SCATS system in terms of traffic flow, delay and other selected MOEs.

STATE-OF-THE-ART LITERATURE REVIEW

A literature review was performed to examine past research on the signal coordination and progression for corridors or networks. In order to identify past results related to the proposed research, literature searches were conducted through Internet queries and traditional library resources for the following subject areas:

- Signal coordination
- SCATS signal system
- SCOOT signal system
- Benefits (tangible and intangible) of signal coordination systems

Intelligent Transportation Systems (ITS) have been widely considered as methods to improve the efficiency and safety of a roadway system through real-time traffic data. For arterials with signalized intersections, the benefit of an ITS implemented strategy is the efficient allocation of green time for each intersection either along a corridor or in a network. While ITS strategies have been implemented, the benefits of such strategies have not been documented in terms of their impact on roadway capacity, operation or safety. In order to understand the benefits of ITS strategies, the United States Department of Transportation's (USDOT) Joint Program Office (JPO) created a National ITS Benefits Database to disseminate the most recent information to all transportation professionals [4].

Arterial management systems are ITS strategies used to reduced congestions and improve mobility along arterial roadways through the use of traffic signal control. Initial arterial management systems included pre-timed signal systems which correlate to specific periods of a day, such as the AM, noon or PM peak hour. Pre-timed signal systems do not change during the period and thereby cannot respond to changing traffic conditions. Therefore, the best pre-timed

system is designed with signal progression through the use of signal offsets which optimizes the system. Actuated signal systems are an improvement to the pre-timed systems due to their ability to allow unused green time to be reallocated. However, the inability to modify the offsets at downstream intersections can create lower levels of progression along a corridor than a pre-timed system even through delay has been reduced. While the actuated signal systems can skip phases, the cycle lengths remain the same. Further improvements to traffic signal coordination have been made with the introduction of adaptive signal control systems which can modify the cycle length, signal phasing and signal timing based upon real-time traffic data. The benefits gained from an adaptive signal control systems have not defined since the ability to generalize the benefits may vary on corridor length, intersection spacing, traffic volumes or volume variation [4]. In addition, the limited number of evaluations conducted further constrains the definition of benefits from such systems. SCOOT (Split, Cycle, and Offset Optimization) and SCATS (Sydney Coordinated Adapted Traffic System) are the two most commonly used adaptive signal control systems. SCOOT was developed in the Transport Research Lab in the United Kingdom [5]. SCOOT measures traffic volumes and modifies the signal timings in order to minimize a performance index which incorporates delay, queue length and number of stops measures of effectiveness [5]. SCOOT has been utilized in Toronto, San Diego, Anaheim, London and Bangkok [6]. SCATS was developed by the Department of Main Roads (Roads and Traffic Authority) of New South Wales in Australia. SCATS collects traffic data near the intersection stop bar to adjust the signal timings to minimize number of stops and delay [5]. The SCATS system has been utilized in Hong Kohn, Sydney, Melbourne and Oakland County, Michigan [6].

Martin et. al. [5,7] conducted an evaluation study to compare three signal systems; Synchro-designed fixed-time system, TRANSYT-designed fixed-time system and SCOOT as simulated with CORSIM. The results of the study indicated that the SCOOT simulated system was more effective than either the Synchro or TRANSYT system. However, the differential between the SCOOT system and the other two signal systems declined as the traffic volumes approached saturation.

The SCATS systems was compared to a dynamic TRANSYT system which modified the signal timing and cycle length at 45 minute intervals in the research study conducted by Liu and Cheu

[8]. The researchers found that in simulations the dynamic TRANSYT system resulted in lower average delays per vehicle. They also found that the simulated SCATS system was replicated with the simulation program designed for the study, PARAMICS.

The SCOOT system in Anaheim, California was compared to a fixed time system. The results of the study ranged from a decrease in travel time by 10 percent with the SCOOT system to an increase in travel time by 15 percent [4]. The preferred location for the vehicle detectors for the SCOOT system is near the upstream intersection. However, existing mid-block vehicle detectors were utilized for the Anaheim system, which may have led to the poor performance of the system.

Abdel-Rahim and Taylor [9] also utilized a simulation program, CORSIM, to compare the benefits of adaptive signal systems to coordinated fixed-time systems. The study was conducted along Orchard Lake Road in Oakland County, Michigan with five signalized intersections. The researchers found that adaptive traffic signal systems reduced travel time along the corridor particularly when the demand was less than capacity. The study also found that actuated signals provided similar results to the adaptive signal system. In addition, the SCATS and SCOOT systems predicted arrivals in a similar fashion.

The comparison of an adaptive traffic signal system with a fixed time system in Vancouver, Washington along Mill Plain Boulevard, a six-lane divided arterial, found that the adaptive signal system performed more efficiently than the fixed time system for the eastbound direction during both the AM and PM peak periods [10]. However, the improvement for the westbound direction was not statistically significant at the 95 percent level of confidence. Eghtedari concluded that future research should incorporate travel time and delay studies for the minor streets as well as left-turn movements. This was one of the few studies that utilized actual field data for the comparison of systems and did not rely on simulation programs.

A study conducted for the Cobb County Department of Transportation found that the SCATS system did not provide significant improvements to the travel time or reductions in delay [11]. A driver satisfaction survey conducted by Petrella et. al. [11] found that a representative sample of the population concurred with the empirical results of the research study conducted by the Georgia Institute of Technology.

The JPO also established various measures of effectiveness in several ITS programs areas, such as mobility and efficiency, in order to assist researchers and practitioners in determining the impact of ITS strategies [4]. For mobility programs, the measures of effectiveness as defined by the JPO include delay and travel time. Delay can be measured in seconds per vehicle or number of stops. Travel time can be measured in the variability in travel time or the reduction in travel time. For efficiency ITS programs, measures of effectiveness include the measurement of effective capacity or throughput. Effective capacity is defined as the "Maximum potential rate at which persons or vehicles may traverse a link, node or network under a representative composite of roadway conditions," including "weather, incidents and variation in traffic demand patterns" [4]. Throughput is defined as "The number of persons, goods, or vehicles traversing a roadway section per unit time" [4]. Based upon the definitions of each possible measure of effectiveness, it is readily possible to measure throughput, while effective capacity can vary depending on various factors. Therefore, the JPO recommends utilizing throughput as a surrogate measure for effective capacity [4].

Past research projects have evaluated signal systems through various measures of effectiveness. Park et. al. [12] utilized travel time to calibrate an urban arterial network with 12 coordinated actuated signalized intersections and maximum queue length to validate the model. Al-Mudhaffar and Bang [13] also utilized travel time and queue length in their analysis as well as intersection delay in an evaluation between fixed time coordination and self-optimizing control for bus priority control. To compare traffic simulation models for a fixed-time system, an actuated-coordinated system, a SCATS system and a SCOOT system utilizing CORSIM, a microscopic simulation model, Abdel-Rahim and Taylor [9] utilized average travel time, intersection delay and average intersection approach delay for the major and minor streets. A similar study was conducted by Martin et. al. [5,7] to compare the delay, queue length and travel time between SCOOT and a fixed-time system with CORSIM. Wolshon and Taylor [14] utilized intersection delay for individual movements in order to analyze the implementation of the SCATS system in South Lyon, Michigan. Liu and Cheu [8] utilized average vehicle delay to compare traffic flow in network between a dynamic TRANSYT system and SCATS control. TRANSYT was also utilized to compare a SCOOT control system with a pre-timed signal system through the comparison of delay by Park and Chang [15]. Girianna and Benekohal [16]

validated a two-way street network with ten signalized intersections utilizing total vehicles discharged and average link speed. To determine the effectiveness of an adaptive signal control system as compared to a time-of-day signal control, Eghtedari [10] examined travel time and average speed for a six-lane divided arterial in downtown Vancouver, Washington. Stevampvoc & Martin [17] utilized the performance index from Synchro, optimization software, to determine the benefits of updating traffic signal timings.

Based upon the literature review, it was determined that appropriate measures of effectiveness to determine the impact of the two signal systems would be travel time, travel time delay, intersection delay, queue length, fuel consumption and emission data.

RESEARCH OBJECTIVES

The objective of this evaluation study was to assess the effectiveness of the SCATS signal system on the reduction of traffic congestion in terms of delay, queue length and other traffic characteristics. The evaluation of the effectiveness of the SCATS system was accomplished through a field experiment to meet the following objectives:

- Select study corridor and intersections for inclusion in the evaluation study
- Determine the traffic volumes along the corridor to design the pre-timed signal system with Synchro, a traffic optimization program
- Collect the measures of effectiveness (MOE) of traffic flow for each of the two signal timing scenarios (pre-timed and SCATS) such as:
    - Travel time
    - Travel speed
    - Fuel Consumption
    - Hydrocarbon Emissions
    - Carbon Monoxide Emissions
    - Nitrogen Oxide Emissions
    - Number of stops
    - Total delay
    - Number of vehicles stopping at intersections along the corridor
    - Maximum Queue length at intersections along the corridor
- Determine the effectiveness of the two signal system scenarios based upon field data collected.

STUDY AREA

A four-mile segment along M-59 between Pontiac Lake Road West to Pontiac Lake Road East was selected as the corridor for the data collection and analysis for the field experiment. The M-59 corridor selected for this research project includes seven intersections as follows:

- Pontiac Lake Road West
- Williams Lake Road
- Oakland Boulevard
- Service Drive
- Airport Road
- Crescent Lake Road
- Pontiac Lake Road East

The M-59 corridor selected for the research project is depicted in Figure 1.

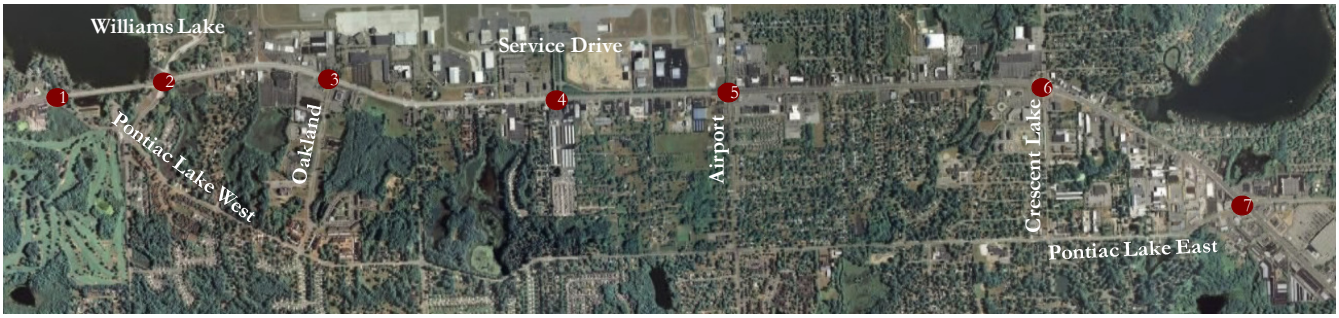

Figure 1. M-59 Corridor for Analysis

Traffic operational data was collected for each intersection as follows:

- Existing geometric conditions
- Traffic volume
- Travel time
- Travel speed
- Fuel Consumption
- Emissions
- Number of stops
- Total delay
- Number of vehicles stopping at intersections along the corridor
- Maximum queue length at intersections along the corridor

Except for the traffic volume data, the data was collected for a typical weekday (Tuesday, Wednesday or Thursday) and Friday during the noon (12 PM to 1 PM) and PM (4 PM to 6 PM) peak periods, as well for a Saturday morning peak (9 AM to 11 AM). The traffic volume data was only collected for a typical weekday noon and PM peak periods. Due to the low traffic volumes at the intersection with Service Drive, traffic operational data, other than traffic volumes and geometric conditions, were not collected at the intersection.

Existing Geometric Conditions and Traffic Volumes

As a part of this study, a field survey was conducted for each intersection. The field survey included visiting the intersection sites, collecting the existing conditions of the intersection, taking photographs in order to capture the existing lane use and other potential physical characteristics in the vicinity of the intersections, and assessing the existing traffic control devices. The existing condition data that was collected included the lane widths, lane use, lengths of turn bays, location of stop bars and crosswalks, length and width of crosswalks, location of overhead signals and post-mounted signals, and signs relating to traffic control. The existing condition data was entered into Synchro, a traffic signal optimization software package, to design the pre-timed signal operation recommended for each intersection for implementation in the field in order to compare the operational characteristics with the SCATS system. The Synchro signal system file was submitted to MDOT for review and implementation. During the course of this study, MDOT has implemented their pre-timed signal design for evaluation.

The manual turning movement volume counts were collected for each intersection using two-person data collection teams between May 22nd and June 7th of 2007. Each team member recorded the through and turning movement traffic separately, for each of the intersection approaches. The counts included the identification of trucks, buses and school buses at the intersection. The counts were taken in 15-minute intervals for the entire duration of the peak periods. Once the turning movement data were finalized, it was analyzed and summarized. Tables were prepared for each intersection and analysis period, including the following:

- Number of passenger cars, trucks, and school buses counted for each 15-minute interval for each approach and each movement.
- Highest hourly volume observed in the period.
- Peak hour factors.
- Percent of trucks and school buses for each movement, approach and intersection.

The noon and PM peak hour diagrams for each intersection are provided in Appendix A.

Travel Time Sample Size Calculation

In order to evaluate the effectiveness of the SCATS system, travel time studies were conducted along the M-59 corridor for the two signal system scenarios (MDOT pre-timed and SCATS) after the area schools began in September. In order to determine the minimum number of required travel time runs during the peak period, preliminary travel time data was collected along M-59 during the week of June 4, 2007. The following equation was used to calculate the number of runs required [18,19]:

$$n = \left\{ \frac{\hat{\sigma} x Z}{\varepsilon} \right\}^2$$

Where,

n = Estimated sample size for number of runs at the desired precision and level of confidence

$\hat{\sigma}$ = Preliminary estimate of the population standard deviation for average travel speed among the sample runs

Z = Two-tailed value of the standardized normal deviate associated with the desired level of confidence (at a 95% level of confidence, Z = 1.96)

ε = Acceptable error (mph) (assumed as 2 mph)

The calculated sample size was based on the intended use of the travel time information. According to Oppenlander [18], the range of permitted errors in the estimate of the mean travel speed (ε) is ± 1.0 mph to ± 3.0 mph for 'before and after' studies involving operational improvements of roadways, such as signal modifications. The allowable error used in this analysis were based upon the preliminary travel time runs conducted in June of 2007. According to Oppenlander, "If no travel time and delay studies have been conducted on the route under evaluation, an initial study of 4 to 5 test runs provides a sample of data for estimating the average range in travel speeds" [18]. Therefore, the preliminary number of runs for the sample size estimation were a minimum of five runs.

The preliminary travel time data were taken during the Noon (12 PM to 1 PM) and PM (4 PM to 6 PM) peak periods on a typical weekday on June 7, 2007. The data used in the analysis to determine the sample size requirements are shown in Table 1 with a summary of the travel data in Table 2. The calculation for the minimum number of runs for the analysis is as follows:

Table 1. Preliminary Travel Time Data

Peak Period and Travel Time Run Number	Travel Time (sec)	Travel Speed (mph)	Travel Time (sec)	Travel Speed (mph)
Noon Peak Period	**Eastbound**		**Westbound**	
1	422	39.07	549	30.03
2	484	34.07	465	35.46
3	489	33.72	463	35.61
4	510	32.33	452	36.48
5	496	33.24	537	30.70
6	402	41.02	502	32.84
7	409	40.31	N/A	N/A
PM Peak Period	**Eastbound**		**Westbound**	
1	451	36.56	625	26.38
2	527	31.29	634	26.00
3	428	38.52	897	18.38
4	431	38.26	849	19.42
5	412	40.02	727	22.68
6	484	34.07	590	27.95
7	481	34.28	716	23.03
8	420	39.26	741	22.25
9	425	38.80	688	23.97
10	463	35.61	N/A	N/A
11	479	34.42	N/A	N/A

Note: Travel time runs were not equal for each direction and scenario based upon the travel conditions in the field. Periods which experienced fewer travel time runs are designated by N/A.

Table 2. Travel Time Statistical Data from Preliminary Runs

Peak Period and Direction of Travel	Number of Runs	Mean Travel Time (sec)	Mean Travel Speed (mph)	Standard Deviation of the Travel Speed (mph)
Noon Peak Period				
Eastbound	8	458.59	35.93	3.71
Westbound	7	494.67	33.33	2.73
PM Peak Hour				
Eastbound	11	454.64	36.27	2.75
Westbound	10	718.56	22.94	3.15

$$\text{Noon Peak Eastbound Minimum Number of Runs} = \left(\frac{3.71 \times 1.96}{2}\right)^2 = 13.22 \text{ runs}$$

$$\text{Noon Peak Westbound Minimum Number of Runs} = \left(\frac{2.73 \times 1.96}{2}\right)^2 = 7.16 \text{ runs}$$

$$\text{PM Peak Eastbound Minimum Number of Runs} = \left(\frac{2.75 \times 1.96}{2}\right)^2 = 7.26 \text{ runs}$$

$$\text{Noon Peak Eastbound Minimum Number of Runs} = \left(\frac{3.15 \times 1.96}{2}\right)^2 = 9.53 \text{ runs}$$

Therefore, ten to fourteen runs should satisfy the sample size requirements for travel time.

Statistical Analyses

Student's t-test with Welch's Modification for the Comparison of Means (Travel Time and Travel Time Delay)

The Student's t-test was considered to determine if the differences in mean travel time, travel speed, total delay or number of stops along the corridor are significant. In order for the Student's t-test to maintain its power and robustness, the data must follow several assumptions. Only continuous data, or data which can assume a range of numerical value should be tested with the Student's t-test [20]. In addition, the data must exhibit a distribution that is approximately normal with variances that are equal between the two groups being tested [20]. The data observations must also be independent, implying that the observations of the first group are different from the observations of the second group [20]. Additional tests were conducted to verify that the data's distribution was normal and the variances of the two groups were equal.

Once the underlying assumptions were verified, a two-tailed Student's t-test was conducted with a null hypothesis stating there was no difference between the two means of the signal systems. The alternative hypothesis states that one signal system is better or worse than the other. A one-tailed test requires the direction of the difference in travel time or delay to be specified prior to the analysis. The two-tailed test was used for this research as the effect on travel time in regards to the signal system is not previously known. Specifically, it cannot be stated whether the SCATS system increases or reduces travel time. If the calculated t-value is greater than the critical t-value obtained in available statistical tables, the difference in means was determined to be statistically significant. The calculated t-value was found with the following equation [20] for $[N_B + N_A - 2]$ degrees of freedom assuming the collection of unequal sample sizes:

$$t_{calc} = \frac{\left(\overline{X}_B - \overline{X}_A\right)}{\sqrt{\sigma^2\left(\frac{1}{N_B} + \frac{1}{N_A}\right)}}$$

Where:

$\overline{X}_B$ = sample mean of signal system one

$\overline{X}_A$ = sample mean of signal system two

N_B = number of observations

N_A = number of observations

σ = common standard deviation

If the data was determined to follow a normal distribution but the variances were not equal, the Welch's modification to the Student's t-test was utilized to test the differences in the means of the signal system groups. The Welch's method has shorter confidence intervals and more power than the Student's t-test when the variances are found to be substantially different. The Welch's test statistic [20] is as follows:

$$W = \frac{\left(\overline{X}_B - \overline{X}_A\right)}{\sqrt{\left(\frac{\hat{\sigma}_B^2}{N_B} + \frac{\hat{\sigma}_A^2}{N_A}\right)}}$$

$$k' = \frac{\left(\frac{\hat{\sigma}_B^2}{N_B} + \frac{\hat{\sigma}_A^2}{N_A}\right)^2}{\frac{\left(\frac{\hat{\sigma}_B^2}{N_B}\right)^2}{N_B - 1} + \frac{\left(\frac{\hat{\sigma}_A^2}{N_A}\right)^2}{N_A - 1}}$$

Where:

$\overline{X}_B$ = sample mean of signal system one

$\overline{X}_A$ = sample mean of signal system two

N_B = number of observations of signal system one

N_A = number of observations of signal system two

$\hat{\sigma}_B$ = standard deviation of signal system one

$\hat{\sigma}_A$ = standard deviation of signal system two

k' = degrees of freedom

One-way Analysis of Variance for the Comparison of Means (Travel Time and Travel Time Delay)

In order to compare several means simultaneously, a one-way analysis of variance (ANOVA) was utilized to determine if the means were similar. Although a Student's t-test could have been conducted on the same data, several iterations of the t-test would be required in order to compare all possible scenarios. However, the Type I error rate is greater when multiple t-tests are conducted and can be calculated as follows [20]:

$$\text{Type I Error Rate} = 1 - (1 - \alpha)^c$$

Where:

α = the level of confidence for each t-test

c = the number of independent t-tests

The ANOVA determines the level of confidence based upon the number of dependent variable categories that are being compared. For instance, if the mean travel time for each roadway type was compared, there would be three individual t-tests that would be conducted; SCATS, pre-timed and MDOT pre-timed. Although a desired Type I error of 0.05 was selected, the calculated Type I error rate would be equal to 0.14. However, the ANOVA would utilize a level of confidence of 31.7 percent or alpha equal to 0.017 for each of the comparisons which would yield an alpha of 0.05 for the entire analysis.

The one-way ANOVA required the comparison of one independent variable, illumination, with several categories of the dependent variable, mean speed, mean speed deviation or lateral placement. The assumptions for the ANOVA were similar to those for the Student's t-test. The

data must be continuous, independent, follow the normal distribution and have equal variances [20]. Violations of these assumptions impact the results of the test; however, the robustness of the ANOVA varied from the Student's t-test. For instance, the ANOVA is considered a very robust test even with the violation of normality, unless the variances and sample sizes are unequal [20]. To perform the ANOVA, an F-statistic is calculated which is equal to the mean squares between the groups divided by the mean squares within the groups. If F- calculated was greater than the F-critical obtained in available statistical tables, the difference in the means was statistically significant. When conducting the ANOVA test, the Levene's test for equal variances was performed simultaneously. When the Levene's test indicated that the variances were equal, the ANOVA calculated F-statistic was reported. If the variances were determined not to be equal, the Welch's modification to the ANOVA was conducted and the calculated F value based upon an asymptotically distribution was reported. The equations used to perform this test are as follows [21]:

$$SS_T = \sum_{k=1}^{K} \sum_{i=1}^{n_k} X_{ik}^2 - \frac{T^2}{N}$$

Where:

SS_T = Total sum of squares

$\sum_{k=1}^{K} \sum_{i=1}^{n_k} X_{ik}^2$ = squared scores summed across all individuals and groups

K = Number of groups

n = Number of observations

T = sum of scores summed across all observations and groups

N = total number of scores

$$SS_B = \sum_{k=1}^{K} \frac{T_k^2}{n_k} - \frac{T^2}{N}$$

Where:

SS_B = Sum of squares between-groups

T_k= sum of observations for kth group

$$SS_W = \sum_{k=1}^{K} \sum_{i=1}^{n_k} X_{ik}^2 - \sum_{k=1}^{k} \frac{T_k^2}{n_k}$$

Where:

SS_W = Sum of squares within-groups

$$MS_B = \frac{SS_B}{K - 1}$$

$$MS_W = \frac{SS_W}{N - K}$$

$$F_{calc} = \frac{MS_B}{MS_W}$$

Where:

MS_B = Mean sum of squares between-groups

MS_W = Mean sum of squares within-groups

When statistically significant results are obtained in the ANOVA, the only conclusion that can be drawn from the test is that differences exist between the means. However, the determination of which two means are in fact not equal cannot be concluded. Therefore, in order to solve this issue, post-hoc tests were utilized to assist in specific comparisons among groups. There are numerous post-hoc tests that have been established for various assumptions or violation of assumptions. Most of the post-hoc tests have been shown in past statistical research to withstand small deviations from normality. The determination of the post hoc tests conducted during this research was based upon summaries of past research [20,22]. For this research, the Bonferroni test was utilized when the sample sizes and variances were equal and a small number of comparisons were needed. For requirements of a larger number of comparisons with equal sample sizes and variances, the Tukey test was utilized. When the samples sizes were not equal but the variances were equal, the Hochberg test was conducted. If the variances were not assumed equal and the sample sizes were not equal, the Games-Howell test was conducted.

Paired t-test for the Comparison of Means (Intersection Delay and Queue Length)

In order to test the effectiveness of the signal systems based upon the mean measure of effectiveness, the paired t-test was used to determine if the differences in the variables are significant. Continuous data, or data which can assume a range of numerical values, such as the variables of intersection delay and queue length, can be tested in the paired t-test. In addition to assuring the data is appropriate for the test, there are two underlying assumptions of the data before the paired t-test can be performed. The data must exhibit a distribution that is approximately normal. In addition, the data observations must be dependent, indicating matched

pairs. For the paired t-test, a two-tailed test was used which utilizes a null hypothesis that states there is no difference between two means. A one-tailed test requires the direction of the difference to be specified prior to the analysis. The two-tailed test will be used for this research as the difference between the effectiveness of the signal systems is not known. Specifically, it cannot be stated whether the use of the SCATS systems would increase or decrease the measure of effectiveness.

The following equations will be used to calculate the paired t-statistic and the sample variance.

$$P_t = \frac{\overline{X}_B - \overline{X}_A}{\frac{s_D}{\sqrt{n}}}$$

$$s_D^2 = s_B^2 + s_A^2 - 2\left[\frac{1}{N-1}\sum_{i=1}^{N}\left(X_{Bi} - \overline{X}_B\right)\left(X_{Ai} - \overline{X}_A\right)\right]$$

Where:

$\overline{X}_B$ = sample mean of signal system one

$\overline{X}_A$ = sample mean of signal system two

N = number of study locations

S_B = standard deviation of signal system one

S_A = standard deviation of signal system two

If the calculated Pt-value is greater than the critical Pt-value obtained in available statistical tables, the difference in means is statistically significant with the degrees of freedom equal to the number of study locations less one.

Wilcoxon Signed Rank Test

If the assumption of normality was violated in the paired t-test, other statistical tests was performed to maintain a Type I error of 0.05 without infinitely increasing the Type II error or loss of power. If the assumption of normality was violated, the Wilcoxon Signed Rank Test was used. This statistical analysis tests the hypothesis that the signal systems have similar distributions for the measures of effectiveness. The first step in the procedure was to calculate the difference between the variables. Any difference of zero was ignored and the remaining number of variables was used as the sample size. The absolute values of the differences was then determined and ranks were assigned to each value. The sign of the differences was then

applied to the ranks. The following test statistic was calculated [22].

$$W = \frac{\sum R_i}{\sqrt{\sum R_i^2}}$$

Where:

R_i= the signed rank values

If there were no ties found among the absolute value differences, the following test statistic is calculated [22].

$$W = \frac{\left(\sqrt{6}\right)\sum R_i}{\sqrt{[n(n+1)(2n+1)]}}$$

Where:

R_i = the signed rank values

n = the final sample size

The null hypothesis, that the distributions were similar, was rejected if the absolute value of the Wilcoxon statistic exceeded the z-value of 1.96 based upon an alpha equal to 0.05.

TRAFFIC OPERATIONAL DATA COLLECTION

Travel Time Data and Travel Speed

The travel time and travel speed for the M-59 corridor were collected for two of the signal systems scenarios (MDOT pre-timed and SCATS). Travel time and travel speed studies were performed along M-59 on a typical weekday and Friday for the noon (12 PM to 1 PM) and PM (4 PM to 6 PM) peak periods, as well for a Saturday morning peak (9 AM to 11 AM). The travel data was collected using computerized equipment available from JAMAR Technologies. The travel data collection methods was based upon the 'Average Vehicle, Floating Car' method as outlined in the Institute of Transportation Engineers (ITE) Manual of Traffic Engineering Studies [19]. In this method, a two-person data collection team was used for each 'test vehicle'. One person was the driver and the second person operated the data recorder. The data recorder was responsible for recording travel time between consecutive signalized intersections, as well as recording of the types, number and location of stops and duration of the stopped time. In the 'Average Vehicle, Floating Car' method the driver of the test vehicle was instructed to pass as

many vehicles as vehicles that passed the test car. This ensured that the average position of the test vehicle in the traffic was maintained, and the measurements reflect average conditions within the traffic stream. The travel runs were conducted only on days in which the weather conditions were clear and dry.

The travel time and travel speed data collected by signal system, peak period and direction of travel for the typical weekday is documented in Table 3, for Friday in Table 4 and for Saturday in Table 5.

Table 3. Typical Weekday Travel Time and Travel Speed Data

Peak Period and Travel Time Run Number	MDOT Pre-timed System				SCATS System			
	Travel Time (sec)	Travel Speed (mph)	Travel Time (sec)	Travel Speed (mph)	Travel Time (sec)	Travel Speed (mph)	Travel Time (sec)	Travel Speed (mph)
Noon Peak Period	**Eastbound**		**Westbound**		**Eastbound**		**Westbound**	
1	457	31.2	438	32.3	359	39.7	407	34.9
2	458	31.1	343	41.3	409	35.0	430	33.0
3	399	35.7	442	32.0	363	39.4	381	37.3
4	437	32.5	437	32.4	328	43.5	403	35.2
5	450	31.7	414	34.2	342	41.7	340	41.5
6	441	32.3	346	40.9	358	39.7	411	34.5
7	363	39.3	381	37.2	370	38.7	360	39.4
8	341	41.9	356	39.7	430	33.3	431	33.0
9	437	32.7	366	35.2	412	34.5	367	38.6
10	419	34.0	371	38.1	442	32.4	415	34.2
11	414	34.5	252	35.8	370	38.5	424	33.4
12	427	33.4	387	36.4	388	36.8	394	36.1
13	N/A	N/A	N/A	N/A	440	32.5	373	38.1
14	N/A	N/A	N/A	N/A	386	37.1	449	31.4
15	N/A	N/A	N/A	N/A	N/A	N/A	398	35.7

Table 3. Typical Weekday Travel Time and Travel Speed Data (continued)

Peak Period and Travel Time Run Number	MDOT Pre-timed System				SCATS System			
	Travel Time (sec)	Travel Speed (mph)	Travel Time (sec)	Travel Speed (mph)	Travel Time (sec)	Travel Speed (mph)	Travel Time (sec)	Travel Speed (mph)
PM Peak Period	**Eastbound**		**Westbound**		**Eastbound**		**Westbound**	
1	426	33.5	467	30.3	421	33.8	414	34.2
2	460	30.9	542	26.1	330	43.0	427	33.2
3	431	33.1	457	31.0	397	35.9	430	32.9
4	305	46.6	452	31.3	408	34.9	446	31.8
5	394	36.2	479	29.6	386	37.0	341	41.5
6	440	32.4	463	30.6	476	29.9	438	32.3
7	456	31.3	388	36.5	366	38.9	345	41.1
8	420	33.9	405	34.9	376	37.9	436	32.4
9	510	28.0	493	28.7	404	35.3	446	31.8
10	409	34.8	480	29.5	420	33.9	495	28.6
11	397	35.9	434	32.5	398	35.8	436	32.4
12	415	34.4	501	28.3	323	44.1	451	31.4
13	N/A	N/A	N/A	N/A	431	33.0	467	30.2
14	N/A	N/A	N/A	N/A	391	36.4	473	29.9
15	N/A	N/A	N/A	N/A	408	34.9	N/A	N/A

Note: Travel time runs were not equal for each direction and scenario based upon the travel conditions in the field. Periods which experienced fewer travel time runs are designated by N/A.

Table 4. Friday Travel Time and Travel Speed Data

Peak Period and Travel Time Run Number	MDOT Pre-timed System				SCATS System			
	Travel Time (sec)	Travel Speed (mph)	Travel Time (sec)	Travel Speed (mph)	Travel Time (sec)	Travel Speed (mph)	Travel Time (sec)	Travel Speed (mph)
Noon Peak Period	**Eastbound**		**Westbound**		**Eastbound**		**Westbound**	
1	447	32.0	343	41.1	427	33.4	327	43.3
2	457	31.3	397	35.5	446	32.0	382	37.0
3	457	31.2	360	39.2	407	35.0	394	35.6
4	457	31.2	397	35.5	378	37.7	412	34.3
5	444	32.1	424	33.3	352	40.4	417	33.9

Table 4. Friday Travel Time and Travel Speed Data (continued)

Peak Period and Travel Time Run Number	MDOT Pre-timed System				SCATS System			
	Travel Time (sec)	Travel Speed (mph)	Travel Time (sec)	Travel Speed (mph)	Travel Time (sec)	Travel Speed (mph)	Travel Time (sec)	Travel Speed (mph)
Noon Peak Period	**Eastbound**		**Westbound**		**Eastbound**		**Westbound**	
6	455	31.3	464	30.4	N/A	N/A	N/A	N/A
7	438	32.5	346	40.8	N/A	N/A	N/A	N/A
8	411	34.7	414	34.1	N/A	N/A	N/A	N/A
9	427	33.4	392	35.9	N/A	N/A	N/A	N/A
10	412	34.6	378	37.4	N/A	N/A	N/A	N/A
11	423	33.8	391	36.1	N/A	N/A	N/A	N/A
12	437	32.6	403	35.1	N/A	N/A	N/A	N/A
13	N/A	N/A	371	38.0	N/A	N/A	N/A	N/A
PM Peak Period	**Eastbound**		**Westbound**		**Eastbound**		**Westbound**	
1	407	35.1	403	35.0	386	36.7	340	41.6
2	405	35.2	489	28.9	406	34.8	467	30.3
3	418	34.2	507	27.7	389	36.3	587	24.1
4	365	39.2	505	28.0	403	35.1	613	23.0
5	463	30.9	486	29.0	453	31.2	632	22.4
6	474	30.2	513	27.5	405	34.9	452	31.1
7	511	27.9	414	34.0	397	35.6	443	31.9
8	456	31.3	474	29.8	409	34.6	467	30.3
9	428	33.4	398	35.3	465	30.4	460	30.8
10	521	27.5	388	28.9	384	36.9	471	30.1
11	N/A	N/A	505	28.0	315	44.9	394	35.9
12	N/A	N/A	470	30.0	384	36.7	497	28.5
13	N/A	N/A	N/A	N/A	296	42.1	532	26.6
14	N/A	N/A	N/A	N/A	394	35.8	435	32.5
15	N/A	N/A	N/A	N/A	384	36.8	459	30.8
16	N/A	N/A	N/A	N/A	347	40.8	571	24.8

Note: Travel time runs were not equal for each direction and scenario based upon the travel conditions in the field. Periods which experienced fewer travel time runs are designated by N/A.

Table 5. Saturday Travel Time and Travel Speed Data

Travel Time Run Number	MDOT Pre-timed System				SCATS System			
	Travel Time (sec)	Travel Speed (mph)	Travel Time (sec)	Travel Speed (mph)	Travel Time (sec)	Travel Speed (mph)	Travel Time (sec)	Travel Speed (mph)
	Eastbound		Westbound		Eastbound		Westbound	
1	431	33.2	378	37.4	401	35.6	404	35.1
2	358	39.9	322	43.9	343	41.6	389	36.3
3	384	38.2	318	44.4	309	46.2	323	43.9
4	438	32.7	362	38.9	395	36.1	383	37.0
5	495	28.9	434	32.4	455	31.3	407	34.8
6	583	24.5	347	40.6	390	36.5	387	36.7
7	369	38.6	326	43.3	383	37.2	389	36.5
8	367	38.9	315	44.9	336	42.4	414	34.1
9	450	31.9	317	44.6	336	42.4	420	33.8
10	462	31.7	370	38.2	312	45.7	333	42.5
11	455	32.2	379	37.2	325	43.8	439	32.3

Note: Travel time runs were not equal for each direction and scenario based upon the travel conditions in the field. Periods which experienced fewer travel time runs are designated by N/A.

Fuel Consumption

The total fuel consumed per directional length of travel for the M-59 corridor was collected for two signal systems scenarios (MDOT pre-timed and SCATS). The data was collected in a similar manner as that of the travel time and travel speed data described in the previous section. The total fuel consumed data collected by signal system, peak period and direction of travel for the typical weekday is documented in Table 6, for Friday in Table 7 and for Saturday in Table 8.

Table 6. Typical Weekday Total Fuel Consumption Data

Peak Period and Travel Time Run Number	MDOT Pre-timed System		SCATS System	
	Fuel Consumption (gal)	Fuel Consumption (gal)	Fuel Consumption (gal)	Fuel Consumption (gal)
Noon Peak Period	**Eastbound**	**Westbound**	**Eastbound**	**Westbound**
1	0.2268	0.2209	0.1865	0.1970
2	0.2225	0.2109	0.2092	0.2094
3	0.2148	0.2231	0.2121	0.2041
4	0.2183	0.2226	0.2113	0.2170
5	0.2251	0.2106	0.1867	0.2058
6	0.2240	0.2199	0.2145	0.2102
7	0.2244	0.2249	0.2083	0.1923
8	0.2217	0.2219	0.2138	0.2265
9	0.2282	0.2182	0.2195	0.2084
10	0.2207	0.2313	0.2311	0.2128
11	0.2170	0.1482	0.1966	0.2010
12	0.2200	0.2148	0.2175	0.2256
13	N/A	N/A	0.2405	0.2101
14	N/A	N/A	0.2330	0.2306
15	N/A	N/A	N/A	0.2039
PM Peak Period	**Eastbound**	**Westbound**	**Eastbound**	**Westbound**
1	0.2140	0.2165	0.2302	0.2227
2	0.2147	0.2465	0.2055	0.2066
3	0.2293	0.2268	0.2170	0.2233
4	0.2010	0.2246	0.1995	0.2232
5	0.2286	0.2361	0.2019	0.2037
6	0.2401	0.2301	0.2292	0.2225
7	0.2383	0.2243	0.2016	0.1978
8	0.2264	0.2163	0.2151	0.2329

Table 6. Typical Weekday Total Fuel Consumption Data (continued)

Peak Period and Travel Time Run Number	MDOT Pre-timed System		SCATS System	
	Fuel Consumption (gal)	Fuel Consumption (gal)	Fuel Consumption (gal)	Fuel Consumption (gal)
PM Peak Period	**Eastbound**	**Westbound**	**Eastbound**	**Westbound**
9	0.2457	0.2339	0.2363	0.2197
10	0.2252	0.2188	0.2268	0.2224
11	0.2278	0.2257	0.2101	0.2149
12	0.2203	0.2336	0.1852	0.2144
13	N/A	N/A	0.2258	0.2235
14	N/A	N/A	0.2134	0.2180
15	N/A	N/A	0.2039	N/A

Note: Travel time runs were not equal for each direction and scenario based upon the travel conditions in the field. Periods which experienced fewer travel time runs are designated by N/A.

Table 7. Friday Total Fuel Consumption Data

Peak Period and Travel Time Run Number	MDOT Pre-timed System		SCATS System	
	Fuel Consumption (gal)	Fuel Consumption (gal)	Fuel Consumption (gal)	Fuel Consumption (gal)
Noon Peak Period	**Eastbound**	**Westbound**	**Eastbound**	**Westbound**
1	0.2292	0.2040	0.2115	0.1857
2	0.2087	0.2087	0.2347	0.2106
3	0.2123	0.1857	0.2217	0.2299
4	0.2410	0.2172	0.1951	0.2219
5	0.2405	0.2356	0.2133	0.2148
6	0.2184	0.2170	N/A	N/A
7	0.2297	0.2059	N/A	N/A
8	0.2358	0.2315	N/A	N/A
9	0.2315	0.2254	N/A	N/A
10	0.2211	0.2181	N/A	N/A
11	0.2322	0.2239	N/A	N/A
12	0.2252	0.2325	N/A	N/A
13	N/A	0.2179	N/A	N/A

Table 7. Friday Total Fuel Consumption Data (continued)

Peak Period and Travel Time Run Number	MDOT Pre-timed System		SCATS System	
	Fuel Consumption (gal)	Fuel Consumption (gal)	Fuel Consumption (gal)	Fuel Consumption (gal)
PM Peak Period	Eastbound	Westbound	Eastbound	Westbound
1	0.2253	0.2148	0.2143	0.1928
2	0.2273	0.2275	0.2187	0.2183
3	0.2271	0.2296	0.1986	0.2429
4	0.2070	0.2349	0.2102	0.2424
5	0.2295	0.2320	0.2165	0.2536
6	0.2447	0.2335	0.2270	0.2281
7	0.2250	0.2194	0.2169	0.2114
8	0.2209	0.2360	0.2013	0.2169
9	0.2094	0.2110	0.2347	0.2246
10	0.2323	0.2298	0.2166	0.2175
11	N/A	0.2235	0.2072	0.2076
12	N/A	0.2231	0.2327	0.2181
13	N/A	N/A	0.1710	0.2496
14	N/A	N/A	0.2258	0.2252
15	N/A	N/A	0.2227	0.2359
16	N/A	N/A	0.2095	0.2608

Note: Travel time runs were not equal for each direction and scenario based upon the travel conditions in the field. Periods which experienced fewer travel time runs are designated by N/A.

Table 8. Saturday Total Fuel Consumption Data

Travel Time Run Number	MDOT Pre-timed System		SCATS System	
	Fuel Consumption (gal)	Fuel Consumption (gal)	Fuel Consumption (gal)	Fuel Consumption (gal)
	Eastbound	Westbound	Eastbound	Westbound
1	0.2230	0.2032	0.2238	0.2099
2	0.2006	0.1769	0.2047	0.2340
3	0.2104	0.1833	0.2090	0.2175
4	0.2273	0.2086	0.2090	0.2014
5	0.2392	0.2374	0.2018	0.2437

Table 8. Saturday Total Fuel Consumption Data (continued)

Travel Time Run Number	MDOT Pre-timed System		SCATS System	
	Fuel Consumption (gal)	Fuel Consumption (gal)	Fuel Consumption (gal)	Fuel Consumption (gal)
	Eastbound	Westbound	Eastbound	Westbound
6	0.2450	0.2119	0.1976	0.2070
7	0.2035	0.1898	0.1925	0.2063
8	0.2180	0.1946	0.1877	0.1793
9	0.2316	0.1932	0.2059	0.2077
10	0.2417	0.2117	0.2084	0.2035
11	0.2257	0.2113	0.1905	0.1915

Note: Travel time runs were not equal for each direction and scenario based upon the travel conditions in the field. Periods which experienced fewer travel time runs are designated by N/A.

Emissions

The hydrocarbon, carbon monoxide and nitrogen oxide emissions for the M-59 corridor were collected, and measured in grams, for two signal systems scenarios (MDOT pre-timed and SCATS). The data was collected in a similar manner as that of the travel time and travel speed data described in the previous section. The hydrocarbon, carbon monoxide and nitrogen oxides emissions data collected by signal system, peak period and direction of travel for the typical weekday is documented in Tables 9 and 10, for Friday in Tables 11 and 12 and for Saturday in Tables 13 and 14.

Table 9. Typical Weekday Hydrocarbon and Carbon Monoxide Emissions Data

Peak Period and Travel Time Run Number	MDOT Pre-timed System				SCATS System			
	HC (gms)	CO (gms)	HC (gms)	CO (gms)	HC (gms)	CO (gms)	HC (gms)	CO (gms)
Noon Peak Period	Eastbound		Westbound		Eastbound		Westbound	
1	21.62	261.74	22.93	276.97	16.54	205.35	15.63	193.80
2	21.23	260.05	18.11	248.84	18.61	235.86	18.16	218.64
3	18.65	246.05	19.23	237.00	19.08	266.55	18.51	234.13
4	20.77	056.73	21.45	260.52	19.31	267.40	20.94	253.63
5	22.62	271.79	19.56	246.41	15.46	200.46	16.42	213.00
6	20.15	250.12	19.63	269.98	17.64	249.55	19.60	253.42
7	18.85	271.45	21.95	290.46	17.95	246.07	16.24	213.51

Table 9. Typical Weekday Hydrocarbon and Carbon Monoxide Emissions Data (continued)

Peak Period and Travel Time Run Number	MDOT Pre-timed System				SCATS System			
	HC (gms)	CO (gms)	HC (gms)	CO (gms)	HC (gms)	CO (gms)	HC (gms)	CO (gms)
Noon Peak Period	**Eastbound**		**Westbound**		**Eastbound**		**Westbound**	
8	16.95	251.05	21.06	284.76	21.27	251.42	20.70	266.37
9	21.83	277.96	23.34	304.52	19.03	254.28	18.59	258.47
10	18.95	253.00	19.06	239.00	22.35	276.01	20.31	257.27
11	17.64	223.14	14.58	190.50	15.16	193.98	15.83	196.46
12	18.90	232.87	19.43	241.56	20.03	268.68	20.04	249.06
13	N/A	N/A	N/A	N/A	23.31	304.59	19.29	249.58
14	N/A	N/A	N/A	N/A	21.28	278.04	21.55	266.63
15	N/A	N/A	N/A	N/A	N/A	N/A	16.92	205.23
PM Peak Period	**Eastbound**		**Westbound**		**Eastbound**		**Westbound**	
1	20.57	244.04	18.92	231.56	21.99	263.69	19.40	249.63
2	20.55	233.99	24.02	288.28	16.91	225.57	17.64	213.73
3	22.78	275.55	20.98	267.25	19.49	250.62	20.84	265.41
4	16.09	229.69	20.54	265.92	18.05	221.20	21.28	267.39
5	20.40	294.33	21.61	273.09	17.49	233.04	17.62	231.83
6	24.06	294.09	20.57	267.53	20.82	260.81	21.19	271.33
7	23.92	299.16	20.36	283.07	16.86	221.21	16.19	211.31
8	21.34	260.69	19.17	244.00	21.14	278.04	21.01	259.76
9	23.88	283.84	23.52	281.22	24.38	326.19	21.02	248.01
10	18.41	236.57	19.92	228.15	21.08	280.42	19.38	227.15
11	21.25	285.12	19.72	255.23	19.45	233.66	18.29	218.99
12	18.36	233.45	22.16	254.12	13.55	185.62	18.86	230.58
13	N/A	N/A	N/A	N/A	21.40	259.53	19.97	230.20
14	N/A	N/A	N/A	N/A	18.05	235.90	19.19	220.00
15	N/A	N/A	N/A	N/A	19.43	239.39	N/A	N/A

Note: Travel time runs were not equal for each direction and scenario based upon the travel conditions in the field. Periods which experienced fewer travel time runs are designated by N/A.

Table 10. Typical Weekday Nitrogen Oxide Emissions Data

Peak Period and Travel Time Run Number	MDOT Pre-timed System		SCATS System	
	NOx (gms)	NOx (gms)	NOx (gms)	NOx (gms)
Noon Peak Period	**Eastbound**	**Westbound**	**Eastbound**	**Westbound**
1	13.83	15.45	10.37	8.49
2	13.34	11.65	11.41	10.84
3	11.41	11.48	12.22	11.92
4	13.25	13.98	13.10	14.20
5	15.10	12.28	9.37	10.31
6	12.44	13.10	10.72	12.28
7	11.73	15.06	11.04	9.80
8	10.17	14.49	14.21	12.99
9	14.19	16.78	11.43	11.62
10	11.33	12.64	14.74	13.03
11	10.34	10.03	8.56	8.39
12	11.59	12.72	12.83	13.20
13	N/A	N/A	15.34	12.69
14	N/A	N/A	14.25	13.74
15	N/A	N/A	N/A	10.12
PM Peak Period	**Eastbound**	**Westbound**	**Eastbound**	**Westbound**
1	13.57	10.85	14.94	11.94
2	13.09	14.79	10.90	10.32
3	15.57	12.84	12.46	13.23
4	10.17	12.43	11.16	13.51
5	12.63	13.13	10.48	11.45
6	16.57	12.19	12.47	13.46
7	16.15	13.06	10.31	9.98
8	14.27	12.00	14.40	13.32
9	15.26	15.37	17.01	13.58
10	11.08	11.96	13.42	10.94
11	13.98	11.87	12.76	10.84
12	11.02	13.94	7.58	11.07
13	N/A	N/A	14.08	12.18
14	N/A	N/A	11.00	11.35
15	N/A	N/A	12.57	N/A

Table 11. Friday Hydrocarbon and Carbon Monoxide Emissions Data

Peak Period and Travel Time Run Number	MDOT Pre-timed System				SCATS System			
	HC (gms)	CO (gms)	HC (gms)	CO (gms)	HC (gms)	CO (gms)	HC (gms)	CO (gms)
Noon Peak Period	**Eastbound**		**Westbound**		**Eastbound**		**Westbound**	
1	20.99	266.85	16.69	218.54	19.02	217.08	13.74	171.83
2	19.39	216.47	17.37	219.83	21.33	284.23	18.86	252.00
3	18.47	216.31	14.30	165.80	21.58	278.61	22.89	302.11
4	22.09	285.62	20.25	255.74	17.06	217.96	21.15	274.88
5	20.38	263.56	23.08	306.38	19.10	250.42	18.11	227.97
6	19.04	231.29	20.59	233.67	N/A	N/A	N/A	N/A
7	20.29	252.31	19.54	262.03	N/A	N/A	N/A	N/A
8	21.66	295.22	21.37	275.01	N/A	N/A	N/A	N/A
9	22.43	303.97	22.00	286.84	N/A	N/A	N/A	N/A
10	20.10	267.23	19.71	252.44	N/A	N/A	N/A	N/A
11	20.70	269.38	20.02	258.33	N/A	N/A	N/A	N/A
12	19.20	237.66	22.47	297.38	N/A	N/A	N/A	N/A
13	N/A	N/A	19.13	246.07	N/A	N/A	N/A	N/A
PM Peak Period	**Eastbound**		**Westbound**		**Eastbound**		**Westbound**	
1	19.89	250.14	18.28	231.05	17.54	235.45	16.03	202.21
2	22.03	293.55	20.96	252.04	21.05	260.85	19.34	223.59
3	18.25	233.40	19.90	227.98	17.11	209.27	23.74	253.80
4	17.89	236.14	21.97	253.64	19.38	243.25	26.66	240.54
5	23.38	268.95	22.16	275.03	19.04	231.31	25.27	258.76
6	24.43	288.42	23.09	268.26	22.43	272.03	22.47	278.90
7	20.04	224.06	17.79	233.20	21.26	268.17	19.42	235.27
8	21.60	242.01	23.09	288.84	17.60	213.41	20.14	238.89
9	19.39	225.09	17.59	220.01	22.18	293.38	21.37	257.07
10	21.10	241.08	22.33	279.96	19.19	256.57	19.99	229.46
11	N/A	N/A	22.39	245.56	16.77	240.59	18.31	242.10
12	N/A	N/A	19.46	239.08	21.73	305.61	20.73	234.87
13	N/A	N/A	N/A	N/A	15.05	201.87	24.81	296.63
14	N/A	N/A	N/A	N/A	21.59	289.79	20.30	258.05
15	N/A	N/A	N/A	N/A	20.06	262.40	23.17	294.43
16	N/A	N/A	N/A	N/A	17.77	249.66	25.83	283.98

Note: Travel time runs were not equal for each direction and scenario based upon the travel conditions in the field. Periods which experienced fewer travel time runs are designated by N/A.

Table 12. Friday Nitrogen Oxide Emissions Data

Peak Period and Travel Time Run Number	MDOT Pre-timed System		SCATS System	
	NOx (gms)	NOx (gms)	NOx (gms)	NOx (gms)
Noon Peak Period	**Eastbound**	**Westbound**	**Eastbound**	**Westbound**
1	13.10	10.45	11.99	7.98
2	12.03	10.33	13.13	11.84
3	10.70	8.23	14.35	15.70
4	13.81	13.31	10.44	13.78
5	12.42	15.35	12.73	10.77
6	11.23	13.04	N/A	N/A
7	12.61	13.22	N/A	N/A
8	13.97	13.92	N/A	N/A
9	14.54	14.97	N/A	N/A
10	12.57	13.00	N/A	N/A
11	13.06	13.01	N/A	N/A
12	11.64	15.11	N/A	N/A
13	N/A	12.53	N/A	N/A
PM Peak Period	**Eastbound**	**Westbound**	**Eastbound**	**Westbound**
1	12.81	11.16	10.44	10.03
2	14.63	12.60	14.05	11.59
3	10.79	11.39	10.48	14.39
4	11.32	13.61	12.38	14.16
5	15.96	13.72	11.25	15.45
6	16.64	14.60	15.63	14.68
7	11.63	10.25	14.34	11.87
8	14.36	14.75	10.69	12.30
9	12.40	10.60	13.74	13.56
10	12.43	13.99	12.12	12.25
11	N/A	14.38	10.61	11.14
12	N/A	11.26	14.24	12.58
13	N/A	N/A	9.66	15.75
14	N/A	N/A	14.31	12.62
15	N/A	N/A	13.11	15.03
16	N/A	N/A	11.20	16.66

Note: Travel time runs were not equal for each direction and scenario based upon the travel conditions in the field. Periods which experienced fewer travel time runs are designated by N/A.

Table 13. Saturday Hydrocarbon and Carbon Monoxide Emissions Data

Travel Time Run Number	MDOT Pre-timed System				SCATS System			
	HC (gms)	CO (gms)	HC (gms)	CO (gms)	HC (gms)	CO (gms)	HC (gms)	CO (gms)
	Eastbound		Westbound		Eastbound		Westbound	
1	18.51	229.47	15.73	204.34	20.17	261.63	17.92	229.74
2	15.92	205.56	12.19	155.82	17.27	228.37	22.75	293.05
3	16.82	204.42	13.73	184.13	17.62	244.37	19.08	234.89
4	20.32	265.37	17.94	230.95	18.27	269.36	15.46	212.50
5	23.70	276.27	22.42	290.80	17.27	234.78	23.84	318.79
6	21.91	241.02	18.65	244.51	16.27	198.68	16.19	206.36
7	17.58	214.69	15.04	199.91	15.93	203.75	16.83	210.58
8	18.69	249.39	14.75	193.61	13.61	189.92	12.75	170.25
9	20.07	251.58	15.74	214.42	17.10	220.93	16.65	212.62
10	22.67	287.99	18.32	228.58	18.18	209.84	16.37	189.04
11	20.28	244.67	18.96	235.09	15.03	181.35	16.63	190.27

Note: Travel time runs were not equal for each direction and scenario based upon the travel conditions in the field. Periods which experienced fewer travel time runs are designated by N/A.

Table 14. Saturday Nitrogen Oxide Emissions Data

Travel Time Run Number	MDOT Pre-timed System		SCATS System	
	NOx (gms)	NOx (gms)	NOx (gms)	NOx (gms)
	Eastbound	Westbound	Eastbound	Westbound
1	10.95	8.89	13.29	11.04
2	9.53	6.44	11.19	15.41
3	10.10	7.88	11.30	11.83
4	12.42	11.45	11.97	9.25
5	15.57	14.53	11.27	15.78
6	12.48	12.38	9.38	8.99
7	11.35	9.12	9.89	9.99
8	11.95	9.03	7.79	6.84
9	12.24	9.86	10.02	9.87
10	14.45	11.85	10.59	9.59
11	12.47	12.42	8.28	10.26

Note: Travel time runs were not equal for each direction and scenario based upon the travel conditions in the field. Periods which experienced fewer travel time runs are designated by N/A.

Number of Stops and Total Delay

The number of stops and total delay for the M-59 corridor were collected for two signal systems scenarios (MDOT pre-timed and SCATS). The data was collected in a similar manner as that of the travel time and travel speed data described in the previous section. The number of stops and total delay data collected by signal system, peak period and direction of travel for the typical weekday is documented in Table 15, for Friday in Table 16 and for Saturday in Table 17.

Table 15. Typical Weekday Number of Stops and Total Delay Data

Peak Period and Travel Time Run Number	MDOT Pre-timed System				SCATS System			
	No. of Stops	Total Delay (sec)	No. of Stops	Total Delay (sec)	No. of Stops	Total Delay (sec)	No. of Stops	Total Delay (sec)
Noon Peak Period	**Eastbound**		**Westbound**		**Eastbound**		**Westbound**	
1	3	171	2	153	0	73	2	121
2	4	171	2	60	2	122	3	145
3	2	112	3	159	1	76	2	95
4	3	152	3	154	1	41	3	119
5	3	164	2	129	0	55	1	61
6	3	154	2	66	1	73	1	126
7	1	80	3	95	1	83	1	74
8	2	69	2	73	2	143	3	146
9	5	151	3	107	2	127	1	82
10	3	133	3	87	5	155	2	129
11	3	132	2	71	1	84	2	139
12	4	141	3	103	1	101	4	109
13	N/A	N/A	N/A	N/A	4	153	2	87
14	N/A	N/A	N/A	N/A	4	98	3	164
15	N/A	N/A	N/A	N/A	N/A	N/A	3	111
PM Peak Period	**Eastbound**		**Westbound**		**Eastbound**		**Westbound**	
1	4	140	3	184	4	134	2	132
2	3	175	6	257	1	43	3	144
3	3	145	3	172	2	112	3	145
4	0	21	3	168	2	121	3	161
5	2	108	4	195	1	101	1	58
6	3	153	3	179	3	190	3	153

Table 15. Typical Weekday Number of Stops and Total Delay Data (continued)

Peak Period and Travel Time Run Number	MDOT Pre-timed System				SCATS System			
	No. of Stops	Total Delay (sec)	No. of Stops	Total Delay (sec)	No. of Stops	Total Delay (sec)	No. of Stops	Total Delay (sec)
PM Peak Period	**Eastbound**		**Westbound**		**Eastbound**		**Westbound**	
7	5	170	2	108	2	81	2	60
8	3	133	2	121	1	90	2	152
9	5	224	5	209	3	118	3	161
10	3	122	4	195	2	134	4	211
11	3	111	2	152	1	111	3	151
12	3	132	6	219	1	36	2	166
13	N/A	N/A	N/A	N/A	4	145	5	183
14	N/A	N/A	N/A	N/A	2	106	4	189
15	N/A	N/A	N/A	N/A	2	122	N/A	N/A

Table 16. Friday Number of Stops and Total Delay Data

Peak Period and Travel Time Run Number	MDOT Pre-timed System				SCATS System			
	No. of Stops	Total Delay (sec)	No. of Stops	Total Delay (sec)	No. of Stops	Total Delay (sec)	No. of Stops	Total Delay (sec)
Noon Peak Period	**Eastbound**		**Westbound**		**Eastbound**		**Westbound**	
1	2	159	2	60	3	141	0	43
2	3	170	2	115	3	160	1	97
3	2	170	2	75	2	120	3	110
4	2	170	2	115	1	90	2	127
5	4	163	4	141	2	66	2	132
6	3	173	4	180	N/A	N/A	N/A	N/A
7	3	151	2	63	N/A	N/A	N/A	N/A
8	2	124	3	132	N/A	N/A	N/A	N/A
9	2	140	3	111	N/A	N/A	N/A	N/A
10	2	125	3	94	N/A	N/A	N/A	N/A
11	3	136	3	107	N/A	N/A	N/A	N/A
12	4	151	3	119	N/A	N/A	N/A	N/A
13	N/A	N/A	3	87	N/A	N/A	N/A	N/A

Table 16. Friday Number of Stops and Total Delay Data (continued)

Peak Period and Travel Time Run Number	MDOT Pre-timed System				SCATS System			
	No. of Stops	Total Delay (sec)	No. of Stops	Total Delay (sec)	No. of Stops	Total Delay (sec)	No. of Stops	Total Delay (sec)
PM Peak Period	**Eastbound**		**Westbound**		**Eastbound**		**Westbound**	
1	4	121	2	123	2	101	1	55
2	3	119	4	207	1	123	3	181
3	3	131	5	229	2	105	6	303
4	1	78	6	220	2	119	8	327
5	5	176	4	202	2	168	8	349
6	6	187	5	230	3	122	3	169
7	3	223	3	130	1	113	2	159
8	6	169	3	191	2	124	3	183
9	4	141	3	119	3	182	4	174
10	4	233	4	204	2	100	4	186
11	N/A	N/A	5	223	1	32	1	110
12	N/A	N/A	3	188	2	104	3	213
13	N/A	N/A	N/A	N/A	0	46	5	247
14	N/A	N/A	N/A	N/A	3	111	3	150
15	N/A	N/A	N/A	N/A	3	101	4	176
16	N/A	N/A	N/A	N/A	2	63	8	286

Note: Travel time runs were not equal for each direction and scenario based upon the travel conditions in the field. Periods which experienced fewer travel time runs are designated by N/A.

Table 17. Saturday Number of Stops and Total Delay Data

Travel Time Run Number	MDOT Pre-timed System				SCATS System			
	No. of Stops	Total Delay (sec)	No. of Stops	Total Delay (sec)	No. of Stops	Total Delay (sec)	No. of Stops	Total Delay (sec)
	Eastbound		**Westbound**		**Eastbound**		**Westbound**	
1	3	143	2	94	2	96	2	105
2	2	71	0	38	1	49	3	129
3	3	88	0	35	2	49	3	135
4	3	151	2	78	0	27	2	50
5	3	207	3	151	0	40	3	154

Table 17. Saturday Number of Stops and Total Delay Data (continued)

Travel Time Run Number	MDOT Pre-timed System				SCATS System			
	No. of Stops	Total Delay (sec)	No. of Stops	Total Delay (sec)	No. of Stops	Total Delay (sec)	No. of Stops	Total Delay (sec)
	Eastbound		Westbound		Eastbound		Westbound	
6	9	295	2	64	2	115	2	119
7	3	83	1	42	1	56	2	105
8	2	80	0	31	0	26	0	37
9	5	160	0	32	2	109	2	100
10	3	167	2	88	3	168	3	122
11	2	162	2	96	1	104	1	101

Note: Travel time runs were not equal for each direction and scenario based upon the travel conditions in the field. Periods which experienced fewer travel time runs are designated by N/A.

Number of Stopped Vehicles

The number of stopped vehicles data was collected for two signal systems scenarios (MDOT pre-timed and SCATS). The number of stopped vehicles was selected as a surrogate measure for intersection delay. Intersection delay is calculated by dividing the cumulative number of stopped vehicles collected in all specified intervals for a peak period by the volume for each critical lane group, such as through or left turn movements, and multiplying by the interval of the data collection period. In order to accurately collect the intersection delay, the volume of each critical lane group would be needed for each day of the data collection as traffic volumes along a roadway can vary substantially by day. Therefore, the number of stopped vehicles was utilized as a surrogate measure for intersection delay. The number of stopped vehicles was collected along M-59 on a typical weekday and Friday for the noon (12 PM to 1 PM) and PM (4 PM to 6 PM) peak periods, as well for a Saturday morning peak (9 AM to 11 AM). The number of stopped vehicles were collected by critical lane group, left turn or through movements, for each of the six intersections studied along the M-59 corridor. The interval selected for data collection was 15 seconds for through movements and 60 seconds for left turn movements. Therefore, the total number of stopped vehicles is the summation of the number of vehicles observed stopped during each interval observed.

The number of stopped vehicles collected by signal system, peak period and direction of travel for the MDOT pre-timed system data is documented in Table 18, and for the SCATS system data in Table 19.

Table 18. MDOT Pre-timed System Number of Stopped Vehicles Data

Intersection by Approach and Movement	Number of Stopped Vehicles During Peak Period				
	Weekday Noon Peak Period	Weekday PM Peak Period	Friday Noon Peak Period	Friday PM Peak Period	Saturday Peak Period
Pontiac Lake West Road					
EB Left Turn	70	66	98	173	52
EB Through	397	403	316	535	381
WB Left Turn	123	221	286	656	99
WB Through	105	420	192	231	143
NB Left Turn	5	15	6	24	8
NB Through	68	128	346	1141	21
SB Left Turn	0	5	6	1	5
SB Through	62	82	177	354	147
Williams Lake Road					
EB Left Turn	125	186	124	180	121
EB Through	886	1587	536	1418	672
WB Left Turn	33	26	12	40	17
WB Through	1249	1753	1230	1921	1009
NB Left Turn	164	417	310	575	231
NB Through	216	395	376	1274	398
SB Left Turn	115	80	116	77	41
SB Through	677	1808	519	1259	990
Oakland Boulevard					
EB Left Turn	157	119	260	186	22
EB Through	782	846	740	683	592
WB Left Turn	160	192	215	223	17
WB Through	516	1211	650	767	457
NB Left Turn	74	127	111	121	22
NB Through	220	190	143	196	91
SB Left Turn	118	157	164	170	21
SB Through	212	206	150	174	118

Table 18. MDOT Pre-timed System Number of Stopped Vehicles Data (continued)

Intersection by Approach and Movement	Number of Stopped Vehicles During Peak Period				
	Weekday Noon Peak Period	Weekday PM Peak Period	Friday Noon Peak Period	Friday PM Peak Period	Saturday Peak Period
Airport Road					
EB Left Turn	270	451	219	403	198
EB Through	1599	3087	1647	2045	1107
WB Left Turn	105	64	53	98	43
WB Through	904	3788	966	2157	720
NB Left Turn	286	370	520	700	117
NB Through	1177	4443	1346	4915	559
SB Left Turn	92	61	42	74	39
SB Through	961	1981	1039	2965	523
Crescent Lake Road					
EB Left Turn	162	489	304	504	127
EB Through	2920	1746	1289	456	743
WB Left Turn	117	122	62	238	44
WB Through	2255	5033	2234	9286	962
NB Left Turn	130	151	111	380	49
NB Through	457	134	500	959	270
SB Left Turn	71	93	73	127	40
SB Through	769	3137	955	1661	269
Pontiac Lake East Road					
EB Left Turn	96	98	88	162	37
EB Through	1254	1099	1498	926	1541
WB Left Turn	24	16	17	27	6
WB Through	2011	7936	3537	6383	840
NB Left Turn	306	287	395	576	335
NB Through	1106	1582	565	1736	470
SB Left Turn	96	210	98	108	68
SB Through	1516	4376	1632	3299	590

Table 19. SCATS System Number of Stopped Vehicles Data

Intersection by Approach and Movement	Number of Stopped Vehicles During Peak Period				
	Weekday Noon Peak Period	Weekday PM Peak Period	Friday Noon Peak Period	Friday PM Peak Period	Saturday Peak Period
Pontiac Lake West Road					
EB Left Turn	48	38	42	37	14
EB Through	441	411	877	584	459
WB Left Turn	3	1	9	3	0
WB Through	220	393	891	415	476
NB Left Turn	131	345	113	283	42
NB Through	14	139	376	99	13
SB Left Turn	4	6	2	11	2
SB Through	80	59	71	38	117
Williams Lake Road					
EB Left Turn	101	218	99	151	140
EB Through	1195	1357	1330	1596	1143
WB Left Turn	24	23	24	27	15
WB Through	1101	2101	1183	2290	1633
NB Left Turn	195	239	215	319	196
NB Through	497	1011	622	1095	730
SB Left Turn	93	128	94	107	113
SB Through	283	772	404	1162	1213
Oakland Boulevard					
EB Left Turn	57	49	52	71	13
EB Through	224	331	263	316	112
WB Left Turn	63	52	43	63	50
WB Through	144	92	156	206	91
NB Left Turn	6	121	16	24	10
NB Through	24	113	61	90	74
SB Left Turn	3	18	50	28	15
SB Through	354	436	92	114	148

Table 19. SCATS System Number of Stopped Vehicles Data (continued)

Intersection by Approach and Movement	Number of Stopped Vehicles During Peak Period				
	Weekday Noon Peak Period	Weekday PM Peak Period	Friday Noon Peak Period	Friday PM Peak Period	Saturday Peak Period
Airport Road					
EB Left Turn	455	384	351	468	179
EB Through	2053	1757	1334	1593	1001
WB Left Turn	81	98	82	120	40
WB Through	2177	3783	2590	4642	1367
NB Left Turn	340	792	251	571	132
NB Through	1049	2354	1217	1912	712
SB Left Turn	52	55	81	79	45
SB Through	1149	1463	954	2452	605
Crescent Lake Road					
EB Left Turn	176	396	209	521	170
EB Through	1705	1387	1575	1826	1004
WB Left Turn	164	115	129	154	63
WB Through	2165	4510	1816	5008	1258
NB Left Turn	152	200	161	184	65
NB Through	779	2208	789	2860	421
SB Left Turn	81	99	75	119	52
SB Through	987	1792	1624	5396	576
Pontiac Lake East Road					
EB Left Turn	80	102	120	121	62
EB Through	1509	2038	2443	2673	907
WB Left Turn	21	27	25	20	22
WB Through	2234	6073	2056	5269	1702
NB Left Turn	365	300	418	459	233
NB Through	806	982	1362	2433	834
SB Left Turn	68	184	94	183	56
SB Through	1461	3103	1479	4676	774

Queue Length

The maximum queue length for each approach's movement for each intersection along M-59 was collected for a typical weekday and Friday for the noon (12 PM to 1 PM) and PM (4 PM to 6 PM) peak periods, as well for a Saturday morning peak (9 AM to 11 AM). The queue length was collected every 15 seconds for each critical lane group, left turn and through movements, to determine the extent of the overflow of vehicles at the intersection. Any vehicle stopped or traveling less than five miles per hour was considered a part of the queue. Due to variation in traffic volumes during a peak period, at least a 60 minute time period was recorded for each approach.

The maximum queue length collected by signal system, peak period and direction of travel for the MDOT pre-timed system data is documented in Table 20, and for the SCATS system data in Table 21.

Table 20. MDOT Pre-timed System Maximum Queue Length Data

Intersection by Approach and Movement	Maximum Queue Length in Vehicles During Peak Period				
	Weekday Noon Peak Period	Weekday PM Peak Period	Friday Noon Peak Period	Friday PM Peak Period	Saturday Peak Period
Pontiac Lake West Road					
EB Left Turn	5	5	6	11	3
EB Through	26	25	15	22	13
WB Left Turn	9	12	9	18	6
WB Through	7	14	16	14	8
NB Left Turn	2	2	2	2	1
NB Through	6	4	10	22	2
SB Left Turn	0	1	6	1	1
SB Through	3	2	9	8	5
Williams Lake Road					
EB Left Turn	8	9	7	7	7
EB Through	20	32	14	32	18
WB Left Turn	3	2	3	3	3
WB Through	22	32	38	28	18
NB Left Turn	10	19	15	26	12
NB Through	8	12	23	22	8
SB Left Turn	5	6	8	5	3
SB Through	14	29	10	35	16

Table 20. MDOT Pre-timed System Maximum Queue Length Data (continued)

Intersection by Approach and Movement	Maximum Queue Length in Vehicles During Peak Period				
	Weekday Noon Peak Period	Weekday PM Peak Period	Friday Noon Peak Period	Friday PM Peak Period	Saturday Peak Period
Oakland Boulevard					
EB Left Turn	9	4	5	5	3
EB Through	29	33	26	26	27
WB Left Turn	5	4	4	5	4
WB Through	22	35	20	27	20
NB Left Turn	2	3	4	4	3
NB Through	6	5	5	7	3
SB Left Turn	4	5	4	4	4
SB Through	8	6	4	5	12
Airport Road					
EB Left Turn	14	16	14	15	9
EB Through	28	48	31	36	25
WB Left Turn	10	4	5	8	4
WB Through	18	52	19	28	28
NB Left Turn	20	16	20	23	6
NB Through	14	31	16	37	10
SB Left Turn	5	5	3	6	6
SB Through	17	31	15	123	12
Crescent Lake Road					
EB Left Turn	9	17	14	22	10
EB Through	39	29	20	11	20
WB Left Turn	7	11	5	11	3
WB Through	39	67	40	92	28
NB Left Turn	8	11	7	16	6
NB Through	13	5	8	14	8
SB Left Turn	5	7	6	8	4
SB Through	17	30	14	22	7

Table 20. MDOT Pre-timed System Maximum Queue Length Data (continued)

Intersection by Approach and Movement	Maximum Queue Length in Vehicles During Peak Period				
	Weekday Noon Peak Period	Weekday PM Peak Period	Friday Noon Peak Period	Friday PM Peak Period	Saturday Peak Period
Pontiac Lake East Road					
EB Left Turn	9	5	4	7	6
EB Through	21	33	26	23	20
WB Left Turn	2	2	4	4	1
WB Through	35	67	35	49	18
NB Left Turn	15	14	16	25	17
NB Through	16	20	11	21	10
SB Left Turn	7	11	7	8	5
SB Through	18	32	20	29	13

Table 21. SCATS System Maximum Queue Length Data

Intersection by Approach and Movement	Maximum Queue Length in Vehicles During Peak Period				
	Weekday Noon Peak Period	Weekday PM Peak Period	Friday Noon Peak Period	Friday PM Peak Period	Saturday Peak Period
Pontiac Lake West Road					
EB Left Turn	4	3	3	3	2
EB Through	19	13	18	15	12
WB Left Turn	1	1	1	1	0
WB Through	12	20	20	18	21
NB Left Turn	8	14	7	13	4
NB Through	3	4	12	3	1
SB Left Turn	1	1	1	8	2
SB Through	5	8	2	2	5

Table 21. SCATS System Maximum Queue Length Data (continued)

Intersection by Approach and Movement	Maximum Queue Length in Vehicles During Peak Period				
	Weekday Noon Peak Period	Weekday PM Peak Period	Friday Noon Peak Period	Friday PM Peak Period	Saturday Peak Period
Williams Lake Road					
EB Left Turn	6	16	6	17	7
EB Through	26	38	36	34	19
WB Left Turn	3	2	4	2	2
WB Through	21	31	21	33	30
NB Left Turn	11	17	18	24	10
NB Through	12	17	16	22	14
SB Left Turn	9	9	8	11	8
SB Through	8	14	11	18	13
Oakland Boulevard					
EB Left Turn	3	4	5	5	2
EB Through	10	16	12	15	10
WB Left Turn	4	4	3	5	30
WB Through	12	11	11	14	12
NB Left Turn	2	2	3	3	2
NB Through	1	4	3	4	3
SB Left Turn	1	3	10	3	2
SB Through	7	7	4	4	3
Airport Road					
EB Left Turn	21	22	28	29	8
EB Through	30	32	27	35	25
WB Left Turn	7	6	5	7	4
WB Through	34	48	39	51	26
NB Left Turn	14	24	12	27	10
NB Through	14	30	19	22	11
SB Left Turn	4	4	7	5	2
SB Through	19	23	19	38	15

Table 21. SCATS System Maximum Queue Length Data (continued)

Intersection by Approach and Movement	Maximum Queue Length in Vehicles During Peak Period				
	Weekday Noon Peak Period	Weekday PM Peak Period	Friday Noon Peak Period	Friday PM Peak Period	Saturday Peak Period
Crescent Lake Road					
EB Left Turn	12	14	13	21	10
EB Through	32	34	25	30	20
WB Left Turn	9	7	9	9	6
WB Through	31	42	27	44	29
NB Left Turn	8	10	9	9	5
NB Through	13	32	14	33	9
SB Left Turn	9	7	9	5	4
SB Through	14	21	27	41	13
Pontiac Lake East Road					
EB Left Turn	6	7	8	7	5
EB Through	33	41	36	35	23
WB Left Turn	2	2	4	2	4
WB Through	29	46	43	64	110
NB Left Turn	16	15	18	19	16
NB Through	13	14	19	28	15
SB Left Turn	8	11	6	13	4
SB Through	21	36	20	44	16

TRAFFIC OPERATIONAL DATA STATISTICAL ANALYSIS

The statistical significance of the effectiveness of the two signal systems (SCATS and the MDOT pre-timed system) were examined to determine whether the changes observed in the measures of effectiveness were attributable to the signal system or chance.

The dependant variable for the statistical tests was the measure of effectiveness while the independent variable was the type of signal system. The dependant variables were considered continuous data or data assuming a range of numerical values. The independent variable was considered discrete and categorical data described by the data belonging to only one group; SCATS or the MDOT pre-timed system.

Statistical tests were conducted to determine the effectiveness of the signal systems for each dependant variable. Due to the assumptions associated with the various statistical tests, the normality of the data and the homogeneity of the variances were examined for each dependant variable.

The statistical analysis is detailed in the following sections, respectively, for each measure of effectiveness including the following:

- Travel time for the corridor
- Travel speed for the corridor
- Travel time total delay for the corridor
- Fuel consumption
- Hydrocarbon, carbon monoxide and nitrogen oxide emissions
- Number of stops along the corridor
- Number of vehicles stopped at the intersections for the corridor and side streets
- Maximum queue length at the intersections for the corridor and side streets

Travel Time Analysis

The travel time data was categorized by eastbound and westbound travel in addition to overall travel (eastbound and westbound combined) for each of the two signal systems; SCATS and the MDOT pre-timed system. The mean travel times for each direction of travel as well as for the overall travel are shown graphically in Figures 2 through 4.

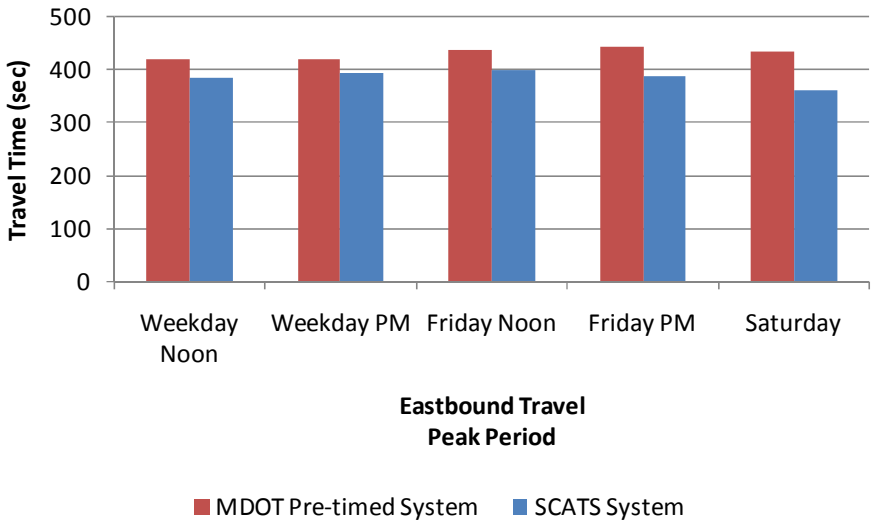

Figure 2. Eastbound Mean Travel Time By Peak Period

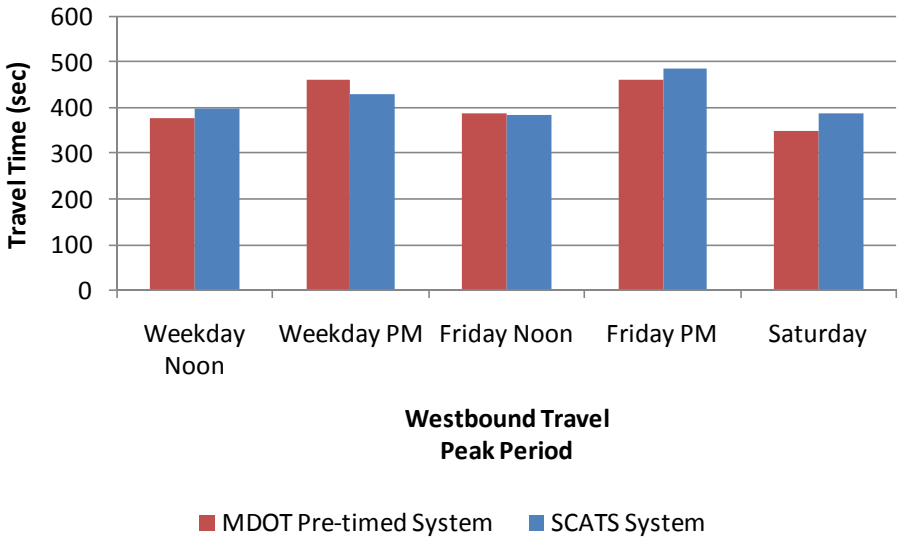

Figure 3. Westbound Mean Travel Time By Peak Period

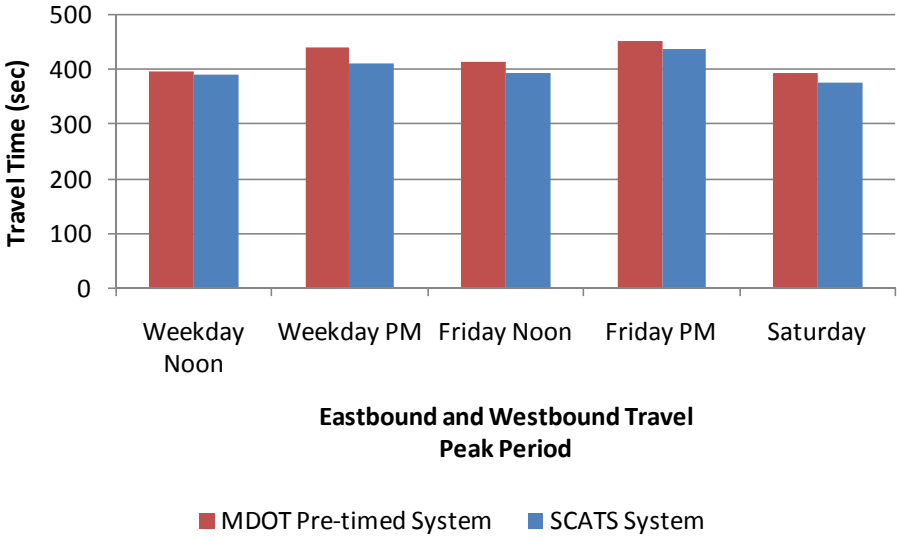

Figure 4. Overall Mean Travel Time By Peak Period

Statistical data calculated, including the mean travel time, standard deviation, are shown in Table 22. A negative value for the percent difference in mean travel time indicates that the travel time in the MDOT pre-timed system was faster than that in the SCATS system. A positive value for the percent difference in mean travel time indicates that the travel time in the SCATS system was faster than that in the MDOT pre-timed system.

Table 22. Travel Time Statistical Data

Day, Peak Period and Direction of Travel	MDOT Pre-timed System		SCATS System		Percent Difference in Mean Travel Time
	Mean Travel Time (sec)	Standard Deviation	Mean Travel Time (sec)	Standard Deviation	
Weekday Noon Peak					
Eastbound	420.25	36.62	385.5	36.21	8.27%
Westbound	377.75	53.40	398.87	30.05	-5.59%
Total	399.00	49.76	392.41	33.27	1.65%
Weekday PM Peak					
Eastbound	421.92	48.70	395.67	38.07	6.22%
Westbound	463.42	41.70	431.79	42.88	6.83%
Total	442.67	49.15	413.10	43.77	6.68%
Friday Noon Peak					
Eastbound	438.75	17.15	402.00	37.62	8.38%
Westbound	390.77	32.94	386.4	36.05	1.12%
Total	413.80	35.72	394.20	35.70	4.74%
Friday PM Peak					
Eastbound	444.80	49.31	388.56	42.48	12.64%
Westbound	462.67	47.85	488.75	79.47	-5.64%
Total	453.81	49.27	438.66	80.74	3.34%
Saturday Peak					
Eastbound	435.64	66.63	362.27	45.69	16.84%
Westbound	351.64	37.29	389.82	34.87	-10.86%
Total	393.64	68.00	376.05	42.09	4.47

The travel time data was analyzed for adherence to the assumption of normality for use in the Student's t-test for determining if the difference in mean travel time is significant. As the number of tests performed upon one data set reduces the power and robustness of each test, the analysis for normality was conducted by reviewing the histogram and a normal probability plot for each data set. A review of the travel time data indicates that the data was not normally distributed and therefore the Student's t-test cannot be utilized while maintaining adequate power and robustness of the test which assures the results of the analysis.

An analysis of variance (ANOVA) test can also be conducted on the travel time data to determine if the difference in the mean travel times between the SCATS and the MDOT pre-

timed system are significantly different. One advantage the ANOVA has over the Student's t-test is the ability to compare several means simultaneously without reducing the power and the robustness of the test.

The assumptions for the ANOVA are similar to those of the Student's t-test; however, the ANOVA is considered a very robust test even with the violation of normality.

The ANOVA was used to determine if the travel time for the SCATS system as compared to the MDOT pre-timed system were statistically significantly different for the following comparisons:

- Eastbound travel time by peak period
- Westbound travel time by peak period
- Total travel time (combined eastbound and westbound travel times) by peak period

The peak periods for the analysis include the weekday noon, weekday PM, Friday noon, Friday PM and Saturday. The null hypothesis for the travel time data for the SCATS and the MDOT pre-timed system was as follows:

> H_o (null hypothesis): There was no difference between the mean travel time between the SCATS and MDOT pre-timed systems for a specified peak period.

For all the comparisons, the variances were found to be different resulting in the reporting of the Welch's modified F-statistic. Due to the unequal sample sizes for each comparison and the non-homogeneous variances, the Games-Howell post-hoc test was conducted.

Based upon the statistical analysis, the null hypothesis was accepted for each comparison between the SCATS and the MDOT pre-timed system. This indicates there was no statistical difference between the two signal systems for any of the peak periods analyzed. A significant result indicating differences between the two systems would be represented by a p-value less than 0.05, representing a level of confidence of 95 percent. The results of the post hoc results are shown in Table 23.

Table 23. Travel Time Statistical Post hoc Analysis Results

Comparison Category of SCATS vs. MDOT Pre-timed Systems	Mean Difference	Standard Error of the Difference	95% Lower Bound Confidence Interval	95% Upper Bound Confidence Interval	Test Result (p-value)
Eastbound Weekday Noon	-34.75	14.33	-91.61	22.11	SCATS=Pre-timed (0.642)
Eastbound Weekday PM Peak	-26.25	17.15	-95.33	42.83	SCATS= Pre-timed (0.985)
Eastbound Friday Noon Peak	-36.75	17.54	-141.55	68.05	SCATS= Pre-timed (0.784)
Eastbound Friday PM Peak	-56.24	18.87	-134.12	21.64	SCATS= Pre-timed (0.335)
Eastbound Saturday Peak	-73.36	24.36	-173.40	26.67	SCATS= Pre-timed (0.319)
Westbound Weekday Noon Peak	21.12	17.26	-50.53	92.76	SCATS= Pre-timed (0.998)
Westbound Weekday PM Peak	-31.63	16.62	-97.49	34.23	SCATS= Pre-timed (0.910)
Westbound Friday Noon Peak	-4.37	18.53	-99.49	90.75	SCATS= Pre-timed (1.000)
Westbound Friday PM Peak	26.08	24.20	-69.20	121.37	SCATS= Pre-timed (1.000)
Westbound Saturday Peak	38.18	15.39	-24.04	100.40	SCATS= Pre-timed (0.608)
Total Weekday Noon Peak	-6.59	11.89	-46.46	33.28	SCATS= Pre-timed (1.000)
Total Weekday PM Peak	-29.56	12.91	-72.44	13.32	SCATS= Pre-timed (0.414)
Total Friday Noon Peak	-19.60	13.36	-67.98	28.78	SCATS= Pre-timed (0.887)
Total Friday PM Peak	-15.15	17.87	-74.27	43.96	SCATS= Pre-timed (0.997)
Total Saturday Peak	-17.59	17.05	-75.13	39.95	SCATS= Pre-timed (0.988)

Travel Speed Analysis

The travel speed data was categorized by eastbound and westbound travel in addition to overall travel (eastbound and westbound combined) for each of the two signal systems; SCATS and the MDOT pre-timed system. The mean travel speeds for each direction of travel as well as for the overall travel are shown graphically in Figures 5 through 7.

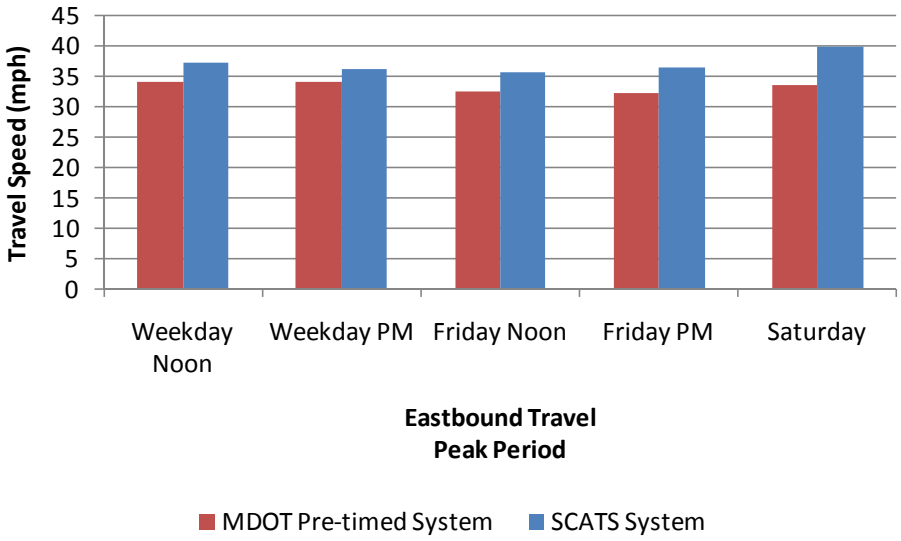

Figure 5. Eastbound Mean Travel Speed By Peak Period

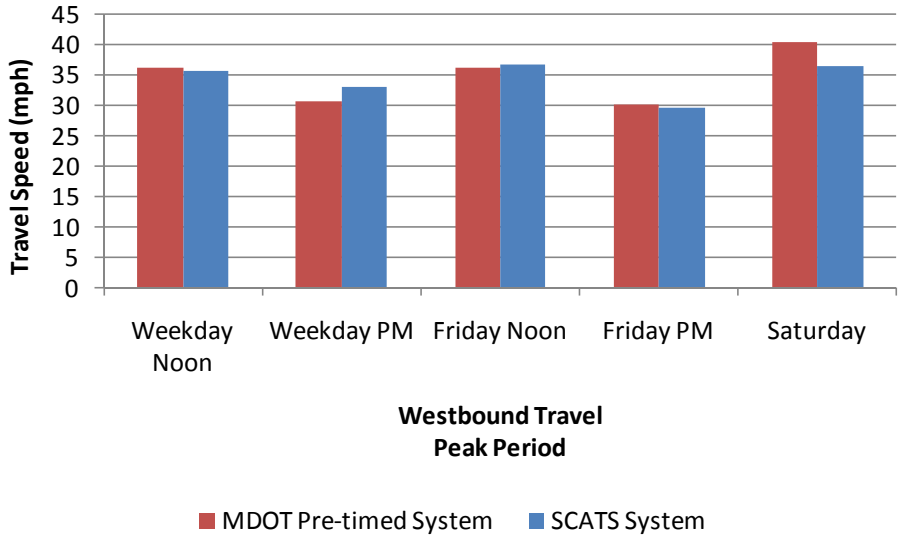

Figure 6. Westbound Mean Travel Speed By Peak Period

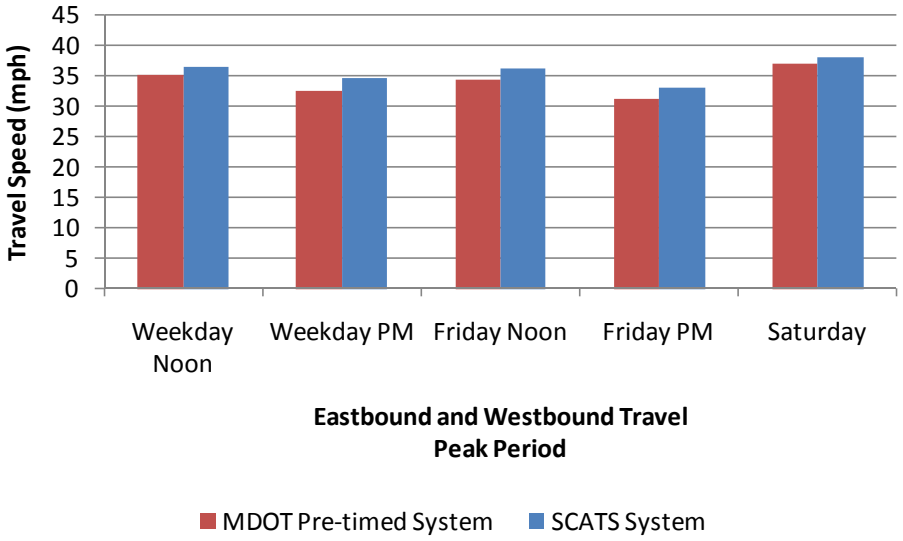

Figure 7. Overall Mean Travel Speed By Peak Period

Statistical data calculated, including the mean travel speed, standard deviation, and the percent difference in mean travel speed, are shown in Table 24. A positive value for the percent difference in mean travel speed indicates that the travel speed in the MDOT pre-timed system was faster than that in the SCATS system. A negative value for the percent difference in mean travel speed indicates that the travel speed in the SCATS system was faster than that in the MDOT pre-timed system.

Table 24. Travel Speed Statistical Data

Day, Peak Period and Direction of Travel	MDOT Pre-timed System		SCATS System		Percent Difference in Mean Travel Speed
	Mean Travel Speed (sec)	Standard Deviation	Mean Travel Speed (sec)	Standard Deviation	
Weekday Noon Peak					
Eastbound	34.19	3.33	37.34	3.44	-9.21%
Westbound	36.29	3.27	35.75	2.77	1.49%
Total	35.24	3.40	36.52	3.16	-3.63%
Weekday PM Peak					
Eastbound	34.25	4.51	36.31	3.63	-6.01%
Westbound	30.78	2.84	33.12	3.75	-7.60%
Total	32.51	4.09	34.77	3.97	-6.95%

Table 24. Travel Speed Statistical Data (continued)

Day, Peak Period and Direction of Travel	MDOT Pre-timed System		SCATS System		Percent Difference in Mean Travel Speed
	Mean Travel Speed (sec)	Standard Deviation	Mean Travel Speed (sec)	Standard Deviation	
Friday Noon Peak					
Eastbound	32.56	1.29	35.70	3.37	-9.64%
Westbound	36.34	2.99	36.82	3.82	-1.32%
Total	34.52	2.99	36.26	3.45	-5.04%
Friday PM Peak					
Eastbound	32.49	3.62	36.48	3.64	-12.28%
Westbound	30.18	2.89	29.67	4.92	1.69%
Total	31.23	3.37	33.07	5.48	-5.89%
Saturday Peak					
Eastbound	33.70	4.78	39.89	3.49	-18.37%
Westbound	40.53	4.06	36.64	3.56	9.60%
Total	37.11	5.56	38.26	4.44	-3.10%

A review of the travel speed data indicates that the data was not normally distributed and therefore the Student's t-test cannot be conducted while maintaining adequate power and robustness of the test which assures the results of the analysis. The ANOVA was used to determine if the travel speeds for the SCATS system as compared to the MDOT pre-timed system were statistically significantly different for the following comparisons:

- Eastbound travel speed by peak period
- Westbound travel speed by peak period
- Total travel speed (combined eastbound and westbound travel speed) by peak period

The peak periods for the analysis include the weekday noon, weekday PM, Friday noon, Friday PM and Saturday. The null hypothesis for the travel speed data for the SCATS and the MDOT pre-timed system was as follows:

> H_o (null hypothesis): There was no difference between the mean travel speed between the SCATS and MDOT pre-timed systems for a specified peak period.

For all the comparisons, the variances were found to be different resulting in the reporting of the Welch's modified F-statistic. Due to the unequal sample sizes for each comparison and the non-homogeneous variances, the Games-Howell post-hoc test was conducted.

Based upon the statistical analysis, the null hypothesis was accepted for each comparison between the SCATS and the MDOT pre-timed system. This indicates there was no statistical difference between the two signal systems for any of the peak periods analyzed. A significant result indicating differences between the two systems would be represented by a p-value less than 0.05, representing a level of confidence of 95 percent. The results of the post hoc results are shown in Table 25.

Table 25. Travel Speed Statistical Post hoc Analysis Results

Comparison Category of SCATS vs. MDOT Pre-timed Systems	Mean Difference	Standard Error of the Difference	95% Lower Bound Confidence Interval	95% Upper Bound Confidence Interval	Test Result (p-value)
Eastbound Weekday Noon	3.15	1.33	-2.12	8.42	SCATS= Pre-timed (0.675)
Eastbound Weekday PM Peak	2.06	1.60	-4.38	8.51	SCATS= Pre-timed (0.998)
Eastbound Friday Noon Peak	3.14	1.55	-6.37	12.65	SCATS= Pre-timed (0.811)
Eastbound Friday PM Peak	3.99	1.46	-1.95	9.92	SCATS= Pre-timed (0.462)
Eastbound Saturday Peak	6.19	2.04	-2.05	14.43	SCATS= Pre-timed (0.300)
Westbound Weekday Noon Peak	-0.54	1.18	-5.27	4.20	SCATS= Pre-timed (1.000)
Westbound Weekday PM Peak	2.35	1.29	-2.78	7.47	SCATS= Pre-timed (0.937)
Westbound Friday Noon Peak	0.48	1.90	-9.71	10.67	SCATS= Pre-timed (1.000)
Westbound Friday PM Peak	-0.51	1.49	-6.36	5.35	SCATS= Pre-timed (1.000)
Westbound Saturday Peak	-3.89	1.62	-10.48	2.70	SCATS= Pre-timed (0.662)

Table 25. Travel Speed Statistical Post hoc Analysis Results (continued)

Comparison Category of SCATS vs. MDOT Pre-timed Systems	Mean Difference	Standard Error of the Difference	95% Lower Bound Confidence Interval	95% Upper Bound Confidence Interval	Test Result (p-value)
Total Weekday Noon Peak	1.27	0.91	-1.73	4.29	SCATS= Pre-timed (0.919)
Total Weekday PM Peak	2.26	1.11	-1.43	5.95	SCATS= Pre-timed (0.584)
Total Friday Noon Peak	1.74	1.24	-2.85	6.32	SCATS= Pre-timed (0.911)
Total Friday PM Peak	1.84	1.21	-2.15	5.83	SCATS= Pre-timed (0.874)
Total Saturday Peak	1.15	1.52	-3.93	6.23	SCATS= Pre-timed (0.999)

Fuel Consumption Analysis

The gallons of fuel consumed along the corridor was categorized by eastbound and westbound travel in addition to overall travel (eastbound and westbound combined) for each of the two signal systems; SCATS and the MDOT pre-timed system. The average gallons of fuel consumed for each direction of travel as well as for the overall travel are shown graphically in Figures 8 through 10.

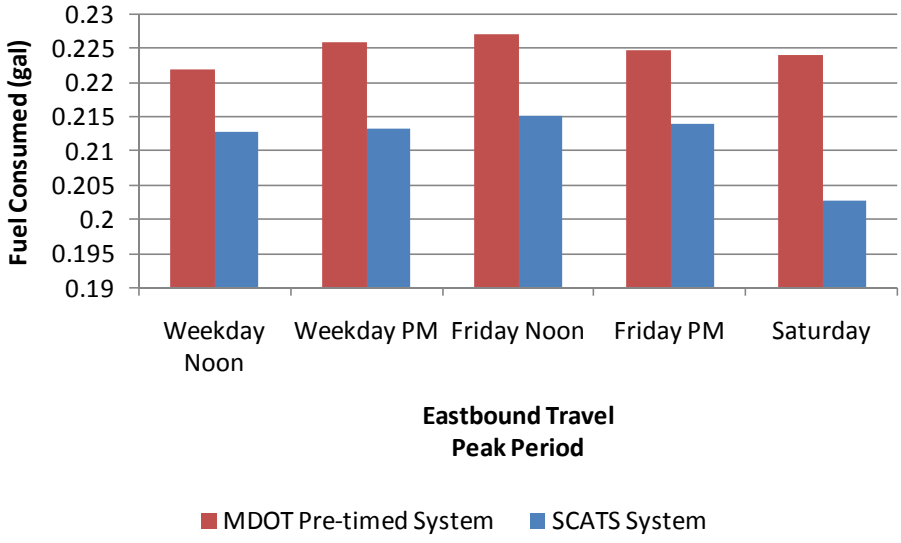

Figure 8. Eastbound Fuel Consumption By Peak Period

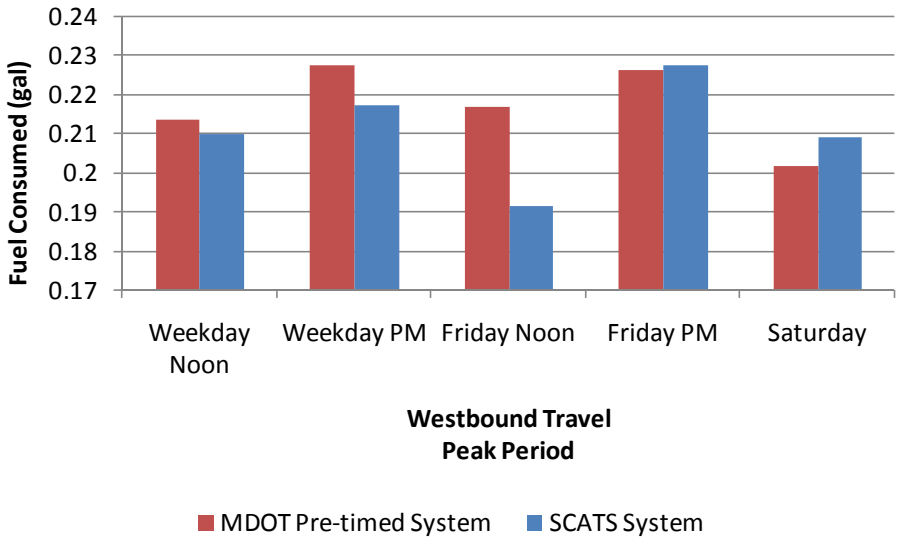

Figure 9. Westbound Fuel Consumption By Peak Period

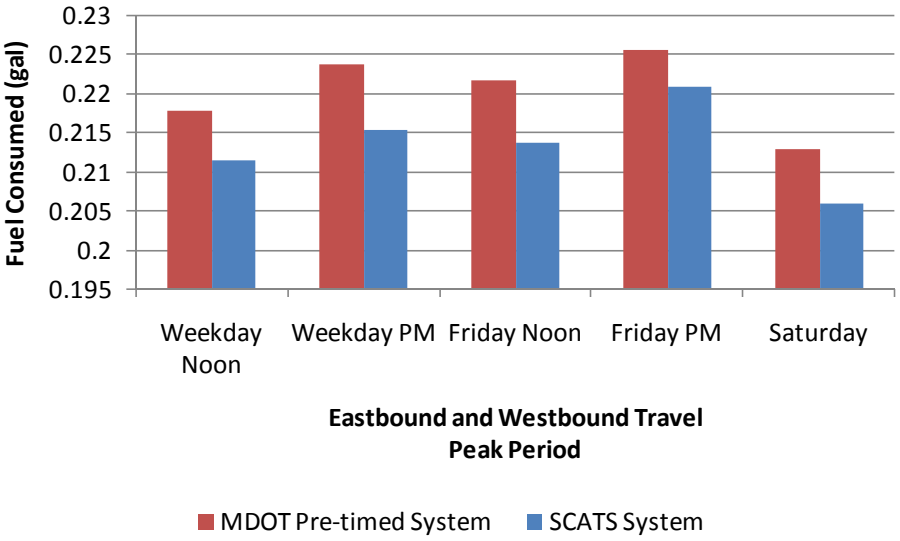

Figure 10. Overall Fuel Consumption By Peak Period

Statistical data calculated, including the average fuel consumption, standard deviation, and the percent difference in average fuel consumed, are shown in Table 26. A negative value for the percent difference in the average fuel consumed indicates that the fuel consumed in the MDOT pre-timed system was lower than that in the SCATS system. A positive value for the percent difference in the average fuel consumed indicates that fuel consumed in the SCATS system was lower than that in the MDOT pre-timed system.

Table 26. Fuel Consumption Statistical Data

Day, Peak Period and Direction of Travel	MDOT Pre-timed System		SCATS System		Percent Difference in Average Fuel Consumed
	Average Fuel Consumed	Standard Deviation	Average Fuel Consumed	Standard Deviation	
Weekday Noon Peak					
Eastbound	0.2220	0.0040	0.2129	0.0158	4.10%
Westbound	0.2139	0.0215	0.2103	0.0109	1.68%
Total	0.2180	0.0157	0.2115	0.1329	2.98%
Weekday PM Peak					
Eastbound	0.2260	0.1239	0.2134	0.0142	5.58%
Westbound	0.2278	0.0089	0.2175	0.0093	4.52%
Total	0.2269	0.0106	0.2154	0.0121	5.07%
Friday Noon Peak					
Eastbound	0.2271	0.0103	0.2152	0.0145	5.24%
Westbound	0.2172	0.0137	0.2126	0.0167	2.12%
Total	0.2220	0.0130	0.2139	0.0148	3.65%
Friday PM Peak					
Eastbound	0.2249	0.0108	0.2140	0.0153	4.85%
Westbound	0.2263	0.0080	0.2279	0.0184	-0.71%
Total	0.2256	0.0092	0.2209	0.0181	2.08%
Saturday Peak					
Eastbound	0.2242	0.0149	0.2028	0.01037	9.55%
Westbound	0.2020	0.1684	0.2093	0.0179	-3.61%
Total	0.2131	0.0193	0.2060	0.0146	3.33%

A review of the fuel consumption data indicates that the data was not normally distributed and therefore the Student's t-test cannot be conducted while maintaining adequate power and robustness of the test which assures the results of the analysis. The ANOVA was used to determine if the fuel consumed under the SCATS system as compared to the MDOT pre-timed system were statistically significantly different for the following comparisons:

- Eastbound fuel consumed by peak period
- Westbound fuel consumed by peak period
- Total fuel consumed (combined eastbound and westbound travel speed) by peak period

The peak periods for the analysis include the weekday noon, weekday PM, Friday noon, Friday PM and Saturday. The null hypothesis for the fuel consumption data for the SCATS and the MDOT pre-timed system was as follows:

> H_o (null hypothesis): There was no difference between the average fuel consumed between the SCATS and MDOT pre-timed systems for a specified peak period.

For all the comparisons, the variances were found to be different resulting in the reporting of the Welch's modified F-statistic. Due to the unequal sample sizes for each comparison and the non-homogeneous variances, the Games-Howell post-hoc test was conducted.

Based upon the statistical analysis, the null hypothesis was accepted for all of the directional comparisons between the SCATS and the MDOT pre-timed system. This indicates there was no statistical difference between the two signal systems for any of the directional peak periods analyzed. However, when the eastbound and westbound fuel consumed data is combined for the weekday PM peak period, a significant result is found. This significance is due to the differences between the eastbound and westbound data and not due to the difference in the SCATS versus the MDOT pre-timed signal systems. A significant result indicating differences between the two systems would be represented by a p-value less than 0.05, representing a level of confidence of 95 percent. The results of the post hoc results are shown in Table 27.

Table 27. Fuel Consumption Statistical Post hoc Analysis Results

Comparison Category of SCATS vs. MDOT Pre-timed Systems	Mean Difference	Standard Error of the Difference	95% Lower Bound Confidence Interval	95% Upper Bound Confidence Interval	Test Result (p-value)
Eastbound Weekday Noon	-0.009	0.004	-0.027	0.009	SCATS= Pre-timed (0.831)
Eastbound Weekday PM Peak	-0.125	0.005	-0.033	0.008	SCATS= Pre-timed (0.630)
Eastbound Friday Noon Peak	-0.119	0.007	-0.051	0.027	SCATS= Pre-timed (0.934)

Table 27. Fuel Consumption Statistical Post hoc Analysis Results (continued)

Comparison Category of SCATS vs. MDOT Pre-timed Systems	Mean Difference	Standard Error of the Difference	95% Lower Bound Confidence Interval	95% Upper Bound Confidence Interval	Test Result (p-value)
Eastbound Friday PM Peak	-0.011	0.005	-0.313	0.010	SCATS= Pre-timed (0.821)
Eastbound Saturday Peak	-0.021	0.005	-0.044	0.001	SCATS= Pre-timed (0.074)
Westbound Weekday Noon Peak	-0.003	0.007	-0.032	0.025	SCATS= Pre-timed (1.000)
Westbound Weekday PM Peak	-0.010	0.004	-0.024	0.004	SCATS= Pre-timed (0.377)
Westbound Friday Noon Peak	-0.005	0.008	-0.049	0.040	SCATS= Pre-timed (1.000)
Westbound Friday PM Peak	0.002	0.005	-0.189	0.022	SCATS= Pre-timed (1.000)
Westbound Saturday Peak	0.007	0.007	-0.227	0.037	SCATS= Pre-timed (1.000)
Total Weekday Noon Peak	-0.006	0.004	-0.198	0.007	SCATS= Pre-timed (0.850)
Total Weekday PM Peak	-0.011	0.003	-0.022	-0.001	**Reject Null**; SCATS≠Pre-timed (0.019)
Total Friday Noon Peak	-0.008	0.005	-0.028	0.012	SCATS= Pre-timed (0.873)
Total Friday PM Peak	-0.005	0.004	-0.017	0.008	SCATS= Pre-timed (0.959)
Total Saturday Peak	-0.007	0.005	-0.243	0.010	SCATS= Pre-timed (0.930)

Hydrocarbon Emissions Analysis

The grams of hydrocarbon emissions along the corridor data was categorized by eastbound and westbound travel in addition to overall travel (eastbound and westbound combined) for each of the two signal systems; SCATS and the MDOT pre-timed system. The average grams of hydrocarbons emitted for each direction of travel as well as for the overall travel are shown graphically in Figures 11 through 13.

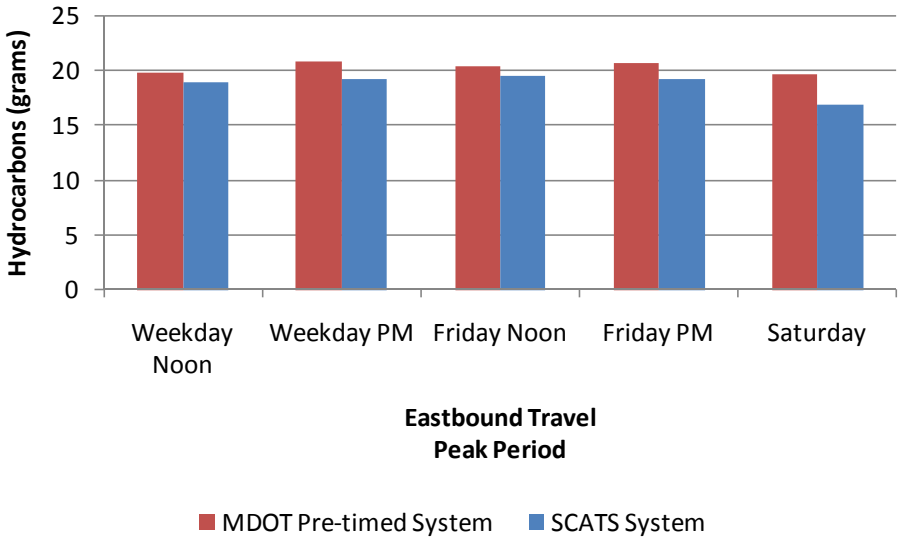

Figure 11. Eastbound Emission of Hydrocarbons By Peak Period

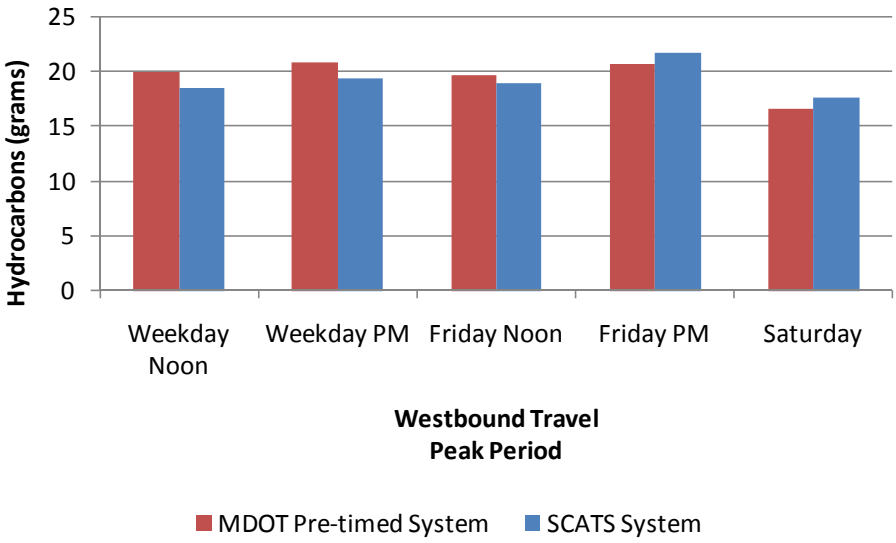

Figure 12. Westbound Emission of Hydrocarbons By Peak Period

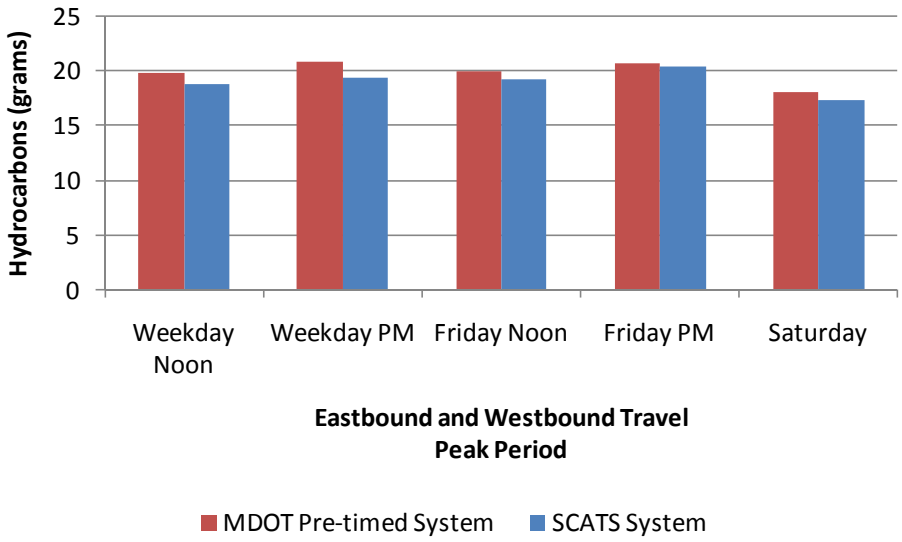

Figure 13. Overall Emission of Hydrocarbons By Peak Period

Statistical data calculated, including the average grams of hydrocarbon emissions, standard deviation, and the percent difference, are shown in Table 28. A negative value for the percent difference in the average grams of hydrocarbon emissions indicates that the hydrocarbons emitted in the MDOT pre-timed system was lower than that in the SCATS system. A positive value for the percent difference in the average grams of hydrocarbon emissions indicates that the hydrocarbons emitted in the SCATS system was lower than that in the MDOT pre-timed system.

Table 28. Hydrocarbon Emissions Statistical Data

Day, Peak Period and Direction of Travel	MDOT Pre-timed System		SCATS System		Percent Difference in HC Emissions
	HC Emissions (grams)	Standard Deviation	HC Emissions (grams)	Standard Deviation	
Weekday Noon Peak					
Eastbound	19.85	1.78	19.07	2.44	3.93%
Westbound	20.03	2.37	18.58	1.98	7.24%
Total	19.94	2.05	18.82	2.19	5.62%
Weekday PM Peak					
Eastbound	20.97	2.49	19.34	2.64	7.77%
Westbound	20.96	1.61	19.42	1.58	7.35%
Total	20.96	2.04	19.38	2.15	7.54%

Table 28. Hydrocarbon Emissions Statistical Data (continued)

Day, Peak Period and Direction of Travel	MDOT Pre-timed System		SCATS System		Percent Difference in HC Emissions
	HC Emissions (grams)	Standard Deviation	HC Emissions (grams)	Standard Deviation	
Friday Noon Peak					
Eastbound	20.40	1.25	19.61	1.87	3.87%
Westbound	19.73	2.46	18.95	3.47	3.95%
Total	20.05	1.96	19.28	2.65	3.84%
Friday PM Peak					
Eastbound	20.80	2.12	19.36	2.23	6.92%
Westbound	20.75	2.06	21.72	2.99	-4.67%
Total	20.77	20.4	20.54	2.86	1.11%
Saturday Peak					
Eastbound	19.68	2.45	16.97	1.75	13.77%
Westbound	16.68	2.89	17.68	3.19	-6.00%
Total	18.18	3.03	17.33	2.54	4.68%

A review of the hydrocarbon emissions data indicates that the data was not normally distributed and therefore the Student's t-test cannot be utilized while maintaining adequate power and robustness of the test which assures the results of the analysis. The ANOVA was used to determine if the hydrocarbon emissions for the SCATS system as compared to the MDOT pre-timed system were statistically significantly different for the following comparisons:

- Eastbound hydrocarbons emitted by peak period
- Westbound hydrocarbons emitted by peak period
- Total hydrocarbons emitted (combined eastbound and westbound travel speed) by peak period

The peak periods for the analysis include the weekday noon, weekday PM, Friday noon, Friday PM and Saturday. The null hypothesis for the number of stops data for the SCATS and the MDOT pre-timed system was as follows:

> H_o (null hypothesis): There was no difference between the average grams of hydrocarbon emitted between the SCATS and MDOT pre-timed systems for a specified peak period.

For all the comparisons, the variances were found to be different resulting in the reporting of the Welch's modified F-statistic. Due to the unequal sample sizes for each comparison and the non-homogeneous variances, the Games-Howell post-hoc test was conducted.

Based upon the statistical analysis, the null hypothesis was accepted for each comparison between the SCATS and the MDOT pre-timed system. This indicates there was no statistical difference between the two signal systems for any of the peak periods analyzed. A significant result indicating differences between the two systems would be represented by a p-value less than 0.05, representing a level of confidence of 95 percent. The results of the post hoc results are shown in Table 29.

Table 29. Hydrocarbon Emissions Statistical Post hoc Analysis Results

Comparison Category of SCATS vs. MDOT Pre-timed Systems	Mean Difference	Standard Error of the Difference	95% Lower Bound Confidence Interval	95% Upper Bound Confidence Interval	Test Result (p-value)
Eastbound Weekday Noon	-0.774	0.832	-4.07	2.52	SCATS= Pre-timed (1.000)
Eastbound Weekday PM Peak	-1.63	0.990	-5.54	2.28	SCATS= Pre-timed (0.973)
Eastbound Friday Noon Peak	-0.777	0.910	-5.81	4.26	SCATS= Pre-timed (1.000)
Eastbound Friday PM Peak	-1.44	0.871	-4.96	2.08	SCATS= Pre-timed (0.968)
Eastbound Saturday Peak	-2.70	0.908	-6.42	1.01	SCATS= Pre-timed (0.333)
Westbound Weekday Noon Peak	-1.45	0.854	-4.86	1.98	SCATS= Pre-timed (0.963)

Table 29. Hydrocarbon Emissions Statistical Post hoc Analysis Results (continued)

Comparison Category of SCATS vs. MDOT Pre-timed Systems	Mean Difference	Standard Error of the Difference	95% Lower Bound Confidence Interval	95% Upper Bound Confidence Interval	Test Result (p-value)
Westbound Weekday PM Peak	-1.54	0.628	-4.02	0.95	SCATS= Pre-timed (0.626)
Westbound Friday Noon Peak	-0.782	1.70	-10.13	8.56	SCATS= Pre-timed (1.000)
Westbound Friday PM Peak	0.973	0.955	-2.78	4.72	SCATS= Pre-timed (1.000)
Westbound Saturday Peak	1.00	1.30	-4.25	6.25	SCATS= Pre-timed (1.000)
Total Weekday Noon Peak	-1.12	0.584	-3.05	0.815	SCATS= Pre-timed (0.660)
Total Weekday PM Peak	-1.58	0.579	-3.50	0.332	SCATS= Pre-timed (0.187)
Total Friday Noon Peak	-0.766	0.926	-4.24	2.71	SCATS= Pre-timed (0.996)
Total Friday PM Peak	-0.232	0.666	-2.43	1.97	SCATS= Pre-timed (1.000)
Total Saturday Peak	-0.852	0.843	-3.67	1.97	SCATS= Pre-timed (0.990)

Carbon Monoxide Stops Analysis

The grams of carbon monoxide emissions along the corridor data was categorized by eastbound and westbound travel in addition to overall travel (eastbound and westbound combined) for each of the two signal systems; SCATS and the MDOT pre-timed system. The average grams of carbon monoxide emitted for each direction of travel as well as for the overall travel are shown graphically in Figures 14 through 16.

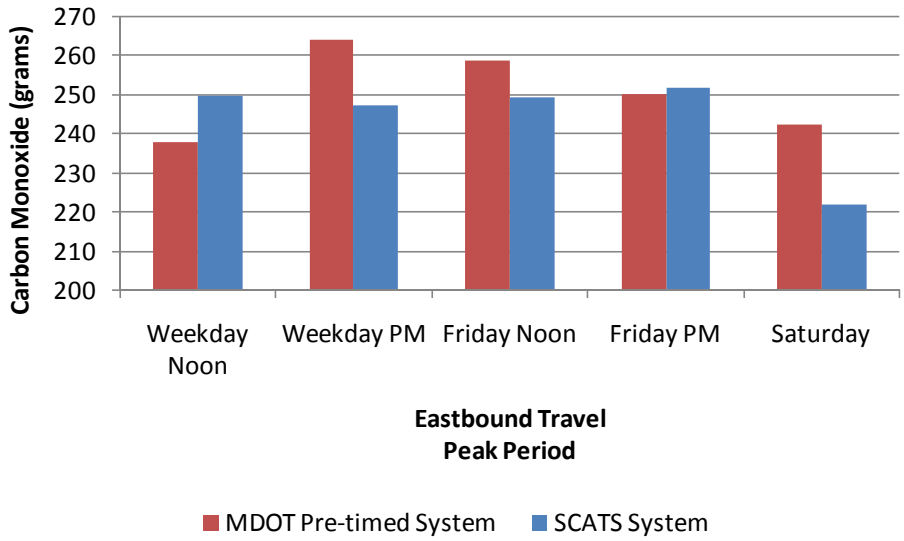

Figure 14. Eastbound Emission of Carbon Monoxide By Peak Period

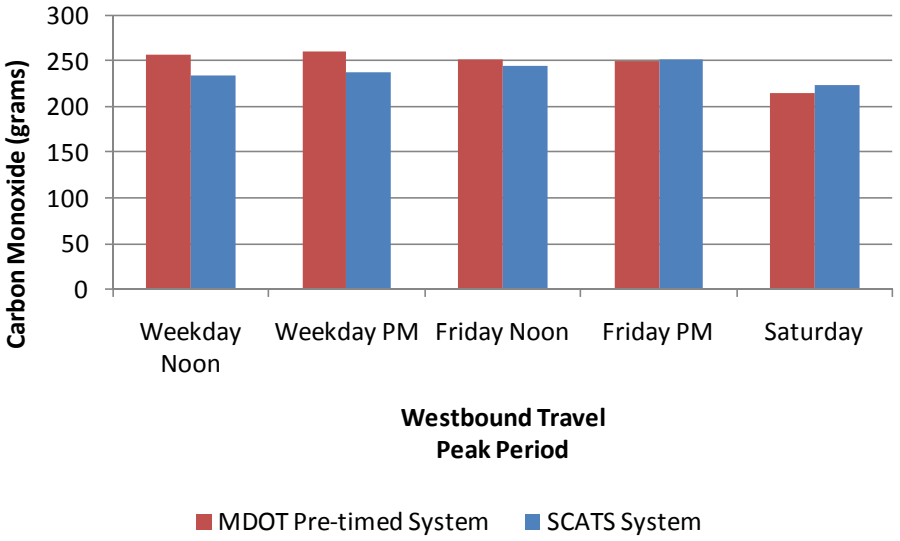

Figure 15. Westbound Emission of Carbon Monoxide By Peak Period

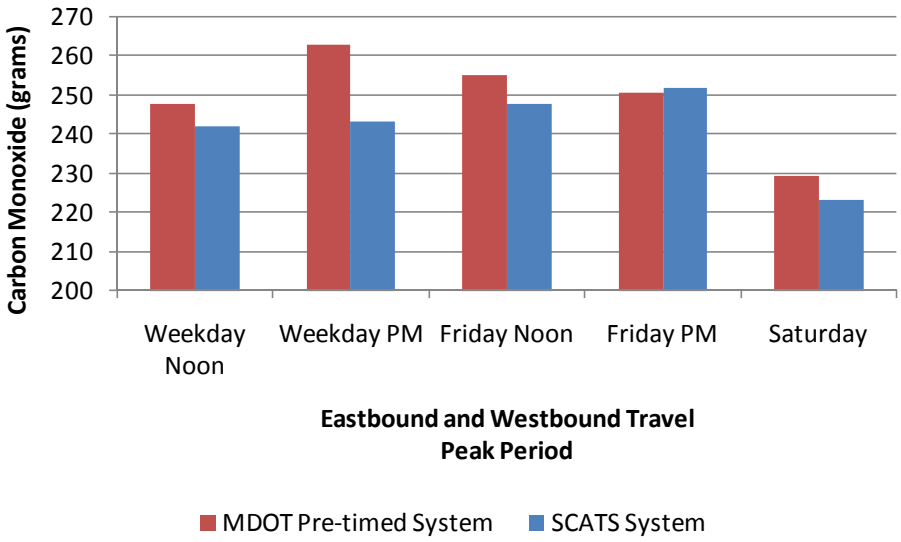

Figure 16. Overall Emission of Carbon Monoxide By Peak Period

Statistical data calculated, including the average grams of carbon monoxide emissions, standard deviation, and the percent difference, are shown in Table 30. A positive value for the percent difference in the average grams of carbon monoxide emissions indicates that the carbon monoxide emitted in the MDOT pre-timed system was lower than that in the SCATS system. A negative value for the percent difference in the average grams of carbon monoxide emissions indicates that the carbon monoxide emitted in the SCATS system was lower than that in the MDOT pre-timed system.

Table 30. Carbon Monoxide Emissions Statistical Data

Day, Peak Period and Direction of Travel	MDOT Pre-timed System		SCATS System		Percent Difference in CO Emissions
	CO Emissions (grams)	Standard Deviation	CO Emissions (grams)	Standard Deviation	
Weekday Noon Peak					
Eastbound	237.99	59.25	249.87	31.85	-4.99%
Westbound	257.54	30.58	235.28	25.93	8.64%
Total	247.77	47.18	242.33	29.37	2.20%
Weekday PM Peak					
Eastbound	264.21	27.31	247.66	32.84	6.26%
Westbound	261.62	19.55	238.95	20.90	8.67%
Total	262.91	23.27	243.46	27.60	7.40%

Table 30. Carbon Monoxide Emissions Statistical Data (continued)

Day, Peak Period and Direction of Travel	MDOT Pre-timed System		SCATS System		Percent Difference in CO Emissions
	CO Emissions (grams)	Standard Deviation	CO Emissions (grams)	Standard Deviation	
Friday Noon Peak					
Eastbound	258.82	29.92	249.66	32.02	3.54%
Westbound	252.16	37.49	245.76	49.61	2.54%
Total	255.36	33.13	247.71	39.42	3.00%
Friday PM Peak					
Eastbound	250.28	25.02	252.10	30.14	-0.73%
Westbound	251.22	22.42	251.78	26.35	-0.22%
Total	250.80	23.06	251.94	27.85	-0.45%
Saturday Peak					
Eastbound	242.77	27.62	222.09	28.68	8.52%
Westbound	216.56	36.62	224.37	44.62	-3.61%
Total	229.66	33.87	223.23	36.62	2.80%

A review of the carbon monoxide emissions data indicates that the data was not normally distributed and therefore the Student's t-test cannot be utilized while maintaining adequate power and robustness of the test which assures the results of the analysis. The ANOVA was used to determine if the carbon monoxide emissions for the SCATS system as compared to the MDOT pre-timed system were statistically significantly different for the following comparisons:

- Eastbound carbon monoxide emitted by peak period
- Westbound carbon monoxide emitted by peak period
- Total carbon monoxide emitted (combined eastbound and westbound travel speed) by peak period

The peak periods for the analysis include the weekday noon, weekday PM, Friday noon, Friday PM and Saturday. The null hypothesis for the number of stops data for the SCATS and the MDOT pre-timed system was as follows:

> H_o (null hypothesis): There was no difference between the average grams of carbon monoxide emitted between the SCATS and MDOT pre-timed systems for a specified peak period.

For all the comparisons, the variances were found to be different resulting in the reporting of the Welch's modified F-statistic. Due to the unequal sample sizes for each comparison and the non-homogeneous variances, the Games-Howell post-hoc test was conducted.

Based upon the statistical analysis, the null hypothesis was accepted for each comparison between the SCATS and the MDOT pre-timed system. This indicates there was no statistical difference between the two signal systems for any of the peak periods analyzed. A significant result indicating differences between the two systems would be represented by a p-value less than 0.05, representing a level of confidence of 95 percent. The results of the post hoc results are shown in Table 31.

Table 31. Carbon Monoxide Emissions Statistical Post hoc Analysis Results

Comparison Category of SCATS vs. MDOT Pre-timed Systems	Mean Difference	Standard Error of the Difference	95% Lower Bound Confidence Interval	95% Upper Bound Confidence Interval	Test Result (p-value)
Eastbound Weekday Noon	11.88	19.11	-67.57	91.32	SCATS= Pre-timed (1.000)
Eastbound Weekday PM Peak	-16.55	11.58	-62.16	29.07	SCATS= Pre-timed (0.993)
Eastbound Friday Noon Peak	-9.16	16.57	-93.63	75.03	SCATS= Pre-timed (1.000)
Eastbound Friday PM Peak	1.82	10.93	-41.84	45.48	SCATS= Pre-timed (1.000)
Eastbound Saturday Peak	-20.68	12.00	-69.19	27.83	SCATS= Pre-timed (0.955)
Westbound Weekday Noon Peak	-22.26	11.08	-66.59	22.06	SCATS= Pre-timed (0.867)

Table 31. Carbon Monoxide Emissions Statistical Post hoc Analysis Results (continued)

Comparison Category of SCATS vs. MDOT Pre-timed Systems	Mean Difference	Standard Error of the Difference	95% Lower Bound Confidence Interval	95% Upper Bound Confidence Interval	Test Result (p-value)
Westbound Weekday PM Peak	-22.67	7.94	-54.10	8.77	SCATS= Pre-timed (0.380)
Westbound Friday Noon Peak	-6.40	24.50	-139.12	126.32	SCATS= Pre-timed (1.000)
Westbound Friday PM Peak	0.564	9.24	-35.74	36.86	SCATS= Pre-timed (1.000)
Westbound Saturday Peak	7.81	17.21	-62.16	77.79	SCATS= Pre-timed (1.000)
Total Weekday Noon Peak	-5.44	11.07	-42.67	31.78	SCATS= Pre-timed (1.00)
Total Weekday PM Peak	-19.46	6.99	-42.57	3.65	SCATS= Pre-timed (0.169)
Total Friday Noon Peak	-7.65	14.12	-59.87	44.57	SCATS= Pre-timed (1.000)
Total Friday PM Peak	1.15	6.96	-21.88	24.18	SCATS= Pre-timed (1.000)
Total Saturday Peak	-6.43	10.63	-41.95	29.09	SCATS= Pre-timed (1.000)

Nitrogen Oxides Emissions Analysis

The grams of nitrogen oxide emissions along the corridor data was categorized by eastbound and westbound travel in addition to overall travel (eastbound and westbound combined) for each of the two signal systems; SCATS and the MDOT pre-timed system. The average grams of nitrogen oxide emitted for each direction of travel as well as for the overall travel are shown graphically in Figures 17 through 19.

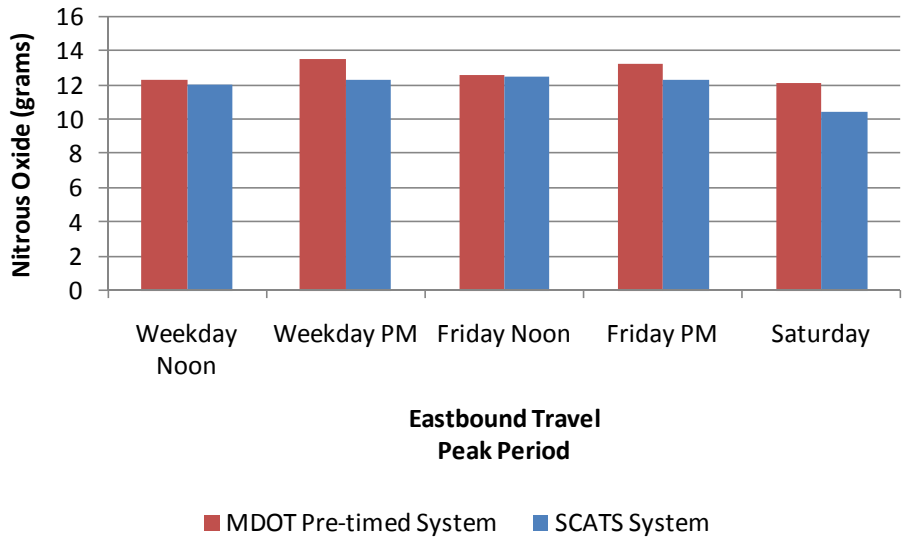

Figure 17. Eastbound Emission of Nitrogen Oxide By Peak Period

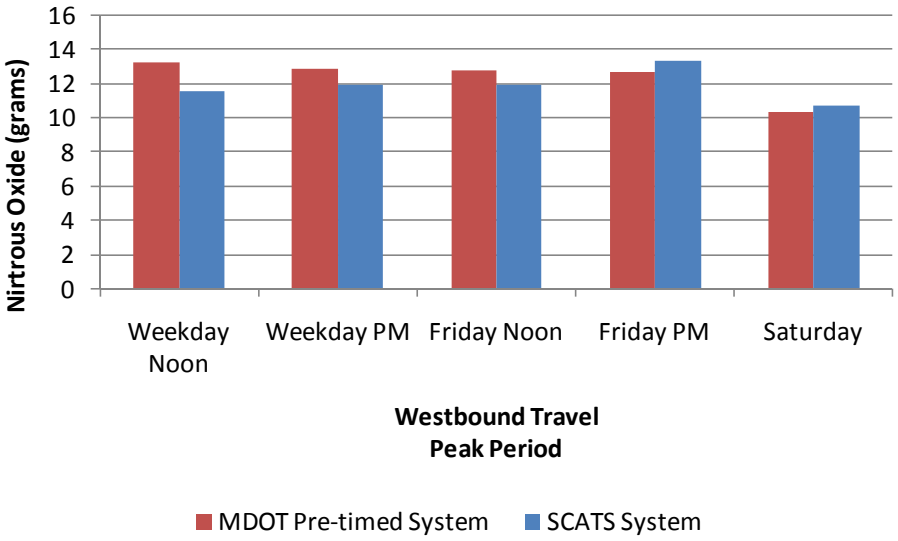

Figure 18. Westbound Emission of Nitrogen Oxide By Peak Period

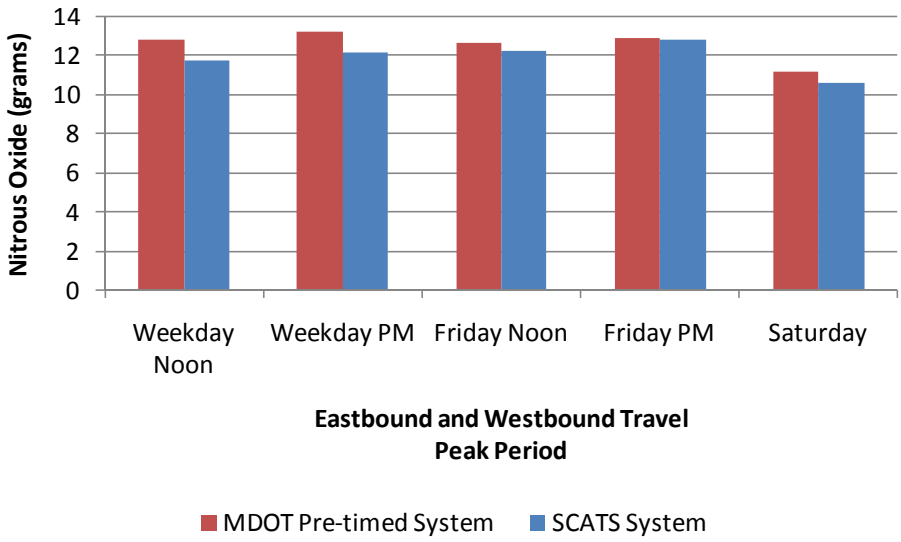

Figure 19. Overall Emission of Nitrogen Oxide By Peak Period

Statistical data calculated, including the average grams of nitrogen oxide emissions, standard deviation, and the percent difference, are shown in Table 32. A negative value for the percent difference in the average grams of nitrogen oxide emissions indicates that the nitrogen oxide emitted in the MDOT pre-timed system was lower than that in the SCATS system. A positive value for the percent difference in the average grams of nitrogen oxide emissions indicates that the nitrogen oxide emitted in the SCATS system was lower than that in the MDOT pre-timed system.

Table 32. Nitrogen Oxide Emissions Statistical Data

Day, Peak Period and Direction of Travel	MDOT Pre-timed System		SCATS System		Percent Difference in NOx Emissions
	NOx Emissions (grams)	Standard Deviation	NOx Emissions (grams)	Standard Deviation	
Weekday Noon Peak					
Eastbound	12.39	1.55	12.11	2.06	2.26%
Westbound	13.31	1.91	11.57	1.84	13.07%
Total	12.85	1.77	11.83	1.93	7.94%
Weekday PM Peak					
Eastbound	13.61	2.10	12.37	2.28	9.11%
Westbound	12.87	1.30	11.94	1.27	7.23%
Total	13.24	1.75	12.16	1.84	8.16%

Table 32. Nitrogen Oxide Emissions Statistical Data (continued)

Day, Peak Period and Direction of Travel	MDOT Pre-timed System		SCATS System		Percent Difference in NOx Emissions
	NOx Emissions (grams)	Standard Deviation	NOx Emissions (grams)	Standard Deviation	
Friday Noon Peak					
Eastbound	12.64	1.14	12.53	1.45	0.87%
Westbound	12.81	2.06	12.01	2.94	6.25%
Total	12.73	1.65	12.27	2.20	3.61%
Friday PM Peak					
Eastbound	13.30	2.00	12.39	1.83	6.84%
Westbound	12.69	1.67	13.38	1.86	-5.44%
Total	12.97	1.81	12.88	1.89	0.69%
Saturday Peak					
Eastbound	12.14	1.75	10.45	1.61	13.92%
Westbound	10.35	2.37	10.80	2.68	-4.35%
Total	11.24	2.23	10.63	2.16	5.43%

A review of the nitrogen oxide emissions data indicates that the data was not normally distributed and therefore the Student's t-test cannot be utilized while maintaining adequate power and robustness of the test which assures the results of the analysis. The ANOVA was used to determine if the nitrogen oxide emissions for the SCATS system as compared to the MDOT pre-timed system were statistically significantly different for the following comparisons:

- Eastbound nitrogen oxide emitted by peak period
- Westbound nitrogen oxide emitted by peak period
- Total nitrogen oxide emitted (combined eastbound and westbound travel speed) by peak period

The peak periods for the analysis include the weekday noon, weekday PM, Friday noon, Friday PM and Saturday. The null hypothesis for the number of stops data for the SCATS and the MDOT pre-timed system was as follows:

> H_o (null hypothesis): There was no difference between the average grams of nitrogen oxide emitted between the SCATS and MDOT pre-timed systems for a specified peak period.

For all the comparisons, the variances were found to be different resulting in the reporting of the Welch's modified F-statistic. Due to the unequal sample sizes for each comparison and the non-homogeneous variances, the Games-Howell post-hoc test was conducted.

Based upon the statistical analysis, the null hypothesis was accepted for each comparison between the SCATS and the MDOT pre-timed system. This indicates there was no statistical difference between the two signal systems for any of the peak periods analyzed. A significant result indicating differences between the two systems would be represented by a p-value less than 0.05, representing a level of confidence of 95 percent. The results of the post hoc results are shown in Table 33.

Table 33. Nitrogen Oxide Emissions Statistical Post hoc Analysis Results

Comparison Category of SCATS vs. MDOT Pre-timed Systems	Mean Difference	Standard Error of the Difference	95% Lower Bound Confidence Interval	95% Upper Bound Confidence Interval	Test Result (p-value)
Eastbound Weekday Noon	-0.280	0.710	-3.09	2.53	SCATS= Pre-timed (1.000)
Eastbound Weekday PM Peak	-1.24	0.845	-4.57	2.09	SCATS= Pre-timed (0.991)
Eastbound Friday Noon Peak	-0.11	0.726	-3.96	3.74	SCATS= Pre-timed (1.000)
Eastbound Friday PM Peak	-1.22	0.760	-4.10	2.29	SCATS= Pre-timed (0.976)
Eastbound Saturday Peak	-1.69	0.715	-4.57	1.21	SCATS= Pre-timed (0.682)
Westbound Weekday Noon Peak	-1.73	0.728	-4.62	1.16	SCATS= Pre-timed (0.672)

Table 33. Nitrogen Oxide Emissions Statistical Post hoc Analysis Results (continued)

Comparison Category of SCATS vs. MDOT Pre-timed Systems	Mean Difference	Standard Error of the Difference	95% Lower Bound Confidence Interval	95% Upper Bound Confidence Interval	Test Result (p-value)
Westbound Weekday PM Peak	-0.928	0.506	-2.94	1.08	SCATS= Pre-timed (0.931)
Westbound Friday Noon Peak	-0.791	1.43	-8.71	7.12	SCATS= Pre-timed (1.000)
Westbound Friday PM Peak	0.686	0.670	-1.96	3.33	SCATS= Pre-timed (1.000)
Westbound Saturday Peak	0.454	1.08	-3.91	4.82	SCATS= Pre-timed (1.000)
Total Weekday Noon Peak	-1.01	0.508	-2.70	0.669	SCATS= Pre-timed (0.607)
Total Weekday PM Peak	-1.08	0.495	-2.72	0.559	SCATS= Pre-timed (0.483)
Total Friday Noon Peak	-0.456	0.770	-3.34	2.43	SCATS= Pre-timed (1.000)
Total Friday PM Peak	-0.083	0.510	-1.78	1.61	SCATS= Pre-timed (1.000)
Total Saturday Peak	-0.615	0.662	-4.34	-0.329	SCATS= Pre-timed (0.994)

Number of Corridor Stops Analysis

The number of stops along the corridor data was categorized by eastbound and westbound travel in addition to overall travel (eastbound and westbound combined) for each of the two signal systems; SCATS and the MDOT pre-timed system. The average number of stops for each direction of travel as well as for the overall travel is shown graphically in Figures 20 through 22.

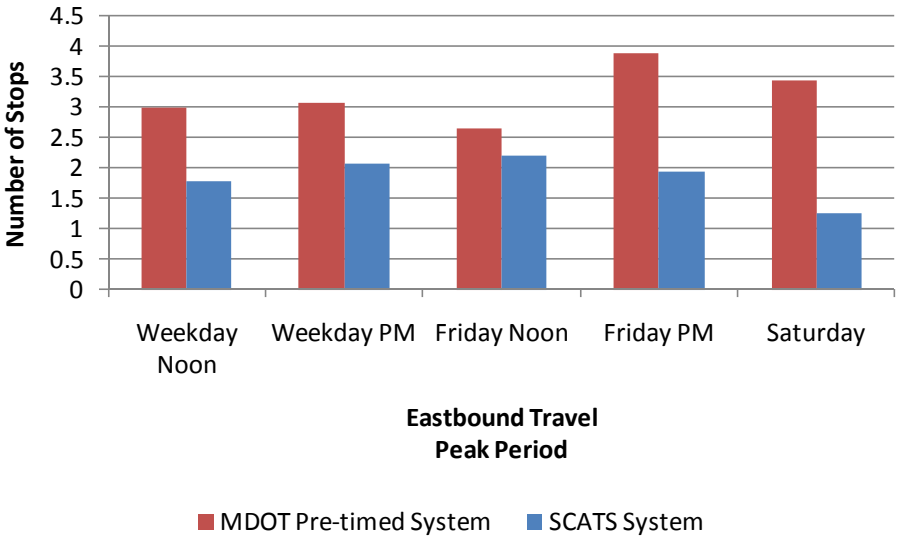

Figure 20. Eastbound Mean Number of Stops By Peak Period

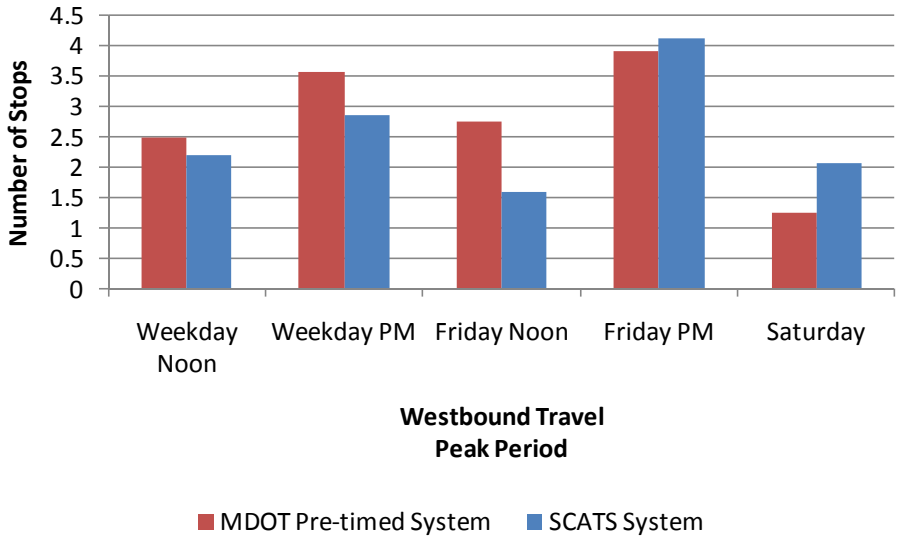

Figure 21. Westbound Mean Number of Stops By Peak Period

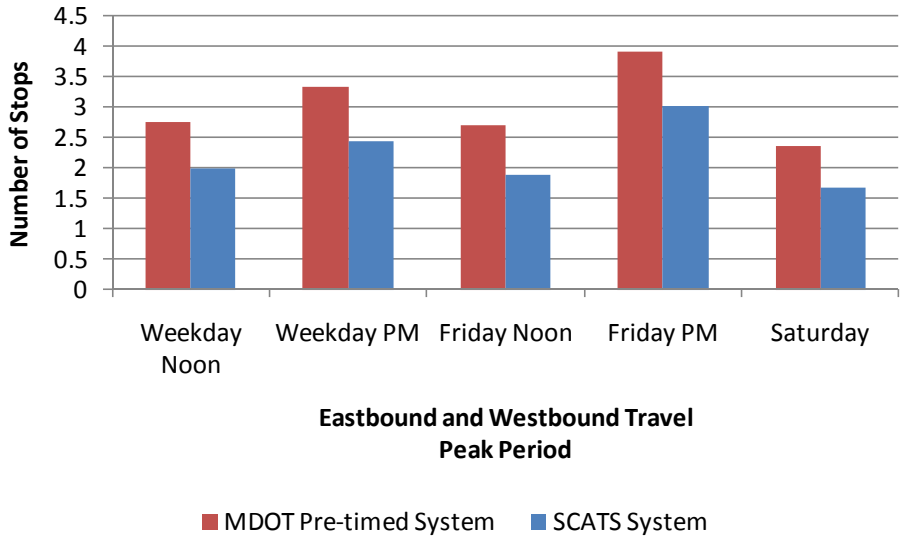

Figure 22. Overall Mean Number of Stops By Peak Period

Statistical data calculated, including the average number of stops, standard deviation, and the percent difference in average number of stops, are shown in Table 34. A negative value for the percent difference in the average number of stops indicates that the number of stops in the MDOT pre-timed system was lower than that in the SCATS system. A positive value for the percent difference in the average number of stops indicates that the number of stops in the SCATS system was lower than that in the MDOT pre-timed system.

Table 34. Number of Stops Statistical Data

Day, Peak Period and Direction of Travel	MDOT Pre-timed System		SCATS System		Percent Difference in Average Number of Stops
	Average No. of Stops	Standard Deviation	Average No. of Stops	Standard Deviation	
Weekday Noon Peak					
Eastbound	3.00	1.04	1.78	1.53	40.67%
Westbound	2.50	0.52	2.20	0.94	12.00%
Total	2.75	0.85	2.00	1.25	27.27%
Weekday PM Peak					
Eastbound	3.08	1.31	2.07	1.03	32.79%
Westbound	3.58	1.44	2.86	1.03	20.11%
Total	3.33	1.37	2.45	1.09	26.43%

Table 34. Number of Stops Statistical Data (continued)

Day, Peak Period and Direction of Travel	MDOT Pre-timed System		SCATS System		Percent Difference in Average Number of Stops
	Average No. of Stops	Standard Deviation	Average No. of Stops	Standard Deviation	
Friday Noon Peak					
Eastbound	2.67	0.78	2.20	0.84	17.60%
Westbound	2.77	0.73	1.60	1.14	42.24%
Total	2.72	0.74	1.90	0.99	30.15%
Friday PM Peak					
Eastbound	3.90	1.52	1.94	0.85	50.26%
Westbound	3.92	1.16	4.13	2.31	-5.36%
Total	3.91	1.31	3.03	2.04	22.51%
Saturday Peak					
Eastbound	3.45	2.02	1.27	1.01	63.19%
Westbound	1.27	1.10	2.09	0.94	-64.57%
Total	2.36	1.94	1.68	1.04	28.81%

A review of the number of stops data indicates that the data was not normally distributed and therefore the Student's t-test cannot be utilized while maintaining adequate power and robustness of the test which assures the results of the analysis. The ANOVA was used to determine if the number of stops for the SCATS system as compared to the MDOT pre-timed system were statistically significantly different for the following comparisons:

- Eastbound number of stops by peak period
- Westbound number of stops by peak period
- Total number of stops (combined eastbound and westbound travel speed) by peak period

The peak periods for the analysis include the weekday noon, weekday PM, Friday noon, Friday PM and Saturday. The null hypothesis for the number of stops data for the SCATS and the MDOT pre-timed system was as follows:

> H_o (null hypothesis): There was no difference between the average number of stops between the SCATS and MDOT pre-timed systems for a specified peak period.

For all the comparisons, the variances were found to be different resulting in the reporting of the Welch's modified F-statistic. Due to the unequal sample sizes for each comparison and the non-homogeneous variances, the Games-Howell post-hoc test was conducted.

Based upon the statistical analysis, the null hypothesis was accepted for each comparison between the SCATS and the MDOT pre-timed system. This indicates there was no statistical difference between the two signal systems for any of the peak periods analyzed. A significant result indicating differences between the two systems would be represented by a p-value less than 0.05, representing a level of confidence of 95 percent. The results of the post hoc results are shown in Table 35.

Table 35. Number of Stops Statistical Post hoc Analysis Results

Comparison Category of SCATS vs. MDOT Pre-timed Systems	Mean Difference	Standard Error of the Difference	95% Lower Bound Confidence Interval	95% Upper Bound Confidence Interval	Test Result (p-value)
Eastbound Weekday Noon	-1.21	0.51	-3.23	0.80	SCATS= Pre-timed (0.662)
Eastbound Weekday PM Peak	-1.02	0.46	-2.88	0.85	SCATS= Pre-timed (0.775)
Eastbound Friday Noon Peak	-0.47	0.44	-2.67	1.74	SCATS= Pre-timed (0.999)
Eastbound Friday PM Peak	-1.96	0.53	-4.25	0.33	SCATS= Pre-timed (0.129)
Eastbound Saturday Peak	-2.18	0.68	-5.06	0.69	SCATS= Pre-timed (0.254)
Westbound Weekday Noon Peak	-0.30	0.29	-1.44	0.84	SCATS= Pre-timed (1.000)
Westbound Weekday PM Peak	-0.73	0.50	-2.75	1.30	SCATS= Pre-timed (0.990)
Westbound Friday Noon Peak	-1.17	0.55	-4.27	1.93	SCATS= Pre-timed (0.772)
Westbound Friday PM Peak	0.21	0.67	-2.44	2.86	SCATS= Pre-timed (1.000)
Westbound Saturday Peak	0.82	0.44	-0.96	2.59	SCATS= Pre-timed (0.916)

Table 35. Number of Stops Statistical Post hoc Analysis Results (continued)

Comparison Category of SCATS vs. MDOT Pre-timed Systems	Mean Difference	Standard Error of the Difference	95% Lower Bound Confidence Interval	95% Upper Bound Confidence Interval	Test Result (p-value)
Total Weekday Noon Peak	-0.75	0.29	-1.71	0.21	SCATS= Pre-timed (0.251)
Total Weekday PM Peak	-0.89	0.35	-2.04	0.27	SCATS= Pre-timed (0.266)
Total Friday Noon Peak	-0.82	0.35	-2.12	0.48	SCATS= Pre-timed (0.414)
Total Friday PM Peak	-0.88	0.46	-2.38	0.63	SCATS= Pre-timed (0.651)
Total Saturday Peak	-0.68	0.47	-2.28	0.91	SCATS= Pre-timed (0.901)

Total Delay Analysis

The travel time total delay data was categorized by eastbound and westbound travel in addition to overall travel (eastbound and westbound combined) for each of the two signal systems; SCATS and the MDOT pre-timed system. The mean total delay for each direction of travel as well as for the overall travel are shown graphically in Figures 23 through 25.

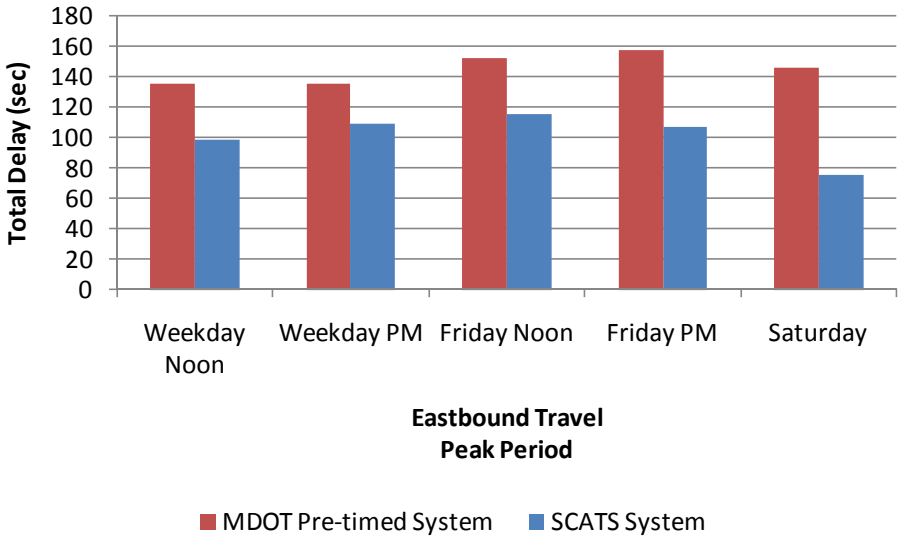

Figure 23. Eastbound Mean Total Delay By Peak Period

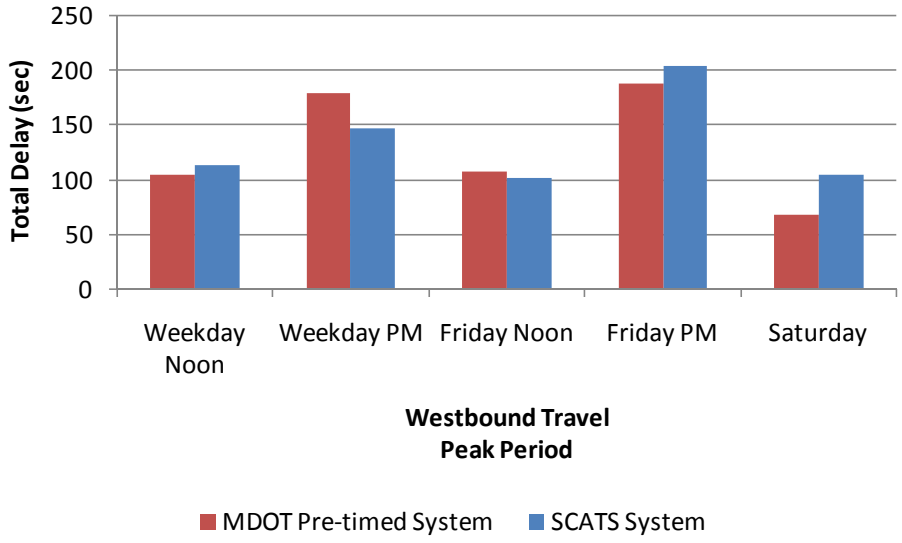

Figure 24. Westbound Mean Total Delay By Peak Period

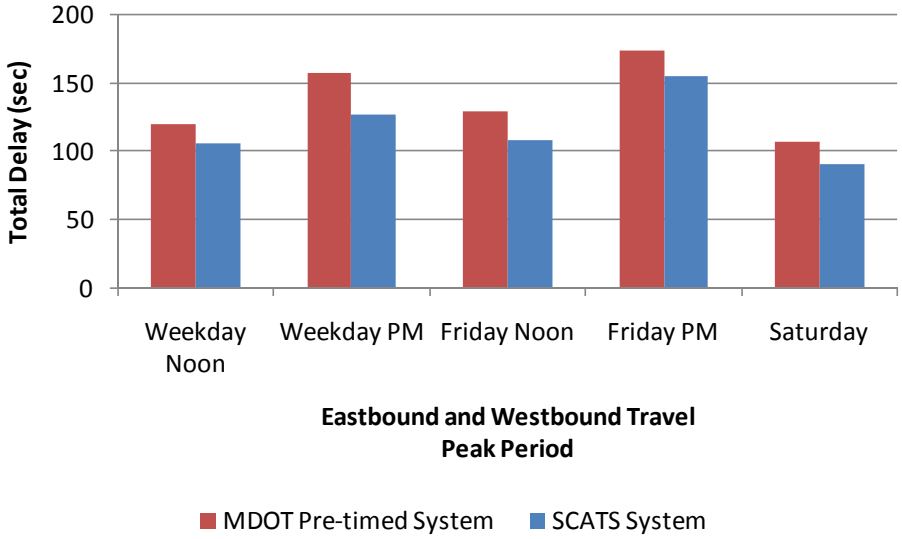

Figure 25. Overall Mean Total Delay By Peak Period

Statistical data calculated, including the mean total delay, standard deviation, and the percent difference in mean total delay, are shown in Table 36. A negative value for the percent difference in mean total delay indicates that the delay in the MDOT pre-timed system was lower than that in the SCATS system. A positive value for the percent difference in mean total delay indicates that the delay in the SCATS system was lower than that in the MDOT pre-timed system.

Table 36. Total Travel Delay Statistical Data

Day, Peak Period and Direction of Travel	MDOT Pre-timed System		SCATS System		Percent Difference in Mean Total Delay
	Mean Total Delay (sec)	Standard Deviation	Mean Total Delay (sec)	Standard Deviation	
Weekday Noon Peak					
Eastbound	135.83	33.43	98.86	36.13	27.22%
Westbound	104.75	36.12	113.87	29.41	-8.71%
Total	120.29	37.56	106.62	33.12	11.36%
Weekday PM Peak					
Eastbound	136.17	48.30	109.60	38.18	19.51%
Westbound	179.92	40.92	147.57	42.71	17.98%
Total	158.04	49.15	127.93	44.14	19.05%
Friday Noon Peak					
Eastbound	152.67	17.82	115.40	37.92	24.41%
Westbound	107.62	33.08	101.80	35.69	5.41%
Total	129.24	34.93	108.60	35.44	15.97%
Friday PM Peak					
Eastbound	157.80	48.81	107.13	38.06	32.11%
Westbound	188.83	41.40	204.25	79.49	-8.17%
Total	174.73	46.57	155.69	78.70	10.90%
Saturday Peak					
Eastbound	146.09	66.46	76.27	45.07	47.79%
Westbound	68.09	37.68	105.18	34.72	-54.47%
Total	107.09	66.12	90.73	41.95	15.28%

A review of the travel delay data indicates that the data was not normally distributed and therefore the Student's t-test cannot be utilized while maintaining adequate power and robustness of the test which assures the results of the analysis. The ANOVA was used to determine if the total delay for the SCATS system as compared to the MDOT pre-timed system were statistically significantly different for the following comparisons:

- Eastbound total travel delay by peak period
- Westbound total travel delay by peak period
- Total travel delay combined (eastbound and westbound travel speed) by peak period

The peak periods for the analysis include the weekday noon, weekday PM, Friday noon, Friday PM and Saturday. The null hypothesis for the total travel delay data for the SCATS and the MDOT pre-timed system was as follows:

> H_o (null hypothesis): There was no difference between the mean travel delay between the SCATS and MDOT pre-timed systems for a specified peak period.

For all the comparisons, the variances were found to be different resulting in the reporting of the Welch's modified F-statistic. Due to the unequal sample sizes for each comparison and the non-homogeneous variances, the Games-Howell post-hoc test was conducted.

Based upon the statistical analysis, the null hypothesis was accepted for each comparison between the SCATS and the MDOT pre-timed system. This indicates there was no statistical difference between the two signal systems for any of the peak periods analyzed. A significant result indicating differences between the two systems would be represented by a p-value less than 0.05, representing a level of confidence of 95 percent. The results of the post hoc results are shown in Table 37.

Table 37. Travel Delay Statistical Post hoc Analysis Results

Comparison Category of SCATS vs. MDOT Pre-timed Systems	Mean Difference	Standard Error of the Difference	95% Lower Bound Confidence Interval	95% Upper Bound Confidence Interval	Test Result (p-value)
Eastbound Weekday Noon	-36.98	13.65	-91.01	17.05	SCATS= Pre-timed (0.464)
Eastbound Weekday PM Peak	-26.57	17.08	-95.27	42.13	SCATS= Pre-timed (0.982)
Eastbound Friday Noon Peak	-37.27	17.72	-142.64	68.11	SCATS= Pre-timed (0.782)
Eastbound Friday PM Peak	-50.68	18.13	-185.34	-8.91	SCATS= Pre-timed (0.433)
Eastbound Saturday Peak	-69.82	24.21	-169.34	29.70	SCATS= Pre-timed (0.381)
Westbound Weekday Noon Peak	9.12	12.90	-42.66	60.89	SCATS= Pre-timed (1.000)

Table 37. Travel Delay Statistical Post hoc Analysis Results (continued)

Comparison Category of SCATS vs. MDOT Pre-timed Systems	Mean Difference	Standard Error of the Difference	95% Lower Bound Confidence Interval	95% Upper Bound Confidence Interval	Test Result (p-value)
Westbound Weekday PM Peak	-32.35	16.42	-97.41	32.72	SCATS= Pre-timed (0.885)
Westbound Friday Noon Peak	-5.82	18.41	-99.93	88.30	SCATS= Pre-timed (1.000)
Westbound Friday PM Peak	15.42	23.19	-76.47	107.31	SCATS= Pre-timed (1.000)
Westbound Saturday Peak	37.09	15.45	-25.37	99.55	SCATS= Pre-timed (0.656)
Total Weekday Noon Peak	-13.67	9.83	-46.32	18.98	SCATS= Pre-timed (0.924)
Total Weekday PM Peak	-30.11	12.96	-73.13	12.91	SCATS= Pre-timed (0.393)
Total Friday Noon Peak	-20.64	13.21	-68.57	27.29	SCATS= Pre-timed (0.848)
Total Friday PM Peak	-19.04	17.09	-75.57	37.49	SCATS= Pre-timed (0.981)
Total Saturday Peak	-16.34	16.70	-72.65	39.93	SCATS= Pre-timed (0.992)

Number of Stopped Vehicles Analysis

The number of vehicles stopping at the study intersections data was categorized by those vehicles stopping along the main roadway (M-59) and those along the minor roadways for each of the two signal systems; SCATS and the MDOT pre-timed system. The number of vehicles stopping at the study intersections for M-59, the minor roadways and the total number of stopped vehicles are shown graphically in Figures 26 through 28.

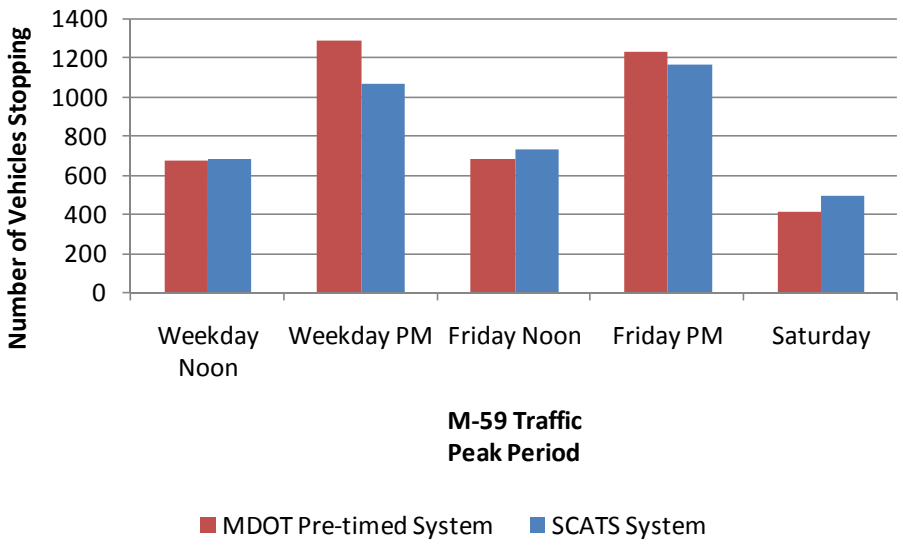

Figure 26. M-59 Number of Stopped Vehicles By Peak Period

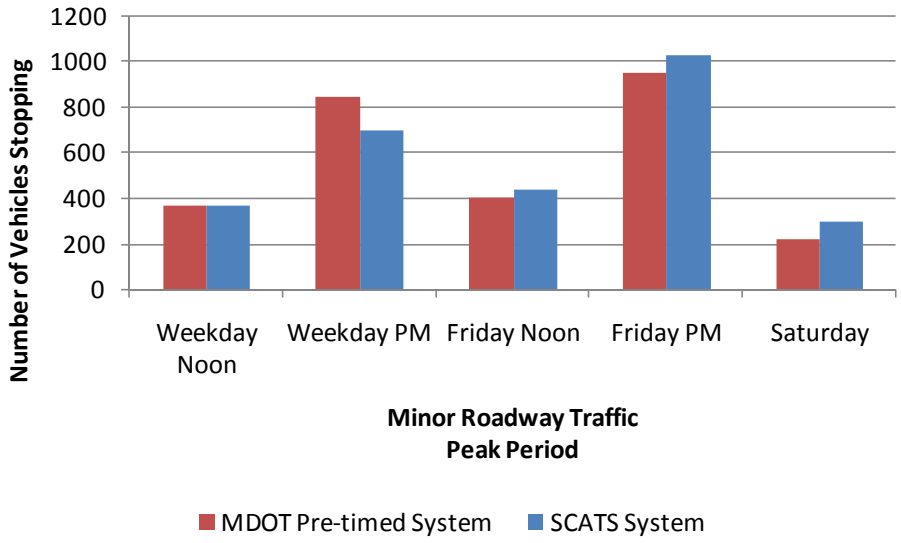

Figure 27. Minor Roadways Number of Stopped Vehicles By Peak Period

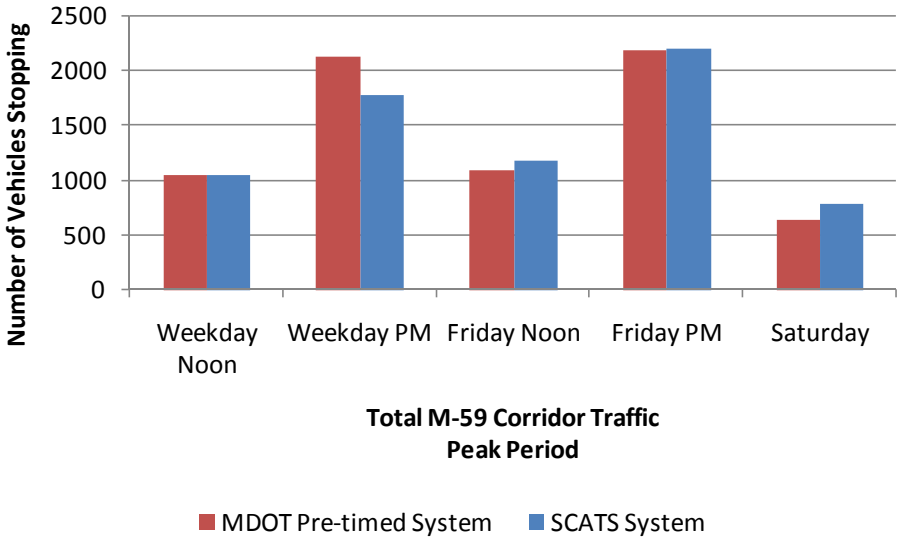

Figure 28. Total Number of Stopped Vehicles By Peak Period

Statistical data calculated, including the average number of stopped vehicles by roadway type, standard deviation, and the percent difference in average number of stopped vehicles, are shown in Table 38. A negative value for the percent difference in the number of stopped vehicles indicates that the MDOT pre-timed system had fewer stopped vehicles than the SCATS system. A positive value for the percent difference in the number of stopped vehicles indicates that the SCATS system had fewer stopped vehicles than the MDOT pre-timed system.

Table 38. Number of Stopped Vehicles Statistical Data

Day, Peak Period and Direction of Travel	MDOT Pre-timed System		SCATS System		Percent Difference in Number of Stopped Vehicles
	Mean Number of Stopped Vehicles	Standard Deviation	Mean Number of Stopped Vehicles	Standard Deviation	
Weekday Noon Peak					
M-59	680.00	810.70	685.04	828.99	-0.74%
Minor Roadways	370.75	429.99	373.88	429.37	-0.84%
Weekday PM Peak					
M-59	1289.96	1925.05	1072.33	1617.69	16.87%
Minor Roadways	851.46	1348.47	704.96	867.01	17.21%
Friday Noon Peak					
M-59	690.54	856.96	737.46	845.87	-6.79%
Minor Roadways	404.17	433.62	442.54	513.19	-9.49%

Table 38. Number of Stopped Vehicles Statistical Data (continued)

Day, Peak Period and Direction of Travel	MDOT Pre-timed System		SCATS System		Percent Difference in Number of Stopped Vehicles
	Mean Number of Stopped Vehicles	Standard Deviation	Mean Number of Stopped Vehicles	Standard Deviation	
Friday PM Peak					
M-59	1237.42	2170.03	1173.92	1659.73	5.13%
Minor Roadways	952.75	1230.46	1028.92	1514.31	-7.99%
Saturday Peak					
M-59	414.58	440.35	496.71	581.76	-19.81%
Minor Roadways	225.92	251.10	299.08	343.41	-32.38%

The number of stopped vehicle data was analyzed for adherence to the assumption of normality for use in the paired t-test for determining if the difference in the average number of stopped vehicles was significant. The paired t-test was selected for the number of stopped vehicle data due to the matched characteristics of the data collection. For the number of stopped vehicle data, data was collected for each intersection's critical lane group for the same period under each signal system. A review of the data indicates that the data was not normally distributed and therefore the paired t-test should not be conducted due to the lack of the test's ability to maintain adequate power and robustness of the test, which assures the results of the analysis.

A non-parametric test can be conducted when the assumption of normality is violated in the paired t-test, such as the Wilcoxon Signed Rank Test. Due to confusion regarding non-parametric tests outside of the academia, both the paired t-test and the Wilcoxon Signed Rank test were conducted to provide further justification for the non-parametric results. The tests was used to determine if the average number of stops for the SCATS system as compared to the MDOT pre-timed system were statistically significantly different for the following comparisons:

- Number of stopped vehicles along M-59 by peak period
- Number of stopped vehicles along the minor roadways by peak period

The peak periods for the analysis include the weekday noon, weekday PM, Friday noon, Friday PM and Saturday. The null hypothesis for the number of stopped vehicle data for the SCATS and the MDOT pre-timed system was as follows:

H_o (null hypothesis): There was no difference between the average number of stopped vehicles between the SCATS and MDOT pre-timed systems for a specified peak period.

Based upon the statistical analysis, the null hypothesis was not accepted for each comparison between the SCATS and the MDOT pre-timed system. For the paired t-test, the comparison of the SCATS system to the MDOT pre-timed system for the minor roadways during the Saturday peak period were found to be statistically different. The MDOT pre-timed system had fewer vehicles stopping along the minor roadways than the SCATS system. The Wilcoxon Signed Rank test found similar results for the Saturday peak period. In addition, the Wilcoxon Signed Rank test found statistically different results in the comparison of the M-59 traffic during the weekday PM peak period. The SCATS system has fewer vehicles stopping along M-59 during the weekday PM peak period. For the remaining of the comparisons, there was no statistical difference between the two signal systems for the remaining peak periods analyzed. A significant result indicating differences between the two systems would be represented by a p-value less than 0.05, representing a level of confidence of 95 percent. The results of the paired t-test results are shown in Table 39 while the results of the Wilcoxon Signed Rank test results are shown in Table 40.

Table 39. Number of Stopped Vehicles Paired t-test Statistical Analysis Results

Comparison Category of SCATS vs. MDOT Pre-timed Systems	Mean Difference	Standard Error of the Difference	95% Lower Bound Confidence Interval	95% Upper Bound Confidence Interval	Test Result (p-value)
M-59 Traffic Weekday Noon	-5.04	85.97	-182.89	172.80	SCATS= Pre-timed (0.954)
M-59 Traffic Weekday PM Peak	217.63	113.96	-18.12	453.37	SCATS= Pre-timed (0.069)
M-59 Traffic Friday Noon Peak	-46.92	121.28	-297.80	203.97	SCATS= Pre-timed (0.702)
M-59 Traffic Friday PM Peak	63.50	240.42	-433.84	560.84	SCATS= Pre-timed (0.794)
M-59 Traffic Saturday Peak	-82.13	69.65	-226.20	61.95	SCATS= Pre-timed (0.250)

Table 39. Number of Stopped Vehicles Paired t-test Statistical Analysis Results (continued)

Comparison Category of SCATS vs. MDOT Pre-timed Systems	Mean Difference	Standard Error of the Difference	95% Lower Bound Confidence Interval	95% Upper Bound Confidence Interval	Test Result (p-value)
Minor Roadways Weekday Noon Peak	-3.13	33.95	-73.36	67.11	SCATS= Pre-timed (0.927)
Minor Roadways Weekday PM Peak	146.50	159.62	-183.70	476.70	SCATS= Pre-timed (0.368)
Minor Roadways Friday Noon Peak	-38.38	50.26	-142.34	65.59	SCATS= Pre-timed (0.453)
Minor Roadways Friday PM Peak	-76.17	235.32	-562.97	410.63	SCATS= Pre-timed (0.749)
Minor Roadways Saturday Peak	-73.17	25.75	-126.44	-19.89	**Reject Null**; SCATS≠ Pre-timed (0.009)

Table 40. Number of Stopped Vehicles Wilcoxon Signed Rank Statistical Analysis Results

Comparison Category of SCATS vs. MDOT Pre-timed Systems	Negative Ranks (SCATS< Pre-timed)	Positive Ranks (SCATS> Pre-timed)	Z-Calculated	Test Result (p-value)
M-59 Traffic Weekday Noon	14	10	-0.057	SCATS= Pre-timed (0.954)
M-59 Traffic Weekday PM Peak	17	7	-2.286	**Reject Null**; SCATS≠ Pre-timed (0.022)
M-59 Traffic Friday Noon Peak	12	12	0.000	SCATS= Pre-timed (1.000)
M-59 Traffic Friday PM Peak	14	10	-0.543	SCATS= Pre-timed (0.587)
M-59 Traffic Saturday Peak	10	14	-1.172	SCATS= Pre-timed (0.241)

Table 40. Number of Stopped Vehicles Wilcoxon Signed Rank Statistical Analysis Results (continued)

Comparison Category of SCATS vs. MDOT Pre-timed Systems	Negative Ranks (SCATS< Pre-timed)	Positive Ranks (SCATS> Pre-timed)	Z-Calculated	Test Result (p-value)
Minor Roadways Weekday Noon Peak	11	13	-0.086	SCATS= Pre-timed (0.932)
Minor Roadways Weekday PM Peak	13	11	-0.829	SCATS= Pre-timed (0.407)
Minor Roadways Friday Noon Peak	14	10	-0.543	SCATS= Pre-timed (0.587)
Minor Roadways Friday PM Peak	15	9	-0.971	SCATS=Ag Pre-timed ed (0.331)
Minor Roadways Saturday Peak	9	15	-2.229	**Reject Null**; SCATS≠ Pre-timed (0.026)

Maximum Queue Length Analysis

The maximum queue length in vehicles at the study intersections data was categorized by those vehicles queued at signals along the main roadway (M-59) and those along the minor roadways for each of the two signal systems; SCATS and the MDOT pre-timed system. The maximum queue length in vehicles at the study intersections for M-59 and the minor roadways are shown graphically in Figures 29 through 30.

Statistical data calculated, including the mean queue length by roadway type, standard deviation, and the percent difference in mean queue length, are shown in Table 41. A negative value for the percent difference in the mean queue length indicates that the MDOT pre-timed system had shorter queues than the SCATS system. A positive value for the percent difference in the mean queue length indicates that the SCATS system had shorter queues than the MDOT pre-timed system.

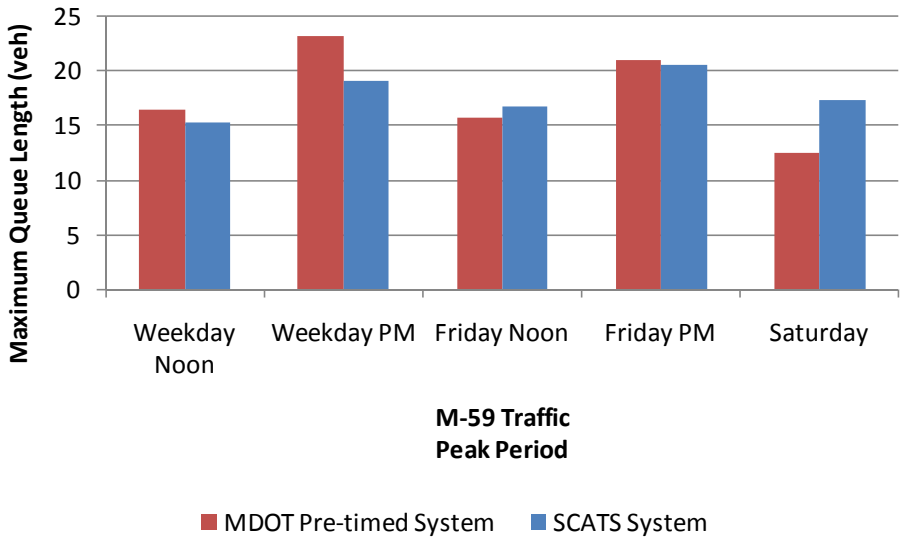

Figure 29. M-59 Maximum Queue Length By Peak Period

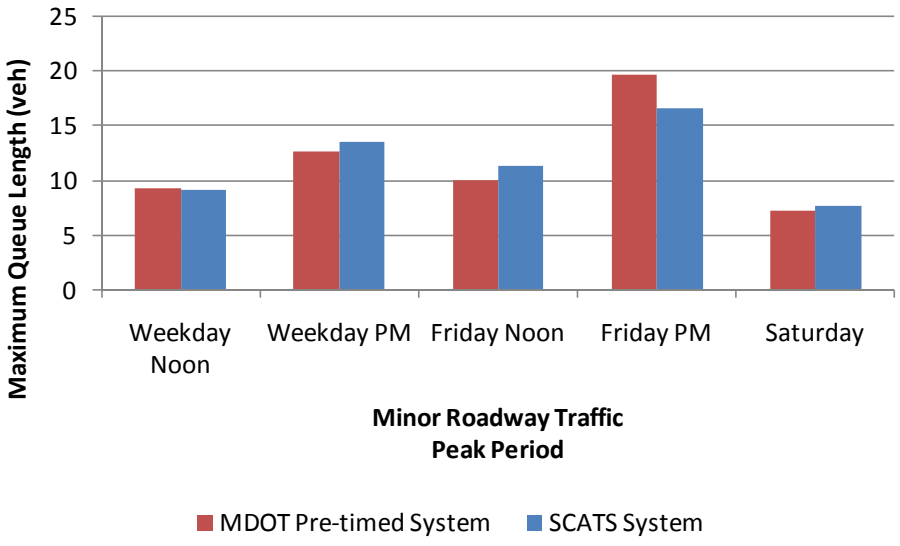

Figure 30. Minor Roadways Maximum Queue Length By Peak Period

Table 41. Maximum Queue Length Statistical Data

Day, Peak Period and Direction of Travel	MDOT Pre-timed System		SCATS System		Percent Difference in Mean Queue Length
	Mean Queue Length	Standard Deviation	Mean Queue Length	Standard Deviation	
Weekday Noon Peak					
M-59	16.50	11.44	15.29	11.55	7.33%
Minor Roadways	9.29	5.87	9.21	5.66	0.86%
Weekday PM Peak					
M-59	23.23	19.92	19.17	15.74	17.48%
Minor Roadways	12.79	10.66	13.63	9.84	-6.57%
Friday Noon Peak					
M-59	15.83	11.60	16.83	13.04	-6.32%
Minor Roadways	10.13	5.94	11.42	6.89	-12.73%
Friday PM Peak					
M-59	21.00	19.13	20.67	17.15	1.57%
Minor Roadways	19.71	24.48	16.63	13.15	15.63%
Saturday Peak					
M-59	12.58	9.08	17.38	22.10	-38.16%
Minor Roadways	7.25	4.59	7.79	5.27	-7.45%

The maximum queue length data was analyzed for adherence to the assumption of normality for use in the paired t-test for determining if the difference in the mean maximum queue length was significant. The paired t-test was selected for the maximum queue length due to the matched characteristics of the data collection where data was collected for each intersection's critical lane group for the same period under each signal system. A review of the data indicates that the data was not normally distributed and therefore the paired t-test should not be conducted due to the lack of the test's ability to maintain adequate power and robustness of the test, which assures the results of the analysis.

A non-parametric test can be conducted when the assumption of normality is violated in the paired t-test, such as the Wilcoxon Signed Rank Test. Due to confusion regarding non-parametric tests outside of the academia, both the paired t-test and the Wilcoxon Signed Rank test were conducted to provide further justification for the non-parametric results. The tests were

used to determine if the mean maximum queue length for the SCATS system as compared to the MDOT pre-timed system were statistically significantly different for the following comparisons:

- Maximum queue length along M-59 by peak period
- Maximum queue length along the minor roadways by peak period

The peak periods for the analysis include the weekday noon, weekday PM, Friday noon, Friday PM and Saturday. The null hypothesis for the queue length data for the SCATS and the MDOT pre-timed system was as follows:

> H_o (null hypothesis): There was no difference between the average maximum queue length between the SCATS and MDOT pre-timed systems for a specified peak period.

Based upon the statistical analysis, the null hypothesis was accepted for each comparison between the SCATS and the MDOT pre-timed system. Therefore, there was no statistical difference between the two signal systems for the peak periods analyzed. A significant result indicating differences between the two systems would be represented by a p-value less than 0.05, representing a level of confidence of 95 percent. The results of the paired t-test results are shown in Table 42 while the results of the Wilcoxon Signed Rank test results are shown in Table 43.

Table 42. Queue Length Paired t-test Statistical Analysis Results

Comparison Category of SCATS vs. MDOT Pre-timed Systems	Mean Difference	Standard Error of the Difference	95% Lower Bound Confidence Interval	95% Upper Bound Confidence Interval	Test Result (p-value)
M-59 Traffic Weekday Noon	1.21	1.52	-1.94	4.35	SCATS= Pre-timed (0.435)
M-59 Traffic Weekday PM Peak	4.08	2.06	-0.19	8.35	SCATS= Pre-timed (0.060)
M-59 Traffic Friday Noon Peak	-1.00	1.96	-5.06	3.06	SCATS= Pre-timed (0.616)
M-59 Traffic Friday PM Peak	0.33	2.89	-5.64	6.31	SCATS= Pre-timed (0.909)
M-59 Traffic Saturday Peak	-4.79	4.11	-13.30	3.71	SCATS= Pre-timed (0.256)

Table 42. Queue Length Paired t-test Statistical Analysis Results (continued)

Comparison Category of SCATS vs. MDOT Pre-timed Systems	Mean Difference	Standard Error of the Difference	95% Lower Bound Confidence Interval	95% Upper Bound Confidence Interval	Test Result (p-value)
Minor Roadways Weekday Noon Peak	0.08	0.659	-1.28	1.48	SCATS= Pre-timed (0.900)
Minor Roadways Weekday PM Peak	-0.83	1.61	-4.16	2.50	SCATS= Pre-timed (0.609)
Minor Roadways Friday Noon Peak	-1.29	1.00	-3.37	0.78	SCATS= Pre-timed (0.210)
Minor Roadways Friday PM Peak	3.08	4.10	-5.39	11.56	SCATS= Pre-timed (0.459)
Minor Roadways Saturday Peak	-0.54	0.71	-2.02	0.93	SCATS= Pre-timed (0.455)

Table 43. Queue Length Wilcoxon Signed Rank Statistical Analysis Results

Comparison Category of SCATS vs. MDOT Pre-timed Systems	Negative Ranks (SCATS< Pre-timed)	Positive Ranks (SCATS> Pre-timed)	Tie Ranks (SCATS= Pre-timed)	Z-Calculated	Test Result (p-value)
M-59 Traffic Weekday Noon	14	8	2	-0.992	SCATS= Pre-timed (0.321)
M-59 Traffic Weekday PM Peak	12	8	4	-1.345	SCATS= Pre-timed (0.179)
M-59 Traffic Friday Noon Peak	10	11	3	-0.522	SCATS= Pre-timed (0.601)
M-59 Traffic Friday PM Peak	12	9	3	-0.191	SCATS= Pre-timed (0.848)
M-59 Traffic Saturday Peak	10	9	5	-0.609	SCATS= Pre-timed (0.542)
Minor Roadways Weekday Noon Peak	9	11	4	-0.038	SCATS= Pre-timed (0.970)
Minor Roadways Weekday PM Peak	11	9	4	-0.113	SCATS= Pre-timed (0.910)

Table 43. Queue Length Wilcoxon Signed Rank Statistical Analysis Results (continued)

Comparison Category of SCATS vs. MDOT Pre-timed Systems	Negative Ranks (SCATS< Pre-timed)	Positive Ranks (SCATS> Pre-timed)	Tie Ranks (SCATS= Pre-timed)	Z-Calculated	Test Result (p-value)
Minor Roadways Friday Noon Peak	7	14	3	-1.323	SCATS= Pre-timed (0.186)
Minor Roadways Friday PM Peak	14	9	1	-0.198	SCATS= Pre-timed (0.843)
Minor Roadways Saturday Peak	10	11	3	-0.875	SCATS= Pre-timed (0.381)

CONCLUSIONS

Beginning in 1992, Oakland County began converting their pre-timed coordinated traffic signal systems to SCATS (Sydney Coordinated Adaptive Traffic System). SCATS uses anticipatory and adaptive techniques to increase the efficiency of the road network by minimizing the overall number of vehicular stops and delay experienced by motorists. The primary purpose of the SCATS system is to maximize the throughput of a roadway by controlling queue formation. The SCATS system has the ability to change the signal phasing, timing strategies and the signal coordination within a network to alleviate congestion by automatically adjusting the signal parameters according to real time traffic demand.

There had not been any comprehensive studies conducted in the past that evaluated the performance of the SCATS system in terms of delay, flow, queue length, fuel consumption, emissions and other characteristics.

The objective of this research was to assess the effectiveness of the SCATS signal system on the reduction of traffic congestion in terms of delay, queue length and other characteristics as compared to a pre-timed signal system.

Traffic operational data was collected for the SCATS signal system and an MDOT pre-timed signal system. The traffic operational data included the following:

- Travel time
- Travel speed
- Fuel consumption
- Hydrocarbon emissions
- Carbon monoxide emissions
- Nitrogen oxide emissions
- Number of stops along the corridor
- Total travel delay
- Number of stopped vehicles at each intersection for M-59 and the minor intersecting roadways
- Maximum queue length at each intersection for M-59 and the minor intersecting roadways

The statistical significance of the effectiveness of the two signal systems were tested to determine whether the changes observed in the measures of effectiveness were attributable to the signal system or chance. Several hypotheses were presented and tested for significance at a 95 percent level of confidence or alpha equal to 0.05. A summary of the findings are as follows:

- The performance of the SCATS system was found to be superior for several of the performance measures for each of the peak periods generally for the eastbound travel direction. At 95 percent confidence level, it was not significant.
- A statistical difference was found between the two signal systems based upon the number of stopped vehicles for the minor roadways during the Saturday peak period. The number of stopped vehicles under the MDOT pre-timed signal system operation was fewer than under the SCATS signal system operation. For the remaining peak period comparisons for the minor roadways, there were not any statistical differences found between the two signal systems based upon the number of stopped vehicles.
- A statistical difference was found between the two signal systems based upon the number of stopped vehicles for M-59 during the weekday PM peak period. The number of stopped vehicles under the SCATS signal system operation was fewer than under the MDOT pre-timed signal system operation. For the remaining peak period comparisons for M-59, there were not any statistical differences found between the two signal systems based upon the number of stopped vehicles.

REFERENCES

1. 2005 Urban Mobility Report, Texas Transportation Institute.
2. National Traffic Signal Report Card, National Transportation Operations Coalition, 2005.
3. "FAST-TRAC: A New Solution to an Old Problem." Road Commission of Oakland County.
4. "Intelligent Transportation System Benefits: 2001 Update." Mitretek Systems, United States Department of Transportation, Washington D.C., June 2001.
5. Martin, Peter T., Joseph Perrin, Bhargava Rama Chilukuri, Chantan Jhaveri and Yuqi Feng. Adaptive Signal Control II. University of Utah Traffic Lab, Department of Civil and Environmental Engineering, Salt Lake City, Utah, January 2003.
6. "Adaptive Road Traffic Control Systems in Use in Ireland." www.iol.ie~discover/traffic.htm.
7. Jhaveri, Chintan S., Joseph Perrin, Peter Martin. "Scoot Adaptive Signal Control: An Evaluation of its Effectiveness over Range of Congestion Intensities." Transportation Research Board 2003 Annual Meeting, Compendium of Papers, January 2003.
8. Liu, Daizong and Ruey Long Cheu. "Comparative Evaluation of Dynamic TRANSYT and SCATS-Based Signal Control Logic using Microscopic Traffic Simulations." Transportation Research Board, 2004 Annual Meeting, Compendium of Papers, November 2003.
9. Adel-Rahim, Ahmed and William Taylor. "Potential Travel Time and Delay Benefits of Using Adaptive Signals." Transportation Research Board, 2000 Annual Meeting, Compendium of Papers, July 31, 1999.
10. Eghtedari, Ali. "Measuring the Benefits of Adaptive Traffic Signal Control: Case Study of Mill Plain Blvd. Vancouver, Washington." Transportation Research Board, 2006 Annual Meeting, Compendium of Papers.
11. Petrella, Margaret, Stacey Bricka, Michael Hunter, and Jane Lappin. "Driver Satisfaction with an Urban Arterial After Installation of an Adaptive Signal System." Transportation Research Board, 2006 Annual Meeting, Compendium of Papers, November 15, 2005.
12. Park, Byungkyu, Jongsun Won and Ilsoo Yun. "Application of Microscopic Simulation Model Calibration and Validation Procedure: A Case Study of Coordinated Actuated Signal System." Transportation Research Board, 2006 Annual Meeting.
13. Al-Mudhaffar, Azhar and Kari-Lennart Bang. "Impacts of Coordinated Traffic Signal Control Strategies and Bus Priority." Transportation Research Board, 2006 Annual Meeting, Compendium of Papers.
14. Wolshon, Brian and William Taylor. "Impact of Adaptive Signal Control on Major and Minor Approach Delay." Journal of Transportation Engineering, Volume 125, Number 1, pp. 30-38, January/February 1999.
15. Park, Byungkyu and Myungsoon Chang. "Realizing Benefits of Adaptive Signal Control at an Isolated Intersection." Transportation Research Board, 2002 Annual Meeting, Compendium of Papers, November 2001.

16. Girianna, Montty and Rahim Benekohal. "Signal Coordination for a Two-Way Street Network with Oversaturated Intersections." Transportation Research Board, 2003 Annual Meeting, Compendium of Papers, January 2003.
17. Stevanovic, Aleksandar and Peter Martin. "Assessing the Ageing of Pre-Timed Traffic Signal Control Using Synchro and SimTraffic." Transportation Research Board, 2006 Annual Meeting, Compendium of Papers, November 15, 2005.
18. Oppenlander, J.C. "Sample Size Determination for Travel Time and Delay Studies." Traffic Engineering Journal, September 1976.
19. Manual of Transportation Engineering Studies, Institute of Transportation Engineers, Prentice Hall, 2000.
20. Hinkle, Dennis, W. Wiersma, and S. Jurs. Applied Statistics for the Behavioral Sciences, Fifth Edition. Houghton Mifflin Company, New York, New York, 2003.
21. "Levene Test for Equality of Variances." Engineering Statistics Handbook, Chapter 1.3.5.10., 1960.
22. Field, Andy. Discovering Statistics Using SPSS, Second Edition. Sage Publications, Limited, Thousand Oaks, CA, 2005.

APPENDIX A

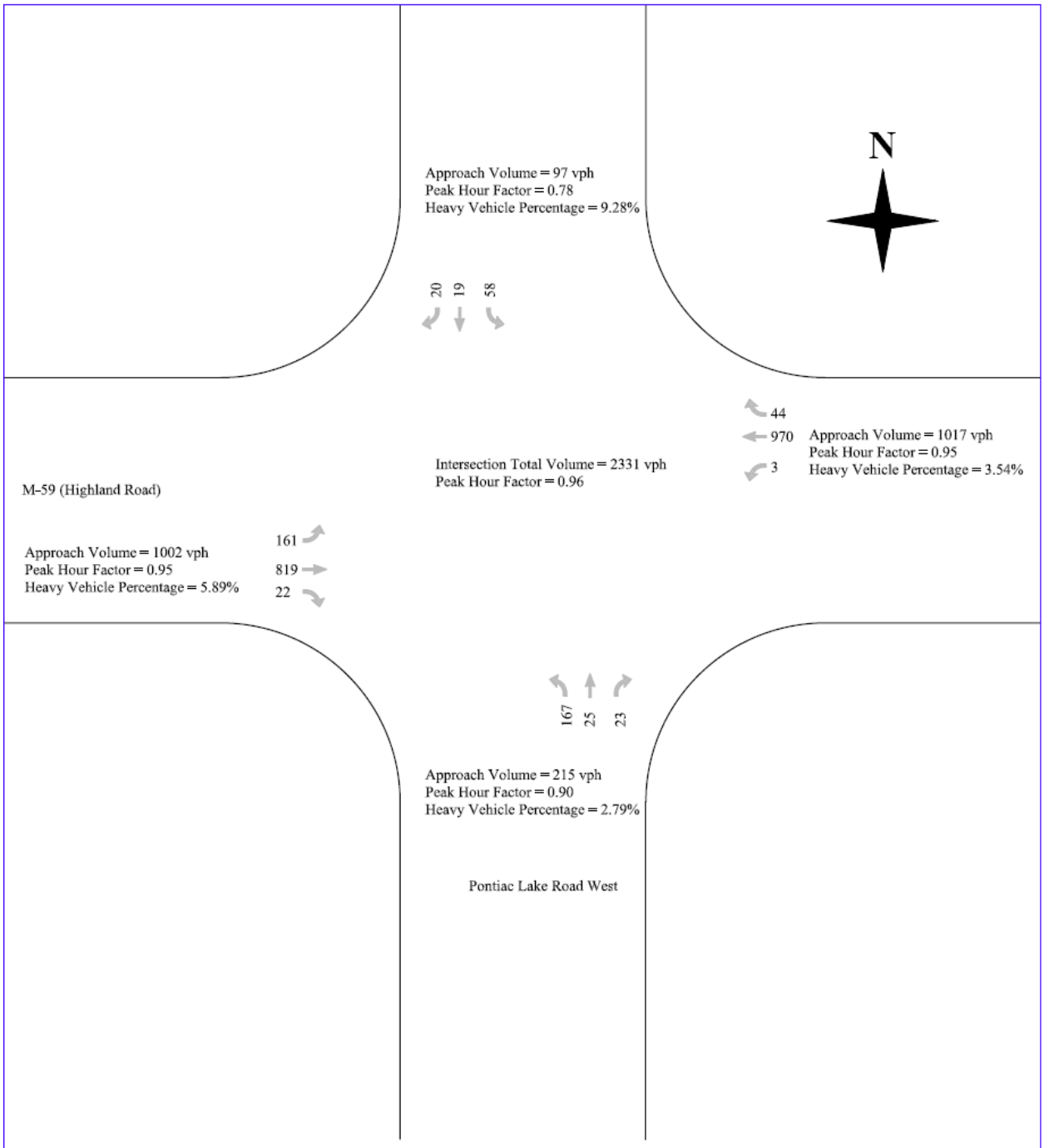

Volume Diagram
M-59 and Pontiac Lake Road West
Noon Peak Hour Volume Diagram

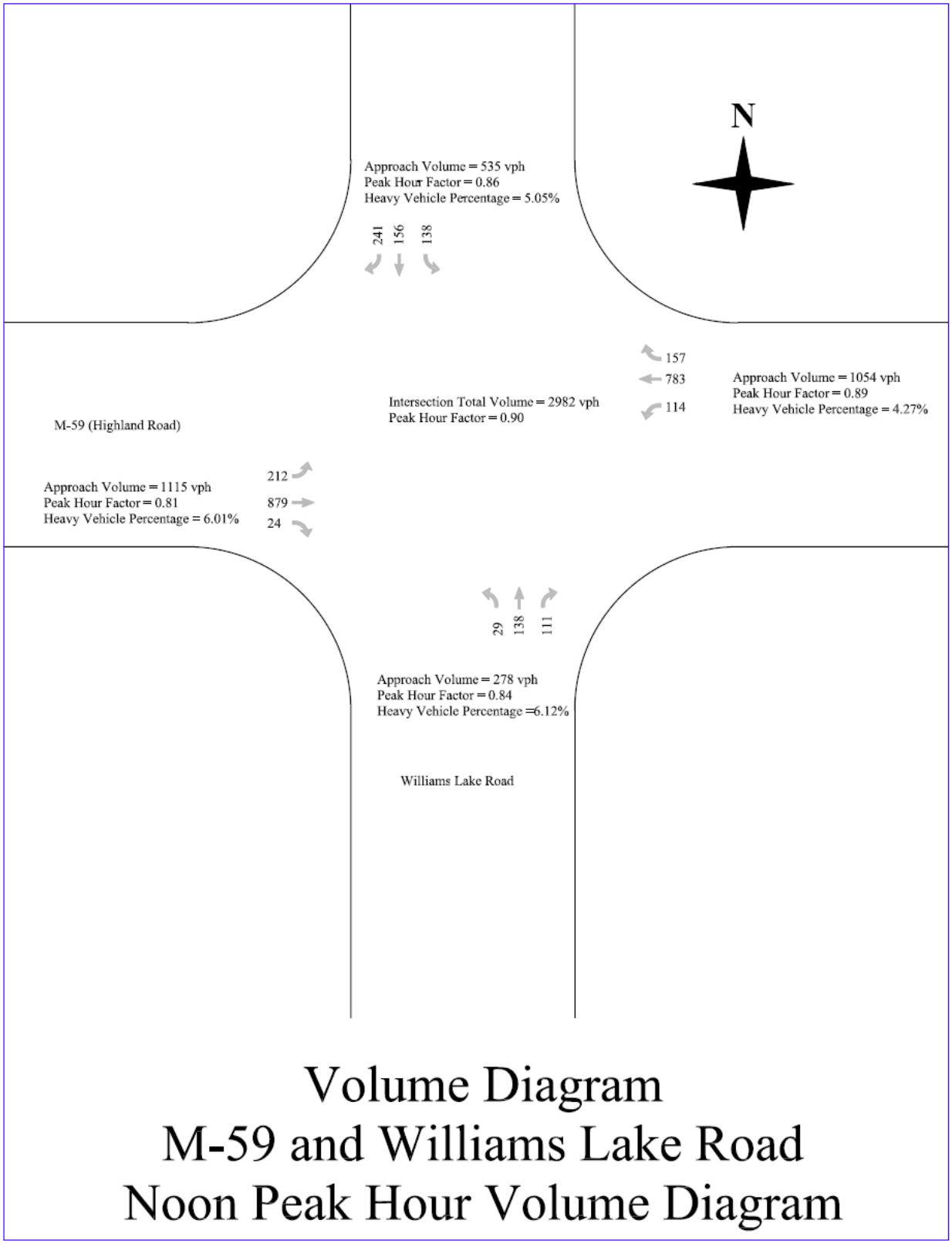

Volume Diagram
M-59 and Williams Lake Road
Noon Peak Hour Volume Diagram

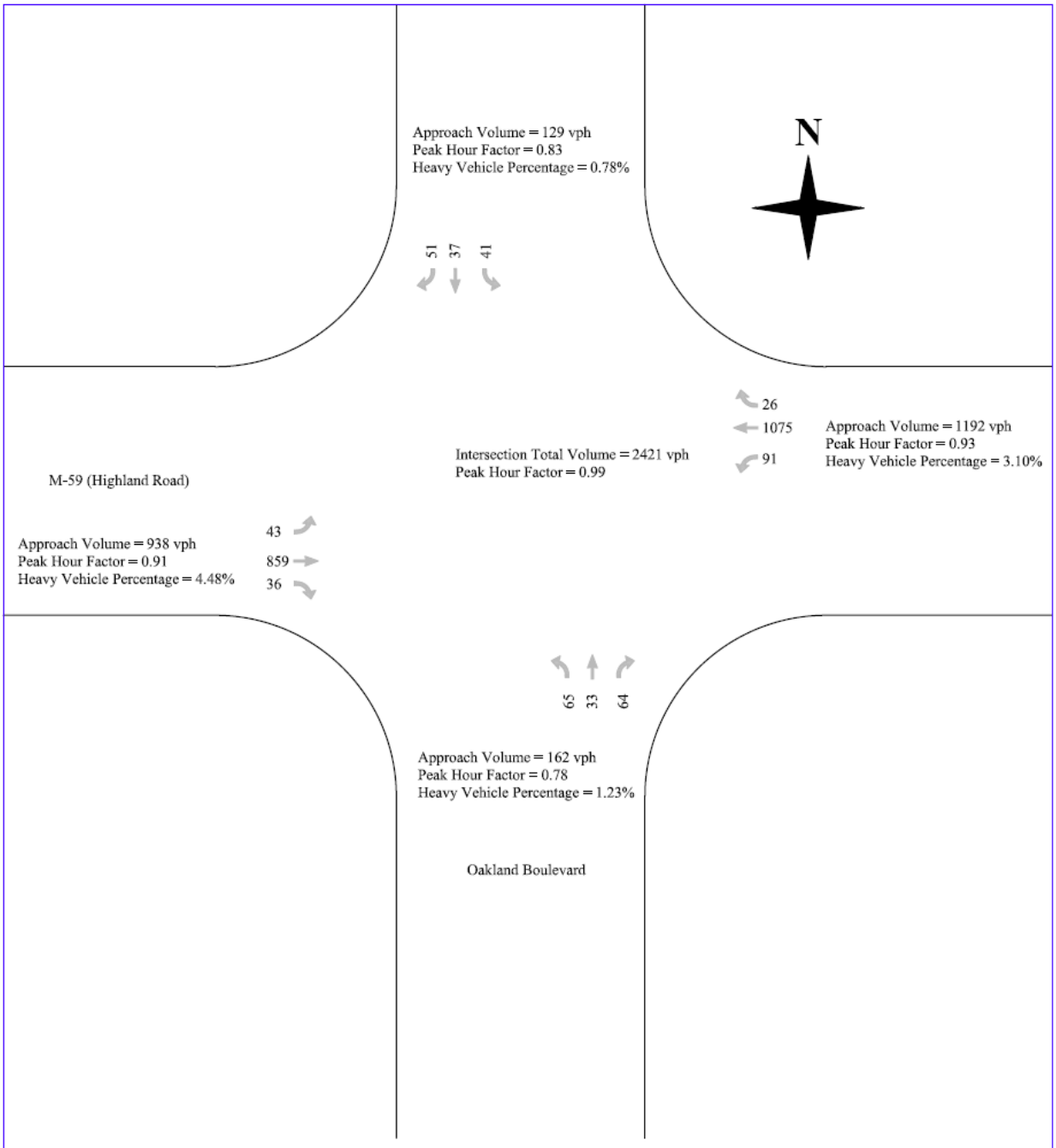

Volume Diagram
M-59 and Oakland Boulevard
Noon Peak Hour Volume Diagram

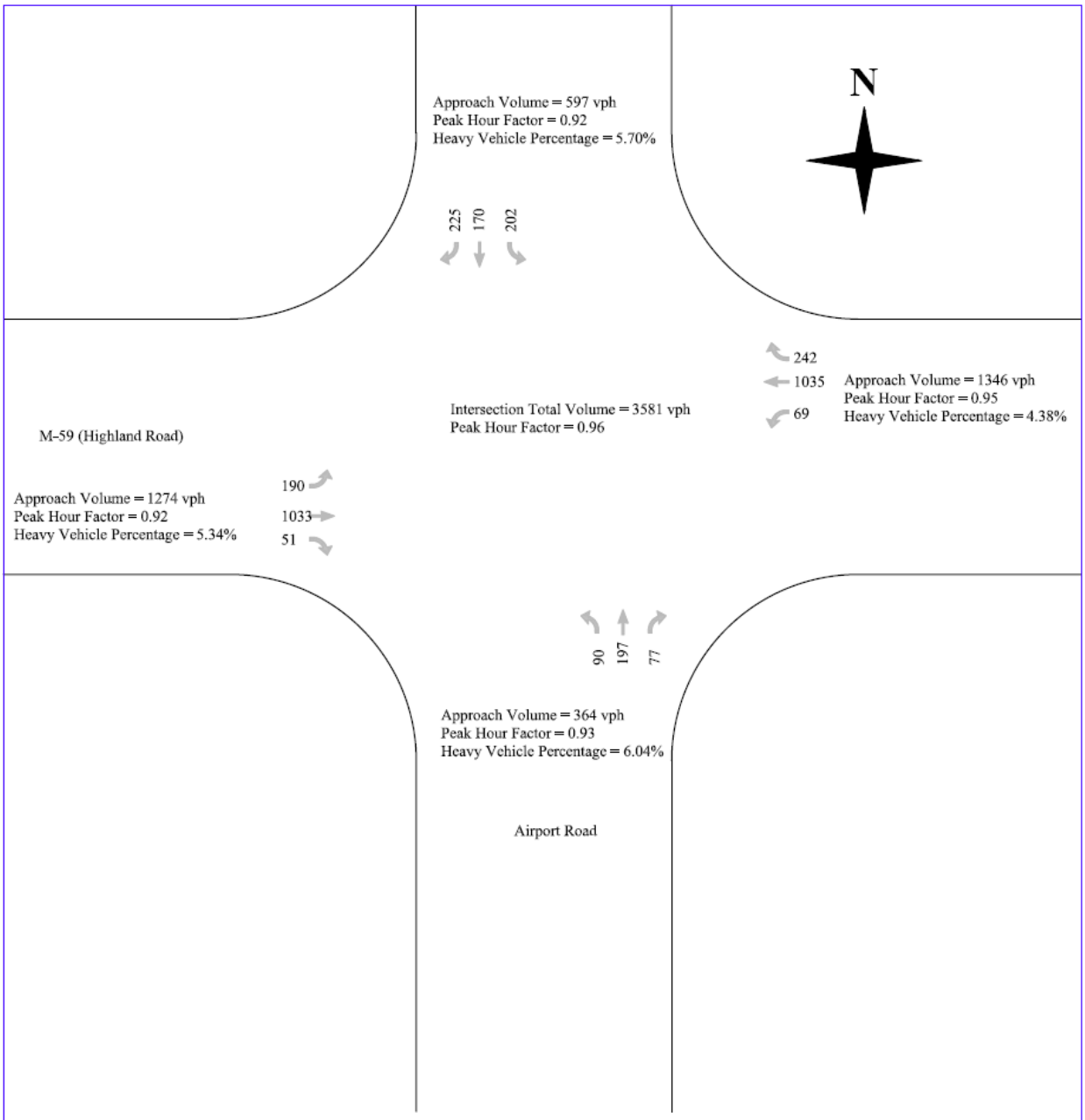

Volume Diagram
M-59 and Airport Road
Noon Peak Hour Volume Diagram

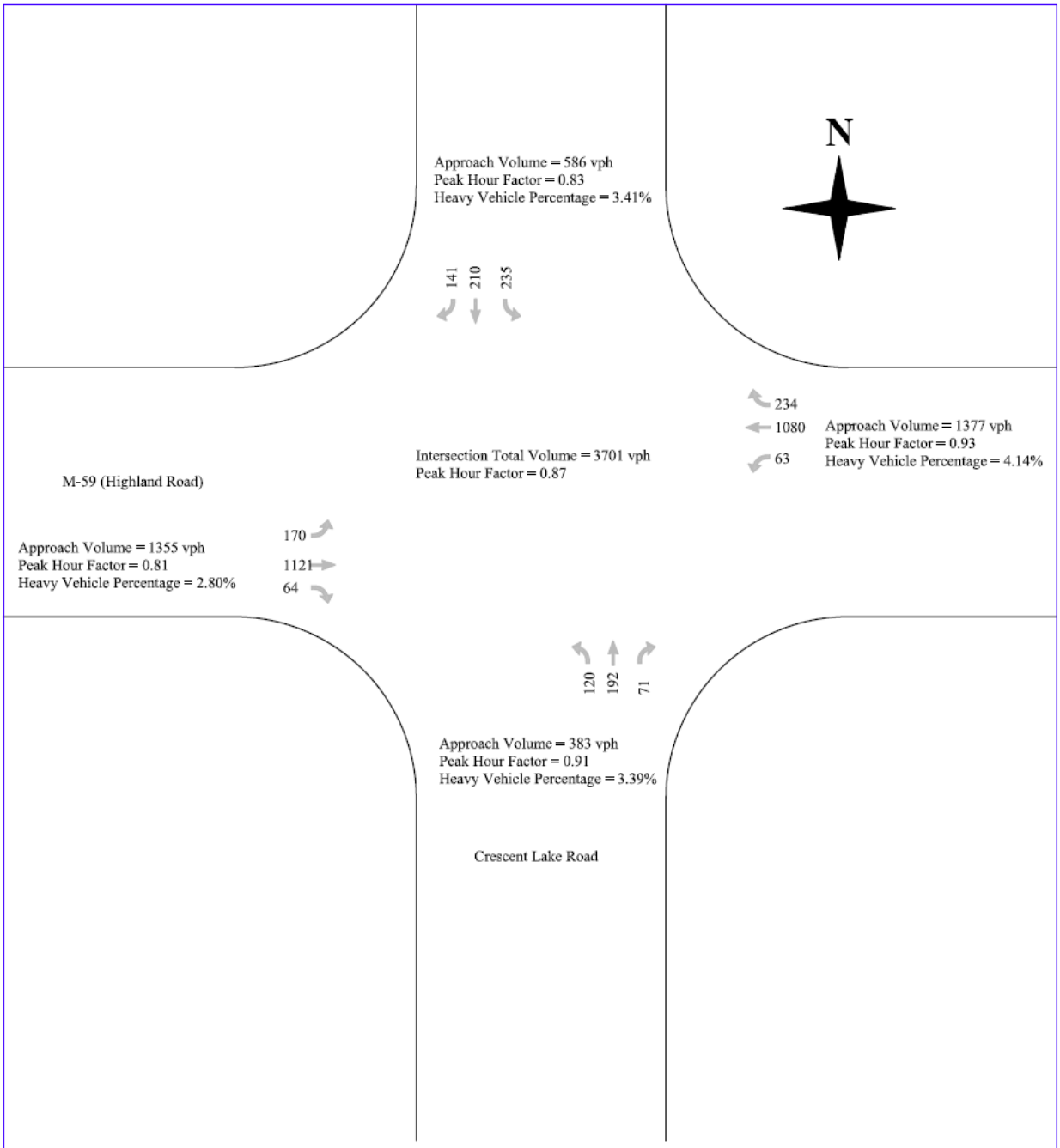

Volume Diagram
M-59 and Crescent Lake Road
Noon Peak Hour Volume Diagram

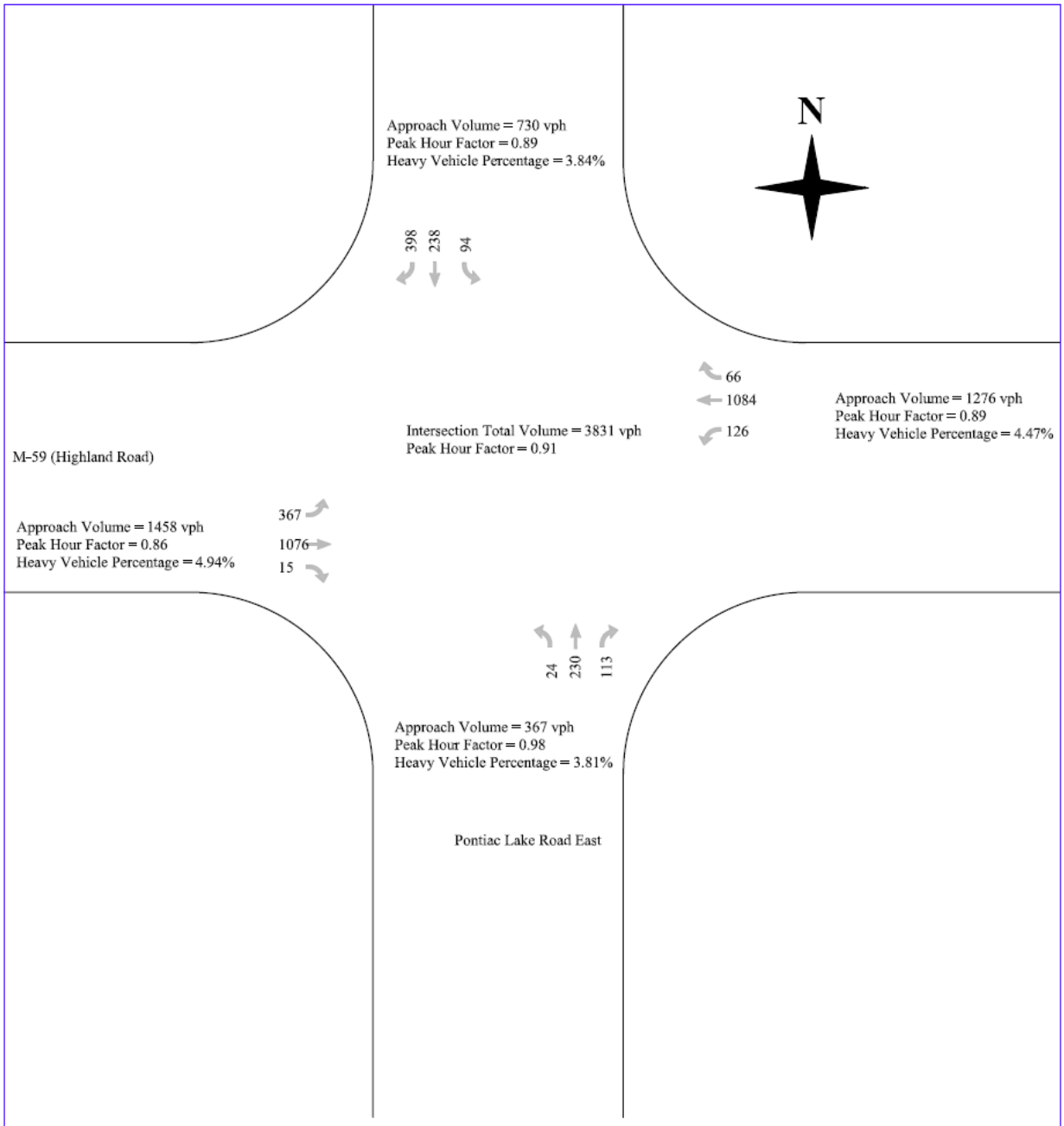

Volume Diagram
M-59 and Pontiac Lake Road East
Noon Peak Hour Volume Diagram

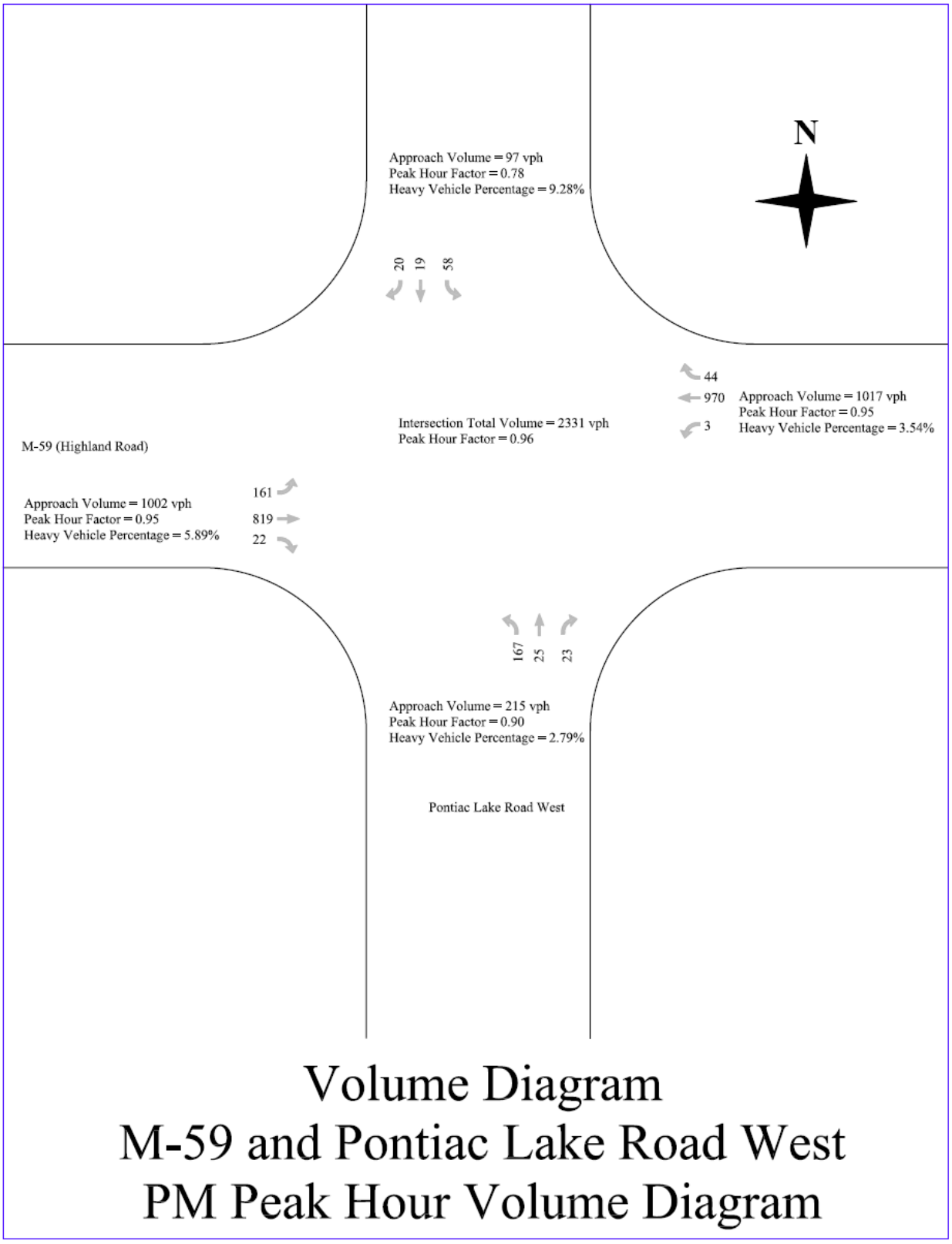

Volume Diagram
M-59 and Pontiac Lake Road West
PM Peak Hour Volume Diagram

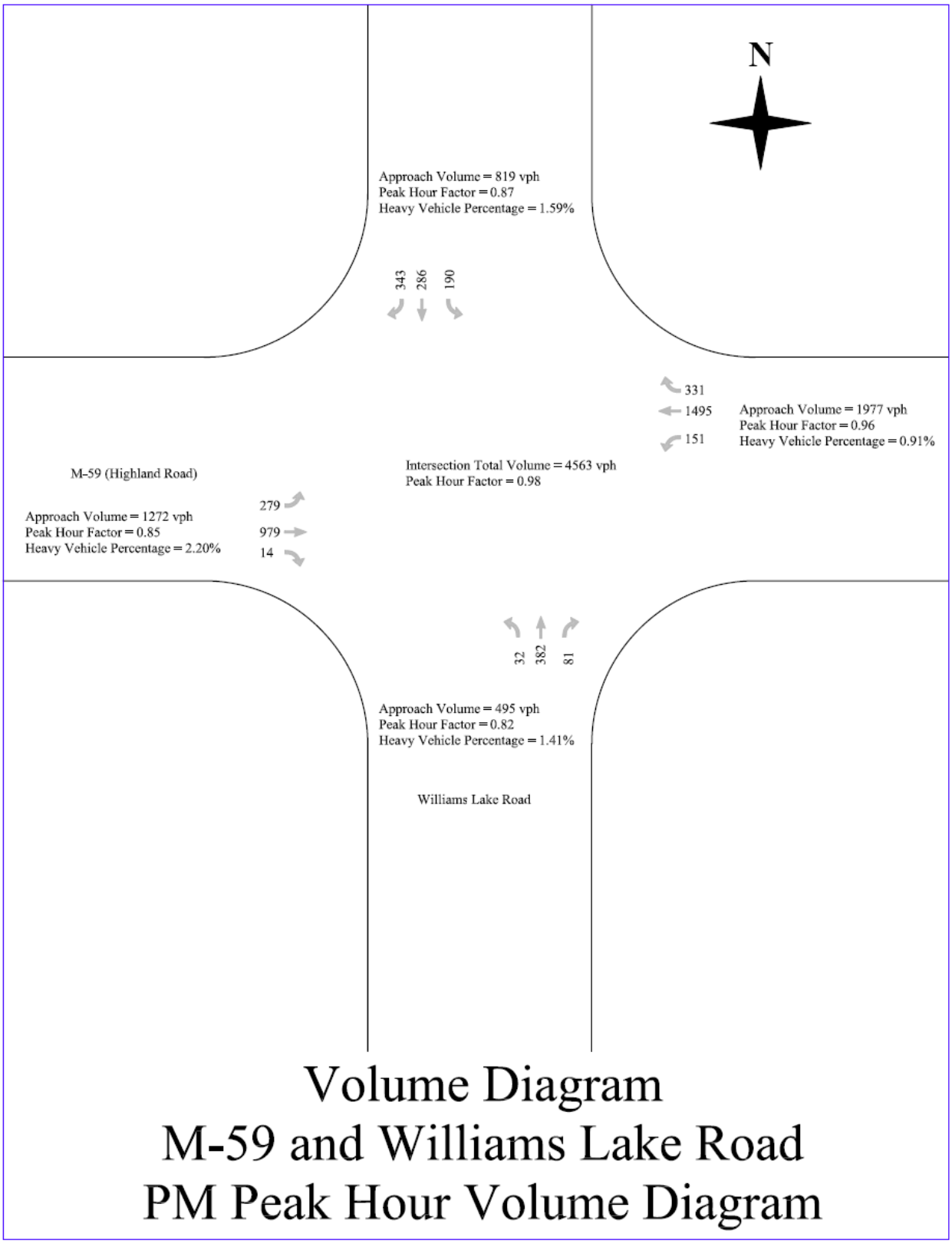

Volume Diagram
M-59 and Williams Lake Road
PM Peak Hour Volume Diagram

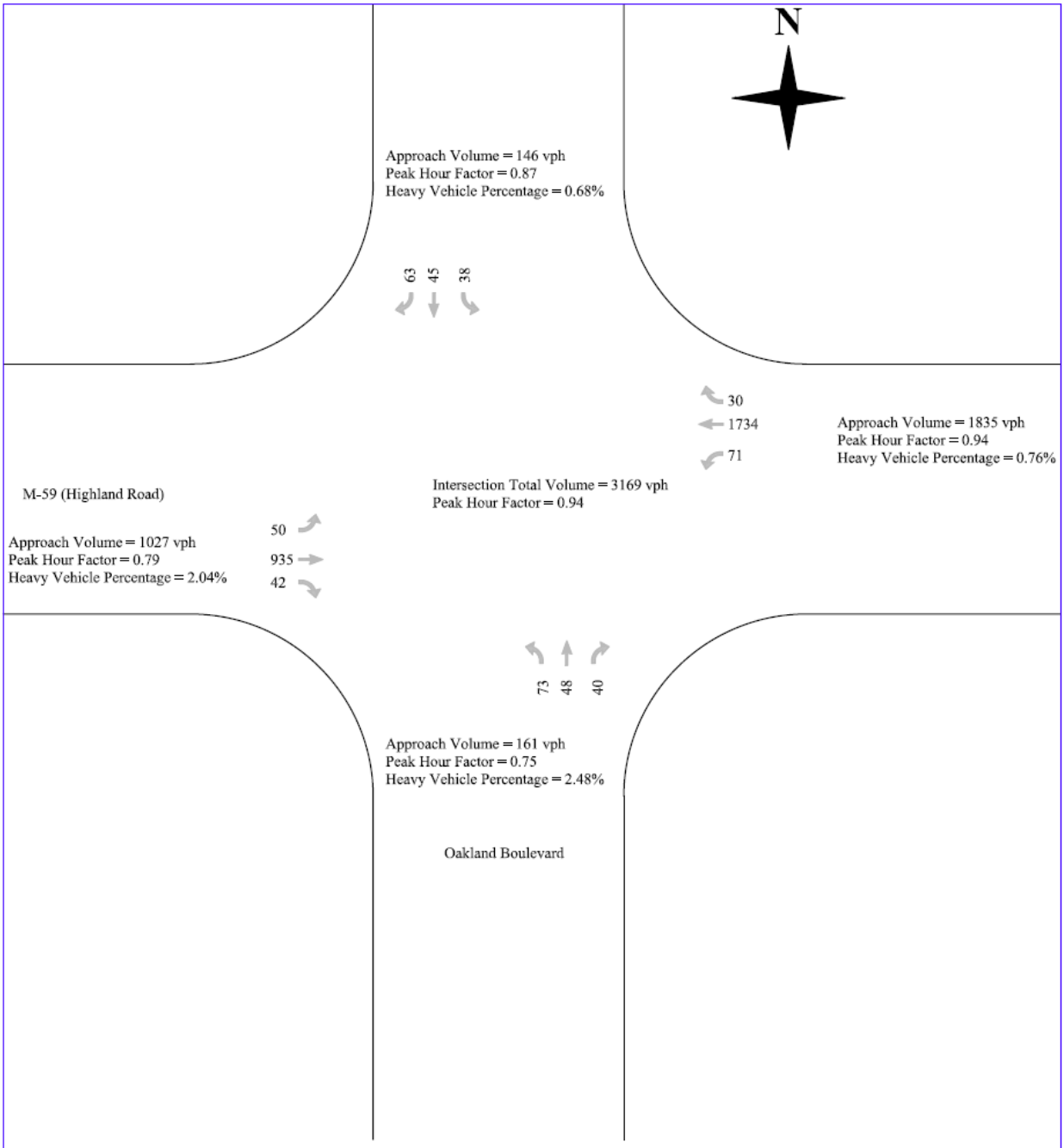

Volume Diagram
M-59 and Oakland Boulevard
PM Peak Hour Volume Diagram

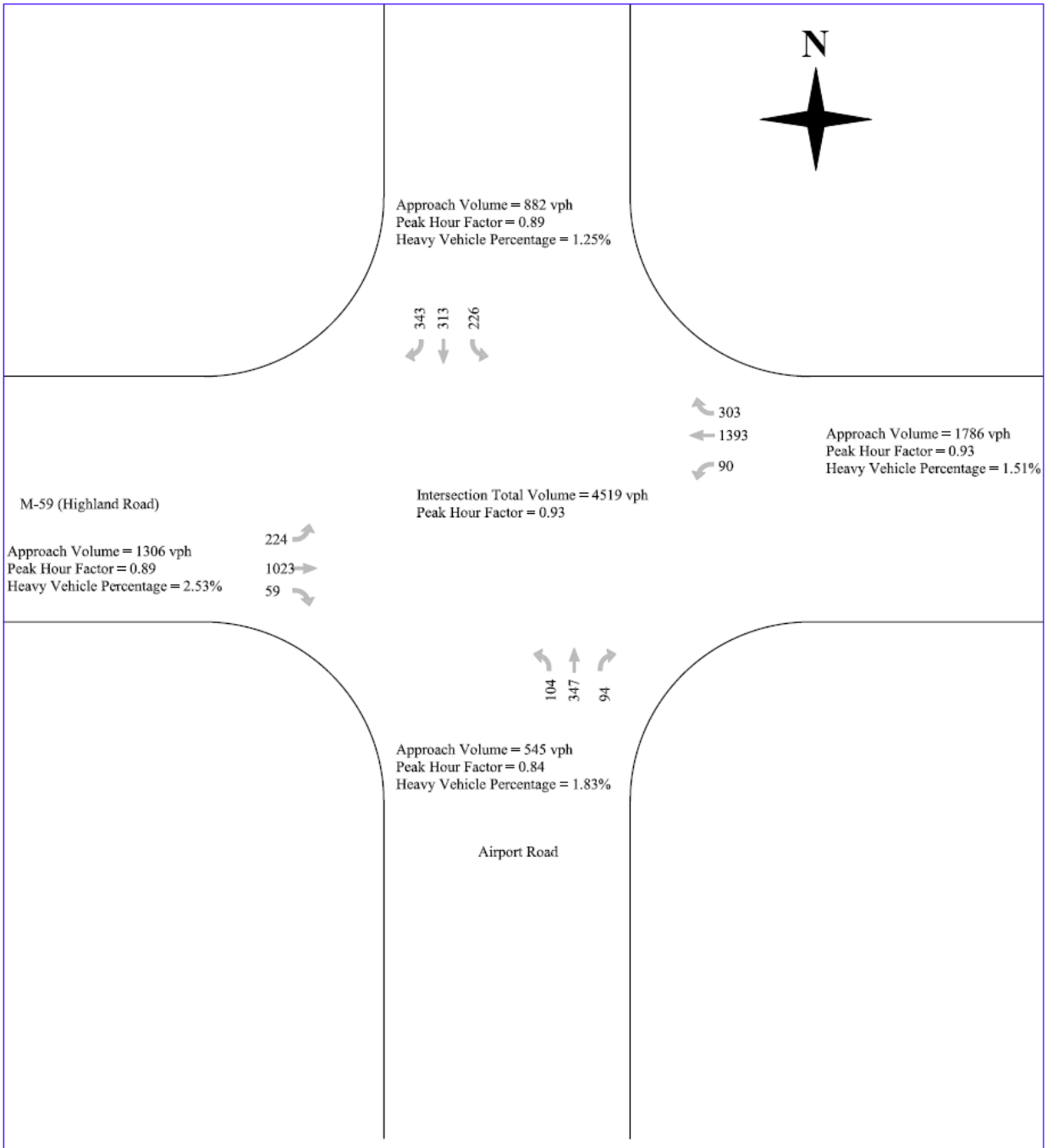

Volume Diagram
M-59 and Airport Road
PM Peak Hour Volume Diagram

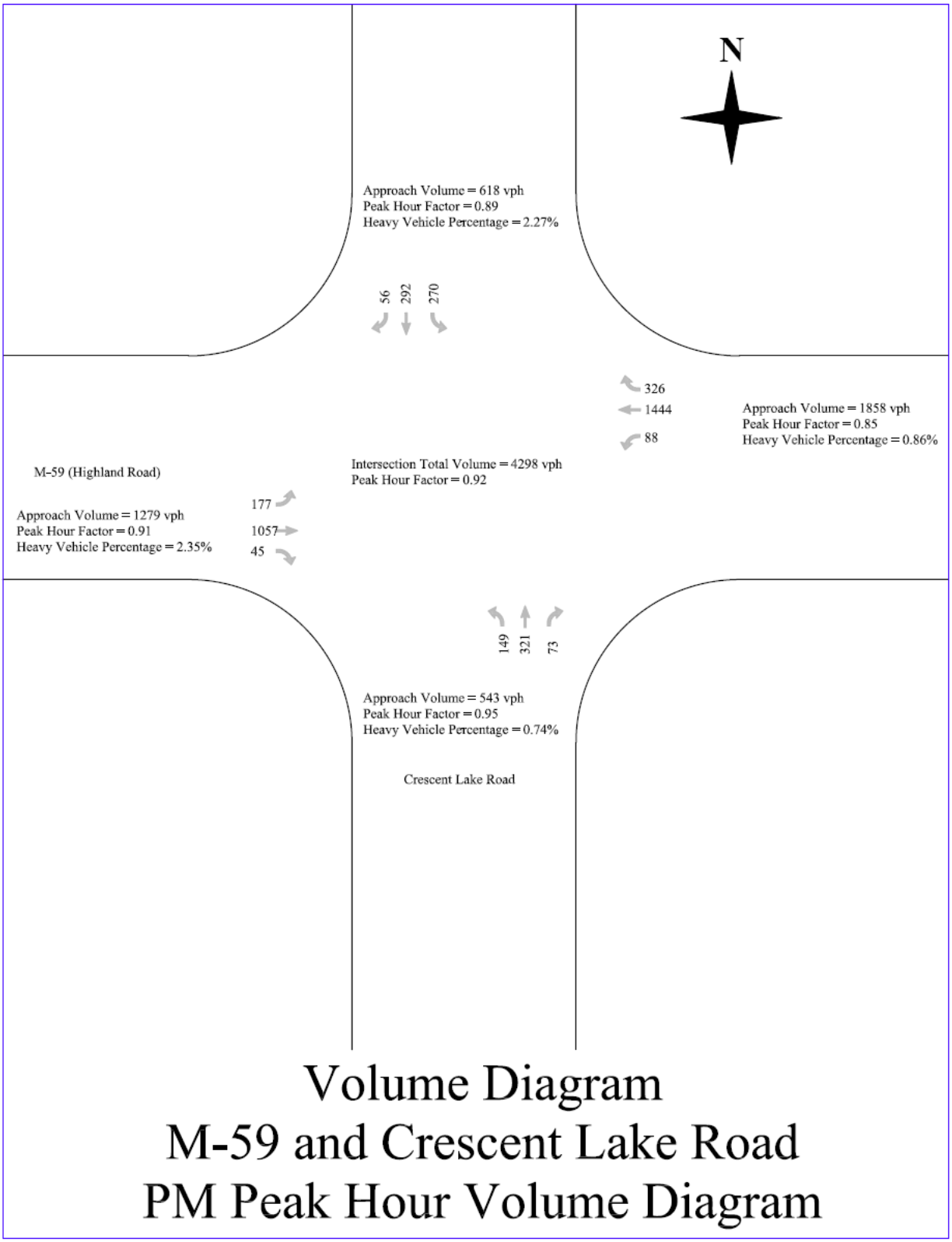

Volume Diagram
M-59 and Crescent Lake Road
PM Peak Hour Volume Diagram

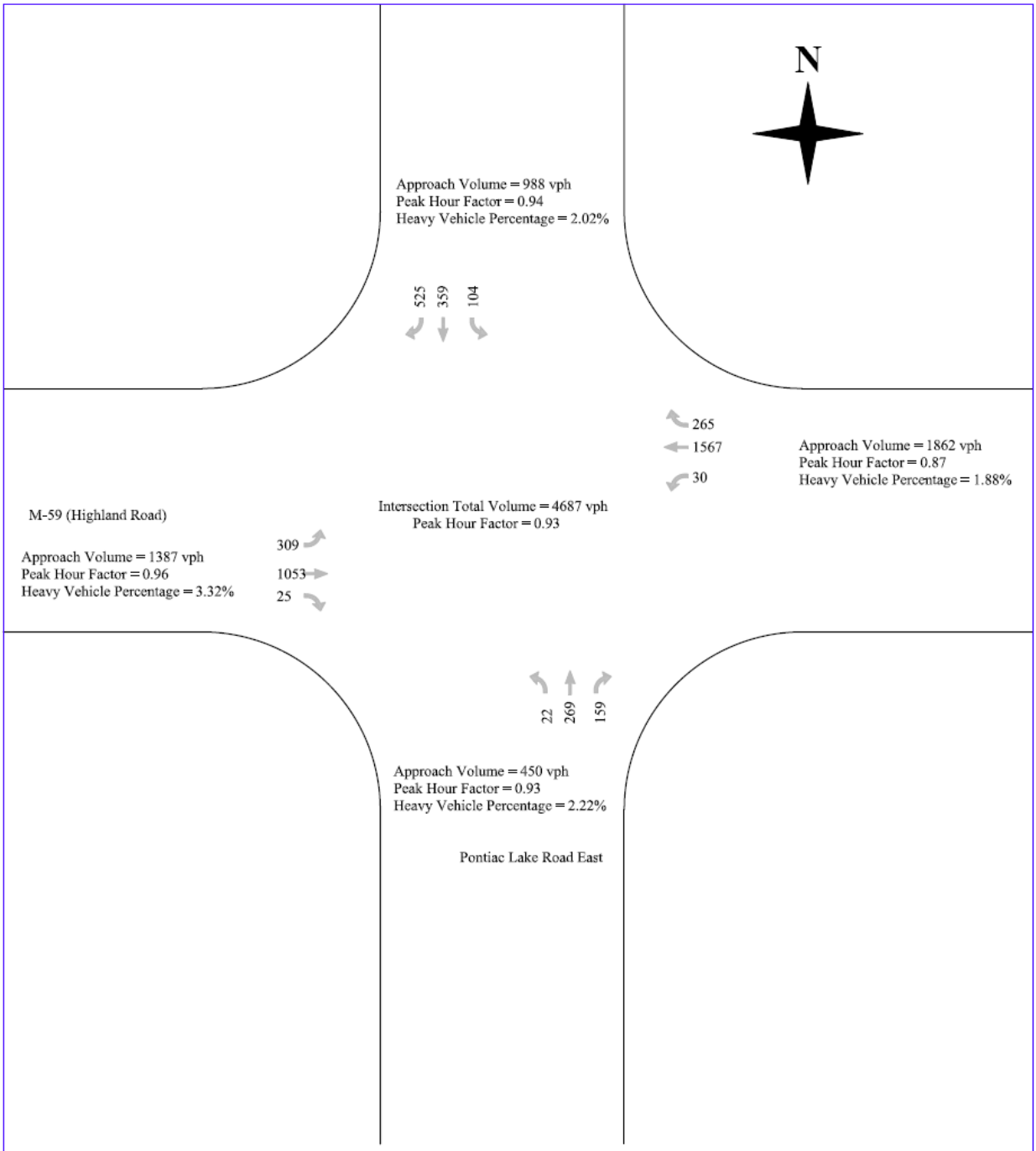

Volume Diagram
M-59 and Pontiac Lake Road East
PM Peak Hour Volume Diagram

MICHIGAN OHIO UNIVERSITY TRANSPORTATION CENTER
Alternate energy and system mobility to stimulate economic development.

Report No: MIOH UTC TS14 2010-Final
MDOT Report No: RC1545

MODELING METROPOLITAN DETROIT TRANSIT

Final Report

Project Team

Snehamay Khasnabis, Ph.D., P.E.
Elibe A. Elibe, E.I.T.
Sabyasachee Mishra, Ph.D., E.I.T.
Subrat K. Swain, E.I.T.
College of Engineering
Wayne State University
5050 Anthony Wayne Drive
Detroit, MI 48202

Utpal Dutta, Ph.D., P.E.
Eric Tenazas, E.I.T
Dept. of Civil & Environmental Engineering
University of Detroit Mercy
4001 W. McNichols Road
Detroit, Michigan 48221

Report No: MIOH UTC TS14 2010-Final

TS14, October, 2010
FINAL REPORT

Developed By:

Dr. Snehamay Khasnabis
Principal Investigator, WSU
skhas@wayne.edu

In conjunction with:

Dr. Utpal Dutta
Co- Principal Investigator, UDM
duttau@udmercy.edu
313-993-1040

SPONSORS

This is a Michigan Ohio University Transportation Center project supported by the U.S. Department of Transportation, the Michigan Department of Transportation, Wayne State University, and the University of Detroit Mercy.

ACKNOWLEDGEMENT

This research was conducted jointly at Wayne State University, Detroit and at the University of Detroit Mercy. Significant matching support was provided by the Michigan Department of Transportation and the two partner universities. The authors would like to express their sincere appreciation to the project sponsors for their support. The authors would also like to thank the Southeast Michigan Council of Governments (SEMCOG) for its assistance with a variety of data and literature. Particularly, the assistance of Alex Bourgeau and Dr. Li-Yang Feng of SEMCOG are thankfully acknowledged.

DISCLAIMERS

Technical Report Documentation Page

1. Report No. RC-1545	**2. Government Accession No.**	**3. MDOT Project Manager** Niles Annelin
4. Title and Subtitle Michigan Ohio University Transportation Center Subtitle: "Modeling Metropolitan Detroit Transit"		**5. Report Date** October 2010 **6. Performing Organization Code**
7. Author(s) Dr. Snehamay Khasnabis, Wayne State University Dr. Utpal Dutta, University of Detroit Mercy		**8. Performing Org. Report No.** MIOH UTC TS14 2010-Final
9. Performing Organization Name and Address Michigan Ohio University Transportation Center University of Detroit Mercy, Detroit, MI 48221 and Wayne State University, Detroit, MI 48202		**10. Work Unit No. (TRAIS)** **11. Contract No.** 2007-0538 **11(a). Authorization No.**
12. Sponsoring Agency Name and Address Michigan Department of Transportation Van Wagoner Building, 425 West Ottawa P. O. Box 30050, Lansing, Michigan 48909		**13. Type of Report & Period Covered** Research, October 2007 – October 2010 **14. Sponsoring Agency Code**

15. Supplementary Notes
Additional Sponsors: US DOT Research & Innovative Technology Administration, Wayne State University, and University of Detroit Mercy.

16. Abstract

MIOH UTC TS14 2010-Final

The seven-county Southeast Michigan region, that encompasses the Detroit Metropolitan Area, ranks fifth in population among top 25 regions in the nation. It also ranks among bottom five in the transit service provided, measured in miles or hours or per capita dollars of transit service. The primary transit agencies in the region essentially cater to 'captive riders'. Cities with a stronger transit base in the nation have two things in common; their ability to draw "choice" riders, and their success in building some type of rail transit system, with capital funds generally provided by the federal government. Over past three decades, a number of studies have examined the feasibility of rapid transit services in the Detroit region including speed link (rubber tired high speed buses), Light Rail Transit (LRT), Commuter Rail Transit (CRT) and High Speed Rail Transit (HRT). Among the many problems associated with building such a rapid transit system in the region, is the lack of a "quick response" tool for preliminary planning for light rail transit along an urban travel corridor. The primary objective of this project is to develop a quick-response tool for sketch planning purposes that may be used by other cities to test the feasibility of building LRT systems along a predefined transit corridor (i.e., a corridor with existing transit service, in form of buses). The primary focus of this study is to maximize the use of available data without any new data collection effort. In the report, the authors present an LRT case study for Detroit, where a number of LRT planning studies are currently underway, each with specific objectives, followed by a set of guidelines that can be used by transit planners for sketch planning of LRT. The guidelines are designed to assist transit planners in the preliminary planning effort for a LRT system on an urban travel corridor with existing bus services.

17. Key Words Light rail transit, Railroad commuter service, Bus rapid transit, High speed trains, Transit operating agencies, Public transit, Quality of service, and Detroit.		**18. Distribution Statement** No restrictions. This document is available to the public through the Michigan Department of Transportation.	
19. Security Classification -report	**20. Security Classification - page**	**21. No. of Pages** 57	**22. Price**

Abstract

The seven-county Southeast Michigan region, that encompasses the Detroit Metropolitan Area, ranks fifth in population among top 25 regions in the nation. It also ranks among bottom five in the transit service provided, measured in miles or hours or per capita dollars of transit service. The primary transit agencies in the region essentially cater to 'captive riders'. Cities with a stronger transit base in the nation have two things in common; their ability to draw "choice" riders, and their success in building some type of rail transit system, with capital funds generally provided by the federal government.

Over past three decades, a number of studies have examined the feasibility of rapid transit services in the Detroit region including speed link (rubber tired high speed buses), Light Rail Transit (LRT), Commuter Rail Transit (CRT) and High Speed Rail Transit (HRT). Among the many problems associated with building such a rapid transit system in the region, is the lack of a "quick response" tool for preliminary planning for light rail transit along an urban travel corridor.

The primary objective of this project is to develop a quick-response tool for sketch planning purposes that may be used by other cities to test the feasibility of building LRT systems along a predefined transit corridor (i.e., a corridor with existing transit service, in form of buses). The primary focus of this study is to maximize the use of available data without any new data collection effort. In the report, the authors present an LRT case study for Detroit, where a number of LRT planning studies are currently underway, each with specific objectives, followed by a set of guidelines that can be used by transit planners for sketch planning of LRT. The guidelines are designed to assist transit planners in the preliminary planning effort for a LRT system on an urban travel corridor with existing bus services.

TABLE OF CONTENTS

LIST OF TABLES

LIST OF FIGURES

1. EXECUTIVE SUMMARY

The seven-county Southeast Michigan region, that encompasses the Detroit Metropolitan Area, ranks fifth in population among the top 25 regions in the nation. It also ranks among the bottom five in the transit service provided, measured in miles or hours or per capita dollars of transit service. The primary transit agencies in the region essentially cater to "captive riders." Cities with a stronger transit base in the nation have two things in common; their ability to draw "choice" riders, and their success in building some type of rail transit system, with capital funds generally provided by the federal government.

Over the past three decades, a number of studies have examined the feasibility of rapid transit services in the Detroit region including speed link (rubber tired high speed buses), Light Rail Transit (LRT), Commuter Rail Transit (CRT) and High Speed Rail Transit (HRT). Among the many problems associated with building such a rapid transit system in the region, is the lack of a "quick response" tool for preliminary planning for light rail transit along an urban travel corridor.

The primary objective of this project is to develop a quick-response tool for sketch planning purposes that may be used by other cities to test the feasibility of building LRT systems along a predefined transit corridor (i.e., a corridor with existing transit service, in the form of buses). The primary focus of this study is to maximize the use of available data without any new data collection effort. In the report, the authors present an LRT case study for Detroit, where a number of LRT planning studies are currently underway, each with specific objectives, followed by a set of guidelines that can be used by transit planners for sketch planning of LRT. The guidelines are designed to assist transit planners in the preliminary planning effort for a LRT system on an urban travel corridor with existing bus services.

The research approach is based upon the development of a generic model, intended to predict the following outputs for a proposed light-rail transit system (LRT):

1. Ridership demand estimation (i.e., passenger demand per operating day)
2. Operating parameters (i.e., travel time, speed)
3. System fleet parameters (i.e., fleet size, minimum headway, service headway)
4. Cost estimates (i.e., capital cost, operating cost)

The generic model is also validated with a set of demonstration exercises for a LRT system along the most dominant travel corridor in the region using the available database. Under ideal circumstances, the methodology should be developed first, followed by the demonstration exercise. The proposed procedure is designed to ensure that all the procedural elements recognize the prevailing data constraints, and the available data is utilized to its maximum potential. Hence, the demonstration exercise is presented first, followed by the procedure, presented in the form of a set of guidelines.

Major Findings:

- LRT travel demand along Woodward Ave. for a 26-mile long corridor connecting the Detroit and Pontiac Central Business Districts (CBDs) in a north-westerly direction was established at 21,437 passengers per day.

- A total of 26 LRT stations have been proposed along Woodward Avenue. Using multiple regression analysis, station specific boarding and alighting estimates was generated. Based upon the station "loadings", the daily LRT demand for the Woodward Avenue corridor is revised at 21,522 passengers per day. Using an assumed 300 day duration for an operating year, the annual ridership for the system is estimated to be approximately 6.5 million passengers . The Maximum Loading Station (MLS) and corresponding Peak Hour Demand (PHD) were also established.

- The operating parameters for the proposed LRT system were investigated in this report.

- The proposed LRT system requirements were calculated along with: an analysis of operating parameters (e.g., LRTV travel speed, acceleration, deceleration etc.), Identification of a suitable LRTV manufacturer and model (Kinkisharyo), fleet size, headways, and commercial speed. Based upon a ten-minute peak and 20 minutes off-peak headway, the required fleet size was calculated as 15 LRTVs.

- Operating cost estimates for the proposed system were calculated using the Fully Allocated Cost (FAC) method. Based upon a review of the current literature, the Gwinnett Village CID (Community Improvement District) model, developed by HDR Inc., was adopted for the proposed Woodward LRT system. The Gwinnett Village CID model was derived from parameters related to operating cost data compiled from nine peer LRT systems in the United States. The operating cost for the proposed LRT system is estimated at $550,000 per mile per year (2010 dollars)

- For sketch planning purpose, the capital cost for the proposed LRT system is estimated at $50 million per mile.

Guidelines:

These guidelines are designed to assist the transit planner in developing a sketch plan for a LRT system along an urban arterial that is currently, used as a major transit (primarily bus system) corridor. These guidelines are based on the authors experience in conducting the Detroit LRT case study presented in the main report.

There are essentially three Right of Way (R/W) categories (C, B, and A) in transit operation that are distinguished by the degree of separation from other traffic on the street. An exact definition of the three categories are given below from Vuchic[1].

[1] Vuchic, V.R, "Urban Public Transportation: Systems and Technology", Prentice Hall, N.J., 1981

- *Category C* represents surface streets with *mixed traffic.* Transit may have preferential treatment, such as reserved lanes separated by lines or special signals, or travel mixed with other traffic, …….. .

- *Category B* includes R/W types that are *longitudinally physically separated* (by curbs, barriers, grade separation, etc.) from other traffic, but with grade crossings for vehicles and pedestrians, including regular street intersections. This R/W category is most frequently used for LRT systems……. .

- *Category A* is a *fully controlled* R/W without grade crossings, or any legal access by other vehicles or persons. It is also referred to as "grade separated," "private," or "exclusive" R/W,…….. . In exceptional cases the R/W may have widely spaced grade crossings with signal override and gate protection of the tracks, and yet be considered as category A, since such crossings have little effect on line performance."

Vuchic points out above that category B, often referred to as Partially controlled access, is most frequently used for LRT systems. The authors of this report recommend that category B should be used for LRT systems. A 14-step process to facilitate LRT sketch planning is presented below (Figure E-1).

Step 1: Identify the major travel corridors in the region (with current transit/Bus services), as possible candidates for an LRT system.

Step 2: Assemble the following data:

- Population, Employment and Land use data (design year forecasts) by TAZ's, along a specified band width (1/2 mile to 1 mile)
- Existing Transit Ridership data along the designated travel corridors
- Projected Transit Ridership for the design year along the designated travel corridors

Step 3: Based upon long term demographic and employment growth and current transit travel patterns, identify the most dominant travel corridor (usually along a major transit corridor), as the preferred LRT corridor. A preliminary ridership estimate for the corridor should be established at this point. A minimum of 15,000 daily ridership (4,500,000 annual ridership) is desired. Based upon the Detroit case study presented, the following two rules may be used in developing a preliminary ridership estimate:

- Transit ridership along an existing bus corridor is likely to increase by 25% to 35% when an LRT is introduced
- The split between LRT and bus ridership is likely to be within a range of 4.5:1 to 5.5:1

Step 4: Identify LRT station locations based upon the following principles:

- Station spacing should be between 0.5 miles to 1.5 miles, with 1 mile as the desired value
- Station spacing need not be the same for the entire corridor. Denser land uses requiring more frequent access make for shorter spacing. Higher mobility needs on the other hand, would result in longer spacing.
- Station locations should reflect the dual consequence of access and mobility (contradictory) requirements
- A number of existing bus stops may be aggregated into specific station locations.
- Major bus stop junctions, transfer points etc. make for ideal station locations.

Step 5: Derive ridership estimates (by boarding and alighting) for each station. Means to attain the goal include:

- An analysis of existing (and predicted) station ridership data, along part of the corridor if any, with socio-economic, employment, transportation as land use variables (example Segment 1 in the case study).
- Literature search in identifying models from similar LRT corridors.
- Development of Alighting and Boarding models using station ridership and socio-economic, land use and transportation data from similar LRT systems elsewhere.

Step 6: Finalize ridership estimate so that:

The sum of all Boardings equals the sum of all Alightings and together equals Total Ridership.

The total ridership thus obtained should be in close proximity with the preliminary ridership estimate established in Step 3. Adjustments may be necessary if there is a significant difference between the two estimates.

Step 7: Develop factors for Peak Direction Flow, Peak Period Flow and Peak Hourly Flow to identify design conditions. Use this information to identify the Maximum Loading Section (MLS) and the corresponding Peak hour Demand (Dp).

Step 8: Review current LRT technologies, as well as those under development to identify operating parameters for the proposed system. These should include, but are not limited to:

- Capital Cost, Operating Cost
- Size and capacity of vehicles/trains
- Max. attainable speed
- Acceleration, Deceleration capabilities
- Ride quality

Step 9: Based upon a review of the operating data, select a system to fit the proposed system.

Step 10: Use the relationships presented in the report in Chapter (5), equations (10) through (13) to establish the maximum peak hour headway, and the required fleet size. A necessary pre-requisite to this step is the completion of T_d, T_s and T_l, and the resulting cycle time θ (being the sum total of T_d, T_s and T_l). A specific headway must be assumed to compute T_l, even though headway is the desired output of this exercise. An iterative process may be needed to "converge" these two headway estimates.

Step 11: Once the maximum peak hour headway is determined, a policy headway must be established from data on current state of practice. In the case study presented, the maximum peak hour headway was calculated as 20 minutes. However, a policy headway of 10 minutes was adopted (compatible with current state of practice). This step, may result in 'overdesign', but is considered necessary to sustain transit demand along the corridor where there is no precedence of LRT system. Fleet size must be adjusted to make it compatible with the policy headway adopted. Note: Policy Headway is less than or equal to Maximum Headway.

Step 12: Based upon the results of Step 11, the final system requirements should be established. This information serves as a critical input to the computation of operating cost.

Step 13: Conduct preliminary cost analysis for sketch planning purposes in two separate categories:

- Capital Cost
- Operating cost (annual)

For sketch planning purposes, capital cost can be estimated based on a unit cost per mile derived from the literature. For operating cost, the use of Fully Allocated Cost technique is suggested.

Step 14: Using the ridership data generated (Step 6) develop an estimate of fare-box revenue, and other sources of revenue. Use the operating cost (Step 13) to estimate the following:

- Fare box revenue (%)
- Other revenue (%)
- Subsidy (%)

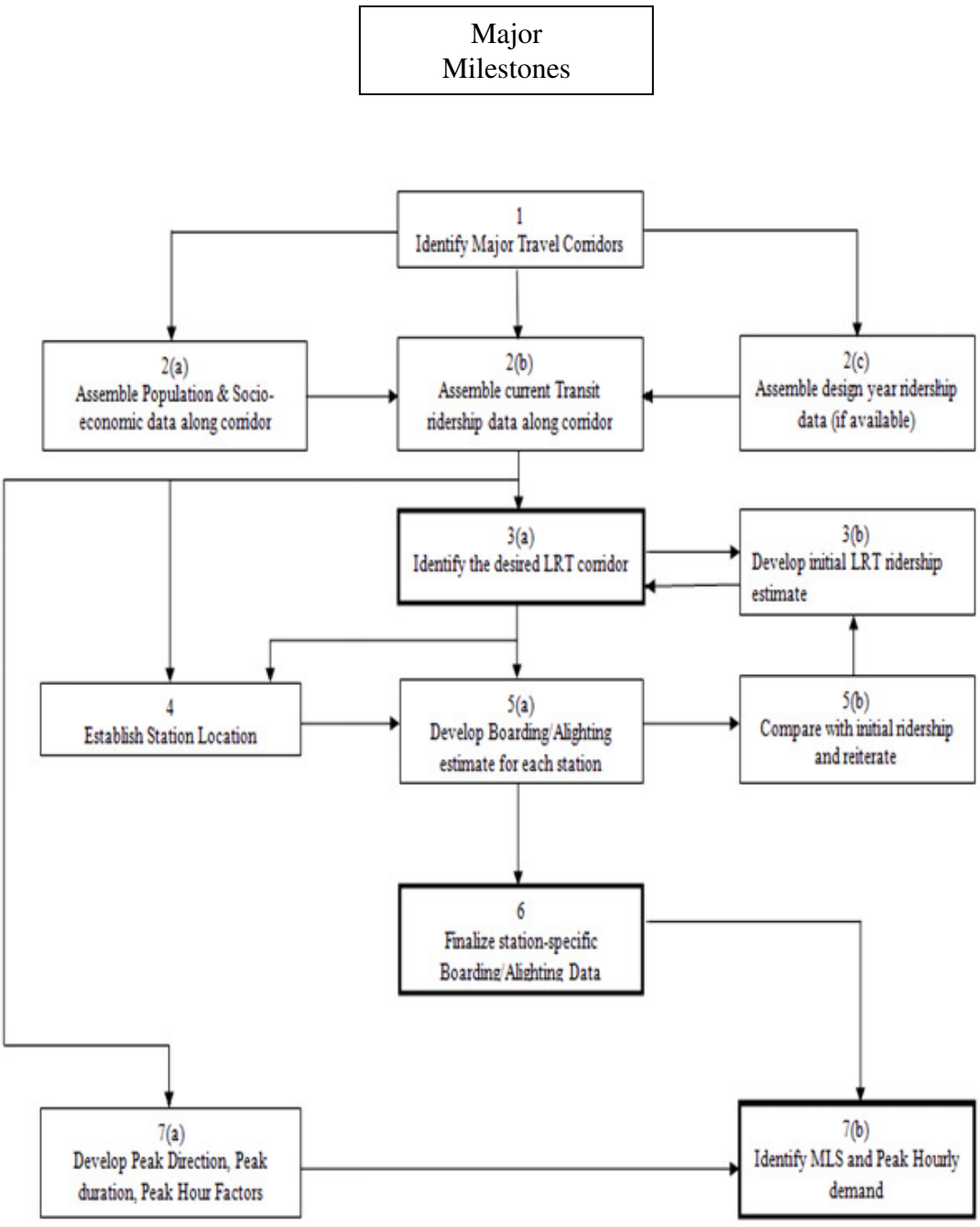

Figure E1. Guidelines for LRT Sketch Planning (Continued next page)

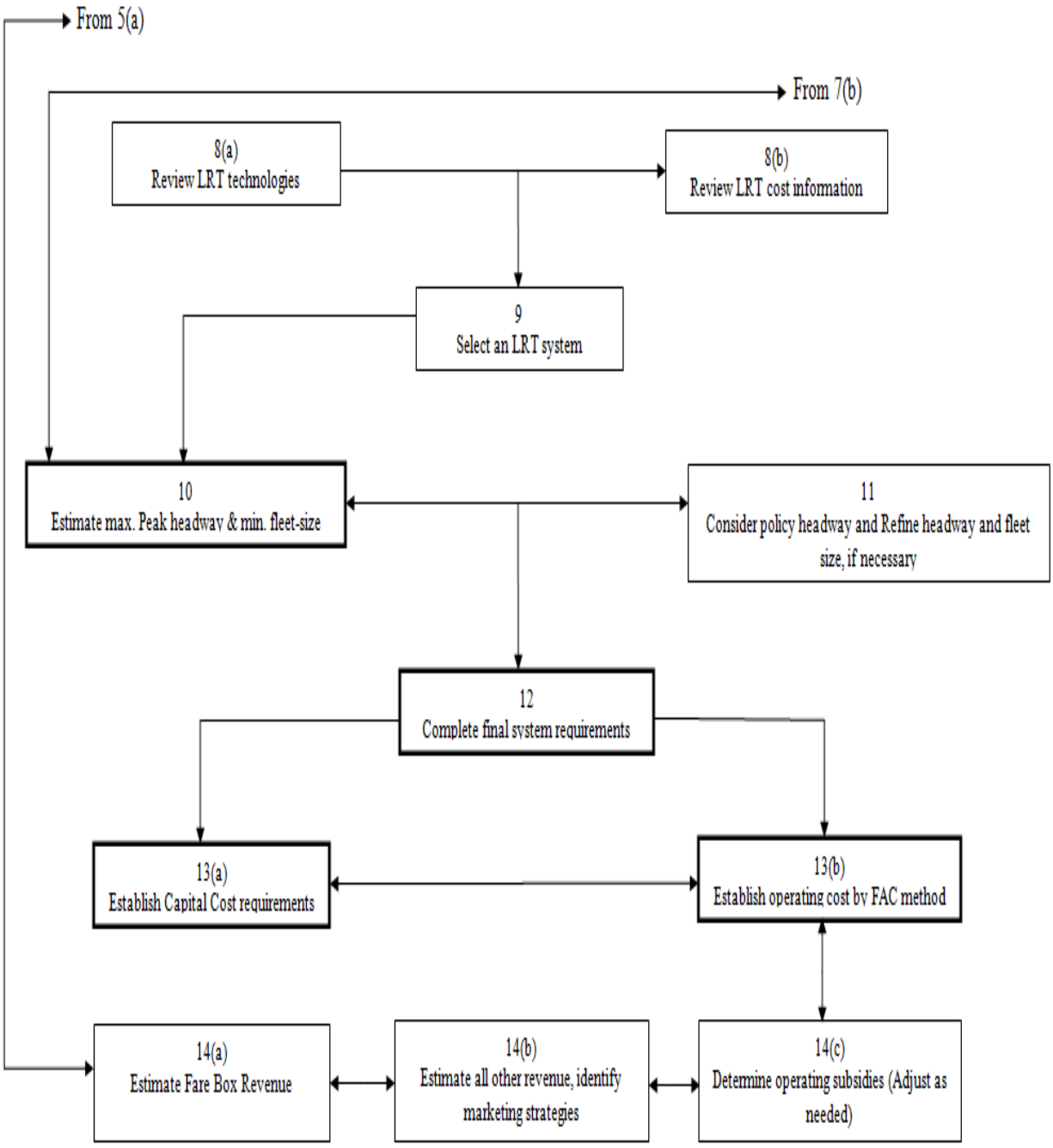

Figure E1. (Continued)

2. BACKGROUND

The seven-county Southeast Michigan region currently has an urbanized area population of approximately 4.0 million, with 1.9 million households that are expected to see a modest growth during the two decades. The region is also expected to add approximately 450,000 jobs over its current base during the same period[2]. Even though 192,000 households in the region do not have access to a private automobile, current use of transit in the region is very limited: only 2 percent of employed residents travel to work using public transit. By contrast, 94 percent employed residents in the Southeast Michigan Council of Governments (SEMCOG) region travel to work by private automobile, van, or light truck.

2.1. Transit in Southeast Michigan

The availability (or lack thereof) of transit service in the region is perhaps the root cause of a small transit mode share. Clearly, the current use of public transit in the SEMCOG region is characterized by a large number of "captive riders". Captive riders are identified as members of the population who do not own, or have access to, a private automobile. This is in contrast to "choice riders", members of the population who use transit modes by choice, despite having access to private automobiles. Other metropolitan regions in North America with similar population (e.g., Washington D.C., San Francisco, CA; Boston, MA; and Toronto, ON, Canada) have successfully created a transit base by attracting choice riders, thereby significantly reducing vehicle congestion levels, dependence on fossil fuel, and environmental pollution.

Very little emphasis, if any, has been placed on attracting choice riders by policymakers in the Southeast Michigan region. This is evident in the fact that, while the region ranks fifth in the country by population among the 25 major metropolitan areas, it ranks 23rd both in the number of miles and number of hours of transit services per capita provided [*1*]. The region also ranks 21st in the amount of local funds spent on transit services. As stated in a report compiled by SEMCOG, many regions in the country spend nearly three times as much per capita for transit services (Detroit: $59.00, Cleveland: $124.000, San Francisco: $255.00). Other factors limiting transit activities in the region are:

1. Lack of consensus between the city of Detroit and its surrounding suburban areas regarding the configuration (i.e., alignment, right-of-way (ROW)), governance, and funding for a transit system, and associated administrative structure.

2. General lack of support from the public at large, for a viable transit base.

This phenomenon is exemplified by a number of "missed opportunities" experienced in obtaining transit resources. For instance, the bulk of a $600 million commitment made by the Federal government in 1974 was lost because of a general lack of consensus on the programming and planning aspects for a transit system. Similarly the first regional transit agency in the Detroit metropolitan area, South-East Michigan Transportation Authority (SEMTA), was created in the early 1970's without a dedicated local transit support base (unlike other metropolitan regions in the country), thereby limiting its ability to compete for federal grants.

[2] These numbers are long-term predictions, and do not reflect the recent economic downturn in the region, and its impact on future population migration.

Lastly, no transit allocations were made out of increased gasoline tax revenues in the state of Michigan, resulting from a 1997 piece of legislation despite the fact that up to ten percent of the funds could have been spent for transit projects.

Transit services are currently provided by three major agencies in the area:

- Detroit Department of Transportation (DDOT): service within the Detroit city limits
- Suburban Mobility Authority for Regional Transportation (SMART): service for the Detroit metropolitan area, with limited service in the Detroit city limits
- Detroit Transportation Corporation (DTC) manages Detroit People Movers.

DDOT and SMART provide bus route service for over 100,000 transit miles per operating day, generating a daily ridership of over 170,000. A number of other transit services are available in the SEMCOG area for their respective local communities:

- Ann Arbor Transportation Authority (city of Ann Arbor)
- Blue Water Area Transportation Commission (city of Port Huron)
- Lake Erie Transit (city of Monroe and Monroe County)

2.2. Past and Current Studies

A brief summary of the recent activities is presented below to provide a basis for this report.

- In 1997, the Metropolitan Affairs Coalition and the Detroit Regional Chamber developed a three-tiered rapid transit system, comprising of both fixed and flexible local services [*2*].
- For many years, the SEMCOG has identified three major travel corridors: Woodward Avenue (connecting Detroit and Pontiac), Interstate 94/Michigan Avenue (connecting Detroit and Ann Arbor), Gratiot Avenue (connecting Detroit and Mt. Clemens) [*3*].
- Past transit studies have identified three travel corridors for viable rapid transit systems, with the first two having the highest potential. Most experts in transportation planning feel that a transit corridor developed along Woodward Avenue could attract riders from parallel corridors (e.g., Interstate 75, Michigan Highway 10 / John C. Lodge Freeway) over and above Woodward Avenue. Similarly, any transit system developed along I-94/Michigan Avenue could also draw riders from the east-west travel routes (e.g., I-96, Ford Road). The potential for transit development along the Gratiot Avenue corridor has never been fully investigated.
- The "Woodward Corridor Transit Alternative Study", conducted in 2000 by the Detroit Transportation Corporation, recommended that both bus-rapid transit (BRT) and light-rail transit be further investigated [*4*].

- A 2001 SEMCOG study recommended rapid transit on 12 regional corridors in the region covering approximately 259 miles. Speed link services, (representing rubber-tired systems on dedicated lanes) were recommended along Woodward Avenue, of the 12 corridors identified [*5*].

- A later study by the Michigan Department of Transportation (MDOT), investigated the potential for deploying signal pre-emption along the Woodward Avenue corridor. The study essentially found that signal pre-emption could be an effective tool for improving the flow of rapid buses over the signalized intersections along Woodward Avenue

- A recent SEMCOG study focused on exploring the possibility of transit development between the cities of Detroit and Ann Arbor, with connection to the Detroit Metropolitan Airport (DTW). A myriad of alternatives, ranging from BRT, LRT, and commuter rail (heavy rail) encompassing a number alignments, were evaluated.

- A recent study conducted by a consultant for SEMCOG and the city of Detroit explored the feasibility of building an LRT system from the Detroit central business district (CBD), to the northern city limits at Eight Mile Road The proposed system would follow the alignment of Woodward Avenue, with an approximate length of nine miles [*6*]. The capital cost of the proposed system, including tracks, train vehicles, and stations was estimated to be $373 million.

3. PROJECT SCOPE

The objective of this research is to develop a quick-response prediction model for sketch planning purposes that may be used by other cities to test the feasibility of building LRT systems along a predefined transit corridor (i.e., a corridor with existing transit service, in the form of buses). In the report, the authors present an LRT case study for Detroit, where a number of LRT planning studies are currently underway, each with specific objectives. The LRT case study is followed by a set of guidelines (Figure E-1). For the purpose of this study, the LRT route from the Detroit CBD (near West Jefferson Avenue) to the northern boundary of the city was designated as Segment 1. The proposed expansion of the LRT route from Eight Mile Road, to E. Huron Street/Michigan Highway 59 (M-59) in the city of Pontiac, was designated as Segment 2.

A map showing Segments 1 and 2 along with cities is shown in Figure 1. The planned LRT system (Segments 1 and 2) will connect the cities of Ferndale, Pleasant Ridge, Royal Oak, Birmingham, Bloomfield Hills, Troy, and Pontiac with the central business district of the city of Detroit and will serve mobility needs of the region along one of its most-heavily travel corridors. For Segment 1, boarding and alighting data for each station were available by day of the week, period of the day (i.e., A.M., MID-DAY, P.M. OFF-PEAK), and direction of travel along Woodward Avenue. Socioeconomic information such as population, employment, and household size were also available for the SEMCOG area, by predefined traffic analysis zones (TAZ).

The research approach is based upon the development of a generic model, intended to predict the following outputs for a proposed light-rail transit system (LRT):

1. Ridership demand estimation (i.e., passenger demand per operating day)
2. Operating parameters (i.e., travel time, speed)
3. System fleet parameters (i.e., fleet size, minimum headway, service headway)
4. Cost estimates (i.e., capital cost, operating cost)

The generic model is also validated with a set of demonstration exercises, using the available database from Segment 1 and Segment 2 of the Woodward Avenue corridor in the SEMCOG region. Under ideal circumstances, the methodology should be developed first, followed by the demonstration exercise. In reality, however, a viable methodology must be developed with due consideration given to data availability. Data constraints often require the methodology development and demonstration to proceed concurrently, with proper and frequent interface between the two phases. The authors used this concurrent procedure in this study to ensure that all the procedural elements recognize the prevailing data constraints, and the available data is utilized to its maximum potential. Hence, the demonstration exercise is presented first, followed by the procedure, presented in the form of a set of guidelines.

3.1. Other Background Information

SEMCOG databases serve as the baseline for ridership estimates, with the assumption that an LRT system would be constructed from the Detroit CBD, northward to the Detroit city limits at Eight Mile Rd (Segment 1). The remainder of the LRT route from Eight Mile Road to E. Huron Street/M-59 is designated as Segment 2 (Figure 1).

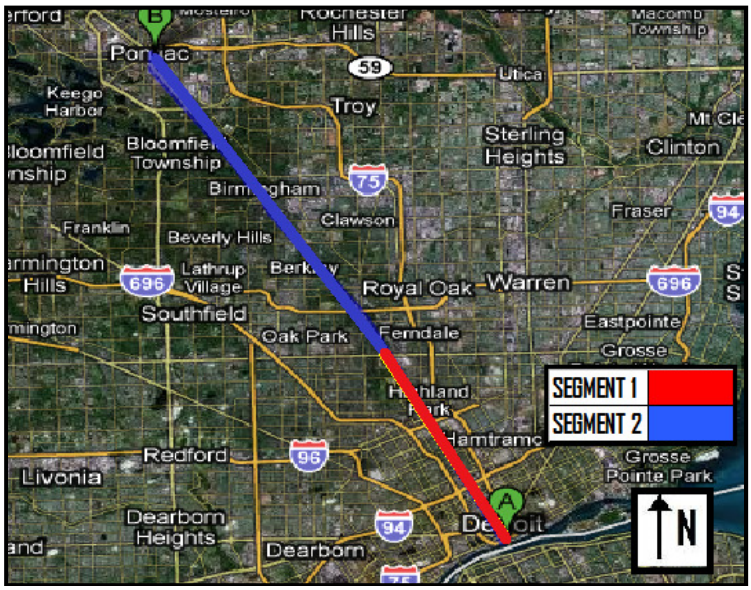

Figure 1. LRT Corridor Along Woodward Avenue (Segments 1 and 2)

Table 1 adapted from a SEMCOG report, contains transit ridership (both bus and LRT) data for a number of scenarios [1]. The original SEMCOG Table is included as Table A1 in Appendix A.

- The range of demand for the Woodward corridor, the subject of this demonstration exercise, is between 19,600 and 22,800 passengers per operating day. The following specific observations can be made relative to the Woodward corridor.

- For the year 2030, daily transit ridership (Bus & LRT) along the Woodward Avenue corridor ('2030 Woodward, Corridor Total') was estimated at 22,800 passengers per operating day, where 11,100 of that total would be contributed from Segment 1 of the LRT ('LRT Woodward').

- DDOT bus route number 53 ('DD 53') along Woodward Avenue was estimated to carry a total daily ridership of 8,300 passengers. However, this particular route is expected to be discontinued under the LRT scenarios.

- The remaining bus service, provided by SMART under the '2030 Woodward, LRT' scenario, is estimated to contribute a combined daily ridership of 11,700 passengers per operating day (SMART bus routes: SM 445, SM 450, SM 460, SM 465, SM 475, SM 495).

- Under the 'NO BUILD' scenario, the expected daily ridership along the Woodward corridor was estimated as 19,600 passengers per operating day. Thus, the net impact of the proposed LRT system (Segment 1) is an additional 3,200 passengers per operating day (net difference 22,800 of 19,600).

The information listed above is presented in a concise form in Figure 2, focusing primarily on the "2030 Woodward" component of Table 1.

3.2. Review of Related LRT Studies

A number of planning studies in the SEMCOG region are currently underway, with the intent of exploring the feasibility of constructing and operating an LRT system along Woodward Ave.:

SEMCOG Study: As a part of the 2035 regional plan for the Southeast Michigan region, SEMCOG's Regional Transit Coordinating Council has agreed upon three corridors for rapid transit, one of which is Woodward Ave. (Detroit CBD to M-59). The SEMCOG study has been conducted using a regional approach, where a combination of BRT, LRT, and arterial rapid transit (ART) would be implemented on each of the aforementioned corridors. ART is an approach to operate conventional buses along existing routes more efficiently, using one or more of the following: signal priority, limited stops between terminal points, and turn-outs at stops.

Table 1. SEMCOG Demand Summary (Woodward Ave. subset)

CORRIDOR	ROUTE NAME	EXISTING RIDERSHIP	2005 BASE	2030 BASE	2030 Woodward			
					NO-BUILD	TSM	BRT	LRT
Woodward	DD53	13,500	9,100	7,700	8,300	8,500		
	SM445	300	200	200	200	200	200	200
	SM450	4,800	3,700	3,800	3,800	3,900	3,900	3,800
	SM460	0	3,900	4,000	4,000	4,000	4,100	4,100
	SM465	300	300	300	300	300	200	200
	SM475	0	200	200	200	200	200	200
	SM495	2,300	2,900	2,800	2,800	2,800	3,100	3,200
	DD53T	0	0	0	0	100	0	0
	BRT Woodward	0	0	0	0	0	9,200	0
	LRT Woodward	0	0	0	0	0	0	11,100
	CORRIDOR TOTAL	**21,200**	**20,300**	**19,000**	**19,600**	**20,000**	**20,900**	**22,800**

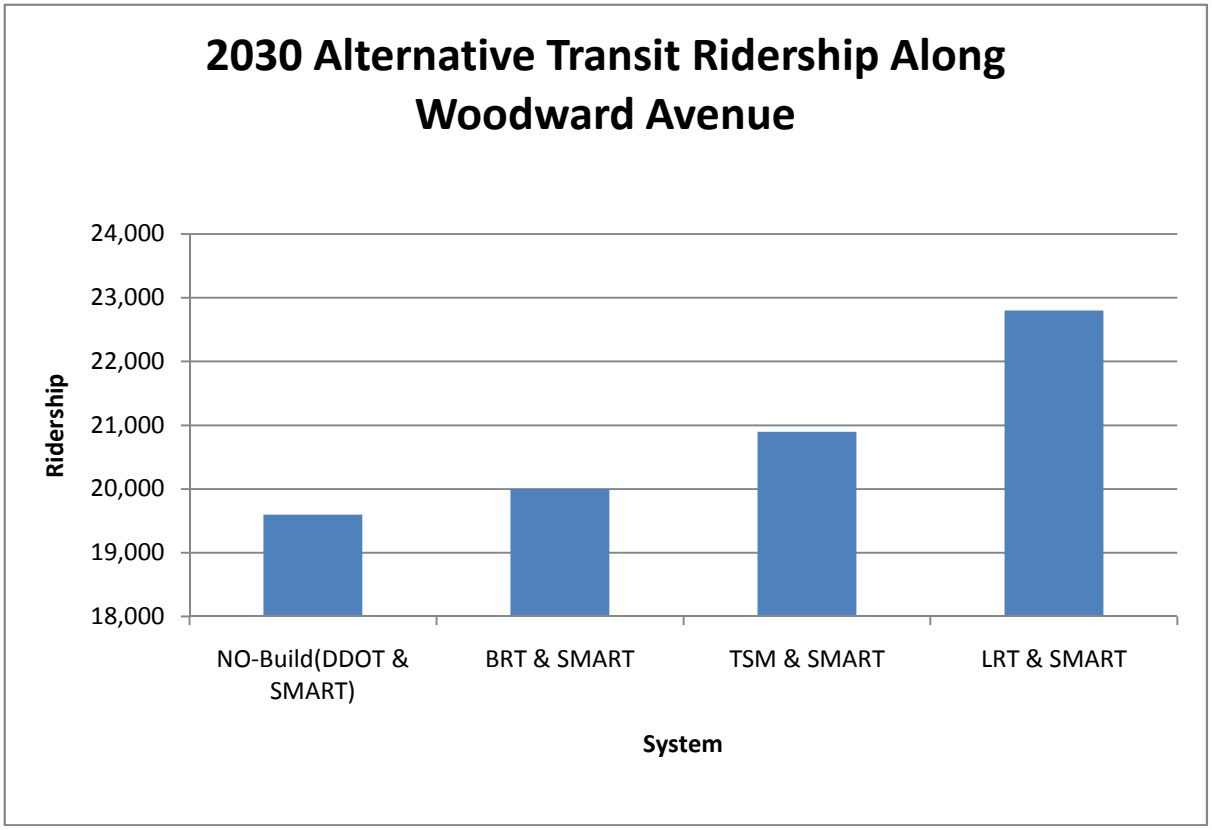

Figure 2. Daily Transit Ridership along Woodward Avenue in 2030 for Various Alternatives

The SEMCOG study plans for LRT to operate along the Woodward corridor from the Detroit CBD to an area just south of Eight Mile Road, near the Michigan State Fairgrounds (Table 1). Officials at SEMCOG have expressed the importance of such a system to have the ability to reach the suburban communities in metro Detroit, where the Eight Mile Road station area could continue to be used as a regional bus transfer center. At the time of this writing, this regional plan has not yet been implemented in the SEMCOG region [*7,8*].

Detroit Transit Options for Growth Study (DTOGS): DTOGS was intended to investigate rapid-transit mobility options for the Detroit metropolitan area. The study followed guidelines established by the Federal Transit Administration (FTA), one of which was to conduct a "Transit Alternatives Analysis". Of the alternatives investigated (bus-rapid, LRT, and conventional bus transit), a plan calling for a Woodward Ave. LRT system prevailed. At the time of its completion, the study predicted that the proposed system (Table 1) would carry approximately 11,000 riders per day. The system, as proposed, is predicted to cost $371 million to construct (2007 estimate) [*9*].

M1-Rail Study: The M1-RAIL is a non-profit, public/private partnership of Detroit business and civic leaders that intend to develop light-rail transit in the city of Detroit to stimulate economic development. The proposed system is expected to operate along Woodward Ave, for approximately 3.4 miles from the Detroit riverfront (W. Jefferson Avenue) to West Grand Blvd. The M1-RAIL proposal differs from the previous studies, in that the planned stations are to be located less than 1/2-mile from one another. Given the smaller distances planned for spacing, the M1-RAIL partnership envisions the proposed system as an urban link rather than a commuter facility. To date, the organization has committed $125 million for the preliminary planning and pre-construction studies of the system [*11*].

The station locations proposed by various studies are presented in Table 2. Because the scope of the LRT system proposed in the M1-Rail study is somewhat different, the corresponding station locations also differ (Table 2).

Even though three studies were done to explore the feasibility of LRT along Woodward corridor, the SEMCOG study is the only one whose detailed modeling data were available to the project team, therefore it serves as benchmark for this study.

Table 2. Proposed Alignments for Woodward Ave. LRT System

SEMCOG	DTOGS	M1-Rail (Private Venture)
8 Mile Rd.	State Fairgrounds (Between 8 and 7 Mile Rd.)	New Center
7 Mile Rd.	7 Mile Rd.	AMTRAK
McNichols Rd.	McNichols Rd.	Wayne State University
Manchester St.	Manchester St.	Cultural Center
E Davison Serv. Dr.	Glendale St.	Detroit Medical Center NORTH
Woodland Heights	Calvert St.	Detroit Medical Center SOUTH
Arden Park	Hazelwood / Holbrook St.	Masonic Temple / Brush Park
Grand Blvd.	Grand Blvd.	Foxtown
Milwaukee	Piquette St.	Grand Circus Park
Warren Ave.	Warren Ave.	Campus Martius
MLK Blvd. / Mack Rd.	MLK Blvd. / Mack Rd.	Congress St.
Montcalm	Foxtown	
Grand River	Downtown*	
Congress	-	
Larned	-	
Jefferson Avenue	Jefferson Avenue	Jefferson Avenue

4. STUDY APPROACH

The intent of this modeling approach is to estimate the LRT ridership demand in Segment 2 of the project area (from Eight Mile Road to M-59, along Woodward Avenue, as shown in Figure 1). The primary basis for this information is the bus ridership data for all routes along the Woodward Avenue corridor. The study plan consists of a number of steps as displayed in Figure 3. The steps are:

- Determine bus ridership for Segments 1 and 2 from SEMCOG data.
- Determine LRT ridership for Segment 1 from SEMCOG data.
- Determine the proportion of bus and LRT ridership for Segment 1. Also compute growth factor of an existing bus transit corridor, when LRT is added.
- Establish a relationship between LRT ridership by station and socioeconomic factors for Segment 1.
- Use developed relationship for Segment 1 to determine LRT ridership for Segment 2.
- Fine tune boarding and alighting data of Segment 2, so that total boarding equals total alighting.
- Compare the regression ridership estimate with the growth factor estimate and make adjustment if necessary.
- Determine peak loading station along peak direction.
- Determine headway during peak and off-peak hours and fleet requirements (# of trains).
- Refine headway (policy) and fleet requirements.
- Determine system capital as well as annual operational and maintenance cost.

4.1. Analysis of Segment 1 Data (Data source SEMCOG)

Passenger boarding and alighting for LRT and bus modes are derived from SEMCOG data as shown in Table 3. The database is broken down into four periods of an assumed eighteen –hour operating day:

- A.M. Peak (three-hour duration; from 6:00 to 9:00 A.M.)
- MID-DAY (six-hour duration; from 9:00 A.M. to 3:00 P.M.)
- P.M. Peak (three-hour duration; from 3:00 to 6:00 P.M.)
- OFF-PEAK (six-hour duration; from 6:00 P.M. to MIDNIGHT)
- **TOTAL** (eighteen-hour day; from 6:00 A.M. to MIDNIGHT)

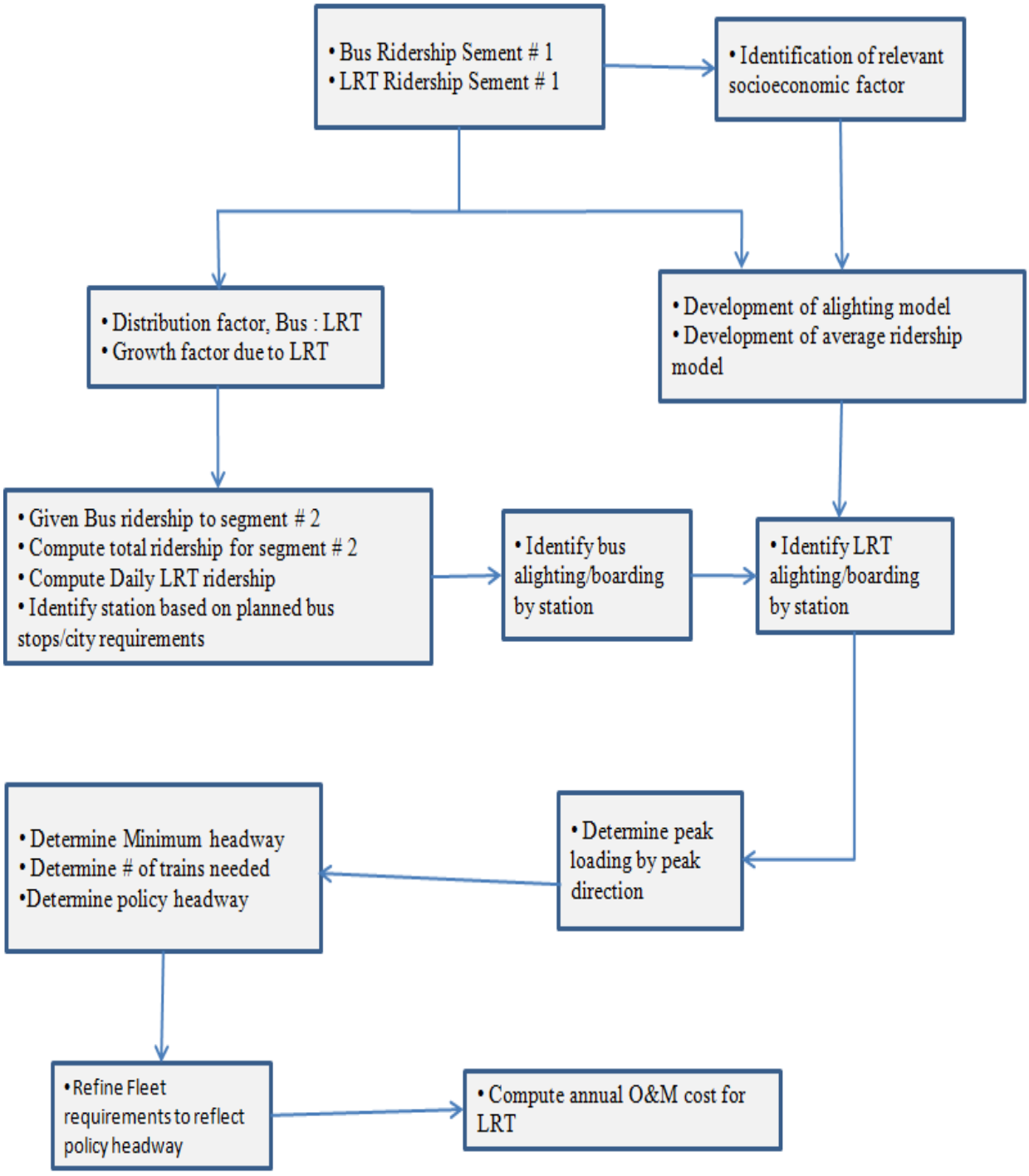

Figure 3. Flow Diagram Study Approach

4.1.1. Bus Ridership for Segment 1

Table 3 shows that for Segment 1, the total daily bus boarding and alighting are 2,624 and 1,532, respectively. For the LRT data in Table 3, there is a perfect match between boarding and alighting (both values round to 11,367 passengers per operating day).

Table 3. Summary of Bus and LRT Demand (2030 SEMCOG Model)

	BUS (Segment 1)		BUS (Segment 2)		LRT (Segment 1)		Proportion of LRT Ridership Per Period
Period	Board	Alight	Board	Alight	Board	Alight	
AM PK	442	232	887	1,160	2,103	2,103	0.19
MIDDAY	1,287	693	2,571	3,299	3,701	3,701	0.33
PM PK	613	439	1,713	1,970	3,100	3,100	0.27
OFF PK	282	168	834	972	2,463	2,463	0.22
TOTAL	**2,624**	**1,532**	**6,005**	**7,401**	**11,367**	**11,367**	**1.00**
AVERAGE	**2,078**		**6,703**		**11,367**		

Total Demand for Segment 1 (LRT & Bus) = 2,078 + 11,367 = 13,445 passengers per day

$$BusDemand\_Contribution = \frac{BusDemand}{TotalDemand} = \frac{2,078}{13,445} x100 \approx 16\% \qquad (1)$$

$$LRTDemand\_Contribution = \frac{LRTDemand}{TotalDemand} = \frac{11,367}{13,445} x100 \approx 84\% \qquad (2)$$

Regarding ridership growth in segment 1 due to addition of LRT service is calculated as follows:

No-build LRT ridership for segment 1 (from Table 1) = 8,300+2,078 = 10,378
LRT build ridership for segment 1 (from Table 3) = 11,367+2,078 = 13,445

$$Growth\_from\_BuildLRT = \frac{13,445 - 10,378}{10,378} x100 = 30\%$$

Summary of Segment 1 Analysis:

- **Bus-LRT ratio = 5.25**
- **Total Transit ridership along an existing transit corridor will increase by 30% after introduction of LRT**

4.1.2. Identification of LRT ridership model for Segment 1

A total of 12 stations are planned along Segment 1. LRT boarding and alighting estimates for each station location on Segment 1 were developed by SEMCOG. A summary of the LRT ridership data by different periods in a day are presented in Table 3. LRT ridership demand data for segment 2 were not developed by SEMCOG. Hence, the project team attempted to develop a regression model relating LRT ridership by stations to socioeconomic factors for Segment 1. This regression model was used to estimate boarding and alighting demand for each LRT station along Segment 2.

The procedure employed involved an attempt to develop separate boarding and alighting demand estimates using a multi-variable regression model for Segment 1. The demand estimates were set as the dependent variable (boarding and alighting data shown for Segment 1 shown in Table 4), while a number of socioeconomic and transportation-related factors for the TAZ surrounding the proposed stations along the Woodward corridor were used as independent variables.

A series of regression models for boarding and alighting demand were tested with combinations of the aforementioned independent variables. As a part of this effort, the authors of the study analyzed three areas of influence surrounding each of the proposed LRT stations along Segment 1: 1/2, 1, and 2 mile radii. The influence areas were referred to as bandwidths for the purposes of this study. The models that were able to describe the most amount of variance in the relationship between the dependent and independent variables for Segment 1 were adopted as final model to predict the ridership demand for Segment 2.

According to the Manual of Uniform Control Devices (MUTCD), normally-paced pedestrian walking speed (*WalkSpeed*) is estimated to be equal to 4.0 feet per second [*12*]. Organizations such as the Maryland DOT, have suggested that new transit-oriented development (TOD) projects are planned within a 15-minute walk of a transit station, in any direction [*13*]. Using these values, the maximum walking distance ($Distance_{MAX}$) for transit riders can be calculated using the following relationship:

$$WalkSpeed = \frac{4\,ft}{\sec} * \frac{3{,}600\sec}{1hr} * \frac{1mi}{5280\,ft} = \frac{2.72mi}{hr}$$

$$Distance_{MAX} = WalkSpeed * WalkTime \qquad (3)$$

$$Distance_{MAX} = \frac{2.72mi}{hr} * 0.25hr = 0.68mi$$

Thus, it was expected that a bandwidth size in proximity to this value would yield a reasonable prediction for transit ridership demand.

4.1.3. Regression Model for Alighting

Three single-variable regression models were developed to estimate alighting demand per station. Each model uses a different bandwidth (1/2, 1, and 2 mile radii surrounding the LRT

station), as shown in Table 5. An examination of the R^2 and F values obtained for each model has indicated that the 1/2-mile bandwidth results in the best fit for the data.

This validated the assumption that the use of a ½-mile bandwidth around Woodward Ave. would yield a reasonable prediction.

Table 4. Segment 1 LRT Ridership Data

STATION NAME	SEMCOG		
	Board	Alight	Average
8 Mile Rd.	2,782	736	1,759
7 Mile Rd.	2,165	695	1,430
McNichols / 6 Mile Rd.	1,291	984	1,138
Manchester St.	477	453	465
Glendale St.	136	145	141
Calvert St.	410	197	303
Hazelwood / Holbrook St.	501	398	450
W. Grand Blvd.	378	974	676
Warren Ave.	1,029	2,141	1,585
MLK Blvd. / Mack Ave.	706	860	783
Foxtown	50	324	187
W. Jefferson	1,442	3,459	2,451
TOTALS	**11,367**	**11,366**	**11,367**

Table 5. Alighting Regression Model Summary

Number of stations (sample size), N = 12				
MODEL NO.	**BANDWIDTH (mi)**	**EQUATION**	**R^2**	**F VALUE**
1	0.5	ALIGHT = 474.548 + 29.274*[Total Empl./acre]	0.820	44.96
2	1	ALIGHT = 449.928 + 45.596*[Total Empl./acre]	0.770	33.52
3	2	ALIGHT = 243.788 + 121.896*[Total Empl./acre]	0.660	19.34

Referring again to Table 5, it was observed that both R^2 and F values decrease as the bandwidth is increased. The independent variable selected for the alighting model is total employment per acre. The model selected was the result of a number of iterations testing both single and multi-variable regression types, considering a range of land-use, demographic, and transportation-related variables of the TAZ's in proximity to the proposed LRT stations.
The models presented in Table 4 represent the best fit among all regression models developed (both single and multiple) for each of the three respective band widths.

4.1.4. Regression Model for Boarding

The project team was not able to develop a reliable boarding model with reasonable ANOVA values (i.e., t-test, F value, R^2, p value). Therefore an alternative approach was employed to estimate boarding data at each station considering following relationship:

- $$AverageRidership = \frac{(Boarding + Alighting)}{2} \quad (4)$$
- $$(2 * AverageRidership) = (Boarding + Alighting)$$
- $$Boarding \cong (2 * AverageRidership) - Alighting \quad (5)$$

A new regression analysis was employed relating the average ridership estimate (dependent variable) to the independent variables, namely employment density and intermodal connectivity (modal-conn). Three multiple regression models were then selected for each of the three bandwidths considered (Table 6). As in the previous section, the ½-mile bandwidth yielded the best performing model. The independent variables used for the model are as follows: total employment per acre and intermodal connectivity. The latter is a binary variable indicating whether or not a proposed transit station was within ½-mile of a facility promoting intermodal travel: bus stations (not stops), commuter train stations (i.e., AMTRAK), or other transit facilities (i.e., Detroit People Mover (DPM)). The list of stations that satisfy this condition are shown in Table 7.

Table 6. Boarding (Alternate Estimate) Model Summary

Number of stations (sample size), N = 12				
MODEL NO.	**BANDWIDTH (mi)**	**EQUATION**	**R^2**	**F VALUE**
1	0.5	AVERAGE Ridership = 579.177 + 14.297*[Total Empl./acre] + 330.033* [Modal_Conn]	0.480	4.154
2	1	AVERAGE Ridership = 585.850 + 21.523*[Total Empl./acre] + 301.686* [Modal_Conn]	0.420	3.426
3	2	AVERAGE Ridership = 520.952 + 47.444*[Total Empl./acre] + 366.00* [Modal_Conn]	0.330	2.182

Based on the ANOVA values these two models were adopted for LRT ridership estimation for segment 2.

$$ALIGHT = 474.548 + 29.274[TotalEmpl./acre] \quad (6)$$

$$AVERAGE = 579.177 + 14.297[TotalEmpl./acre] + 330.033[Modal\_Conn] \quad (7)$$

Station specific boarding can be computed from equation (5), once the alighting and average are computed using equations (6) and (7) respectively.

Table 7. Proposed LRT Stations with Intermodal Connectivity

	NO.	STATION NAME (Connection Description)	INTERMODAL CONNECTION?
SEGMENT 1	1	Jefferson Ave. (Tunnel Bus to Windsor)	YES
	2	Foxtown	NO
	3	MLK Blvd. / Mack Ave.	NO
	4	Warren Ave.	NO
	5	W. Grand Blvd. (AMTRAK)	YES
	6	Hazelwood / Holbrook St.	NO
	7	Calvert St.	NO
	8	Glendale St.	NO
	9	Manchester St.	NO
	10	McNichols Rd.	NO
	11	7 Mile Rd. (SMART-DDOT Transfer Center)	YES
	12	8 Mile / Baseline Rd. (SMART-DDOT Transfer Center)	YES

4.1.5. Demand Estimates for LRT Ridership Segment 1

LRT ridership demand estimates for Segment 1 as predicted by the equations 6 and 7 are presented in Table 8 along with SEMCOG data. Predicted boarding data were adjusted to make total alighting equals total boarding. .

Table 8. Segment 1 LRT Demand Comparison

STATION NAME	SEMCOG			Predicted LRT ridership		
	Board	Alight	Average	Board[3]	Alight[1]	Average[2]
8 Mile Rd.	2,782	736	1,759	1,341	572	957
7 Mile Rd.	2,165	695	1,430	1,343	506	925
McNichols / 6 Mile Rd.	1,291	984	1,138	683	501	592
Manchester St.	477	453	465	682	551	616
Glendale St.	136	145	141	681	574	628
Calvert St.	410	197	303	683	513	598
Hazelwood / Holbrook St.	501	398	450	682	553	617
W. Grand Blvd.	378	974	676	1,338	706	1,022
Warren Ave.	1,029	2,141	1,585	662	1,374	1,018
MLK Blvd. / Mack Ave.	706	860	783	673	916	795
Foxtown	50	324	187	1,330	1,055	1,192
W. Jefferson	1,442	3,459	2,451	1,269	3,545	2,407
TOTALS	**11,367**	**11,366**	**11,367**	**11,367**	**11,366**	**11,367**

[1]Based on equation (6). [2] based on Equation 7, [3]based on equation 5.

When the predicted boarding and alighting data are compared with the SEMCOG data, a reasonable correspondence has been observed between the two, and was expected. The authors of the study have concluded that such a phenomenon confirms the soundness of the two regression models used.

5. RIDERSHIP ANALYSIS: SEGMENT 2

The first task as a part of this effort is to identify LRT stations for Segment 2. Bus stops location information for Segment 2, along with boarding and alighting were collected from SEMCOG. LRT stations are selected by combining a number of bus stops and following these developed rules:

- An intersection of East-West and North-South bus route is a potential station location.
- Each city must have at least one LRT station.
- Spacing between the stations should be approximately one mile.
- Select a station where bus ridership demand is significant.

Considering the above rules, 15 LRT station are selected for segment 2 and presented in Table 9.

Table 9. Proposed LRT Stations with Intermodal Connectivity

	NO.	STATION NAME (Connection Description)	INTERMODAL CONNECTION?
SEGMENT 2	13	9 Mile Rd.	NO
	14	Washington / Allenhurst St. Near 10 Mile Rd.	NO
	15	Lincoln St.	NO
	16	11 Mile Rd. (Royal Oak Transit Center)	YES
	17	12 Mile Rd.	NO
	18	Coolidge Hwy.	NO
	19	Normandy St.	NO
	20	Lincoln St.	NO
	21	15 Mile / Maple Rd.	NO
	22	Oak Blvd.	NO
	23	Lone Pine Rd.	NO
	24	Long Lake Rd.	NO
	25	Square Lake Rd.	NO
	26	MLK / South Blvd.	NO
	27	E. Pike St. (AMTRAK)	YES
	28	E. Huron St. / M-59	NO

5.1. Total Bus Ridership for Segment 2

Table 3, presented before shows that for Segment 2, the total daily bus boarding and alighting are 6,005 and 7,401 respectively. Corresponding data for Segment 1 are 2,624 and 1,532, respectively. Total bus boarding for Segment 1 and Segment 2 (combined) are 8,629, while total alighting for Segment 1 and 2 (combined) is 8,933. Table 3 shows that the Segment 2 bus average ridership (average of boarding and alighting) can be estimated as 6,703 passengers per operating day. Alternatively, Segment 2 bus ridership can also be estimated indirectly as:

- Segment 2 bus ridership: ridership under "no-build" option, minus DD 53 ridership, minus Segment 1 bus ridership. Using the data presented in Tables 1 and 3:

  Segment 2 bus ridership = 19,600 – 8,300 – 2,078* = 9,222 passengers per operating day
  (*the value of 2,078 is the mean of boarding: 2,624 and alighting: 1,532)

- Alternative Segment 2 Bus Ridership Demand = 19,600 – 8,300 – 2,624 = 8,676
  (Substituting Boarding (2,624) for ridership (2,078))

Thus, the range of Segment 2 bus ridership was estimated to be between 6,703 and 9,222 passengers per operating day, or a mean value of 7,962 (close to 8,000). The value of 9,222 (higher of the two estimates) was used in developing ridership values, per station.

5.2. Projecting Segment 2 Transit Ridership Demand (Bus, LRT)

From segment 1 analysis, it is determined that growth factor due to LRT is 1.30. Also the split between LRT and bus ridership was estimated at 5.25:1. Using those factors, the projected total transit ridership for segment 2 and corresponding bus and LRT ridership are computed below:

Segment 2 transit ridership demand = 1.30 x 9,222 = 11,988

LRT: 84% of 11,988 = 10,070 passengers per day
Bus: 16% of 11,988 = 1,918 passengers per day

For the purpose of this research, a preliminary estimate of Segment 2 LRT ridership was established at 10,070 passengers per day. Preliminary estimate for corridor LRT ridership was established at 21, 437 per day (10,070+11,367). This estimate was further refined by considering socioeconomic factors and modal connectivity.

5.3. LRT Ridership by Station

The alighting and average ridership by station for segment 2 are computed using equations 6 and 7 and presented in Table 8. Once validated, the models were used to predict boarding and alighting demand for the proposed LRT stations along Segment 2. These estimates are listed in Table 10. The intermodal connectivity factors are presented earlier in Table 9 for segment 2. Because of the indirect procedure employed in the estimation of boarding data, the boarding prediction (12,198 passengers per day) is different from the alighting prediction (10,155 passengers per day). Hence, the boarding data required adjustment so that the boarding and alighting estimates are equal to one another. The total ridership estimate that was derived (10,155) is little higher than the estimate of 10,070.

Table 10. Predicted LRT Boarding and Alighting for Segment 2

STATION NAME (Intermodal Connectivity)	PREDICTED AVERAGE DEMAND[2]	2*(PREDICTED AVERAGE DEMAND)	PREDICTED ALIGHT[1]	PREDICTED BOARD [3]	ADJUSTED BOARD[4]
9 Mile Rd.	617	1,234	552	682	568
Washington / Allenhurst St. Near 10 Mile Rd.	609	1,218	535	682	568
Lincoln St.	689	1,379	700	679	565
11 Mile Rd. (Royal Oak Transit Center)	950	1,900	558	1,342	1,117
12 Mile Rd.	804	1,609	936	673	560
Coolidge Hwy.	642	1,284	604	680	567
Normandy St.	606	1,211	529	682	568
Lincoln St.	703	1,407	729	678	564
15 Mile / Maple Rd.	663	1,326	646	680	566
Oak Blvd.	596	1,193	510	683	569
Lone Pine Rd.	654	1,307	627	680	566
Long Lake Rd.	599	1,199	516	683	568
Square Lake Rd.	705	1,410	732	678	564
MLK / South Blvd.	771	1,543	868	675	561
E. Pike St. (AMTRAK)	945	1,891	549	1,342	1,117
E. Huron St. / M-59	622	1,243	561	682	567
Total	**11,175**	**22,354**	**10,152**	**12,201**	**10,155**

[1] based on equation 6,[2] based on equation 2,[3] based on 2*predicted average demand-predicted alight, [4]based on (10,152/12,201)*predicted board

6. CORRIDOR STUDY

Once boarding and alighting data for Segment 2 are computed, LRT ridership by station along Woodward corridor from downtown Detroit to M-59 is finalized by adopting SEMCOG data for segment 1 and predicted data for Segment 2. Total LRT boarding and alighting data is presented in Table 11. Once ridership data is computed, then peak loading by peaking direction, headway, fleet size and operating costs are calculated. These are presented in the following sections:

6.1. Peak Demand for Computing LRT System Requirements

The boarding and alighting data presented in Table 11 was used to compute demand (D_P) at the maximum loading section (MLS) for the proposed alignment (i.e., Segments 1 and 2).

The procedure consists of the following steps, executed in sequential order:

Step 1: Peak Directional Demand (PDD) was assumed to be equal to 60 percent of the daily demand (as opposed to an equal split of demand, or 50 percent of daily demand) to incorporate a factor of safety for system capacity requirements.

Step 2: The number of passengers on the system (i.e., on-line) between LRT station locations is calculated using Equations 8 and 9:

For Trip Origin Station: $Pass\_Online_N = BOARD_N$ (*8*)

For remaining Stations Other than last one:

$$Pass\_Online_{N+1} = BOARD_N + BOARD_{N+1} - ALIGHT_{N+1} \quad (9)$$

For Last Station: Pass_Online = 0

where:

Pass_Online: the number of passengers on-line
BOARD: the peak passenger boarding demand, based on the daily boarding calculated using the method discussed in *Projecting Segment 2 Transit Ridership Demand (Bus, LRT).*
ALIGHT: the peak passenger alighting demand, based on the daily alighting calculated using the method discussed in *Total Bus Ridership for Segment 2*.
N: point along the LRT alignment corresponding to a station location

Equation 8 is used at the starting terminal point of the route. Equation 9 is used to compute the number of passengers on-line at each successive station location. It has been assumed that no alighting will occur at the starting terminal point, and that no boarding will occur at the ending terminal point of the LRT route.

Table 11. Woodward Corridor LRT boarding and alighting Data (Segments 1 & 2)

	NO.	STATION NAME (Intermodal Connectivity)	AVERAGE	ALIGHTING	BOARDING
SEGMENT 1	1	Jefferson Ave. (Tunnel Bus to Windsor)	2,451	3,459	1,442
	2	Foxtown	187	324	50
	3	MLK Blvd. / Mack Ave.	783	860	706
	4	Warren Ave.	1,585	2,141	1,029
	5	W. Grand Blvd. (AMTRAK)	676	974	378
	6	Hazelwood / Holbrook St.	450	398	501
	7	Calvert St.	304	197	410
	8	Glendale St.	141	145	136
	9	Manchester St.	465	453	477
	10	McNichols Rd.	1,138	984	1
	11	7 Mile Rd.(SMART-DDOT Transfer Center)	1,430	695	2,165
	12	8 Mile / Baseline Rd. (SMART-DDOT Transfer Center)	1,759	736	2,782
SEGMENT 2	13	9 Mile Rd.	617	552	568
	14	Washington / Allenhurst St. Near 10 Mile Rd.	609	535	568
	15	Lincoln St.	689	700	565
	16	11 Mile Rd.(Royal Oak Transit Center)	950	558	1,117
	17	12 Mile Rd.	804	936	560
	18	Coolidge Hwy.	642	604	567
	19	Normandy St.	606	529	568
	20	Lincoln St.	703	729	564
	21	15 Mile / Maple Rd.	663	646	566
	22	Oak Blvd.	596	510	569
	23	Lone Pine Rd.	654	627	566
	24	Long Lake Rd.	599	516	568
	25	Square Lake Rd.	705	732	564
	26	MLK / South Blvd.	771	868	561
	27	E. Pike St. (AMTRAK)	945	549	1,117
	28	E. Huron St. / M-59	622	561	567
CORRIDOR TOTALS			**22,542**	**21,518**	**21,522**

Step 3: The boarding and alighting daily ridership data (totaled over both directions of travel, northbound and southbound) were used as the baseline for computing the demand for the periods of an assumed 18-hour operating day. The proportions of ridership contributed by each period of the day were derived from the SEMCOG model for LRT Segment 1.

Step 4: In order to practice conservative estimation, the hourly distribution of the passenger demand during the four periods of the operating day was assumed to be non-uniform. The following additional assumptions have been made:

a. Distribution of LRT ridership during various peak and off-peak periods are presented in Table 12. Please note that they were presented before in Table 3.
b. Peak Hourly Demand (PHD) for the AM and PM Peak periods (each period having three-hour durations) equal to 0.40 times the Peak Period Demand (PPD) (as opposed to 0.33).
c. PHD for MID-DAY and OFF-PEAK periods (each period having six-hour durations) equal to 0.20 times the MID-DAY (or OFF-PEAK) demand (as opposed to 0.167).

d. From Table 12, the hourly peak occurs during the PM peak (27 percent of estimated total daily ridership), and is equal to 0.27 times (PHD of 40 percent). This value has been used as the design load to calculate the PHD (D_P), discussed in the next section.

Table 12. Ridership Distribution by Periods of LRT Operating Day

PERIOD	DURATION (hrs)	PROPORTION OF DAILY RIDERSHIP (%)
AM Peak	3	19
MID-DAY	6	33
PM Peak	3	27
OFF-PEAK	6	21
TOTALS	**18**	**100.00**

Columns 1 and 2 of Table 13 contain the PDD values resulting from this method, for the southbound direction of travel. The peak period demand (according to the percentages shown in Table 12) has been used to determine similar data for each station in Segments 1 and 2. These data are listed in columns 4, 6, 8, and 10 of Table 13. The hourly demand data (and the resulting values for passengers on-line) obtained for the four periods of the assumed operating day are listed in columns 5, 7, 9, and 11 of Table 13.

The Maximum Loading Section (MLS) was established for the Woodward corridor for the peak direction of travel. The peak direction demand D_p at the MLS was calculated as 363 passengers per hour, occurring during the PM peak hour period between stations 5 and 6: W. Grand Blvd. and Hazelwood/Holbrook Street, respectively (Table 13 and Figure 4). This demand value was used to estimate the system requirements (i.e., headway, travel time, fleet size). This value is

also known as the design hourly volume (DHV). The procedure used in identifying the MLS, and in estimating the peak demand was adopted from Vuchic [*14*], and presented in Figure 5.

Table 13. Peak Direction LRT MLS Database

			1	2	3	4	5	6	7	8	9	10	11
		STATION NAME	BOARD (60%)	ALIGHT (60%)	Pass On-Line	AM Peak	AM Peak Hourly	MID-DAY	MID-DAY Hourly	PM Peak	PM Peak Hourly	OFF-PEAK	OFF-PEAK Hourly
SEGMENT 2	28	E. Huron St. / M-59	838		838	155	62	272	54	229	92	182	36
	27	E. Pike St.	670	329	1,179	218	87	383	77	322	129	256	51
	26	MLK / South Blvd.	337	521	995	184	74	323	65	272	109	216	43
	25	Square Lake Rd.	338	439	894	165	66	291	58	244	98	194	39
	24	Long Lake Rd.	341	310	925	171	68	301	60	253	101	201	40
	23	Lone Pine Rd.	340	376	889	164	66	289	58	243	97	193	39
	22	Oak Blvd.	341	306	924	171	68	300	60	252	101	201	40
	21	15 Mile / Maple Rd.	340	388	876	162	65	285	57	239	96	190	38
	20	Lincoln St.	338	437	777	144	57	253	51	212	85	169	34
	19	Normandy St.	341	317	800	148	59	260	52	219	87	174	35
	18	Coolidge Hwy.	340	362	778	144	58	253	51	212	85	169	34
	17	12 Mile Rd.	336	562	553	102	41	180	36	151	60	120	24
	16	11 Mile Rd.	670	335	888	164	66	289	58	242	97	193	39
	15	Lincoln St.	338	420	806	149	60	262	52	220	88	175	35
	14	Washington / Allenhurst St. (Near 10 Mile Rd.)	341	321	826	153	61	269	54	226	90	179	36
	13	9 Mile Rd.	341	331	836	155	62	272	54	228	91	181	36
SEGMENT 1	12	8 Mile / Baseline Rd.	1,669	442	2,063	382	153	671	134	563	225	448	90
	11	7 Mile Rd.	1,299	417	2,945	545	218	957	191	804	322	639	128
	10	McNichols Rd.	775	590	3,130	579	232	1,017	203	854	342	679	136
	9	Manchester St.	286	272	3,144	582	233	1,022	204	858	343	682	136
	8	Glendale St.	82	87	3,139	581	232	1,020	204	857	343	681	136
	7	Calvert St.	246	118	3,266	604	242	1,062	212	892	357	709	142
	6	Hazelwood / Holbrook St. *	301	239	3,328	616	246	1,082	216	909	363*	722	144
	5	W. Grand Blvd. *	227	584	2,971	550	220	965	193	811	324	645	129
	4	Warren Ave.	617	1,285	2,303	426	170	749	150	629	252	500	100
	3	MLK Blvd. / Mack Ave.	424	516	2,211	409	164	719	144	604	241	480	96
	2	Foxtown	30	194	2,047	379	151	665	133	559	223	444	89
	1	Jefferson Ave.		2,047	0	0	0	0	0	0	0	0	0
		TOTALS	**12,545**	**12,546**	**44,331**	**8,201**	**3,281**	**14,408**	**2,882**	**12,102**	**4,841**	**9,620**	**1,924**

**** The section between stations 6 and 5 represent the Maximum Loading Section with corresponding Peak Hourly Demand (D_p) of 363.***

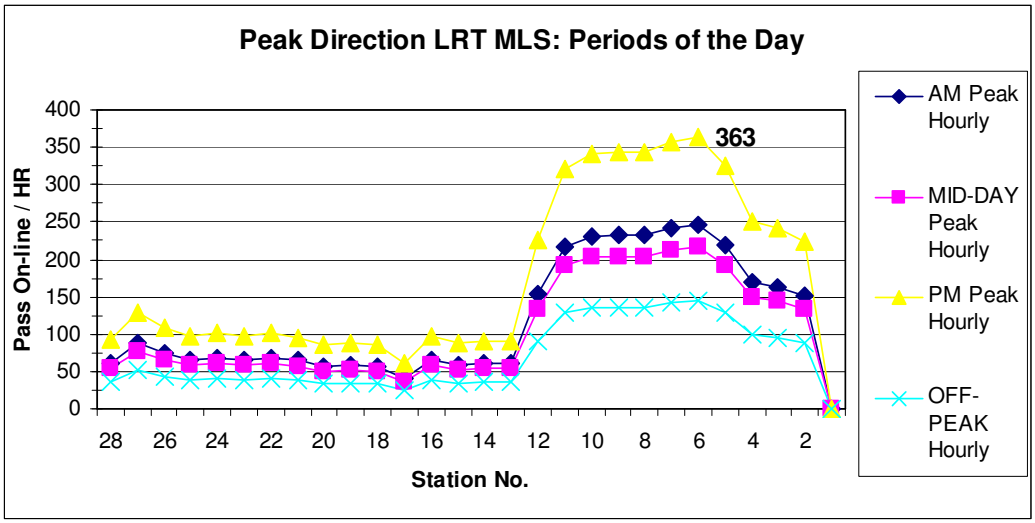

Figure 4. Peak Direction LRT MLS Database

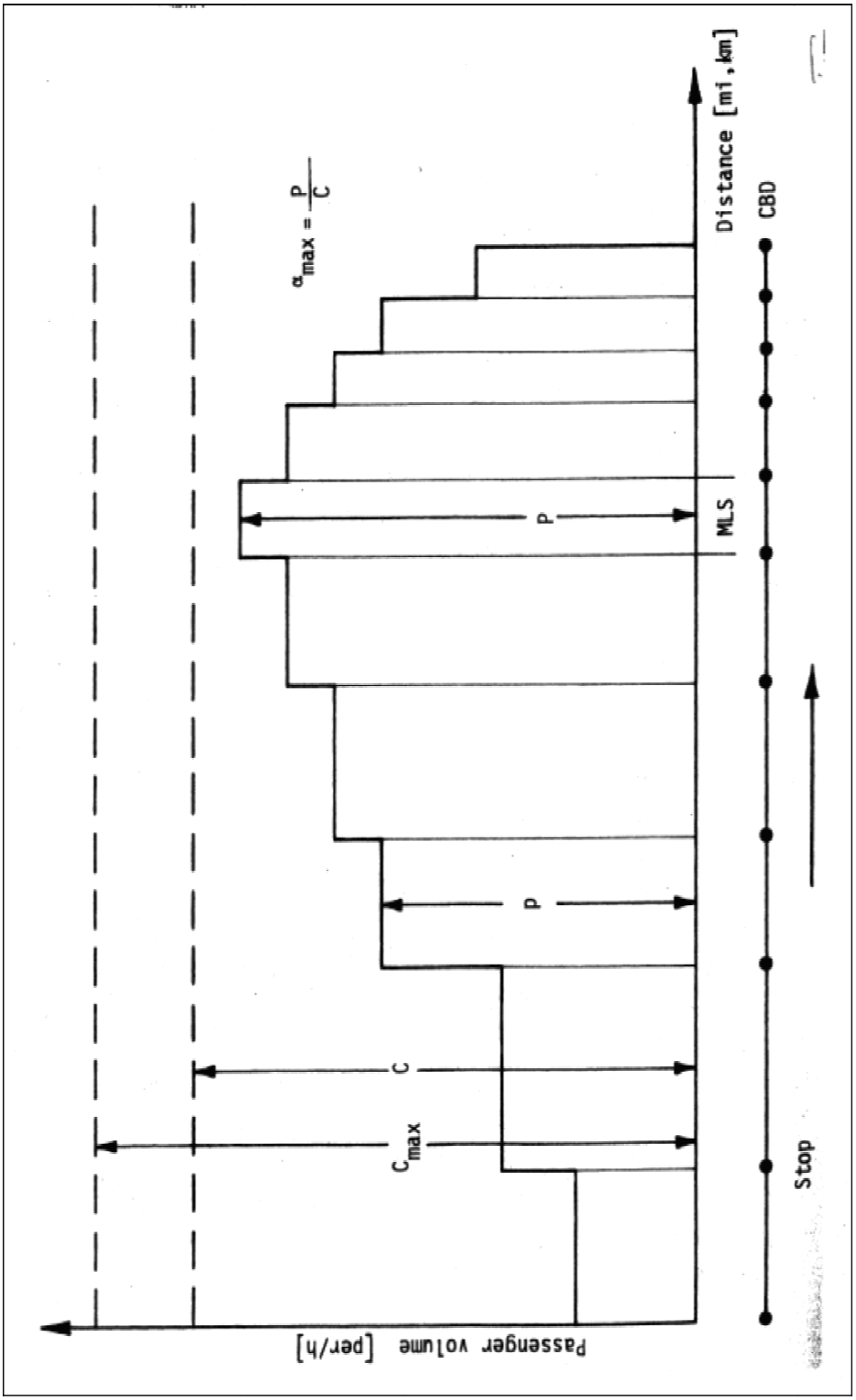

Figure 5. Graphical Representation of Terms Related to Maximum Loading Section Distribution (Source: Vuchic[14])

7. LRT SYSTEM REQUIREMENTS

7.1. Operating Parameters: Introduction

The system requirements for the proposed LRT system were calculated using the demand data, as reported in the previous section, along with information on station location (i.e., station spacing). The following equations were used [*15*]:

$$N_V \geq \frac{(D_P * C)}{(V_C * 60)} \qquad (10)$$

$$H = \frac{C}{N_V} = \frac{60 * V_C}{D_P} \qquad (11)$$

$$C = 2 * (T_D + T_S + T_C) \qquad (12)$$

where:

N_V: the number of LRT vehicles (LRTV) required; fleet size (number of LRTVs)
D_P: the hourly passenger demand at the MLS (passengers on-line, during the peak hour of the peak period)
C: the time required for an LRTV to travel from a starting terminal point A, to an ending terminal point B, and then reach point A again; cycle time (min)
T_D: the time required for an LRTV to travel between points A and B; driving time (min)
T_S: the total time required, between points A and B, for passenger boarding and alighting (min)
T_C: the downtime allotted after an LRTV has completed an A-to-B trip, usually planned to accommodate: breaks for vehicle operations, shift changes, or minor vehicle maintenance; layover time (min)
H: the duration of time between LRTV departures from point A; minimum service headway (LRTV per min headway)
V_C: LRTV capacity, including standing passengers (number of passengers)

Furthermore, the driving time, T_D, is calculated using the following equation:

$$T_D = \frac{(60 * D)}{V_{MAX}} + \left\{ n * \left(\frac{V_{MAX}}{2} \right) * \left(\frac{5{,}280}{3{,}600} \right) * \left[\frac{(a+b)}{60ab} \right] \right\} \qquad (13)$$

where:

D: the distance between the two terminal points of the LRT route (miles)
V_{MAX}: the maximum traveling velocity of an LRTV during normal operation (mph)
n: the number of stops between the two terminal points of the LRT route
a: the acceleration rate of an LRTV during normal operation (fps^2)
b: deceleration of an LRTV during normal operation (fps^2)

Equation 10 shows that for a given demand D_P and LRTV size V_C, the fleet size can be minimized by reducing the cycle time C. Furthermore, cycle time, being the total of driving time (T_D), boarding/alighting time (T_S), and layover time (T_C), can be minimized by reducing any of the three components or any combination thereof.

7.2. Operating Parameters: Assumptions

Equations 10-13 were used to determine the minimum requirements for the LRT system proposed for the metro Detroit region, considering the following assumptions [*16, 17, 18*]:

1. The project team is recommending Kinkisharyo LRTV manufactured by the Kinkishharyo Company Limited, of Osaka, Japan. Kinkisharyo has produced LRTVs for LRT systems in Dallas (Dallas Area Rapid Transit), Phoenix (METRO), Seattle (Sound Transit Central Link), and New Jersey (Hudson-Bergen). The selection LRTVs that are currently in production, rather than seeking customized specifications of another vehicle type, is expected to minimize capital costs related to the fleet size (Table 14, Figure6)

2. LRTVs operating along the Woodward corridor will be given traffic signal pre-emption through all intersections in the metropolitan Detroit area.

3. Boarding and alighting will only occur at the front and rear of the LRTVs, respectively, to facilitate efficient passenger flow.

Source: Dallas Area Rapid Transit (DART), Fact Sheet

Figure 6. Kinkisharyo LRTV [16]

As the result of the assumptions above, the following values have been selected as inputs for Equations 10-13:

D_P = 363 passengers on-line, during the peak hour of the peak period
D = 26 miles
N = 26 LRT stations
a = 3.2 fps^2
b = 4.4 fps^2

Table 14. Kinkisharyo LRTV Specifications [16,17,18]

PARAMETER	VALUE
Location	Osaka, Japan
Length (ft)	92.67
Height (ft)	12.5
Width (ft)	8.83
Weight (1,000 lbs)	107
Seating capacity (seated, plus standees)	150
Top speed (mph)	65
Design life (yrs)	30
Cost ($ million; 2008)	3.2
Maximum # of vehicles for multi-unit operation	4
(normal) Acceleration (fps^2)	3.2
(normal) Deceleration (fps^2)	4.4

With the assumption of exclusive boarding and alighting from separate doors and the average boarding and alighting time per passenger being the same, T_s can be calculated as follows:

$$T_S = n * Av.\ \#\ of\ passengers\ boarding\ per\ stop * Av.\ Boarding\ time \quad (14)$$

-OR-

$$T_S = n * Av.\ \#\ of\ passengers\ alighting\ per\ stop * Av.\ Alighting\ time \quad (15)$$

In order to use equation (14) or (15), the average # of passengers boarding or alighting needs to be estimated. Table 13 shows that the number of passengers boarding per day and the number of passenger alighting per day are the same, being 12, 545. Thus the use of equation (14) or (15) will result the same number. Hence equation (14) is used.

Average # of passengers boarding during peak hour = 12, 545*0.27*0.40= 1,355

Hence, the number of passengers boarding per hour per train = (# of passengers boarding/hr)/ (# of Trains/hr)

With an assumed headway of 10 minutes (peak- hour),

# of passengers boarding per hour per Train = 1355/6= 226

Assuming an even distribution of passengers boarding per stop,
# of passengers boarding/stop = 226/(# of Stops) = 226/26 = 8.7

Hence, using equation (14),

T_s = 26*8.7*2 = 452.4 seconds (Average time to board = 2 sec/passenger)
T_s is raised to 465 second, because of higher initial delays in the boarding process. Thus
T_s = 465 seconds = 7.75 minutes = 8 minutes

The maximum speed capacity of the Kinkisharyo LRTV has been listed at 65 mph, but it is not likely that such speeds will be attainable in a mixed-traffic ROW, where station spacing averages one mile. Thus, a lower value has been assumed for the top speed reached by the LRTV: 50 mph (note that this value is not the travel speed). The downtime provided at each terminal point along the route, T_C, has been estimated at ten minutes so that shift changes and operator breaks may occur:

V_{MAX} = 50 mph
T_C = 10 min

7.3. Operating Parameters: Resulting Values

Considering the variables and inputs discussed in *Operating Parameters: Assumptions,* the operating parameters for the proposed Woodward LRT system can be calculated. Using Equation 13, driving time is calculated and presented in Table 15. Please note that Cycle time can be calculated using Equation 12 as shown in Table 16.

Table 15. Driving Time, T_D

PARAMETER	VALUE
Distance (mi)	26.0
Max. velocity (mph)	50.0
Number of stops	26.0
Acceleration rate (fps^2)	3.5
Deceleration rate (fps^2)	4.4
Driving Time (min)	**39.8**

Table 16. Cycle Time, C

PARAMETER	VALUE
Driving Time (min)(T_d)	39.8
Board/Alight Time (min) (T_s)	8.0
Layover Time (min) (T_c)	10.0
Cycle Time (min)*	**116**

*$C=2(T_d+T_s+T_c)$ =115.6 minutes = 116 minutes (assumed)

The minimum fleet size is calculated using Equation 10 and presented in Table 17. It should be noted, however, that resulting value (15 trains) does not include additional LRTVs that may be required for system maintenance and special events (i.e., providing additional capacity in the event that ridership is significantly higher than that of the peak hour of a normal operating day).

Table 17. Minimum Fleet Size, N_V

PARAMETER	VALUE
MLS (pass/hr)	363.0
Cycle time (min)	116
Vehicle capacity (pass/vehicle)	150.0
Minimum fleet size (Train)	**4.67≈5(assumed)**

The final parameter of this process is the minimum service headway provided by the system, and is calculated using Equation 11 (Table 18). However, it should be noted that this value (23.2 seconds) has been calculated for planning purposes, and that a smaller value for headway is likely to be employed for the sake of convenience for those using the system: policy headway. The development and planning of establishing this value is discussed in the next Section.

Table 18. Minimum Service Headway, H

PARAMETER	VALUE
Minimum service headway (min)	**23.2**

The operating speed, $V_{O,}$ defined as the average speed of the transit vehicle including stopping time at LRT stations is calculated as:

$$V_O = \frac{60L}{(T_D + T_S)} \qquad (16)$$

where:

L: the distance between the two terminal points of the LRT route; takes the same value of *D*, used previously (miles)

The commercial speed, V_C, on the other hand, is the average speed of the transit vehicle for a complete round trip and is calculated as:

$$V_C = \frac{120L}{C} = \frac{120L}{2*(T_D + T_S + T_C)} = \frac{60L}{(T_D + T_S + T_C)} \qquad (17)$$

Using Equations 16 and 17:

$$V_O = \frac{60*(26mi)}{(39.8 + 8.0)} = 32.82mph \qquad (16)$$

$$V_C = \frac{60*(26mi)}{(39.8 + 8.0 + 10.0)} = 27mph \qquad (17)$$

In the transit industry, the commercial speed, V_C, is considered to be a more suitable measure of system performance when compared to operating speed, V_O. The logic for Equations 16 and 17 are schematically represented in Figure 7 [*14*].

7.3.1. Policy Headway

The equations presented in the previous section (*Operating Parameters: Resulting Values*) show that with a minimum headway of 23 minutes, and maximum LRTV capacity of 150 passengers, the passenger demand for the system can be met. However, it is customary to use policy headways for new transit operations. Policy headways are typically shorter than (i.e., more frequent service) the minimum headways. This practice is intended to build and sustain a long-term demand for transit services.

In order to obtain a suitable value for the policy headway for the Woodward LRT system, a list of similar LRT systems around the United States were reviewed by the research team. A summary of this data, derived from the National Transit database and other sources, is presented in Table 19.

A review of this information presented in Table 19 shows that:

1. The peak headways employed for each of the 14 transit systems range from 3 to 15 minutes.

2. For the LRT systems in the Minneapolis and Charlotte areas (average weekday demand of 26,500 and 19,700, respectively), peak headways range from seven to ten minutes. These areas are of interest since their average daily ridership values are comparable to the estimated value for the Woodward LRT system (Detroit area): approximately 22,000.

3. None of the peak headways are larger than 15 minutes. This does not compare favorably with the minimum headway value calculated for the Detroit area: 23 minutes.

4. The off-peak headways are generally twice as large as the peak headways.

Considering the items discussed above, the research team has recommended the following policy headways for the peak, and off-peak periods of the day: ten minutes and 20 minutes, respectively.

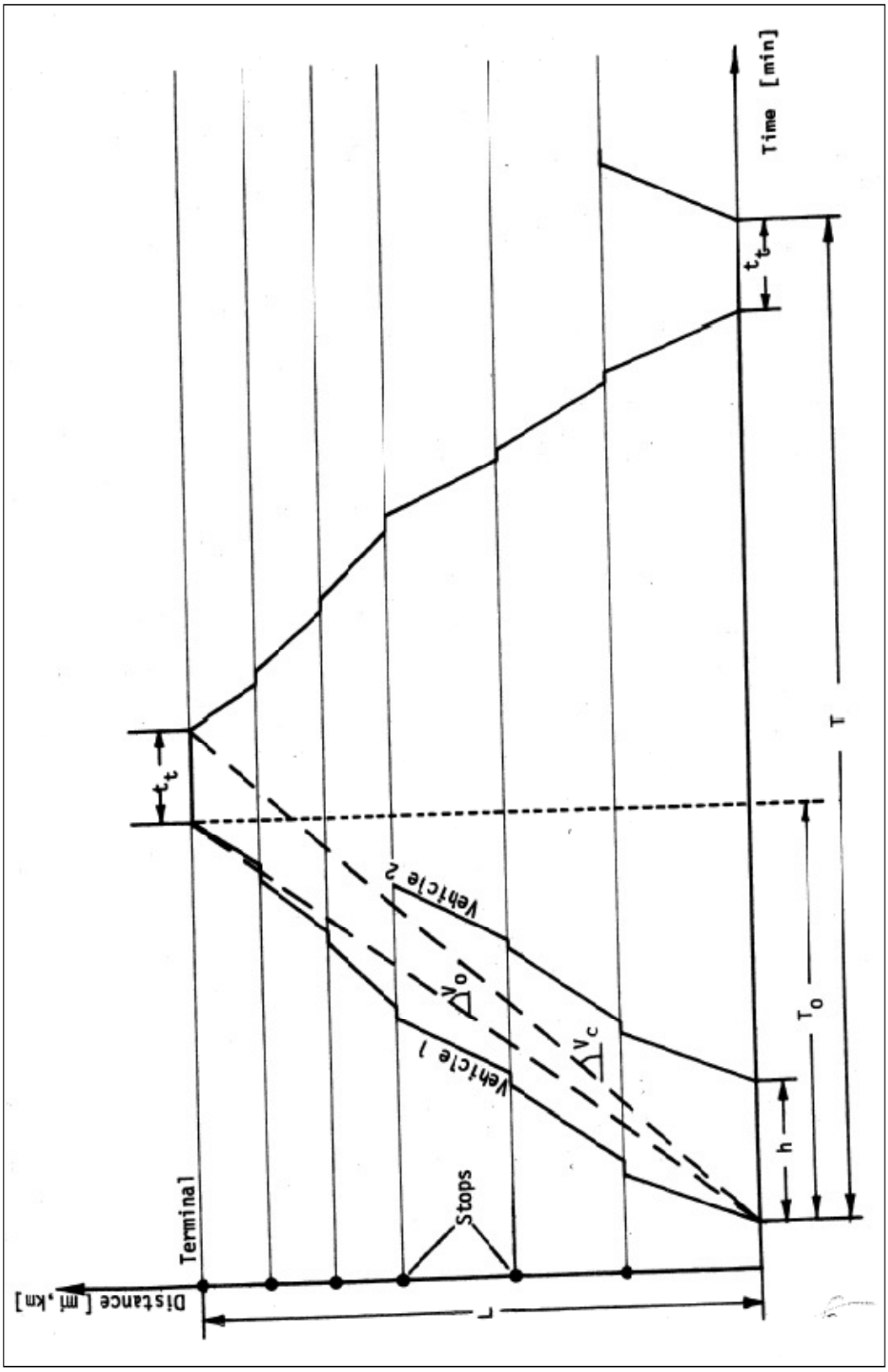

Figure 7. Graphical Representation of Terms Related to Vehicle Travel and Scheduling (Source: Vuchic [14])

Table 19. Comparison of LRT Systems in the United States[1]

SERVICE AREA	TRANSIT AUTHORITY	RIDERSHIP (pass)		HEADWAYS (min)	
		ANNUAL (x 1,000)	AVG. Daily (x 1,000)	PEAK	OFF-PEAK
Phoenix, AZ	Valley Metro Rail Inc.	10,020	33.4	10	20
Los Angeles, CA	Los Angeles County Metropolitan Transportation Authority (LACMTA)	40,740	135.8	4--6, 10	12—20
Sacramento, CA	Sacramento Regional Transit District	17,400	58	15	30
San Diego, CA	San Diego Trolley Inc.	28,800	96	15	30
San Jose, CA	Santa Clara Valley Transportation Authority	9,870	32.9	15	25—30
Denver, CO	Regional Transportation District (RTD)	20,640	68.8	5—10	15—30
Baltimore, MD	Maryland Transit Administration (MTA)	10,920	36.4	3—10	8—15
Minneapolis, MN	Metro Transit (MT)	7,950	26.5	7—10	15+
St. Louis, MO	Bi-State Development Agency (METRO)	15,720	52.4	15	20
Charlotte, NC	Charlotte Area Transit Authority (CATS)	5,910	19.7	7.5	15
Portland, OR	Tri-County Metropolitan Transportation District (TriMET)	31,050	103.5	4—9	15
Philadelphia, PA	Southeastern Pennsylvania Transit Authority	32,760	109.2	4—9	12—15
Dallas, TX	Dallas Area Rapid Transit (DART)	18,330	61.1	10	20+
Salt Lake City, UT	Utah Transit Authority (UTA)	12,960	43.2	15	15

[1]**Source: National Transit Data Base [30]**

7.3.2. Fleet Size

Previous calculations for the operating parameters of the proposed system (*Operating Parameters: Resulting Values*) revealed that the minimum fleet size is equal to 5 LRTVs (based on a minimum headway of 25 minutes). This topic required additional consideration because of the policy headway value that has been recommended above. Intuitively speaking, it is expected that when LRTVs are dispatched at a more frequent rate, additional vehicles will be required to meet the needs of the system. This relationship is derived from Equation 11:

$$H = \frac{C}{N_V} \qquad (11)$$

So that, $$N_V = \frac{C}{H} = \frac{116\,\text{min}}{\left(\frac{1\,LRTV}{10\,\text{min}}\right)} = 11.6 = 12\,trains(assumed)$$

Using the other part of Equation 11:

$$H = \frac{60 * V_C}{D_P} \qquad (11)$$

$$D_P = \frac{60 * 150}{H} = \frac{60 * 150}{12} = 900\, passengers / hr$$

The version of Equation 11 above, results in a value for system capacity equal to 900 passengers per hour (during the peak hour of the peak period), compared to the estimated demand (Dp) of 363 passengers per hour at the MLS (during the peak hour of the peak period).

Finally, the final fleet size ($N_{V,\ FINAL}$) for the proposed system would be most efficient when a contingency factor of 30 percent of the policy fleet size ($N_{V,\ POLICY}$) was added (Equation 18). The intent for the contingency is to accommodate the following scenarios for the system: vehicle repair, scheduled maintenance, emergency repairs, and special events (i.e., sports event, parade, etc.).

$$N_{V,FINAL} = N_{V,POLICY} * 1.30 \qquad (18)$$

$$N_{V,FINAL} = 12 * 1.30 = 15.6 \cong 16 LRTV's$$

8. COST ESTIMATION

The cost elements associated with the delivery of transit services can be broadly classified under two categories: fixed costs and variable costs. Fixed costs are those that hold constant over a large range of service, and do not vary with modest changes in transit level of service. Examples include, but are not limited to, the following: all facility-related capital costs, administrative labor costs, and material costs other than those required to support revenue services. Variable costs, on the other hand, are directly related to the level of transit service provided and include driver wages, vehicle operating costs, etc. The bulk of the fixed cost variables include what is often referred to as the capital expense, which is typically derived from a capital budget, separate from operating revenue and expenses. Variable costs, on the other hand, are generally associated with the operating and maintenance expenses.

The prevailing practice in the transit industry is to include only operating and maintenance expenses, ignoring capital expenses, in computing cost estimates. The prevailing practice is to omit the annualized portion of the capital cost for any proposed transit system into the FAC. However, it can be included in the model by simply allocating the capital cost elements into the appropriate cost variables into the FAC, if necessary. While capital costs represent a large fraction of the total system costs, funds for capital improvements are typically derived from inter-governmental loans, Federal and state subsidies, etc.

Two conflicting factors further confound the relationship between capital and operating costs [*20, 21*]:

- Capital costs associated with fixed facilities (i.e., land, structures, equipment, etc.) are not affected by incremental changes in transit services levels.

- Modest changes in transit service levels may require some changes in the allocation of certain capital resources (e.g., number of transit vehicles on-line).

A review of the current literature has revealed the existence of two methods for estimating transit services: partially-allocated cost (PAC) and fully-allocated cost (FAC).

8.1. Partially-Allocated Cost Models

A partially-allocated cost (PAC) model incorporates a limited number of items for the operating expenses in the estimation process. The most common and simple example is based upon the use of one service variable, typically the number of vehicle-hours (V_H) or vehicle-miles (V_M). The estimated cost can be calculated using Equations 19 and 20:

$$EstimatedCost = U_{VH} * VH \qquad (19)$$

$$EstimatedCost = U_{VM} * VM \qquad (20)$$

where the unit costs have been empirically-derived from data sources:

U_{VH}: unit cost per vehicle-hour traveled
U_{VM}: unit cost per vehicle-miles traveled
VH: number of vehicle-hours of travel
VM: number of vehicle-miles of travel

The advantage of the PAC method is in its relatively simplistic data requirement. The disadvantage, however, lies in the quality of the results obtained, which could be considered to be a crude estimate at best. The choice of the variable for the PAC model (i.e., *VH* versus *VM*) often depends upon the availability of data, and the type of expense (hour-related or mile-related) that comprises the dominant expenditure for the case analyzed. Sometimes, the breadth of the PAC is expanded by including two pertinent variables, as follows:

$$EstimatedCost = (U_{WAGES} * VH) + (U_{POWER} * VM) \qquad (21)$$

where:

U_{WAGES}: the unit cost for wages associated with vehicle-hours traveled
U_{POWER}: the unit cost of power used per vehicle-mile traveled

Results obtained from PAC models are not precise, but they provide a preliminary estimate of costs, that may be appropriate for planning purposes.

8.2. Fully-Allocated Cost Models

A fully-allocated model (FAC) is an expanded version of its predecessor, the PAC, and has been designed to allocate the cost among a larger number of variables. The variables used for the model are those that conceivably affect transit operation. A typical example of FAC model is shown in Equation 22:

$$EstimatedCost = (U_{VH} * VH) + (U_{VM} * VM) + (U_{PV} * PV) \qquad (22)$$

where:

PV: the number of transit vehicles required for operation during the peak hour
U_{PV}: the unit cost per peak vehicle

It should be noted that in multi-variable cost models (as opposed to single-variable models), the unit costs must be calculated to include the expenses for those inputs associated with each service characteristic, avoiding duplication. Table 20 is a typical representative of how cost items are allocated in a typical FAC model [*22*]. The following FAC has been derived for the Los Angeles County Metropolitan Transportation Authority (LACMTA)

$$AnnualCost = \left[(U_{VH} * VH) + (U_{VM} * VM) + (U_{PV} * PV) + (U_{TP} * TP)\right] * F_1 \qquad (23)$$

where:

U_{TP}: the unit cost per passenger
*T*P: the total number of passengers traveling on the system, per year
F: a multiplication factor used to incorporate a number of alternate costs related to operations (e.g., administration, contingency, changes in consumer price index, etc.)

Table 20. Recommended Expense Assignment for Three-Variable Cost Model

	ASSIGNMENT VARIABLE		
EXPENSE OBJECT CLASS	**VEHICLE-HOURS**	**VEHICLE-MILES**	**VEHICLE**
Transportation Expense			
Driver Wages & Salaries	X		
Driver Fringe Benefits	X		
Fuel & Oil		X	
Tires & Tubes		X	
Vehicle Insurance			X
Vehicle Lease			X
Purchased Transportation	X		
Other	X		
Maintenance Expense			
Mechanic Wages & Salary		X	
Mechanic Fringe Benefits		X	
Materials & Supplies		X	
Contracted Maintenance		X	
Facility Rental			X
Utilities			X
Contracted Services			X
Other			X
Call Taking & Dispatching Expense			
Dispatcher Wages & Salary			X
Dispatcher Fringe Benefits			X
Telephone Expenses			X
Computer Expenses			X
Rent			X
Other			X
Administrative Expense			
Administrative Salaries			X
Administrative Fringe Benefits			X
Materials & Supplies			X
Non-Vehicle Insurance			X
Professional Services			X
Travel			X
Office Rental			X
Utilities			X
Equipment Rental/Service			X
Other			X

Source: Improving Transit Performance Using Information based Strategies [22]

8.3. Fully-Allocated Cost and Capital Cost

As mentioned previously, FAC's, originally introduced in the cost analysis framework, did not include capital costs. The process of obtaining capital funds for building transit systems has historically been quite different from that of operating expenses. On the other hand, it has been argued that independent of the source of funding, transit cost models should include capital costs because they are real costs. Furthermore, their incorporation into such cost models will help future cost-containment efforts by transit officials and policymakers.

The capital costs for transit systems include, but are not limited to, the following: vehicles, real estate, structures, and operating equipment (i.e., signals, signage, etc.). For rail transit, additional costs may be incurred in the acquisition of ROW, rail tracks, switching/signal equipment, service stations, and rail yards. The following FAC model has been proposed for estimating the costs related to rail transit systems:

$$FAC = \left[(U_{RH} * VH) + (U_{VM} * VM) + (U_{PV} * PV) + (U_{RM} * RM)\right] * F_1 \qquad (24)$$

where:

U_{RM}: the directional route-miles of travel

8.4. LRT Cost Models

While in the past, most FAC models have been developed for various types of bus systems, there are some rail transit cost models that have been discussed in the current literature. The majority of these models only account for operation and maintenance (O&M) costs.

8.4.1. LRT Operations and Maintenance Cost: METRORail, Red Line

Harris County is the most populous county in the state of Texas, where the city of Houston serves as the county seat. The Metropolitan Transit Authority of Harris County, Texas (METRO) serves the Houston metropolitan area with the following transportation services: light-rail, high-occupancy vehicle lanes (HOV), commuter rail, standard bus, and transit centers. METRO Solutions is a regional transit plan for Harris County, intended to alleviate travel congestion by improving the transportation infrastructure for all modes [*23*].

The 7.5-mile METRO Red Line is an LRT system operated within shared ROW in the Houston area. The Red Line began normal operation in January of 2004 serving 16 stations, traveling between two major terminal stations: University of Houston-Downtown Campus and Reliant Park (home of the Houston Texans, a National Football League team). The following five-factor operations and maintenance (O & M) cost model was developed for METRO. The model was developed for the year 2007 (originally developed for the year 2004, then inflated to reflect current costs for the year 2007) [*24*] (Table 21).

Using the approach depicted in Table 21, the estimated range of O & M costs for a one-car METRO Red Line rail transit system was estimated as: $6.9 to 10.5 million per year.

Table 21. LRT Build Alternative Operation and Maintenance Cost Factors (2007)

O & M COST FACTORS	LRT, ONE-CAR TRAINS ($)
Cost per Revenue Train-Hour	57.46
Cost per Revenue Car-Mile	6.17
Cost per Peak Vehicle	19,699
Cost per Station	118,332
Cost per Guideway-Mile	315,968

Source: METRO Cost Allocation Model [24]

8.4.2. LRT Operations and Maintenance Cost: Metropolitan Atlanta

The city of Atlanta is the 33rd largest in the United States, with an estimated population of 537,958. While the city proper does not compare with the larger cities (e.g., Los Angeles, Chicago, New York City), the metropolitan Atlanta area has experienced significant growth during the last decade. The Atlanta-Sandy Springs-Marietta metropolitan statistical area (MSA) is the 9th largest in the United States, with an estimated population of 5.5 million [*25*].

The Atlanta city proper is served by the Metropolitan Atlanta Rapid Transit Authority (MARTA), which operates heavy-rail and standard bus services throughout the region. However, no heavy-rail service is provided to the suburban counties surrounding the city of Atlanta. The lack of a regional heavy-rail transit network, combined with a booming population that is heavily reliant on private automobiles, places Atlanta among MSAs having the worst commute times in the United States [*26*].

Said commute times are likely to be longer in the suburban and exurban areas of the Atlanta MSA, where transit service is nearly non-existent. For instance, Gwinnett Village, a group of communities located in southwest Gwinnett County (approximately 20 miles northwest of the Atlanta CBD) has expressed a desire to investigate the feasibility of an LRT system for the area. Gwinnett Village is a typical decentralized suburban/exurban population center, consisting of a significant amount of low-density development: 100,000 residents, 60,000 employees, and 5,000 businesses [*27*].

An O & M cost model was developed for the Gwinnett County Community Improvement District (CID) because LRT had not been constructed there previously (similar to the current situation in Detroit, and its suburbs). The model was developed from available system data from nine comparable LRT systems, considered to be peer systems by the model developers: Baltimore (MD), Dallas (TX), Denver (CO), Houston (TX), Minneapolis (MN), Portland (OR), Sacramento (CA), Salt Lake City (UT), St. Louis (MO). Table 22 lists the O & M costs associated with each of the nine aforementioned peer systems[2], where total costs range from $15.0 to 79.8 million (Houston and Dallas, respectively). The unit costs per directional mile, calculated from the National Transit Database, range from $0.565 to $0.913 million (St. Louis and Minneapolis respectively) [*28, 29, 30*]. It was observed that the unit costs are inversely related to the length of the transit system. The FAC O & M model proposed for the Gwinnett Village CID is listed in Figure 7.

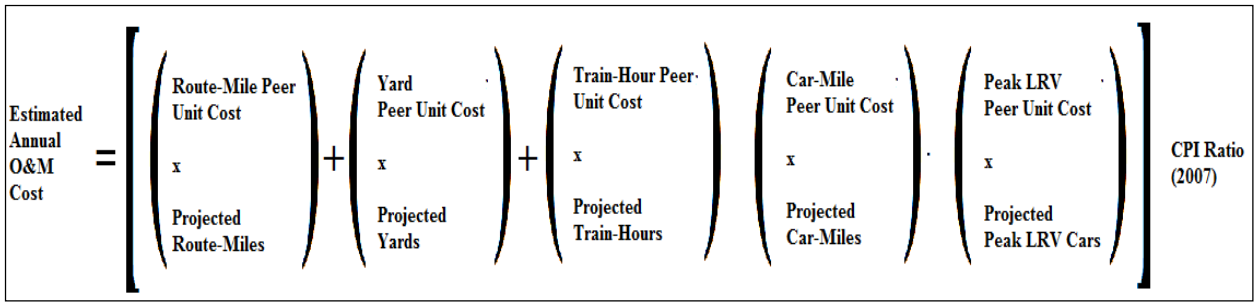

Source: I-85 Corridor LRT Feasibility Study, Phase I, Final Report (HDR Engineering Inc.) [28]

Figure 8. Gwinnett Village O & M Cost Model

where:

Route-Miles: the total number of directional route miles.
Yards: the total number of LRTV maintenance and storage facilities.
Annual Revenue Train-Hours: the total number of hours of revenue service operated by all trains in one year.
Annual Revenue Car-Miles: the total number of miles of revenue service operated by all trains in one year.
Peak LRV Cars: The maximum number of passengers vehicles scheduled in service, at the same time.

Table 22. Peer LRT System Productivity (Year 2007)

	Baltimore (MTA)	Dallas (DART)	Denver (RTD)	Houston (METRO)	Minneapolis (METRO)	Portland (TriMET)	Sacramento (RT)	Salt Lake City (UTA)	St. Louis (METRO)	TOTALS
2007 Units of Service Supplied										
Peak Passenger Cars in Operation	18	85	91	13	27	81	56	46	56	**473**
Train Revenue-Hours	77,449	123,819	201,478	57,660	66,946	261,675	81,641	88,858	134,505	**1,094,031**
Car Revenue-Miles	2,797,732	5,224,548	8,721,165	877,433	1,903,780	6,564,411	4,127,718	2,818,235	6,193,455	**39,228,477**
Directional Route-Miles	58	88	70	15	24	95	74	37	91	**552**
No. of Yards	2	1	1	1	1	1	1	1	2	**11**
Annual Passenger Trips	6,740,923	17,892,532	18,655,496	11,708,960	9,101,036	36,123,810	14,489,691	16,272,468	21,783,634	**152,768,550**
2007 Costs										
Vehicle Operations ($)	20,248,485	28,270,203	18,825,913	6,120,990	6,333,921	25,958,428	18,468,196	8,602,748	19,556,566	**152,385,450**
Vehicle Maintenance ($)	6,791,757	16,623,466	8,825,675	3,212,386	2,877,329	15,091,287	9,906,179	7,361,881	6,887,441	**77,577,401**
Non-Vehicle Maintenance ($)	10,260,675	14,816,022	5,485,171	4,666,814	3,666,297	16,215,291	6,286,302	7,380,353	13,205,449	**81,982,374**
General Administration ($)	2,448,606	20,106,218	7,363,673	1,049,633	9,049,291	16,391,168	12,763,378	2,845,932	11,747,815	**83,765,714**
TOTAL COSTS	**39,749,523**	**79,815,909**	**40,500,432**	**15,049,823**	**21,926,838**	**73,656,174**	**47,424,055**	**26,190,914**	**51,397,271**	**395,710,939**
Productivity Factors (2007)										
Cost per Revenue Train-Hour ($)	513.23	644.62	201.02	261.01	327.53	281.48	580.89	294.75	382.12	
Cost per Revenue Train-Mile ($)	14.21	15.28	4.64	17.15	11.52	11.22	11.49	9.29	8.3	
Cost per Passenger-Trip ($)	5.9	4.46	2.17	1.29	2.41	2.04	3.27	1.61	2.36	
Cost per Directional Route-Mile ($ million)	0.686	0.901	0.578	1	0.913	0.775	0.64	0.708	0.565	

Source: I-85 Corridor LRT Feasibility Study, Phase I, Final Report (HDR Engineering Inc) [28]

The O & M cost data for the peer systems (in 2007 costs), when fully-allocated among the five variables, result in different unit cost values as listed in Table 23. Furthermore, the grand average for the nine systems, results in the following unit costs: yard ($4,157,759), route-miles ($101,888), train-hours ($120.89), car-miles ($3.36), cars ($131,048). These values are listed in the last row of Table 23.

The unit costs, when applied to six LRT alternatives (i.e., track alignments) for the Gwinnett Village CID, result in a set of total annual costs ranging from $25.05 (Alternative 5) to 25.63 million (Preferred 1). The costs have been listed in Table 24. It should be noted that the unit costs outlined above only represent the O & M costs, and that no capital costs were included.

Table 23. Peer Systems Service Provided, Unit Costs

SERVICE AREA	YARDS		ROUTE-MILES		TRAIN-HOURS		CAR-MILES		CARS	
(TRANSIT AUTHORITY)	UNITS	UNIT COST ($)	UNITS	UNIT COST ($)	UNITS	UNIT COST ($)	UNITS	UNIT COST ($)	UNITS	UNIT COST ($)
Baltimore, MD (MTA)	2	2,397,299	58	111,503	77,449	219.98	2,797,732	3.19	18	143,005
Dallas, TX (DART)	1	8,418,502	88	90,698	123,819	161.31	5,224,548	4.60	85	228,837
Denver, CO (RTD)	1	2,285,620	70	47,892	201,478	71.98	8,721,265	1.49	91	81,217
Houston, TX (METRO)	1	4,491,122	15	190,267	57,660	92.56	877,433	4.65	13	43,708
Minneapolis, MN (METRO)	1	2,224,172	24	103,512	66,946	75.89	1,903,780	5.30	27	74,575
Portland, OR (TriMet)	1	8,044,587	95	103,574	261,675	87.77	6,564,411	2.44	81	207,101
Sacramento, CA (RT)	1	3,098,640	74	52,767	81,641	181.55	4,127,718	4.11	56	154,647
Salt Lake City, UT (UTA)	1	3,637,705	37	118,699	88,858	71.05	2,818,235	2.53	46	101,514
St. Louis, MO (METRO)	2	2,822,185	91	98,077	134,505	125.93	6,193,455	1.90	56	144,831
AVERAGE UNIT COST ($)		**4,157,759**		**101,888**		**120.89**		**3.36**		**131,048**

Source: I-85 Corridor LRT Feasibility Study, Phase I, Final Report (HDR Engineering Inc.) [28]

Table 24. Estimated Operating and Maintenance Costs by Alternative

ALTERNATIVE	YARDS	ROUTE-MILES	TRAIN-HOURS	CAR-MILES	CARS	TOTAL ANNUAL O & M COST (2009)	UNIT COST PER DIRECTIONAL MILE
Peer Unit Costs ($)	**4,157,759**	**101,888**	**120.89**	**3.36**	**131,048**		
Preferred 1	1	27.7	46,160	2,382,100	24	**25,629,365**	0.925
O & M Cost by Variable ($)	4,157,759	2,818,210	5,580,295	7,994,360	3,145,164		
Alternative 1	1	27.5	46,160	2,366,600	24	**25,553,266**	0.929
O & M Cost by Variable ($)	4,157,759	2,799,871	5,580,295	7,942,342	3,145,164		
Alternative 2	1	27.2	46,160	2,339,100	24	**25,418,180**	0.935
O & M Cost by Variable ($)	4,157,759	2,767,267	5,580,295	7,850,052	3,145,164		
Alternative 3	1	26.8	46,160	2,309,800	24	**25,274,356**	0.943
O & M Cost by Variable ($)	4,157,759	2,732,625	5,580,295	7,751,721	3,145,164		
Alternative 4	1	26.9	46,160	2,320,100	24	**25,324,968**	0.941
O & M Cost by Variable ($)	4,157,759	2,744,851	5,580,295	7,786,287	3,145,164		
Alternative 5	1	26.3	46,160	2,263,300	24	**25,046,059**	0.952
O & M Cost by Variable ($)	4,157,759	2,677,606	5,580,295	7,595,666	3,145,164		
AVERAGE							**0.938**

Source: I-85 Corridor LRT Feasibility Study, Phase I, Final Report (HDR Engineering Inc.) [28]

where:

$$DirectionalRoute - Miles \cong 2 * RouteLength(one - way) \qquad (25)$$

8.4.3. LRT Operations and Maintenance Cost: Metropolitan Detroit

The FAC O & M model developed for the Gwinnett Village CID study, was used to estimate the costs associated with the proposed Woodward Ave. LRT system in metropolitan Detroit:

$$\begin{aligned} AnnualCost(O\ \&\ M) &= [4{,}157{,}759 * (\#Yards)] + [101{,}888 * (DirectionalRoute - Miles)] \\ &+ [120.89 * (AnnualRevenueTrain - Hours)] + [3.36 * (AnnualRevenueCar - Miles)] \\ &+ [131{,}048 * (PeakLRTCars)] \end{aligned} \qquad (26)$$

Members of the research team found that the following items, related to the Gwinnett Village CID study, were conducive to Gwinnett Village CID model's application to the Woodward LRT system:

1. The directional length values ranged from 15 to 91 miles, compared to 52 miles for the Detroit area.

2. The peak number of train cars ranged from 13 to 91, compared to 22 equivalent cars for the Detroit area (the concept of equivalent train cars will be discussed in the next section).

3. The number of annual passenger trips ranged from 6.7 to 36.1 million, compared to 6.5 million for the Detroit area.

In order to estimate the variables required for Equation 26, and to assure that the values derived are reasonable, a review of LRT operating data for a number of transit systems was conducted. The transit system data was derived from the Federal Transit Administration's National Transit Database, and has been listed in Table 23 [*30*]. It should be noted that the system length values reflect the track network in one direction, and is approximately half of the directional length used in the previous tables ('Route-Miles' fields in Tables 23 and 24).

8.4.4. Number of Yards

Table 24 lists the number of yards provided in each of the nine peer systems. It has been observed that this value ranges between one and two yards, thus it has been assumed that the proposed Woodward Ave. LRT system will utilize one yard. It should be noted that the inclusion of each additional yard increases the estimated annual O & M cost by $4.5 million, according to the Gwinnett Village FAC model selected.

8.4.5. Number of Directional Route-Miles

This value has been calculated as two times the one-way system route length:

$$DirectionalRoute - Miles \cong 2 * RouteLength(one - way) \qquad (25)$$

$$DirectionalRoute - Miles \cong 2 * 26 = 52$$

Entering the system route length into Equation 25 results in a total directional route-mile value of 52 miles.

8.4.6. Number of Annual Revenue Train-Hours

- Each train (LRTV) completing a cycle will complete 116 minutes or 1.93 hours of travel time, where 116 minutes is the cycle time as calculated in Equation 12 and Table 16.
- At a peak headway of ten minutes, for each peak hour, six cycles will have been completed.
- During the six hours of peak periods (i.e., AM and PM peak periods, each with a three-hour duration), a total of 36 cycles will have been completed (6 cycles, times 6 hours equals 36 total cycles).
- During the 12 hours of off-peak periods (i.e., MID-DAY and OFF-PEAK periods, each with a six-hour duration), at a 20 minute headway, a total of 36 cycles will have been completed.
- Over an 18-hour operating day there will be 72 cycles (36 cycles, times two equals 72 cycles), or 72 times 1.93 train-hours.
- Assuming an operating year with a duration of 300 operating days, the total number of revenue vehicle-hours is calculated to be 41,688 train-hours per year (72 times 1.93 times 300).

8.4.7. Number of Annual Revenue Vehicle-Miles

- Each vehicle will complete 52 directional miles of travel per cycle.
- Following the process presented above, the number of vehicle-miles per year is calculated as 1,123,200 (72 times 52 times 300).
- For cost estimation purposes, each Kinkisharyo model LRTV with a maximum capacity of 150 passengers, has been assumed to be equivalent to two vehicles to be conservative.
- Thus, the total vehicle-miles per year is estimated to be 2,246,400, rounded to 2,250,000 (2 times 1,123,200).

8.4.8. Number of Peak LRT Vehicles

- In the previous section, the number of LRTV unit vehicles, required to provide 10 minute peak headways, was calculated as 11. After applying a 30 percent spare factor, however, this value increases to 15 vehicles.

- Using two combined unit LRTVs, the number of peak LRTVs is estimated as 30 (2 times 15 vehicles).

Thus, the annual O & M cost for the proposed system is estimated as (Equation 26):

$$AnnualCost(O\ \&\ M) = [4{,}157{,}759 * 1] + [101{,}888 * 52] + [120.89 * 41{,}688] + [3.36 * 2{,}250{,}000] + [131{,}048 * 30] \quad (26)$$

$$AnnualCost(O\ \&\ M) = \$25{,}987{,}037 / year$$

When adjusted for a 3% inflation above figure translate to $28,403,383/year or $546,228/mile/year in 2010

8.5. LRT Capital Cost

The capital cost of any rail system is likely to vary widely depending primarily on the cost of right away, the type, extent and quality of stations and the type of technology used in the vehicles and infrastructures. Table 25 shows cost of LRT construction per mile in 2010 after considering 3 percent inflation factor for various cities across US. It is observed that the equivalent cost per mile is around $50 million[3].

Table 25. Cost of LRT Construction by Various Cities [31]

CITY	TYPE OF CONS.	LENGTH (MILES)	YEAR OF CONS.	COST/MILE (MILLIONS)	ADJUSTMENT FACTOR (3% PER YEAR)	COST/MILE IN YEAR 2010 (MILLIONS)
Portland	Street	6	2004	63	1.194	75.225
San Diego	Street	4	1998	30	1.426	42.777
San Francisco	Street	2	1998	37	1.426	52.753
San Jose	Street	6	2004	54	1.194	64.479
Denver	Street	6	1994	21	1.605	33.699
Denver	Street	9	2000	22	1.344	29.566
San Jose	Street	8	1999	42	1.384	58.138
San Jose	Street	6	1988	25	1.916	47.903

[3]=∑((Cost/mile in year 2010 in million)*Length of mile)/∑(Length of miles)

9. SUMMARY

In the previous six sections of this report the research team has documented the (Detroit area) Woodward LRT case study, starting with a brief discussion of the background of transit in the region, and ending with a detailed operating cost analysis. A set of conclusions in the form of guidelines for sketch planning an LRT system (along a travel corridor in a metropolitan area), were developed and have been included in the executive summary. The sketch plan represents a synthesis of the case study that has been presented. The specific set of summaries for the case study are as follows:

- The scope of the study has been presented in the *Project Scope* of this report, along with a discussion of current planning efforts in the study area and travel demand estimates along the major corridors. Woodward Avenue has clearly been established as the major travel corridor (excluding Interstate freeways) in the study area.

- LRT travel demand along Woodward Avenue for a 26-mile corridor connecting the Detroit and Pontiac CBD's in a north-westerly direction has been established in *Ridership Analysis: Segment 2*. Total daily LRT demand, for Segments 1 & 2 combined, has been estimated at 21,437 passengers per day.

- A total of 26 LRT stations have been proposed along Woodward Avenue. Using multiple regression analysis, boarding and alighting estimates for each proposed station have been generated. Based upon the station "loadings," the daily LRT demand for the Woodward Ave. corridor is revised at 21,522 passengers per day. Using an assumed 300 day duration for an operating year, the annual ridership for the system is estimated to be 6.5 million passengers (*Corridor Study*). The MLS and corresponding PHD have also been established in this section.

- The operating parameters for the proposed LRT system have been investigated in section: *Corridor Study* of this report.

- The proposed LRT system requirements have been calculated in *LRT System Requirements*, along with: an analysis of operating parameters (e.g., LRTV travel speed, acceleration, deceleration, etc.), identification of a suitable LRTV manufacturer and model (Kinkisharyo), fleet size, headways, and commercial speed. Based upon a ten-minute peak headway, the required fleet size was calculated as 15 LRTVs.

- Operating cost estimates for the proposed system have been calculated in *Cost Estimation*, using the FAC cost method. Based upon a review of the current literature, the Gwinnett Village CID model, developed by HDR Inc., has been adopted for the proposed Woodward LRT system. The Gwinnett Village CID model is derived from parameters related to operating cost data compiled from nine peer LRT systems that have been constructed in the United States.

- For sketch planning purpose, the capital cost for the proposed LRT system is estimated at $50 million per mile.

10. REFERENCES

1. "Improving Transit in Southeast Michigan: A Framework for Action". Southeast Michigan Council of Governments (SEMCOG). Final Report. Detroit, MI: July 2001.

2. "Speed-Link: A Rapid Transit Option for Greater Detroit", prepared for the Metropolitan Coalition, by Transportation Management and Design, 2001.

3. Khasnabis, S., Opiela K.S., and Arbogast, R.G. "Feasibility Analysis for Joint development for Transit Stations in the Detroit Area", Final Report, Wayne State University, prepared for UMTA, USDOT, NTIS#PB 295-374/AS, 1978.

4. "Woodward Corridor Transit Alternative Study", prepared by the Detroit Transportation Corporation by IBI Group, 2000.

5. "Transit Operating Manual", prepared for PENNDOT by University of Pennsylvania, V.K, Vuchic, principal author, 1975.

6. Vuchic, V. "Urban Public Transportation Systems and Technology", Prentice Hall, 1981.

7. Illinois Department of Transportation (IDOT). *Elgin O'Hare West Bypass: Glossary of Terms.* Web. 10 May 2010. < http://www.elginohare-westbypass.org/portals/57ad7180-c5e7-49f5-b282-c6475cdb7ee7/EOHB_Glossary_of_Terms_v3.pdf>.

8. Southeast Michigan Council of Governments (SEMCOG). *SEMCOG General Assesmbley.* p.41. Detroit, MI: 22 Oct 2009. Web. 10 May 2010. < http://library.semcog.org/InmagicGenie/DocumentFolder/GA1009.pdf>

9. Detroit Department of Transportation (DDOT), Detroit Transit Options for Growth Study (DTOGS). DTOGS Study Results. Detroit, MI: Aug 2008. Web. 10 May 2010. <http://www.woodwardlightrail.com/StudyResults.html>.

10. Dutta, U.; et al. "A Quick Response Technique for Estimating Passenger Demand for LRT". University of Detroit Mercy, Wayne State University. Detroit, MI: 1 Aug 2009.

11. M1-RAIL. Web. 10 May 2010. < http://www.m-1rail.com/>

12. United States Department of Transportation (USDOT), Federal Highway Administration (FHWA). *Manual on Uniform Traffic Control Devices for Streets and Highways (MUTCD).* Washington, D.C.: 2003 version, amended.

13. Maryland Department of Transportation (MDOT). *About Transit-Oriented Development*. Office of Real Estate. Hanover, MD. Web. 24 June 2009. <http://www.mdot-realestate.org/tod.asp>.

14. Vuchic, V. *Transit Operating Manual*. Ch. 5: Operations. Pennsylvania Department of Transportation (PennDOT). 1978.

15. Khasnabis, S.; Reddy, G. V.; and Hoda, S.K. "Evaluating The Operating cost Consequences of Bus Pre-Emption" as an IVHS Strategy". Transportation Research Record No. 1390. pp. 3-9. National Research Council. 1993.

16. <http://en.wikipedia.org/wiki/Kinki_Sharyo>.

17. Dallas Area Rapid Transit (DART). *DART Rail Facts*. Dart.org. Dallas, TX: 23 June 2008. <http://www.dart.org/newsroom/dartrailfacts.asp>.

18. Mitsubishi Heavy Industries Limited. *First 100 Percent Domestic Low-Floor Tram*. Technical Review Vol. 43, No. 1. Jan 2006.

19. Lam, William H.K.; Cheung, C-Y; Lam, C.F. “A Study of Crowding Effects at the Hong Kong Light-Rail Stations”. The Hong Kong Polytechnic University, Department of Civil and Structural Engineering: Kowloon, Hong Kong. 8 April 1997.

20. "Fully Allocated Cost Plan" From Audited Expenses for the Fiscal Year Ending 30 June 2004. Adapted from United States Department of Transportation (USDOT). *Fully Allocated Cost Analysis*. Web: 29 April 2010. <http://www.ltd.org/pdf/finance/14%20-%20Fully%20Allocated%20Cost%20Plan%2007.pdf>.

21. Lem, L.L; Li, J.; and Wachs, M. "Comprehensive Transit Performance Indicators". UCTC No. 225, Working Paper. University of California Transportation Center. Berkeley, CA: July 1994.

22. Reilly, J.; Beimborn, E.; Schmitt, R. "Improving Transit System Performance: Using Information-Based Strategies". National Transit Institute (NTI), University of Wisconsin-Milwaukee (UWM). Milwaukee, WI: 1998. Web: 29 April 2010. <http://www4.uwm.edu/cuts/utp/cost.pdf>.

23. "METRO Solutions History". Metropolitan Transit Authority of Harris County, Texas. Houston, TX. Web: 3 June 2010. <http://www.piersystem.com/go/doc/1068/261812/>.

24. "University Corridor Draft: Environmental Impact Statement". METRO Solutions. Houston, TX: July 2007. Web: 20 May 2010. <www.piersystem.com/university_DEIS_volume>.

25. <http://en.wikipedia.org/wiki/Atlanta>.

26. “Forbes: Atlanta Traffic the Worst in America”. Atlanta Business Chronicle. Atlanta, GA: 1 May 2008. <http://atlanta.bizjournals.com/atlanta/stories/2008/04/28/daily97.html>.

27. “About the CID”. Gwinnett Village Community Improvement District. Norcross, GA. Web. 26 May 2010. <http://gwinnettvillage.com/index.php?option=com_content&task=view&id=171&Itemid=120>.

28. "I-85 Corridor LRT Feasibility Study: Phase , Final Report". Gwinnett Village Community Improvement District (CID). HDR Engineering Inc. Atlanta, GA: June 2009.

29. USDOT. *Fully Allocated Cost Analysis: Guideline for Public Transit Providers.* Washington, D.C.

30. Federal Transit Administration (FTA). *National Transit Database., 2008 Light Rail Data*. <http://www.ntdprogram.gov/ntdprogram/data.htm>.

31. Baum-Snow, N and Kahn, T “Effect of Urban Transit Expansions : Evidence from Sixteen Cities, 1970-2000” Brookings-Wharton Paper on Urban Affairs, 2005

11. APPENDICES

Table 1A. SEMCOG & URS Database: Detroit Options for Growth Study (DTOGS)

CORRIDOR	ROUTE NAME	EXISTING RIDERSHIP	2005 BASE	2030 BASE	2030 Gratiot				2030 Michigan				2030 Woodward			
					NO-BUILD	TSM	BRT	LRT	NO-BUILD	TSM	BRT	LRT	NO-BUILD	TSM	BRT	LRT
	DD34	6,900	7,700	6,500	6,700	6,300										
	DD76	600	200	100												
	SM510	2,900	3,900	4,000	4,000	4,000	4,000	3,900								
	SM530	200	100	100	100	100	100	100								
	SM560	5,700	4,900	4,800	4,900	4,900	5,500	5,600								
	SM580	100	400	200	200	200	200	200								
	DD34T	0	0	0	0	100	0	0								
	BRT Gratiot	0	0	0	0	0	8,200	0								
	LRT Gratiot	0	0	0	0	0	0	9,900								
GRATIOT	**CORRIDOR TOTAL**	**16,400**	**17,200**	**15,700**	**15,900**	**15,600**	**18,000**	**19,700**								
	DD37	1,400	1,600	1,800					2,400	700						
	SM200	2,700	3,100	3,300					3,200	3,200	3,300	3,300				
	DD37T	0	0	0					0	1,800	0	0				
	BRT Michigan	0	0	0					0	0	5,200	0				
	LRT Michigan	0	0	0					0	0	0	6,400				
MICHIGAN	**CORRIDOR TOTAL**	**4,100**	**4,700**	**5,100**					**5,600**	**5,700**	**8,500**	**9,700**				
	DD53	13,500	9,100	7,700									8,300	8,500		
	SM445	300	200	200									200	200	200	200
	SM450	4,800	3,700	3,800									3,800	3,900	3,900	3,800
	SM460	0	3,900	4,000									4,000	4,000	4,100	4,100
	SM465	300	300	300									300	300	200	200
	SM475	0	200	200									200	200	200	200
	SM495	2,300	2,900	2,800									2,800	2,800	3,100	3,200
	DD53T	0	0	0									0	100	0	0
	BRT Woodward	0	0	0									0	0	9,200	0
	LRT Woodward	0	0	0									0	0	0	**11,100**
WOODWARD	**CORRIDOR TOTAL**	**21,200**	**20,300**	**19,000**									**19,600**	**20,000**	**20,900**	**22,800**
TOTAL OF THREE CORRIDORS		**41,700**	**42,200**	**39,800**	**40,000**	**39,700**	**42,100**	**43,800**	**40,300**	**40,400**	**43,200**	**44,400**	**40,400**	**40,800**	**41,700**	**43,600**

Table 2A. Transit Ridership along Woodward Under Various Options

OPTIONS	**SEGMENT 1**		**SEGMENT 2**		**TOTAL**
	Bus	**LRT**	**Bus**	**LRT**	
No Build	8,300	X	11,300	X	19,600
LRT(Seg. 1) Bus (Seg. 2)	2,078	11,367	9,222	X	22,667
LRT (Seg. 1 & 2) (preliminary Estimate)	2,078	11,367	1,918	10,070	25,433
LRT (Seg. 1 & 2) Final Estimate)	2,078	11,367	1,918	10,155	25,518

12. List of Acronyms

ART	Arterial Rapid Transit
BRT	Bus Rapid Transit
CBD	Central Business District
CID	Community Improvement District
CRT	Commuter Rail Transit
DDOT	Detroit Department of Transportation
DPM	Detroit People Mover
DTC	Detroit Transportation Corporation
DTW	Detroit Metropolitan Airport
FAC	Fully-Allocated Cost
FTA	Federal Transit Administration
HOV	High-Occupancy Vehicle lanes
HRT	High Speed Rail Transit
LACMTA	Los Angeles County Metropolitan Transportation Authority
LRT	Light Rail Transit
LRTV	Light Rail Transit Vehicles
MARTA	Metropolitan Atlanta Rapid Transit Authority
MDOT	Michigan Department of Transportation
MLS	Maximum Loading Station
MSA	Metropolitan Statistical Area
MUTCD	Manual of Uniform Control Devices
O&M	Operation and Maintenance
PAC	Partially-Allocated Costs
PDD	Peak Directional Demand
PHD	Peak Hour Demand
PPD	Peak Period Demand
ROW	Right of Way
SEMCOG	Southeast Michigan Council of Governments
SEMTA	Southeast Michigan Transportation Authority
SMART	Suburban Mobility Authority for Regional Transportation
TAZ	Traffic Analysis Zone
TOD	Transit-Oriented Development

MICHIGAN OHIO UNIVERSITY TRANSPORTATION CENTER

Alternate energy and system mobility to stimulate economic development.

Report No: MIOH UTC TS15p1-2 2010-Final
MDOT Report No: RC1545

NEW APPROACH TO ENHANCE AND EVALUATE THE PERFORMANCE OF VEHICLE-INFRASTRUCTURE INTEGRATION AND ITS COMMUNICATION SYSTEMS

Final Report

Project Team

Nizar Al-Holou, Ph.D.
Utayba Mohammad
Baraa Alyusuf
Khaldoun Albarazi
Samer Fallouh
Mohamad Abdul-Hak
Rami Sabouni
Fadi Saadeh
Department of Electrical and Computer Engineering
University of Detroit Mercy
4001 W. McNichols Road
Detroit, MI 48221

Report No: MIOH UTC TS15p1-2 2010-Final

TS15, Series, Projects 1 & 2, September 2010
FINAL REPORT

Developed by: **Dr. Nizar Al-Holou**
Principal Investigator, UDM
alholoun@udmercy.edu

In conjunction with: **Prof. Utayba Mohammad**
UDM
mohammut@udmercy.edu

SPONSORS

This is a Michigan Ohio University Transportation Center project supported by the U.S. Department of Transportation, the Michigan Department of Transportation and the University of Detroit Mercy.

ACKNOWLEDGEMENT

This work was supported by the U.S. Department of Transportation through the University Transportation Center (UTC) program, MIOH, at the University of Detroit Mercy. Significant matching support was provided by the Michigan Department of Transportation, the Center for Automotive Research/Connected Vehicle Proving Center (CAR/CVPC) and UDM. The authors would like to express their sincere appreciation to the project sponsors for their support.

DISCLAIMERS

Technical Report Documentation Page

1. Report No. RC-1545	**2. Government Accession No.**	**3. MDOT Project Manager** Niles Annelin
4. Title and Subtitle Michigan Ohio University Transportation Center Subtitle: "New Approach to Enhance and Evaluate the Performance of Vehicle-Infrastructure Integration and its Communication Systems"		**5. Report Date** September 2010 **6. Performing Organization Code**
7. Author(s) Dr. Nizar Al-Holou Prof. Utayba Mohammad		**8. Performing Org. Report No.** MIOH UTC TS15 p1-2 2010-Final
9. Performing Organization Name and Address Michigan Ohio University Transportation Center University of Detroit Mercy, Detroit, MI 48221		**10. Work Unit No. (TRAIS)** **11. Contract No.** 2007-0538 **11(a). Authorization No.**
12. Sponsoring Agency Name and Address Michigan Department of Transportation Van Wagoner Building, 425 West Ottawa P. O. Box 30050, Lansing, Michigan 48909		**13. Type of Report & Period Covered** Research, January 2008 - September 2010 **14. Sponsoring Agency Code**

15. Supplementary Notes
Additional Sponsors: US DOT Research & Innovative Technology Administration and University of Detroit Mercy.

16. Abstract

MIOH UTC TS15 p1-2 2010-Final

Initial research studied the use of wireless local area networks (WLAN) protocols in Inter-Vehicle Communications (IVC) environments. The protocols' performance was evaluated in terms of measuring throughput, jitter time and delay time. This research has developed a unique setup to evaluate IEEE802.11 protocols. This setup will reduce the cost of test beds that might be deployed to evaluate the performance of new IEEE802.11 protocols. To validate the concept, researchers have implemented the test bed at University of Detroit Mercy and evaluated the performance of IEEE802.11b/g. The developed WLAN-based test bed allows the testing of different IEEE802.11 protocols and yet keeps the cost at a reasonable level. Researchers investigated the impact of Doppler shift on the quality of the transmitted/received signal in an Orthogonal Frequency Division Multiplexing (OFDM) communication system. The developed channel model that combines Additive White Gaussian Noise (AWGN) and Rayleigh channel representations to resemble a realistic transmission medium is presented. The model is validated by showing that the relation between Energy of Bit to Noise Ratio (E_b/N_0) and Bit Error Rate (BER) is consistent with theoretical formulas. The degradation in signal quality as a result of increased vehicle speed is presented through graphical and analytical representation of BER with respect of applied Doppler shift. Moreover, a new methodology to reduce the impact of Doppler shift is proposed and simulations are performed to confirm the reduction of Doppler shift impact on the signal quality.

17. Key Words Dedicated short range communications, Wireless communication systems, Intelligent transportation systems, Driver information systems, Intervehicle communications, Vehicle to vehicle communications, Test beds, and Research projects.	**18. Distribution Statement** No restrictions. This document is available to the public through the Michigan Department of Transportation.

19. Security Classification - report	**20. Security Classification - page**	**21. No. of Pages** 59	**22. Price**

Abstract

This report describes our contribution to the Intelligent Transportation System (ITS). A summary of our work vision, objectives and approach to build and deploy the UDM test bed is presented along with recommendations to enhance system performance.

Organization of the Final Report

The UDM research program final report is organized into five sections:

Section 1: Final Report: UDM Research, Executive Summary
This section provides an overview of the UDM research as well as brief background of ITS along with goals and objectives of our research. Moreover, this section illustrates the action plan of our research. This section does not provide the detailed test results. However, it is recommended for general managers of transportation agencies who are concerned with the overall vision of ITS.

Section 2: Final Report: UDM Research, WLAN Evaluation for IVC Application
This section shows the evaluation of using WLAN protocols in Inter-Vehicle Communication (IVC) environments. Moreover, it includes all technical information. This section is recommended for researchers, research-group leaders and research assistants who are concerned with the deployment of WLAN protocols in IVC environments.

Section 3: Final Report: UDM Research, UDM Test Bed
This section provides the details and results of the two approaches investigated in our research. UDM test bed and architecture, however, were described with the test bed component. Example of how to evaluate the performance of an IVC is also provided in this section. This section is recommended for researchers, research-group leaders and research assistants who are concerned with the deployment of the test bed concept to evaluate different IEEE802.11 protocols.

Section 4: Final Report: UDM Research, Doppler Shift Investigation
This section provides information on how Doppler shift can affect the performance of WLAN protocols in IVC environments. A new method to enhance the performance of these protocols for such a dynamic environment is presented as well. This section is recommended for researchers, research-group leaders and research assistants who are concerned with Doppler shift and its impact on performance.

Section 5: Final Report: UDM Research, Traffic Light Scenario Evaluation
This section evaluates traffic flow at intersections relative to number of nodes and communication metrics. A study is conducted to compare adaptive traffic light and fixed-time traffic light controllers to the number of vehicles. This section is recommended for researchers, research-group leaders and research assistants who are concerned with traffic light control systems and their impact on traffic flow.

Table of Contents

List of Tables

List of Figures

1. UDM Research, Executive Summary

1.1. UDM Research Overview

1.1.1. Executive Summary

With the rapid advances in wireless communication and the introduction of Dedicated Short-Range Communications (DSRC) as an enhanced protocol for Vehicular Ad hoc NETwork (VANET) communications, promising opportunities for increased vehicle safety and an enhanced driving experience are available. With opportunities, however, come numerous technical challenges. In order to investigate and overcome these challenges, we started our research with studying the use of wireless local area networks (WLAN) protocols in Inter-Vehicle Communications (IVC) environments. Moreover, the protocols' performance was evaluated in terms of measuring throughput, jitter time and delay time.

In our research, we have come up with a unique setup to evaluate IEEE802.11 protocols. This setup will reduce the cost of test beds that might be deployed to evaluate the performance of new IEEE802.11 protocols. In order to validate our concept, we have implemented the test bed at University of Detroit Mercy and evaluated the performance of IEEE802.11b/g. The developed WLAN-based test bed allowed us to test different IEEE802.11 protocols and yet keep the cost at a reasonable level.

Moreover, we investigate the impact of Doppler shift on the quality of the transmitted/received signal in an Orthogonal Frequency Division Multiplexing (OFDM) communication system. The developed channel model that combines Additive White Gaussian Noise (AWGN) and Rayleigh channel representations to resemble a realistic transmission medium is presented. The model is validated by showing that the relation between Energy of Bit to Noise Ratio (E_b/N_0) and Bit Error Rate (BER) is consistent with theoretical formulas. The degradation in signal quality as a result of increased vehicle speed is presented through graphical and analytical representation of BER with respect of applied Doppler shift. Moreover, a new methodology to reduce the impact of Doppler shift is proposed and simulations are performed to confirm the reduction of Doppler shift impact on the signal quality.

1.1.2. Background

In the United States, in 2003, there were 42,643 vehicle-related fatalities. Of these, 25,136 were a result of road departure, and 9,213 were intersection-related. The problem of highway deaths is a "national epidemic" and costs society $230.6 billion a year, about $820 per person [1]. Moreover, a traveler is more likely to die in a car than on an airplane, in a train or in a terrorist attack [2]. The question is: how can we use technology to create a safe and efficient highway system? Inter-Vehicle Communications (IVC) is a system that allows vehicles to communicate their data between each other and coordinate their maneuvers safely and smoothly. IVC is an example of intelligent transportation systems (ITS), which are a combination of intelligent vehicles and intelligent transportation infrastructure.

The U.S. Department of Transportation (USDOT) proposed ITS initiative: "ITS improves transportation safety and mobility and enhances productivity through the use of advanced information and communications technologies" [9].

Vehicle-Infrastructure Integration (VII) is an emerging IVC and ITS initiative aimed at creating communication links between vehicles (V2V) and between vehicles and the infrastructure (V2I). Traditional ITS technologies rely on infrastructure-based systems to collect and process data. However, VII systems enable vehicles to collect and communicate data to the infrastructure. Moreover, VII systems will allow drivers to receive communication regarding safety hazards and relevant travel information [3].

VII has three main components, as shown in Figure 1:

- On-Board Equipment (OBE), including all components that are installed in the vehicle. This equipment includes wireless subsystems to be able to communicate with other vehicles (V2V), and with infrastructure (V2I).
- Road Side Equipment (RSE), including the wireless subsystem to allow infrastructure and the Network Subsystem to communicate with vehicles.
- Network Subsystem that enables roadside units to communicate with each other and to access the Internet.

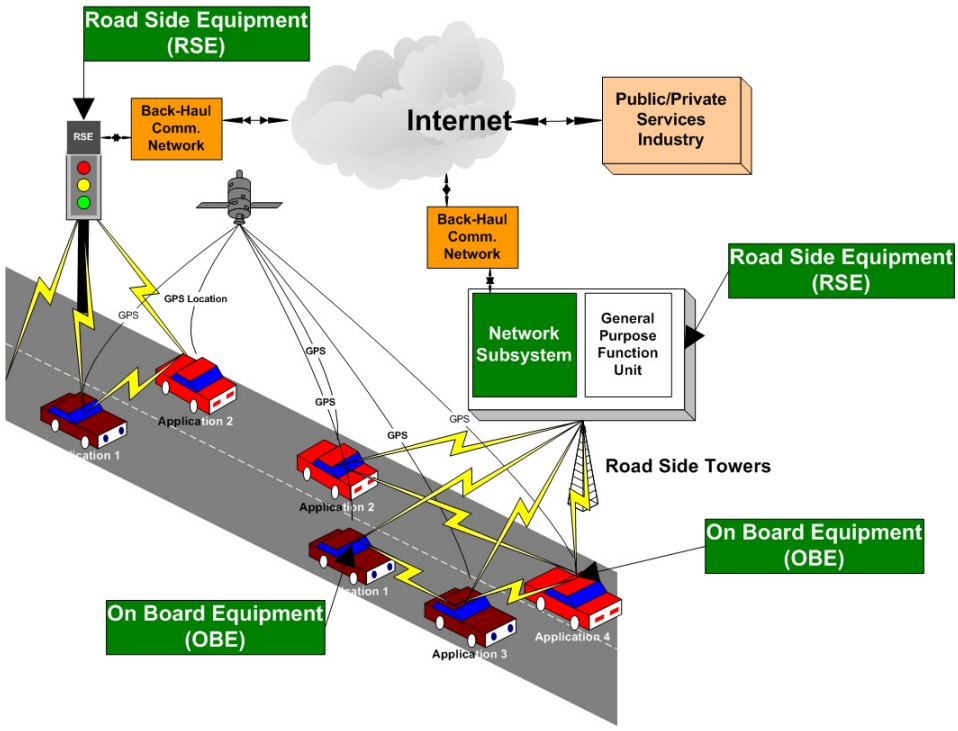

Figure 1. VII Consists of Three Interconnected Components

Graphic created by UDM Student Mahmoud Haidar

The ITS concept has received enormous attention all over the world especially in Japan, Europe, and the United States. In Japan, the ITS vision focuses on enhancing road safety, smoothing traffic, and being environmentally friendly [10]. ITS Japan deals with nine major areas in transportation including electronic toll collection, providing assistance for safe driving, improving the efficiency of the road management, supporting emergency vehicles, and supporting pedestrians. The goal is to achieve a transportation system of three traffic zones by the end of 2011. These zones are: a zero traffic fatalities zone, a zero traffic congestion zone, and a comfortable transportation experience zone [11].

In Europe, different approaches for ITS have been proposed and investigated. FleetNet and Drive-thru Internet are two of the main projects in Europe. FleetNet uses the ad-hoc concept to create a platform for IVC [12]. Its vision addresses safety and non-safety related applications and can be divided into three main categories: cooperative driver-assistance, local flouting car data, and communication and information services applications [13]. The Drive-Thru Internet project uses the infrastructure approach to provide distinct hot spots of WLAN connectivity for vehicles. However, this connectivity is planned to be a short life-time intermittent connectivity [14], which is achieved by creating so-called connectivity islands along the road. Drivers might slow down or stop by these spots to get the services they need [15].

In the process of developing an appropriate communication protocol for ITS, the DSRC was first proposed, in the unlicensed 902-928 MHz frequency range, to support electronic toll collection systems. However, in 1999, the Federal Communications Commission (FCC) assigned 75MHz bandwidth in the 5.9GHz band for DSRC to support ITS services and applications [16, 17, 18]. The ASTM group E17.51 then introduced the E2213 standard, based on the IEEE 802.11a [17, 19, 20], a standard that the FCC referenced as a base line for developing the DSRC protocol. Afterwards, IEEE initiated a new task group (TGP) and released a draft of IEEE 802.11p as their proposed standardized version of DSRC. Since all proposed solutions for DSRC are based on IEEE 802.11 standards, this paper evaluates the performance of two of the most commonly used protocols, IEEE 802.11b and g.

The IEEE 802.11 standards have two modes of operation: centralized (with infrastructure) and distributed/Ad-Hoc (without infrastructure) [17, 21, 22]. The centralized mode has two schemes with which to access the channel: a primary contention-based access scheme, called Distributed Coordination Function (DCF), and an optional contention-free scheme, called Point Coordination Function (PCF). On the other hand, the distributed mode has only one access scheme which is the DCF. DCF uses the Carrier Sense Multiple Access with Collision Avoidance (CSMA/CA) scheme. This means that every station (STA) has to sense the medium before transmitting any data-frame. If the channel was free for a minimum period of time, called Distributed InterFrame Space (DIFS), the STA gets access to the medium and starts sending its data. Otherwise, the STA goes through a back-off procedure. On the other hand, PCF is basically a round-robin scheduler scheme in which the PCF access point, usually called Point Coordinator (PC), polls all the stations in the network giving each one of them a contention-free time slot to send its data [23].

Two of the main challenges in DCF scheme are known as the hidden terminal and exposed terminal problems. Adding the Request-To-Send and Clear-To-Send (RTS/CTS) handshaking mechanism solves the hidden terminal problem, while adding the Data Send (DS) and Data Acknowledgment (ACK) confirmation messages solves the exposed terminal problem [21]. However, these approaches create other problems in VANET applications, such as increasing the overhead of any message, increasing the delay before transmission, and extending the range of blocked terminals [24].

Although IEEE 802.11, based standards deploy similar MAC protocols, they differ in the other physical layer's details such as operating frequencies and modulation schemes. IEEE 802.11a operates in the 5.18-5.825 GHz band, which is close to the DSRC band (5.85-5.925 GHz). Although both standards use Orthogonal Frequency Division Multiplexing (OFDM) technology, DSRC has a maximum data rate of 27 Mbps whereas IEEE 802.11a reaches a maximum bit-rate of 54Mbps. DSRC reduces the channel bandwidth to 10 MHz to reduce the impact of multipath propagation and Doppler shift effects. Moreover, DSRC adds four maximum allowable Effective Isotropic Radiated Power (EIRP) levels to extend its communication range [20]. IEEE 802.11g uses the OFDM technology with a maximum bit-rate of 54Mbps, while IEEE 802.11b uses the Direct Sequence Spread Spectrum (DSSS) technology with a maximum bit-rate of 11Mbps [25]. Both IEEE 802.11b/g operate in the 2.4 GHz ISM unlicensed band, which causes performance degradation when both co-exist.

The effects of different vehicular traffic and mobility scenarios on WLAN performance were studied in [18, 26, 27, 28, 29]. The results in [19] show that under suitable driving conditions, a 1000 m connectivity range can be achieved with IEEE 802.11b; keeping in mind that vehicles' relative speed heavily affects the connection performance. Other research groups showed that using external antennas mounted on the roof of each vehicle extends the Line of Sight (LOS) and improves signal strength [18]. Accordingly, the vehicle speed becomes less important as long as it is less than 180 Km/h and LOS is available.
The multipath propagation effect creates areas of extremely low signal strength, so-called null zones, where the signal cannot be sensed most of the time, and the network throughput suffers significant degradation [27].

Wireless channels with multipath propagation effect are usually described using the Rayleigh fading model. Although vehicular environments suffer from this effect, many other factors contribute to the channel mode. Therefore, many researchers tried to model the channel under different conditions for both V2V and V2I situations, and for single-hop and multiple-hop communication scenarios [28, 29]. The results showed that the performance of single-hop communication depends largely on the distance between vehicles. Once the single-hop communication between vehicles attains a poor connection because of large distance, multiple-hop communication becomes an alternative path that enhances connection performance.

1.1.3. The Vision

VII has many applications; however, our research focuses on those related to a traffic control system [4, 5]. It formulates some vehicle-to-vehicle and vehicle-to-infrastructure communication scenarios and develops a test bed platform to evaluate the network characteristics necessary to service such applications. We envision the project to be of two stages:

- The first stage of the project was defining the test bed requirements, capabilities and constraints, and then building the test bed and using it in the second stage of the project. IEEE 802.11p protocol is being developed for IVC networks, and is still a draft protocol [6]. Therefore, creating a generic test bed that can be used to evaluate the IVC performance for different IEEE 802.11-based protocols is an important task.

  The IEEE 802.11 protocols family uses Carrier Sense Multiple Access/Collision Avoidance (CSMA/CA) technique to access the medium [7]. In CSMA/CA, nodes within the transmission range of each other contend for the medium, and only one node wins it at a time, while others back off randomly, and contend for the medium later. In real life, we have many nodes, vehicles and infrastructure, communicating with each other using 802.11x protocols, hence, making the contention process of a serious impact on the network communications' metrics such as packet delay, throughput, network connectivity…etc. From this perspective, there is a need to develop a test bed that reflects the real life communications. However, it is impossible to bring as many nodes in the test bed as there would be in a real-life scenario, due to high cost. This research envisions a low- cost realistic test bed that allows for testing the different emerging protocols for vehicular applications. Figure 2 illustrates how dense the IVC environment could be, and thereby highlights the need for a representative test bed.

Figure 2. A Busy Highway Merge Section that Gives an Idea of How Dense an IVC Environment Could Be

- The second stage was to investigate the communication characteristics necessary to allow VII to help prevent a running a red traffic-light scenario at a traffic light intersection. Running a red traffic light is a common behavior and a major source of accidents at traffic intersections. Drivers run a red traffic-light for three reasons. First, they misjudge the vehicle's speed, i.e., the driver tries to run the yellow light, speeds up, and cannot stop when the light switches to red. Second, the driver is distracted, i.e., the driver does not pay attention to the light because he or she is distracted with a different task. Third, the driver intentionally runs the red light, i.e., violates the traffic laws on purpose. VII can be helpful in solving all three of these problems. With VII, the vehicle periodically reports its speed and position to the roadside equipment (RSE). The RSE, in turn, periodically reports the traffic-light schedule, such as current traffic light status, when the light will turn to yellow, and when the light will turn to red. The vehicle then can calculate whether it has to decelerate to stop before the light goes red, accelerate to avoid crossing the red light if a stop cannot be performed with the current speed, or warn the driver of an impending traffic-light violation. The implementation of this interaction can go further; a first stage would be an interactive warning system to alert the driver of the traffic light status and advise the proper action. A second stage would be to automate the vehicle reaction at some point and override the driver's control (i.e., prohibit the driver from running a red light). Moreover, in the case of sensing a traffic light potential violation, the RSE can adjust the other traffic-light schedules at the intersection so that it prevents other vehicles from colliding with the errant vehicle. In this case, the errant vehicle will still be violating the law by running a red light, but other vehicles will not be allowed to continue driving until the road is clear. Figure 3 shows the data flow block diagram for the traffic-light scenario.

Looking at the investigated problems as isolated scenarios simplifies them to some extent. The traffic-light scenario, however, is part of an overall system and its communication demands will be allocated from the overall system resources; therefore, challenges must be overcome for this scenario to be tenable. The next section highlights some of the challenges related to implementing VII and IVC systems and addresses those that we will explore in our research.

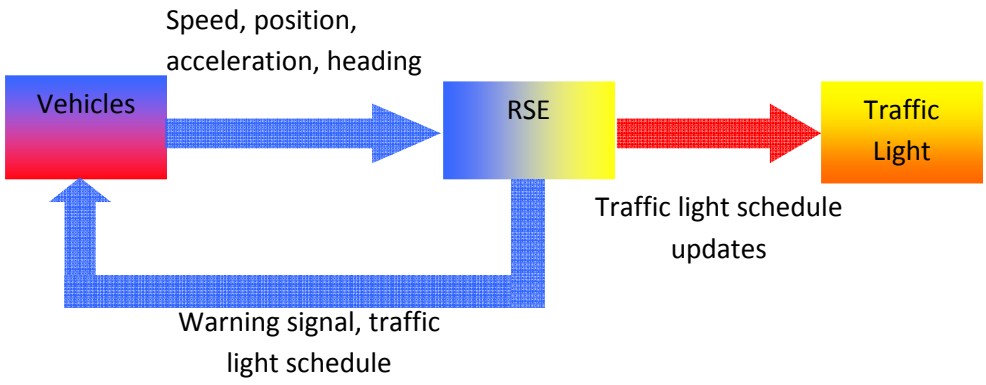

Figure 3. Data Flow Diagram for an ITS Traffic Light Scenario

1.1.4. Objectives of the Work

The purpose of this research was to develop new methodologies that would provide low delay and high throughput. The activities that will be performed as a part of the research are as follows:

1. Develop a Wi-Fi-based test bed for inter-vehicle communication
2. Evaluate the emerging wireless protocols using the developed test bed
3. Evaluate different traffic light scenarios and their impact on communication characteristics
4. Investigate Doppler shift effect on the inter-vehicle communication and possible solutions that would alleviate the problems

1.2. Support of Objectives to MDOT

Our research addresses many of the concerns and priorities of both the USDOT and the Michigan Department of Transportation (MDOT). Both agencies seek a safer road and highway environment with fewer fatal crashes and less unexpected delay due to incidents and non-recurrent congestion. The work proposed here contributes to faster and more effective VII systems that reduce the risk and occurrence of crashes, thereby saving lives and reducing delay. An efficient VII system is expected to improve highway efficiency and reduce unexpected delay and the potential for crashes at a lower cost than is achievable by additional roadway construction. Furthermore, adding additional lanes to roadways is not always possible or feasible due to the lack of land availability, environmental concerns, citizen opposition and financial concerns. Therefore, VII promises to be a viable alternative solution to safety and travel delay problems. The success of VII in Michigan also may help build a VII industry in the state and assist other states in understanding the positive impact of the system on our congested arterial roadway network.

1.3. Action Plan for Research

Task 1: Perform a literature and technology survey to investigate what has been done in the inter-vehicle communication field.

Task 2: Develop a generic test bed that forms a foundation to evaluate wireless technologies (i.e. 802.11x) for inter-vehicle communications.

Task 3: Perform intensive measurements in the test bed to evaluate different performance metrics such as bit error rate (BER), Packet Error Rate (PER) and Packet Delay.

Task 4: Evaluate the communication metrics in our test bed when using one node to load the channel with constant bit rate packets while the others communicate useful data among themselves.

Task 5: Evaluate inter-vehicle communications performance with the help of additional Wi-Fi transceivers. The Wi-Fi nodes will emulate the contention of the medium.

Task 6: Equip the test bed with new wireless technology that has been used recently for inter-vehicle communication such as 802.11n and 802.11p (DSRC).

Task 7: Compare the recent technology performance with the Wi-Fi performance in outdoor environments.

Task 8: Simulate the traffic-light scenario using a network simulator, such as, NS-2, VIILAB …etc.

Task 9: Validate the traffic-light scenario for different number of moving vehicles.

Task 10: Study the Doppler Shift effect encountered in the outdoor high-speed vehicle environment.

2. UDM Research, WLAN Evaluation for IVC Application

2.1. Introduction

With the rapid development of the Intelligent Transportation System, Vehicular Ad-Hoc Networks (VANET) have gained significant importance in the research community. VANET deploys the concept of infrastructureless (ad-hoc) networks in the ITS environment, thereby enabling Vehicle-to-Vehicle (V2V) and Vehicle-to-Road Side Unit (V2R) communications. Still, many issues need to be studied when building VANET, such as mobility, range, bit-rate, security and Doppler shift effect. IEEE 802.11 standard protocols have the potential to serve VANET. However, they were not designed to operate in highly dynamic outdoor environments, such as ITS. Therefore, an extensive evaluation of the IEEE 802.11 family is necessary to reveal its pros and cons. This section shows the results of the tasks of the first year in our research. During the first year our research concentrated on evaluating the performance of the use of IEEE 802.11b/g protocols in Inter-Vehicle Communications (IVC). The evaluation was conducted in terms of measuring time-to-login to the network, range, throughput and jitter time.

2.2. Performance Metrics

In order to evaluate the protocol adequacy for ITS applications, we evaluate its communication range, time-to-login to a network, throughput, jitter time, delay time, and the impact of passive vehicles on the protocol performance.

We define the communication range as the maximum distance a WLAN signal can travel and still be successfully received at the destination, or the distance beyond which the connection between two communicating devices will be lost. The time-to-login is the time needed by a node to join a network, which includes the discovery time, authentication time and association time.
To avoid confusion, we define performance metrics such as data rate, throughput and goodput. The main difference among these performance metrics is that they relate to different OSI layers. The data rate represents the transmitted/received bit rate at the physical layer. The throughput represents the bit rate at the TCP layer with the IP/data link headers. Finally, the goodput measures the bit rate at the application layer. For example, if a 5 Mbyte file takes 5 seconds to be sent over the network, the goodput will be reported as 1 Mbps. Clearly, the goodput is less than the throughput, which is less than the data rate, primarily because each layer adds its own header. Telecommunication engineers usually consider average throughput value and average goodput value, whereas maximum values are considered when talking about data rate. For example, IEEE 802.11b has a data rate of 11 Mbps and the throughput is less than 11 Mbps. Throughput is not fixed in WLAN, and its value is affected by different parameters such as the number of users on the network, the propagation and latency [22]. Obviously, this creates a need for multiple data rate values, which is the case in all WiFi protocols.

To evaluate the protocol ability to serve real-time communication, we measure two timing values: the jitter time and the delay time. The jitter time is the variations in arrival times of periodically sent packets. When a transmitter sends packets periodically, the arrival time of these packets, at the receiver, is expected to follow the same period. However, the arrival time may deviate from its expected value because of channel congestion, and packets may even be received out of order. On the other hand, the delay time is the time between transmitting the packet and receiving it successfully at the destination.

The number of passive vehicles is the number of vehicles that exist in the test field, which are not sending or receiving any data on the wireless channel. The number of vehicles on roads affects the characteristics of wireless channel for vehicular environments even if they are not functioning as transceivers. The known reason for this is the multipath propagation problem that might be represented in the Rayleigh model. However, the Rayleigh model does not fully describe the behavior vehicular environments.

Throughout this task, Windows XP-based laptops and desktops were used. IEEE 802.11b/g were evaluated using both internal and external-USB wireless cards in each machine. To evaluate different protocols in ITS applications, we used the following performance metrics, communication range, time-to-login, and throughput and jitter-time measurements.

The tests were done using four laptops (nodes) running Windows XP. Three laptops were equipped with external and internal WiFi cards. The external cards have IEEE 802.11b/g/n capabilities (Linksys WUSB600N); whereas the internal cards only have IEEE 802.11b/g capabilities. One of the laptops was set up as a sniffer and/or a Signal to Noise Ratio (SNR) tester. A high accuracy DGPS receiver (Novatel ProPak-LBplus) was used to track the distance between nodes so we were able to measure the communication range. Kperf, Wireshark and NetStumbler are the software tools that were used for measuring throughput, sniffing the wireless channel and performing the SNR measurement respectively. Figure 4 depicts the basic setup of the network in both indoor and outdoor environments. The following subsections will show the setup and then will discuss the results for each measurement.

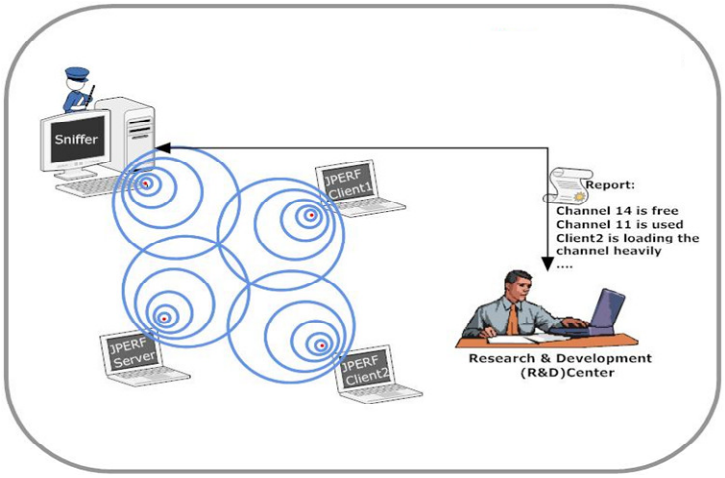

Figure 4. Basic Setup of the Network Used for Performance Evaluation

2.3. IEEE 802.11b/g Communication Range

The communication range is the maximum distance that vehicles can communicate with each other, regardless of the throughput at that distance. This experiment was conducted using two vehicles. One of the vehicles is moving and the other one is stationary. Both vehicles were equipped with laptops. The laptop in the moving vehicle was equipped with a DGPS receiver. The two laptops were communicating with each other. The connection was monitored to determine the distance between vehicles at which the connection was lost. The theoretical and measured values of the connection range of IEEE 802.11b/g standards are compared in Table 1.

For the internal network adapters, the IEEE 802.11b and IEEE 802.11g connections were lost when the communication range became more than 82.85 m and 154.06 m respectively. The communication range was considerably extended to 190.67 m and 251.3 m when using the external adapters.

The communication range plays an important role in determining the availability time and the connectivity time. The availability time is how long the vehicle is going to stay within the communication range, while the connectivity time is how long the vehicle takes to discover the network, establish connection, transfer data and finally terminate the connection. It is good to notice that the availability time changes according to the vehicle speed. As a rule of thumb, the connectivity time has to be less than the availability time. Table 1 shows the communication range values and Table 2 shows the corresponding availability time values for different vehicle speeds. 70 mph was considered as speed limit on highways, whereas 140 mph is the maximum relative speed between two vehicles driving in opposite directions on a highway.

Table 1. Expected VS Experimental Ranges of IEEE802.11b/g

Protocol	Communication Range		
	Expected (theoretical)	Experimental External WiFi adapters	Experimental Internal WiFi adapters
802.11b	~140 Meters	190.67 Meters	82.85 Meters
802.11g	~140 Meters	251.31 Meters	154.06 Meters

Table 2. Availability Time for Different Vehicle Speeds

Speed	IEEE 802.11b		IEEE 802.11g	
	External card	Internal card	External card	Internal card
45 MPH	18.96sec	8.24sec	25sec	15.32sec
65 MPH	13.12sec	5.7sec	17.3sec	10.6sec
70 MPH	12.2sec	5.3sec	16sec	9.9sec
140MPH	6.4 sec	2.65sec	8sec	4.95sec

2.4. Time-to-Login to the Network

To join a WiFi network, a vehicle has to go through an authentication process. During this process, Delay is introduced from all the network stack layers, including: the physical layer queuing, transmission and propagation times; MAC layer delays involving RTS/CTS/ACK handshake; and the network layer association and authentication handshake. After a successful association, the vehicle will be identified on the network by its IP address.

In this experiment, three laptops were used, and a peer-to-peer network was set up between two of them. The third laptop tried to join the network, and the time to join the network was measured. This scenario represents a vehicle that is trying to join other vehicles' network on the highway. WireShark, which is a network protocol analyzer developed by an international team of networking experts [31], was used to monitor the traffic on the network and to measure the third laptop's time-to-login to the network.

The effect of channel loading on both network performance and time-to-login was evaluated by increasing the traffic on the network. The software tool that was used for evaluating the network performance is Kperf. It is an open-source software developed by the University of Illinois in Champaign [32] as a modern tool to measure TCP/UDP performance. This tool is also capable of generating UDP traffic to increase the traffic on the network, and we used this feature to load the wireless channel.

The time-to-login was measured for both static and dynamic IP address allocations, In the static IP allocation method, the network administrator has to manually assign IP addresses to the PCs, while in the dynamic method, the Dynamic Host Configuration Protocol (DHCP) assigns IP addresses to devices that join the network. Figure 5 shows the average values for static and dynamic IP address allocation.

Measurements show that a vehicle took an average of 62.3 sec to join the network when DHCP was used, which is a very long time from a VANET perspective. On the other hand, it took 1.4 sec on average when static IP addresses were used.

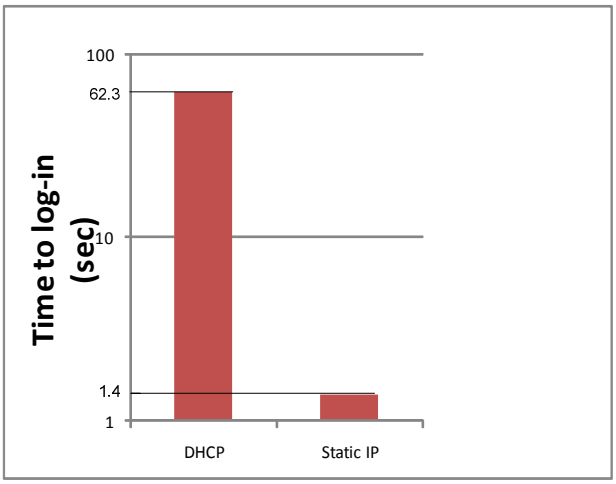

Figure 5. Shows the Time-to-Login for Static and Dynamic IP

3. UDM Research, UDM Test Bed

3.1. Introduction

IEEE802.11p amendment was only approved on Jan 17, 2010. Therefore, the cost of DSRC products available in the market is still very high. As of 2010 there were three major suppliers for DSRC terminals: DENSO, TechnoCom and Mark-IV and the access to their products is still limited. Table 3 shows the price range and availability of some DSRC products.

Table 3. DSRC Market Availability and Prices in 2008-2009

Manufacturer	Cost	Notes
TechnoCom	$28,000	Too expensive
Mark-IV	$4,500	Not for sale
DENSO	N/A	Not available

Because of the high cost and limit access to DSRC products, there has been a need for a low-cost test bed in order to evaluate the different IEEE802.11 protocols including 802.11p in vehicular and laboratory environments.

We came up with two methodologies to set up a low-cost test bed that can be used to evaluate different WLAN protocols.

3.2. Test Bed Concepts

3.2.1. First Method

In this method the network scalability test is addressed. To study the effect of having many vehicles in a road segment on the performance of different MAC/PHY protocols, a large number of nodes is needed. However, we can use fewer nodes as long as those nodes compensate for the absence of the rest of the nodes. In other words, instead of having 100 nodes - two of them are communicating useful data and the rest are loading the channel with 100kbps traffic - we can use only half of that number, i.e. 50 nodes, with double the traffic load that will be 200kbps in our example. Therefore, 50 nodes can compensate for 100 nodes if they generate double the traffic.

We can keep decreasing the number of nodes while increasing the traffic they generate until we reach a network of three (3) nodes. Two of these three nodes are communicating useful data with each other, while the third one is loading the network with different traffic data. This approach significantly cut the cost of setting up the network.

The aforementioned concept was tested and validated in the “first-method test bed”. This test bed consists of four (4) nodes running Windows XP, configured to work in Peer-to-Peer mode as well as infrastructure mode. Any node is ready to communicate with other nodes or to load the network with TCP/UDP traffic. One (1) of the nodes is capable of sniffing the traffic on wireless medium and listing the used channels. The figures 6 through 8 below show the first proposed approach.

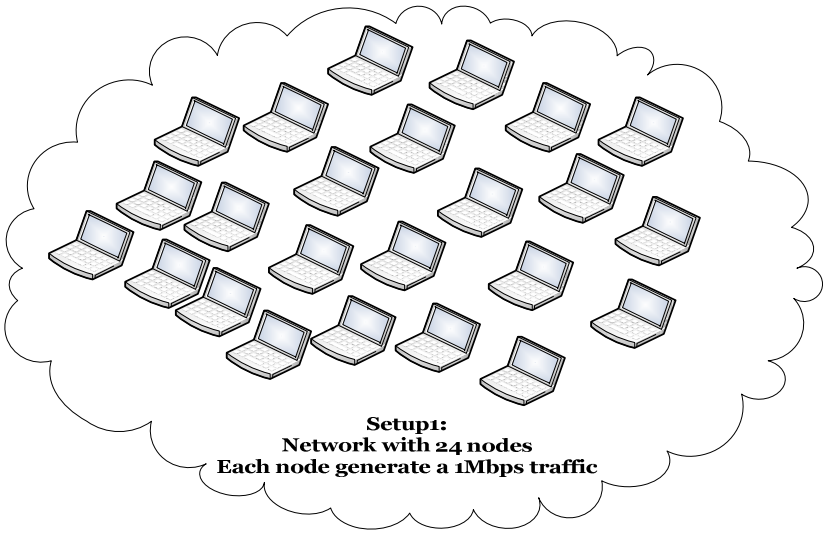

Figure 6. Network with 24 Nodes

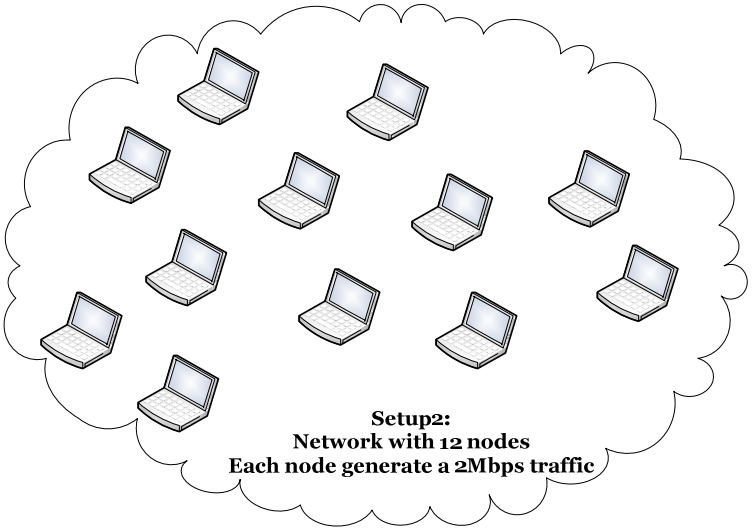

Figure 7. Network with 12 Nodes

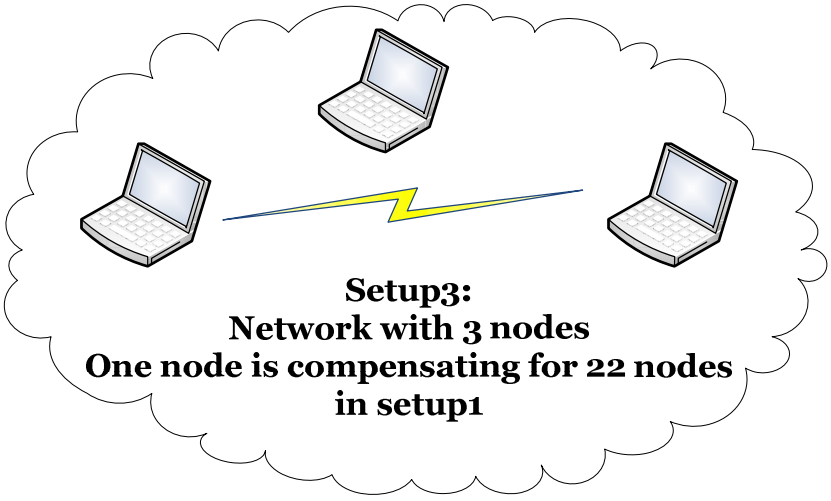

Figure 8. Network with only 3 Nodes

3.2.2. First Method Evaluation

In order to evaluate the validity of this method, we compare the performance of the network when using one node to load the channel with the performance of the network when using multiple nodes to load the channel. i.e. we compare the network throughput, jitter time, and delay time for a single loading node vs. many loading nodes and for the same loading volume.

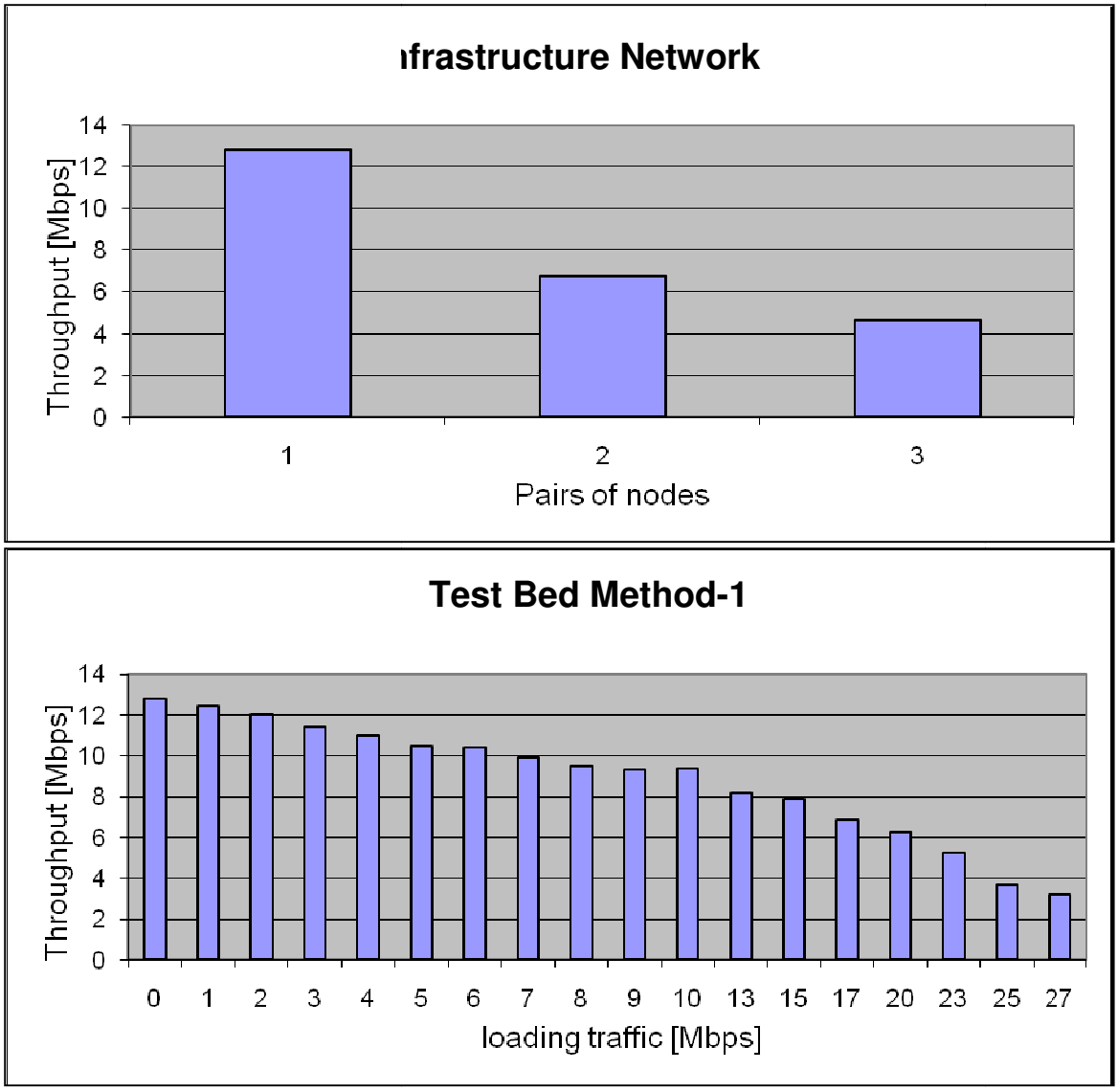

Figure 9. Throughput in a Regular Network VS. One Node Loading the Channel

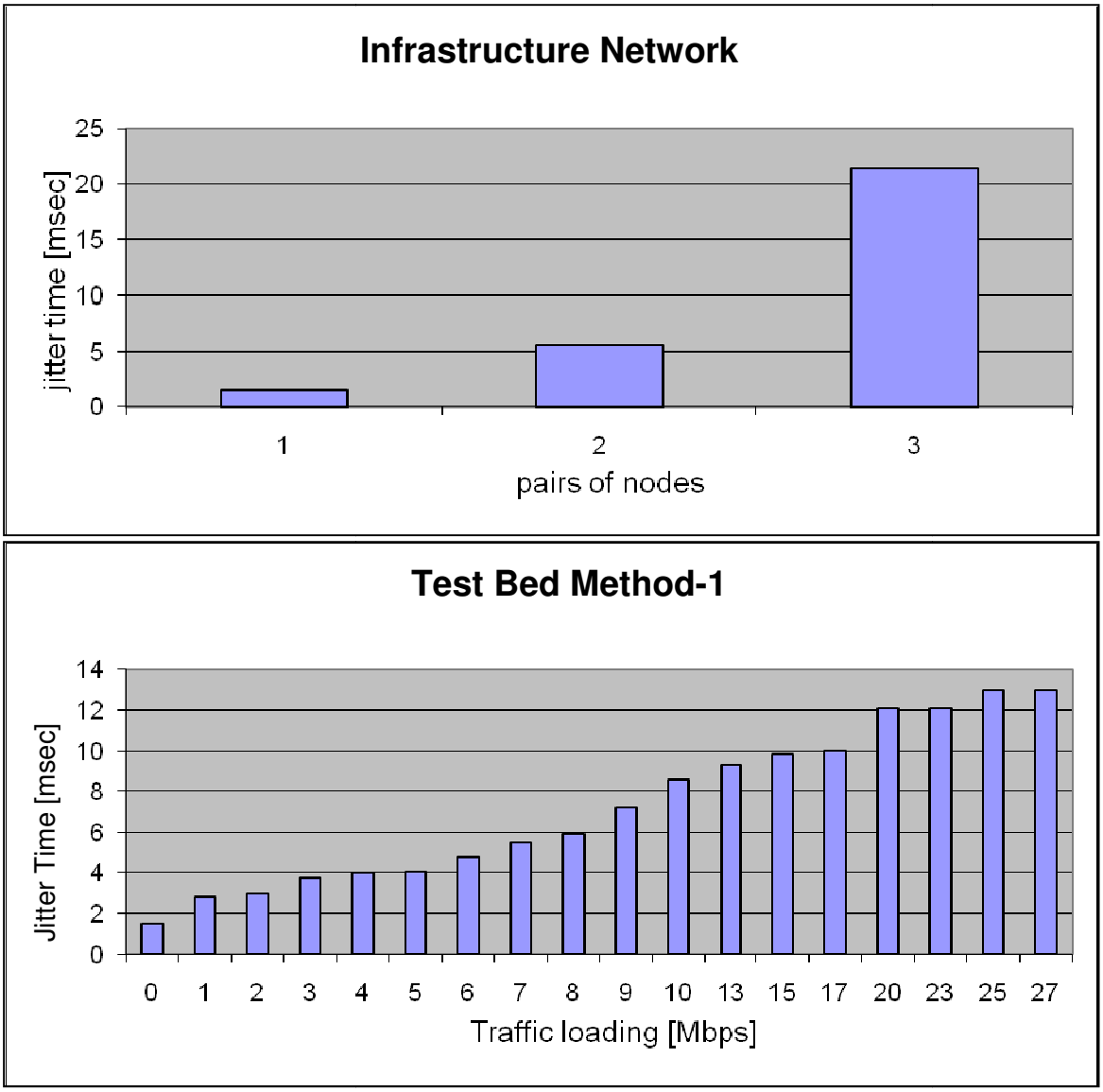

Figure 10. Jitter Time in Regular Network VS. One Node Loading the Channel

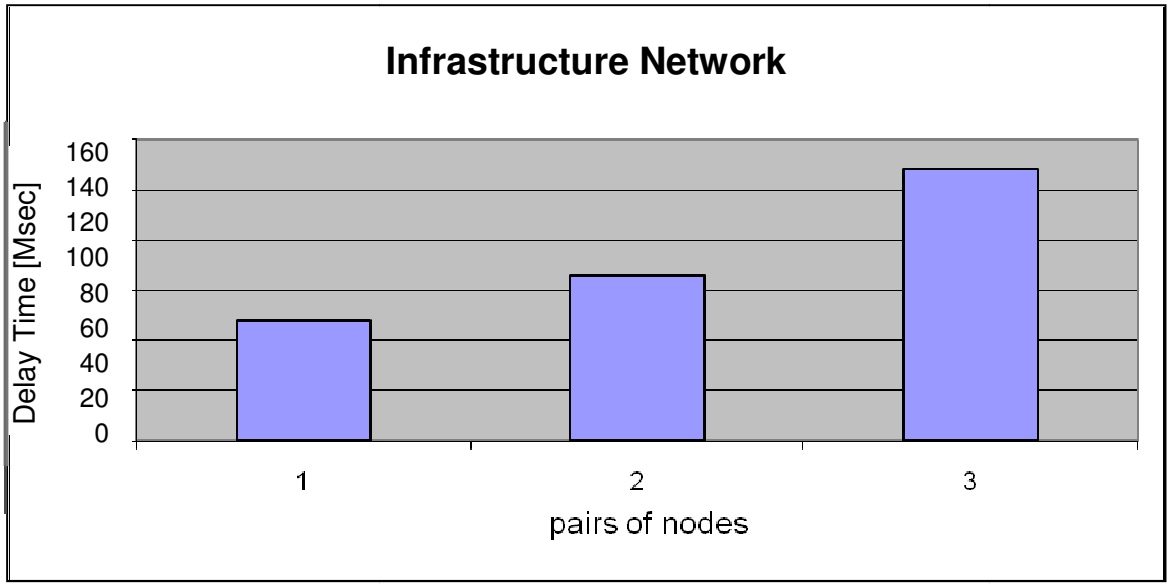

Figure 11. Delay Time in Regular Network VS. One Node Loading the Channel

The results above show that one node may not be used to compensate for the existence of other nodes in the network. That is mainly because of losing the randomness in accessing the channel when using one node for loading. When using one node for loading, it would compete to access the channel only at the beginning of its transmission and when it got access it would dominate. That is, once the node got access to the channel, no other nodes would be able to access the channel. Therefore, other methodologies are needed.

3.2.3. Second Method

In this method, the number of nodes could be kept relatively high, but instead of using high cost new technology nodes, we will use the low-cost popular Wi-Fi transceivers. The Wi-Fi network will serve as a realistic mirror network to reflect the contention process. However, a few nodes of the mirror network are wired directly to a high tech protocol transceiver (under evaluation), and we call these nodes "active nodes" versus those that only work to load the network and hence are called "passive nodes." Once an active node gets access to the channel, it forwards its message to the attached high tech transceiver, which in turn performs the communication. Hence, the new protocols will be evaluated in a more realistic environment at a low cost. Figure 12 depicts the proposed test bed layout.

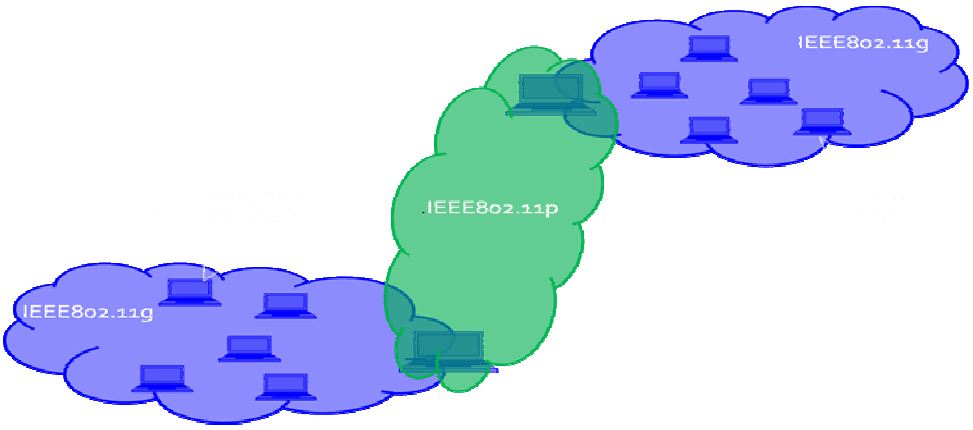

Figure 12. Test Bed Setup

In other words, the main idea behind this method is splitting the large expensive network into two low-cost subnets, which are bridged together using one expensive connection (802.11P).
We implemented this method using two access points, wireless router and three nodes running Windows XP, which is called second-method test bed. Figure 13 shows the network setup where PC_A communicates with PC_B through the access points and the router. PC_C is the one that loads the channel with traffic, thus reflecting the channel contention in the network.

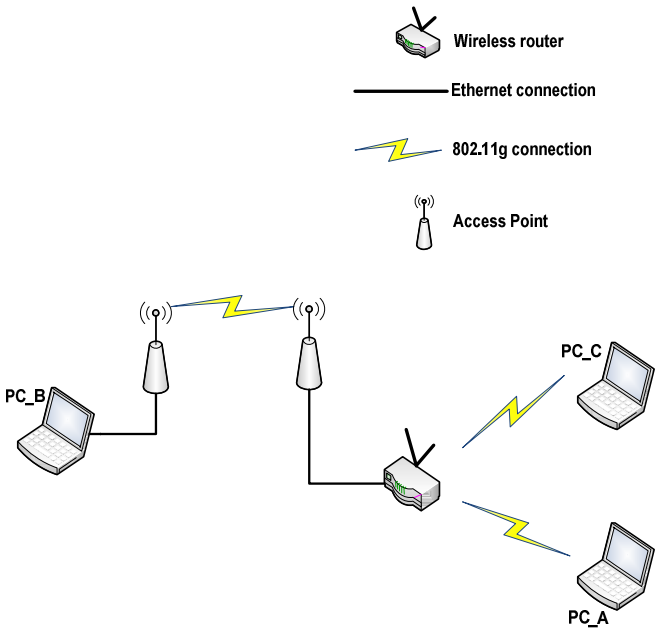

Figure 13. Test Bed Implementation

3.2.4. Second Method Validation

In our research, we have been trying to come up with a new setup to reduce the cost of the test bed needed for evaluation purposes. We have come up with two setups (mentioned in task2); the result of the first setup will be discussed in tasks4 and task5. However, here we will discuss the results of the second approach. As shown in Figures 12 and 13, we split the network into two sub-networks by using two access points, one wireless router and PCs equipped with Wi-Fi transceiver.

In order to validate the concept, we measured the throughput, jitter time and delay time of two network setups. The first setup was one large IEEE802.11g network with a different number of nodes. The second setup was two IEEE802.11g sub-networks bridged with an IEEE802.11g connection. The same two setups, with different protocol IEEE802.11b, were also built and the results ensure that the test bed concept is valid and can be used for evaluation purposes. Figures 14, 15 and 16 show the throughput, jitter time and delay time measurements for the two setups for IEEE802.11g.

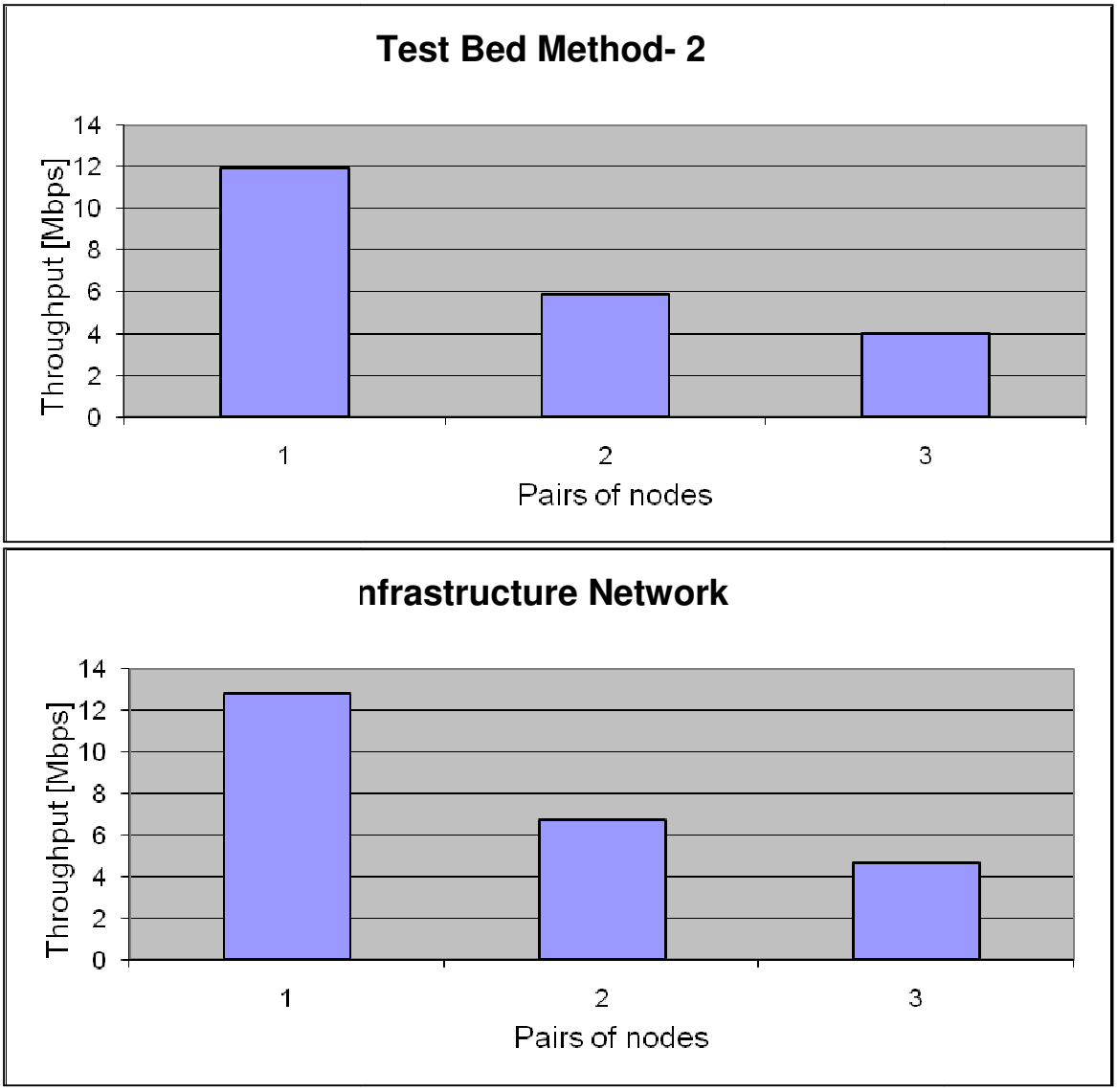

Figure 14. Throughput of IEEE802.11g in Infrastructure-Based Network VS. Test Bed

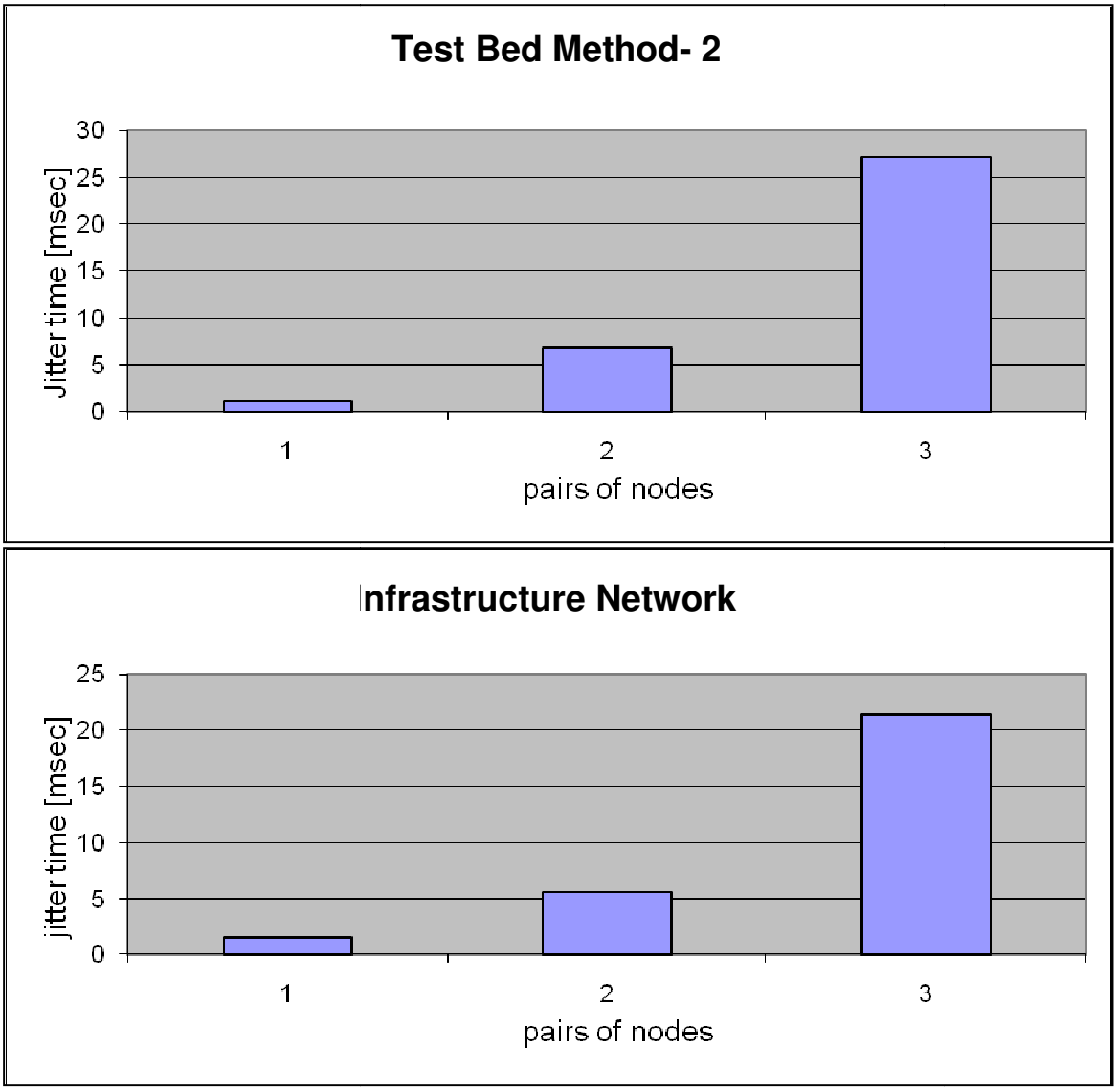

Figure 15. Jitter Time for IEEE802.11g in Infrastructure-Based Network VS. Test Bed

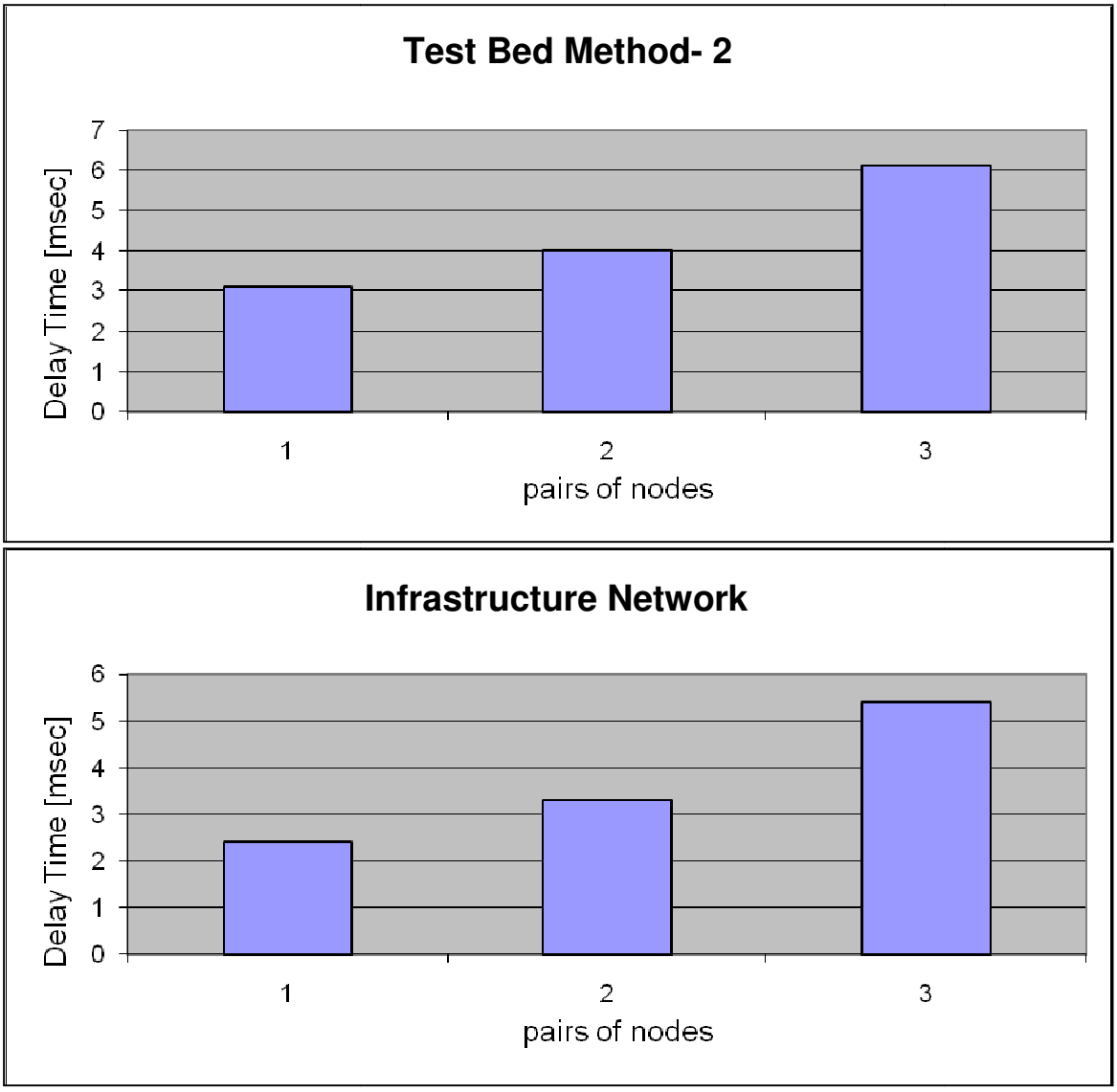

Figure 16. Delay Time in IEEE802.11g in Infrastructure-Based Network VS. Test Bed

3.2.5. Third Method

The last employed method in our test bed was developed to study the impact of distance between vehicles on channel throughput. Therefore, an experiment was designed to be able to acquire data samples from a real-world scenario.

The experiment took a place in the racing track in Michigan. It consisted of:

1. Roadside Unit: laptop running Mac OS placed at a stationary location (Unit A).
2. On-Board Unit: laptop running Windows XP placed in a mobile vehicle (Unit B).
3. Communication Links: Wireless access point to provide Wi-Fi communication and Differential Global Positioning System (DGPS) to provide position of the vehicle.

The following is a summary of the experiment:

1. RSU setup:
    - Unit A is running Jperf to generate random TCP packets
    - Unit A's GPS position is recorded and considered as a reference point
    - Unit A is connected to a wireless module via Ethernet cable which allows it to broadcast generated packets wirelessly
    - Wireless module operates on 802.11g and has large coverage

2. OBU setup:
    - Unit B is equipped with wireless network interface card to receive broadcasted TCP packets
    - Unit B is running Jperf to keep track of received packets and measure the channel throughput
    - Jperf is configured to record samples of channel throughput every time interval
    - Unit B is connected to a DGPS module via USB cable to obtain a precise position of moving vehicle
    - Unit B is running MATLAB program to record samples of vehicle position and calculate the distance from the reference point for every time interval as configured in Jperf

As a result, at each time interval we had a sample of channel throughput and a sample of the vehicle's distance from the RSU. Collected data were organized in a table format to match each throughput sample with its corresponding distance sample. The same experiment was repeated four times with the same maximum distance. Consequently, averaging of throughput samples at a specific distance was taken to obtain higher accuracy. Figure 17 shows results plot where channel throughput is a function of relative distance where the throughput is measured in Mbps and the distance is measured in meters.

A quick look at Figure 16 shows that the channel throughput has dropped from 13 Mbps at distance of 25 meter to less than 4 Mbps at distance of 350 meter. That is due to several factors such as channel delay, signal-to-noise ratio, Doppler shift effect and signal interference.

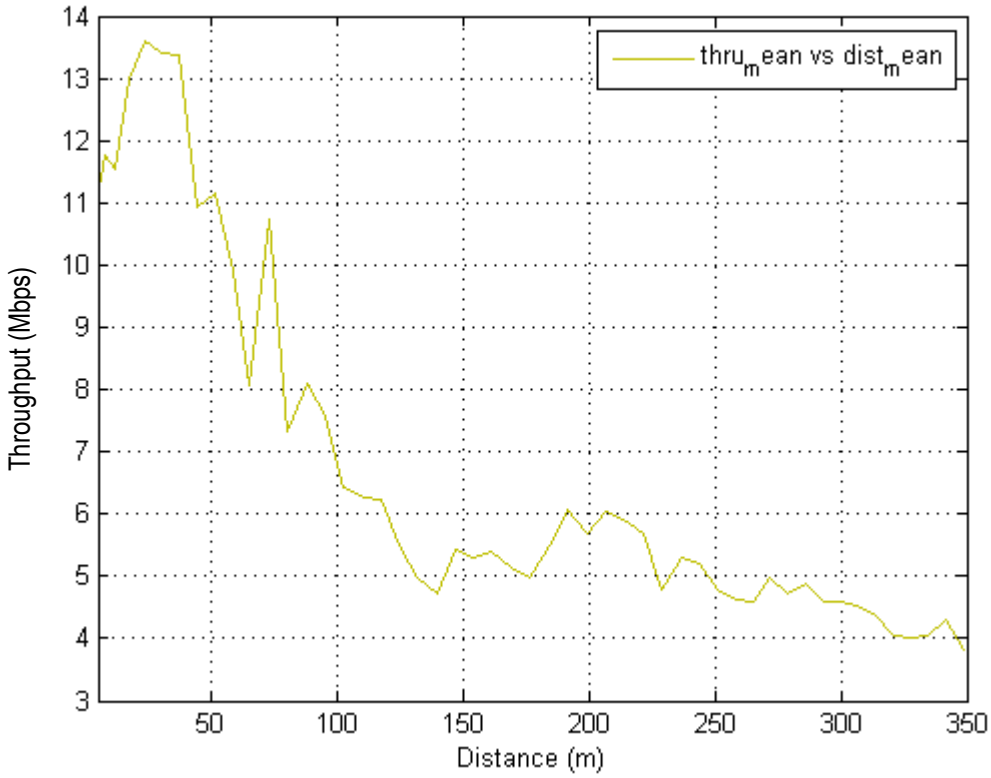

Figure 17. Throughput VS. Distance in Outdoor Environment

4. UDM Research, Doppler Shift Investigation

4.1. Introduction

With the recent trend toward transforming vehicles from simple means of transportation into a moving information platform, wireless communications have become the lifeblood of the Intelligent Transportation System (ITS) [40]. In this context, Intelli-Drive/Vehicle-Infrastructure Integration (VII) was proposed [41]. Intelli-Drive is an emerging Inter-Vehicle Communication (IVC) and ITS initiative that attempts to establish communication links between vehicles (V2V) and between vehicles and the infrastructure (V2I). Exchanging information through V2V and V2I communications aims to improve traffic safety, enhance mobility and reduce traffic jams. Therefore, several protocols of wireless communications for ITS applications have been proposed [42]. Moving vehicles impose a set of requirements on wireless communication systems. Many applications, especially safety-related, cannot tolerate long delays in connection establishment and communication. Moreover, fast moving vehicles and complex roadway environments present challenges at the PHY layer [43]. In addition, high-density roadways along with vehicle speed require a robust and high-speed communication protocol that allows sharing warning messages in real-time.

The IEEE 802.11 family of protocols [44] is a good candidate to provide Wireless Access in Vehicular Environment (WAVE) [60]. The IEEE 802.11a [45] offers a high data rate, up to 54 Mbps, at the 5 GHz band (5.15 – 5.825 GHz) allocated by the Federal Communications Commission (FCC). IEEE 802.11a uses OFDM with 52 subcarriers and a variable modulation scheme.

Although OFDM was primarily standardized for Digital Audio Broadcasting (DAB) [55] and Digital Video Broadcasting (DVB) [46], it was recently proposed for both fixed and mobile wireless applications such as Wireless Local Area Network (WLAN), Ultra WideBand (UWB), and 4th Generation (4G) cellular communication [47]. OFDM utilizes 52 spaced, orthogonal subcarriers to provide payload capabilities of 6, 9, 12, 18, 24, 36, 48, and 54 Mbps at the 20 MHz bandwidth. Subcarriers are modulated using different modulation techniques which can be Binary Phase-Shift Keying (BPSK), Quadratic Phase-Shift Keying (QPSK), 16-Quadratic Amplitude Modulation (16-QAM), or 64-Quadratic Amplitude Modulation (64-QAM). The modulation scheme is followed by a convolutional Forward Error Correction (FEC) with 1/2, 2/3 or 3/4 coding rate. That forms a total of eight combinations, as listed in Table 4.

Table 4. OFDM Modulation/Coding Parameters

Mode	Modulation	Coding Rate	Coded bits per Subcarrier	Coded bits per OFDM Symbol	Data bits per OFDM Symbol	Data Rate [Mbps]
1	BPSK	1/2	1	48	24	6
2		3/4			36	9
3	QPSK	1/2	2	96	48	12
4		3/4			72	18
5	16-QAM	1/2	4	192	96	24
6		3/4			144	36
7	64-QAM	2/3	6	288	192	48
8		3/4			216	52

Distribution of transmitted data over multiple subcarriers increases the adaptation of OFDM to severe channel conditions as well as robustness against Inter-Symbol Interference (ISI). Moreover, the orthogonality between subcarriers, which allows an uncomplicated receiver to separate the subcarriers, eliminates the crosstalk between sub-channels, known as Inter-Carrier Interference (ICI). However, this imposes a strict demand on the accuracy of frequency synchronization between transmitter and receiver as well as sensitivity to frequency offset.

In the wireless mobile environment, Doppler shift emerges due to the motion of a transmitter relative to a receiver. When a vehicle transmits/receives a signal while moving, the transmitted/received signal is subjected to an offset in its frequency. The higher the vehicle speed, the larger the frequency distortion. As a result, frequency shifting increases and leads to a loss in orthogonally between subcarriers causing inter-carrier interference. Low ICI can be eliminated by prefixing each OFDM symbol with a repetition of its end, referred to as cyclic prefix [48]. However, higher values of ICI make signal restoration extremely difficult. Therefore, several methods have been proposed to provide an estimation of Doppler shift. In [49], two main Doppler estimators, level crossing rate-based and covariance-based estimators, were analyzed in detail to study the impact of modeling error, noise error and insufficient number of samples on estimator performance. Another estimation technique was proposed in [50] and used an auto-correlation function of two OFDM symbols in the time domain. The resulting estimator was designed for frequency-selective Rayleigh channels and evaluated at several constellation schemes. However, Doppler shift analyses based on channel estimation in frequency domain are likely to be affected by noise and ICI. Therefore, a Doppler shift analysis based on channel estimation in time domain was proposed in [51]. The auto-correlation function was used once again but this time to correlate several OFDM symbols in time domain. Simulation results showed that the proposed technique improved performance of the estimation process and reduced processing time and memory usage. A novel iterative Doppler shift estimator for low Signal-to-Noise Ratio (SNR) environments was proposed in [52]. The proposed method is based on the Logarithm Envelope (LE) of mobile propagation channel, where the Minimum Mean Square Error (MMSE) of estimation for Doppler shift is derived. Results were obtained from multiple simulation runs under heavy noise distortion, and showed advantages of the developed estimator. Experimental results on path-loss, power-delay and delay-Doppler were presented in [53]. The results were obtained from actual measurements performed at high vehicle speed on a highway in Sweden. The measurements were taken at a carrier frequency of 5.2 GHz while communicating vehicles were traveling. As a result, the delay-Doppler at a given path was investigated. An analysis of radar-based Doppler measurements for ground vehicles was proposed in [54]. Radar measurements were compiled from stationary radar observing moving ground vehicles. The recorded data was analyzed for the purpose of classifying a tracked vehicle. The results indicated that Doppler signature can be used for classification; however, further knowledge regarding the target is required to interpret Doppler signature.

4.2. System Model

In order to study the impact of Doppler shift in a wireless mobile environment, we propose a system model that simulates the PHY layer of IEEE 802.11a, represented in the OFDM. The developed model aims to form a sort of a testbed that can be used as groundwork for development, evaluation or validation of different communication protocols, methodologies and theoretical concepts. Moreover, such a testbed enables the rapid prototyping and manufacturing of wireless transceivers.

With a top-down analysis, an end-to-end baseband wireless communication system can functionally be broken down into three subsystems: IEEE 802.11a transmitter subsystem, IEEE 802.11a receiver subsystem, and wireless channel subsystem as shown in Figure 18. Transmitter and receiver subsystems are closely consistent with the IEEE 802.11a PHY layer as described in 2007-revision of IEEE 802.11a standard [45].

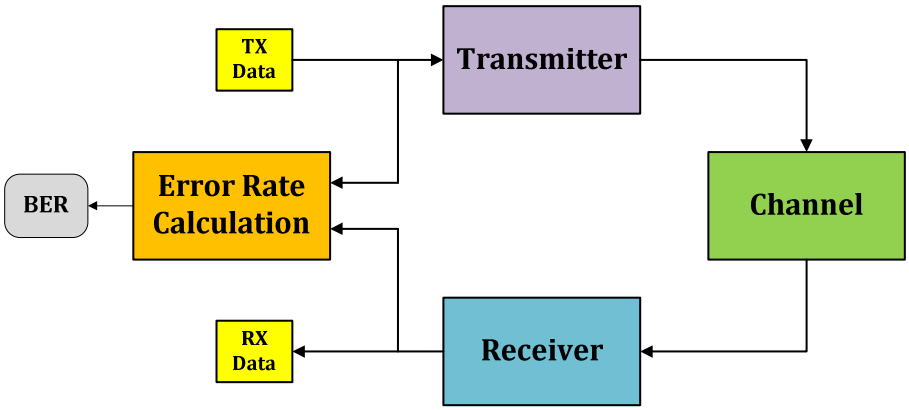

Figure 18. End-to-End System Model Block Diagram

4.2.1. IEEE 802.11a Transmitter Subsystem

Transmitter subsystem implementation can be summarized as follows. The process of transmitting a frame starts with PHY Layer Convergence Procedure (PLCP) to form a PLCP Protocol Data Unit (PPDU) out of the Medium Access Control (MAC) payload, called the PLCP Service Data Unit (PSDU). In this model, TX data was randomly generated by a variable-rate data source and assumed as PSDU. Following the PPDU frame formation, data bits are scrambled by a frame synchronous scrambler. A scrambled data string is encoded with a convolution encoder according to a coding rate (1/2, 2/3 or 3/4) defined in advance. The encoded bit string is divided into groups of coded bits per OFDM symbol, indicated previously in Table 4, to perform an interleaving based on two-step permutation. Subsequently, resulting coded and interleaved groups are modulated into a complex number using BPSK, QPSK, 16-QAM, or 64-QAM, as requested. The resulting complex number string is divided into 48 complex numbers, each of which is associated with one OFDM symbol. Four pilot signals are inserted into each OFDM symbol to create a total of 52 numbers, which is mapped into OFDM subcarriers. Conversion of 52 subcarriers into time domain is accomplished by a 64-point Inverse Fast Fourier Transform (IFFT). Cyclic prefix is pretended to the Fourier-transformed waveform to form a guard interval. Finally, time domain-OFDM symbols are appended one after another, starting after PLCP preamble and signal symbols to multiplex a complete PPDU ready for wireless channel up-conversion. Figure 19 shows a block diagram of the transmitter subsystem.

Figure 19. Transmitter Subsystem Block Diagram

4.2.2. IEEE 802.11a Receiver Subsystem

Receiver subsystem implementation is an inversion of transmitter implementation with the addition of channel estimation and equalization, as illustrated in Figure 20. Upon the detection of PLCP preamble, the receiving process starts by frame synchronization. Then, demultiplexing and cyclic prefix removal are applied on the received frame. Data carried over the 52 subcarriers is transformed back to frequency domain through 64-point Fast Fourier Transform (FFT).

Thereafter, the frame is disassembled into OFDM symbols, pilot signals are removed, and signal field is decoded to determine the desired mode and rate for the demodulation and decoding processes, respectively. Next, appropriate demodulation, which may include signal compensation based channel estimation, and de-interleaving of OFDM symbols are carried out. OFDM symbols are decoded into data bits through the use of Viterbi algorithm, as recommended by the standard. Finally, received data bits are descrambled and assembled into octets to present the RX data.

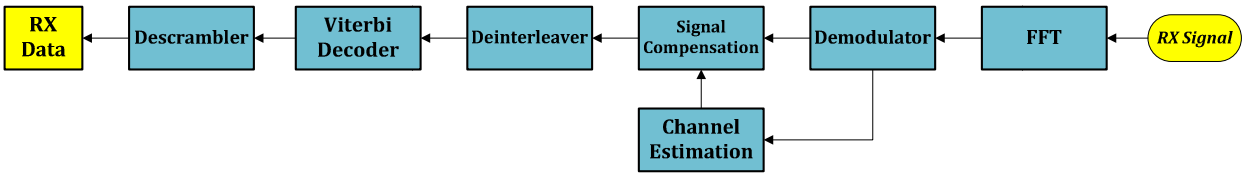

Figure 20. Receiver Subsystem Block Diagram

4.2.3. Wireless Channel Subsystem

The channel subsystem has been developed to simulate a wireless channel in a mobile environment. Therefore, the proposed model, shown in Figure 21, combines two traditional channel models, Additive White Gaussian Noise (AWGN) and Rayleigh, to imitate a real-world wireless medium. The first model is the AWGN channel, which accounts for degradation due to wideband noise. The AWGN channel model perturbs the transmitted waveform by adding a white noise that follows the Gaussian distribution. The added noise values are uncorrelated and Gaussian with zero-mean and predefined variance. Noise variance is set based on the following equations (1) and (2):

$$VAR = \frac{SignalPower\ x\ SymbolPeriod}{SampleTime\ x\ 10^{\frac{\frac{E_s}{N_0}}{10}}} \quad (1)$$

$$E_s/N_0 = E_b/N_0 + 10.\log_{10}(k) \quad (2)$$

Where: E_s/N_0 : ratio of symbol energy to noise spectral density.

E_b/N_0 : Ratio of bit energy to noise spectral density.

k : Number of bits per symbol.

The second model is the Rayleigh fading channel, which accounts for the various effects that the wireless mobile environment has on wave propagation. A transmitted signal is subject to fading, which results from multipath propagation, shadowing or motion of the transmitter and/or receiver. Rayleigh fading channel is a statistical and relatively accurate model commonly used to simulate multipath fading with no dominant line-of-sight path, based on Rayleigh distribution. Multipath fading may result from random delay, reflection, scattering and diffraction of signal components.

Moreover, the model characterizes frequency-flat or frequency nonselective fading, by which all spectral components of the transmitted signal are affected uniformly. As typically assumed, we consider that the fading amplitude is statically independent of the additive white Gaussian noise modeled in the previously discussed AWGN channel model. Furthermore, the relative motion between the transmitter and receiver is expressed by a range of frequency shifts, known as the Doppler spectrum. Doppler shift f_d is related to relative speed v_r in the following equation:

$$f_d = \frac{v_r}{c} f_0 \qquad (3)$$

Where: c : speed of light.
f_0 : transmission carrier frequency.

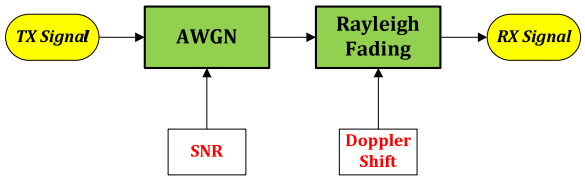

Figure 21. Channel Subsystem Block Diagram

4.3. Model Validation

The performance of wireless communication systems can be evaluated by a simulation model without the need for prototype development or field experiment design. Computer simulation has impacted research and development in the engineering industry due to its economic significance and rapid development. Our testbed has been implemented in a MATLAB/SIMULINK environment from MathWorks [61]. SIMULINK is a graphical block diagramming tool, which extends MATLAB for advanced modeling and simulation capabilities. This makes MATLAB/SIMULINK a very efficient tool to be used for developing communication systems, evaluating in real-time, and obtaining baseline performance analyses.

Our system model has been carried out as proposed in Section 2 with the addition of testbench components that provide signal flow control, data visualization and measurement, and control interface. Model control is accomplished through static and run-time parameters. Static parameters are processed at model initialization prior to execution and remain the same during simulation, while run-time parameters may be manipulated through the graphical interface during simulation. The model is driven by a MATLAB code that presets system configurations, runs the model in a finite iterative loop, and records performance measures. Each measurement is obtained through averaging samples resulting from multiple simulation runs. Moreover, different seeds have been used for data and noise sources to assure the randomness and generalization of the evaluation process.

In order to verify the performance of the proposed mode, we have simulated the proposed framework of the IEEE 802.11a communication system with the following configuration: channel bandwidth of 20 MHz, 20 OFDM symbol per transmitted block, variable modes as specified in Table 4, 64-point FFT/IFFT, and 16-sample cyclic prefix. AWGN and Rayleigh channel models have been developed to simulate the impact of additive white Gaussian noise and flat fading with the ability to specify the desired SNR as well as maximum Doppler shift.

Simulation has been performed with a setup as shown in Figure 17 to measure the BER while varying the E_b/N_0 between 0 and 30 dB. Measurements have been taken for both channel models and compared with the corresponding theoretical formulas.

4.3.1. AWGN Channel Model

The most commonly used technique for evaluating the performance of channel models is the probability of bit error rate, which is one of the most revealing criterions of system behavior. The probability of bit error depends on the constellation set of the used modulation scheme. The following analytical discussion has been concluded from [56-59]. For AWGN channel model and Phase-Shift Keying (PSK) scheme, a general formula, derived in [56], describes the probability of symbol error P_M of M-ary PSK as an integral of the probability density function $p(\theta)$ of the phase random variable θ :

$$P_M = 1 - \int_{-\pi/M}^{\pi/M} p(\theta).d\theta \tag{4}$$

Where the equivalent bit error probability P_b can be approximated to (5) when Gray code is used in symbol mapping:

$$P_b \approx \frac{1}{k} P_M \tag{5}$$

Generally, the integral in (4) is to be evaluated numerically; however, it reduces to a simple form when $M = 2$ and $M = 4$, which represents BPSK and QPSK, respectively. Since there is no interference between signals on the quadratic carriers, the probability of bit error of QPSK is identical to BPSK. Hence, the bit error probability is:

$$P_{b,BPSK} = P_{b,QPSK} = Q\left(\sqrt{\frac{2E_b}{N_0}}\right) \tag{6}$$

Where Q is the tail probability of Gaussian distribution, defined as:

$$Q(x) = \frac{1}{\sqrt{\pi}} \int_x^{\infty} e^{-t^2/2}.dt \tag{7}$$

The Q-function can be expressed in terms of the error function as:

$$Q(x) = \frac{1}{2} - \frac{1}{2}\mathrm{erf}\left(\frac{x}{\sqrt{2}}\right) \tag{8}$$

When Quadratic Amplitude Modulation (QAM) scheme is used over an AWGN channel model, the probability of symbol error for M-ary QAM is:

$$P_M = 2\left(1 - \frac{1}{\sqrt{M}}\right).Q\left(\sqrt{\frac{3}{M-1}\frac{E_s}{N_0}}\right) \tag{9}$$

With Gray code mapping, the bit error for 16-QAM and 64-QAM is approximately expressed in (10) and (11), respectively:

$$P_{b,16QAM} = \frac{3}{4}Q\left(\sqrt{\frac{12E_b}{15N_0}}\right) \quad (10)$$

$$P_{b,64QAM} = \frac{7}{12}Q\left(\sqrt{\frac{18E_b}{63N_0}}\right) \quad (11)$$

Figure 22 shows the probability of BER in both theoretical and simulated results for BPSK, QPSK, 16-QAM, and 64-QAM, all over the AWGN channel model.

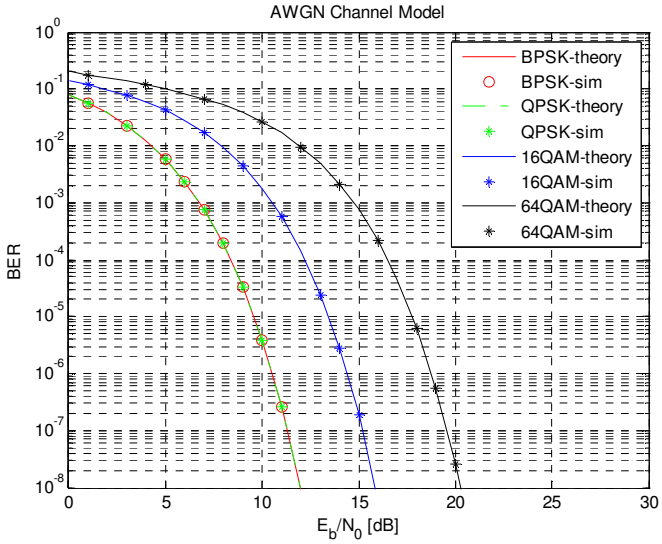

Figure 22. Theoretical and Simulated Probability of BER vs. E_b/N_0 for BPSK/QPSK/16QAM/64QAM Over the AWGN Channel Model

4.3.2. Rayleigh Channel Model

Similar to the AWGN channel model, the Rayleigh channel model is to be validated in terms of the probability of BER. However, derivations of bit error probability are more complicated in the Rayleigh channels compared to the AWGN channels, due to the non-linear relation between BER and SNR. A general formula for the probability of symbol error in M-ary PSK is presented in [56]:

$$P_M = 2\int_{\pi/M}^{\pi} p(\theta).d\theta \quad (12)$$

Similar to the discussion of probability of bit error in the AWGN channel and based on the same assumptions, the probability of bit error in the presence of a fading Rayleigh channel h can be described in (13):

$$P_b = \int_0^{\infty} Q\left(\sqrt{2.\gamma}\right).p(\gamma).d\gamma \quad (13)$$

Where: $\bar{\gamma}$: ratio of bit energy to noise spectral density.

$\gamma = |h^2|.\gamma$: ratio of bit energy to noise spectral density in the presence of a channel h.

$p(\gamma) = \frac{1}{\bar{\gamma}} e^{\gamma/\bar{\gamma}}$: the probability density function of γ .

Hence, (13) can be reduced to:

$$P_b = \frac{1}{\bar{\gamma}} \int_0^{\infty} Q\left(\sqrt{2.\gamma}\right).e^{\gamma/\bar{\gamma}}.d\gamma \qquad (14)$$

The expression in (14) can be evaluated numerically to compute the BER for BPSK and QPSK. As for the QAM scheme, it's significantly more complicated to derive a closed-form formula that describes BER in the Rayleigh channel. However, similar to the BER derivations for the QAM under the AWGN channel, computations begin with the probability of bit error. This can be evaluated in terms of $p(D)$, the probability density function of D , where D is the decision variable of multichannel communication systems, expressed as a general quadratic form. Therefore, $p(D)$ is the Fourier transform of $\psi_D(jv)$, the characteristic function D . Thus, the probability of bit error is:

$$P_b = -\frac{1}{2\pi}\int \frac{\psi_D(jv)}{v} dv \qquad (15)$$

The probability in BER of both theoretical and simulated results for BPSK, QPSK, 16-QAM, and 64-QAM over the Rayleigh channel model is shown in Figure 23.

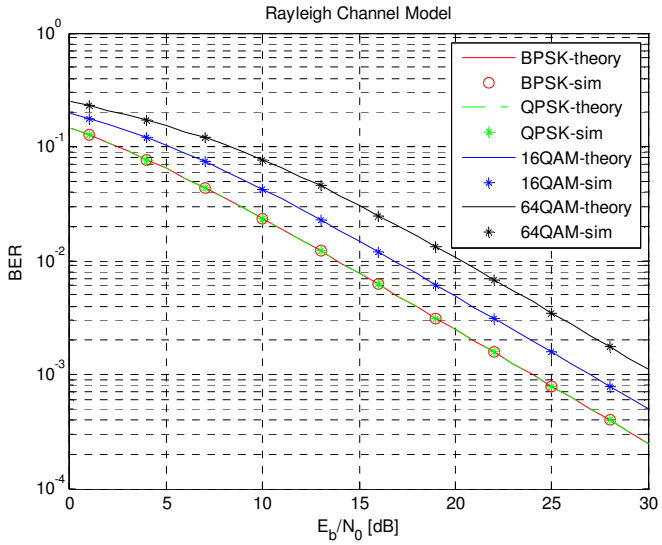

Figure 23. Theoretical and Simulated Probability of BER vs. E_b/N_o for BPSK/QPSK/16QAM/64QAM Over the Rayleigh Channel Model

As shown in Figures 21 and 23, as the energy of bit-to-noise ratio increases, the probability of bit error decreases. PSK has better BER performance than QAM. The probability of BER occurring in BPSK and QPSK is identical, as expected. Additionally, multipath fading in the Rayleigh channel increases the probability of bit error. Comparing the simulation results of BER versus E_b/N_o for the AWGN as well as the Rayleigh models, with the corresponding theoretical formulas described in equations (6, 8, 9, 14 and 15), we find that the performance of the proposed models perfectly agrees with the expected analytical performance for all four modulation schemes. Thus, the developed model is valid to be used to analyze the impact of Doppler shift.

4.4. Doppler Shift Impact Analyses

In this section we present detailed analyses regarding the impact of Doppler shift on signal quality. A systematic approach was adopted to investigate the performance of the communication system. A series of structured experiments was designed, in which changes were made to the input variables and the effects of these changes on performance measures were evaluated. We will start with the comprehensive experiment design; then, the obtained simulation results are presented and discussed, and finally we extend the analyses into mathematical and analytical modeling.

4.4.1. Design of Experiment (DoE)

DoE is widely used in engineering research and development due to its importance as a method for maximizing gathered information, minimizing the cost, and/or optimizing the number of conducted experiments. In this context, our DoE was developed by carefully choosing a number of needed experiments that provided sufficient knowledge about the measure in concern. Variables, to be controlled during the experiment, were defined to guarantee a thorough range of effect. Variables to be observed were defined to provide a meaningful, precise outcome.

The proposed framework was employed to investigate the impact of Doppler shift on signal quality. Computer simulations have been performed in MATLAB/SIMULINK to evaluate the Doppler shift impact for different modulation schemes. The same OFDM system, proposed in Section 2 and validated in Section 3, will be used with additional capabilities to manually configure multiple simulation parameters such as SNR, Doppler shift, and desired modulation scheme. Varying the SNR parameter controls the addition of the white Gaussian noise through the AWGN channel model, while varying the Doppler shift parameter changes the frequency offset of the signal passed through the Rayleigh channel model. To better explore the Doppler shift impact, SNR was set to a fixed value in order to minimize the effect of noise and highlight the effect of frequency shifting. The AWGN channel model was configured to apply an additive noise with SNR of 30 dB. On the other hand, Doppler shift was varied from 0 to 500 Hz. Choosing 500 Hz as the maximum applied frequency shift was based on the corresponding relative speed of two vehicles. According to equation (3), when the transmission carrier frequency f_0 is considered as the central frequency of the IEEE 802.11a band, the 500 Hz frequency shift results from 61.104 MPH relative speed.

Moreover, in each experiment the modulation scheme was set to one of the eight modes as described in Table 4. In each simulation run, a total of 12,500 data blocks were generated to be encoded, modulated, and transmitted over the combined channel model. The number of bits per block varies based on the preset coding rate and mapping technique from 480 bits in BPSK 1/2 to 4,320 bits in 64-QAM 3/4, which produces an approximated transmission payload of 0.57 Mb to 51.50 Mb, respectively. Subsequently, transmitted and received data were fed into an error-calculation block to evaluate the resulted BER. BER was chosen as a performance measure due to its efficiency in assessing the quality of a communication system, especially at the PHY layer. For a specific modulation scheme and Doppler shift value, each BER sample was computed by averaging the BER results obtained from 10 simulation runs with different seeds for data generation.

4.4.2. Simulation Results

The performance of BER versus Doppler shift for the PSK and QAM schemes was evaluated and is presented in Figures 24 and 25, respectively. The modulation technique used along with the associated coding rate are indicated in the figure legend.

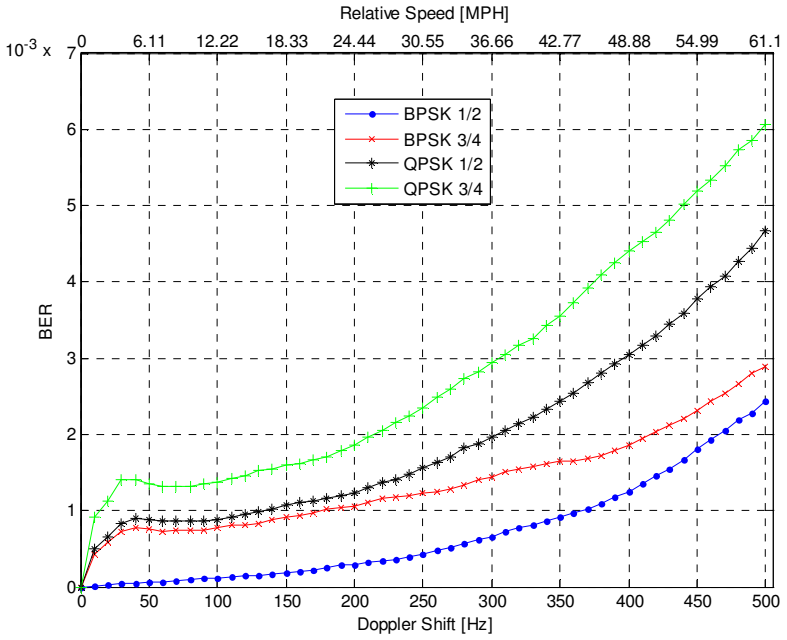

Figure 24. BER VS. Doppler Shift for BPSK and QPSK

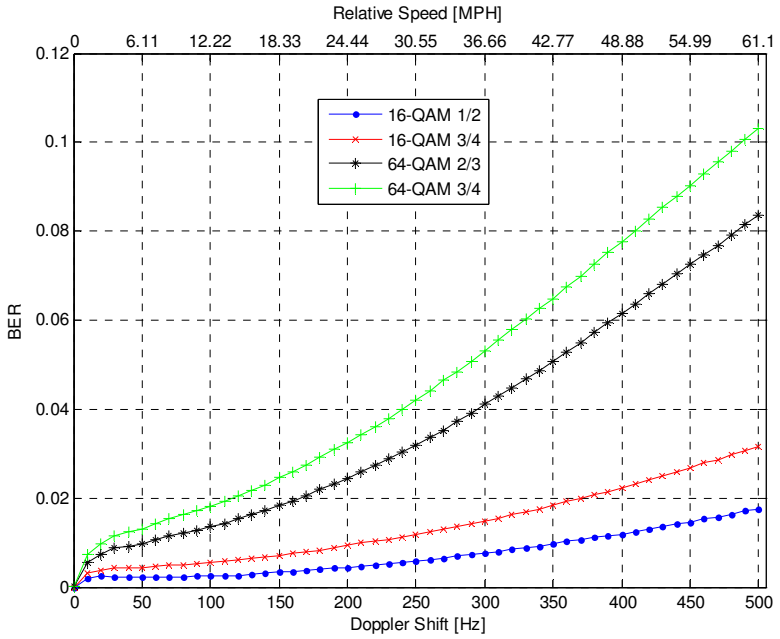

Figure 25. BER VS. Doppler Shift for 16-QAM and 64-QAM

Simulation results show that Doppler shift impact degrades signal quality. As relative speed between two vehicles increases, higher frequency shifting evolves, and as a result BER increases. In addition, the modulation scheme has a considerable impact on BER performance. The QAM scheme seems more sensitive to Doppler shift than the PSK scheme, which is evident from the BER samples, especially when evaluated for high values of Doppler shift. For instance, when Doppler shift is 300 Hz, BER in the PSK scheme is less than 3.10^{-3}, while BER in the QAM is less than 6.10^{-2}, resulting in about 20 times increased degradation. Analytically, the QAM scheme provides a higher data rate than the PSK scheme, which also corresponds with a higher BER. Furthermore, a glance at the characteristic functioning of the AWGN and the Rayleigh channel in Figures 21 and 22, respectively, confirms that the resulting BER is higher in the QAM than it is in the PSK. Moreover, since the used coding rate reflects the efficiently of the FEC, then a lower coding rate, which adds more redundant error-correction bits, should theoretically provide a lower BER. As we notice from Figures 23 and 24, we have obtained agreeable results which present a better BER performance in the case of the lower coding rate over all four modulation techniques (BPSK, QPSK, 16-QAM and 64-QAM). For example, at the 300 Hz frequency shift and QPSK, BER jumps from about 2.10^{-3} in 1/2 coding to about 3.10^{-3} in 3/4 coding. Finally, the performance of BPSK with 1/2 coding seems to be the most resistant to frequency shifting since its curve has the slowest rising of all modes. Contrarily, 64-QAM with 3/4 coding is the least resistant to frequency shifting since its curve has the fastest rising of all modes.

4.4.3. Mathematical Modeling

Data obtained through simulation can be represented mathematically. An accurate mathematical model that relates the potential Doppler shift to the corresponding BER over a particular modulation/coding mode allows for the determination of important characteristics of the given data. Curve fitting technique provides a remarkable tool to construct a function whose curve best approximates a given data set. The constructed function summarizes the relation between input and output variables, allows inferring output values based on input data, and, most importantly, makes it possible to obtain data beyond the range of the observed data, referred to as data extrapolation. To extract the mathematical models of our results, we have used curve fitting with cubic polynomial fitting. First, data resulting from using each mode has been processed to determine the best fitting method. Second, a 3rd degree polynomial equation, described in (16), has been formed for each mode by determining its coefficients (p1, p2, p3 and p4) using the non-linear least square method.

$$BER(f_d) = p1.f_d^{\,3} + p2.f_d^{\,2} + p3.f_d + p4 \qquad (16)$$

Then, curves of derived equations have been plotted for graphical visualization. Finally, the goodness of each fit has been computed to examine how well the model fits the actual data. The goodness of a fit is evaluated using two measures: Sum Squared Error (SSE) and R-square (R^2). SSE is a statistic that measures the total deviation of the fit from the actual data, as described in (17):

$$SSE = \sum_{i=1}^{n} (y_i - \hat{y}_i)^2 \qquad (17)$$

R^2 is the square of the correlation between the actual and fitted data, and defined as the ratio of the Sum of Squares of Regression (SSR) to the Total Sum of Squares (SST):

$$SSR = \sum_{i=1}^{n} (\hat{y}_i - \bar{y})^2 \qquad (18)$$

$$SST = \sum_{i=1}^{n} (y_i - \bar{y})^2 \qquad (19)$$

$$R^2 = \frac{SSR}{SST} = 1 - \frac{SSE}{SST} \qquad (20)$$

Where: y_i: actual data sample.

$\hat{y}_i$: fitted data sample.

$\bar{y}$: mean value.

n : number of data samples.

The closer the SSE is to zero, the smaller the random error component in the model. On the other hand, the closer the R^2 gets to one, the better the model explains the data.

Table 5. Polynomial Coefficients and Goodness-of-Fit Parameters of Fitted Curves

Mode	Polynomial Coefficients				Goodness-of-Fit	
	p1	p2	p3	p4	SSE	R^2
1	-5.96E-11	2.49E-07	8.54E-05	6.67E-03	1.87E-08	0.9992
2	3.42E-11	-1.92E-08	6.08E-06	3.68E-04	3.15E-07	0.9851
3	3.37E-11	-9.05E-09	4.50E-06	5.01E-04	4.53E-07	0.9935
4	1.75E-11	5.02E-09	3.62E-06	9.16E-04	1.40E-06	0.9884
5	1.57E-11	4.85E-08	3.99E-06	1.65E-03	4.13E-06	0.9965
6	7.02E-11	3.22E-08	2.50E-05	2.60E-03	1.02E-05	0.9973
7	-1.54E-11	2.08E-07	5.86E-05	5.15E-03	4.50E-05	0.9984
8	-5.96E-11	2.49E-07	8.54E-05	6.67E-03	7.41E-05	0.9983

Table 5 lists polynomial coefficients of derived equations along with goodness-of-fit parameters for each mode. Figures 26(a) through 26(h) demonstrate the graphical representation of actual data (in blue) and its fitted model (in red) for all eight modes, where modulation scheme and coding rate, as well as resulting R^2, are indicated on top of each figure.

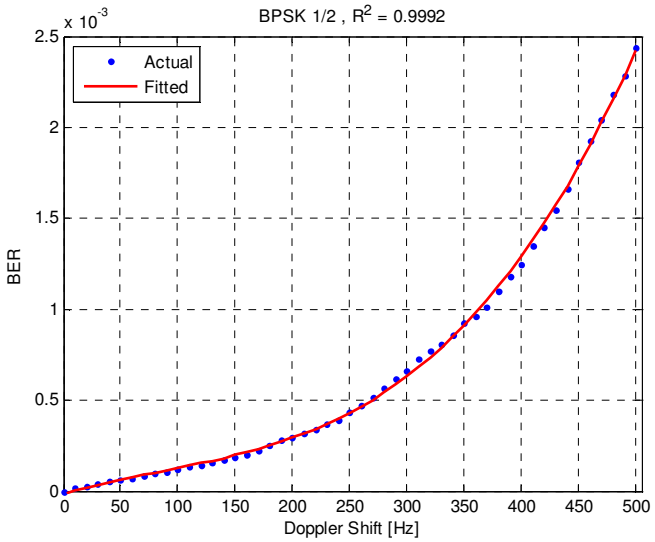

Figure 26 (a). BPSK ½

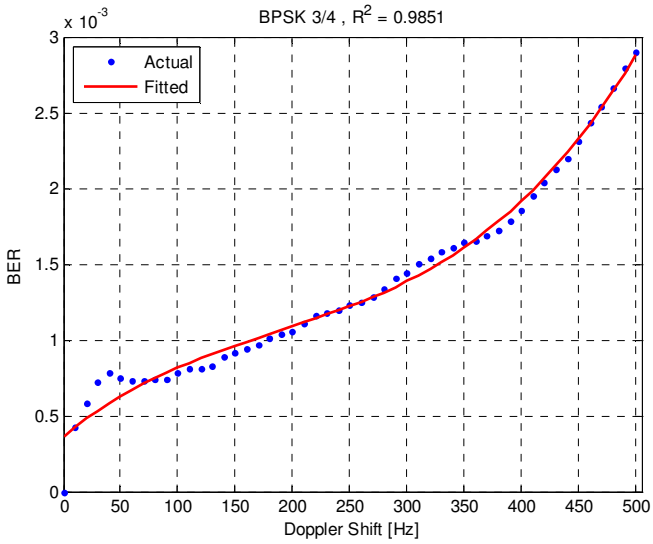

Figure 26 (b). BPSK 3/4

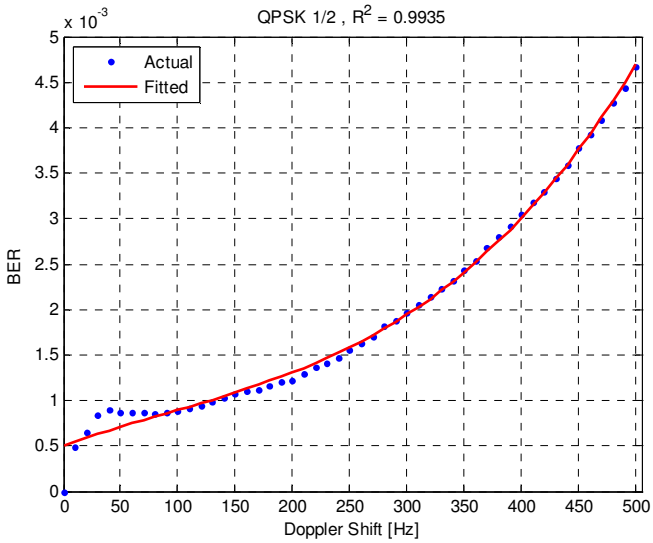

Figure 26 (c). QPSK 1/2

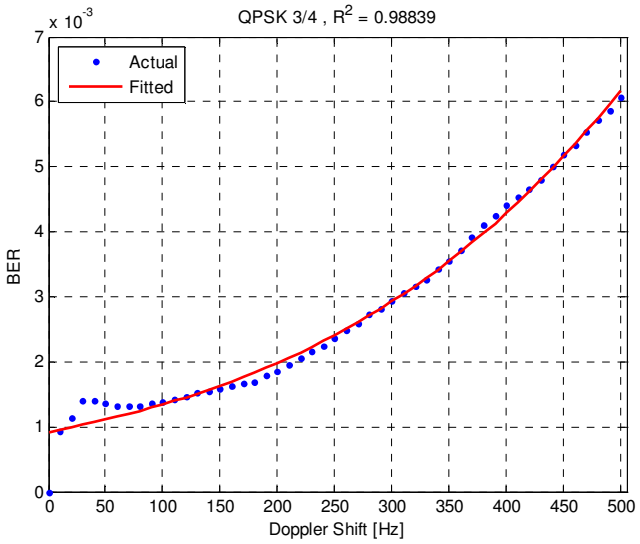

Figure 26 (d). QPSK 3/4

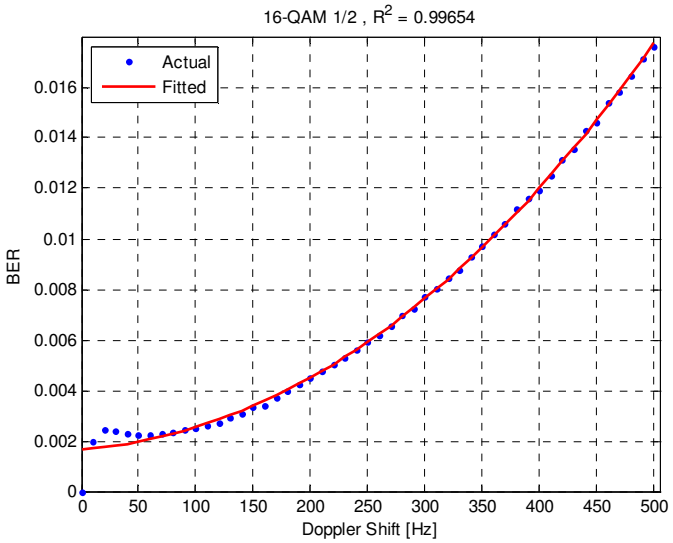

Figure 26 (e). 16-QAM ½

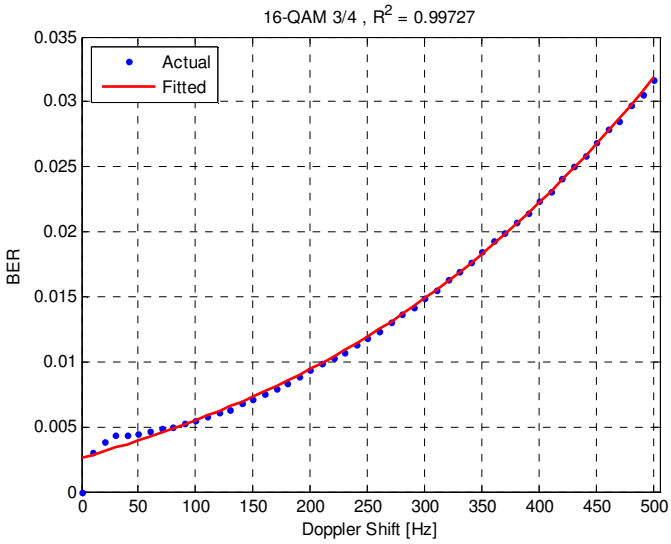

Figure 26 (f). 16-QAM 3/4

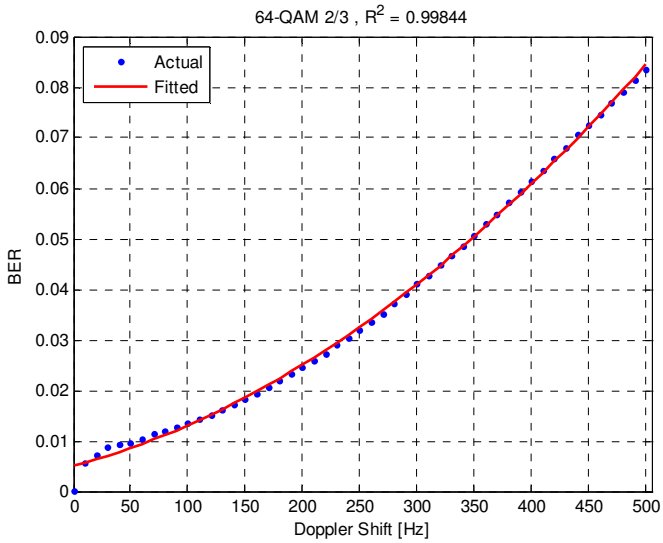

Figure 26 (g). 64-QAM 2/3

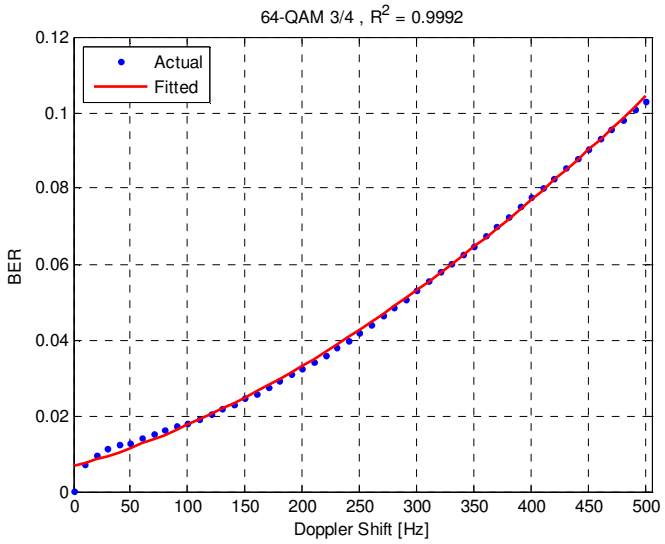

Figure 26 (h). 16-QAM 3/4

Figure 26 (a-h). Curve Fitting of BER vs. Doppler Shift

Based on R^2 values listed in Table 5, goodness-of-fit varies from 99.35% for mode 3 to 99.92% for mode 1. Hence, the derived fits are closely related to the original data. Therefore, 3rd degree equations can be used to mathematically relate the impact of Doppler shift with the resulting BER in an OFDM communication system.

4.5. Adaptive Modulation and Coding

To improve the robustness of the communication system to the encountered frequency shift, we proposed a new methodology that reduces the impact of Doppler shift on signal quality. The proposed methodology is based on an adaptive algorithm that adjusts the modulation scheme according to any Doppler shift that might occur. The developed algorithm establishes communication in the lowest data rate under Mode 1. As Doppler shift changes, the corresponding BER is computed through the appropriate equation that links the BER with the Doppler shift at a particular mode, as summarized in Table 5. These closed-form equations provide the BER for any given Doppler shift value; therefore, the BER can be found not only at the current Doppler shift value, but also at a posterior value, which produces a sort of predicted BER. Consequently, the current and subsequent BERs are compared to a predefined threshold to determine whether to switch to a higher or lower modulation mode. A flow chart of the developed algorithm is illustrated in Figure 27.

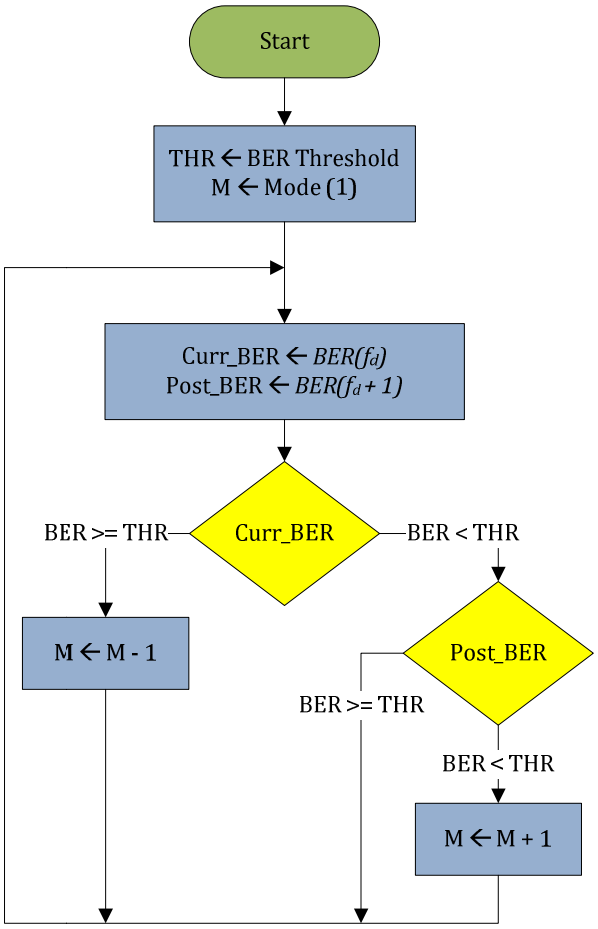

Figure 27. Adaptive Algorithm Flow Chart

The desired BER threshold is set to match the acceptable BER, defined by IEEE. According to the IEEE 802.11a standard [45], the minimum sensitivity of a receiver should fall in the range of (-82 , -65 dBm) to detect the transmitted signal and demodulate it with a Packet Error Rate (PER) of less than 10% at a PSDU length of 1000 octets. A rule of thumb to relate the PER to the BER is:

$$P_p = 1 - (1 - P_b)^N \qquad (21)$$

Where: P_p : probability of packet error.

P_b : probability of bit error.

N : number of bits per packet.

As a result, the acceptable probability of bit error in IEEE 802.11a should be less or equal to 10^{-5}, which can be expressed as a percentage BER of 10^{-3}. This agrees with the analyses and conclusions that were presented in [62].

Applying the proposed adaptive methodology while varying Doppler shift frequency from 0 to 500 Hz causes dynamic mode switching, and as a result, the corresponding BER performs in a different manner, as graphed in Figure 28. As shown, transmission initially begins with the first mode. As long as the computed BER is below the threshold, the communication mode is adjusted to the next higher mode providing a higher data rate. However, whenever the BER exceeds the desired limit, the communication mode is readjusted to the previous lower mode, providing a better robustness.

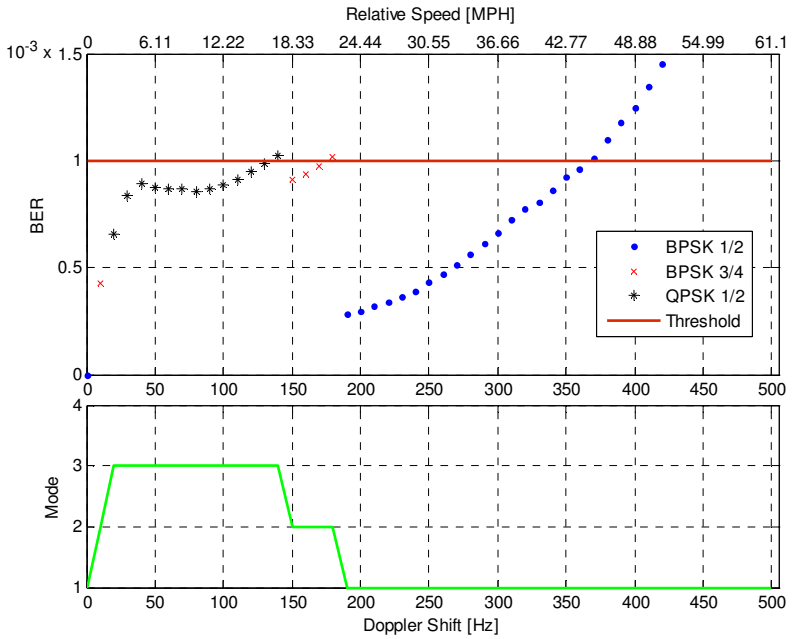

Figure 28. BER VS. Doppler Shift With Adaptive Methodology

We notice that QPSK with a 1/2 coding rate is the highest mode that is to be reached in order to keep the BER in the acceptable range. Moreover, the BER goes beyond the acceptable boundary, despite the mode of adjustment, as Doppler shift exceeds 370 Hz. Hence, we may consider that the proposed methodology is valid for up to 370 Hz of frequency shift, or in other words, up to 45.22 MPH of relative speed. In summary, mode adjustment can be divided into multiple levels based on Doppler shift or relative speed as shown in Table 6.

Table 6. Mode Adjustment Leveling

Doppler Shift f_d [Hz]	Relative Speed v_r [MPH]	Suitable Mode
f_d <= 140	v_r <= 17.11	QPSK 1/2
140 < f_d <= 180	17.11 < v_r <= 22.00	BPSK 3/4
180 < f_d <= 370	22.00 < v_r <= 45.22	BPSK 1/2
370 < f_d	45.22 < v_r	N/A

Mode adjustment in the proposed adaptive methodology has to be used in both the transmitter and receiver to allow an agreement on communication parameters. By that means, the adaptive methodology is only suitable for duplex communication between two vehicles.

5. UDM Research, Traffic Light Scenario Evaluation

5.1. Introduction

Several studies by the U.S. Department of Transportation (USDOT) have shown that traffic congestion conditions continue to deteriorate on a yearly basis, particularly in urban areas. Traffic volumes have been outgrowing road capacity in urban areas; in addition, the unconstructive financial and environmental impacts for developing additional roadway required policy makers to seek alternative solutions to further address traffic congestion. The emergence of new technologies has allowed transportation agencies to improve traffic flow and avoid roadway expansion through adaptive traffic light intersection control. Adaptive traffic light control systems such as the Sydney Coordinated Adaptive Traffic System SCATS[62]- and Split Cycle Offset Optimization Technique SCOOT [63]- have been deployed at major urban intersections. Such adaptive traffic management systems control traffic signals to increase traffic flow using road sensory networks. Recent evolution in wireless communication technologies is allowing for vehicle-to-vehicle (V2V) and vehicle-to-infrastructure (V2I) communication, further supporting the objective of reducing traffic congestion.

The objective of this study is to evaluate the wireless communication network performance as a function of the number of nodes, the communication technologies and the message characteristics. The limited availability of wireless equipped vehicles and the complexity of empirically evaluating wireless communication technologies led us to the use of a simulator. For this evaluation, a simulation tool combining traffic and network simulation capabilities is necessary.

This study is presented in two parts:

Part I: Provides an overview of the study, the evaluation tool and the evaluation method.

Part II: Develops a simulation to simulate different scenarios and discusses simulation results.

5.2. Part I

5.2.1. Related Work

A large number of recent studies have focused on the performance evaluation of wireless communication in vehicular applications. In [64]- , research was conducted to evaluate the reliability of vehicles' ad-hoc networks using a traffic/network simulation tool (VNSim) developed by University Politehnica of Bucharest. The research results demonstrated the advantages of implementing the DSRC (Dedicated Short-Range Communications) communication protocol rather than the 802.11 communication protocol at the physical, MAC and application layers. The research limits the average number of nodes being evaluated to 90 vehicles/minute. Our simulation extends the study beyond 90 vehicles/minute to evaluate the performance of data communication in areas such as highly congested intersections, accidents or construction zones.

Other efforts have focused on developing dynamic traffic light algorithms. In [66]- , researchers developed a genetic algorithm-based traffic light controller to enhance traffic and pedestrian flow performance at traffic lights. This algorithm was based on two parameters: the queue of vehicles and pedestrians at the red light, relative to the number of vehicles and pedestrians that pass through a green light. The performance comparison revealed the proposed controller to have a performance advantage relative to other dynamic traffic light algorithms. The research does take the impact of data communication performance on the proposed traffic light algorithm.

5.2.2. Simulation Tools

In order to study the efficiency of the DSRC communication protocol, traffic and network simulators are needed. In the following section, we discuss a few simulation tools to identify a suitable tool for our simulation goals.

Simulation tools such as TSIS-CORSIM and Paramics are two of several microscopic traffic simulators. This type of simulator provides accurate traffic data; nevertheless, these simulators do not include any network simulation capabilities. Integrating a network simulator is essential to evaluate the impact of the communication network performance with high user rates.

High performance network simulators such as NS-2 are available. NS-2 is an open source simulation tool that runs on Linux. JiST/SWANS is yet another platform-independent network simulator with high performance in discrete evaluation simulation. These types of tools are good for network simulation; however, these tools do not include a traffic simulator, which is equally essential for our study.

ViiLab is a new traffic/network simulator whose development is still being enhanced. Further exploration was required to validate the capabilities of this tool, thus rendering it unqualified for this study.

The evaluation of these simulation tools led us to concentrate our efforts on utilizing VNSim. VNSim is an integrated network/traffic-simulating tool developed by University Politehnica of Bucharest [67]- . We would like to thank Professor Valentin Cristea and Professor Liviu Iftode at University Politehnica of Bucharest for their support during the use of this tool. VNSim was developed utilizing the TrafficView simulator which simulates the vehicular wireless communication network. VNSim provides traffic and vehicle information such as the maximum / average delay of vehicles, fuel consumption and emissions. Furthermore, VNSim's network simulation capabilities provide network communication data such as the number of transmitted messages, rate of received messages, cause of non-received messages, and source of messages-forward vehicle, next forward vehicle, left adjacent vehicle and right adjacent vehicle as shown in Figure 28.

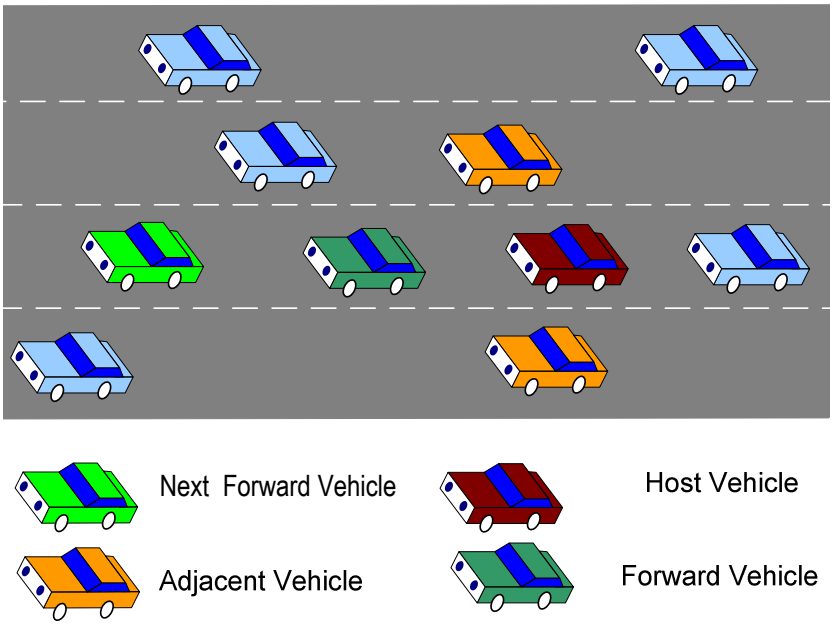

Figure 29. Communication Environment

5.2.3. VNSim: Radio Propagation Models in TrafficView

VNSim offers several radio propagation models and data dissemination models to allow studying of the impact of radio wave propagation. In an ideal communication medium, there is only one direct line of communication between the sender and the receiver units. In a real world application, there are random obstacles such as buildings and other radio wave communication that interfere with the communication path between a sender and a receiver. As a result, it is challenging to model the communication interference and analyze its characteristics. Several radio propagation models have been developed to model the different phenomena that influence the received signal such as:

- *The Shadowing Model:* This model seeks to solve the fading effects that occur on the signal, and loss of signal power that occurs on the long distance path. The model can measure the loss in received signal power using a logarithmical equation that depends on distance. In addition, the model adds a Gaussian random variable to counteract the loss caused by obstacles in the communication medium.

- *The Two Ray Ground Model:* Two paths were considered in this model: the direct line of sight, and the ground reflection path between the sender and the receiver as shown in Figure 30. Therefore, the power of the received signal is simply the sum of these two paths. It is important to note that for short distances between the sender and the receiver, such as a traffic signal, this model does not provide good-quality results.

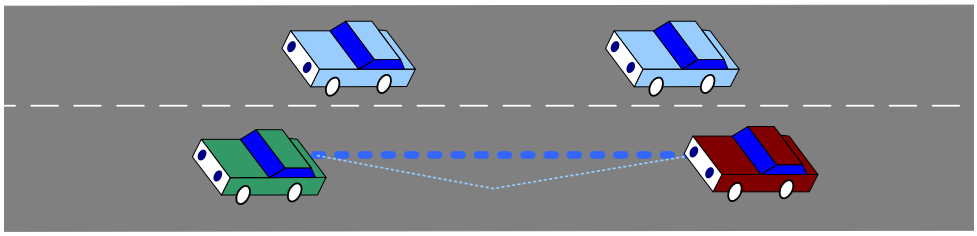

Figure 30. Two Ray Ground Model

- *The Ricean Fading Model:* The radio signal in this case tends to partially cancel itself due to the multi-path interference. This kind of fading occurs when the signal coming from generally the line of sight signal overpowers all other signals.

5.2.4. VNSim: Data Dissemination Models in TrafficView

Data dissemination models in vehicle communication networks are very important to ensure effective data sharing. TrafficView (VNSim) offers three different types of data dissemination models:

- Probabilistic Forwarding (PF)
- Complete Forwarding (CF)
- Neighbor Discovery (ND)

The communication data or packet is sent with a fixed period every 100 milliseconds, but the types of packets differ among the three data dissemination models.

1. In Probabilistic Forwarding, the vehicle can send one of two packets:
   - Packet with vehicle data, containing information about itself
   - Packet with vehicle data, containing information about itself and all other vehicles in its communication range

The application will choose which packet to send in a probabilistic way depending on the size of the platoon. Another enhancement is achieved using the following model: when a vehicle stops at a red light, the vehicle sends a message indicating that it is still in the platoon but it will not be active. This will ensure that the vehicle's information stays in the platoon packet and consequently the number of overall packets will be reduced.

2. The Complete Forwarding model does not use different types of packets. In this model, the only packet that will be sent from each vehicle is the platoon packet in which the vehicle broadcasts its database, which includes information about the other vehicles it identifies.

3. On the other hand, the Neighbor Discovery model does not deal with vehicle platoons. Each vehicle sends a static packet in a static period of time. These packets contain information about the vehicle that sends it (ID, timestamp, speed, road, point, offset, lane, direction, signal and state). The packet size is fixed to 27 bytes. The application adds two extra Bytes to this packet containing information that defines its type. Therefore, the packet size will be 29 bytes [67]-

In summary, Probabilistic and Complete Forwarding deal with large numbers of vehicles where drivers tend to travel as platoons (highway or intersection). In the Forwarding models, the packet contains general information about the road and detailed information about each vehicle in the platoon. Nevertheless, there are two constraints on the platoon packets: the information about each vehicle should not be outdated and the total size of the packet should not exceed 2300 bytes (Ethernet 802.11 frame size).

5.2.5. Performance Measures

In order to evaluate the DSRC protocol at intersections, we apply the three different data dissemination models: PF, CF and ND. In addition, we select several test cases to compare the dissemination models to communication performance in terms of the ratio of successfully received to lost packets.

For each data dissemination model, we present the ratio of successfully received/lost packets as a function of number of nodes per simulation minute. To analyze the reasons behind losing packets we evaluate each category:

- Collision: two packets arrive at the same time to the node and the ratio of the first packet to the sum of the two packets is lower than the collision threshold.
- Corrupted: the received packet does not have enough power to decode the Physical and PCLP header.
- RX (Receiving): the received packet was rejected because the node is engaged in receiving another packet (receiving mode).
- TX (Transmitting): the received packet was rejected because the node is engaged in transmitting another packet (transmitting mode).
- PER: the received packet does not have enough power to decode the data.
- Weak: the received packet does not have enough power to be detected and it is too weak to be received; it would normally be detected as noise.

5.3. Part II

5.3.1. Simulation Setup

The VNSim Simulator environment was selected to run different traffic light scenarios. These scenarios differ by number of nodes; the same simulated scenarios were repeated for the three different data dissemination models PF, CF and ND.

The simulated road is a simple cross intersection: one cross road has three lanes north/south and the other two lanes east/west as shown in Figure 31. On each side of the intersection, approximately 15 to 25 percent of all traveling vehicles will turn left; similarly the same number will turn right and the remaining will continue straight. We ran each experiment for 60 simulation minutes. The average number of nodes varied between 35 and 290 vehicles per simulation minute. Modifying the number of vehicles per lane per simulation hour generated the number of nodes used in each experiment. We divided the drivers' driving behaviors equally into very calm, regular and aggressive. We selected a pre-timed traffic light controller; the cycle's length of time was 70 seconds: green 30 seconds, yellow 3 seconds, and red on all sides of the intersection 2 seconds; hence the Red was 35 seconds long.

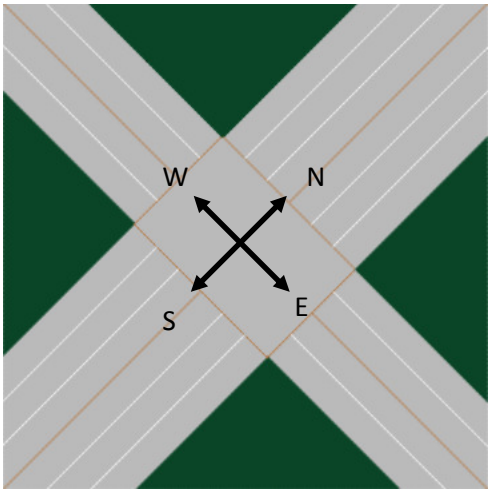

Figure 31. The Simulated Intersection

All of the simulated vehicles were equipped with a wireless device to communicate among themselves (V2V) and with the infrastructure (V2I). The communication range was set to 200 meters between the vehicles and 1,000 meters between vehicle and infrastructure. The selected radio propagation model is the shadowing model.

5.3.2. Scenarios Description

We ran seven scenarios for each different data dissemination model. The number of nodes is different for each scenario and follows the possible paths illustrated in Figure 32:

- Vehicles/Lane/Hour turning left
- Vehicles /Lane/Hour going straight
- Vehicles /Lane/Hour turning right

The selected intersection's traffic flow scenarios are as follows:

- Scenario 1: 25 (Left), 50 (Straight) and 25 (Right)
- Scenario 2: 35 (Left), 70 (Straight) and 35 (Right)
- Scenario 3: 30 (Left), 100 (Straight) and 30 (Right)
- Scenario 4: 50 (Left), 150 (Straight) and 50 (Right)
- Scenario 5: 35 (Left), 180 (Straight) and 35 (Right)
- Scenario 6: 90 (Left), 180 (Straight) and 90 (Right)
- Scenario 7: 110 (Left), 220 (Straight) and 110 (Right)

The simulation time was fixed to 60 minutes which translates into different real run time based on the selected scenario. The real run time varied between 10 and 60 minutes.

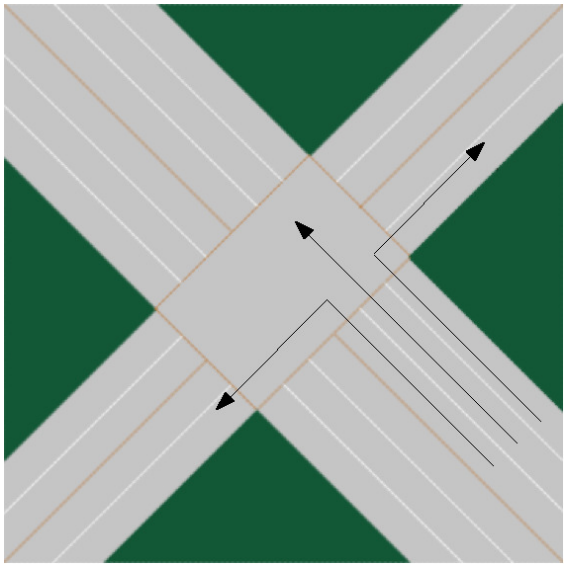

Figure 32. Traffic Direction: Vehicles Turning Left, Right and Going Straight

5.3.3. The Overall Traffic Data

We have run the simulation for all seven scenarios to study the average vehicle density of vehicles at the intersection for different data dissemination models as illustrated in Figure 33. We found that the average waiting time of the three dissemination models performs equally well for the first six scenarios. In scenario seven we can clearly identify that the CF dissemination model results in an improved performance.

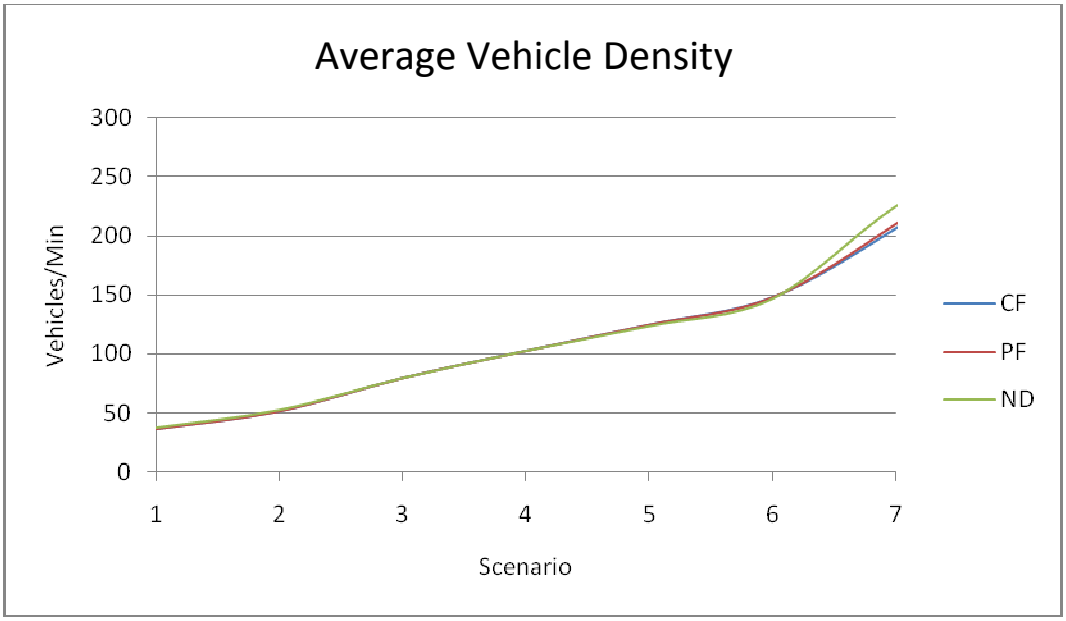

Figure 33. The Average Number of Vehicles at the Intersection for Each Scenario

Figure 34 presents the maximum waiting time of vehicles at the intersection. It can be seen that the pre-timed intersection control can no more offer an equalized control for clearing traffic with volumes identified in scenario six and beyond. The results also show that the PF and CF dissemination models perform equally and surpass the ND model performance.

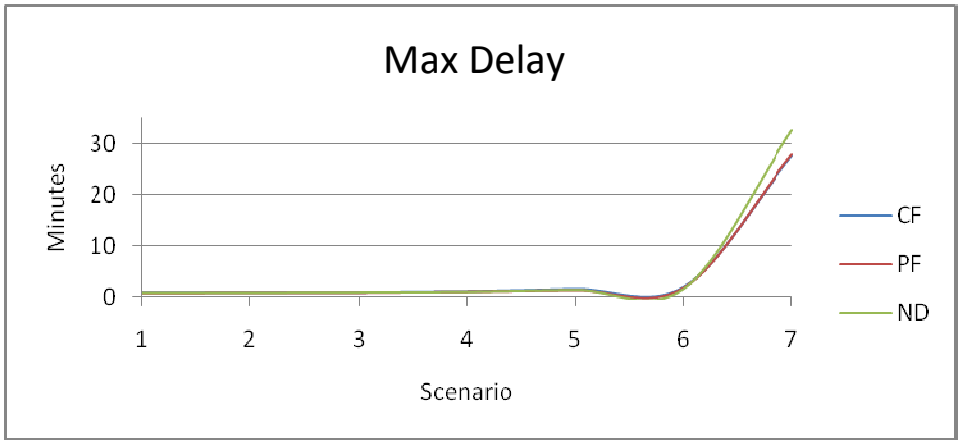

Figure 34. The Maximum Waiting Time at Intersection

An additional measure to portray the enhanced performance of the CF and PF dissemination models was "intersection average delay." We evaluated the vehicle average delay at the intersection, and the results reflected in Figure 35 clearly show the underperformance of the ND dissemination model.

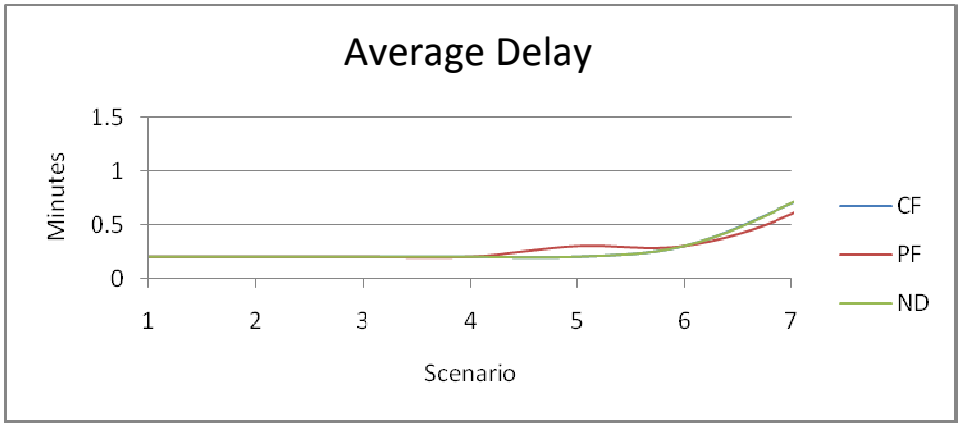

Figure 35. The Average Delay Time at Intersection

Next, the ratio of the successfully received and lost packets for each data dissemination model is discussed. This study will help identify which of the dissemination models could offer enhanced communication performance at intersections. This decision will be based on the largest number of nodes that the model can serve. The simulation results are illustrated in Figure 36. The most interesting aspect is the intersecting point of the successfully received versus lost packet curves for each of the dissemination models. The representative model's plot intersection point identifies where half of the transmitted messages are getting lost. Half of the packets were lost at around 110 nodes when using Neighbor Discovery and Complete Forwarding, while the Probabilistic Forwarding reached approximately 130 nodes before losing half of the transmitted packets. These results lead us to conclude that the Probabilistic Forwarding model offers an improved performance compared to the Complete Forwarding and the Neighbor Discovery dissemination models.

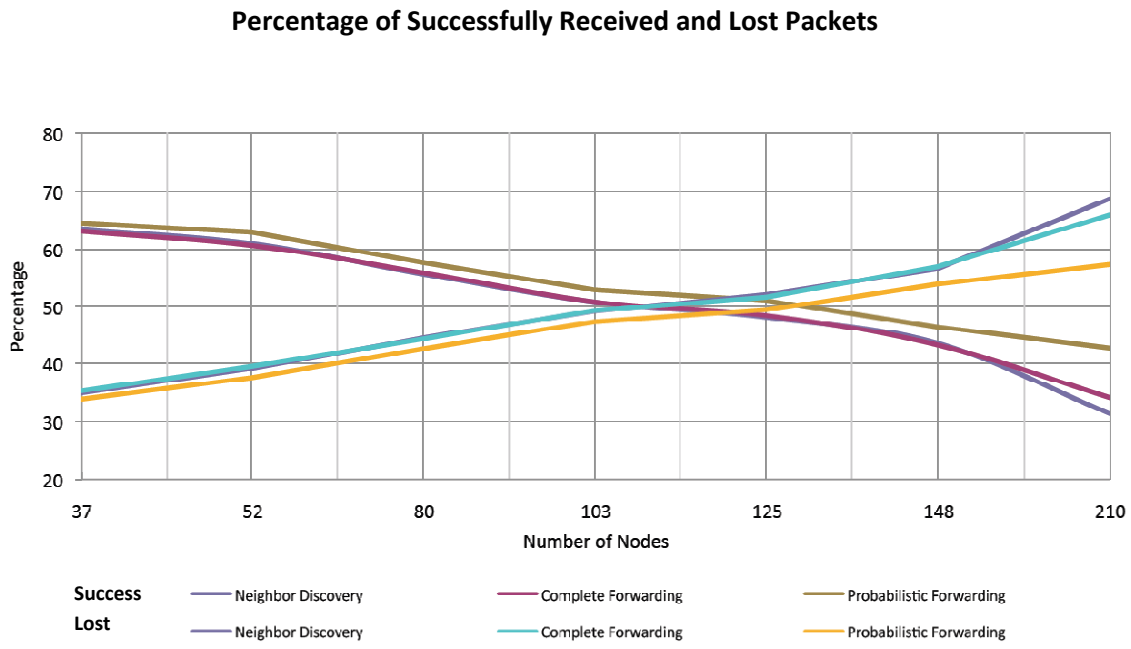

Figure 36. The Percentages of Successfully Received Packets Using the Three Data Dissemination Models

6. Conclusion

In this research, we have defined the requirements of the development of a test bed that has been used to evaluate and validate different wireless protocols. WLAN communication protocols have been evaluated for vehicular applications. Multiple performance measures, such as communication range, time-to-login, throughput and jitter time, have been used to determine the effectiveness of wireless protocols in the ITS environment. Experimental results showed that the practical communication range may vary from the theoretical value according to the type of Wi-Fi transceiver used. Another measure, time-to-login, showed the importance of having a static assignment of a unique address for network nodes, where the dynamic addressing resulted in significant delays.

Newly developed methodologies have been proposed to reduce the cost of test bed implementation. The first method aims to use a single node to generate a network load that is similar to the load of multiple nodes. As a result, it was proven that this method is not valid due to the inconsideration of the random access of the large number of nodes. The second method divides the network with costly wireless transceivers into two or more subnets with low-cost transceivers, where all subnets are bridged together using the costly link. Throughput, jitter time and delay time were used as measures to validate the proposed methodology. The last method was to evaluate the impact of the distance between vehicles on the communication throughput. Several experiments were designed and implemented at a racing track to measure the throughput while the relative distance between the transmitter and receiver varied. Results illustrated the degradation of channel throughput as the relative distance increased.

We have implemented an end-to-end OFDM communication system using MATLAB/SIMULINK with all required configuration. The consistency between simulation results and analytical solutions has validated the proposed system. A comprehensive design of the performed experiments has been presented. The main focus of this section was to analyze the impact of Doppler shift, as a function of relative speed, on the signal quality. PSK schemes have presented greater resistance for Doppler shift impact in comparison with QAM schemes; however, with a lower data rate. Moreover, an explicit, precise mathematical model has been derived for each mode to provide a close-form relation between Doppler shift and BER. An adaptive methodology has been developed to improve system robustness to Doppler shift impact. Simulation results showed the enhanced performance of the proposed methodology and indicated the possible range of operation in term of frequency shift as well as relative speed.

In Section 5, we have showed with simulation that the probabilistic forwarding dissemination model in vehicle communication is the optimal dissemination model. The probabilistic forwarding dissemination offers improved performance in achieving successful data communication between nodes in all traffic flow conditions.

7. Resulting Publications

1. Baraa Alyusuf, Rami Sabouni, Utayba Mohammad, and Nizar Al-Holou, "Performance Evaluation of IEEE 802.11b/g for Inter-Vehicle Communication (IVC)," accepted for presentation at ITS-America 2010.
2. Baraa Alyusuf, Utayba Mohammad and Nizar Al-Holou, "Performance Evaluation of IEEE802.11 Family Protocols," poster presentation at the 2009 ITS-Michigan Annual Meeting & Exposition.
3. Khaldoun Albarazi, Fadi Saadeh, Utayba Mohammad and Nizar Al-Holou, Ghassan Shahine, "Development and Evaluation of the Next Generation Traffic Light System," poster presentation at the 2009 ITS-Michigan Annual Meeting & Exposition.
4. "Development of Test Bed to Evaluate the Performance of Intelligent Transportation Systems (ITS)," poster, UDM Faculty and Student Research symposiums, April 15, 2008.
5. "Wireless Networks for the Next Generation Vehicles," poster, UDM Faculty and Student Research symposiums, April 15, 2008.
6. Khaldoun Albarazi, Utayba Mohammad and Nizar Al-Holou, "Doppler Shift Impact on Vehicular Ad-hoc Network," accepted for publication at the Canadian Journal on Multimedia and Wireless Networks.

8. Glossary of Acronyms

AWGN	Additive White Gaussian Noise
BER	Bit Error Rate
COTS	Commercial Off-the-Shelf
DSRC	Dedicated Short-Range Communications
E_b/N_0	Energy of Bit-to-Noise Ratio
FCC	Federal Communications Commission
FHWA	Federal Highway Administration
FPGA	Field Programmable Gate Array
Gbps	Gigabit Per Second
GHz	Giga-Hertz
GPS	Global Positioning System
IP	Internet Protocol
IPv4	Internet Protocol Version 4
IPv6	Internet Protocol Version 6
ISO	International Standards Organization
IVPS	In-Vehicle Payment Service
IVTP	In-Vehicle Toll Processing
ITS	Intelligent Transportation Systems
MAC	Medium Access Control
MDOT	Michigan Department of Transportation
MHz	Mega-Hertz
MTU	Maximum Transmission Unit
OBU	On-Board Unit
OEM	Original Equipment Manufacturer
OFDM	Orthogonal Frequency Division Multiplexing
OS	Operating System
PC	Personal Computer
PER	Packer Error Rate
RF	Radio Frequency
RITA	Research and Innovative Technology Administration
RSU	Roadside Unit
SNR	Signal to Noise Ratio
TCP/IP	Transmission Control Protocol/ Internet Protocol
UDP	Universal Datagram Protocol
URL	Uniform Resource Locator
USDOT	United States Department of Transportation
V2I	Vehicle to Infrastructure
V2V	Vehicle to Vehicle
WAVE	Wireless Access in Vehicular Environments

9. References

[1]- http://safety.fhwa.dot.gov/

[2]- C. J. Merlin, W. B. Heinzelman, “A Study of Safety Applications in Vehicular Networks,” proceedings of the IEEE International Workshop on Heterogeneous Multi- Hop Wireless and Mobile Networks 2005, November 2005.

[3]- VII Michigan Test Bed Program concepts of operations, MDOT, revised draft, October 10, 2005.

[4]- Jun Luo, Jean-Pierre Hubaux, “A Survey of Inter-Vehicle Communication,” 2004.

[5]- Ioan Chisalita, Nahid Shahmehri, “A Peer-to-Peer Approach to Vehicular Communication for the Support of Traffic Safety Applications.”

[6]- Lothar Stibor, Yunpeng Zang, Hans-Jürgen Reumerman,“Neighborhood evaluation of vehicular ad-hoc network using IEEE 802.11p.” www.ew2007.org/papers/1569014956.pdf

[7]- ANSI/IEEE Std 802.11, 1999 Edition, “Part 11: Wireless LAN Medium Access Control (MAC) and Physical Layer (PHY) Specifications.”

[8]- http://safety.fhwa.dot.gov/

[9]- http://www.its.dot.gov/its_overview.htm

[10]- http://www.its-jp.org/english/about_e/

[11]- "ITS Strategy in Japan," Report of the ITS Strategy Committee, June 2003.

[12]- W. Franz, H. Hartenstein, and B. Bochow, “Internet on the Road via Inter-Vehicle Communications,” Workshop der Informatik 2001:Mobile Communications over Wireless LAN: Research and Applications, Gemeinsame Jahrestagung der GI und OCG, pp. 26-29, September 2001.

[13]- http://www.et2.tu-harburg.de/fleetnet/english/applications.html

[14]- J. Ott, and D. Kutscher, "A Modular Access Gateway for Managing Intermittent Connectivity in Intermittent Communications," European Transactions on Telecommunications; 2006

[15]- http://www.drive-thru-internet.org/motivation.html

[16]- "VII Michigan Test Bed Program concepts of operations," MDOT, revised draft, October 10, 2005.

[17]- http://wireless.fcc.gov/services/index.htm?job=service_home&id=dedicated_src

[18]- M. Wellens, B. Westphal, and P. Mahonen, "Performance Evaluation of IEEE 802.11-based WLANs in Vehicular Scenarios," Vehicular Technology Conference, IEEE 65th, Dublin, pp. 1167-1171, April 2007.

[19]- Proxim, Inc. ,“What is a Wireless LAN?” White-Paper, March 1998.

[20]- L. Stibor, Y. Zang, and H. J. Reumerman, "Neighborhood evaluation of vehicular ad-hoc network using IEEE 802.11p," p. 5, April 2007.

[21]- H. Menouar, M. Lenardi , and F. Filali, "A Survey and Qualitative Analysis of MAC Protocols for Vehicular Ad hoc NETworks (VANETs)," IEEE Wireless Communications, vol. 13, Issue: 5, pp. 1-4, October 2006.

[22]- P. Roshan, and J. Leary, "802.11 Wireless LAN Fundamentals," USA-IN: Cisco Press, January 2004.

[23]- Q. Ni, L. Romdhani, and T. Turletti, "A Survey of QoS Enhancements for IEEE 802.11 Wireless LAN," Wiley Journal of Wireless Communication and Mobile Computing (JWCMC), John Wiley and Sons Ltd., vol. 4, Issue 5, pp. 547-566, 2004.

[24]- J. Zhu, and S. Roy, "MAC for Dedicated Short Range Communications in Intelligent Transport System," IEEE Communications Magazine, vol. 41, pp. 60-67, December 2003.

[25]- ANSI/IEEE Std. 802.11, "Part 11: Wireless LAN Medium Access Control (MAC) and Physical Layer (PHY) Specifications," 1999 Edition.

[26]- J. P. Singh, N. Bambos, B. Srinivasan, and D. Clawin, "Wireless LAN Performance under Varied Stress Conditions in Vehicular Traffic Scenarios," Vehicular Technology Conference, IEEE 56th, vol. 2, pp. 743- 747, 2002.

[27]- D. N. Cottingham, I. J. Wassell, and R. K. Harle, "Performance of IEEE 802.11a in Vehicular Contexts," Vehicular Technology Conference, IEEE 65th, Dublin, pp. 854-858, 2007.

[28]- H. Abdulhamid, "Channel Estimation for 5.9 GHz DSRC Applications," Master Thesis, University of Windsor, January 2007.

[29]- H. Wu, M. Palekar, R. Guensler, and M. Hunter, J. Lee, J. Ko, "An Empirical Study of Short Range Communications for Vehicles," in Proceedings of the 2nd ACM international workshop on Vehicular ad hoc networks, Cologne, Germany, September 2005.

[30]- http://en.wikipedia.org/wiki/IEEE_802.11n

[31]- http://www.wireshark.org/

[32]- http://dast.nlanr.net/projects/Iperf/

[33]- J. Hua, J. Bao, Z. Xu, L. Meng, G. Li "Doppler shift estimation for low signal-noise-ratio environment in mobile communication systems" Proceedings of wireless communication, networking, and mobile computing 4th international conference 2008, pp. 1-4.

[34]- X. Wang, Z. Tan, G. Zhu, Z. Zhong "Doppler frequency shift estimation for Rician channel in high-speed mobile communication" Proceedings of signal processing 8th international conference 2006, vol. 3.

[35]- A. Paier, J. Karedal, N. Czink, C. Dumard, T. Zemen, F. Tufvesson, A. Molisch, C. Mecklenbrauker "Characterization of vehicle-to-vehicle radio channels from measurement at 5.2 GHz" Springer science and business media, LLC. 2008.

[36]- J. Kjellgren, S. Gadd, N. Jonsson, J. Gustavsson "Analysis of Doppler measurements of ground vehicles" Proceedings of radar conference IEEE international 2005, pp. 284-289.

[37]- A. Aguiar, J. Gross “Wireless channel models” Technical report, Technical University Berlin, Telecommunication networks group, April 2003.

[38]- M. Grag “Statistical wireless channel model” [Online], available: http://mohitgarg.vectorstar.net

[39]- S. D. Elliott and D. J. Dailey, Wireless Communications for Intelligent Transportation Systems, Boston, London: Artech House, 1995.

[40]- (2009) IntelliDrive website. [Online]. Available: http://www.intellidriveusa.org

[41]- R. Bishop, Intelligent Vehicle Technology and Trends, Boston, London: Artech House, 2005.

[42]- D. Jiang and L. Delgrossi, “IEEE 802.11p: towards an international standard for wireless access in vehicular environments,” in Proc. VTC, 2008, pp. 2036-2040.

[43]- B. Gallagher, H. Akatsuka, and H. Suzuki, “Wireless communications for vehicle safety: radio link performance and wireless connectivity methods,” IEEE Vehicular Technology Magazine, pp. 4-16+24, Oct. 2006.

[44]- Wireless LAN Medium Access Control (MAC) and Physical Layer (PHY) Specifications, IEEE Std. 802.11, 2007.

[45]- European Telecommunication Standard Institute, Digital Video Broadcasting (DVB); Framing structure, channel coding and modulation for digital terrestrial television (DVB-T), March 1997. ETSI ETS 300 744 ed.

[46]- M. Yabusaki, “Asia Pacific Viewpoint and Activities: Introduction,” 4G Forum, May. 2003.

[47]- W. Henkel, G. Taubock, P. Odling, P.O. Borjesson, and N. Petersson, “The cyclic prefix of OFDM/DMT – an analysis,” in Proc. Broadband Communications, 2002, pp. 22.1-22.3.

[48]- J.M. Holtzman and A. Sampath, “Adaptive averaging methodology for handoffs in cellular systems,” in Proc. Vehicular Technology, 1995, vol. 44(1), pp. 59–66.

[49]- C. Tepedelenlioglu, A. Abdi, G. B. Giannakis, and M. Kaveh, “Estimation of Doppler spread and signal strength in mobile communications with applications to handoff and adaptive transmission,” in Proc. WCNMC, 2001, pp. 221-241.

[50]- T. Yucek, R. M. A. Tannious, and H. Arslan, “Doppler spread estimation for wireless OFDM systems,” U.S. Patent 7599453, Oct. 6, 2009.

[51]- J. Hua, J. Bao, Z. Xu, L. Meng, and G. Li, “Doppler shift estimation for low signal-noise-ratio environment in mobile communication systems,” in Proc. WCNMC, 2008, pp. 1-4.

[52]- A. Paier, J. Karedal, N. Czink, C. Dumard, T. Zemen, F. Tufvesson, A. Molisch, and C. Mecklenbrauker, “Characterization of vehicle-to-vehicle radio channels from measurement at 5.2 GHz,” Wireless Personal Communication, vol. 50(1), pp. 19-32, Jul. 2009.

[53]- J. Kjellgren, S. Gadd, N. Jonsson, and J. Gustavsson, “Analysis of Doppler measurements of ground vehicles,” in Proc. Radar, 2005, pp. 284-289.

[54]- European Telecommunication Standard Institute, Digital Audio Broadcasting (DAB); DAB to mobile, portable and fixed Receivers, February 1995. ETSI ETS 300401 ed.1.

[55]- J. Proakis, Digital Communications, 4th ed, NY, USA: McGraw-Hill, 2001.

[56]- M. K. Simon and M. S. Alouini, Digital Communication over Fading Channels: A Unified Approach to Performance Analysis, NY, USA: John Wiley & Sons, Inc., 2000.

[57]- U. Madhow, Fundamentals of Digital Communication, NY, USA: Cambridge University Press, 2008.

[58]- (2009) Signal Processing for Communication website. [Online]. Available: http://www.dsplog.com

[59]- (2009) IEEE 1609 - Family of Standards for Wireless Access in Vehicular Environments (WAVE). [Online]. Available: http://www.standards.its.dot.gov/fact_sheet.asp?f=80

[60]- (2010) MathWorks website. [Online]. Available: http://www.mathworks.com

[61]- J. Yee and H. P. Esfahani, "Understanding wireless LAN performance trade-offs," Communication System Design, Nov. 2002.

[62]- http://www.scats.com.au

[63]- http://www.scoot-utc.com

[64]- Cristian Gorgorin, "Information Dissemination in Vehicular Ad-hoc" Graduation Project, June 2006

[65]- Victor Gradinescu, Cristian Gorgorin, Raluca Diaconescu, Valentin Cristea, and Liviu Iftode "Adaptive Traffic Lights Using Car-to-Car Communication", 2007.

[66]- Ayad M. Turky, M.S. Ahmad, M.Z.M. Yusoff1, and Baraa T. Hammad "Using Genetic Algorithm for Traffic Light Control System with a Pedestrian Crossing", 2009.

[67]- Cristian Aurelian Petroaca, "Vehicle Ad-Hoc Networks, Dedicated Short-Range Communication Protocol" Graduation Project, June 2007.

MICHIGAN OHIO UNIVERSITY TRANSPORTATION CENTER
Alternate energy and system mobility to stimulate economic development.

Report No: MIOH UTC TS18p2 2010-Final-UDM
MDOT Report No: RC-1545

TRANSPORTATION INFORMATICS: ADVANCED IMAGE PROCESSING TECHNIQUES FOR AUTOMATED PAVEMENT DISTRESS EVALUATION

FINAL REPORT

PROJECT TEAM

Dr. James Lynch
Dr. Utpal Dutta
Civil & Environmental Engineering
College of Engineering & Science
University of Detroit Mercy
4001 W. McNichols Road
Detroit, MI 48221

Undertaken in conjunction with a project led by
Dr. Ezzatollah Salari and Dr. Eddie Chou
The University of Toledo

Report No: MIOH UTC TS18p2 2010-Final-UDM

TS18, Series, UDM Project 2, September, 2010
FINAL REPORT

Developed By: **James Lynch**
Principal Investigator, UDM
lynchjj@udmercy.edu
313-993-3361

In conjunction with: **Dr. Ezzatollah Salari**
Co-Principal Investigator, UT
esalari@utoledo.edu
419-530-6002

SPONSORS

This is a Michigan Ohio University Transportation Center project supported by the U.S. Department of Transportation, the Michigan Department of Transportation (for the University of Detroit Mercy portion of the project), The University of Toledo, and the University of Detroit Mercy.

ACKNOWLEDGEMENT

The project team would like to acknowledge support from the Michigan Department of Transportation (MDOT) during the course of this research. Also the project team would like to acknowledge collaboration with researchers from The University of Toledo.

DISCLAIMERS

Technical Report Documentation Page

1. Report No. RC-1545	2. Government Accession No.	3. MDOT Project Manager Niles Annelin
4. Title and Subtitle Michigan Ohio University Transportation Center Subtitle: "Transportation Informatics: Advanced Image Processing Techniques for Automated Pavement Distress Evaluation"		5. Report Date September 2010 6. Performing Organization Code
7. Author(s) Dr. James Lynch, University of Detroit Mercy		8. Performing Org. Report No. MIOH UTC TS18p2 2011-Final-UDM
9. Performing Organization Name and Address Michigan Ohio University Transportation Center University of Detroit Mercy, Detroit, MI 48221 and University of Detroit Mercy, Detroit, MI 48221		10. Work Unit No. (TRAIS) 11. Contract No. 2007-0538 11(a). Authorization No.
12. Sponsoring Agency Name and Address Michigan Department of Transportation Van Wagoner Building, 425 West Ottawa P. O. Box 30050, Lansing, Michigan 48909		13. Type of Report & Period Covered Research, January 2009- April 2010 14. Sponsoring Agency Code

15. Supplementary Notes
Additional Sponsors: US DOT Research & Innovative Technology Administration, University of Detroit Mercy

16. Abstract

MIOH UTC TS18p2 2011-Final-UDM

Pavement condition assessment is a critical part of infrastructure management. Methods to reduce the time required to collect and analyze the data or to reduce the subjectivity in the interpretation of the data could be beneficial to parties responsible for the management of pavement structures. Two methods have been proposed, each of which addresses one of the limitations of the existing methods of pavement condition assessment.

The first method is the development of a computerized interface and database for pavement condition assessment from digital photographs. The intent of using digital photographs rather than a windshield survey for data collection is to allow easier identification of conditions and re-evaluation in the event of discrepancies among results obtained by individual inspectors.

The second method is to apply image processing techniques to the pavement condition assessment process from digital photographs. The intent of using digital photographs and image processing techniques is to automate the pavement condition assessment process, thereby removing the subjective nature of manual assessment.

The researchers at the University of Detroit Mercy developed a computer interface which allows the user to review digital photographs from Google Earth, identify defects present.

17. Key Words	18. Distribution Statement
Informatics, Infrastructure, Aging infrastructure, Intermodal terminals, Asset management, Rehabilitation (Maintenance), Image analysis, Pavement maintenance	No restrictions. This document is available to the public through the Michigan Department of Transportation.

19. Security Classification - report	20. Security Classification - page	21. No. of Pages	22. Price
		14	

Abstract

Pavement condition assessment is a critical part of infrastructure management; however, the process of collecting and analyzing the necessary data is time consuming. Furthermore, the conclusions obtained from the analysis of pavement condition data are subjective. Methods to reduce the time required to collect and analyze the data or to reduce the subjectivity in the interpretation of the data could be beneficial to parties responsible for the management of pavement structures. Two methods have been proposed, each of which addresses one of the limitations of the existing methods of pavement condition assessment.

The first method is the development of a computerized interface and database for pavement condition assessment from digital photographs. The intent of using digital photographs rather than a windshield survey for data collection is to allow easier identification of conditions and to allow easy re-evaluation in the event of discrepancies among the results obtained by individual inspectors.

The second method is to apply image processing techniques to the pavement condition assessment process from digital photographs. The intent of using digital photographs and image processing techniques is to automate the pavement condition assessment process, thereby removing the subjective nature of manual assessment.

This project began in January 2009, and this report covers work completed through December 2009, which is the time period during which the project received support from the Michigan Department of Transportation. The work continued beyond December 2009, using funds from the United States Department of Transportation and the University of Detroit Mercy. During that time period, the researchers at the University of Detroit Mercy developed a computer interface which allows the user to review digital photographs from Google Earth, identify defects present.

TABLE OF CONTENTS

LIST OF FIGURES

1. Introduction

Roads are part of the infrastructure that must be constructed, maintained, repaired, and eventually replaced, and each of these tasks require resources. The resources associated with road construction, maintenance, and repair includes the labor, equipment, and material associated with design services, material testing, demolition, and construction. During a project consisting of road maintenance, repair, or reconstruction, the traffic that normally uses that road will be delayed (at the least) and possibly re-routed, and these delays will have an economic impact on drivers, residents, and businesses. The general state of the infrastructure in the United States is poor, and the cost of upgrading the nation's infrastructure to acceptable levels is $2.2 trillion (1). Specifically, roads were rated as D- (1). Given the amount of resources, including money, associated with upgrading the nation's infrastructure, including roads, to acceptable levels, and the amount of resources associated with new road projects, the stakeholders in these projects need to carefully allocate these resources.

Asset management is a formalized process that allows stakeholders to optimize the allocation of resources for activities such as construction, maintenance, repair, and replacement of their systems or infrastructure. Asset management principles applied directly to pavement is generally called pavement management. A pavement management program includes collecting and analyzing data on the use and condition of roads within the subject network (2). The results of the use and condition analysis could be used to forecast future use and condition, to make strategic decisions, and to prioritize resource allocation.

Pavement condition is determined by identifying the type, severity, and extent of various defects or modes of deterioration and assigning a condition value to the pavement. Some of the common pavement condition assessment methods include the Federal Highway Administration (FHWA) method, the Pavement Surface Evaluation and Rating (PASER) method, and pavement condition index (PCI) method. In all of these methods, a condition number is assigned from the results of a windshield survey, which is a visual inspection of the pavement performed while driving the subject road.

Some limitations of this visual inspection are the effort required to obtain the results, trade-offs between the data collection process and the quality of the data, and the variability in the results. Furthermore, if the assessment data are collected from a windshield survey, the survey could interfere with traffic flow or traffic flow could obscure some of the conditions that the evaluators would need to note.

The trade-offs between the effort required to obtain the results and the quality of the data can be illustrated through the results of a study performed by the Kent County Road Commission (KCRC) in 2001 (3). Prior to 2001, the KCRC had been using the PCI method for pavement condition assessment. Based on the procedures associated with the PCI method and the size of the KCRC network, only one-third of the network could be evaluated in any given year. The KCRC undertook a research project that involved evaluating the roads using both the PCI and PASER method and comparing the results in terms of cost of data collection and processing, type of data collected, and recommended action from the results. The outcomes were that effort associated with data collection and processing using the PASER method were such that the entire

network could be evaluated in one year, compared to three years by the PCI method; and that the recommended course of action based on the evaluation results were generally similar. The downside of assessing pavement condition with the PASER method is that the PASER method does not provide the level of detail of the PCI method.

The repeatability of pavement evaluation can be addressed by having several inspectors evaluate the same subject road several times and by different methods. In one such study, a team of three inspectors evaluated the same road twice using visual inspection of the subject road and twice using visual inspection of digital photographs of the subject road. The results were that the variability between inspections ranged from 41 to 43 percent for visual inspection of the subject road, compared to 8 to 19 percent from visual inspection of digital photographs of the subject road (4).

Assessing pavement condition by visual inspection, whether the data are collected from a windshield survey or from photographs, is subjective in that it relies on interpretation from a human inspector. Non-destructive test methods, such as the falling weight deflectometer (FWD) and the international roughness index (IRI) have been developed to provide pavement condition. The FWD is performed with an impulsive force applied with a drop weight and a series of transducers to measure the response of the pavement-soil system. The results are analyzed to determine the elastic constants of the pavement, aggregate base, and subgrade (5). The results of the IRI are the roughness (6). Both of these methods require trained operators and instrumented vehicles, and will cause some traffic delay during testing.

Techniques from digital signal processing have been proposed and tested as a method to automatically identify and quantify various types of defects in pavement (7). The intent of these methods is to remove the subjective nature of human interpretation from the pavement condition assessment process.

As the size of the nation's road network increases, the resources required to maintain this network will increase, and that includes inspection. Some challenges for those agencies responsible for condition assessment include obtaining enough data to make strategic and specific decisions, and obtaining those data economically and reliably.

This is a report on the first phase of a project that will result in a computerized interface for the evaluation of pavement condition using digital photographs and the development of a computerized database of the pavement condition assessment results.

2. Background

Asset management allows stakeholders to systematically collect, organize, and analyze data related to the performance and condition of buildings, utilities, pavements, etc., for which that stakeholder is responsible. Ultimately, decision-makers can better allocate resources related to the operation of that asset.

Pavement is an asset that stakeholders, such as state and local governments, must construct, maintain, repair, and eventually replace. A pavement management system is a specific form of asset management that allows the stakeholders to allocate resources for the pavement system.

A key element of a pavement management system is collecting and analyzing pavement condition data. The traditional methods of pavement evaluation rely on teams of investigators driving the subject site and making notes as they drive. This method is time-consuming and subject to operator error. An attempt to improve pavement evaluation is to use digital photographs, typically taken with specially instrumented vehicles.

3. Pavement Management Systems

Medina et al. (1999) cited a portion of the *Pavement Policy for Highways* that defines pavement management as, "a set of tools or methods that can aid decision-makers in finding cost-effective strategies for providing and maintaining pavements in a serviceable condition" (8). The pavement management system must address methods, schedules, and budgets associated with achieving the goals.

The three main components of a pavement management system are data collection, data analysis, and implementation. One approach to pavement management is shown schematically in Figure 1.

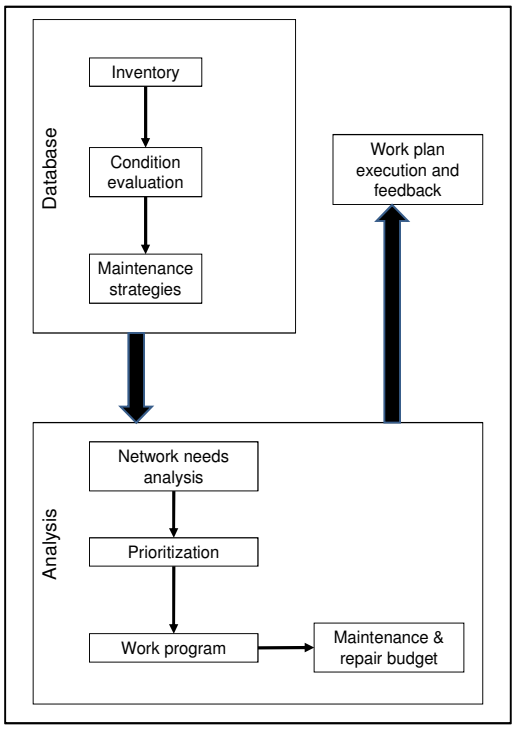

Figure 1: Pavement Management Structure
(after Medina et al., 1994)

The data collection component is summarized in a database which includes the inventory, condition evaluation, and maintenance strategies. The analysis portion of the Pavement Management Structure requires the synthesis of the pavement condition assessment, which is determined from the condition evaluation and the maintenance strategies, along with global concerns related to the network. Based on the results of the network need, one can prioritize the work and develop a work plan, which is, of course, constrained by budgets. Once projects have been selected that are high on the priority list and feasible within the budget, they are implemented.

4. Pavement Condition Assessment

Pavement condition assessment is the process by which existing pavement structures are evaluated to identify conditions that could affect ride quality, rider safety, or structure life. Numerous pavement condition assessment methods have been developed, but all of them have common features such as:

- Type of condition
- Severity of condition
- Extent of condition

Once the assessment has been completed, decisions could be made related to maintenance, repair, or reconstruction of the pavement.

The PASER method is the pavement condition assessment that was developed by researchers at the University of Wisconsin-Madison (9). Pavement structures evaluated by the PASER method are rated from 10 (excellent condition) to 1 (failed pavement), based on the type, severity, and extent of the observed conditions. In general, structural problems of low severity result in a lower PASER rating than non-structural problems of higher severity. For example, a longitudinal crack that develops along a construction joint derives from quality during construction and is not a structural condition. If the longitudinal crack width is small, i.e., less than one-quarter inch, the PASER rating is 8, which is considered "Good." On the other hand, rutting represents structural failure of the pavement. Even minor rutting, i.e., depth less than one-half inch, results in a PASER rating of 3, which is considered "Poor."

In the method developed by the FHWA, the conditions that could affect ride quality or ride safety, or that represent structural defects, have been identified and classified as Low Severity, Medium Severity, or High Severity (10). The presence of different conditions, their severity, and extent are used to determine the overall pavement condition.

In the PCI method, the type, severity, and extent of each condition is identified and the overall pavement condition is rated from 1 (failed) to 100 (no defects) using the evaluation procedures of the PCI method (3).

5. Database Types and Characteristics

A database is a model that stores values such that relationships can be easily identified and results can be easily analyzed. According to Ullman and Widom (2008), all data models, whether databases or otherwise, require the developer to define:

- The structure of the data
- Operations on the data
- Constraints on the data (11)

In a database, the structure of the data is a two-dimensional array called a *table*. The table is comprised of *records*, and each record contains *fields*. The data in a particular field could be numeric, string, logical, etc. The fields in a record can contain mixed data types, but once a data type is selected, all records for that field must follow the selected data type. The

operations on the data are called *queries*, and can include isolating certain records or fields within each record based on user-defined criteria. For example, the user may decide to identify all records for which a field is greater than a threshold value. The constraints on the data depend on the type of data. For example, if a particular field is the month, it must fall between 1 and 12 for numerical data or must contain the name of a month for string data.

The results of data operations performed on a data structure that meets the defined constraints are presented as *reports*. Common report formats include tabular and graphical. Furthermore, graphical reports could be graphs or drawings.

Graphical information system (GIS) is a software package that combines database functions with computer-aided drafting (CAD) and mapping capabilities. It is well-suited to analyze data from a database and generate graphical reports as drawings. The drawings could be generated with the CAD features of the GIS software or could be overlain on maps that are imported from another software package.

6. Image Processing

The content of a photograph will contain one or more objects of interest, i.e., the subject of the photograph, but also will contain a background, and may contain objects that are not part of the subject of the photograph. The interpretation of photographs includes identifying and

classifying objects of interest captured in the photograph, and may include quantifying these objects.

In the case of digital photography, the image is discretized into a set of pixels. The number of pixels in a photograph depends on the resolution of the camera, the size of the lens, and the distance from the camera to the subject of the photograph. Another way of thinking about a digital photograph is the scale of the pixel. Each object in the photograph is a certain size and is captured by a certain number of pixels. From this information, the scale of each pixel can be computed. In theory, the objects of interest in a digital photograph can be quantified by determining the scale of the photograph and counting the number of pixels required to capture each object of interest.

Some challenges in quantifying the contents of a digital image are illumination, noise, and ill-defined boundaries between objects and background. Image processing is a field that attempts to improve the probability of identifying, quantifying, and analyzing objects of interest within a digital photograph.

The basic steps in the processing of a digital image are coding, enhancement, restoration, and feature extraction (12). Image coding is the process of collecting the data. Image enhancement includes isolating features of interest or removing items that are not of interest. Image restoration can include reducing the effects of uneven illumination and of noise. Image feature extraction consists of determining the desired characteristics of the objects of interest. A common method of removing noise from images is filtering (13).

7. Results of Investigation

The goal of this project is to develop an interactive pavement condition database system that could be used as part of a pavement management system. This project, which is being conducted in conjunction with a similar project at the University of Toledo (UT), was first funded in January 2009 and is presently funded through August 2009. At the beginning of the UDM portion of this project, the researchers at UT are currently in Year 2 funding through the MIOH UTC.

The activities of the project completed thus far by the researchers at UDM have been to:

- Review general topics within pavement condition assessment;
- Review general topics within databases;
- Review the methods used for pavement condition assessment within the state of Michigan; and
- Design an interface and database that incorporates aspects of successfully developed pavement condition assessment systems but meets the criteria used within the state of Michigan.

The researchers at UDM met with researchers at UT, who had begun their research a year in advance of the researchers at UDM. The outcomes of the meetings at UT were:

1) Pavement Condition Assessment
   a) The researchers at UT use the FHWA method of pavement evaluation.
   b) The researchers at UT analyze digital photographs to assess the pavement condition (some of these photographs have been collected by the researchers and some have been collected from Google Map.)
   c) The researchers at UT have developed a computerized database and interface to analyze the digital photographs of pavement sections and to determine the condition of those pavement sections using the FHWA method.
2) Digital Image Processing applied to Digital Images of Pavement
   a) The researchers at UT have collected digital images of pavements sections with varying types of defects.

b) The researchers at UT have developed methods to automatically isolate the defect portion on a digital photograph of pavement surface that contains defects.
c) Quantify the defects identified in Step 2b.

8. Pavement Condition Assessment

The standard method of pavement condition assessment in the state of Michigan is the PASER method. The PASER rating is most often determined through a windshield survey, although the use of digital photographs for manual interpretation is becoming more common (3).

The inspectors collect the data by driving the subject road, recording observations, and rating the road. The inspectors compare their results and, if the results are acceptably close to each other, the average of the results becomes the rating. If the results are not acceptably close to each other, the road would be evaluated again, presumably by driving it again.

One method of improving the evaluation of road is to collect digital photographs of the road and determine the pavement condition from the photographs. The evaluation could be performed at the office or laboratory after all photographs have been collected. An advantage of this method over evaluation during driving is that if the results do not match, the team of inspectors could re-evaluate the road from the photographs rather than by driving the subject road again.

The method of evaluating roads from digital photographs is, theoretically, less expensive than evaluating the roads by driving them; however, it is still expensive in that it requires specially instrumented vehicles. Researchers at UT have developed a method of evaluating pavement from digital photographs collected through Google Earth.

The UDM researchers have met with the UT researchers to review their procedures and interface. The UT researchers evaluate their pavement using the FHWA method; whereas, the UDM researchers would use the PASER method. Because the pavements are evaluated by different methods, the UDM researchers would need to develop a new interface and database. At this time, the UDM researchers have identified a set of criteria for the interface and database and have begun the design of these systems.

The UDM researchers used the requirements of the PASER method and the concepts presented during the meeting with the UT researchers to develop a computerized interface for pavement evaluation and database for the management of that pavement evaluation data. The interface was coded in visual basic and the details of that interface are shown in Figure 2.

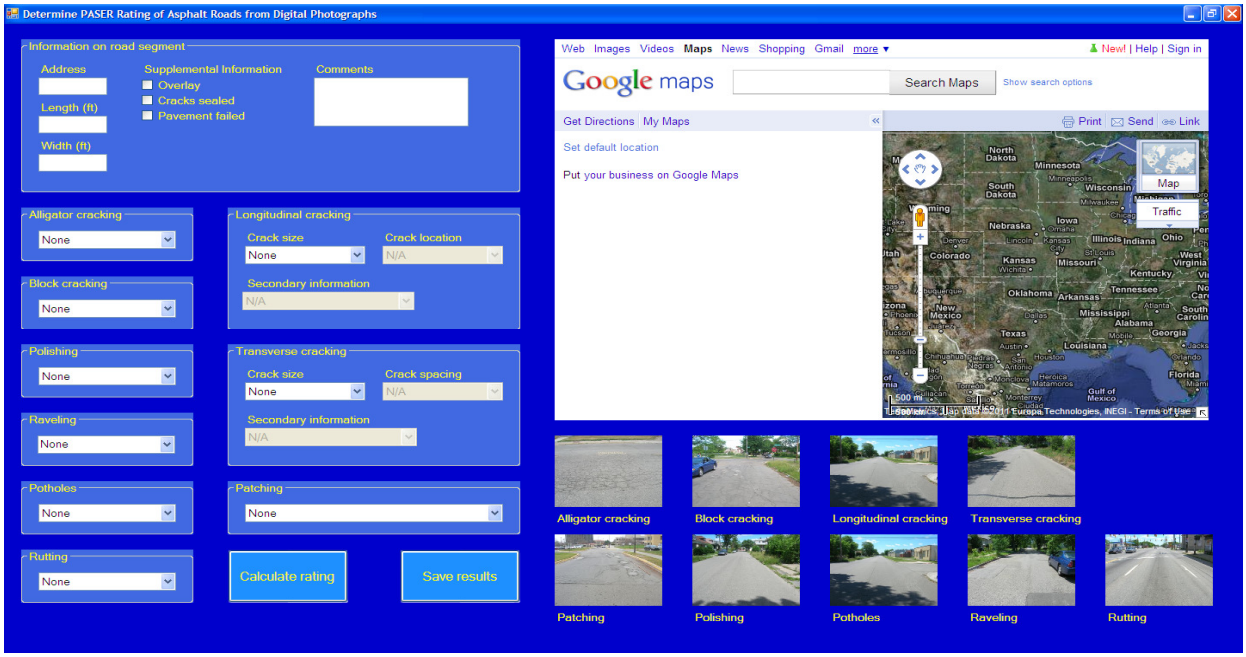

Figure 2: Computerized interface for pavement evaluation by PASER method

The interface has distinct areas related to the general information on the road segment, the image of the road segment, the conditions identified in the evaluation, and conditions. The upper left-hand corner of the interface has a set of text boxes in which the user can enter basic information on the segment, such as address, width, and length. This portion also includes check boxes for specific conditions that automatically define the PASER value, i.e., "Recent Overlay" and "Failed." The upper right-hand corner is a Web browser that allows the user to review the photographs. Below the Web browser are sample photographs of the nine conditions considered in the PASER method. Most of the left side contains drop-down menus in which the user selects the conditions present and the severity of these conditions. The "Calculate rating" button executes code that parses the contents of the drop-down menus and check boxes to determine the PASER number. The "Save results" button executes code that performs the same function as the "Calculate rating" button but it also writes the results to the database.

The functionality of the interface and the concept of using digital photographs from Google Earth were tested by evaluating several stretches of road for which PASER results were available and then comparing the two sets of results. The city of Novi, Mich., was selected and the results of the 2008 evaluation of that city's road network were used as the test case (14). Several roads of low, medium, and high traffic were selected. The results indicate that the pavement evaluation using digital images found on Google Earth were ±1 of the results presented in the 2008 evaluation. Other road segments were evaluated, but those results could not be compared to published values because the researchers did not have access to reports on the evaluation of those roads.

From the results of the Novi evaluation and of other roads, a preliminary finding is that digital images available on Google Earth provide a good first pass at pavement evaluation but will probably not replace digital images collected with specially instrumented vehicles designed for the collection of pavement condition data, nor will they replace windshield surveys. Not every road of interest will be in the Google Earth database, and the quality of photographs in that database could vary significantly. A particular concern is the availability of images of wide roads or divided roads. The images collected for Google Earth appear to be collected as the vehicle drives one direction in one lane of the road. If the road is wide or divided, the pavement on the opposite side of the road may not be visible.

The researchers at UDM have begun working with Arc Map GIS to develop methods of graphically presenting results from pavement condition assessment projects.

9. Digital Image Processing Applied to Digital Images of Pavement

The researchers at UT have developed a method of automatically identifying and quantifying cracks in pavement by applying techniques from digital image processing to digital photographs of pavement. The images were collected with a digital camera. The image enhancement was performed with median filtering. After the image was enhanced, pixels corresponding to cracks were identified. The pixels corresponding to cracks were analyzed to determine direction and connectivity, and to determine the size of the cracks.

10. Next Steps

The next steps in this research project are to add functionality to the computerized interface and database, and to link the contents of the pavement condition database to an Arc Map GIS database. Once all of the functions have been added to the database, a formal study will be undertaken to identify advantages and disadvantages of pavement condition assessment using digital images available through Google Earth.

11. References

[1] ASCE, "Report Card for America's Infrastructure," http://www.infrastructurereportcard.org/, American Society of Civil Engineers, 2009.

[2] Tsai, Y. and Lai, J. S. (2002). "Framework and Strategy for Implementing an Information Technology-based Pavement Management System," *Transportation Research Record, 1816*, TRB, National Research Council, Washington, D.C., pp. 56-64.

[3] Kent County Road Commission Planning Division, (2001). "Comparison of Pavement Condition Rating Systems PASER vs. PCI".

[4] Lee, H. and Kim, J. (2007). "Analysis of Error in Pavement Ground Truth Indicators for Evaluating the Accuracy of Automated Image Collection and Analysis System," *Pavement Surface Condition/Performance Assessment: Reliability and Relevancy of Procedures and Technologies, ASTM STP 1486*, ASTM International, West Conshohocken, PA, 2007, pp. 12 – 26.

[5] Huang, Y. H. (1993). *Pavement Analysis and Design*, Pearson Prentice Hall, Upper Saddle River, NJ.

[6] IRI, International Roughness Indicator.

[7] Koutsopoulos, H. N. and Downey, A. B. (1993). "Primitive-based Classification of Pavement Cracking Images," *Journal of Transportation Engineering*, ASCE 119(3), pp 402 – 418.

[8] Medina, A., Flintsch, G. W., and Zaniewski, J. P. (1999). "Geographic Information Systems-based Pavement Management System: A Case Study," *Transportation Research Record, 1652*, TRB, National Research Council, Washington D.C., pp. 151-157.

[9] Walker, D., Entine, L., and Kummer, S., (2002). *Pavement Surface Evaluation and Rating: Asphalt Roads*, Transportation Information Center University of Wisconsin-Madison, Madison, WI.

[10] Miller, J. S. and Bellinger W. Y., (2003). "Distress Identification Manual for the Long-Term Pavement Performance Program," Publication Number FHWA-RD-03-031, U. S. Department of Transportation Federal Highway Administration.

[11] Ullman, J. D. and Widom, J. (2008). *A First Course in Database System, 3rd Edition*, Prentice Hall, Upper Saddle River, NJ.

[12] van der Heijden, F. (1994). *Image Based Measurement Systems: Object Recognition and Parameter Estimation*, John Wiley & Sons, Chichester, England.

[13] Gonzalez, R. C., Woods, R. E., and Eddins, S. L., (2004). *Digital Image Processing using Matlab ®,* Pearson Prentice Hall, Upper Saddle River, NJ.

[14] "Pavement Condition Survey - City of Novi, Novi, MI" SME Project Number PP58667, Jan. 28, 2009.

12. List of Acronyms

CAD	Computer-aided drafting
FWD	Falling weight deflectometer
FHWA	Federal Highway Administration
GIS	Graphical information system
IRI	International roughness index
KCRC	Kent County Road Commission
PASER	Pavement Surface Evaluation and Rating
PCI	Pavement condition index

MICHIGAN OHIO UNIVERSITY TRANSPORTATION CENTER
Alternate energy and system mobility to stimulate economic development.

Report No: MIOH UTC TS21p1 2010-Final
MDOT Report No: RC1545

MANAGEMENT AND ANALYSIS OF MICHIGAN INTELLIGENT TRANSPORTATION SYSTEMS CENTER DATA WITH APPLICATION TO THE DETROIT AREA I-75 CORRIDOR

FINAL REPORT

PROJECT TEAM

Dr. Charles Standridge
Dr. Shabbir Choudhuri
School of Engineering

Dr. David Zeitler
Department of Statistics

Grand Valley State University
301 West Fulton
Grand Rapids, MI 49504

With Contributions By
Dr. Snehamay Khasnabis
College of Engineering
Wayne State University
2168 Engineering Building
Detroit, MI 48202

Report No: MIOH UTC TS21p1 2010-Final

TS 21, Series, Project 1, September 2008 through August 2009
FINAL REPORT

Developed By:

Charles R. Standridge
Principal Investigator, GVSU
standric@gvsu.edu
616-331-6750

Shabbir Choudhuri
Investigator, GVSU
choudhus@gvsu.edu

David Zeitler
Investigator, GVSU
zeitlerd@gvsu.edu

With Contributions By:

Snehamay Khasnabis
Co-Principal Investigator, WSU
skhas@wayne.edu

SPONSORS

This is a Michigan Ohio University Transportation Center project funded by the U.S. Department of Transportation, the Michigan Department of Transportation, Grand Valley State University, and Wayne State University.

ACKNOWLEDGEMENT

In addition to the Sponsors, the Project Team would like to acknowledge support from the Michigan Intelligent Transportation Systems Center (MITSC), and the Southeastern Michigan Council of Governments (SEMCOG) during the course of this research. This support is gratefully acknowledged.

DISCLAIMERS

Abstract

An understanding of traffic flow in time and space is fundamental to the development of strategies for the efficient use of the existing transportation infrastructure in large metropolitan areas. Thus, this project involved developing the methods necessary to systematically describe, explain, and predict the flow of traffic with respect to time and space. The utility of this knowledge was demonstrated in routing voluminous traffic. Achieving these objectives required the collection, management, and analysis of traffic data concerning volume, speed, and traffic sensor occupancy. Management of this data required the design and implementation of a large scale database management system as well as assuring the quality of the collected data. Descriptive, explanatory, and predictive statistical models were developed to help gain the desired understanding of traffic flow. Application efforts focused on the Detroit metropolitan area. Traffic data was regularly obtained from the Michigan Intelligent Transportation Systems Center. Statistical models of traffic flow in the Detroit area I-75 corridor were constructed. A previously developed routing model was extended and adapted to the I-75 corridor and the newly developed statistical models incorporated to help compute traffic flow metrics. Both a software solver and a hardware solver for the model were implemented. In addition, a framework for traffic simulation was developed and applied to the development and calibration of a micro-simulation model including the same part of the I-75 corridor. This model was used to demonstrate the benefits of guidance in re-routing traffic as a result of a traffic incident.

Technical Report Documentation Page

1. Report No. RC-1545	2. Government Accession No.	3. MDOT Project Manager Niles Annelin
4. Title and Subtitle Michigan Ohio University Transportation Center Subtitle: "Management and Analysis of Michigan Intelligent Transportation Systems Center Data with Application to the Detroit Area I-75 Corridor", Project 1.		5. Report Date November 2010 6. Performing Organization Code
7. Author(s) Dr. Charles R. Standridge, Grand Valley State University Dr. Shabbir Choudhuri, Grand Valley State University Dr. David Zeitler, Grand Valley State University Dr. Snehamay Khasnabis, Wayne State University		8. Performing Org. Report No. MIOH UTC TS21p1 2010-Final
9. Performing Organization Name and Address Michigan Ohio University Transportation Center University of Detroit Mercy, Detroit, MI 48221 and Grand Valley State University, Grand Rapids, MI 49504 and Wayne State University, Detroit, MI 48202		10. Work Unit No. (TRAIS) 11. Contract No. 2007-0538 11(a). Authorization No.
12. Sponsoring Agency Name and Address Michigan Department of Transportation Van Wagoner Building, 425 West Ottawa P. O. Box 30050, Lansing, Michigan 48909		13. Type of Report & Period Covered Research, September 2008 – August 2009 14. Sponsoring Agency Code

15. Supplementary Notes

Additional Sponsors: US DOT Research & Innovative Technology Administration, Grand Valley State University, and Wayne State University. Additional Support: the Michigan Intelligent Transportation Systems Center (MITSC), and the Southeastern Michigan Council of Governments (SEMCOG).

16. Abstract

MIOH UTC TS21p1 2010-Final

An understanding of traffic flow in time and space is fundamental to the development of strategies for the efficient use of the existing transportation infrastructure in large metropolitan areas. Thus, this project involved developing the methods necessary to systematically describe, explain, and predict the flow of traffic with respect to time and space. The utility of this knowledge was demonstrated in routing voluminous traffic. Achieving these objectives required the collection, management, and analysis of traffic data concerning volume, speed, and traffic sensor occupancy. Management of this data required the design and implementation of a large scale database management system as well as assuring the quality of the collected data. Descriptive, explanatory, and predictive statistical models were developed to help gain the desired understanding of traffic flow. Application efforts focused on the Detroit metropolitan area. Traffic data was regularly obtained from the Michigan Intelligent Transportation System Center. Statistical models of traffic flow in the Detroit area I-75 corridor were constructed.

Continued On Next Page…

A previously developed routing model was extended and adapted to the I-75 corridor and the newly developed statistical models incorporated to help compute traffic flow metrics. Both a software solver and a hardware solver for the model were implemented. In addition, a framework for traffic simulation was developed and applied to the development and calibration of a micro-simulation model including the same part of the I-75 corridor. This model was used to demonstrate the benefits of guidance in re-routing traffic as a result of a traffic incident.

17. Key Words	**18. Distribution Statement**
Intelligent transportation systems, Traffic flow, Time, Traffic data, Data collection, Transportation infrastructure, Traffic volume, Detroit (Michigan), Research projects.	No restrictions. This document is available to the public through the Michigan Department of Transportation.

19. Security Classification - report	**20. Security Classification - page**	**21. No. of Pages**	**22. Price**
		20	

Table of Contents

List of Tables

List of Figures

1. Executive Summary

As investment in construction and expansion decreases, making better use of urban traffic infrastructure is essential. One important aspect of doing so is developing an understanding of the movement of traffic in time and space, including how to re-route large volumes of traffic in case of an incident. Meeting this need requires developing traffic data analysis methods, dynamic re-routing models, and simulation-based incident management system assessment tools. The development of such tools was the focus of this project. In addition, validation of the tools was performed through their application to I-75 corridor in Detroit. The project team consisted of faculty and students from Grand Valley State University and Wayne State University supported by staff from the Michigan Department of Transportation and the Southeast Michigan Council of Governments. The project was divided into three components, each of which will be discussed in turn.

Statistical analysis of intelligent transportation systems data, in particular the data from the Michigan Intelligent Transportation Systems Center, was one project component. Data from one 12-month period was graphed. By examination of the graphs, it was determined that non-holiday weekday data was homogeneous and of the most interest. A multi-level regression model was employed to predict traffic speed update to 30 minutes in the future using only the current speed and the speed one minute in the past. The coefficients of the regression were themselves equations whose parameters were estimated by regression as a function of prediction interval. Predicted speeds were compared to actual speeds with the largest median error being 5.4% over the 30-minutes time horizon.

A dynamic re-routing model for large volumes of traffic around one or more freeway incidents was developed and applied. The model was implemented in software using MATLAB. Results showed the proper change in routes as more traffic was re-routed. A prototype hardware solver for the model, an analog computer, was developed as well. This addressed the issue of computational speed of the re-routing algorithm in order to produce routes repeated in near-real time.

A five-step framework for constructing, calibrating, and applying a micro-simulation model to assess incident management strategies has been developed. Calibration was successfully performed in light of no-traffic incidents and selected traffic incidents using both graphs and standard metrics of performance. Application of the modeled showed that incident management strategies improved traffic flow in terms of both volume and speed.

2. Action Plan for Research

The action plan was designed to help the research team meet its fundamental goals of understanding traffic flow in time and space as well as to apply this understanding in routing voluminous traffic. The research team sought to transform the speed, volume, and occupancy data collected by the Michigan Intelligent Transportation Systems Center (MITSC) concerning the interstate system in the Detroit metropolitan area into a highly usable public resource. Meeting this objective involved the following:

1. Systematically acquire the MITSC data, which has been accomplished and is ongoing via FTP twice a month.
2. Design and implement a database management system for this voluminous data, about 50 gigabytes per year within a MySQL database as well as demonstrate this capability for a small, less than 10percent, subset of the data concerning the Detroit area I-75 corridor.
3. Evaluate the quality of the data. This included determining missing data values and evaluating the effectiveness of the traffic sensors in consistently collecting data.
4. Develop and implement procedures for descriptive, explanatory, and predictive statistical model building to represent the movement of traffic in time and space as well as building models.
5. Apply these results to voluminous traffic re-routing in the Detroit area I-75 corridor, thus demonstrating their utility.
    a. Continue refining routing models that take into account time and space.
    b. Continue refining both hardware and software based solvers for these models.
    c. Develop a procedure to assist an intelligent transportation systems (ITS) in finding alternate routes in an efficient manner in response to traffic incidents.
6. Develop a procedure for developing, calibrating, and applying micro-simulation to traffic incident management scenario (IMS) assessment. Apply this procedure to the Detroit area I-75 corridor.

3. Introduction

A team of university-based transportation system experts, simulation experts, optimization experts, and applied statisticians has been assembled to develop, implement, and validate an approach to reducing congestion in integrated transportation corridors. This team has been working together since November 2006 with funding provided by the Michigan-Ohio University Transportation Center (MIOH-UTC) through the U.S. Department of Transportation (USDOT) with matching funds supplied by the Michigan Department of Transportation (M-DOT), Grand Valley State University (GVSU), and Wayne State University (WSU). This report covers the period from September 2008 through August 2009.

The team has been working in three areas:

1. Statistical analysis of intelligent transportation systems data, in particular, the data from MITSC.
2. Optimal re-routing of traffic due to traffic incidents on a freeway.
3. Micro-simulation to assess the ability of incident management strategies to effectively re-route traffic around an incident.

As a proof of concept of the procedures and methods we have developed, the above have been applied to a selected portion of the I-75 corridor in Detroit.

The effort has been lead by faculty in the GVSU School of Engineering (SOE) and Department of Statistics as well as the WSU Department of Civil and Environmental Engineering (CEE). The organization of the project is shown in Figure 1.

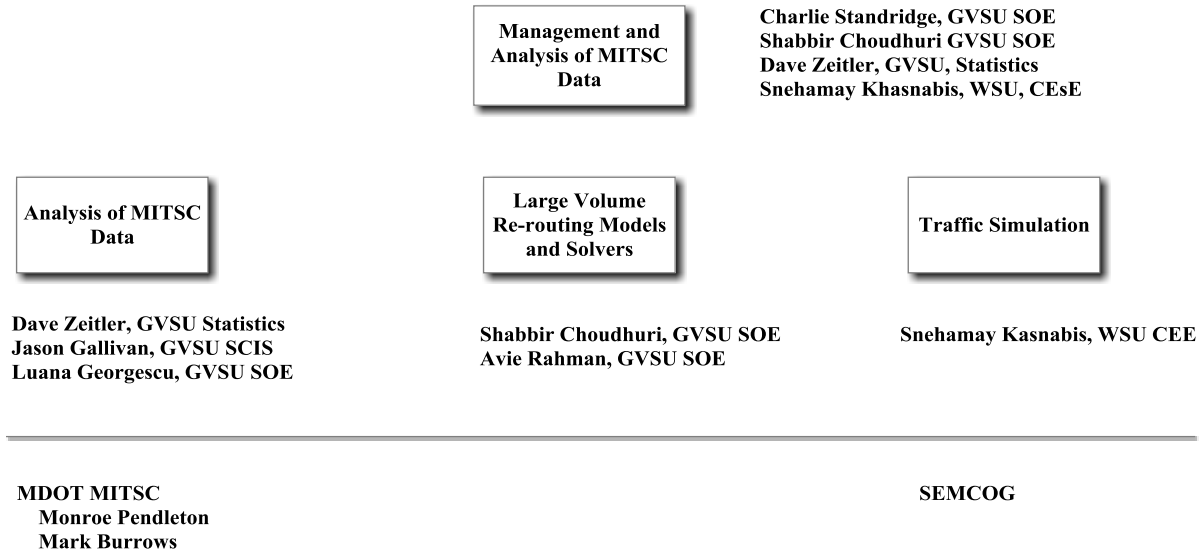

Figure 1. Project Organization

Support for our work has been provided by the Southeastern Michigan Council of Governments (SEMCOG) as well as MDOT, particularly the staff of the MITSC.

Project activities have been supported by graduate assistants and undergraduate students. All students who have participated in this project and related research are listed in Table 1.

Table 1. Student Participation

Student	Faculty Mentor	Department	Degree Program	Status on Project	When on Project
Vishnu Yada	Shabbir Choudhuri	GVSU, Computer Information Systems	Master of Science	20 hours weekly, Graduate Assistant	January – December 2007
Ashfaq Rahman	Shabbir Chouduri	GVSU, School of Engineering	Master of Science	20 hours weekly, Graduate Assistant	August 2007 – present
Andrew Even	Shabbir Chouduri	GVSU, School of Engineering	Master of Science in Engineering	Capstone project, unpaid	January – December 2007
S. Mishra	Snehamay Khasnabis	WSU, Civil & Environmental Engineering	Ph.D.	Hourly, Graduate Assistant	January 2007 – August 2009
A. Manori	Snehamay Khasnabis	WSU, Civil & Environmental Engineering	Master of Science	Hourly, Graduate Assistant	September 2007- December 2007
S. Swain	Snehamay Khasnabis	WSU, Civil & Environmental Engineering	Master of Science	Hourly, Graduate Assistant	February 2008- August 2010
E. Elibe	Snehamay Khasnabis	WSU, Civil & Environmental Engineering	Master of Science	Hourly, Graduate Assistant	September 2008 – August 2010
S. Vuyyura	Snehamay Khasnabis	WSU, Civil & Environmental Engineering	Master of Science	Hourly, Graduate Assistant	September 2008 – August 2010
Jason Gallivan	Charlie Standridge	GVSU, Computer Information Systems	Master of Science	20 hours weekly, Graduate Assistant	January 2007 – present
Andrew Van Garderen	Dave Zeitler	GVSU, Statistics Department	Bachelor of Science	Semester stipend	August 2007 – May 2008
Allison Wehr	Dave Zeitler	GVSU, Statistics Department	Bachelor of Science	Semester stipend	January – May 2008
Ryan Masselink	Dave Zeitler	GVSU, School of Engineering	Bachelor of Science in Engineering	Semester stipend	May 2009 – April 2010

4. Objective

The team has established that its primary research objectives are:

- *To describe, explain, and predict the flow of traffic in a corridor with respect to time and space.*
- *To apply these results in the routing of voluminous traffic.*

The team has addressed the former through the statistical analysis of traffic data obtained from MITSC. Achieving the latter has to do with developing re-routing models for voluminous traffic in response to traffic incidents, particularly on freeways, as well as assessing IMS using micro-simulation.

5. Scope

In pursuit of its objectives, the team has developed methods in the statistical analysis of traffic data, optimization modeling of voluminous traffic re-routing, and micro-simulation analysis of traffic IMS. Proof of concept for these methods has been accomplished by applying them to the I-75 traffic corridor in Detroit, specifically southbound I-75 between 8 Mile Road on the north and Clay on the south for statistical analysis as shown in Table 2, as well as Baldwin Avenue on the north and 8 Mile Road on the south, as shown in Figure 2, for optimization modeling and micro-simulation.

Table 2. Location of the Sensors for Statistical Analysis

Location	Sensor ID	Latitude	Longitude
SB I-75 S of 8 Mile Road	68865	42.44226000000	-83.09524000000
SB I-75 S of 8 Mile Road	68612	42.43976105390	-83.09518743310
SB I-75 S of 7 Mile Road	68353	42.43219393	-83.09489812000
SB I-75 S of Mc Nichols (6 Mile) Road	67841	42.41632659650	-83.08648851500
SB I-75 S of Davison	67333	42.40634558200	-83.07608999730
SB I-75 S of Holbrook	66561	42.38444669210	-83.06696384570
SB I-75 S of Clay	66305	42.37999518890	-83.06403518030

Traffic data of interest was from the period November 2006 through August 2009. Sub-periods were selected in which to demonstrate each method.

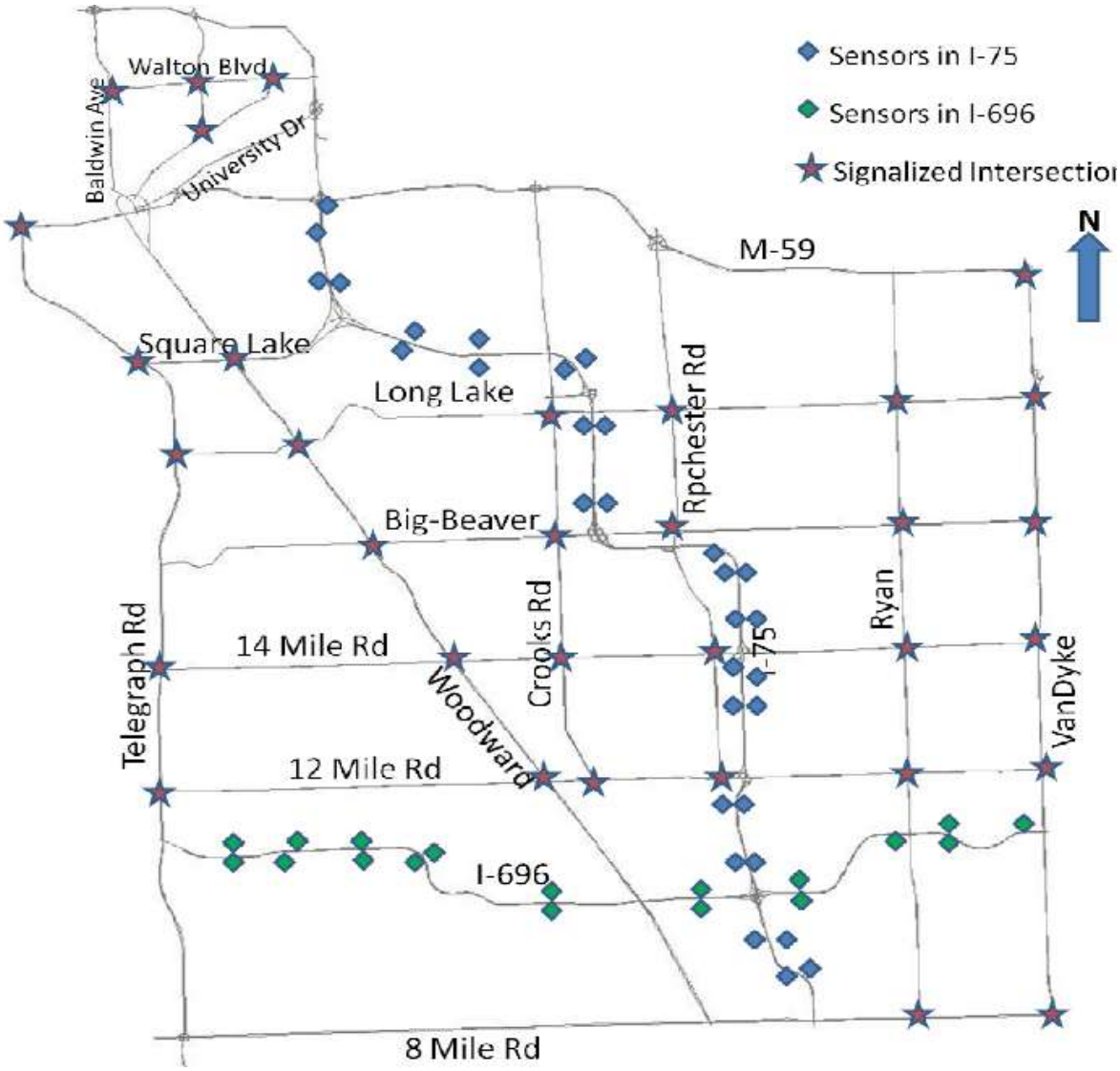

Figure 2. Northern Portion of I-75 Corridor in Detroit

6. Methodology

6.1. Statistical Analysis

The statistical analysis of the MITSC data was done in two stages. In the first stage, the data was examined and graphed. Upon examination of the data, it became apparent that some of the sensors transmit erroneous data that is not useful. Only about seven of them, those listed in Table 2 above, transmitted data that could be used in statistical analysis.

The traffic data was graphed for each day of the year for each sensor. Data from November 2006 through October 2007 was employed. It was clear from these graphs that weekday traffic patterns were different from weekend patterns and holidays. No differences were noted among the days of the week or the months of the year. Thus, the second stage statistical analysis used all non-holiday weekdays.

For each minute, the average across days was computed and subtracted from each day's observed value. The statistical analysis of these residuals proceeded as follows. An explanatory / predictive multi-level model (MLM) for traffic speed was developed using regression. The variance in the residuals can be explained based on the current speed and the speed at one time unit previous, in other words by the current speed and the acceleration. The intercept, b_{0n}, is the average of the residuals which must be 0.

$$S_{t+n} = \underbrace{\bar{S}_{t+n}}_{\text{1st level of MLM}} + \underbrace{b_{0n} + b_{1n} * r_{s_t} + b_{2n} * r_{s_{t-1}}}_{\text{2nd level of MLM}}$$

n is prediction horizon

S_{t+n} is the future speed at time t+n

$\bar{S}_{t+n}$ are the means for every minute calculated at t+n

r_{s_t} are the residuals of the speed calculated at the current time t

$r_{s_{t-1}}$ are the residuals of the speed calculated at the past time t-1

b_{0n} is the constant term or the intercept

b_{1n}, and b_{2n} are regression coefficients

The coefficients b_{1n} and b_{2n} are themselves estimated by regression equations, thus the MLM. The prediction horizon n ranged from 1 to 30 minutes with intervals 1, 2,.., 10, 15, and 30 minutes used to estimate the parameters of the regression equations of the coefficients in the above equation.

6.2. Re-Routing Models

The re-routing model previously developed was extended and tailored to the traffic corridor shown in Figure 2. This previous model is shown in Figure 3.

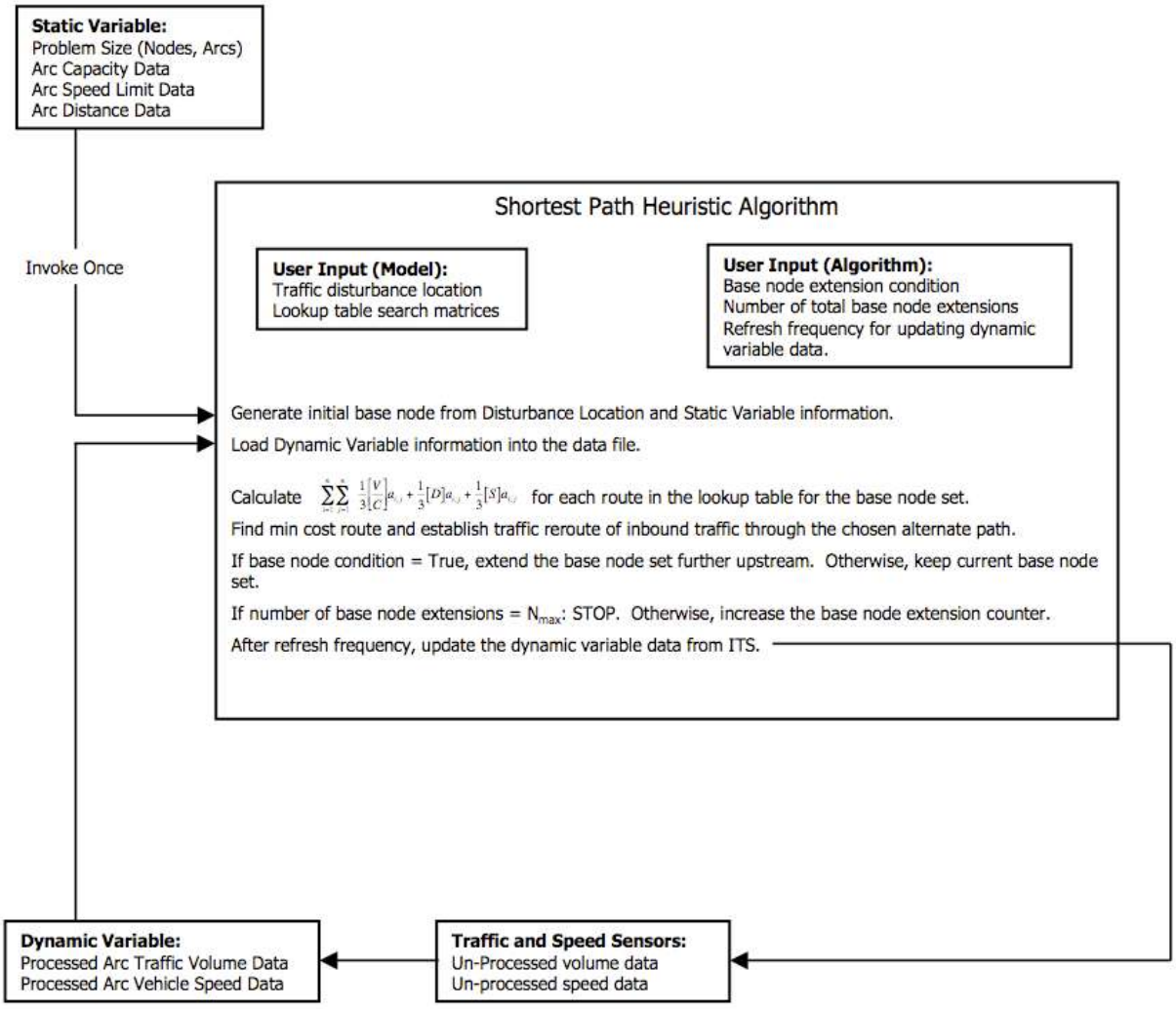

Figure 3. Previous Re-Routing Model

The revised model is called DETSIM and has the following features:

- Graphical Road Network Editor
- Graphical output
- Interactive selection of one or more incidence locations
- Partial closure of a freeway segment
- Usage of standard data interchange format
- A simple simulator of traffic flow
- An improved solver written in MATLAB

The size of the traffic network in Figure 2 raised the issue of whether a software model solver could always compute re-routing information in near real-time. Thus, a hardware implementation was proposed. An electrical network has stark similarities with a traffic network. If the traffic flow of arc can be modeled as a resistor in the electrical network, then the electrical system itself becomes an analog of the traffic system. The re-routing solution can be obtained as quickly as electricity will flow through the network.

6.3. Micro-Simulation for Incident Management Assessment Strategies

A framework for the assessment of incident management strategies using micro-simulation has been developed. The five-step methodology encompassing policy and operational strategies associated with IMS can be summarized as follows:

1. Network creation and assembling various databases.
2. Identification of the policies and development of algorithm that comprise the IMS.
3. Calibration of the micro-simulation model.
4. Conducting micro-simulation-based experiments, by creating incidents on the network, and by using the databases, algorithm and policies identified in the earlier steps.
5. Analysis of the results.

The experimental design used in testing the framework encompasses two major components: Model Calibration (Step 3) and Model Application (Step 4). Table 3 gives the measures of calibration.

Table 3. Measures of Calibration

GOODNESS-OF-FIT MEASURES	DESIRABLE
RMSE (Measures Overall % Error)	Close to 0
Correlation Coefficient: *r*	Close to 1
Theil's Inequality Coefficient: *Ui* (Disproportionate Weight of Large Errors)	Close to 0
Theil's Component: *Us* (Measure of Variance Proportion)	Close to 0
Theil's Component:*Uc* (Measure of Covariance Proportion)	Close to 1
Theil's Component:*Um* (Measure of Bias Proportion)	Close to 0

Calibration is done with respect to both traffic volume and traffic speed, both with no traffic incidents and in the presence of traffic incidents.

To test the framework, a model of the traffic network shown in Figure 2 was developed using AIMSUN. Data sources included Traffic.com, MITSC, SEMCOG, and MDOT's Freeway Courtesy Patrol.

7. Discussion of Results

7.1. Statistical Analysis

The graphs in Figure 4 show speed and occupancy for one weekday for sensor 68855. Occupancy is increasing between about 6-10am with a minimal speed decrease. Speed is low (about 30 mph) at a congestion point between 3:30-6:00pm.

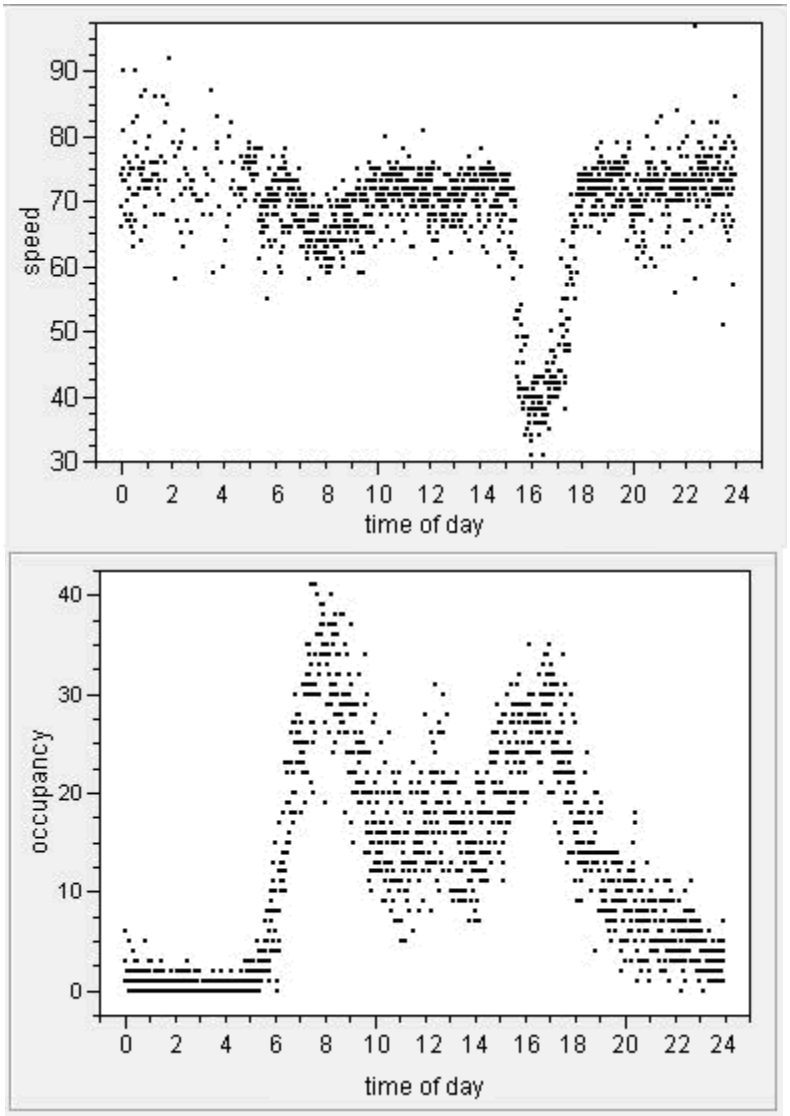

Figure 4. Speed and Occupancy for One Day for the Sensor 68865

Figure 5 show the results of estimating the regression coefficients b_{1n} and b_{2n} in the MLM.

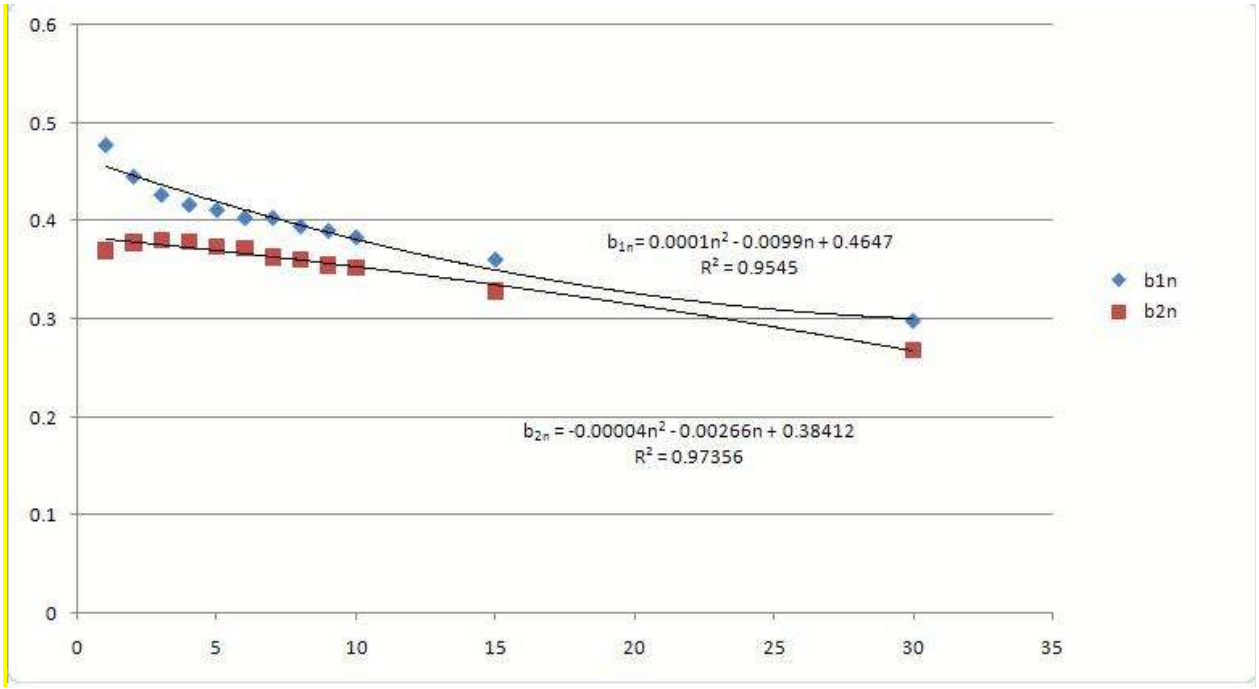

Figure 5. Regression Equations for Coefficients

To evaluate the model, predicted speeds were compared with observed speeds. The median error (ME) for the five prediction horizons ranged from 2.6 to 5.4 percent, with smaller percentages associated with smaller prediction horizons. Figures 6 and 7 show the prediction errors for time intervals of one minute and 30 minutes.

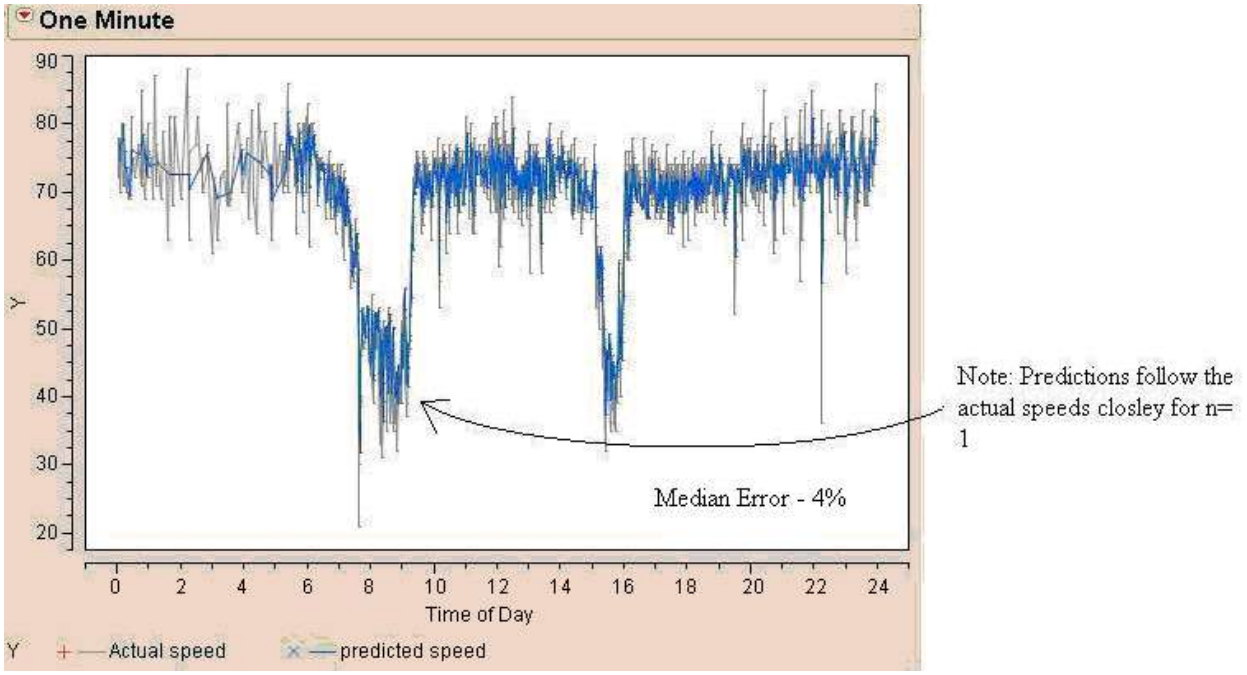

Figure 6. Prediction Error for One-Minute Time Interval

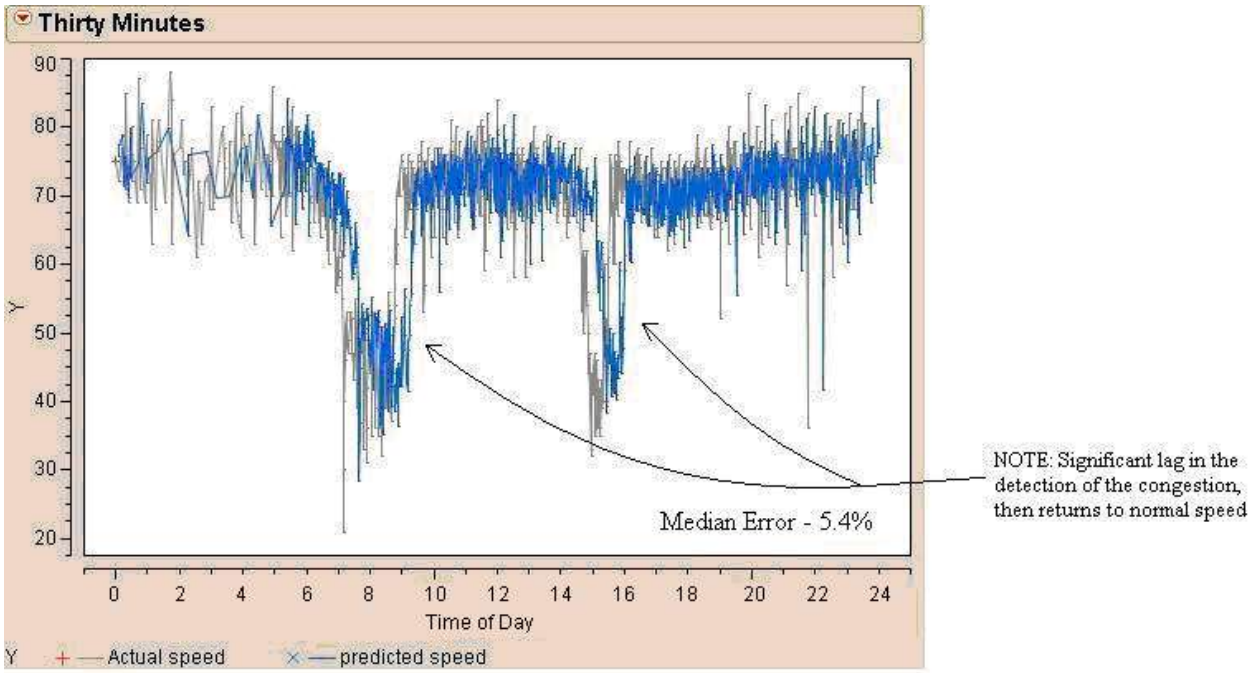

Figure 7. Prediction Error for 30 Minute Time Interval

7.2. Re-Routing Models

With respect to the improved software solver, results showed that the best detour path, with respect to avoiding congestion, changes frequently. This was expected as the traffic flow metric on each arc in the traffic network is constantly recomputed, which allows the re-routing to adapt to changes in volume and speed due to previous traffic re-routing.

With respect to the hardware solver, the traffic corridor shown in Figure 2 was implemented as an electric circuit whose schematic is shown in Figure 8. By locating the highest current paths, the best routes with respect to traffic flow can be determined. To measure current, the voltage drop across a fixed value resistor was amplified by an instrumental amplifier, and then sensed by a micro-controller's Analog-to-Digital Converter (ADC). The ADC values were then compared for each segment to find the optimal path.

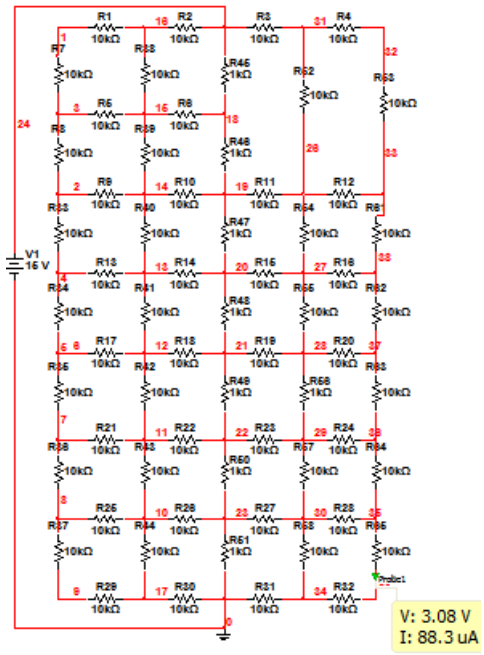

Figure 8. Electrical Schematic Representation of the Traffic Corridor of Figure 2

7.3. Micro-Simulation for Incident Management Assessment Strategies

The model was first calibrated with no incidents considered. Traffic volume data was collected from Traffic.com in the form of sensor data for three hours on 7/12/2008, from 3:00 to 6:00 P.M. This volume data, when input to AIMSUN was instrumental in creating a 185 X 185 origin-destination (O-D) matrix for this three-hour duration. A sub-area O-D matrix (185 X 185) is generated for the network under consideration from SEMCOG'S large regional matrix for the year 2015. The two 185 X 185 O-D matrices developed using two different tools from two different sources are input back to AIMSUN and are subjected to dynamic traffic assignment (DTA), while adjusting the DTA parameters.

Sensors present in the model are used to record traffic volumes at five-minute intervals. These traffic volumes are compared to achieve a reasonable correspondence. DTA parameters are adjusted until a desired degree of correspondence is achieved between the two data sources.

Figures 9, 10, 11 and 12 show typical graphs used to determine calibration. Tables 4 and 5 show the statistical results. These graphs and tables show a close enough correspondence between simulation results and collected data to verify calibration.

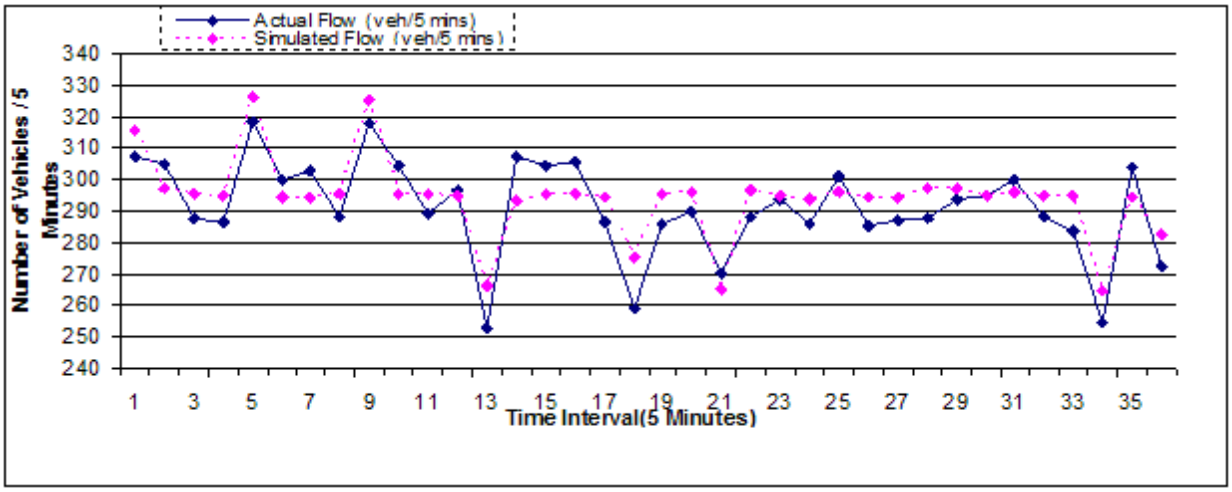

Figure 9. No Incident Scenario
Sensor: MI075200N (I-75 South of 12 Mile Road), Date: 7/12/2008, Time: 3:00 - 6:00 P.M.

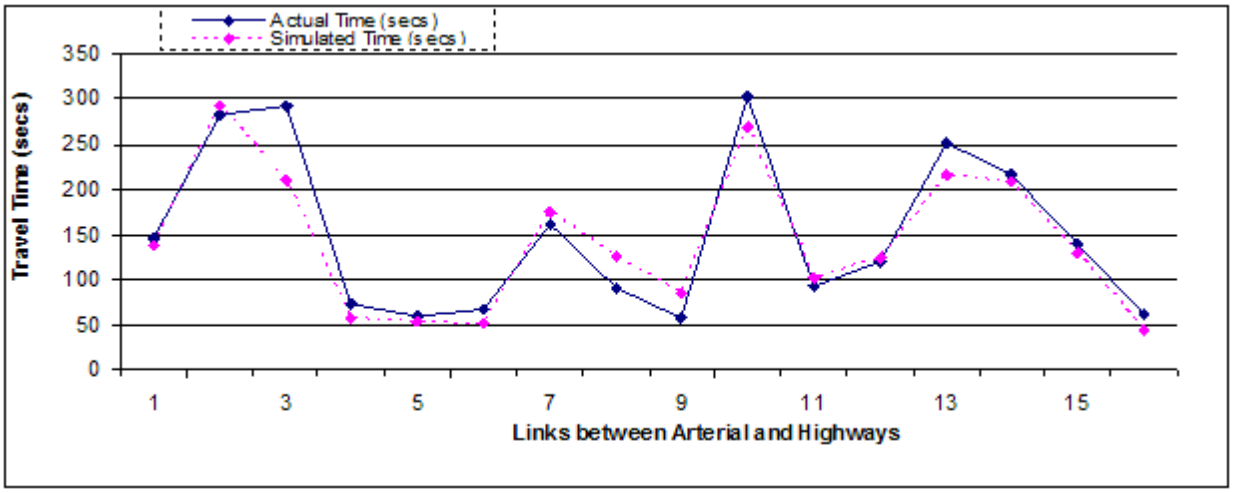

Figure 10. No Incident Scenario
Date: 7/12/2008, Time: 3:00 - 4:00 P.M.

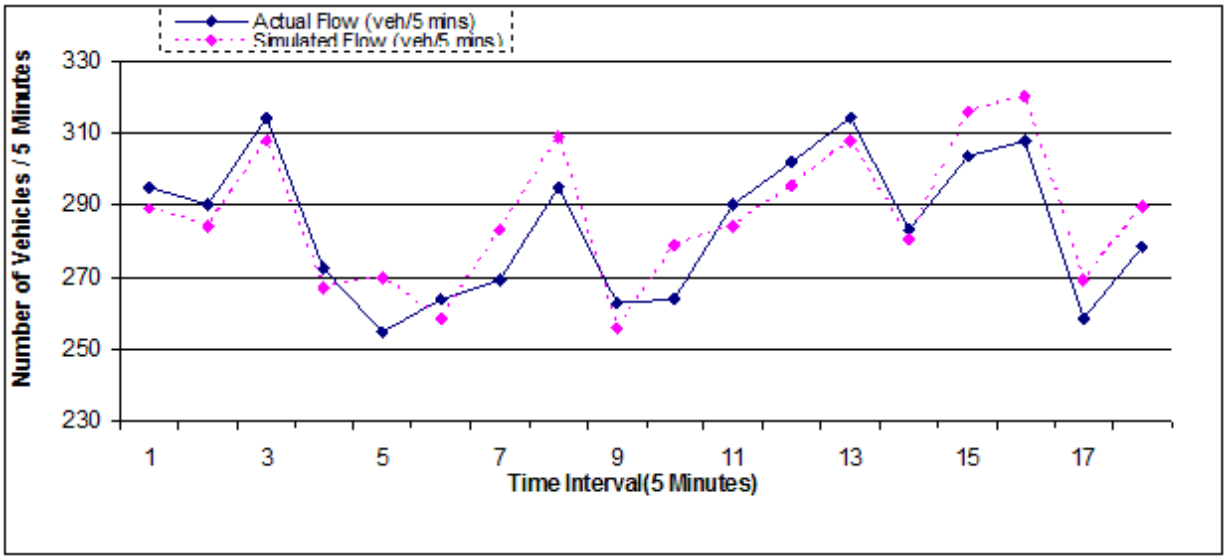

Figure 11. Incident Scenario: Abandoned Vehicle
Right-Lane Closure: SB I-75 @ 12 Mile Road
Sensor: MI075180S (I-75 South of 14 Mile Road), Date: 1/19/2009, Time: 8:35 - 10:00 A.M.

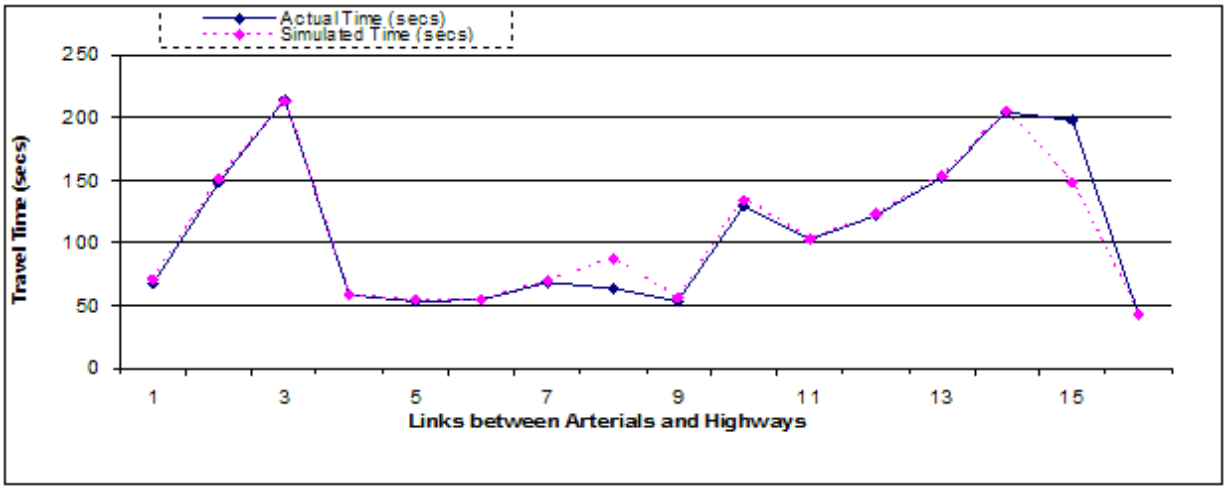

Figure 12. Incident Scenario: Abandoned Vehicle
Right-Lane Closure: SB I-75 @ 12 Mile Road

Table 4. Summary of Calibration Test Results – Traffic Volume

WITH/WITHOUT INCIDENT	TYPES OF INCIDENTS	DATE, TIME OF THE INCIDENT	LOCATION OF THE INCIDENT	LOCATION OF THE SENSOR	FIGURE	ROOT MEAN SQUARE ERROR (RMSE) % ERROR	CORRELATION COEFFICIENT (R)	THEIL'S WEIGHT OF LARGE ERRORS (UI)	THEIL'S VARIANCE PROPORTION (US)	THEIL'S COVARIANCE PROPORTION (UC)	THEIL'S BIAS PROPORTION (UM)
No Incident	No incidents	7/12/2008, 3PM-6PM	No Incident	S of 12 Mile at I-75	1A	0.03	0.85	0.01	0.12	0.89	0.12
				S of 14 Mile at I-75	1B	0.07	0.95	0.03	0.05	0.98	0.10
				S of 12 Mile at I-75	1C	0.03	0.86	0.02	0.29	0.84	0.02
		9/22/2008, 3PM-6PM	No Incident	S of 12 Mile at I-75	2A	0.02	0.95	0.01	0.03	0.98	0.12
				S of 14 Mile at I-75	2B	0.02	0.86	0.01	0.23	0.87	0.04
				S of 14 Mile at I-75	2C	0.03	0.95	0.01	0.26	0.86	0.02
With Incident	Abandoned Vehicles	1/19/2009, 8:35AM-10:00AM	SB-I-75 @ 12 Mile (Right Lane)	North of I-696 at I-75	4A	0.03	0.92	0.02	0.01	0.97	0.14
				S of 14 Mile at I-75	4B	0.04	0.88	0.02	0.00	0.98	0.07
	Flat Tire	1/19/2009, 5:40PM-7:05PM	SB-I-75 @ 12 Mile (Right Lane)	S of 12 Mile at I-75	4C	0.03	0.97	0.02	0.12	0.80	0.13
				S of 14 Mile at I-75	4D	0.03	0.98	0.02	0.06	0.81	0.18
	No Gas	1/24/2009, 3:15PM-4:40PM	NB-I-75 @ 13 Mile (Right Lane)	S of 14 Mile at I-75	4E	0.03	0.90	0.01	0.14	0.90	0.04
				S of 12 Mile at I-75	4F	0.02	0.92	0.01	0.20	0.86	0.01
	Mechanical Problems	1/26/2009, 2:25PM-3:50PM	SB-I-75 @ 12 Mile (Right Lane)	S of 12 Mile at I-75	4G	0.03	0.95	0.01	0.11	0.89	0.09
				S of 14 Mile at I-75	4H	0.03	0.97	0.01	0.15	0.89	0.03
	Debris on Road	2/6/2009, 4:25PM-5:50PM	SB-I-75 @ 14 Mile (Right Lane)	S of 14 Mile at I-75	4I	0.02	0.91	0.01	0.02	0.98	0.11
				S of 15 Mile at I-75	4J	0.02	0.96	0.01	0.10	0.95	0.01
	Accident	1/13/2009, 8:10AM-9:35AM	SB-I-75 @ 13 Mile (Right Lane)	S of 12 Mile at I-75	4K	0.03	0.93	0.01	0.02	0.86	0.34
				S of 14 Mile at I-75	4L	0.03	0.96	0.01	0.02	0.90	0.26

Table 5. Summary of Calibration Test Results – Travel Time

WITH/WITHOUT INCIDENT	TYPES OF INCIDENTS	DATE, TIME OF THE INCIDENT	LOCATION OF THE INCIDENT	FIGURE	ROOT MEAN SQUARE ERROR (RMSE) % ERROR	CORRELATION COEFFICIENT (R)	THEIL'S WEIGHT OF LARGE ERRORS (UI)	THEIL'S VARIANCE PROPORTION (US)	THEIL'S COVARIANCE PROPORTION (UC)	THEIL'S BIAS PROPORTION (UM)
No Incident	No incidents	7/12/2008, 3PM-4PM	No Incident	3A	0.21	0.96	0.08	0.16	0.82	0.09
		9/22/2008, 3PM-4PM	No Incident	3B	0.15	0.97	0.07	0.10	0.80	0.15
With Incident	Abandoned Vehicles	1/19/2009, 8:35AM-10:00AM	SB-I-75 @ 12 Mile (Right Lane)	5A	0.12	0.97	0.06	0.13	0.94	0.00
	Flat Tire	1/19/2009, 5:40PM-7:05PM	SB-I-75 @ 12 Mile (Right Lane)	5B	0.06	0.99	0.04	0.19	0.85	0.03
	No Gas	1/24/2009, 3:15PM-4:40PM	NB-I-75 @ 13 Mile (Right Lane)	5C	0.11	0.98	0.04	0.03	0.89	0.14
	Mechanical Problems	1/26/2009, 2:25PM-3:50PM	SB-I-75 @ 12 Mile (Right Lane)	5D	0.07	0.98	0.05	0.04	0.94	0.07
	Debris on Road	2/6/2009, 4:25PM-5:50PM	SB-I-75 @ 14 Mile (Right Lane)	5E	0.18	0.96	0.07	0.01	0.87	0.17
	Accident	1/13/2009, 8:10AM-9:35AM	SB-I-75 @ 13 Mile (Right Lane)	5F	0.06	0.99	0.02	0.00	0.98	0.08

The model, calibrated along with the appropriate parameters, was used to test the effectiveness of alternative IMS on the same network. The two types of IMS were adapted from AIMSUN, then tested, lane closure, and forced turning (FT). Lane closure refers to a scenario where single or multiple lanes are closed for a given freeway section. FT refers to scenarios where vehicles are forced to divert from their original intended path, due to the occurrence of a road closure. For each IMS tested, two types of performance data are gathered, unit travel time and unit delay, both measured in seconds per kilometer per vehicle. In all the cases recorded, both travel time and delay measures are reduced under guided conditions signifying a positive impact of the IMS in alleviating congestion.

8. Conclusions

8.1. Statistical Analysis

MLM can be use to predict traffic speed up to 30 minutes in the future. Only two speed values are required to make such predictions, making computations fast and data storage requirements minimal.

8.2. Re-Routing Models

Dynamic re-routing models can be used with an ITS to route traffic around incidents in near real-time, including changing alternative routes in response to traffic flow. A hardware-based model solver may be needed to perform needed computations in near-real time.

8.3. Micro-Simulation for Incident Management Assessment Strategies

Micro simulation analysis shows that managed routing of traffic improves traffic volume and travel time in dealing with a traffic incident.

9. Recommendations for Future Research

9.1. Statistical Analysis

Additional validation of the MLM model can be obtained by re-estimating the parameters using data from a later 12-month period.

In addition, the MITSC data can be used to indicate the potential benefits of avoiding turbulent conditions such as those caused by non-metered entry during rush hour.

9.2. Re-Routing Models

For the re-routing model of the I-75 corridor, a formal comparison of the computational speed of the hardware and software solvers would be helpful.

A test of the re-routing model with respect to re-routing traffic around a freeway incident at MITSC is a necessary next step. This would involve obtaining the data needed by the model in near-real time and transmitting re-routing information via message signs or other electronic means to vehicles. Performance metrics would need to be developed.

9.3. Micro-Simulation for Incident Management Assessment Strategies

The role of traffic simulation in regional modeling should be explored.

10. Recommendations for Implementation

10.1. Statistical Analysis

MLM models can be straightforwardly developed from traffic data on speed. Speed prediction from MLM models can be used in software to compute the freeway travel time from one location to another. Such times are often displayed on message signs.

10.2. Re-Routing Models

Implementation would depend on the results of the test of the model at the MITSC described in the preceding section.

10.3. Micro-Simulation for Incident Management Assessment Strategies

Traffic routing policies should be assessed using micro-simulation before implementation.

11. List of Acronyms, Abbreviations, and Symbols

ADC	Analog-to-Digital Converter
CEE	Civil and Environmental Engineering
DTA	Dynamic Traffic Assignment
FT	Forced Turning
GVSU	Grand Valley State University
IMS	Incident Management Scenario
ITS	Intelligent Transportation Systems
MDOT	Michigan Department of Transportation
ME	Median Error
MIOH-UTC	Michigan Ohio University Transportation Center
MITSC	Michigan Intelligent Transportation Systems Center
MLM	Multi-Level Model
O-D	Origin Destination Matrix
SEMCOG	Southeastern Michigan Council of Governments
SOE	School of Engineering
USDOT	United States Department of Transportation
WSU	Wayne State University

12. Bibliography

Even, A. 2007. Multi-Commodity Dynamic Vehicle Routing Subject to Capacity Constraints With Real Time Transportation Information. Unpublished Masters Project. School of Engineering, Padnos College of Engineering and Computing, Grand Valley State University.
Even, A., S. Choudhuri, and C. Standridge. 2007. Dynamic Traffic Rerouting with Feedback from Infrastructure, INFORMS Annual Meeting, Seattle.

Georgescu, L. 2009. Applied Analysis Of Urban Interstate Highway Traffic Data. Unpublished Masters Thesis. School of Engineering, Padnos College of Engineering and Computing, Grand Valley State University.

Khasnabis, S., S. Mishra, S. Swaim, E. A. Elibe, and S. Vuyyuru. 2010. Management and Analysis of Michigan Intelligent Transportation System Center Data with Application to the Detroit Area I-75 Corridor. Working Paper. Department of Civil and Environmental Engineering, Wayne State University. Detroit, MI.

Mishra, S., and S. Khasnabis. 2007. Survey of Literature Review: Congestion Relief by Travel Time Minimization in Near Real Time. Working Paper. Department of Civil and Environmental Engineering, Wayne State University. Detroit, MI.

Mishra, S., S.Khasnabis., S.K.Swain., and A.Manori. 2009. A Framework for Evaluating Incident Management Strategies on Freeways. 2nd International Symposium for Freeway and Tollway Operations (ISFO), Honolulu, Hawaii.

Rahman, A., S. Choudhuri, and C. Standridge. 2008. A Real-Time Hardware-Based Solver for the Large-Scale Traffic Rerouting Problem Using ITS Data. INFORMS Annual Meeting, Washington, DC.

Rahman, A. 2009. Unpublished Masters Thesis. School of Engineering, Padnos College of Engineering and Computing, Grand Valley State University.

Standridge, Charles, J. Gallivan, and S. Choudhuri. 2009. Simulation Software Interoperability, Simulation Environments, and Extensions. Proceedings of the 2009 Industrial Engineering Research Conference.

Yada, V., S. Choudhuri, and C. Standridge. 2007. Web-Based Data Repository for Collaboration among ITS Researchers. INFORMS Annual Meeting, Seattle.

MICHIGAN OHIO UNIVERSITY TRANSPORTATION CENTER
Alternate energy and system mobility to stimulate economic development.

Report No: MIOH UTC TS22p1-2 2010-Final

MDOT Report No: RC1545

SAFETY EVALUATION OF SCATS CONTROL SYSTEM

FINAL REPORT

PROJECT TEAM

Dr. Utpal Dutta
Sujay Bodke
Brian Dara
Dr. James Lynch
Department of Civil & Environmental Engineering
University of Detroit Mercy
4001 W. McNichols Road
Detroit, MI 48221

Report No: MIOH UTC TS22p1-2 2010-Final

TS22, Series, Projects 1 and 2, September 2010
FINAL REPORT

Developed by: **Dr. Utpal Dutta**
Co- Principal Investigator, UDM
duttau@udmercy.edu

In conjunction with: **Dr. James Lynch**
Co-Principal Investigator, UDM
lynchjj@udmercy.edu

Graduate Research Assistants: **Sujay Bodke and Brian Dara**

SPONSORS

This is a Michigan Ohio University Transportation Center project supported by the U.S. Department of Transportation, the Michigan Department of Transportation and the University of Detroit Mercy.

ACKNOWLEDGEMENT

The Project Team would like to acknowledge support from the Michigan Department of Transportation (MDOT), the Road Commission for Oakland County (RCOC), and the Southeastern Michigan Council of Governments (SEMCOG) during the course of this research.

DISCLAIMERS

Technical Report Documentation Page

1. Report No. RC-1545	**2. Government Accession No.**	**3. MDOT Project Manager** Niles Annelin
4. Title and Subtitle Michigan Ohio University Transportation Center Subtitle: "Safety Evaluation of the SCATS Control System", Project 1.		**5. Report Date** September 2010 **6. Performing Organization Code**
7. Author(s) Dr. Utpal Dutta, University of Detroit Mercy Dr. James Lynch, University of Detroit Mercy		**8. Performing Org. Report No.** MIOH UTC TS22p1-2 2010-Final
9. Performing Organization Name and Address Michigan Ohio University Transportation Center University of Detroit Mercy, Detroit, MI 48221		**10. Work Unit No. (TRAIS)** **11. Contract No.** 2007-0538 **11(a). Authorization No.**
12. Sponsoring Agency Name and Address Michigan Department of Transportation Van Wagoner Building, 425 West Ottawa P. O. Box 30050, Lansing, Michigan 48909		**13. Type of Report & Period Covered** Research, January 2009 - September 2010 **14. Sponsoring Agency Code**

15. Supplementary Notes
Additional Sponsors: US DOT Research & Innovative Technology Administration and University of Detroit Mercy. Additional Support: the Road Commission for Oakland County (RCOC), and the Southeastern Michigan Council of Governments (SEMCOG).

16. Abstract MIOH UTC TS22p1-2 2010-Final

Since 1992, traffic signals in Oakland County and a portion of Macomb and Wayne Counties of Michigan have been converted to the Sydney Coordinated Adaptive Traffic System (SCATS). County traffic engineers have been adjusting various SCATS parameters to improve its effectiveness in terms of delay, traffic flow, queue length, and crash and injury occurrences. In 2008, a study was conducted to evaluate the performance of the SCATS system on M-59, between Pontiac Lake East to Pontiac Lake West in Waterford Township, Michigan, in terms of delay, flow, queue length, fuel consumption and emission. As a part of this study various performance parameters of SCATS system were compared with the Pre-timed signal system. Performance of the SCATS system was found to be superior for several of the performance measures during each Peak period. When compared to Pre-timed signal, installation and maintenance cost of SCATS system is almost two times greater. Therefore, there is a need to determine the added related benefits of SCATS system. In this context, determination of crash benefit of SCATS can play a significant role. If we can combine congestion and crash related benefits, then it is most likely combined benefits will overweigh the cost. Crash data from 1999 to 2008 of two corridors, one controlled by the SCATS and other by the Pre-timed signal system were examined to determine the effectiveness of SCATS system. In order to evaluate the effectiveness of SCATS signal system, intersections as well as segment crash data before and after the installation of SCATS signals were compared. In addition, a series of statistical tests were performed to compare safety performance of SCATS and pre-timed signal systems. It was observed that there was shift in severity types A and B to C, which is noteworthy. However, statistical tests were not able to identify any difference of significance at 95 percent confidence level. Finally, cost related information for both SCATS as well as Pre-timed was also computed and compared.

17. Key Words SCATS (Computer program), Intelligent transportation systems, Adaptive traffic systems, Measures of effectiveness, Traffic control devices, Traffic signals, Traffic signal control systems, Mobility, Traffic congestion, Michigan, and Research projects.		**18. Distribution Statement** No restrictions. This document is available to the public through the Michigan Department of Transportation.	
19. Security Classification - report	**20. Security Classification - page**	**21. No. of Pages** 29	**22. Price**

Abstract

Since 1992, traffic signals in Oakland County and a portion of Macomb and Wayne Counties of Michigan have been converted to the Sydney Coordinated Adaptive Traffic System (SCATS). County traffic engineers have been adjusting various SCATS parameters to improve its effectiveness in terms of delay, traffic flow, queue length, and crash and injury occurrences.

In 2008, a study was conducted to evaluate the performance of the SCATS system on M-59, between Pontiac Lake East to Pontiac Lake West in Waterford Township, Michigan, in terms of delay, flow, queue length, fuel consumption and emission. As a part of this study various performance parameters of SCATS system were compared with the Pre-timed signal system. Performance of the SCATS system was found to be superior for several of the performance measures during each Peak period. When compared to Pre-timed signal, installation and maintenance cost of SCATS system is almost two times greater. Therefore, there is a need to determine the added related benefits of SCATS system. In this context, determination of crash benefit of SCATS can play a significant role. If we can combine congestion and crash related benefits, then it is most likely combined benefits will overweigh the cost.

Crash data from 1999 to 2008 of two corridors, one controlled by the SCATS and other by the Pre-timed signal system were examined to determine the effectiveness of SCATS system. In order to evaluate the effectiveness of SCATS signal system, intersections as well as segment crash data before and after the installation of SCATS signals were compared. In addition, a series of statistical tests were performed to compare safety performance of SCATS and pre-timed signal systems. It was observed that there was shift in severity types A and B to C, which is noteworthy. However, statistical tests were not able to identify any difference of significance at 95 percent confidence level. Finally, cost related information for both SCATS as well as Pre-timed was also computed and compared.

Table of Contents

List of Tables

List of Figures

1. Introduction

Increasing travel demand and lack of sufficient highway capacity is a serious problem in most major metropolitan areas in the United States. Large metropolitan cities have been experiencing increased traffic congestion problems over the past several years. The total delay that drivers experience has increased from 0.7 billion hours in 1982 to 3.7 billion hours in 2003. [1] Combining the 3.7 billion hours of delay and 2.3 billion gallons of fuel consumed, due to congestion, leads to a total congestion cost of $63 billion dollars for drivers in 85 of the largest metropolitan areas of the nation. [1]

In spite of the implementation of many demand management measures, the congestion in most urban areas is still increasing. In many areas congestion is no longer limited to two peak hours in a day; instead, it is extended to two to three hours in the morning, afternoon and evening. Thus, the congestion experienced on urban and suburban freeways and arterial streets results in delays to the motorist, excess fuel consumption and a high level of pollutant emission not only during the peak hours in a day, but also for several hours throughout the day.

As many urban areas across the nation, Oakland County, one of the largest county in the State of Michigan has been experiencing congestion for the past two decades. During the 1990's, Oakland County experienced a surge of population growth and economic development. Associated growth in traffic required in excess of a billion dollar in road improvement needs. At the current level of funding, it will take 70 years to meet the capacity needs of Oakland County roadways [2]. Looking for innovative and cost effective ways to improve road user mobility and safety, the Road Commission for Oakland County (RCOC) began investigating innovative traffic control strategies associated with Intelligent Transportation Systems (ITS). Subsequently, the County Board of Commissioners approved $2 million for the development of an advanced traffic management system in the South East Oakland County. This commitment by Oakland County toward congestion mitigation, prompted the United States Congress to financially support this effort as a Federal demonstration project with $10 million in funding. The innovative traffic control system created in Oakland County with the Federal and County funds is called "FAST-TRAC", an acronym which stands for Faster and Safer Travel through Traffic Routing & Advanced Controls.

As a part of a field demonstration project traffic signals at 28 intersections in the city of Troy within Oakland County were converted from pre-time coordinated traffic signal control to SCATS (Sydney Coordinated Adaptive Traffic System) control in 1992. SCATS is a computer controlled traffic signal system developed in Australia and used widely in the Pacific Rim. SCATS uses anticipatory and adaptive techniques to increase the efficiency of road network by minimizing the overall number of vehicular stops and delay experienced by motorists. The primary purpose of the SCATS system is to maximize the throughput of a roadway by controlling queue formation.

Since 1992, traffic signals in Oakland County and a portion of Macomb and Wayne Counties have been converted to the SCATS signal system. County traffic engineers have been adjusting various SCATS parameters to improve its effectiveness in terms of delay, traffic flow, queue length, and crash and injury occurrences.

In 2007, a study was conducted to evaluate the performance of the SCATS system on M-59, between Pontiac Lake East to Pontiac Lake West in Waterford Township, Michigan, in terms of delay, flow, queue length, fuel consumption and Emission [8]. As a part of this study various performance parameters of SCATS system were compared with the Pre-timed signal system. Some of the findings of this study are displayed in Figures 1, and 2.

Performance of the SCATS system was found to be superior for several of the performance measures during each Peak period as shown in Figures 1 and 2. However, this study did not examine the crash effectiveness of SCATS system. In fact, no in-depth study has been done to quantify the crash effectiveness of SCATS system. When compared to Pre-timed signal, installation and maintenance cost of SCATS system is almost two times greater. Therefore, there is a need to determine the added related benefits of SCATS system if any. In this context, determination of crash benefit of SCATS can play a significant role. If we can combine congestion and crash related benefits, then it is most likely combined benefits will overweigh the cost. Also, a 2008 Cambridge Systematic study determined that the cost of crashes is almost two to seven times more than the cost of congestion depending on the size of cities as shown in Figures 3 and 4 [9]. However, there have not been any comprehensive studies conducted that evaluated the safety performance of SCATS control system. To determine the safety effectiveness of SCATS system a study was conducted. The purpose of this study was two folds:

- Examine the crash experience of a corridor before and after the installation of SCATS system.
- Compare the safety performance of SCATS controlled corridor with a similar Pre-timed controlled corridor.

This report documents the findings of this study.

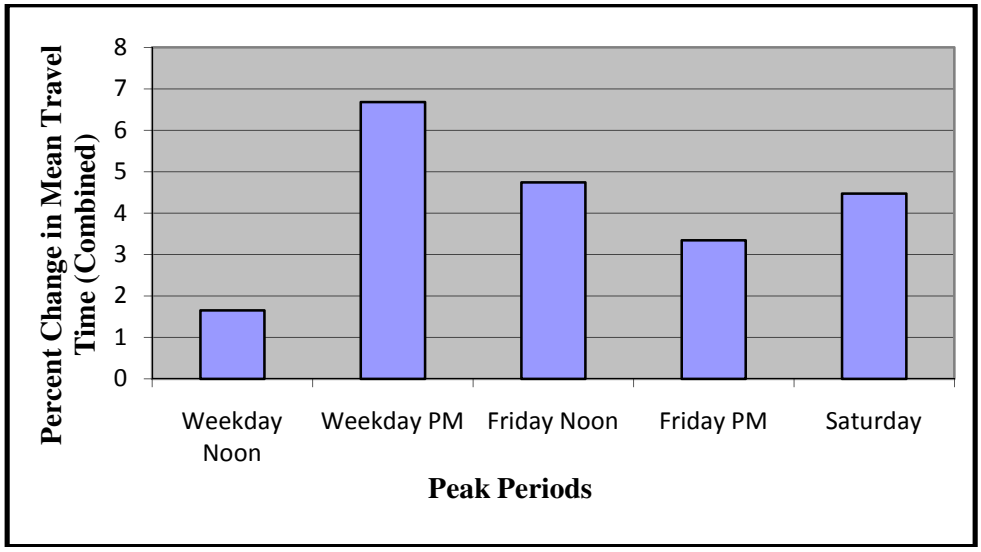

Figure 1. Difference in Travel Time between SCATS and Pre-Timed System

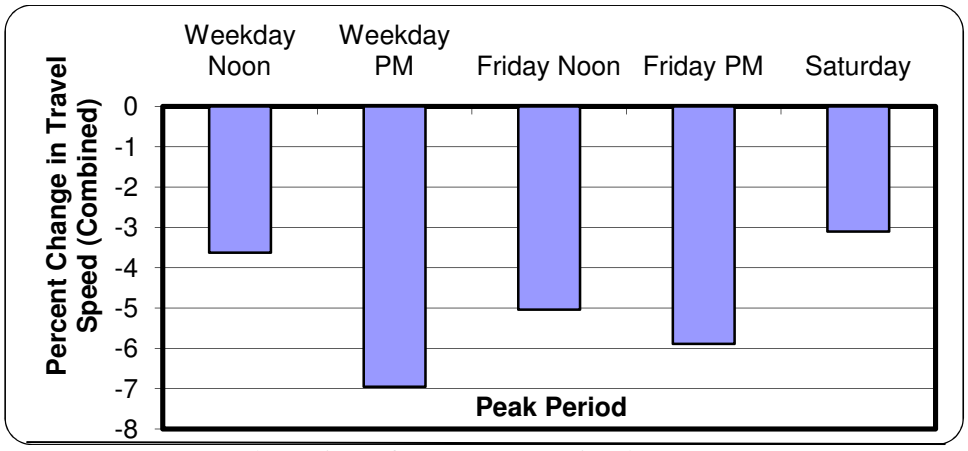

Note: Percent Change in Performance= ((Pre-timed-SCATS)/SCATS)*100

Figure 2. Difference in Mean Speed between SCATS and Pre-Timed System

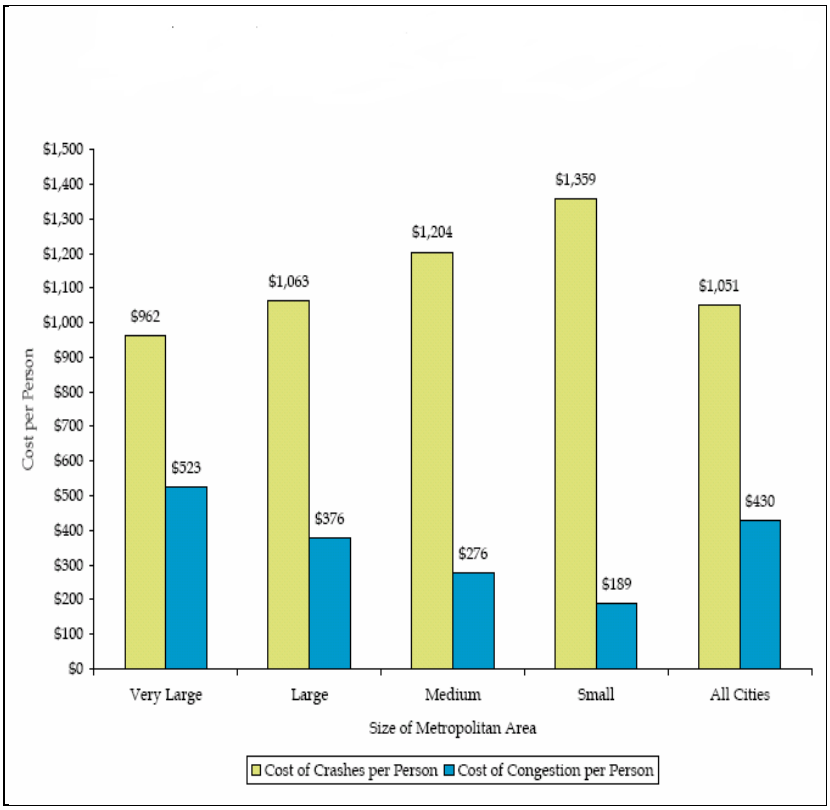

Figure 3. Cost of Crash and Congestion per Person by Size of Metropolitan Area [9]

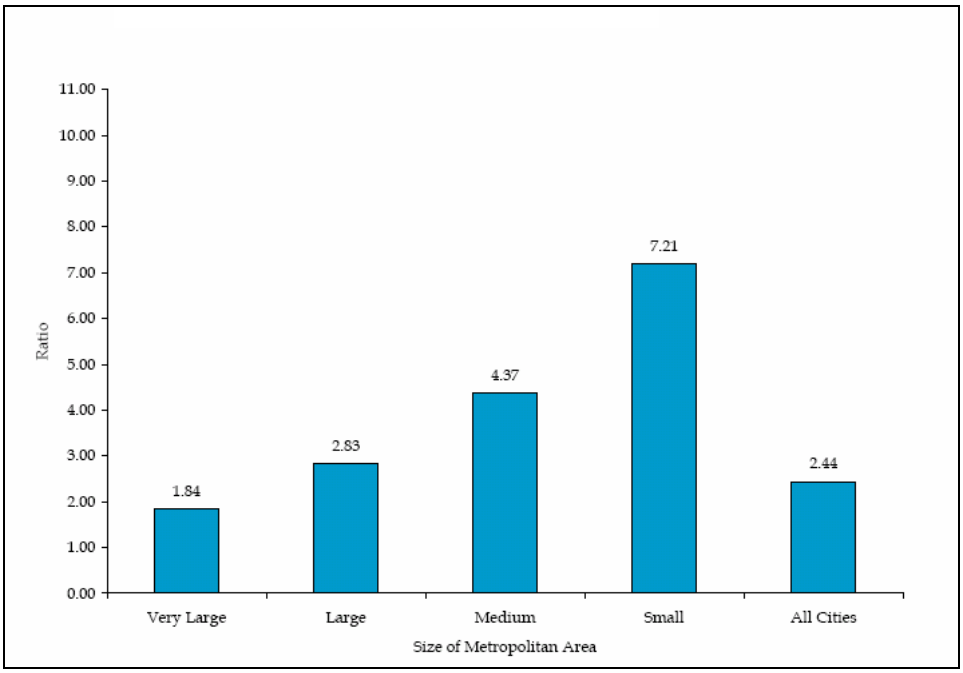

Figure 4. Ratio of Crash cost over Congestion by Size of Metropolitan Area [9]

2. Study Area

A 6.186 mile segment (mile points 12.354-18.54) along M-59 from Pontiac Lake East to Voorheis Road and an 8.03 mile segment (mile points 0.579-8.609) of Dixie Highway from Telegraph to Englewood Road, in Oakland County, Michigan were selected as a SCATS controlled and a Pre-timed controlled corridor respectively for data collection and analysis purpose. M-59 was converted to SCATS signal system in 2002. Bird's eye views of two segments are presented in Figures 5 and 6. Various attributes of these two corridors are presented in Table 1.

Table 1. Various Attributes of SCATS and Pre-timed Controlled Corridors

Attributes	**SCATS Corridor**	**Pre-timed Corridor**
Length	6.186 miles	8.03 miles
Number of Lanes	5	5
Center lane	Yes	Yes
Land use	Mostly Retail	Mostly Retail
Number of Signals	9	14
Year of conversion	2002	Not applicable
Average ADT	28,380-42,378	23,996-38, 974

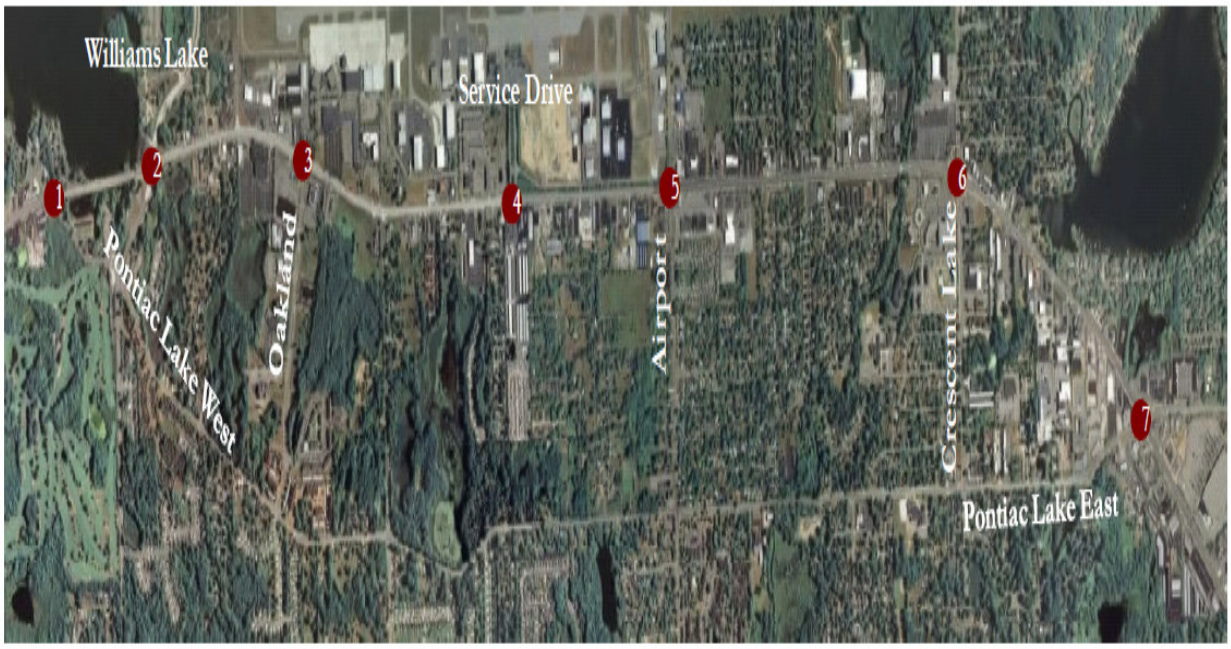

Figure 5. M-59 Corridor (SCATS Controlled Segment)

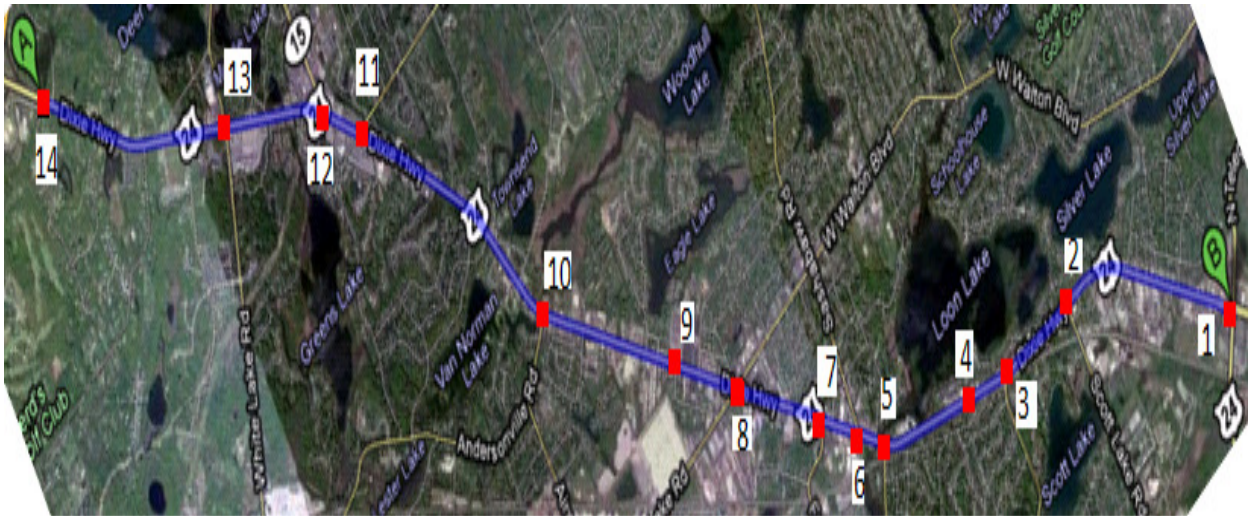

Figure 6. Dixie Corridor (Pre-timed Controlled Segment)

3. Data Collection

Crash data and traffic volume data of each corridor along with all signalized intersections within the corridor from 1999 to 2008 were collected. South East Michigan Council of Government (SEMCOG), as well as the Michigan Department of Transportation (MDOT), data sites were used to data as a part of this effort. Data were sorted by year and severity type. According to SEMCOG, various types of Crash severity are defined as follows:

Fatal: Any injury that results in death.

Injury-A (Incapacitating Injury, permanent injury): Any injury other than a fatal injury that prevents the injured person from driving, walking or normally continuing activities the person was capable of performing before the injury occurred.

Injury-B (Non-incapacitating Injury, temporary Injury): Any injury not incapacitating but evident to observers at the scene of crash in which injury occurred.

Injury-C (Possible injury, slight bruises and cuts): Any injury other than F, A or B.

Property Damage Only (PDO): Any crash that results in no fatality or injures but damage of property at least $400.00

The SCATS controlled corridor consists of nine segments of various lengths totaling 6.186 miles. Whereas the Pre-timed controlled corridor has fourteen segments of various lengths totaling 8.03 miles. Please note that Fatal accident was observed rarely, therefore, most instances it was not included as a part of analysis.

4. Data Analysis

4.1. SCATS Controlled Corridor

A 6.186 mile segment of M-59 was selected as a SCATS controlled corridor for the purpose of this study. This segment of M-59 is a five lane east-west arterial in Oakland County, Michigan and consists of nine smaller segments of varied length. Crash data and traffic volume data of each segment was collected from years 1999-2001 and 2003-2008. This corridor was converted to SCATS control system in 2002.

4.2. SCATS Segment Analysis

Crash data including severity from 1999 to 2008 (excluding the year 2002, year of switch) were presented in Table 2. For the purpose of this study, years between 1999-2001 were considered as before period and years between 2003-2008 were considered as after period. A review of mean data before and after the installation of SCATS signal indicated the followings:

- Total crash per mile per year was reduced by 16.8 percent after the installation of SCATS system.
- SCATS was able to reduce crash severity type A, B and C per year per mile by 31.032, 42.50 and 10.19 percent respectively.
- Property Damage Only crash type per year per mile went down by 16.48 percent.

Table 2. Crash Data M-59 from 1999-2008 (Segment length: 6.186 Mile)

Crash type	1999	2000	2001	Mean (99-01)	2003	2004	2005	2006	2007	2008	Mean (03-08)	Difference
Total crash	610	572	572	584.67	530	531	541	455	443	416	486	16.88%
(per mile)	98.61	92.47	92.47	94.51	85.68	85.84	87.46	73.55	71.61	67.25	78.56	
A-level	10	10	9	9.67	3	10	5	12	1	9	6.67	31.03%
(per mile)	1.62	1.62	1.45	1.56	0.48	1.62	0.81	1.94	0.16	1.45	1.08	
B-level	32	38	30	33.33	26	23	22	16	16	12	19.17	42.50%
(per mile)	5.17	6.14	4.85	5.39	4.2	3.72	3.56	2.59	2.59	1.94	3.1	
C-level	106	120	93	106.33	113	102	103	86	81	88	95.5	10.19%
(per mile)	17.14	19.4	15.03	17.19	18.27	16.49	16.65	13.9	13.09	14.23	15.44	
ABC	148	168	132	149.33	142	135	130	114	98	109	121.33	18.75%
(per mile)	23.92	27.16	21.34	24.14	22.96	21.82	21.02	18.43	15.84	17.62	19.61	
PDO	462	403	440	435	387	396	410	338	344	305	363.33	16.48%
(per mile)	74.68	65.15	71.13	70.32	62.56	64.02	66.28	54.64	55.61	49.3	58.73	
Total Injured	211	255	191	219	198	191	175	156	136	136	165.33	24.51%
(per mile)	34.11	41.22	30.88	35.4	32.01	30.88	28.29	25.22	21.99	21.99	26.73	

4.2.1. Crash Severity Analysis

Figure 7, represents crash severity in percent during before and after periods. For both time periods crash severity type C was the predominant type. Crash types B and A were reduced by close to one percent after the installation of SCATS system. Other types remained identical. Table 3 presents the proportion of each severity type during the before and after period.

While examining the distribution of severity types A, B and C during the before and after periods, it is noted that a shift from higher severity crashes to lower severity crashes was realized, which is very significant. A previous study also observed a similar trend [6].

Table 3. Distribution of Severity in Percent for Before and After Periods

Severity Type	Segment	
	Before (1999-2001)	After (2003-2008)
F	0.17%	0.27%
A	1.65%	1.37%
B	5.7%	3.94%
C	18.19%	19.65%
PDO	74.40%	74.78%

4.2.2. Computation of Before and After Crash Rate Considering Traffic Exposure

Traffic volume data were used to compute crash rate per 100 million vehicles miles for each of the ten segments as well as for complete segment. Total, as well as severity type crash rate before and after the insatllation of SCATS system are presented in Table 4 and Figure 8. Crash rate of injury type B is reduced by 34 percent, followed by a 22 percent reduction in injury type A. Reduction in types B and A crash rate resulted a slight rate increase in case of type C. However, mean total crash rate was reduced by only 5.6 percent. It is to be noted that nation wide mean crash rate has been on the decline for more than 10 years.

4.3. SCATS Intersection Analysis

There are nine signalized intersections within the 6.18 mile segment of M-59. They are:

- Pontiac Lake East
- Williams Lake road
- Oakland Blvd.
- Airport Road
- Crescent Lake Road
- Pontiac Lake West
- Cass Lake Road
- Elizabeth Lake Road
- Voorheis Road

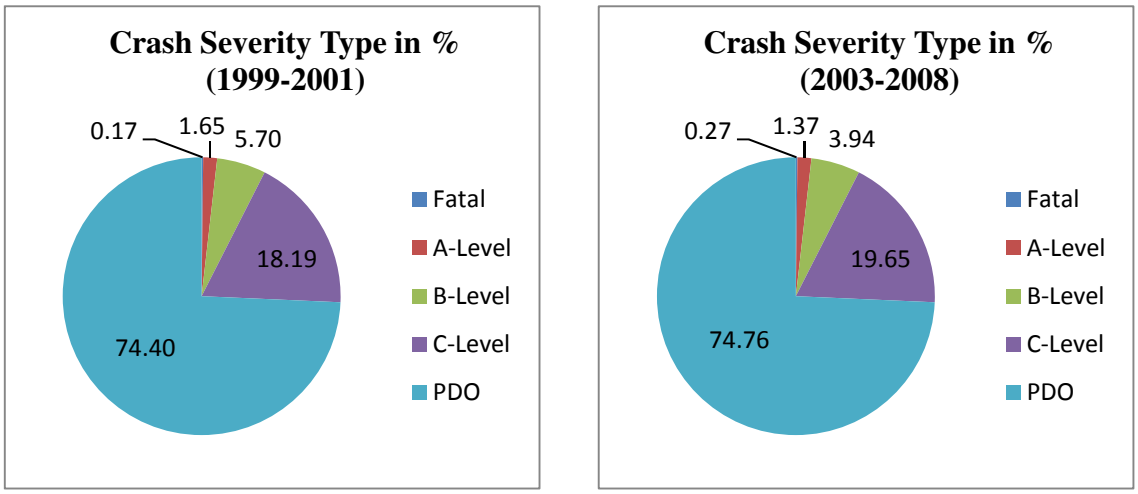

Figure 7. Various types of Severity in Percent within M-59 Corridor : Before and after the installation of SCATS system

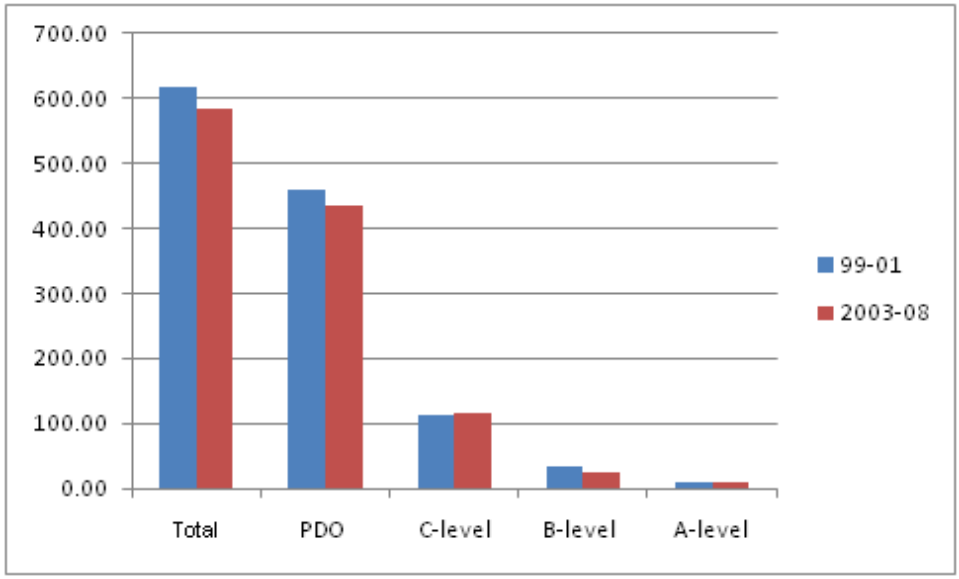

Figure 8. Graphical representation of Before-After Crash Rate

Table 4. Crash Rate by Each Segments of M-59 Corridor

Segment Number	Segment Length in Miles	Mean Crash rate/ 100 Million Vehicles Miles									
		Total Crash		Severity Type A		Severity Type B		Severity Type C		PDO	
		Before	After	Before	After	Before	After	Before	After	Before	After
1	0.351	913.97	663.87	39.4	11.85	63.03	23.71	126.07	126.45	685.48	501.85
2	0.281	1653.43	1179.7	19.68	4.94	88.58	29.62	255.89	236.93	1279.44	908.22
3	0.098	343.27	634.68	19.07	25.91	38.14	25.91	57.21	155.43	228.85	427.44
4	0.457	552.09	533.3	12.27	11.11	36.81	30.55	94.06	97.22	404.86	388.86
5	1.007	339.64	451.27	1.86	7.56	22.27	22.69	76.09	86.98	239.41	334.04
6	1.006	804.4	812.28	6.65	11.89	39.89	29.73	172.85	164.12	582.81	602.97
7	0.754	739.15	648.99	11.83	11.11	32.52	26.97	141.92	111.07	552.89	498.24
8	1.27	468.68	394.72	7.02	4.71	28.09	16.02	78.99	83.84	354.58	288.27
9	0.248	1159.59	849.07	17.98	4.82	62.92	33.77	161.8	188.15	925.87	622.33
10	0.714	408.25	386.05	13.06	1.73	26.13	10.39	68.59	70.98	303.73	302.96
Mean Rate		617.4	582.8	10.2	8	35.2	23	112.3	114.5	459.4	435.7
Difference (percent)		**-34.6(-5.61%)**		**-2.2(-21.69%)**		**-12.2(-34.71%)**		**+2.5(1.98%)**		**-23.7(-5.15%)**	

Total crash within 250ft of all intersections controlled by SCATS system along with severity type during 1999-2001 and 2003-2008 are presented in Table 5. A review of Table 5 reveals the following.

- Total crash per intersection per year is reduced by more than 24 percent after the installation of the SCATS system.
- Severity type B per intersection is reduced by 53 percent between these two study periods, followed by severity A and C respectively.

4.3.1. Share of Crash Severity

Pie charts in Figure 9, represents the percent distribution of crash severity in all intersections combined during the before and after periods. Similar to the segment analysis Property Damage Only (PDO) is the predominant type followed by severity type C. Table 6, represents percent share among severity A, B and C before and after the installation of the SCATS system. There is a drastic shift of severity type B during the after period, from 4.62 percent to 2.82 percent. A similar trend was also observed in the case of segment analysis as presented before.

4.3.2. Computation of Before and After Crash Rate for Intersections considering Traffic Exposure

Before and after crash data for each intersection controlled by the SCATS system within the 6.186 mile corridor of M-59 were used to compute the crash rate in Millions of vehicles. Crash rate by total as well as severity type before and after the installation of the SCATS system are presented in Table 7. A review of Table 7 indicates the following:

- Total crash rate per millions of vehicles is reduced by 14.98 percent after the installation of the SCATS signals.
- Crash rate of severity type B showed the highest reduction of 47.78 percent, followed by a reduction of 39.98% of severity type A.

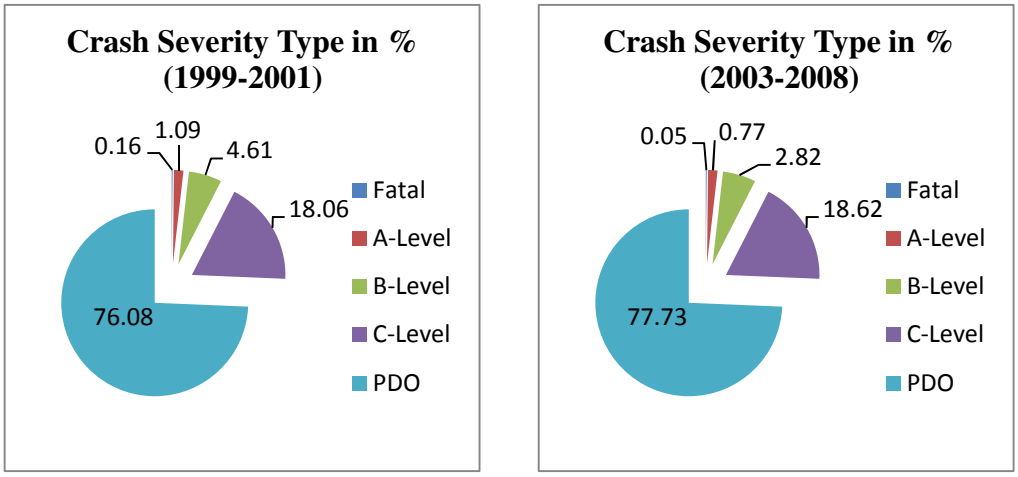

Figure 9. Various types of Severity of all Intersections in Percent within M-59 Corridor Before and after the installation of SCATS system

Table 5. Crash Data of All intersection within SCATS Corridor from 1999-2008 (without 2002)

Crash type	1999	2000	2001	Mean (99-01)	2003	2004	2005	2006	2007	2008	mean (03-08)	Difference
Total crash	418.00	467.00	394.00	426.33	386.00	318.00	358.00	292.00	288.00	307.00	324.83	-23.81%
(per intersection)	(46.44)	(51.89)	(43.78)	(47.37)	(42.89)	(35.33)	(39.78)	(32.44)	(32.00)	(34.11)	(36.09)	
A-level	4.00	5.00	5.00	4.67	3.00	1.00	3.00	5.00	0.00	3.00	2.50	-46.43%
(per intersection)	(0.44)	(0.56)	(0.56)	(0.52)	(0.33)	(0.11)	(0.33)	(0.56)	(0.00)	(0.33)	(0.28)	
B-level	15.00	30.00	14.00	19.67	12.00	7.00	11.00	8.00	7.00	10.00	9.17	-53.39%
(per intersection)	(1.67)	(3.33)	(1.56)	(2.19)	(1.33)	(0.78)	(1.22)	(0.89)	(0.78)	(1.11)	(1.02)	
C-level	66.00	104.00	61.00	77.00	75.00	65.00	59.00	52.00	59.00	53.00	60.50	-21.43%
(per intersection)	(7.33)	(11.56)	(6.78)	(8.56)	(8.33)	(7.22)	(6.56)	(5.78)	(6.56)	(5.89)	(6.72)	
ABC	85.00	139.00	80.00	101.33	90.00	73.00	73.00	65.00	66.00	66.00	72.17	-28.78%
(per intersection)	(9.44)	(15.44)	(8.89)	(11.26)	(10.00)	(8.11)	(8.11)	(7.22)	(7.33)	(7.33)	(8.02)	
PDO	333.00	327.00	313.00	324.33	296.00	245.00	285.00	227.00	221.00	241.00	252.50	-22.15%
(per intersection)	(37.00)	(36.33)	(34.78)	(36.04)	(32.89)	(27.22)	(31.67)	(25.22)	(24.56)	(26.78)	(28.06)	
Total Injured	121.00	190.00	111.00	140.67	128.00	103.00	97.00	85.00	84.00	83.00	96.67	-31.28%
(per intersection)	(13.44)	(21.11)	(12.33)	(15.63)	(14.22)	(11.44)	(10.78)	(9.44)	(9.33)	(9.22)	(10.74)	

Table 6. Severity Distribution in Percent for SCATS Controlled Intersections during Before and After periods

Severity Type	Before	After
F	0.16%	0.05%
A	1.09%	0.77%
B	4.61%	2.82%
C	18.06%	18.62%
PDO	76.08%	77.73%

5. Analysis of Pre-timed Controlled Segments

5.1. Pre-timed Controlled Corridor

An 8.03 mile-stretch of Dixie Highway in Oakland County, Michigan was considered in this study as the Pre-timed controlled corridor. This corridor consists of 14 Pre-timed signalized intersections. Crash data including severity for this corridor from 1999 to 2008 (excluding year 2002) are presented in Table 8. For the purpose of this study the period between 1999-2001 was designated as before period and years between 2003-2008 was considered as after period. A review of mean data during the before and after periods indicates the followings:

- Total crash per mile per year was reduced by 28.84 percent between 1999-2001 and 2003-2008.
- Between these two periods crash severity type A, B and C per year per mile were reduced by 48.8, 51.13 and 36.36 percent respectively.
- Property damage only crash type per year per mile was decreased by 24.58 percent.
- Following the national trend the crash rate of this corridor also decreased.

5.1.1. Crash Severity Distribution

Table 8 represents various types of crash severity during period 1999-2001 and 2003-2008. For both time periods, crash severity type C was the predominant type among the three severity type. However, PDO captured the highest share of crashes at 78 percent.

Table 7. Intersection Crash data M-59

Intersection	Mean Crash rate/ Million Vehicles									
	Total Crash		Severity A		Severity B		Severity C		PDO	
	Before	After	Before	After	Before	After	Before	After	Before	After
Pontiac lake rd	1.63	1.36	0.08	0.01	0.11	0.03	0.28	0.28	1.13	1.04
Williams lake rd	5.01	3.50	0.06	0.04	0.28	0.13	0.89	0.67	3.79	2.66
Oakland Blvd N	1.91	1.69	0.06	0.01	0.13	0.13	0.36	0.28	1.35	1.27
Airport rd	4.17	5.10	0.02	0.01	0.09	0.08	0.77	0.84	3.29	4.16
Crescent Lake Rd	3.77	3.34	0.00	0.01	0.11	0.07	0.69	0.55	2.97	2.70
Pontiac lake rd.	3.86	3.33	0.00	0.02	0.27	0.10	0.69	0.75	2.90	2.45
Cass Lake Rd	3.61	2.21	0.05	0.00	0.13	0.07	0.56	0.46	2.88	1.69
Elizabeth Lake Rd	2.88	2.76	0.07	0.06	0.16	0.08	0.45	0.53	2.21	2.09
Voorheis Rd	1.89	1.13	0.000	0.01	0.07	0.01	0.51	0.20	1.31	0.90
Mean Rate	3.19	2.71	0.04	0.02	0.15	0.08	0.58	0.51	2.42	2.11
Difference(percent)	0.48(-14.98%)		0.02(-39.98%)		0.07(-47.78%)		0.07(-11.97%)		0.31(-13%)	

Table 8. Segment Crash Data Dixie Highway

Type/year	1999	2000	2001	Mean (99-01)	2003	2004	2005	2006	2007	2008	Mean (03-08)	Difference
Total Crash	593.00	516.00	442.00	517.00	415.00	452.00	373.00	299.00	328.00	340.00	367.83	-28.85%
(per mile)	(73.85)	(64.26)	(55.04)	(64.38)	(51.68)	(56.29)	(46.45)	(37.24)	(40.85)	(42.34)	(45.81)	
A-level	9.00	13.00	8.00	10.00	2.00	7.00	8.00	9.00	2.00	3.00	5.17	-48.33%
(per mile)	(1.12)	(1.62)	(1.00)	(1.25)	(0.25)	(0.87)	(1.00)	(1.12)	(0.25)	(0.37)	(0.64)	
B-level	35.00	33.00	28.00	32.00	18.00	22.00	16.00	13.00	15.00	10.00	15.67	-51.04%
(per mile)	(4.36)	(4.11)	(3.49)	(3.99)	(2.24)	(2.74)	(1.99)	(1.62)	(1.87)	(1.25)	(1.95)	
C-level	112.00	103.00	72.00	95.67	73.00	79.00	59.00	47.00	58.00	49.00	60.83	-36.41%
(per mile)	(13.95)	(12.83)	(8.97)	(11.91)	(9.09)	(9.84)	(7.35)	(5.85)	(7.22)	(6.10)	(7.58)	
ABC	156.00	149.00	108.00	137.67	93.00	108.00	83.00	69.00	75.00	62.00	81.67	-40.68%
(per mile)	(19.43)	(18.56)	(13.45)	(17.14)	(11.58)	(13.45)	(10.34)	(8.39)	(9.34)	(7.72)	(10.17)	
PDO	436.00	366.00	333.00	378.33	319.00	343.00	290.00	229.00	253.00	278.00	285.33	-24.58%
(per mile)	(54.30)	(45.58)	(41.47)	(47.11)	(39.73)	(42.71)	(36.11)	(28.52)	(31.51)	(34.62)	(35.53)	
Total Injured	232.00	226.00	167.00	208.33	145.00	140.00	125.00	102.00	113.00	85.00	118.33	-43.20%
(per mile)	(28.89)	(28.14)	(20.80)	(25.94)	(18.06)	(17.43)	(15.57)	(12.70)	(14.07)	(10.59)	(14.74)	

Table 9. Distribution of Severity in Percent for Before and After Periods for Segment and Intersection

Severity Type	Pre-timed Segment		Pre-timed Intersections	
	Before	After	Before	After
F	0.19%	0.23	0.10%	0.20%
A	1.93%	1.40%	1.91%	0.81%
B	6.19%	4.26%	5.15%	3.63%
C	18.50%	16.54%	17.84%	16.62%
PDO	73.18%	77.57%	75.00%	78.73%

5.1.2. Computation of Crash Rate Considering Traffic Exposure

Traffic volume and segment length were used to compute the crash rate per 100 million vehicle miles for Dixie Highway segments during 1999-2001 and 2003-2008. Crash rates are presented in Table 10 and Figure 10. For the Pre-timed controlled corridor, it was observed that:

- Total Crash per mile was reduced by 24.94 percent between 1999-2001 and 2003-2008.
- Crash rate of severity type B was reduced by 48.35 percent, followed by types A (45.49%) and C (32.9%).

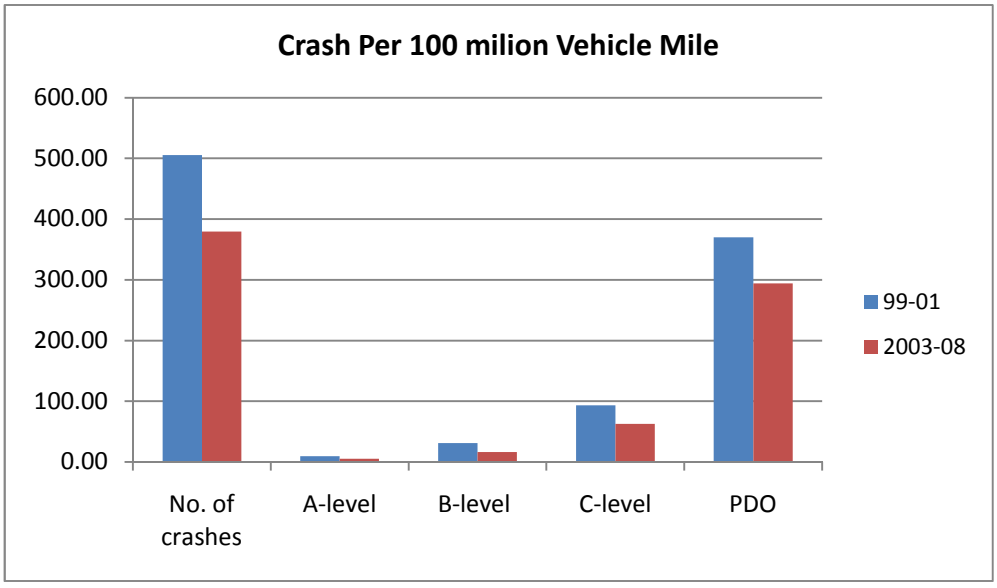

Figure 10. Crash per 100 million Vehicle Mile for Dixie Highway during 1999-2001 and 2003-2008

Table 10. Crash rate within each segments of Dixie Highway

Segment Number	Segment Length	Mean Crash rate/ 100 Million Vehicles Miles									
		Total Crash		Severity A		Severity B		Severity C		PDO	
		Before	After	Before	After	Before	After	Before	After	Before	After
1	0.49	1056.82	681.75	9.56	11.65	114.77	20.39	224.75	160.24	707.73	489.46
2	0.626	288.22	282.78	0.00	4.56	18.72	13.68	37.43	36.49	232.07	228.05
3	0.455	365.64	291.79	5.15	9.41	30.90	15.69	77.25	53.34	252.34	213.35
4	0.833	143.46	125.11	8.44	0.00	8.44	0.00	36.57	23.99	90.01	101.11
5	0.16	1158.43	1098.87	47.61	8.02	111.08	32.08	269.77	216.57	729.97	842.20
6	0.239	371.82	327.55	0.00	5.37	10.62	16.11	95.61	48.33	180.60	257.74
7	0.559	699.48	358.14	9.08	4.59	45.42	22.96	131.72	66.58	513.25	264.02
8	1.25	540.30	389.11	2.03	6.16	26.41	19.51	93.44	55.44	416.40	308.00
9	1.275	554.68	389.47	16.23	7.54	32.47	15.08	97.41	64.07	405.86	300.27
10	0.237	2096.11	1493.73	72.78	6.76	58.23	47.31	262.01	202.77	1703.09	1236.89
11	0.654	859.82	499.67	31.65	2.45	26.37	22.04	184.62	78.38	617.17	394.34
12	1.252	234.58	260.26	2.58	4.84	15.47	14.53	30.93	37.53	183.02	200.95
Mean crash rate		505.4	379.41	9.78	5.33	31.28	16.16	93.53	62.75	369.87	294.31
Difference (Percent)		125.99(-24.94%)		3.4(-45.49%)		15.1(-48.35%)		30.8(-32.91%)		75.76(-20.43%)	

5.2. Intersection Analysis

Dixie highway corridor has the following 14 pre-timed controlled intersections:

- Telegraph Road South
- Silver Lake Road
- Scott Lake Road
- Watkins Lake Road
- Hatchery Road
- Sashabaw Road
- Frembes Road
- Williams Lake Road
- Hatfield Dr.
- Andersonville Road
- Maybee Road
- Ortonville Road
- White Lake Road
- Englewood Road

Crash data of all 14 Pre-timed controlled intersections for the periods 1999-2001 and 2003-2008 were collected and then converted into crashes per intersection. Crash per intersection data are presented in Table 11. It was observed that:

- Total crashes per Pre-time signal were reduced by 29.10 percent between 1999-2001 and 2003-2008.
- Severity type A per intersection was reduced by 70 percent followed by types B and C.

5.2.1. Share of Crash Severity

Table 9 (presented before) and Figure 11 include the percent distribution of crash severity in all intersections combined during before and after periods. Similar to Pre-timed segment analysis Property Damage Only (PDO) is the predominant type followed by severity type C**.**

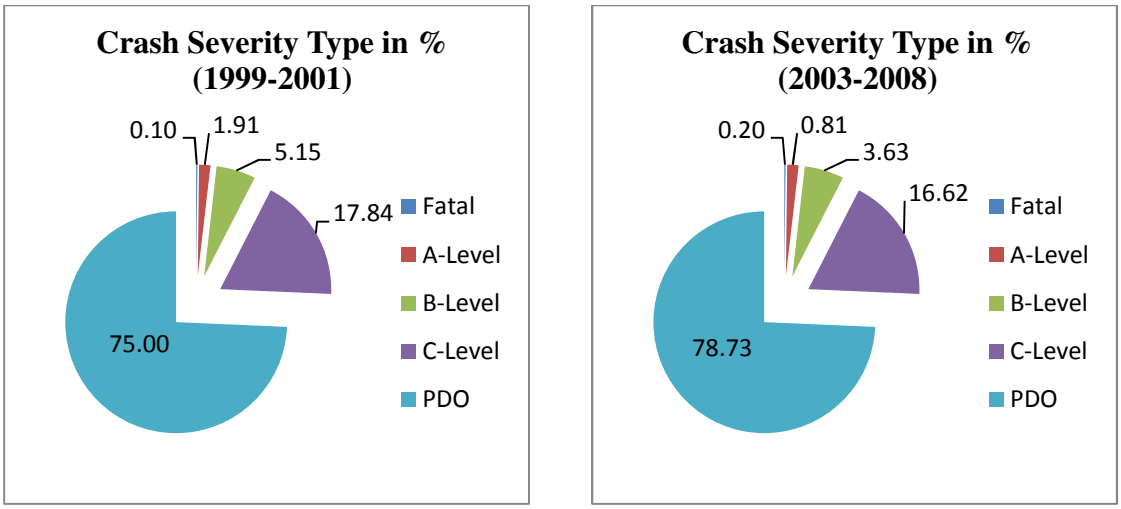

Figure 11. Distribution of Crash Severity of all Intersections in Percent between periods 1999-2001 and 2003-2008 (Dixie Highway)

5.2.2. Computation of Before and After Crash Rate for Intersections considering Traffic Exposure

Before and after crash data of each intersection controlled by the Pre-timed system within the 8.03 mile corridor of Dixie Highway were used to compute the crash rate in million of vehicles. Crash rate by total as well as severity type between 1999-2001 (before) and 2003-2008 (after) are presented in Table 12. A review of Table 12 indicates the following:

- Total crash rate per millions of vehicles is reduced by 25.77 percent between the two tested time periods.
- Crash rate of severity type A showed highest reduction of 71.05 percent, followed by a reduction of 38.08 percent for severity type C.

Table 11. Crash Data of All Intersections within Pre-Timed controlled Corridor from 1999-2008 (without 2002)

Type/year	1999	2000	2001	mean (99-01)	2003	2004	2005	2006	2007	2008	mean (03-08)	Difference
Total crash	369.00	372.00	307.00	349.33	276.00	296.00	242.00	219.00	211.00	242.00	247.67	-29.10%
(per intersection)	(26.36)	(26.57)	(21.93)	(24.95)	(19.71)	(21.14)	(17.29)	(15.64)	(15.07)	(17.29)	(17.69)	
A-level	7.00	7.00	6.00	6.67	0.00	3.00	4.00	4.00	0.00	1.00	2.00	-70.00%
(per intersection)	(0.50)	(0.50)	(0.43)	(0.48)	(0.00)	(0.21)	(0.29)	(0.29)	(0.00)	(0.07)	(0.14)	
B-level	19.00	19.00	16.00	18.00	13.00	13.00	10.00	8.00	6.00	4.00	9.00	-50.00%
(per intersection)	(1.36)	(1.36)	(1.14)	(1.29)	(0.93)	(0.93)	(0.71)	(0.57)	(0.43)	(0.29)	(0.64)	
C-level	61.00	76.00	50.00	62.33	41.00	55.00	36.00	38.00	41.00	36.00	41.17	-33.96%
(per intersection)	(4.36)	(5.43)	(3.57)	(4.45)	(2.93)	(3.93)	(2.57)	(2.71)	(2.93)	(2.57)	(2.94)	
ABC	87.00	102.00	72.00	87.00	54.00	71.00	50.00	50.00	47.00	41.00	52.17	-40.04%
(per intersection)	(6.21)	(7.29)	(5.14)	(6.21)	(3.86)	(5.07)	(3.57)	(3.57)	(3.36)	(2.93)	(3.73)	
PDO	282.00	269.00	235.00	262.00	221.00	225.00	192.00	168.00	164.00	200.00	195.00	-25.57%
(per intersection)	(20.14)	(19.21)	(16.79)	(18.71)	(15.79)	(16.07)	(13.71)	(12.00)	(11.71)	(14.29)	(13.93)	
Total Injured	133.00	145.00	100.00	126.00	75.00	89.00	76.00	73.00	69.00	52.00	72.33	-42.59%
(per intersection)	(9.50)	(10.36)	(7.14)	(9.00)	(5.36)	(6.36)	(5.43)	(5.21)	(4.93)	(3.71)	(5.17)	

Table 12. Intersection Crash Data Dixie Highway

Intersection	Mean Crash rate/ Million Vehicles									
	Total Crash		Severity A		Severity B		Severity C		PDO	
	Before	After	Before	After	Before	After	Before	After	Before	After
Telegraph Rd S	2.014	2.127	0.07	0.014	0.187	0.228	0.328	0.356	1.429	1.684
Silver Lake Rd	2.319	1.341	0	0	0.141	0.171	0.445	0.271	1.733	1.042
Scott Lake Rd	1.335	1.428	0	0.043	0.07	0.086	0.141	0.214	1.125	1.156
Watkins Lake Rd	0.843	0.657	0	0.014	0.07	0.086	0.234	0.128	0.538	0.499
Hatchery Rd	0.984	1.053	0.07	0.012	0.07	0.077	0.257	0.206	0.586	0.822
Sashabaw Rd	1.472	1.155	0.076	0.012	0.126	0.128	0.33	0.27	0.939	0.847
Frembes Rd	1.345	0.783	0.025	0.012	0.076	0.077	0.254	0.154	0.99	0.564
Williams Lake Rd	3.046	1.925	0	0.012	0.152	0.154	0.66	0.27	2.234	1.54
Hatfield Dr	0.735	0.449	0	0.012	0.025	0.025	0.101	0.044	0.609	0.372
Andersonville Rd	1.726	1.053	0.025	0	0.025	0.025	0.381	0.218	1.295	0.795
Maybee Rd	2.894	2.258	0.025	0	0.126	0.128	0.33	0.372	2.412	1.823
Ortonville Rd	2.843	2.387	0.05	0	0.076	0.077	0.431	0.27	2.285	2.054
White Lake Rd	4.13	2.607	0.161	0.015	0.097	0.091	0.807	0.47	3.065	1.955
Englewood Dr	1.484	0.955	0.032	0.015	0.129	0.121	0.129	0.106	1.162	0.712
Mean Rate	1.94	1.441	0.038	0.011	0.097	0.089	0.344	0.213	1.355	1.133
Difference (Percent)	0.50(-25.77%)		0.027(-71.05%)		0.008(-8.24%)		0.131(-38.08%)		0.222(-17.87%)	

6. Comparative Safety Performance Analysis

When compared, the safety performance of the SCATS and the Pre-timed corridors between 1999-2001 and 2003-2008, the higher reduction in total crash per intersection and severity combined per intersection were observed in case of the SCATS system. The performance of the Pre-timed system was superior in other categories as displayed in Table 13. However, during 2003-2008, the SCATS controlled segment and intersections experienced lower percent of severity type A and B crashes (Table 14 and Figure 12) when compared to the Pre-timed segment and intersections, which is noteworthy.

Table 13. Percent of Severity for SCATS and Pre-Timed Corridors and Intersections between 2003-2008

Severity Type	Segment		Intersections	
	M-59	Dixie Highway	M-59	Dixie Highway
A	5.5%	6.3%	3.46%	3.83%
B	15.8%	19.2%	12.7%	17.25%
C	78.7%	74.5%	83.8%	78.9%

7. Statistical Analysis

The statistical significance of the effectiveness of the SCATS signals was examined by comparing

- Crash data of 1999-2001(before period) and 2003-2008(after period) on M-59 and
- Crash data of Dixie Highway (Pre-timed corridor) and M-59 (SCATS corridor) during 2003-2008.

The purpose of this analysis was to determine whether the changes observed in the measure of effectiveness were attributable to the signal system or chance. The student t-test was used to determine whether the difference in mean crash rate between before and after periods and also between the Pre-timed corridor and the SCATS corridor were significant or not. The following is the equation used to calculate the t-statistic and degrees of freedom (k') for unequal sample sizes.

$$t_{calculated} = \frac{x_b - x_a}{\sqrt{\frac{\sigma_b^2}{n_b} + \frac{\sigma_a^2}{n_a}}}$$

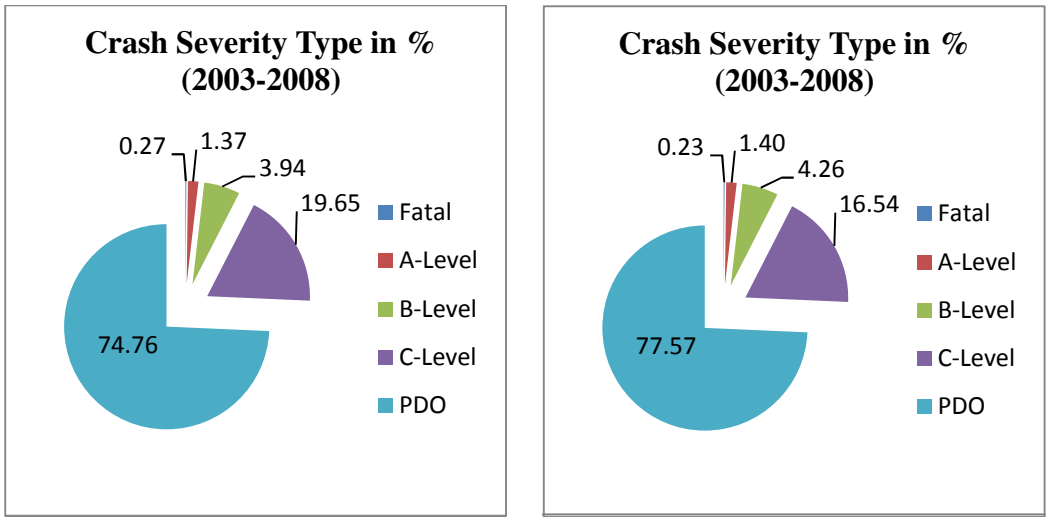

M-59 (SCATS) **Dixie (Pre-timed)**

Figure 12. Distribution of Crash Severity of all Intersections in Percent Controlled by SCATS (M-59 Highway) and Pre-timed System (Dixie Highway) during 2003-2008

Table 14. Reduction in Crash Rate between 1999-2001 and 2003-2008 for M-59 (SCATS) And Dixie Highway (Pre-timed)

Attributes	SCATS(Percent)	Pre-timed (Percent)
Reduction in crash/mile/year	15.95 (-16.87%)	18.58(-28.95%)
Reduction in Severity (A+B+C) /mile/year	4.53(-18.75%)	6.97(-40.68%)
Reduction in crash/100 million vehicle mile	34.64(-5.61%)	126.1(-24.94%)
Reduction in Severity(A+B+C)/100 million vehicle mile	12.2(-7.73%)	50.4(-37.44%)
Reduction in crash/intersection	11.28(-23.8%)	7.26(-29.10)
Reduction in Severity (A+B+C)/Intersection	3.24(-28.78%)	2.48(-40.04%)
Reduction in crash/million Vehicle	0.477(-14.97%)	0.499(-25.7%)
Reduction in Severity (A+B+C)/Million Vehicle reduction	0.153(-20.0%)	0.166(-34.65%)

Where:
x_b= sample mean of test sites (Before Data)
x_a= sample mean of control sites (After Data)
n_b= number of test sites
n_a= number of control sites
σ_b= standard deviation of test sites
σ_b= standard deviation of control sites

If the calculated t-value is greater than the critical t-value, the difference in means is statistically significant. For the student's t-test, a two-tailed test was used which utilizes a null hypothesis that states there is no difference between the two means or treatments. The alternative hypothesis would state that one of the means is higher or lower than the other, or that one treatment is better or worse than the other treatment. The two-tailed test was used for this research, as the differences between the effectiveness of the tested systems were not known. Specifically, it could not be stated prior to this analysis that the use of the SCATS system was better or worse than the corridor that did not use the SCATS system. Statisticians in traffic engineering have consistently used an alpha equal to 0.05 or a level of confidence of 95 percent for evaluations of various treatments. Alpha is simply equal to 95 percent subtracted from 100 percent.

Based upon the statistical analysis (presented in Table 15), null hypotheses were accepted for all comparison between before and after periods of SCATS installation except severity type B due to p-values greater than 0.05. While comparing the SCATS and Pre-timed systems, other than total crash rate for intersection, null hypotheses were accepted. The acceptance of the null hypothesis for the majority of statistical tests indicates that there is no statistical difference between before and after periods of SCATS signal installation. For comparison between the systems, it means there was statistical difference between the two signal systems for any type of crash rate during the period analyzed. A significant result indicating differences between the periods or systems would be represented by a p-value less than 0.05, representing a level of confidence of 95 percent.

8. Economic Analysis

Cost, life, and salvage related information of both SCATS and Pre-timed signal systems were collected from the Road Commission for Oakland County (RCOC). While computing present worth cost and equivalent annual cost, a discount rate of four percent was considered. Present worth cost, equivalent annual cost and corridor cost per year per mile are presented in Table 16. The SCATS system cost $6,798 more in comparison to the Pre-timed system. The per mile cost of the SCATS corridor is $9,376 higher.

Table 15. Results of Statistical Analysis

Type	Parameters	M-59			
		Segment		Intersection	
		Before	After	Before	After
Total	Std. Mean	738	655	3.19	2.71
	Std. Deviation	429	244	1.18	1.26
	P-Value	0.597		0.419	
	Test Result	Before = After		Before = After	
A	Std. Mean	14.9	9.59	0.0361	0.021
	Std. Deviation	10.4	6.79	0.032	0.0185
	P-Value	0.195		0.245	
	Test Result	Before = After		Before = After	
B	Std. Mean	43.8	24.94	0.15	0.078
	Std. Deviation	21	7.13	0.0734	0.0385
	P-Value	0.021		0.021	
	Test Result	Before ≠ After		Before ≠ After	
C	Std. Mean	123.3	132.1	0.576	0.505
	Std. Deviation	61.7	53.2	0.199	0.224
	P-Value	0.738		0.489	
	Test Result	Before = After		Before = After	
		Segment (03-08)		Intersection(03-08)	
		M-59	Dixie	M-59	Dixie
Total	Std. Mean	655	517	2.71	1.421
	Std. Deviation	244	398	1.26	0.647
	P-Value	0.328		0.017	
	Test Result	M-59 = Dixie		M-59 ≠ Dixie	
A	Std. Mean	9.56	5.95	0.021	0.0118
	Std. Deviation	6.79	3.09	0.0185	0.011
	P-Value	0.146		0.204	
	Test Result	M-59 = Dixie		M-59 = Dixie	
B	Std. Mean	24.94	19.9	0.0768	0.0518
	Std. Deviation	7.13	11.4	0.0385	0.0382
	P-Value	0.227		0.146	
	Test Result	M-59 = Dixie		M-59 = Dixie	
C	Std. Mean	132.1	87	0.505	0.236
	Std. Deviation	53.2	66.9	0.224	0.102
	P-Value	0.094		0.007	
	Test Result	M-59 = Dixie		M-59 ≠ Dixie	

Table 16. Cost Information of SCATS and Pre-Timed System

Attributes	SCATS System	Pre-Timed	Difference in Cost
Initial Cost	$120, 000	$100,000	$20, 000
Maintenance cost/year	$9,000	$4,000	$5,000
Life	15 years	15 years	15 years
Salvage	0	0	0
Discount Rate	4%	4%	4%
Present Worth of Cost	$220, 062	$144,472	$75, 590
Cost/Year	$19, 788	$12, 990	$6,798
Corridor cost/mile/year[1]	$28, 789	$19, 412	$9,376

[1]= (Cost/year)*number of signal within corridor/Length of corridor in miles

Note: Length of SCATS and Pre-Timed corridors are 6.186 and 8.03 miles respectively.

8.1. Cost of Crash by Signal System Computation

The expected cost of crash by signal system per year during 2003-2008 was computed by combining percent reduction data and cost of crashes by type. Cost of crashes by type was obtained from the National Highway and Traffic Safety Administration report [7]. The mean expected cost of crash by corridor and intersections controlled by SCATS and Pre-timed signal are included in Table 17. A lower cost of crash on SCATS corridor as well as intersection was observed. Please note that the expected costs were computed by summing the percent per severity type times the cost of severity types as cited in reference [7].

9. Conclusions

In this study the safety effectiveness of the SCATS controlled signal was evaluated by performing a before and after analysis and also by comparing a SCATS controlled corridor with a Pre-timed controlled corridor. This effort compared a section of M-59 (SCATS corridor) with a section Dixie Highway (Pre-timed corridor) to assess the effectiveness of the SCATS control system on the reduction of crashes. Total crashes, as well as severity types A, B, C and PDO data were examined to quantify related benefits. The crash rate in million vehicles and 100 million vehicle miles were computed. The statistical significance of the effectiveness of the two types of signal systems were tested to determine whether the observed difference in performances were attributable to the signal system or chance. Several hypotheses were presented and tested for significance at a 95 percent level of confidence or alpha equal to 0.05.

The findings of this study can be summarized as follows:

- In case of the SCATS signal system, there was shift in severity from types A and B to C.
- Even though, the installation of SCATS system cost more, by transforming from more severe crashes to less severe crashes, it would result in savings to the travelling public.
- In most cases, statistical analysis did not prove the superiority of SCATS system at the 95 percent confidence level, when before and after data were compared. Similar results were also observed when compared between SCATS and Pre-timed signal's crash experience.

Table 17. Expected Unit Cost of Crash For SCATS And Pre-Timed Corridors And Intersections Between 2003-2008

Severity Type	Cost in year 2000 dollars	Percent of Crash by Segment on		Percent of Crash by Intersections on	
		M-59 SCATS	Dixie Hwy Pre-timed	M-59 SCATS	Dixie Hwy Pre-timed
F	$977,208	0.27%	0.23%	0.05%	0.20%
A	$1,096,161	1.37%	1.4%	0.77%	0.81%
B	1$186,097	3.94%	4.26%	2.82%	3.63%
C	$10,562	19.65%	16.54%	18.62%	16.62%
PDO	$2,532	74.76%	77.57%	77.73%	78.73%
Expected Unit Cost of [1] Crash by Control System		$28,956	$29,232	$18,111	$21,337

[1] computed by combining percent of crash by severity type and related cost

10. References

1. Texas Transportation Institute, The 2002 Urban Mobility Report, June 2002.
2. Dutta, U., “Safety Potential of Smart Control System”, Proceedings of the Fifth International Conference on Application of Advanced Technologies in Transportation, ASCE, 1998.
3. FHWA/UTC workshop on Urban/ Suburban Mobility and Congestion Mitigation Research, June 6-7, 2006.
4. Taylor, W., et al., “Evaluation of SCATS corridors”, Project Report 1998.
5. Oppenlander, J.C., “Sample Size Determination for Travel Time and Delay Studies”, Traffic Engineering Journal, September 1976.
6. Quiroga, C.A. and Bullock, D., “Determination of Sample Sizes for Travel Time Studies”, ITE Journal, August 1998.

7.Dutta, U., "Life Cycle Costing in the Transit Industry," Transportation Research Record No. 1011, 1984 (with Cook, A.R., Maze, T.H., and Glandon, M.)

8.Dutta, U. "Evaluation of SCATS System", Final Report submitted to MIOH UTC, April, 2009.

9.Cambridge Systematics " Crashes vs. Congestion: What is the Cost to Society", A Report prepared for AAA by Cambridge Systematics, March 2008.

10. Dutta, U., "Traffic Signal Installation and Accident Experience", Journal of Institute of Transportation Engineers, Vol. 60, No. 9, Sept. 1990 (with T.K. Datta).

11. List of Acronyms

FAST-TRAC	Faster and Safer Travel through Traffic Routing & Advanced Controls
ITS	Intelligent Transportation Systems
MDOT	Michigan Department of Transportation
PDO	Property Damage Only
RCOC	Road Commission for Oakland County
SCATS	Sydney Coordinated Adaptive Traffic System
SEMCOG	South East Michigan Council of Government

MICHIGAN OHIO UNIVERSITY TRANSPORTATION CENTER
Alternate energy and system mobility to stimulate economic development.

Report No: MIOH UTC TS23p1 2010-Final

MDOT Report No: RC1545

TRANSIT-ORIENTED DEVELOPMENT ON DETROIT RAIL TRANSIT SYSTEM

FINAL REPORT

PROJECT TEAM

Snehamay Khasnabis, Ph.D., P.E.
Elibe A. Elibe, E.I.T.
College of Engineering
Wayne State University
5050 Anthony Wayne Drive
Detroit, MI 48202

Utpal Dutta, Ph.D., P.E.
Eric Tenazas, E.I.T.
Dept. of Civil & Environmental Engineering
University of Detroit Mercy
4001 W. McNichols Road
Detroit, MI 48221

Report No: MIOH UTC TS23p1 2010-Final

TS23, Series, Project 1, October, 2010
FINAL REPORT

Developed By:

Dr. Snehamay Khasnabis
Principal Investigator, WSU
skhas@wayne.edu

In Conjunction With:

Dr. Utpal Dutta
Co- Principal Investigator, UDM
duttau@udmercy.edu
313-993-1040

Graduate Research Assistants:

Elibe A. Elibe
Wayne State University
ec1735@wayne.edu

Eric Tenazas
University of Detroit Mercy
tenazaer@udmercy.edu

SPONSORS

This is a Michigan Ohio University Transportation Center project supported by the U.S. Department of Transportation, the Michigan Department of Transportation, Wayne State University, and the University of Detroit Mercy.

ACKNOWLEDGEMENT

This research was conducted jointly at Wayne State University and at the University of Detroit Mercy. Significant matching support was provided by the Michigan Department of Transportation and the two partner universities. The authors would like to express their sincere appreciation to the project sponsors for their support. A number of agencies and individuals extended their support for the project by sharing their thoughts on various issues related to the project. Those that lent their support are listed in the second acknowledgement section.

DISCLAIMERS

Technical Report Documentation Page

1. Report No. RC-1545	**2. Government Accession No.**	**3. MDOT Project Manager** Niles Annelin
4. Title and Subtitle Michigan Ohio University Transportation Center Subtitle: "Transit-Oriented Development on Detroit Rail Transit System"		**5. Report Date** October 2010 **6. Performing Organization Code**
7. Author(s) Dr. Snehamay Khasnabis, Wayne State University Dr. Utpal Dutta, University of Detroit Mercy		**8. Performing Org. Report No.** MIOH UTC TS23 p1 2010-Final
9. Performing Organization Name and Address Michigan Ohio University Transportation Center University of Detroit Mercy, Detroit, MI 48221 and Wayne State University, Detroit, MI 48202		**10. Work Unit No. (TRAIS)** **11. Contract No.** 2007-0538 **11(a). Authorization No.**
12. Sponsoring Agency Name and Address Michigan Department of Transportation Van Wagoner Building, 425 West Ottawa P. O. Box 30050, Lansing, Michigan 48909		**13. Type of Report & Period Covered** Research, January 2009 – October 2010 **14. Sponsoring Agency Code**
15. Supplementary Notes Additional Sponsors: US DOT Research & Innovative Technology Administration, Wayne State University, and University of Detroit Mercy.		

16. Abstract

MIOH UTC TS23 p1 2010-Final

This study, conducted jointly at Wayne State University (WSU) and the University of Detroit Mercy (UDM), develops transit-oriented development (TOD) programs around two selected stations along the planned light-rail transit (LRT) route in Metropolitan Detroit. This study identifies two transit stations along the Woodward Avenue corridor, proposes TOD packages for these sites, and identifies planning, economic, and institutional mechanisms for their effective implementation. The study integrates TOD with the planning and design of selected stations in the Detroit area, with the intent to maximize economic growth potential and to improve the quality of life of the citizens of the local communities and the users of the LRT facility.

17. Key Words		**18. Distribution Statement** No restrictions. This document is available to the public through the Michigan Department of Transportation.	
19. Security Classification -report	**20. Security Classification - page**	**21. No. of Pages** 81	**22. Price**

Abstract

The term transit-oriented development (TOD) is being used increasingly in transit literature, particularly in studies related to planning and design of urban rail-transit. TOD relates to the integration of diverse (but desirable) land uses with transit, both temporally and spatially, and is designed to increase transit ridership and to promote desirable land uses surrounding the station areas. Light-rail transit (LRT) stations appear to be ideal sites for TOD programs, primarily because of compatibility in their scale of operation. Currently, there are a number of transit initiatives in the Detroit metropolitan region that, if implemented, may significantly change the transportation characteristics in the southeast Michigan area.

The purpose of this study, conducted jointly at Wayne State University (WSU) and the University of Detroit Mercy (UDM), is to develop TOD programs on two selected stations along the planned LRT route in Metropolitan Detroit (Chapter 1). This study identifies two transit stations along the Woodward Avenue corridor, proposes TOD packages for these sites, and identifies planning, economic, and institutional mechanisms for their effective implementation. The study integrates TOD with the planning and design of selected stations in the Detroit area, with the intent to maximize economic growth potential and to improve the quality of life of the citizens of the local communities and the users of the LRT facility.

After network-level analysis, the project team selected, within the City of Detroit, the Masonic Temple site based primarily upon the availability of a large amount of vacant land adjacent to Woodward Avenue presumed to be at reasonable prices. For the suburban station, the Troy-Birmingham site was selected because of the steady growth in the area, the excellent level of intergovernmental cooperation by the two cities in promoting new development, and the proposed development of the Multi-modal Transit Center (MTC) and much-needed private developer support. The project team felt the site lends itself to pedestrian friendliness, considered vital for TOD.

The project level analysis, demonstrating the development of TOD packages at the two selected stations are presented in the full report along with a discussion of a set of mechanisms that can be used to implement/expedite the respective TOD packages at the two sites. In developing the TOD packages, the project team reviewed the zoning and associated regulations, and the current land uses, along with the site characteristics, both from their land use and transportation point of view, and proposed land uses that would "blend" with the current fabric.

A set of mechanisms (both general and station-specific) is also presented in recognition of the probability that the implementation of any new program, encompassing transportation-land use interface such as TOD, is likely to be hindered by different institutional barriers. A "mechanism" in this case can be looked upon as a strategy or a group of strategies (planning, economic, financial, etc.) that can be deployed through proper intergovernmental cooperation to implement the proposed development. Finally, a set of conclusions are presented at the end of the report.

TABLE OF CONTENTS

LIST OF TABLES

LIST OF FIGURES

EXECUTIVE SUMMARY

The term transit-oriented development (TOD) is being used increasingly in the literature, particularly in studies related to planning and design of urban rail-transit. TOD relates to the integration of diverse (but desirable) land uses with transit, both temporally and spatially, and is designed to increase transit ridership and to promote desirable land uses surrounding the station areas. Over the last decade, there has been increased interest in North American cities, to construct light-rail transit (LRT) systems to improve mobility. LRT stations appear to be ideal sites for TOD programs, primarily because of compatibility in their scale of operation. Currently, there are a number of transit initiatives in the Detroit metropolitan region that, if implemented, may significantly change the transportation characteristics in the southeast Michigan area. A number of studies are currently underway with the intent of exploring the feasibility of constructing an LRT system along Woodward Avenue, one of the most dominant travel corridors in Metropolitan Detroit.

The purpose of this study, conducted jointly at Wayne State University (WSU) and the University of Detroit Mercy (UDM), is to develop TOD programs on two selected stations along the planned LRT route in Metropolitan Detroit (Chapter 1). Reducing the cost of transportation and congestion on our highways, and creating opportunities for economic development, are major challenges in metro Detroit at this time. TOD programs can contribute to these goals by reducing the public's dependence on automobile travel and revitalizing the local economy. An LRT system would present great opportunities to the community to address these critical needs. This study identifies two transit stations along the Woodward Avenue corridor, proposes TOD packages for these sites, and identifies planning, economic, and institutional mechanisms for their effective implementation. The focus of this study is to integrate TOD with the planning and design of selected stations in the Detroit area, with the intent to maximize economic growth potential and to improve the quality of life of the citizens of the local communities and the users of the LRT facility.

Following a comprehensive review of the current literature on TOD and recent planning efforts on LRT in the Detroit metropolitan area, the project team adopted a two-stage procedure (Network Level and Project Level) to select two stations for TOD along the proposed and current rail corridors in the region. The purpose of the network level analysis is to develop measures for identifying a set of candidate stations where TOD may be feasible based upon factors such as:

- Availability of land
- Proximity to a transit mode/station
- Proximity of adjacent land use conducive to TOD
- Pedestrian "friendliness"

The purpose of the project level analysis, on the other hand, is to develop specific TOD projects at the two selected sites within the area of influence.

The network-level analysis resulted in the initial identification of the following for sites for preliminary consideration:

1. New Center Area, city of Detroit
2. Masonic Temple Theater District, city of Detroit
3. Dearborn Amtrak station, city of Dearborn
4. Troy-Birmingham Amtrak station, cities of Troy & Birmingham

While each of the four sites were found to be appropriate for TOD, project requirement called for the selection of one site in the city of Detroit, and the other in the suburbs for the consideration of TOD. Among the two Detroit stations identified above, the project team selected the Masonic Temple site, based primarily upon the availability of a large amount of vacant land adjacent to Woodward Avenue presumed to be at reasonable prices. The New Center site, while considered more walkable and more vibrant than the Masonic Temple site, was omitted from consideration based primarily upon the nature of local real estate characterized by smalls plots of land that are spatially discontinuous, that may not lend themselves to creative and new development. The project team fully recognizes that the New Center area remains a viable candidate for TOD, based upon the current land uses and their vibrancy. The team, however, felt that the cost of assembling large tracts of land for TOD might be prohibitive.

For the suburban station, the Troy-Birmingham site was selected because of the steady growth in the area, the excellent level of intergovernmental cooperation by the two cities in promoting new development, and the proposed development of the Multi-modal Transit Center (MTC) and much-needed private developer support. The project team felt the site lends itself to pedestrian friendliness considered vital for TOD. While the exact location of the nearest LRT station on Woodward is not known at this time, the project team felt that with proper planning, the station can be integrated with the Amtrak station-site through appropriate pedestrian interfaces, thereby increasing the overall vibrancy of the general area. In the long-run, the site could have a significant and positive impact on the local economy. The Dearborn Amtrak station, even though it met all the fundamental criteria (Table 4), was considered somewhat deficient in pedestrian access.

The project-level analysis, demonstrating the development of TOD packages at the two selected stations are presented in this report along with a discussion of a set of mechanisms that can be used to implement/expedite the respective TOD packages at the two sites. The analysis presented considers the inherent similarities and differences between the two sites within the analytic framework that calls for the same intent, i.e., to propose development packages that would be pedestrian friendly; that could promote land use resulting in economic benefits, increased vibrancy, and higher quality of life; which in turn, would contribute to higher transit ridership. In developing the TOD packages, the project team reviewed the zoning and associated regulations, and the current land uses, along with the site characteristics, both from their land use and transportation point of view, and proposed land uses that would “blend” with the current fabric.

The developments proposed at the two sites encompass a variety of land uses including multi-family residential, retail, service-oriented, and other uses within the area of influence of the proposed station. Pedestrian friendliness serves as a common thread in designing the future development. The availability of large amounts of vacant land is considered a key factor at the Masonic Temple site. Much of the activity proposed at the Troy-Birmingham Amtrak site will be enhanced by the proposed MTC that would serve as the much-needed access point for SMART buses, automotive traffic, and pedestrians.

A set of mechanisms (both general and station-specific) is also presented in Chapter in recognition to the probability that the implementation of any new program, encompassing transportation-land use interface such as TOD, is likely to be hindered by different institutional barriers. A "mechanism" in this case can be looked upon as a strategy or a group of strategies (planning, economic, financial, etc.) that can be deployed through proper intergovernmental cooperation to implement the proposed development. First, a set of general mechanisms is presented that may be applied to transportation projects in general, and that may require interface with land use planning and economic development. This discussion is followed with station-specific mechanisms that attempt to relate the proposed development with strategies that may be deployed to expedite their effective implementation. Finally, a set of conclusions are presented at the end of the report.

1. INTRODUCTION

1.1. What is Transit-Oriented Development?

The term transit-oriented development (TOD) is being used increasingly in the transit literature, particularly in studies related to planning and design of urban rail transit. TOD relates to the integration of diverse (but desirable) land uses with transit, both temporally and spatially, designed to increase transit ridership and to promote desirable land uses surrounding the station areas. A desirable feature of TOD is pedestrian orientation, as demonstrated in number of recent studies. A TOD complex is typically centered on a transit station with gradually decreasing density contour lines, characterized by high density development in the center with "progressively lower density development spreading outward from the center". A formal definition available in literature is as follows [*1*]:

> "*A transit-oriented-development (TOD) is a mixed-use residential and commercial area designed to maximize access to public transport and often incorporates features to encourage transit ridership...TOD's generally are located within a radius of one quarter to one-half mile from a transit stop, as this is considered appropriate for pedestrians*."

Although the above definition of TOD does not mention any specific transit mode, current development patterns in North America suggest that urban rail transit, particularly light-rail transit (LRT) is most conducive to TOD. The focus of this study is on the integration of TOD with the planning and design of selected stations in the Detroit area, along Woodward Avenue. For the remaining sections of this report, the term "pedestrian" has been used to describe all forms of non-motorized travel (e.g., rollerblading, bicycling, skateboarding, and walking).

1.2. The Relationship Between TOD and LRT

Over the last decade, there has been an increased interest in North American cities (i.e., the United States and Canada) in constructing LRT systems in metropolitan areas with the intent of improving mobility. Other factors that have driven this trend include, but are not limited to, the following:

- Reduced negative environmental impact, compared to standard buses (powered by fossil fuels).
- Ability to carry larger passenger volumes efficiently.
- Better service reliability than standard buses.
- Reduced dependence on foreign-sourced fossil fuels (i.e., crude oil).
- Ability to generate significant economic development.
- Less capitally-intensive than rapid-rail transit (RRT) systems.
- Better societal image than standard buses.

A preliminary search conducted by the project team indicated that there are [*2*]:

- 27 cities in North America that have LRT systems in operation.
- 13 cities under extension or under construction for LRT
- Another 40 cities where LRT systems have been approved or proposed (including the Detroit metropolitan area).
- At least 20 of the 27 cities that have constructed LRT have implemented some type of TOD program surrounding transit station locations.

The current literature indicates that many of the TOD programs are on their way to achieving their desired goals of generating higher passenger ridership than (standard) buses, creating significant economic development, and reducing travel congestion. One recent study found that a major economic advantage of TOD is a significant reduction in transportation costs for households located in or around TOD areas [*3*]. The study shows that households with sufficient access to transit stations (i.e., considered to be within a five-minute walk of the transit station), spend about nine percent of their household income on transportation, while the corresponding figures of the average household and households in the suburbs in the United States are 19 percent and 25 percent, respectively. The recent increases in crude oil prices are likely to cause this gap to increase even further.

Another study found that TOD-type housing options in four metropolitan areas produced significantly less traffic than what is generated by a comparable conventional development [*4*]. At the national level, these savings are likely to result in less dependence on foreign oil. Lastly, recent experience with LRT in different cities show that for every dollar of investment in LRT, there is an additional five to six dollars worth of economic development generated by TOD programs [*5*].

Thus, the major benefits of TOD can be summarized as follows:

- Reduced traffic congestion, traffic hazards, and environmental pollution.
- Increased transit ridership resulting from denser development near the station areas.
- Potential for significant economic development in proximity to TOD.
- Reduced household spending on transportation, with a focus on lower-income households.
- Reduced dependence on non-renewable energy.
- Promoting walkable communities and desirable land uses.
- Potential to reduce urban sprawl.
- Vibrant station centers, conducive to pedestrian travel.

The rendering in Figure 1 depicts an ideal configuration for a TOD, a mixed-use redevelopment proposed in the city of Beaverton, OR (a suburb of Portland) [*6*]. In the foreground, passenger boarding platforms and shelters for an LRT system can be observed, while in the background a number of high-density buildings (presumably mixed-use, where both retail and residential land uses are represented) have been sited within a pedestrian plaza. The TOD site has been complemented by street lighting, landscaping, and wide walking paths, all at pedestrian scale.

Figure 1. Ideal TOD Site Configuration
(Source: The Urban Renaissance Group and Group Mackenzie)

1.3. Transit in Metropolitan Detroit, Michigan

1.3.1. Overview:

The Southeast Michigan Council of Governments (SEMCOG) is the metropolitan planning organization (MPO) designated for the southeast Michigan region encompassing seven counties: St. Clair, Macomb, Wayne, Oakland, Livingston, Washtenaw, and Monroe (Figure 2) [*7*]. The current population of the southeast Michigan area of four million places it among the top five regions in the country. Long-term predictions conducted in the early 2000s indicate significant growth in population, households, and employment during the upcoming two decades.

Figure 2. SEMCOG Area Map
(Source: SEMCOG Website)

Approximately 192,000 households in the SEMCOG region have been identified as households without access to a private automobile. Despite this figure, the modal split for transit in the region is very low: only 2.5 percent of people commuting to their place of employment do so using public transit (mostly captive riders). In contrast, 94 percent of commuters travel to work by car, van, or light truck. Thus, the Detroit metropolitan area cannot be designated as a transit-oriented community.

Regions with similar population bases in North America (e.g., Washington, D.C., San Francisco, CA; Boston, MA; and Toronto, Canada) have successfully created and maintained a transit base by attracting choice riders, thereby significantly reducing congestion levels, environmental pollution, and dependence on fossil fuels. The common ingredient among these cities is some type of rail-based travel mode, either LRT or RRT. Choice riders are those commuters who choose to travel by way of public transit, despite the fact that they own at least one private automobile. Very little emphasis, if any, has been placed by policy makers in this region to attract these riders. This is evident from the fact that, while the region ranks fifth in population in the country, it ranks 23rd both in the number of miles and hours of transit services provided [*8*]. Furthermore, the region ranks 21st in the amount of local dollars spent on transit.

1.3.2. Historical Perspective:

As stated in the SEMCOG report, many regions in the United States spend more than three times as much, per capita, for transit services than in the Detroit metropolitan area (Detroit: $59.00, Cleveland: $124.00, San Francisco: $255.00) [8]. Other factors that have limited the availability of transit activities in the region include: the lack of consensus among the city of Detroit and adjoining counties/townships about the structure, governance and funding of a regional transit system, and lack of support among the public at large for a viable transit base.

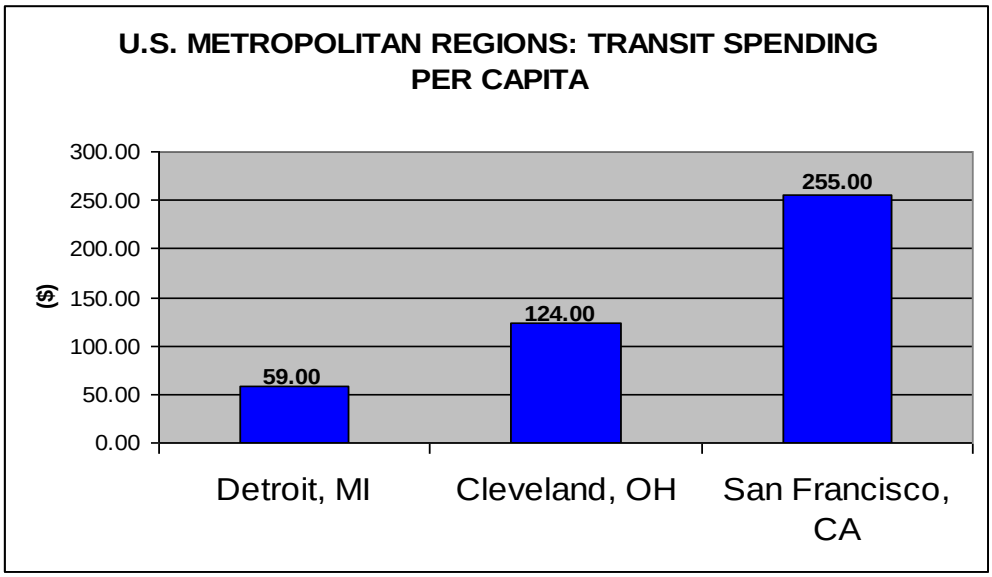

Figure 3. United States Metropolitan Regions: Transit Spending Per Capita

This phenomenon is exemplified by a number of missed opportunities experienced in obtaining transit resources. For instance, the bulk of a $600 million commitment made by the Federal government in 1974 was "lost" because of a general lack of consensus on the programming and planning aspects for a transit system. Similarly, the first regional transit agency in the Detroit metropolitan area, Southeast Michigan Transportation Authority (SEMTA), was created in the early 1970s without a dedicated local transit support base (unlike other metropolitan regions in the country), thereby limiting the region's ability to compete for federal grants. Lastly, no transit allocations were made out of increased gasoline tax revenues in the state, resulting from 1997 legislation, despite the fact that up to ten percent of these funds could be dedicated for transit. Transit services are currently provided by three major agencies in the Detroit metropolitan area:

1. Detroit Department of Transportation (DDOT): service within the city limits of Detroit, Hamtramck, and Highland Park.
2. Suburban Mobility Authority for Regional Transportation (SMART): service for the Detroit metropolitan area, with limited service within the Detroit city limits (including the cities Hamtramck and Highland Park).
3. Detroit Transportation Corporation (DTC): Service for the people mover system.

DDOT and SMART provide bus route service for over 100,000 transit miles per operating day, generating a daily ridership of over 170,000. A number of other transit services are available in the SEMCOG area for their respective local communities:

4. Ann Arbor Transportation Authority (AATA): service for the city of Ann Arbor.
5. Blue Water Area Transportation Commission (BWATC): service for the city of Port Huron.
6. Lake Erie Transit (LET): service for the city of Monroe and Monroe County

1.3.3. Current Developments:

Lately, there has been some renewed interest in rail transit investments within the SEMCOG region. This interest has resulted in a number of studies conducted by both public and private sector stakeholders [*8,9,10,11,12,13,14*]:

- SEMCOG has identified three major travel corridors: Woodward Avenue (connecting the cities of Detroit and Pontiac), Interstate 94/Michigan Avenue (connecting the cities of Detroit and Ann Arbor), and Gratiot Avenue (connecting the cities of Detroit and Mt. Clemens) [*8*].
- A 2001 SEMCOG study recommended rapid transit on 12 regional corridors in the region covering approximately 259 miles. Speed-link services, which would consist of rubber-tired systems on dedicated lanes (i.e., BRT) were recommended along Woodward Avenue, of the 12 corridors identified [*8*].
- A later study, conducted by the Michigan Department of Transportation (MDOT) investigated the potential for deploying traffic signal pre-emption along the Woodward Avenue corridor. This study indicates that signal pre-emption can be an effective tool for improving the flow for BRT through signalized intersections along Woodward Avenue.
- The Metropolitan Affairs Coalition and the Detroit Regional Chamber (DRC) developed a three-tiered rapid transit system, comprising of both fixed and flexible-route local services [*9*].
- Past transit studies have identified the three travel corridors for viable rapid-transit systems, with the first two having the highest potential for success. Transportation experts have expressed that a transit corridor developed along Woodward Avenue could attract riders from corridors parallel to it (e.g., Interstate 75, Michigan Highway 10/John C. Lodge Freeway), over and above Woodward Avenue. Similarly, any transit system developed along I-94/Michigan Avenue could also draw riders from its parallel east-west travel routes (e.g., Interstate 96, Ford Road/Michigan Highway 153). The potential for transit development along the Gratiot Avenue corridor has never been fully investigated.
- The "Woodward Corridor Transit Alternative Study", conducted in 2000 by the Detroit Transportation Corporation, recommended that both bus-rapid transit (BRT) and LRT be further investigated [*10*].
- A recent SEMCOG study explored the possibility of commuter rail transit (CRT) development between the cities of Detroit and Ann Arbor, with a connection to the Detroit Metropolitan Wayne County Airport (DTW), located in the city of Romulus. A myriad of alternatives, ranging from BRT, LRT, and CRT, (following several of alignments) were examined.[1]
- A recent study conducted by a consultant for both SEMCOG and the city of Detroit, explored the feasibility of constructing an LRT system in the city of Detroit from the central business district (CBD) to the northern city limits at Eight Mile Road The proposed system would follow the alignment of Woodward Avenue with an approximate track length of nine miles [*11*]. The capital cost for the system (including rail track, train vehicles, and station structures) was estimated at $373 million.

[1] "Ann Arbor-Downtown Detroit-Metro Airport Transit Study," prepared for SEMCOG, Parsons Corporation, August 2006.

- The M1-RAIL organization is a non-profit, public/private partnership of Detroit-area business and civic leaders that intends to plan and construct an LRT system within the city of Detroit to stimulate economic development. The proposed system will operate along a 3.4-mile route on Woodward Avenue from the Detroit riverfront (W. Jefferson Avenue), northward to the New Center district (W. Grand Boulevard). The proposed LRT system differs from that of the previous studies, in that the planned stations are to be located less than 1/2-mile from one another. Given the shorter distances planned for spacing, the M1-RAIL partnership envisions the proposed system as an urban connector rather than a commuter facility. The organization has so far raised $125 million for the preliminary planning and pre-construction studies of the system [*12*].
- The cities of Troy and Birmingham (located in Oakland County), along with their respective chambers of commerce, have collaborated with one another to acquire funding for the construction of a multi-modal transit center: the Troy-Birmingham Multi-modal Transit Center (MTC). The proposed MTC is located along a railroad route shared by Canadian National Railway (CN) and Amtrak that borders the two cities. The cities have successfully combined their efforts to gain political support at the local, state, and Federal government levels. Such efforts have resulted in the allocation of approximately $8.5 million in Federal funding from the American Recovery and Reinvestment Act of 2009 (ARRA), dedicated to the MTC. The MTC will provide access to SMART, Amtrak, private sedan services, and the Oakland/Troy airport [*13*,*14*].

1.4. Objectives

The objectives of this study are as follows:

1. Identify factors that contribute to the realization of TOD benefits at LRT transit stations.
2. Identify two stations in proximity to the proposed Woodward Avenue LRT corridor, with one located in the city of Detroit and another in the suburban Detroit area that could serve as candidates of TOD, based upon factors identified.
3. For each station identified, develop separate TOD packages (i.e., a combination of mixed uses) in a functional form with due consideration given to the zoning and land use plans of the respective city which will improve quality of life for the surrounding residents.
4. Quantify the packages into appropriate units of development for sketch planning purposes and conduct economic analysis for testing viability of these TOD projects.
5. Develop a set of strategies for implementing TOD packages around LRT station areas (e.g., tax increment financing (TIF), land banking, density booms).

Reducing the cost of transportation, minimizing congestion of our highways, reducing dependency on foreign fossil fuel, and reducing adverse environmental impact are the primary national priorities of today. By exploring the feasibility of implementing TOD programs around proposed LRT stations along the Woodward corridor, this study contributes to the attainment of objectives and priorities of the U.S. Department of Transportation (USDOT) and other federal agencies: Federal Highway Administration (FHWA), Environmental Protection Agency (EPA), Department of Energy (DOE), and Department of Housing and Urban Development (HUD).

2. STATE OF THE PRACTICE

In order to propose techniques, mechanisms, tools, and configurations for transit station locations in Metropolitan Detroit, the project team endeavored to review the current state of the practice for TOD planning. Significant effort has been exerted to seek out information for TOD's that have been planned in metropolitan areas with new LRT systems, particularly in areas where transit service (prior to the construction of LRT) was limited. Lastly, this section focuses on ideal, rather than developments that are simply adjacent to transit facilities. The latter of the two types of developments are typical of land uses in proximity to newly constructed transit facilities.

2.1. Center for Transit-Oriented Development

Funded by Congress in 2005, the Center for Transit-Oriented Development (CTOD) serves as a national clearinghouse on best practices for TOD. It is a national nonprofit effort that works with the Federal Transit Administration (FTA) and the U.S. Department of Housing and Urban Development in matters related to transit and land use policy and funding.
Along with best practices, CTOD also provides research and tools to support market-based TOD and also provides communities with technical assistance regarding TOD [*15*]. The project team received valuable information from CTOD concerning development around transit stations.

CTOD studied neighborhoods located near transit and notes that they were more racially and socio-economically diverse than other neighborhoods.

Through research, CTOD has found that the demand for housing in areas that are near public transportation and that feature walkable neighborhoods with mixed-uses is on the rise due to changes in demographics and increasing traffic problems. Table 1 is a modified table taken from the CTOD brochure *5 Years of Progress* that shows the expected increase of system size of each region from the year 2005 to the projected sizes in the year 2030. Whether a system is small, medium, large, or extensive depends on the number of stations in the system. The designations are as follows: small (24 or few stations), medium (25-69 stations), large (70-200 stations), extensive (201 or more stations). The transit zone households from the year 2000 to the projected totals in the year 2030 are also shown in the table. It is observed that growth in household near transit zone will vary from as low as 56.39 percent (Galveston) to as high as 3969.44 percent (Sacramento) during next 30 years (base line year 2000). This trend will create a tremendous potential for TOD around transit stations [*16*].

Table 1. National Demand for TOD Housing

NATIONAL DEMAND FOR TOD HOUSING						
TRANSIT REGION	**TRANSIT ZONES 2005**	**SYSTEM SIZE 2005**	**SYSTEM SIZE 2030**	**TRANSIT ZONE HOUSEHOLDS 2000**	**2030 PROJECTED TRANSIT ZONE HOUSEHOLDS**	**PERCENT INCREASE IN TRANSIT ZONE HOUSEHOLDS**
New York	955	Ext.	Ext.+	2,876,160	5,371,866	86.77
Los Angeles	113	Large	Ext.	261,316	1,708,447	553.79
Chicago	401	Ext.	Ext.+	787,204	1,503,638	91.01
San Francisco Bay	286	Ext.	Ext.+	409,497	832,418	103.28
Philadelphia	370	Ext.	Ext.+	506,058	809,058	59.87
Boston	288	Ext.	Ext.+	396,261	750,726	89.45
Washington	127	Large	Ext.	234,202	688,582	194.01
Portland	108	Large	Ext.	72,410	279,891	286.54
Miami	60	Med.	Large	62,595	271,326	333.46
Dallas	48	Med.	Large	46,429	270,676	482.99
Atlanta	38	Med.	Large	44,542	228,430	412.84
Baltimore	61	Med.	Large	70,303	198,594	182.48
San Diego	56	Med.	Large	65,743	187,300	184.90
Houston	18	Small	Med.	12,259	181,331	1379.17
Seattle	29	Med.	Large	29,492	159,781	441.78
Denver	24	Small	Large	17,881	138,207	672.93
Minneapolis-St. Paul	17	Small	Med.	18,703	123,776	561.80
Tampa Bay Area	10	Small	Med.	3,024	117,012	3769.44
Sacramento	55	Med.	Large	51,179	107,441	109.93
Pittsburgh	68	Med.	Large	42,792	98,349	129.83
St. Louis	28	Med.	Med.	21,438	94,475	340.69
Cleveland	49	Med.	Large	53,649	86,733	61.67
Las Vegas	9	Small	Med.	8,257	79,448	862.19
Charlotte	10	Small	Large	3,752	76,931	1950.40
New Orleans	18	Small	Med.	31,685	64,160	102.49
Salt Lake City	22	Small	Med.	20,023	63,328	216.28
Memphis	23	Small	Med.	7,269	56,303	674.56
Buffalo	16	Small	Small	19,183	32,616	70.03
Little Rock	11	Small	Med.	1,100	26,434	2303.09
Galveston	15	Small	Med.	5,821	12,029	106.65
Syracuse	8	Small	Small	6,489	10,147	56.37
Total	3349	-	-	6,189,147	15,209,786	145.75*

** Note: Percent increase of transit households from 2000 to 2030. This is not the total percentage of the column.*

(Source: http://www.reconnectingamerica.org/public/display_asset/ctod5yearbrochure)

2.2. Successful Implementation of TOD

In the planning literature, there is no universally-accepted premise about what a TOD should accomplish. Therefore, past projects that have been completed, but labeled as failures, may only have been recognized as such since there is no benchmark for success [*17*]. For the purpose of this study, the project team has considered successful TODs to be characterized by meeting the following benefits:

1. A strong relationship between the land use surrounding a transit station, and the transit facility itself (e.g., more dense development close to the facility, less dense away from it).
2. Developments where facilities have been planned with pedestrians and transit riders in mind.
3. Developments that have had a positive impact on the areas adjacent to transit stations, following their completion (e.g., increased property values, new development, increased pedestrian activity).

2.2.1. Ohlone/Chynoweth TOD - San Jose, CA:

The Ohlone/Chynoweth TOD is located along the Ohlone/Chynoweth-Almaden LRT route, operated by the Santa Clara Valley Transportation Authority (VTA) in San Jose, CA. The route is just over one mile in length, serving three stations, where the Ohlone/Chynoweth station serves as transfer point to the Alum Rock/Santa Teresa line. The Ohlone/Chynoweth-Almaden route was opened for service in 1991 [*18,19*].

Historically, most of the San Jose area has experienced land development that has been largely driven by developers. Thus, the area surrounding the Ohlone/Chynoweth TOD reflects a suburban pattern around a single-family residential neighborhood. However, the city government began to implement more transit-friendly policies after the development of the VTA LRT system: transportation demand management, zoning regulations, master plans, etc.. Those political and institutional mechanisms, along with a $250,000 grant obtained (by VTA) from the Federal Transit Administration, facilitated the planning for this particular station TOD [*20*]. The Ohlone/Chynoweth TOD once existed as a park-and-ride facility, where the bulk of the land was utilized as surface parking with more than 1,000 spaces. The station area was reconfigured with the intent to better utilize the available land for transit-based mobility, to reduce auto-orientation, and to incorporate a mix of land uses:

- Reduction of park-and-ride spaces from 1,100 to 240.
- Medium-density affordable housing development made up of 330 units.
- Addition of 4,400 square feet of retail space.
- Child daycare facility.
- Transit-friendly amenities, such as indoor bicycle parking (with lockers), HVAC, low-floor boarding platforms, and payphones.

In a study conducted by the Mineta Transportation Institute (MTI), the Ohlone/Chynoweth TOD was determined to have had a positive impact on the single-family residences. Using a distance-based empirical relationship, the study found that for every 100 ft decrease in the distance between a home and the TOD, the average sale price for the home increased by $10,500. Additionally, the number of automotive trips generated by the TOD is expected to be somewhat lower than those generated by the original park-and-ride facility [*21*]. Because each of the three conditions listed above have been realized, the Ohlone/Chynoweth TOD has been considered a success.

2.2.2. Center Commons TOD - Portland, OR:

The Center Commons TOD is located along the Red, Blue, and Green lines of Portland's Metropolitan Area Express (MAX) LRT system operated by the Tri-County Metropolitan Transportation District of Oregon (TriMet) [*22*]. The MAX Blue line, connecting suburban Gresham with the Portland CBD was constructed in 1986 as the first LRT system in the area. Today, Portland's regional governing body, Metro, is renowned for having the most aggressive smart-growth, sustainable development and TOD policies in the United States and has been used as a benchmark for other planning agencies for implementing similar policies [*23*].

Prior to the implementation of Metro's TOD policies, most development that took place near transit stops was merely transit-adjacent, where densities were often lower than those typical of single use, saturated with surface parking facilities. Metro's current policies encourage developers to construct multi-story structures with retail space on the lower floors and significantly reduced surface parking facilities.

The Metro planning process has also been successful in creating financing options to facilitate land-use planning. Center Commons, for instance, was one of nine LRT stations that utilized a $3.5 million FTA grant for TOD implementation. This TOD has also successfully integrated a mix of mixed-income rental and for-sale residential units in the same 4.9 acre parcel of land. Additionally, 75 percent of the units constructed were marketed toward residents earning less than the area's median income. The Center Commons TOD boasts the following amenities:

- 314 residential units (combination of affordable rentals and for-sale units, as well as market-rate units).
- Improved pedestrian paths between the TOD site and the adjacent transit station.
- Conservation of a number of large, mature oak trees that remained from the previously abandoned site.
- Located five miles outside of Portland CBD (strategic location for city workers), with an estimated 19 minute travel time.
- Proximity to both MAX and bus services (located approximately 1/4-mile and 1/3 miles away, respectively).
- Infill location in an area where mature flora (trees), a large grocer, a stable single-family residential neighborhood, and a hospital had already existed.

Based on the results of a survey conducted within the TOD, it has been determined that transit mode share for work trips increased from 31 to 46 percent after residents moved into the units, while that for non-work trips increased from 20 to 31 percent [*24*]. Because Center Commons has targeted and attracted occupants that were interested in having better access to transit, and because amenities have been developed to suit transit riders, the TOD program has been considered to be very successful.

2.3. Additional General TOD Information

Upon review of TOD experience of other cities, the project team concluded the following:

- Neighborhoods near transit are more racially and socio-economically diverse than other neighborhoods.
- The growth of households within transit zone will be significant in next 20 years.
- For every 100-foot-decrease in distance between a home and the TOD, the average sale price of the home increased by $10,500.
- After implementation of TOD, the transit mode share of work trips increase from 31 to 46 percent, while non-work trip increase from 20 to 31 percent.

3. METHODOLOGY

The TOD project team initiated the study by seeking objective metrics regarding the possible implementation of TOD in the Detroit metropolitan area. The most critical of such metrics was the location of the area of interest relative to a transit line, proposed or existing. Methods used for this analysis in this effort were conducted on two separate levels: network and project. The network level approach was used to select two station sites for TOD. The project-level approach was used to prescribe probable TOD packages for each station.

3.1. Network-Level Analysis

The purpose of the Network-Level analysis is to develop a measure for identifying a set of candidate stations where TOD programs may be feasible. Potential stations were judged against a set of criteria in order to determine possible TOD eligibility.

3.1.1. Overview:

A set of candidate TOD sites in the Detroit metropolitan area were identified based on the following criteria:

1. Availability of blighted parcels of vacant land.
2. Proximity to a transit mode or facility that is along, or in proximity to, a well-defined travel corridor.
3. Proximity to land uses that may be improved by TOD, through increased foot traffic from growth in transit ridership (e.g., major centers of employment, tourist attractions, and entertainment facilities).
4. Availability of facilities that are conducive to pedestrian mobility: sidewalks, pedestrian-scale land development, street lighting, pedestrian crosswalks.

Criterion number one relates to the assumption that a new development would be less capital intensive if it were to be constructed from the "ground up", as opposed to seeking the redevelopment of an existing structure through demolition. For instance, the J.L Hudson department store, formerly located on Woodward Avenue in the Detroit CBD, was at one time the tallest store in the United States and the second largest by total square footage (second only to the Macy's flagship store located in New York City). In October of 1998, the 33-level (23 of which were above street-level) 2.2 million square foot building was imploded at an upfront cost of $15 million.

Additional societal costs were incurred upon the completion of the implosion, primarily the cleanup of demolition debris, as well as, structural and utility damage incurred by the Detroit People Mover system located nearby [*25*,*26*]. Using the J.L. Hudson department store as (an upper boundary example), the cost of imploding the building (in 1998 dollars) was approximately $6.82 per square foot of space.

$$UnitCost_{IMPLOSION} = \left(\frac{TotalCost}{TotalArea} \right) = \left(\frac{\$15{,}000{,}000}{2.2E6\, ft^2} \right) = \frac{\$6.82}{ft^2} \qquad (1)$$

This estimation, while an extreme case, was considered relevant to the areas in and around the Detroit CBD, where a number of vacant high-density, high square footage buildings remain. The purpose of this example is to illustrate the prohibitive cost associated with the demolition of old structures, thereby increasing the capital cost of the project.

The second criterion reflects one of the most critical intended effects of TOD: accessibility. Most riders access transit modes using park and ride facilities, which require connectivity via an automotive travel corridor (e.g., major freeways, arterials) or by walking (or bicycling). In each of the two methods of access, the TOD serves as a portal to the transit mode in question (e.g., CRT, LRT, RRT, BRT). The third criterion places greater value on potential sites where the use of existing transit services has been observed (e.g., SMART, DDOT, Amtrak). The use of this criterion would imply that the addition of TOD would have a positive effect on transit ridership and the quality of life for those communities served. It has been assumed that the addition of facilities and land uses conducive to non-vehicular travelers in an area around transit activity centers would improve the walkability and increase mobility for all demographics of the affected population (e.g., captive and choice riders, disabled, elderly).

The final criterion relates to the physical layout of the potential TOD site. From a pedestrian standpoint, the walkability of an area is derived from the facilities in place there. For instance, a typical "big-box" retailer located on a high-speed divided arterial highway (e.g., a posted speed limit of 45 MPH along Eight Mile Road) is unlikely to be welcoming to pedestrians in the area. Such developments are often surrounded by large surface parking facilities, without paths or clearance for pedestrians to travel from the side of the road to the structure. Thus, sites with poor access for pedestrians are not suited for TOD.

In order to quantify the walkability of a candidate site for TOD, Walk Score (a tool developed with the intent of scoring geographic locations on their pedestrian-friendly attributes) was utilized. The algorithm used by its developers ranks addresses on an additive scale ranging from 0 to 100 (representing descriptions of "Car-Dependent" to "Walker's Paradise," respectively; Table 2) [*27*]. Using this approach, points are awarded to the address in question according to the number of destinations in its proximity, and their relative distance to them as well. Points of pedestrian attraction beyond one mile from the entity in are not counted in the "Walk Score."

Table 2. Walk Score Thresholds

WALK SCORE	DESCRIPTION	
90 - 100	"Walker's Paradise"	Daily errands do not require a car.
70 - 89	"Very Walkable"	Most errands can be accomplished on foot.
50 - 69	"Somewhat Walkable"	Some amenities within walking distance.
25 - 49	"Car-Dependent"	A few amenities within walking distance.
0 - 24	"Car-Dependent"	Almost all errands require a car.

(Source: Walk Score, "How it Works")

The types of destinations considered in calculating the walk score include, but are not limited to, the following [*28*]:

1. **Transit Modes**
2. **Retail Land Uses**
    a. Grocery
    b. Restaurants
    c. Coffee Shops
    d. Bars
    e. Movie Theaters
    f. Bookstores
    g. Drug Stores
    h. Hardware Stores
    i. Clothing & Music
3. **Municipal Land Uses**
    a. Libraries
    b. Parks
    c. Schools

3.1.2. Additional Criteria for TOD Site Selection:

The following criteria, in addition to proximity to transit (as mentioned in section: *Methodology*), were considered for the selection of candidate TOD sites in the Detroit area. These criteria are intended to capture characteristics of a site that may be most critical to transit riders. Additionally, Walk Score developers have identified many of these criteria as weaknesses in the algorithm used to calculate scores [*28*]:

- **Aesthetics**: refers to street landscaping, outdoor artwork/sculptures, and architectural quality and design of structures in proximity to areas where pedestrians may travel. Neighborhoods that are aesthetically pleasing are expected to have a positive effect on the pedestrian experience.
- **Sidewalk quality and condition:** refers to the actual width of the walking path as well as the condition of the pavement (i.e., cracks, surface friction). Walking areas that are in poor condition, or without pavement at all, are expected to inhibit pedestrian mobility.
- **Topography:** refers to the change in elevation between any two points. Drastic changes in elevation or steep inclines/declines are expected to inhibit pedestrian mobility.
- **Climate:** areas having climates with extreme weather conditions are not likely to be conducive to pedestrian mobility (e.g., high heat and dry winds typical of the climate in Yuma, AZ).
- **Land development configuration:** streetscape and curb designs may potentially influence the travel behavior for pedestrians. For instance, sidewalks that are farther from developments may not generate the same amount of foot traffic as those in a typical urban environment where sidewalks and structures are immediately adjacent to one another.

- **Safety/Crime:** the frequency and severity of crimes committed in a neighborhood are expected to have a significant effect on the amount of pedestrian travel generated by the land uses there. Choice transit riders and consumers may be particularly sensitive to this attribute.
- **Roadway geometry and classification:** the types of roadways in the areas where pedestrians may travel may adversely affect their travel behavior (choosing one walking route in favor of another). For instance, a sidewalk near an intersection of two arterial roads with high posted speed limits and poor-maintained crosswalks may not be attractive. The elderly and young children are particularly sensitive to such areas.

3.2. Project Level Analysis

The purpose of the Project Level analysis is to develop a TOD package for each selected site (an outcome of Network level analysis). The process of identifying TOD packages at each selected site would require detailed analyses of the existing conditions (e.g., population, land ownership) and the possible barriers that may inhibit TOD implementation (e.g., zoning definitions and classifications).

3.2.1. Development Inventory:

In order to develop a TOD package at any site, it is first necessary to assess the type of existing development within some pre-defined influence boundary. For TOD projects, that pre-defined boundary should be established as no greater than a 1/2-mile walking distance (to capture the upper boundary of comfortable walking distance for transit riders and TOD inhabitants), and the types of development that may be of interest include, but are not limited to, the following:

- Residential (e.g., for-sale, rental, senior, low-income)
- Retail/Service/Commercial (e.g., eateries, apparel, drugstore)
- Public/Civic/Institutional (e.g., parks, pedestrian plazas/common areas, schools, churches, hospitals)

This data will enable developers to determine what type of new businesses to include among the existing development to allow for growth and expansion.

Table 3. Sample TOD Site Ranking Matrix

#	LOCATION NAME	CITY	MAJOR THOROUGHFARES	TRANSIT SERVICE?		TRANSIT MODES (AGENCY)	MAJOR ATTRACTIONS / EMPLOYMENT CENTERS / LANDMARKS?	VACANT / BLIGHTED LAND?		# ACRES	SIDEWALKS?		WALKSCORE (out of 100)
				YES	NO			YES	NO		YES	NO	

3.2.2. Population Characteristics:

Along with noting the existing developments in a TOD area, the characteristics of the surrounding area's population must be analyzed when considering development/redevelopment. Developments that cater to the needs of this population, while attracting new population would be considered highly desirable. For example, if part of the population in a TOD area consists of people of a certain demographic (elderly, low-income, etc.), one may consider including businesses that not only accommodate their interests, but also those that are likely to attract new people.

3.2.3. Land Ownership:

Available land may have to be transferred from an existing owner to a developer in order for development to occur. Rather than owning several parcels of land scattered throughout an area, a developer may wish to assemble parcels of land in close proximity into larger blocks to facilitate desirable development patterns.

3.2.4 Zoning:

Zoning is a primary determinant of the types of land uses permissible under the current law, and may be a major issue when dealing with any type of development/redevelopment project. With the TOD goal in mind, zoning definitions/classifications may have to be adjusted to allow for a specific type of building/project. The feasibility of such zoning changes under the current city ordinances must be carefully assessed.

3.2.5. Funding:

A key factor to the successful implementation of any TOD program is the availability of funding. Funding can come in various forms, such as: grants, special tax provisions, incentives, private donations, etc. Amidst all the planning barriers, funding may be the last hurdle to be cleared before project ground-breaking takes place.

3.2.6. Barriers to Implementation:

Although there are many factors in each of the TOD sites that are believed to ease the implementation process (e.g., high transit ridership, existing vibrant community, proximity to frequently-traveled travel corridors), there may also be underlying factors that could inhibit TOD implementation as well. Examples of those factors include:

1. Assembly of disaggregate and scattered land parcels (properties may be difficult to purchase or obtain)
2. Costs of infrastructure improvements (e.g., sidewalk/curb construction, storm water drainage, pedestrian and vehicular traffic signals, street lighting)
3. Vehicular and pedestrian traffic issues (e.g., capacity, safety, operations).
4. Financing challenges (e.g., sources of funding, tax revenue)
5. Lack of coordination between TOD stakeholders (e.g., public versus private organizations; local/state/federal governments, private property owners).
6. Market conditions (lack of demand for new developments)

With regard to real estate, the acquisition of land for development projects may be delayed, and in some cases blocked altogether, by land owners who are unwilling to negotiate. On the other end of the spectrum, the topic of eminent domain often invokes considerable opposition from the public. For instance, the Poletown industrial development located in the city of Detroit displaced a community of more than 4,000 residents for the construction of a new General Motors plant in the 1970's. A small group of those displaced challenged the city of Detroit and General Motors, and would eventually take their argument to the Michigan Supreme Court, only to be defeated in a 1981 ruling: Poletown Neighborhood Council v. City of Detroit. The power of eminent domain has been a sensitive and controversial topic, and has been challenged in many cities in the U.S. [*29*].

The use of eminent domain for the sake of economic development remains blocked by the state of Michigan constitution, as the result of the 2004 Michigan Supreme Court ruling in the case of County of Wayne v. Edward Hathcock. In that case, the court justices expressed that the state law allowing eminent domain for public use was interpreted, at the time, to favor those leading the movement for the Poletown development. The law generally allows land to be taken if it is to be used for purposes benefiting the public [*30*].

Although the ruling was considered a victory for those supporting the rights of private property owners, it simultaneously became a barrier to the planning and implementation of development projects, particularly, TOD projects that often require significant amounts of (often disaggregate) land parcels. In the following sections, factors that may inhibit efforts to implement TOD at each of the locations selected for this study will be discussed.

Another potential mechanism is use of tax abatement, zoning modification, etc. through the concept of consent judgment. This can be applied in a legal sense, and an example of use is the land designation for the Troy-Birmingham Multimodal Transit Center. In this case, Grand Sakwa (the land owner) agreed to give a piece of land to the cities of Troy and Birmingham, with a major stipulation; they had to start development on the site within a specified time frame or else the land would revert back to Grand Sakwa ownership. The cities of Troy and Birmingham were able to secure sufficient funding to allow for development on the land within the specified time frame, thus fulfilling the agreement set forth by Grand Sakwa.

4. NETWORK LEVEL ANALYSIS / SITE SELECTION[2]

Based on a set of factors (as presented in *Network Level Analysis*) such as availability of vacant land, proximity of transit corridor, pedestrian friendly environment and others, the following four sites were selected for the preliminary consideration of this study:

1. New Center - New Center District, city of Detroit
2. Masonic Temple Theater District - Midtown/Downtown District, city of Detroit
3. Dearborn Amtrak station - Fairlane Town Center District, city of Dearborn
4. Troy-Birmingham Amtrak station - Rail District, cities of Troy and Birmingham

The site locations, relative to the Detroit metropolitan area, are depicted as black stars in Figure 4. All but one of the sites considered are located within Wayne County, the exception, site 4, is located in Oakland County. Eight Mile Road, depicted as a grey line in the east-west direction, serves as a physical boundary that mirrors the county line. Site numbers 1, 2, and 4 are located along the proposed Woodward LRT alignment, where Woodward Avenue has been highlighted by the red line in Figure 4. Site number three, the Dearborn Amtrak station, is located along the proposed Interstate 94/Michigan Avenue CRT alignment. Each of the four candidate locations are shown below:

Figure 4. Location of Candidate TOD Sites

[2] Data collected for this chapter were obtained in the period between August 2009 and March 2010.

4.1. New Center

Detroit's New Center district is home to a number of centers of employment and entertainment. The area was first developed in the early 1920's by a group of automotive pioneers wishing to construct their offices within the city of Detroit. At that time, the City was experiencing an economic boom fueled by the private automobile industry and it was difficult to acquire large tracts of land in the central business district. Hence, the New Center area is regarded by many as one of the first major suburban centers in the United States.

The New Center is located near the intersection of Woodward Avenue and W. Grand Blvd., approximately 3.4 miles north of the Detroit River. The most prominent buildings/attractions are described as follows. Their locations, as well as the location of the Amtrak CRT route (depicted as a purple line) are shown in Figure 5. Images of the three buildings considered major landmarks within the city are listed below, and shown in Figure 6 [*31*,*32*,*33*]:

- **Cadillac Place**: this building is located at the southeast quadrant of the intersection of M-10 and W. Grand Boulevard, and served as the world headquarters for the General Motors Company (GM) from 1923, when the building was constructed, until 1996 when the company relocated into the Renaissance Center along the Detroit River in the Detroit CBD. The building is currently occupied by the State of Michigan.
- **Fisher Building:** this building, as well as Cadillac Place, has been listed on both the National Historical Landmarks (NHL) and National Register of Historic Places (NRHP) and in 1978 and 1989, respectively. The Fisher Building houses the headquarters for the Detroit Public School district, as well as 30 floors of office space and the historic Fisher Theater.
- **Henry Ford Hospital:** located at the northwest quadrant of the same intersection, the Henry Ford Hospital is a part of the Henry Ford Health System, a regional center for medical care based in Metropolitan Detroit. The hospital houses more than 900 beds, and typically responds to nearly 20 percent of ambulatory care in southeast Michigan.

Figure 5. New Center District Location

Figure 6. New Center District: Cadillac Place (upper-left), Fisher Building (upper-right), and Henry Ford Hospital (bottom)
(Sources: Skyscrapercity.com; Flickr.com, Henry Ford Hospital Photostream; UrbanToronto.ca)

4.2. Masonic Temple Theater

The Masonic Temple, the largest theater of its kind in the world, is located at the intersection of 2nd Avenue and Temple Street, less than one-half mile west of Woodward Avenue and less than one-half mile north of the Detroit CBD (Figure 7). The Temple was constructed in 1922 and encompasses a number of connected structures: Ritualistic Building, Moslem Temple Tower, Scottish-Rite Cathedral, two ballrooms, and a large drill-hall space. In 1980, the Masonic Temple was added to the NRHP [*34,35,36,37*].

The Temple has historically hosted a number of theatrical and musical performances held by globally-renowned acts throughout the year. Additionally, the property is strategically located along the Woodward Avenue corridor where a number of entertainment centers have been completed within the past decade. Some of the most prominent developments are described below and illustrated in Figure 8:

- **Woodward Place Townhouses at Brush Park:** this development is located at the corner of Woodward Avenue and Adelaide Street, less than one-half of a mile west of the Masonic Temple property. The Woodward Place Townhouses were constructed by the Crosswinds Communities, a major homebuilder in the Detroit area, in a strategic location between the Detroit Medical Center (to the north) and the Detroit CBD (to the south). The development was constructed at a minimal setback from Woodward Avenue, providing good access to the adjacent sidewalks.

- **Ford Field:** home to the Detroit Lions of the National Football League (NFL), construction was completed in 2002 after the franchise relocated from its previous home, the Pontiac Silverdome in Pontiac, MI. The stadium is located in Detroit's CBD, at the intersection of Brush and E. Montcalm streets, which is just east of the Comerica Park complex, located near Woodward Avenue and I-75. Ford Field was constructed for a cost of approximately $500 million, with a seating capacity of 65,000. In addition to the NFL season, many concerts and events are held throughout the year in the stadium space. In recent years, Ford Field has hosted a few special events, most notably the NFL Super Bowl XL, 2009 NCAA Men's Final Four, etc.
- **Comerica Park:** home to the Detroit Tigers of Major League Baseball (MLB), construction on the Comerica Park complex was completed in 2000, after the team moved from their previous home, Tiger Stadium, on Michigan Avenue in the outskirts of the Detroit CBD. The ballpark is located at the intersection of Woodward Avenue and Montcalm Street, just south of I-75. In addition to the MLB regular season, Comerica Park hosts a number of entertainment events throughout the calendar year.

Figure 7. Midtown/Downtown District Location

The areas in the city of Detroit north of I-75, near the Masonic Temple have undergone some redevelopment in the past decade, particularly along the Woodward Avenue corridor. Those developments have included residential, mixed-use, and retail buildings, and have added significantly to the economic vibrancy of the area.

Figure 8. Midtown/Downtown District: Masonic Temple (upper-left), Woodward Place Townhouses (upper-right), Ford Field (lower-left), Comerica Park (lower-right)
(Sources: Wikipedia.com, Wikipedia Commons; Crosswinds Communities; Metro-Melt.com; ExperienceDetroit.com)

4.3. Dearborn Amtrak Station

The Fairlane Town Center district, located in the city Dearborn is home to a number of economic and cultural places of interest, most notably the world headquarters for the Ford Motor Company, located across from the Dearborn Amtrak station near the interchange of Southfield Fwy. (M-39) and Michigan Avenue (Figure 9). The Ford Motor Company is ranked as the sixth largest company in the nation, based on the Fortune 500 listings for the year 2009 [*38*]. Many of Ford assembly plants and research and development facilities are located in the vicinity of the area depicted in Figure 10.

The city of Dearborn has two business districts: West Dearborn and East Dearborn. The Fairlane district is nearly central to both locations, however unlike those downtowns, pedestrian mobility within the Fairlane district is constrained by limited sidewalk connections. Other major attractions in the district include the following [*39,40,41,42,43*] in Figure 10:

- **The Henry Ford Museum and Greenfield Village:** located approximately 2 miles southwest of the Amtrak station, the complex houses a vast collection of memorabilia, structures, and machinery from America's Industrial Revolution period. The museum and village (outdoor portion) were listed as a NRHP and NHL district in 1981. Prominent pieces of the collection include the limousine of Former President John F. Kennedy and Thomas Edison's laboratory.
- **Fairlane Town Center Mall:** located in the area bounded by M-39, Evergreen Road, Michigan Avenue, and Hubbard Drive, the mall is within a 15-minute drive from the major population centers in the region. Constructed in 1976, Fairlane Town Center consists of three floors of retail space, totaling approximately 1.5 million square feet, more than 8,000 surface parking spaces, and 150 tenants.
- **Hyatt Regency Hotel:** located adjacent to the Fairlane Town Center complex, the AAA four-diamond-rated hotel offers 772 guest rooms, 62,000 feet^2 of event facilities. The Hyatt Regency is strategically located between the city of Detroit and the Detroit Metropolitan airport.
- **UM-Dearborn:** located just west of the Fairlane Town Center complex, this branch of the University of Michigan educational system was founded in 1959. It has an enrollment of approximately 8,600 students, offering undergraduate and master's degrees in arts and sciences, education, engineering and computer science, and management.
- **Henry Ford Community College:** located just north of the UM-Dearborn campus, this college was founded in 1938 and has been fully accredited since 1949. Approximately 13,000-14,000 students are enrolled in various disciplines, which include liberal arts, science, fine arts, culinary arts and health science disciplines.

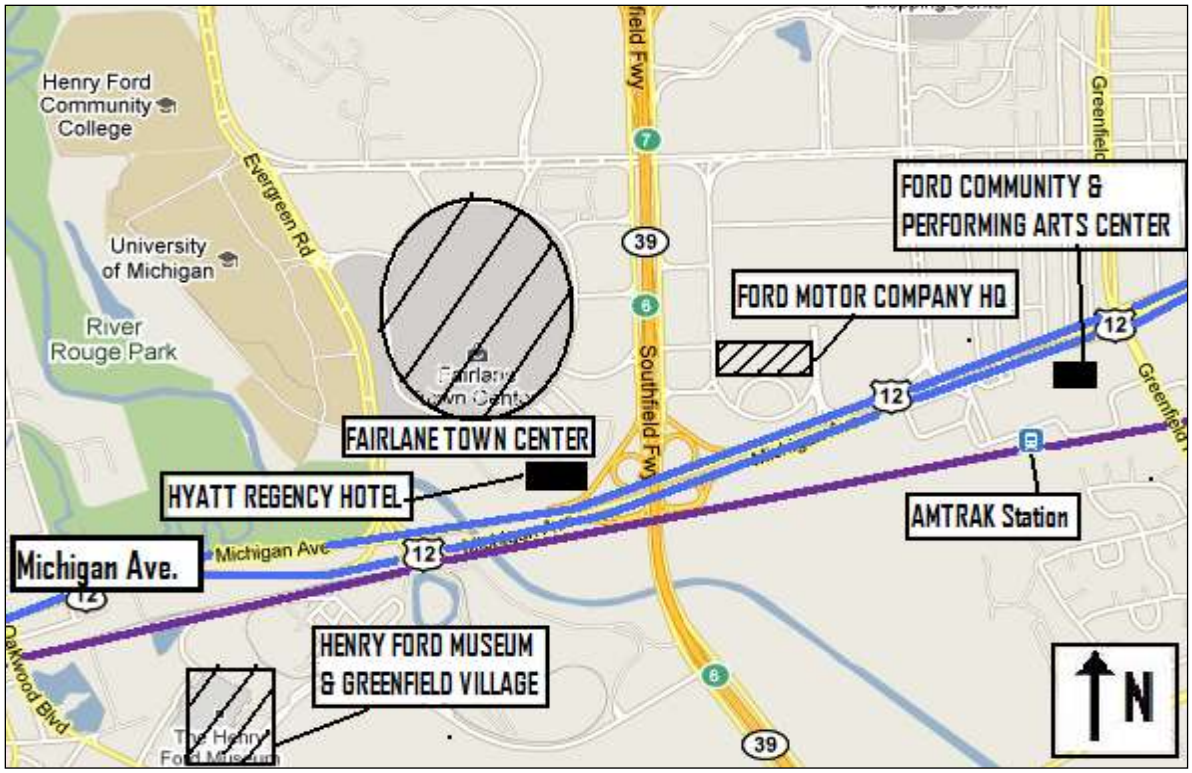

Figure 9. Fairlane Town Center District Location

Figure 10. Fairlane Town Center District: Greenfield Village (upper-left), Fairlane Town Center Mall (upper-right), Ford Motor Company Headquarters (lower-left), Hyatt Regency Hotel (lower-right)
(Sources: City-Data.com, Dearborn; Detroit Travel Guide; Flickr.com; Wikipedia.com, Wikipedia Commons)

4.4. Troy-Birmingham Amtrak Station

The Rail District is an emerging development market that is located in the cities of Troy and Birmingham in Oakland County. The district area has been created through the redevelopment of land parcels once occupied by heavy industrial land uses. Major travel corridors such as I-75 (to the east), Woodward Avenue (to the west), and the lines shared by CN and Amtrak (immediately adjacent) are easily accessible (Figure 11). Overall the area surrounding the Rail District offers a mix of land uses, with varying levels of density.

The Rail District is expected to be further improved by the construction of the Multi-modal Transit Center (MTC). Access to this area from the city of Troy is currently inhibited by the physical barrier caused by the double set of railroad tracks that are located between the Troy-Birmingham boundary. This barrier requires Troy residents to access the site by vehicles through the easement located on S. Eton Street. A preliminary site plan for the new MTC, obtained from the city of Troy is shown in Figure B1 of the Appendix B. Plans for the MTC and the adjoining areas include the following (Figure 11) [*44,45*]:

1. Relocation of the existing Amtrak station south, along the eastern set of tracks on which Amtrak operates.
2. The proposed MTC includes a staging area for storage of four SMART buses, a small pedestrian plaza, passenger parking facilities, bicycle storage, and a hybrid vehicle charging station.
3. Construction of an ADA-compliant pedestrian tunnel under the railroad ROW, that connects the relocated Amtrak station (along eastern tracks) and the MTC (along the western tracks).

Figure 11. Troy-Birmingham Rail District, Birmingham CBD Location

A stable residential community that largely consists of single-family homes with a small cluster of rental units, is located immediately south of the Rail District. Within the past two years, the city of Birmingham has improved pedestrian mobility along S. Eton Street and Maple Road. Some of the attractions near this area have been located in Figure 11, described in the list below, and depicted in Figure 12 [*46*]:

- **Birmingham Theater:** also known as the "Birmingham 8" which reflects the number of movie screen available, has been a part of the city of Birmingham since 1927. The building housing the theater experienced a complete reconstruction and renovation in the mid-1990's and has improved to compete with newer theaters with updated sound and seating systems. First run movies can also be viewed at the theater.
- **Rail District Lofts:** this high-density, four-story residential development has been constructed near the heart of the Rail District, at the intersection of S. Eton and Villa Streets in the city of Birmingham. The development has been designed in contemporary architecture and is made up of larger rental apartments within walking distance to the Amtrak station.

- **Midtown Square Shopping Center:** this shopping center is typical of the North American "big-box" development with a cluster of retail outlets surrounded by a significant amount of surface parking. Midtown Square, located in the Troy portion of the rail district, offers a diverse group of shopping options such as The Home Depot (hardware), Kroger (grocery), and Old Navy (apparel).

- **The Village at Midtown Square:** this multi-family residential development is located in the city of Troy, adjacent to the Midtown Square Shopping Center. The units here have been styled more traditionally than those on the Birmingham side of the Rail District, utilizing a brownstone town home façade. Although the Troy side of this area is less pedestrian-oriented than its Birmingham counterpart, this development offers abundant sidewalks and the units are within (short) walking distance to the shopping center.
- **Oakland-Troy Airport:** the Oakland-Troy Airport allows for private, corporate, and charter flights. Business travelers and tourists can benefit from the airport's proximity to business, recreation, and entertainment venues.

Figure 12. Troy-Birmingham Rail District, Birmingham CBD: Birmingham Theater (upper-left), Birmingham Rail District (upper-right), Midtown Square Shopping Center (lower-left), The Village at Midtown Square (lower-right)
(Sources: Water Winter Wonderland; Masonry Institute of Michigan; Berridge Manufacturing Company; MichiganHomes.net)

4.5. Candidate TOD Site Ranking

The information compiled for the four sites has been used to complete the ranking matrix composed in *Network Level Analysis* (Table 3). The matrix serves as an objective documentation from which the final two TOD sites were selected (Table 4). The data collected in Table 4 can be summarized, as follows:

- All of the sites were serviced by at least one bus transit authority (SMART or DDOT).
- Only one of the sites was not within one-half mile of the proposed Woodward LRT route: the Dearborn Amtrak station.
- Only one of the sites was not in proximity to vacant or undeveloped land (at least one acre): the Birmingham Amtrak station.
- Sidewalks were abundant in all but one of the sites: the Dearborn Amtrak station.

4.6. Selection of the two TOD Sites

Based on the data presented in Table 4 and the requirements set forth in the proposal (one of the two stations selected for TOD to be located in the city of Detroit, the other being in the suburbs) the following two sites were selected:

2. Masonic Temple Theater District - Midtown/Downtown District, city of Detroit
4. Troy-Birmingham Amtrak station - Rail District, cities of Troy and Birmingham

Site numbers 2 and 4 best satisfied the conditions described in *Network Level Analysis: Overview*; availability of vacant or blighted parcels of land, proximity to a transit facility along, or in proximity to, a well-defined travel corridor, proximity to land uses that may be improved by TOD, and the availability of facilities that are conducive to pedestrian mobility.

Site number 2 (Masonic Temple) is a strong candidate for TOD implementation because of its location with respect to the proposed Woodward LRT route, as well existing transit services provided by SMART and DDOT. Furthermore, a sizeable amount of vacant land was identified and located adjacent to Woodward Avenue. This location is expected to be a critical factor in any TOD implementation because it would be a suitable place for a transit station in the least ambitious scenario (e.g., a minimal amount of development). The strategies used to catalyze development near this area are discussed later in this report.

Site number 4, the Troy-Birmingham Amtrak station located in the Rail District, was selected for consideration because of the steady growth that has taken place as of late. The early commitment made by both cities to plan and develop medium-density residential and mixed land uses has resulted in a revitalization of the area. The completion of the MTC is expected to further facilitate the revitalization process, where both cities will be connected along the Troy-Birmingham border, resulting in improved accessibility for the local residents. Considering these factors, site number 4 was identified as a suitable location for TOD implementation.

Table 4. TOD Site Ranking Matrix

#	LOCATION NAME	CITY	MAJOR THOROUGHFARES	TRANSIT		TRANSIT MODES (AGENCY)	MAJOR ATTRACTIONS / EMPLOYMENT CENTERS / LANDMARKS?	VACANT /		# ACRES	SIDEWALKS?		WALKSCORE (out of 100)
				YES	NO			YES	NO		YES	NO	
1	New Center	Detroit	Woodward Ave. I-75, M-10, I-94	X		BUS (DDOT, SMART) LRT (Proposed)*	Henry Ford Health Systems Detroit Public Schools Detroit Police Dept. Fisher Theater	X		4.1	X		77
2	Masonic Temple Theater	Detroit	Woodward Ave. I-75, M-10	X		BUS (DDOT, SMART) LRT (Proposed)*	Masonic Temple Theater Ford Field (NFL - Lions) Comerica Park (MLB - Lions)	X		5.5	X		75
3	Dearborn AMTRAK Station	Dearborn	Michigan Ave. Southfield Fwy./M-39	X		BUS (SMART, DDOT) CRT (AMTRAK)	Ford Motor Company World HQ Hyatt Regency Hotel Fairlane Town Center Ford Community & Performing Arts Center Henry Ford Museum & Greenfield Village	X		5.2		X	57
4	Birmingham AMTRAK Station	Birmingham	Woodward. Ave.	X		BUS (SMART) CRT (AMTRAK) LRT (Proposed)*	Birmingham CBD Troy Shopping Center		X	< 1.0	X		80

The project team realizes that site number 1, the New Center district, is the most walkable and vibrant of the four sites considered. They also felt that while vibrancy has been observed within the New Center district, that the existing development may be prohibitive to new TOD projects. This sentiment was based on the nature of the local real estate characterized by small plots of land that are spatially discontinuous, and that do not lend themselves to creative new development. Thus, the New Center was omitted from consideration of this study. However, if an LRT system were constructed along Woodward, the New Center area is expected to retain the vibrancy, utilizing the current land use patterns.

The Dearborn Amtrak area, on the other hand, was difficult to consider for this study since there were no concrete plans to begin CRT service along the Amtrak route. At the time of this writing, local governments along the route (i.e., the city of Detroit, city of Dearborn, city of Ann Arbor), county governments (i.e., Wayne and Washtenaw counties), and regional governments (e.g., SEMCOG) have been unable to secure adequate funding to begin CRT services. Furthermore, the area surrounding the station is solidly automotive-oriented in design, where the sidewalks along Michigan Avenue are adequate but somewhat disconnected with the land uses there. Thus, the "sidewalks" entry in Table 4 reflected the connectivity of said sidewalks in addition to their existence. Any funds that have been granted for Amtrak or commuter rail in the state of Michigan do not have any application for a CRT service between Detroit and Ann Arbor. That proposed service would NOT be operated by Amtrak, but along Amtrak tracking. Considering these factors, the Dearborn Amtrak station was omitted from consideration of this study.

5. PROJECT LEVEL ANALYSIS / TOD PACKAGES

In the previous chapter, the network level analysis that resulted in the selection of two stations in the Detroit metropolitan area for implementing TOD was presented. The objective of this section is to propose a set of TOD packages for each station, along with a set of institutional, planning, and economic mechanisms to aid the implementation of the respective TOD packages. As a part of this effort, first TOD packages are developed for each station and then a general discussion of various sets of mechanisms relevant to both sites is presented, followed by station-specific discussion.

5.1. Masonic Temple Theater

This is one of the two stations selected based primarily on the availability of vacant land, proximity to a transit line, and the location of major activity/employment centers within a short distance. Detailed information about the location of the center, site characteristics, and the proposed TOD packages/mechanisms are presented below.

5.1.1. General Overview:

Figures 13 and 14 are modified revisions of maps obtained from the records maintained by the City of Detroit Geographic Information Systems (GIS) and Planning and Development Departments. These maps depict the current zoning patterns of the area surrounding the Masonic Temple site which is bisected by Woodward Avenue [47]. Each of the maps has been overlaid with descriptions of the current land uses.

Referring to Figures 13 and 14, the city of Detroit has made provisions for denser, infill-type development to occur in proximity of the Masonic Temple Theater area, particularly along the east side of Woodward Avenue (as reflected in R5 and R6 zoning classifications). Many of these parcels of land directly east of the Woodward Place Townhomes have been zoned as "Planned Development" and may be best described as medium-density residential development (Figure 13).

The land use definition "Planned Development District" (PD) refers to a zone established under Article XI, Division 2 of the Detroit Zoning Ordinance: Specialty Purpose Zoning Districts and Overlay Areas. The description for the PD zoning definition generally states that those plots of land classified as such may be useful when urban renewal and infill development projects are being considered. Furthermore, the PD zoning may be applied to allow a variety of land uses: residential, public/civic/institutional, retail/service/commercial, etc. [*48*].

The Masonic Temple Theater area located west of Woodward Avenue and south of Temple Street, on the other hand, is entirely zoned as "General Business." Additionally, nearly half of those parcels of land have been observed to be vacant properties. The project team felt that this section of the Temple area would have the most opportunity for TOD implementation because of the availability of vacant land directly along Woodward Avenue. Furthermore, the parcels are physically contiguous and are likely to be owned by the same entity, whether public (e.g., Wayne County, city of Detroit) or private (e.g., real estate holding company, business owner). Single-ownership of contiguous parcels of land (as opposed to multiple-ownership of scattered parcels) are better suited for planned development projects.

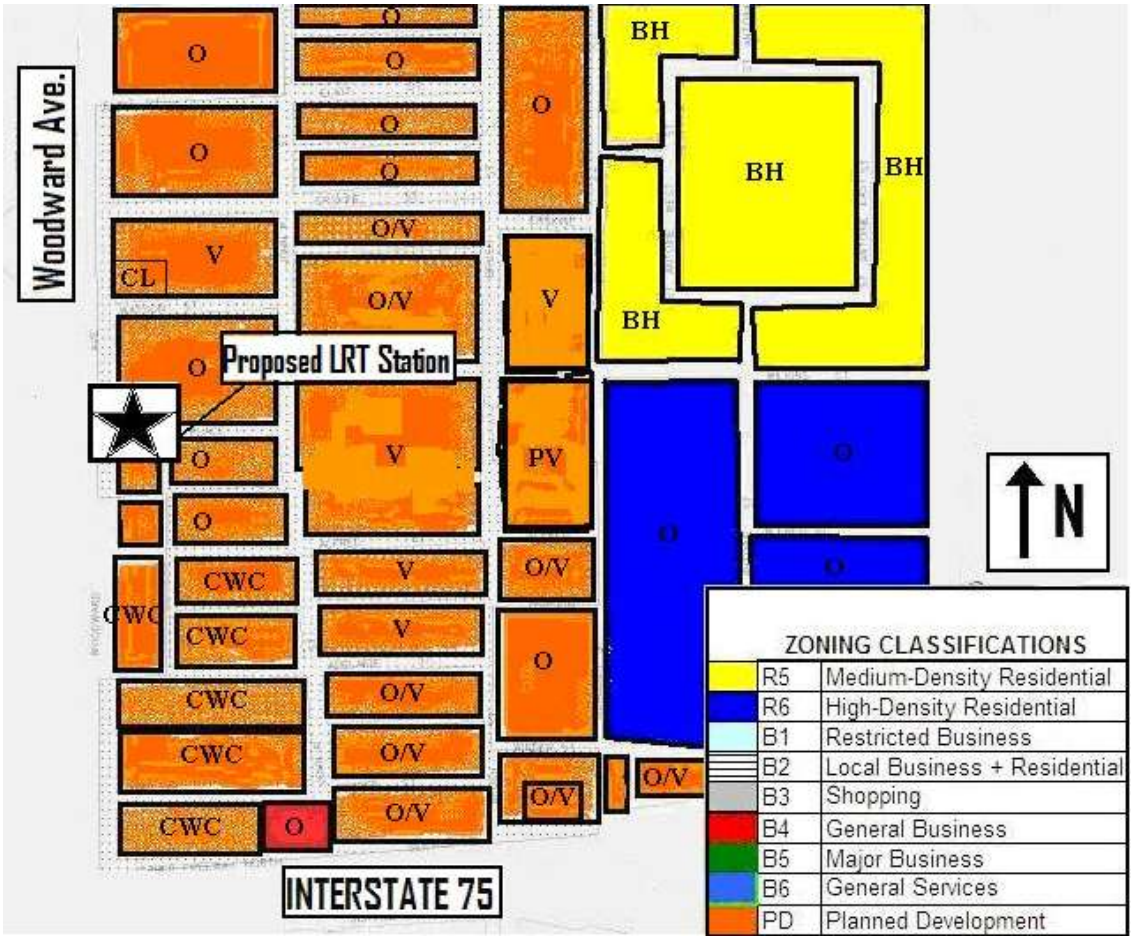

Figure 13. Masonic Temple Theater, East of Woodward Avenue

- O: occupied land, building(s) on-site
- V: mostly vacant land, building may be on-site
- O/V: building(s) on-site, mixed with vacant land
- CL: Crystal Lofts
- PV: Village-Brush Park Manor: Paradise Valley (Senior-Living Community)
- CWC: Crosswinds Communities, Woodward Place Townhomes at Brush Park
- BH: Brewster Homes

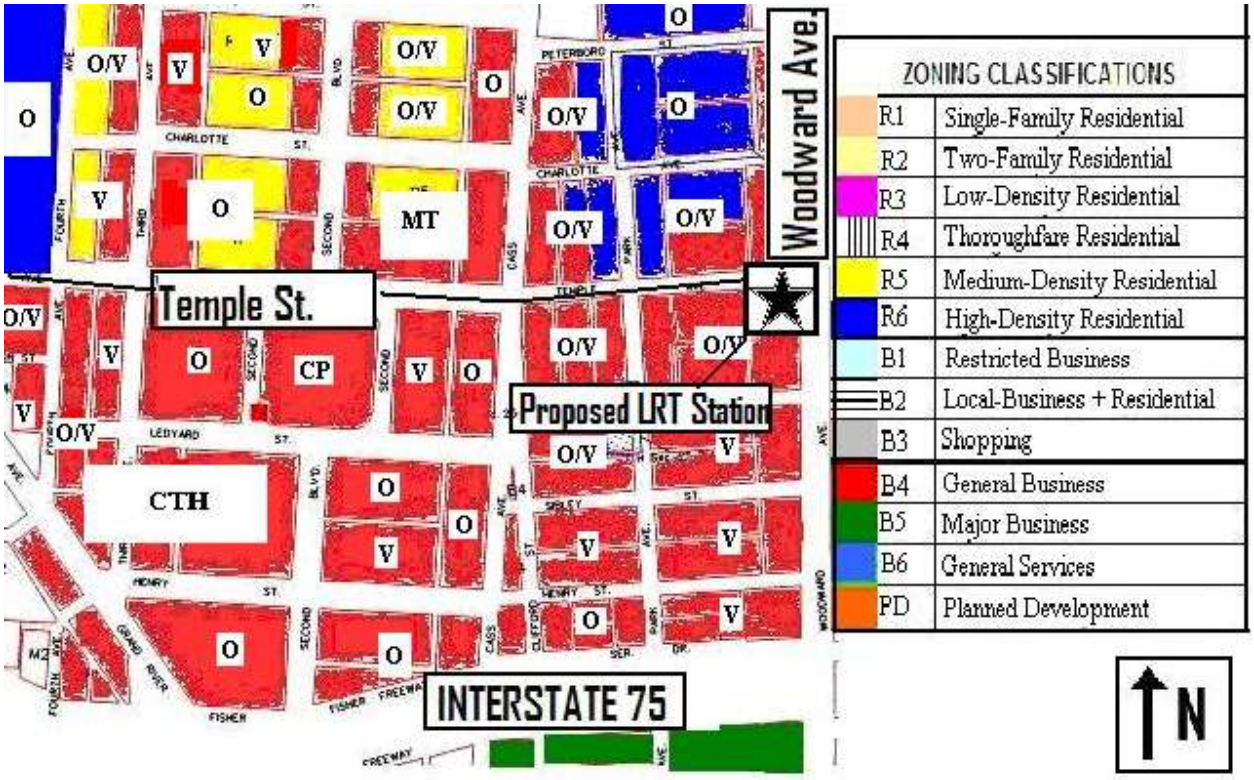

Figure 14. Masonic Temple Theater, West of Woodward Avenue

- O: occupied land, building(s) on-site
- V: mostly vacant land, building may be on-site
- O/V: building(s) on-site, mixed with vacant land
- MT: Masonic Temple Theater property
- CP: Cass Park
- CTH: Cass Technical High School

Aerial images of the vacant properties and occupied parcels of land with respect to Woodward Avenue and Temple Street are shown in Figures 15 and 16. The total land area of the vacant land depicted is estimated at 5.5 acres (Table 4).

Figure 15. Masonic Temple Theater, West of Woodward Avenue and North of Temple Street: Aerial View

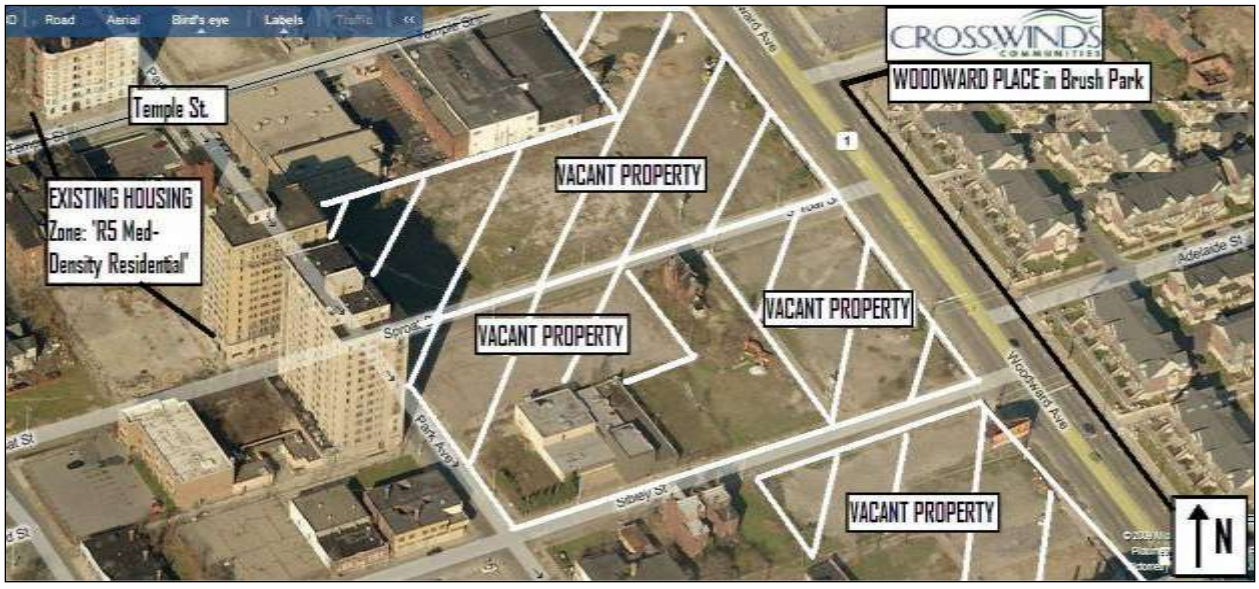

Figure 16. Masonic Temple Theater, West of Woodward Avenue and South of Temple Street: Aerial View

5.1.2. Site Characteristics and Land use activities Inventory:

In the Masonic Temple Theater area, the influence area is centered around the intersection of Woodward Avenue and Temple Street. The residential development in the Masonic Temple area has experienced significant growth in supply during the past decade, particularly along the Woodward Avenue corridor. Those new developments have largely been marketed toward individuals wishing to live closer to Detroit's Cultural Center (to the north) and Detroit CBD (to the south), consisting of a mix of contemporary loft-styled condominiums (i.e., The Ellington, Crystal Lofts) and more traditional-styled townhomes (i.e., Woodward Place at Brush Park). A summary of the residential market development inventory, within the influence area, is shown in Table 5 [*49,50,51,52*].

Table 5. Residential Market

NAME	WALK DISTANCE TO STATION [mi]	TYPE	MARKET	TOTAL # FLOORS	TOTAL # UNITS	ADDITIONAL INFO
Woodward Place at Brush Park	< 0.1	Condo, Townhome	For-Sale	NA	180	2,3-bedroom units (1,300 - 2,002 ft^2)
Village-Brush Park: Manor Paradise Valley	0.3	Senior	Rent	3	113	1-bedroom apts.
Heritage Senior Living	0.5	Senior	Rent	4	50	
Carlton Lofts	< 0.2	Condo	For Sale	7	51	Studio (1 or 2-level), 1-2 bedroom units (700-1,800 ft^2)
Crystal Lofts	0.1	Condo	For Sale	4	17	Studio, 1,2-bedroom units (1,137-1,885 ft^2)
Ellington Lofts	0.4	Condo	For Sale	4	55	1,2-bedroom units (860-1500 ft^2)
Peterboro Place Apartments	0.2	Rent	Rent	6	?	

Commercial development in the Masonic Temple, by contrast, has not experienced much growth during the past. Most of the new commercial developments constructed have been focused along the Woodward corridor, and are attached to the aforementioned residential developments as mixed-use facilities: first-floor commercial, second-floors and higher residential. The real estate market for residential and commercial spaces remains weak, as the hardships faced by the American automotive manufacturers (historically, the backbone of the Detroit-area economy) have had a ripple effect on the metro area and the state of Michigan as a whole. Furthermore, the world economic crisis of 2008-2009 has severely deepened those effects. As a result, many of the newer residential developments (especially along the Woodward corridor) are sparsely occupied.

A summary of the commercial market development inventory, within the influence area, is shown in Table 6.

Table 6. Retail/Service/Commercial Market

NAME	WALK DISTANCE TO STATION (mi)	TYPE	MARKET	ADDITIONAL INFO
Park Sibley Market	0.2	Retail	Convenience	
Big Eagle Market	0.4	Retail	Convenience	
Source Apparel	< 0.1	Retail	Apparel	Woodward Ave. corridor
Detroit 1 Coney Island	0.2	Service	Restaurant (Casual)	
People's Records & Collectibles	0.2	Retail	General	
FedEx Kinko's	0.4	Service	General	Mixed Use Development (Ellington Lofts Structure)
Starbucks Coffee	0.4	Service	Restaurant	
T-Mobile	0.4	Retail	General	
Temple Bar	0.2	Service	Pub, Lounge	
Atlas Global Bistro	< 0.1	Service	Restaurant	

Public/civic/institutional land uses near a TOD are expected to improve the quality of life of the local residents. Many of these land uses, such as hospitals, schools, and libraries may present employment opportunities within the community as well. Considering these factors, the Masonic Temple area is strategically located near the Detroit Medical Center (DMC) (approximately one mile north), a campus of medical research institutions that have strong relationships with many institutions of higher learning within the state of Michigan: University of Michigan, Michigan State University, and Wayne State University (located approximately one mile north of the proposed Temple transit stop). A summary of the public/civic/institutional land uses in the influence area (within one-half mile) surrounding the Masonic Temple is shown in Table 7.

Table 7. Public/Civic/Institutional Market: Masonic Temple Area

NAME	WALK DISTANCE TO STATION (mi)	TYPE	ADDITIONAL INFO
Cass Park	0.3	Public Park	
University of Michigan - Detroit Center	0.4	Higher Learning	Satellite campus
Ecumenical Theological Seminary	< 0.1	Place of Worship	Training center
Cass Park Baptist Church / Hope Baptist Center	0.4	Place of Worship	
St. Patrick's Parrish Catholic Church	0.5	Place of Worship	
Jehovah's Witnesses Woodward	0.4	Place of Worship, hall	
St. John's Episcopal Church	0.4	Place of Worship	NRHP, 1982

One of the most prominent places listed is the St. John's Episcopal Church, located at the intersection of Woodward Avenue and the I-75 service drive (Figure 17). St. John's is the oldest functioning church located along Woodward Avenue in the Detroit metropolitan area and in 1982 it was added to the NRHP [*53*]. Currently, the church remains as a local landmark of the Detroit lower Woodward Avenue/CBD area.

Figure 17. St. John's Episcopal Church

In summary, the data presented in Tables 5-7 has indicated the following, with regard to the Masonic Temple influence area:

- The residential housing stock is diverse, but the newer developments are sparsely occupied (particularly the Ellington Lofts and Crystal Lofts).
- The commercial development market is largely open. The city of Detroit lacks a major chain-based grocery chain (e.g., Meijer, Kroger). Within the influence area, there are no developments consisting of: chain-based hardware retailer (e.g., Home Depot, Lowe's, Menards, ACO Hardware), drugstore (e.g., CVS, Walgreen's, Rite-Aid), casual dining restaurant (e.g., Applebee's, TGI Friday's, Chili's, Red Lobster), or general apparel (e.g., Old Navy, H & M, Marshall's, Kohl's, Target).
- There is a wealth of institutional land uses nearby (WSU, DMC, places of worship), but there is a lack of pedestrian facilities in the area, particularly along the Woodward Avenue corridor. The sidewalks located are in good condition but are relatively narrow, considering the urban location. Aside from the Cass Park property, located across from the Masonic Temple, there are no common areas or pedestrian plazas within the influence area.
- There are more than six churches within half-a-mile radius of the temple that attract in excess of 1000 worshipers during Sundays. However, there is no nearby quality eating establishment for those patrons.

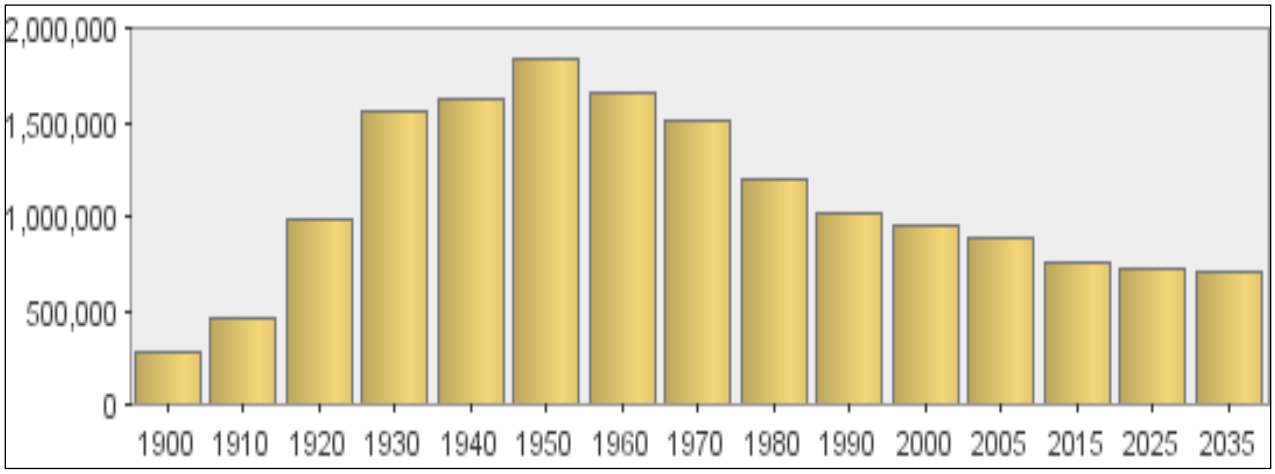

Figure 18. Population Forecast: City of Detroit
(Source: U.S. Census Bureau, SEMCOG 2035 Forecast)

5.1.3. Pedestrian Access:

From an engineering standpoint, the configuration of the Woodward Avenue corridor and its adjacent streets in the Masonic Temple area are not conducive to pedestrian mobility or TOD. The most challenging issue in this regard is that the total width of the Woodward Avenue. The right-of-way consists of nine lanes:

- Through movements (six lanes): three lanes in each direction of travel (northbound and southbound)
- Left-turn movements (LT): one center lane
- Curbside parking (two lanes): one lane in each direction of travel

According to aerial imagery obtained for the area, the crossing width for the Woodward Avenue. ROW is approximately 10 feet per lane, or a total of 90 feet [*54*]. Although traffic along this corridor is not particularly heavy along this highway segment (ADT: 10,168 vehicles per day (vpd), PHV: 971 vehicles per hour (vph)), pedestrian safety would be questionable even under non-peak traffic conditions due to the large crossing width that pedestrians must overcome when traveling from one side of Woodward Avenue to another [*55*] (Figures 19-21). Further analysis of geometric highway and traffic signal design in this area revealed the lack of the following pedestrian-friendly features:

1. Properly delineated crosswalks
2. Pedestrian relief center island
3. Pedestrian crossing signals

The T-shaped intersection configuration for cross-streets in the area (moving from north to south: Charlotte Street, Edmund Place, Temple Street, Alfred Street, and Sproat Street; represented

by locations 1-5 in Figure 19), make it difficult to implement pedestrian crossing signals, while simultaneously maintaining vehicular traffic along Woodward Avenue. The cross-streets at locations 1-5 are controlled by 'STOP' signs only. Past efforts to improve pedestrian safety at un-signalized intersections have included the installation of pavement markings/delineation and warning signs. Such improvements, however, have had limited success in achieving goals to increase pedestrian safety. One of the most challenging problems in solely relying on signage and markings is that they may be ignored by drivers and pedestrians [*56*].

Although the technology used in traffic and pedestrian signals has increased dramatically in the past 20 years (i.e., video detection), and methods to stop vehicular flow along Woodward Avenue in order to allow safer pedestrian crossing movements are achievable, the main function of Woodward is that of a primary arterial roadway. Thus, the addition of five traffic signals within a distance less than one-quarter mile (the exact distance between Charlotte and Sproat Streets is one-sixth of a mile) is likely to have adverse effects on throughput capacity.

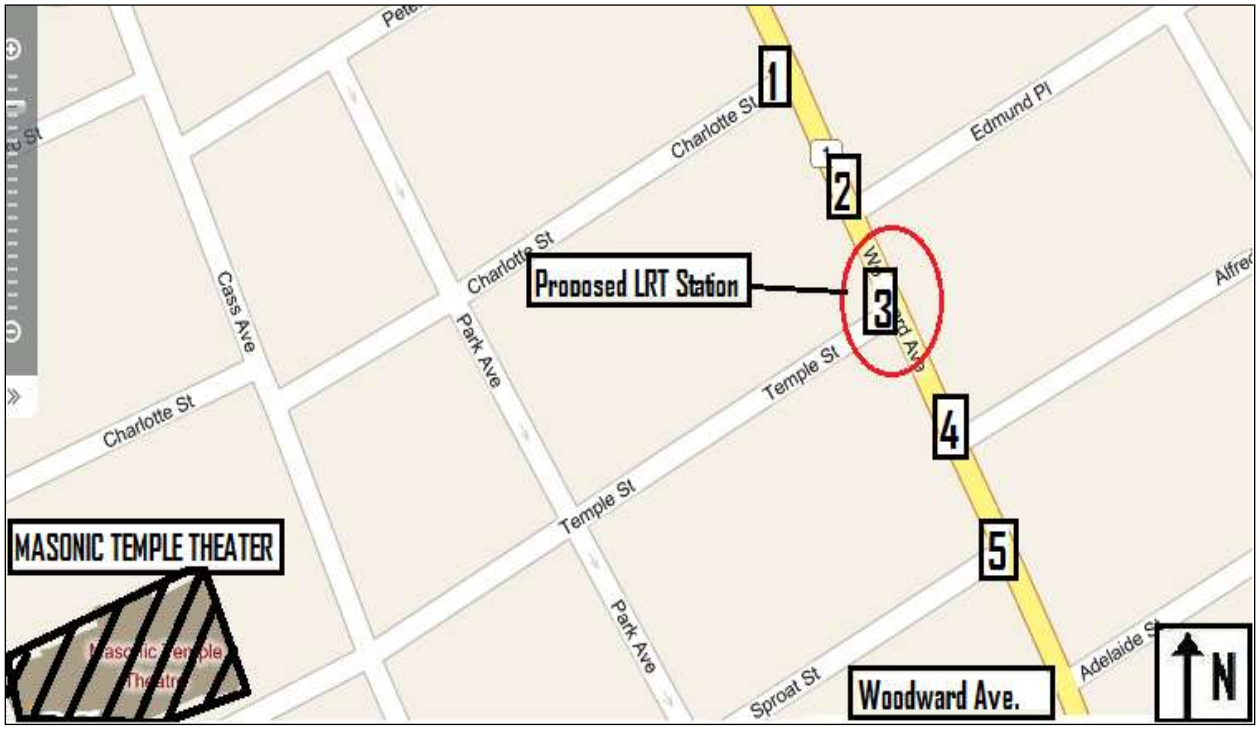

Figure 19. Proposed LRT Station Locations

Preliminary plans for the M-1 Rail LRT system, call for the LRT vehicles (LRTV) to travel along Woodward Avenue by utilizing the second travel lane from the curbside. Using this convention, northbound LRT passengers would need to access the east side curb of Woodward Avenue, so that they may board the system, and vice versa. Based upon the existing conditions of the site, it would appear that successful implementation of LRT would require significant improvement in pedestrian safety.

In order for the area near the Masonic Temple LRT station to function as a true TOD, the east and west sides of the Woodward Avenue must be better connected for pedestrian movement.

Figure 20. Aerial View of Woodward Avenue ROW

Figure 21. Street View of Woodward Avenue, Looking South (Figure 19, Location 3)

5.1.4. TOD's Proposed:

The records maintained by the city of Detroit related to the real property surrounding the proposed LRT station at Woodward Avenue and Temple Street (referred to as location 3 in Figures 19 and 22), indicate that a total eight parcels are currently city-owned. The total area of those parcels, located adjacent to Woodward Avenue and north of Sproat Street, is approximately 2.63 acres (Figure 22). Those parcels are conducive to any efforts taken by the city to construct passenger boarding/alighting facilities for the proposed LRT system, and are strategically located to support a system that operates LRTVs through the median (where two sets of track are laid side-by-side), or along travel lanes (where one track is laid in a traveled lane, for each direction of travel). In regard to future development in the Masonic Temple area, this scenario would largely represent the most conservative scenario.

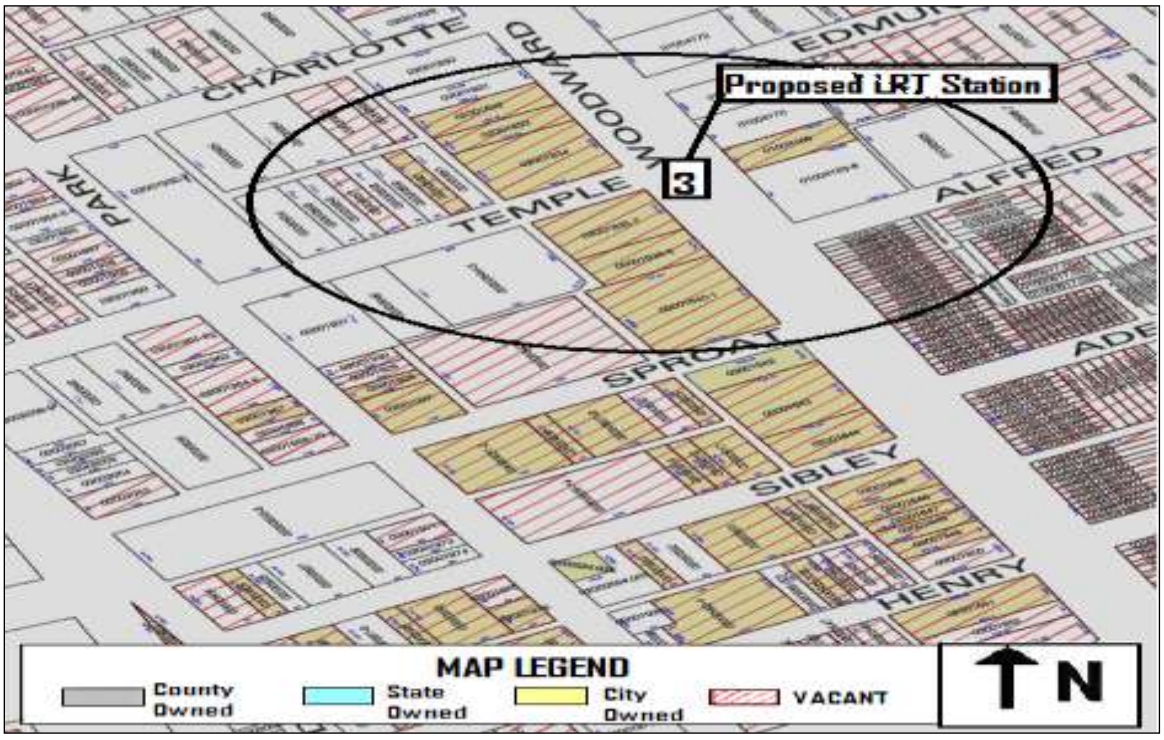

Figure 22. Land Use and Property Ownership

The Temple area was selected for consideration in this study for its potential for future growth. The area currently lacks many features that are typical of an ideal TOD. Of particular importance is the lack of connectivity across Woodward Avenue, as well as, the land uses within walking distance of the proposed LRT station. Table 8 lists land uses that may be added to the area with the intent to improve the quality of life and livability for the local residents. A discussion of possible mechanisms to complement proposed land uses is provided in the next section.

Lastly, a spatial reference with respect to the area near the proposed Masonic Temple LRT station is provided for each proposed land use. It should be noted that the proposed changes for the area are subject to change and other alternatives may be implemented for TOD.

Table 8. Proposed Land Uses

	LAND USE TYPE	DESCRIPTION	ADDITIONAL INFO
1	Retail/Service/Commercial	Child Care Center	
2		Bookstore	e.g., Borders Books & Music, Schuler's Books & Music
3		Casual Dining Restaurant	e.g., Chili's, Applebee's, TGI Friday's, Denny's
4		Grocery or General	e.g., Meijer, Kroger, Target, Wal-Mart
5	Public/Civic/Institutional	Transit Station w/ Shelter	May be integrated into mixed-use structure, located on street-level
6	Residential	Apartment Complex	For Rent, Marketed toward students (WSU, UM, MSU)
7	Public/Civic/Institutional	Traffic calming/Pedestrian facilities	e.g., pedestrian relief island (Woodward Ave.), HAWK pedestrian signals, capacity reduction (Woodward Ave.), "zebra" crosswalk markings

The land uses and improvements listed in Table 8 are all proposed for the area encircled in Figure 22. Items 1-6 could be sited in the circled area, on the west side of Woodward Avenue, if they were incorporated into a large, mixed-use structure. Using this convention, land uses that generally generate pedestrian traffic (such as the non-residential types of development listed), could be located at street-level of such mixed-use structures. Residential units (preferably rentals) or additional retail (such as a large grocery chain) could then be planned for the higher floors of the proposed structure. The amount of first-floor space available for tenants, such as a large grocery chain or general retailer, may be a limiting factor when implemented in the area encircled in Figure 22. To mitigate this, additional parcels of land (located south of Sproat Street and west of Woodward Avenue) could be released from city ownership. Examples of mixed-use structures are depicted in Figures 23 and 24. The density of such a development and its precise location would largely depend on the willingness of the administration/policy makers of the city of Detroit to release the city-owned land parcels and the willingness of developers to pursue such projects.

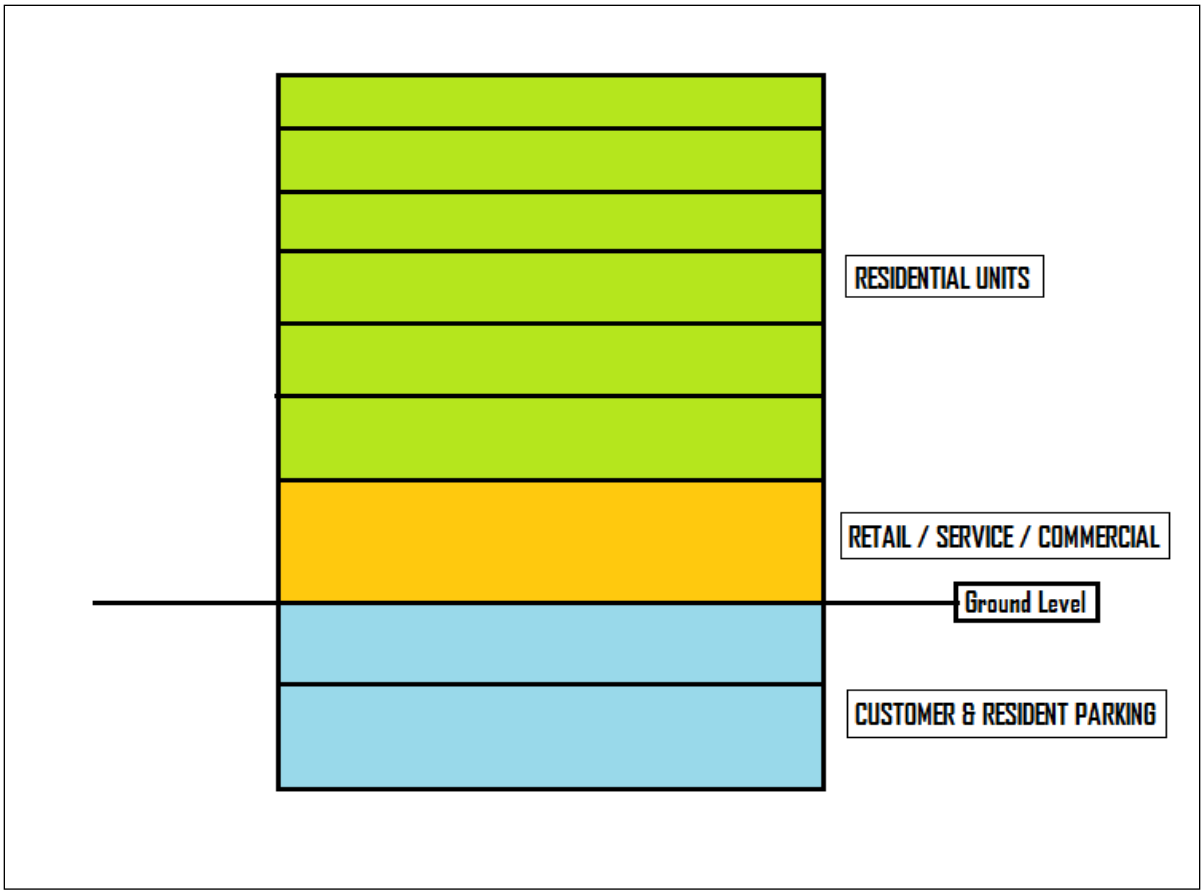

Figure 23. Diagram of Typical Mixed-Use Structure

In the spirit of TOD, it is also suggested that plans for additional parking facilities are significantly reduced or omitted if possible. This suggestion parallels research conducted for Transit Cooperative Research Program (TCRP) Report 128: Effects of TOD on Housing, Parking, and Travel. In the study, trip generation and parking data were collected from 17 completed TOD projects located in four metropolitan areas in the United States: Philadelphia/NE New Jersey, Portland, San Francisco Bay, and Washington, D.C. It was determined that residential TOD's generate approximately 50 percent less vehicle trips, during the peak periods (i.e., A.M. and P.M. peaks), than the most current rate estimates established by the Institute of Transportation Engineers (ITE) [*57*]. Furthermore, it is suggested that if additional parking is considered absolutely necessary for the development, that such parking be located as an underground facility (blue portion of Figure 23), to maintain the pedestrian friendliness of the general area at the street level.

Each of the land uses proposed in Table 8 are intended to complement, and in many cases to provide for the needs of the community living in proximity to the Masonic Temple area (community areas listed in Table 5). For instance, there is a lack of a major bookstore chain in the area. With the added advantage of the proximity of the MSU and UM-based facilities, and those currently maintained by WSU, UDM, and the DMC, additional book sellers could be valuable to metro Detroit residents affiliated by those institutions.

Another example would be the lack of a major grocer or general retail chain within the city limits. The lack of such a facility requires the residents of the city, including the temporary student populations and existing Temple-area residents, generally must travel outside of the city of Detroit (e.g., Dearborn, Warren, Redford Township) for such retailers or settle for limited options available at local convenience stores.

Figure 24. Completed Mixed-Use Structure
(Source: http://yochicago.com/mixed-use-shops-and-lofts-in-grand-boulevard-to-feature-140-new-apartments/13924/)

5.2. Troy-Birmingham Amtrak Station

The second site selected for possible implementation of TOD, was based primarily upon the proximity to a rail station, potential interface with the proposed LRT station on Woodward, strong pedestrian friendliness in the design of the streetscape of the partner city of Birmingham, potential to incorporate a pedestrian orientation with the retail development in Troy, and the availability of a relatively large high-density residential development around the station area. Detailed discussion of these features and proposed TOD and associated institutional mechanisms are presented below.

5.2.1.General Overview:

Figure 25 is an aerial photograph obtained from the city of Troy Planning Department that displays what the area looked like in 1990, when a Ford plant occupied the land and before major development occurred. Zoning maps for the cities of Troy and Birmingham were also obtained from records maintained by their respective city planning departments. Figures 26 and 27 have been modified from those records, and depict the current zoning definitions and their distribution for the cities of Troy and Birmingham, respectively [*58,59*]. Each of the zoning maps has been overlaid with descriptions of the current land uses that have been observed in the area.

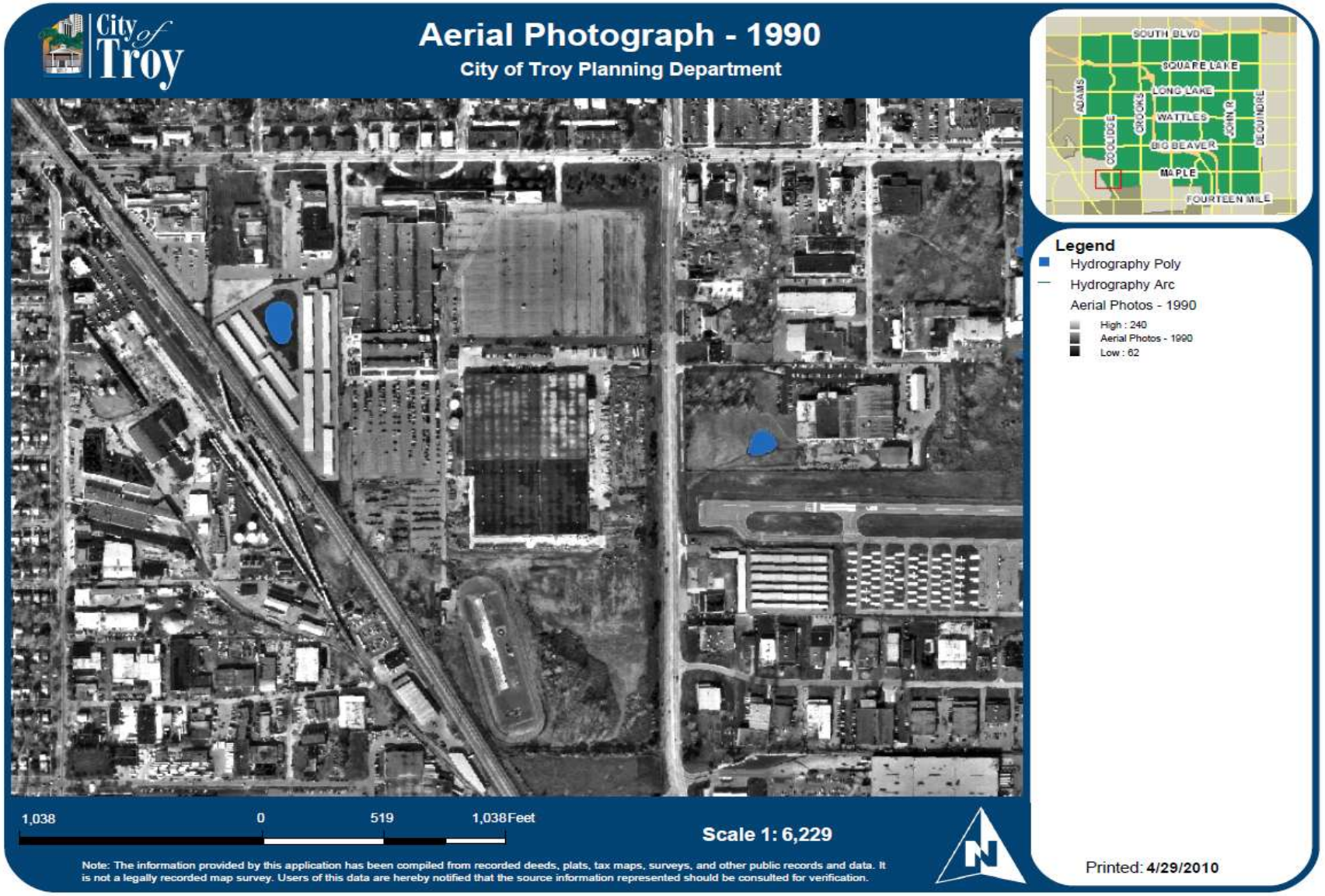

Figure 25. Ford Tractor Plant – Circa 1990

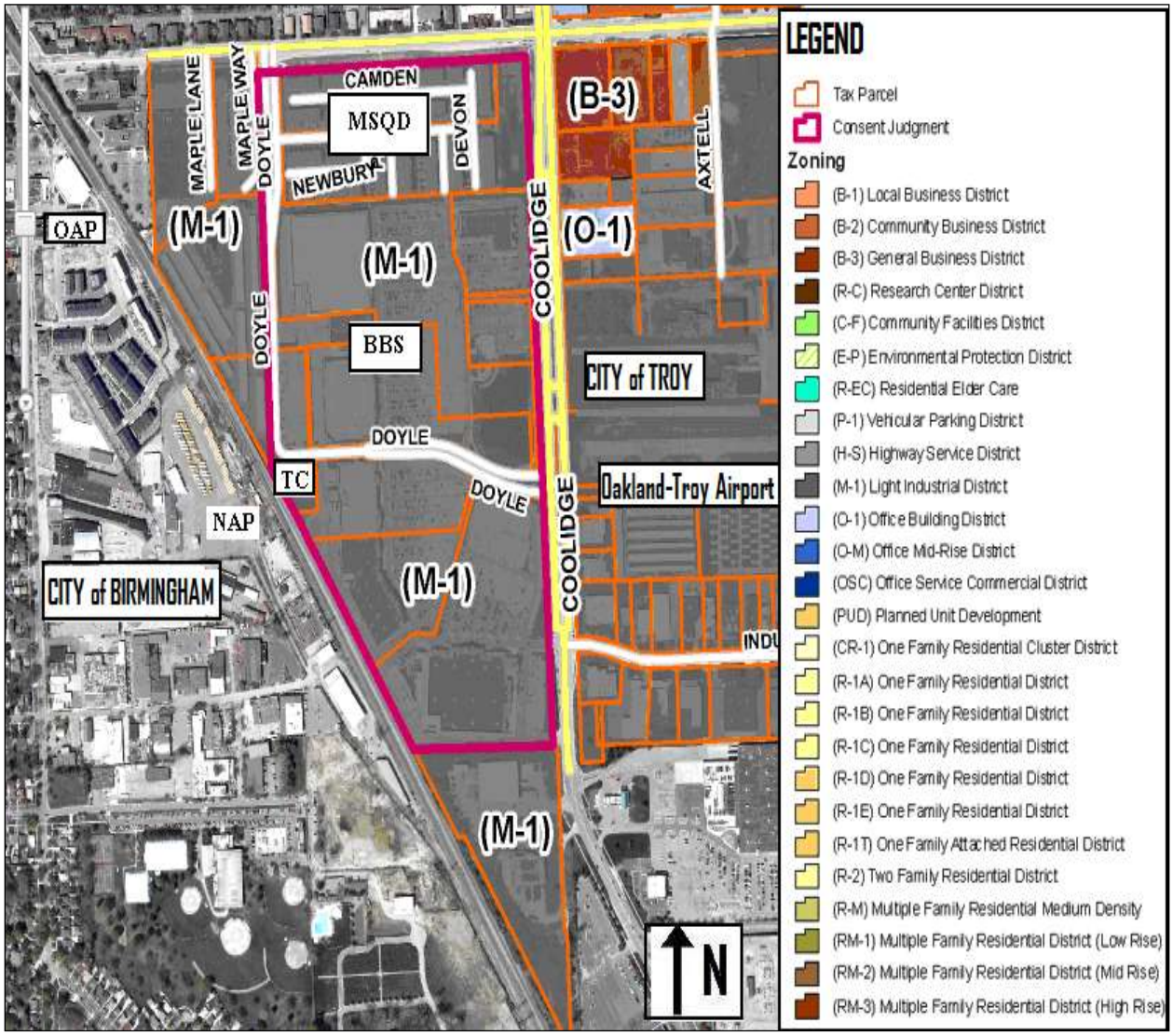

Figure 26. Troy-Birmingham Amtrak Station: City of Troy (North of Railroad Tracks)

- TC: proposed Troy-Birmingham Multi-modal Transit Center (MTC)
- OAP: existing Amtrak station
- NAP: proposed Amtrak platform
- BBS: Midtown Square Shopping Center (big-box retailers)
- MSQD: The Village at Midtown Square

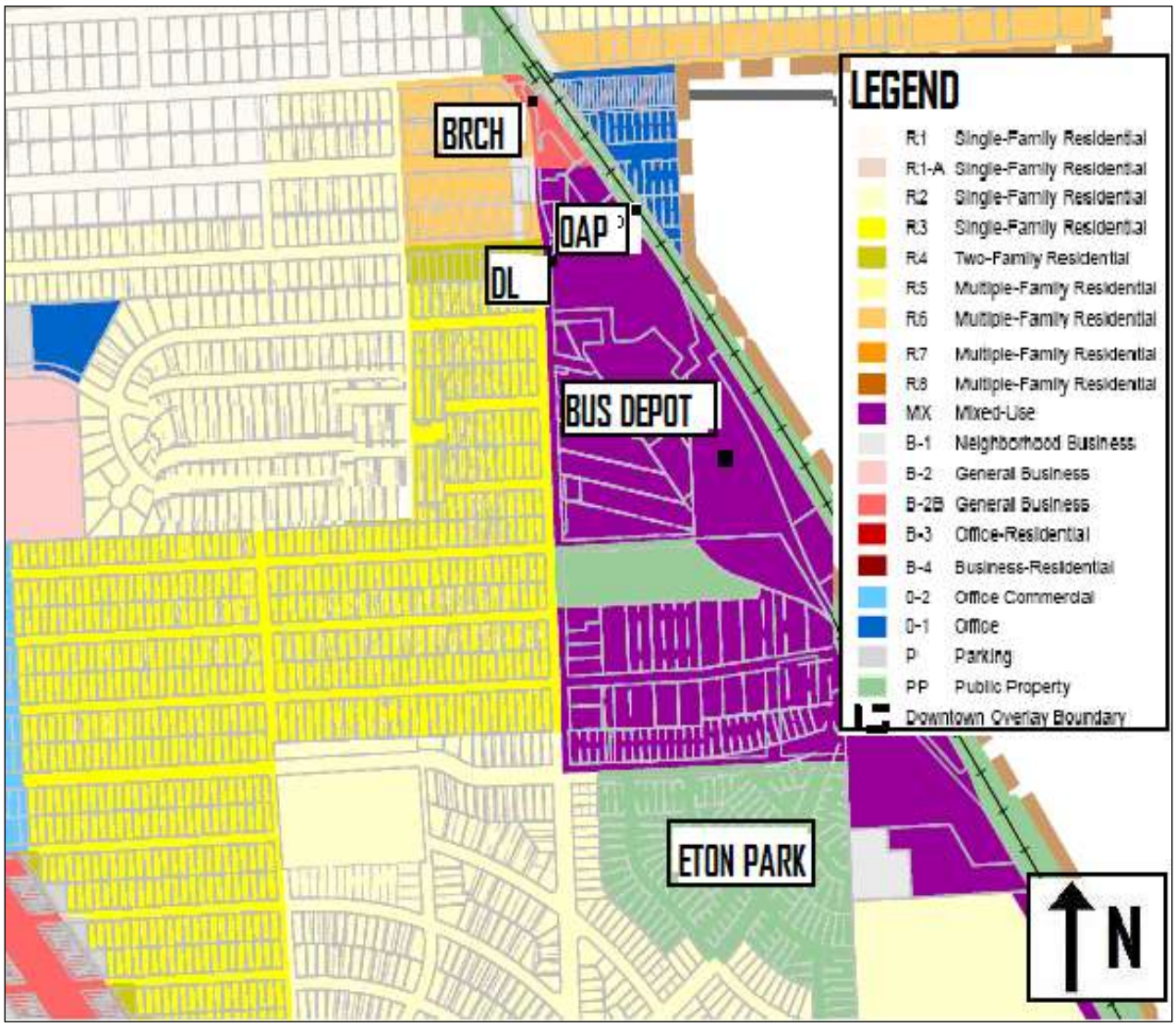

Figure 27. Troy-Birmingham Amtrak Station: City of Birmingham (South of Railroad Tracks)

- BRCH: Big Rock Chop House
- OAP: existing Amtrak platform
- DL: The District Lofts
- BUS DEPOT: surface school bus parking and maintenance facility for the City of Birmingham School District.

An aerial image of the Rail District, near the proposed Multi-modal Transit Center (MTC) is shown in Figure 28. The boundary of the MTC site is depicted as the white triangular area north of the railroad tracks, which are depicted by purple lines. The location of the Birmingham School District bus depot and Midtown Square Shopping Center can also be identified to the west and east of the railroad tracks, respectively. The records maintained by the cities of Troy and Birmingham appear to indicate that the bulk storage area (located just south of the bus depot in Figure 28) will remain as such.

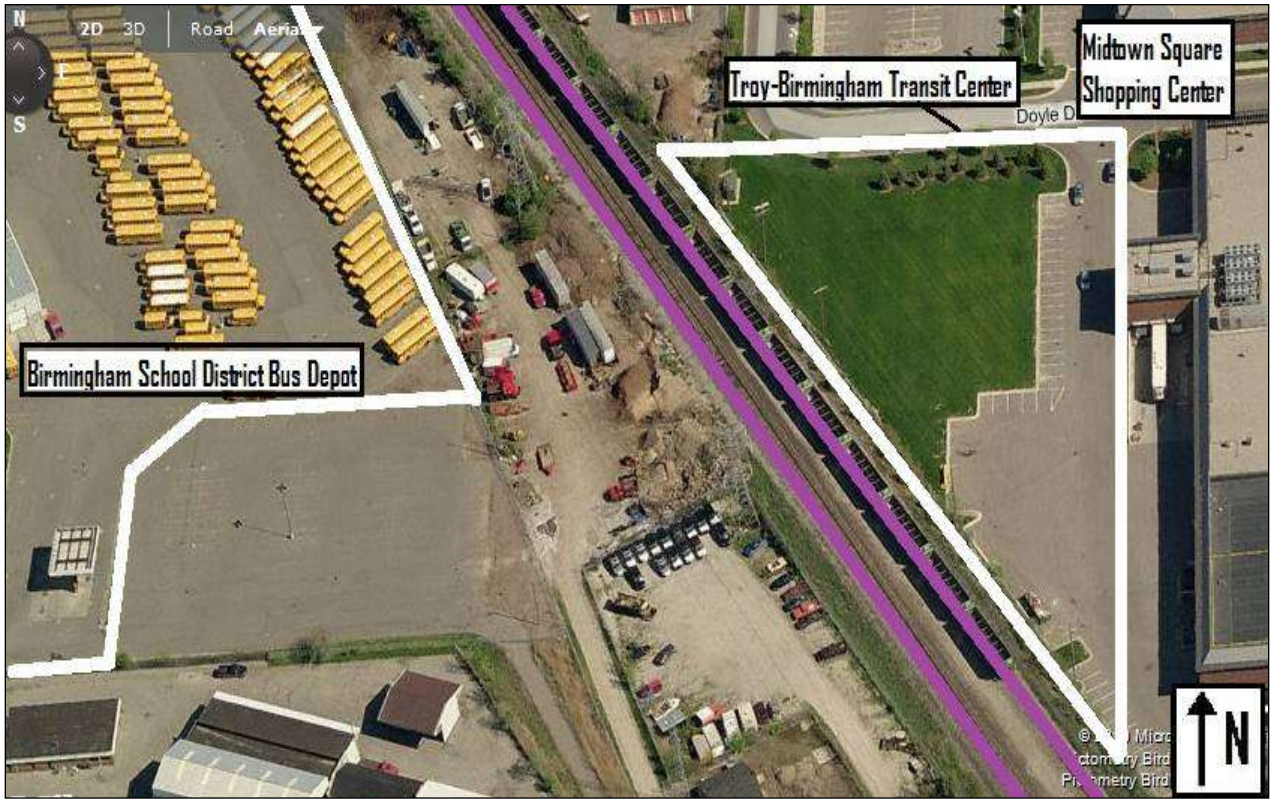

Figure 28. Proposed Troy-Birmingham Multi-modal Transit Center (MTC) Site

The lack of vacant property within the Rail District has been validated and was based on field observations made by the project team and aerial imagery. Although the amount of vacant land in the Rail District has diminished as the result of the completion of development projects (e.g., The District Lofts, Lofts at Eton Street Station), the addition of pedestrian-friendly features is expected to further improve the quality of life for those who frequent the area. In particular, pedestrian activities will be greatly facilitated on the Troy portion of the district, along the Midtown Square Shopping Center that border the proposed MTC site. For the Troy-Birmingham Amtrak station, the influence area is centered around the proposed MTC site, along the railroad tracks located there (Figures 11, 26, and 28).

Two local organizations have a key role in the development programs currently underway at this site. The descriptions of those organizations have been listed below [*60,61*]:

- **Birmingham-Bloomfield Chamber of Commerce (BBCC):** The BBCC is an organization that intends to build strong relationships with the government, education, and communities to create and maintain a prosperous business climate for its members: cities of Beverly Hills, Bingham Farms, Birmingham, Bloomfield Hills, Bloomfield Township, and Franklin. Among those cities, the city of Birmingham is of particular interest because of the speculation of rail transit in the Detroit metropolitan area.
- **Troy Chamber of Commerce (TCOC):** An organization formed with the intent to promote an environment that builds successful businesses and a thriving community, through service and regional collaboration.

In the midst of the proposals for rail transit investments in the Detroit metropolitan area, the BBCC, TCOC, and the cities that they represent, have collaborated to ensure that their member cities are able to capitalize on new mobility improvements. One of such collaborations was the planning and execution of a transit design charrette, intended to bring groups of professionals (e.g., designers, architects, engineers, and planners) together to share ideas and thoughts about the (then) proposed Troy-Birmingham Multi-modal Transit Center (MTC). Although the participants of the charrette were rather diverse (with respect to their fields of interest and profession), it was generally understood that the implementation of TOD was critical in meeting the mobility needs in the Detroit metropolitan region.

5.2.2. Site Characterization and Planning Perspectives:

The residential market in the area surrounding the rail district is very diverse in nature. The relative proximity to the city of Troy, which is generally known to be more affordable and less walkable than the city of Birmingham, creates additional diversity in housing type (rentals versus for-sale), price ranges (senior, low-cost, moderate, or upscale), and development configuration (apartment, townhome, loft, or single-family).

A telephone survey of the residential developers (leasing management companies, and sales offices for for-sale units) appears to indicate that vacancy rates in the influence area surrounding the proposed MTC are relatively low. A partial list of multi-family residential developments within the influence area for the MTC has been presented in Table 9 [*62,63,64*].

TABLE 9 Residential Market

NAME	WALK DISTANCE TO STATION (mi)	TYPE	MARKET	TOTAL # FLOORS	TOTAL # UNITS	ADDITIONAL INFO
The District Lofts	< 0.1	For Sale, Rent	Upscale condo	4	24	all units are 2 bedoom, 2 bath (1,500 - 1,950ft^2)
Eton Street Station	0.1 - 0.2	For Sale	Townhomes (40), Live/Work Studio (60)		110	Studio units are live/work artisan units, offering commercial retail space on first floor.
Eton Square Apartments & Townhomes	0.3	Rent	Apartments, townhomes		158	Troy side; Apartments (1,2 bedrooms), Townhomes (3 bedrooms)
Maplecrest Apartments	0.3	Rent	Apartments		68	Troy side; 1 bedroom (64 units), 2 bedroom (4 units)
2755 E. Maple Rd.	0.5	Rent	Apartments		6	Troy side; 1 bedroom
The Village at Midtown Square	0.3	For Sale	Townhomes		285	Troy side; 2 bedroom (1,480 - 2,321 ft^2)

The commercial markets in the cities of Troy and Birmingham are one of the most coveted areas in the Detroit metropolitan region, and arguably in the entire state of Michigan. In the city of Troy, the Somerset Collection is located approximately two miles north of the proposed MTC. This retail development is renowned as the most upscale commercial center in the state of Michigan. For the city, the mall serves as a local landmark, where a number of office buildings, hotels, and restaurants have been constructed in the last decade as the result of its success. In Birmingham on the other hand, the most attractive shopping destination is located in the CBD, located approximately one mile west of the Rail District. Like the Somerset Collection, the Birmingham CBD is considered a desired destination for shoppers in the Detroit metropolitan area, and a local center of lifestyle for the residents of both Troy and Birmingham.

Table 10. Commercial Market

NAME	WALK DISTANCE TO STATION (mi)	TYPE	MARKET	ADDITIONAL INFO
Whistle Stop	0.3	Service	Restaurant (Casual)	Birmingham side
Big Rock Chophouse / The Reserve	0.4	Service	Restaurant (Upscale)	Built on the site of the former Birmingham rail depot
Baja Fresh	0.4	Service	Restaurant (Casual)	Troy side
Target	> 0.4	Retail	General, Apparel	Troy side; Midtown Square Shopping Center
Dunham's		Retail	Apparel, Sports	
Kohl's		Retail	Apparel	
Old Navy		Retail	Apparel	
Petco		Retail, Service	Pets	
Famous Footwear		Retail	Apparel	
The Home Depot		Retail	Hardware, Tools, Materials	
Cole St. Salon & Spa	0.5	Service	Beauty parlor	Birmingham side (Cole St.)
Moran's Flora		Retail	Florist	

The Rail District has been marketed toward a younger and affluent demographic, a stark comparison to the demographics of Troy and Birmingham: older, conservative, affluent residents often living with at least one child in a single-family home. Much of the land uses located on Cole Street (Birmingham side), have been renovated and redeveloped from what were once industrial-related structures: warehouses, factories, etc. Table 10 summarizes the commercial developments located in the influence area for the Rail District.

Public/civic/institutional land uses in the Troy-Birmingham MTC influence area include the Goldfish Swimming School, located on Cole Street. Although there are a number of parks in both cities, there is a general lack of pedestrian facilities around the proposed MTC area.

In summary, collection of the data obtained for this section has indicated the following:

- Residential housing market is robust, despite the economic downturn, where newer developments (for-sale) have been successful and older ones (rental) have largely remained occupied. Additionally, the newer developments in the Rail District have successfully attracted a younger, more urban-influenced (e.g., a desire to reside in walkable communities, reduced dependence on private automobiles for travel) demographic sector.
- Commercial developments have been successful. The group of offerings within the Rail District is diverse, but will remain separated from one another until completion of the MTC.

5.2.3. Population Characteristics:

The populations of the cities of Troy and Birmingham are characterized by the relatively high median household incomes that they earn (according to the 2000 Census). The incomes are well above the averages for both Oakland County and the seven-county SEMCOG region [*65*].

Table 11. Comparison of Median Incomes in Oakland County, SEMCOG Region

COMMUNITY	POPULATION	MEDIAN HH INCOME ($ in 1999)
Birmingham	20,570	80,861
Troy	80,084	77,538
Oakland County	1,204,053	61,907
SEMCOG Region	4,782,407	49,979

Considering these data, it is expected that the development market in these cities would be stronger than the market in other parts of the Detroit area. The strength of that market may be a sign of hope for Metropolitan Detroit land developers; however, it may also be the biggest barrier to the success of new developments. The challenge for these two affluent cities to implement TOD will be to attract and retain a demographic that is naturally attracted to transit service and TODs.

Although, there are rental options available for those demographic groups that typically earn less than their wealthy counterparts (i.e., senior citizens, young professionals), there does not seem be many that cater to those that typically inhabit TOD's. Since the housing market in the area has fared better than most communities in the SEMCOG region, it could be argued that additional housing developments would have success here.

The Troy portion of the Rail District generally lacks features expected to promote pedestrian-oriented development. One exception is the Village at Midtown Square Development. This high-density community has been constructed with sidewalks adjacent to every unit of the development, but those facilities do not sufficiently connect pedestrians and shopping center. The sheer size of the parking capacity at Midtown Square may be prohibitive to those travelers. To mitigate this, an additional set of walkways could be constructed that "criss-cross" the large parking area, so that pedestrian travel time is shortened.

While the exact measures that may be used to mitigate these issues have not been determined, the project team has expressed that improvements in pedestrian safety and walkability and can be realized. Examples of those improvements and the mechanisms that may ease their implementation will be discussed later in this report.

The proposed MTC, as planned, would expose Amtrak passengers that enter or exit trains in the area to the (rear) service-entry elevations of the retail outlets located in the Midtown Square Shopping Center: Target, Kroger, Dunham's, etc. These areas are often used for the storage of waste dumpsters, recycling containers, loading docks and platforms, and building utilities (e.g., HVAC, water control). Additionally, the shopping center has been constructed using a layout that is typical of "big-box" retail outlets: large expanses of surface parking facilities, limited pedestrian facilities, limited common/green spaces, and significant separation between the development and the roadways adjacent to it.

The existing layout of the Midtown Square Shopping Center is shown below in Figure 29, in which the lack of pedestrian-friendly facilities can be observed. The posted speed limits in the parking area have not been determined, but it is expected that overall pedestrian safety could be improved upon. .

Figure 29. Midtown Square Shopping Center: Street-Level View

5.2.4. TOD's Proposed:

The Rail District has undergone significant changes in the last 20 years, but more may be needed so that it may approach an idyllic TOD. As mentioned in the previous sections, the amount of undeveloped land here is limited. Projects such as The District Lofts, Eton Street Station, and Midtown Square have consumed the vacant land in the area. However, additional growth may be realized along Cole Street, located at the southern end of the Rail District in the city of Birmingham. The city planning department has rezoned most of the Cole Street corridor as "Mixed Use," according to records maintained by the city government (shown as the purple-shaded area, located south of the proposed MTC, in Figure 27). Cole Street has lately undergone significant development and property reinvestment. The Rail District is now considered an affordable alternative to the Birmingham CBD for entrepreneurs wishing to relocate their operations to the city.

New businesses that have relocated to this growing community are diverse and include architects, engineers, florists, swim instructors, interior designers, and beauty salons. Considering this trend, the area may be the most viable option for redevelopment projects in the Rail District because most of the remaining sections in Birmingham and Troy have been occupied.

Suitable areas for new development and reconstruction may be the low-density developments that are adjacent to Cole Street, shown in Figure 30. The area shown in the image has historically been utilized for light-to-medium industrial land uses (e.g., warehousing, auto repair), but is now well-equipped to accommodate TOD, as a result of zoning modifications by the city of Birmingham (institutional mechanism). It should also be noted, that much of the Cole Street corridor is strategically located within half a-mile walking distance from the proposed MTC across the CN ROW.

The addition of affordable, medium to high-density residential land uses along the corridor may be a boon to the MTC investment, and the quality of life for those living there.

Figure 30. Rail District: Cole St. Corridor

It has been observed that there is a lack of a major bookstore or bookseller within an approximate one-mile radius surrounding the Rail District. While such retail outlets can be found near the Somerset collection in Troy and the Birmingham CBD, it would be expected that demand for an additional bookstore would be generated by growth in the area. Oakland County boasts a demographic of highly-educated residents, more than 23 percent hold a bachelor's degree and an additional 15 percent hold graduate or professional degrees (relatively high values compared to Wayne County: corresponding values of 10.9 and 6.4 percent respectively) [*65*].

Again, the most critical limiting factor for redevelopment in the Birmingham section of the Rail District is the availability of vacant land. Although additional development is possible, its magnitude and pattern (in terms of acres redevelopment) would ultimately be subject to the willingness of the entities that own the properties discussed to participate in the project.

In order to create a more people-friendly environment, existing stores such as Target, Kohl's, Kroger, Old Navy, and others should consider adding another exit/entry point at the other side of the store, so that transit patrons may get in/out from both side.

Pedestrian improvements, on the other hand, may be the missing link in connecting both communities in the Rail District. Some of these improvements could include but are not limited to the following: speed bumps, improved pedestrian crossing markings, widened walkways dedicated to pedestrians, ADA-compliant curb cuts, and traffic calming measures (e.g., narrowed lanes, warning signal/signs). Those facilities, in addition to the CN right of way (ROW) pedestrian tunnel planned for the MTC project, would truly connect the two cities of Birmingham and Troy, and would have the potential to stimulate additional economic investment. A complete list of the proposed land uses suggested for the area is shown in Table 12.

Table 12. Proposed Land Uses

	LAND USE TYPE	DESCRIPTION	ADDITIONAL INFO
1	Retail/Service/Commercial	Bookstore	e.g., Borders Books & Music, Schuler's Books & Music
2		Child Care Center	
3	Public/Civic/Institutional	Common spaces (Troy)	e.g., pedestrian plaza, small park, landscaping, sidewalks/pathways
4		Traffic Calming/Pedestrian Facilities (Both cities)	e.g., pedestrian crossing signals & crosswalks, curb cuts, pedestrian lighting, wayfinding facilities
5	Residential	Apartment complex (Birmingham)	e.g., Affordable senior living community, affordable rental units

5.3. Mechanisms Deployed to Implement TOD

5.3.1. General Mechanisms:

The implementation of any new programs (e.g., TOD, joint development, etc.) is often hindered by different barriers. In order to overcome these barriers, it may be necessary to deploy a different set of mechanism or techniques. The mechanisms described below may be executed by TOD stakeholders, a broad range of groups and organizations that may include but are not limited to: local governments (e.g., planners, city council, public works), federal/state/regional governments (e.g., FHWA, HUD, MDOT, SEMCOG), private developers, transit providers/agencies, and financial institutions. The deployment of these mechanisms requires significant intergovernmental cooperation at different levels. Mechanisms have been classified into three categories:

1. **Planning:** relates to strategies that may be used to change zoning definitions or master plans for communities to facilitate the implementation of TOD programs. Examples include creating overlay zoning districts, benefit assessment districts, empowerment zones, and re-zoning properties.
2. **Institutional:** relates to strategies involving a planned arrangement for the coordination of efforts and/or resources exerted between different TOD stakeholders. Examples of this mechanism include the creation of project-specific planning commissions (i.e., TOD), joint-development programs, municipal powers, development rights, and court rulings.
3. **Economic:** relates to strategies that may be used by TOD stakeholders to overcome economic barriers through a commitment of public monetary resources. Examples include property leasing, public private partnerships (PPP), TIF, land banking, alternative sources of funding, land acquisition, and grants (local, state, or federal).

There have been numerous examples, in the Detroit metropolitan area, where such mechanisms have been utilized for the execution of development projects. Mechanisms that may be used for the implementation of TOD projects in the state of Michigan, the SEMCOG region, or counties and local governments are listed in Table 13 [*66*].

The state of Michigan, the SEMCOG region, and the city governments represented by each of the two station areas selected, all are eligible for varying degrees of development incentives. For instance, although the city of Detroit has experienced a decrease in population over the past three decades, the city government and the Detroit Economic Growth Corporation (DEGC) have established well-defined mechanisms to promote developments expected to improve the quality of life for the remaining population. Programs intended to attract nationally-recognized casual dining restaurants and grocery stores are likely to be of particular interest in this context. Such programs are examples of local support for new development.

On the other side of the scale, the current federal administration has expressed a strong desire to incorporate smart growth, sustainability, and livability into new developments in the nation's communities. Federal monies are largely available though a competitive process, rewarding the most suitable projects with grants. The marriage of local incentives, on the lower scale, federal incentives, on the upper scale, and state and regional programs, in between, may be highly attractive to stakeholders wishing to pursue development projects.

The project team has assembled packages for mixed-use TOD implementation at each of the two sites that have been selected. Each package addresses the following items, with regard to the site location:

- Changes in zoning definitions
- New land uses
- Geometric constraints and safety issues (i.e., traffic control, pedestrian facilities)
- Mechanisms for effective implementation (i.e., planning, institutional, economic)
- Real property available for new construction

Table 13. Mechanisms: General

	JURISDICTION	AGENCY	PROGRAM	APPLICATIONS	FINANCING (TYPE)
1	Federal	FHWA / FTA	Metroplotan & Statewide Planning Formula Grant	Regional planning, decision-making	Grants (Formula)
2			Transportation Planning Capacity Building Program	Land use and scenario planning, TOD, non-motorized transportation, safety	
3		FTA	Urbanized Areas Formula Grant Program (Transit agencies in urbanized areas population of 200,000+)	Planning, engineering design, and evaluation of transit projects; 1%+ of funds used for historic preservation, landscaping, public art, pedestrian access, disabilities access	
4			Bus & Bus Facilities Discretionary Grant Program (Transit agencies in urbanized areas population of 200,000+)	New and replacement buses, equipment, facilities, intermodal transit centers	Grants (Competitive)
5		FHWA	Transportation Enhancement (TE) Program	Expand transportation mode choices, safety programs, historic preservation, environmental mitigation, scenic beautification	Grants (Formula)
6			Congestion Mitigation and Air Quality (CMAQ) Program	Reduce pollution, transportation system efficiency, non-motorized transportation facilities, travel demand management	General fund
7		EPA	Smart Growth Implementation Assistance (SGIA) Program	Technical assistance for resolving transportation and parking issues, affordable housing, storm water management, infill and redevelopment.	Competitive
8		EDA	Economic Development Program	Aid in financing economic development.	Grants, loans
9			Economic Development Planning	Provides assistance to public agencies for economic development planning	Grants
10	State of Michigan	MSHDA	Housing Development Authority (PA 346 of 1966)	Study housing issues, acquire and release real property	Grants, bonds, appropriation, operation revenues

Table 13. Mechanisms: General (cont.)

	JURISDICTION	AGENCY	PROGRAM	APPLICATIONS	FINANCING (TYPE)
11	State of Michigan	MEDC	Economic Development Corporations (PA 338 of 1974)	Plan/acquire/prepare sites, loan guarantees, equip facilities for private enterprise	Grants, bonds, operation revenues
12		DDA	Downtown Development Authorities (PA 197 of 1975)	Devise and maintain plans, acquire/hold/develop property, enter PPP, operation of projects	Grants, bonds, operation revenues, TIF, tax proceeds
13		MTA	Metropolitan Transit Authorties (PA 204 of 1967)	Plan/acquire/operate transit and related facilities, utilize eminent domain for land needs	

The city of Detroit utilizes a number of organizations and authorities in planning for development limits intended to improve economic growth and quality of life for its citizens. The Detroit Economic Growth Corporation (DEGC) is a private, non-profit organization that provides the city with the following services with the intent of creating new investments and employment: project management, financial assistance, planning, and development assistance.

The DEGC was founded in 1978 to circumvent many of the bureaucratic obstacles that may slow the progress of a planned project by combining the resources of both the private and public sector. The 35 members of the DEGC collectively serve as the authority governing other organizations, all of which are intended to boost economic activity within the city of Detroit. An organization chart depicting the structure of the DEGC is shown in Figure 31.

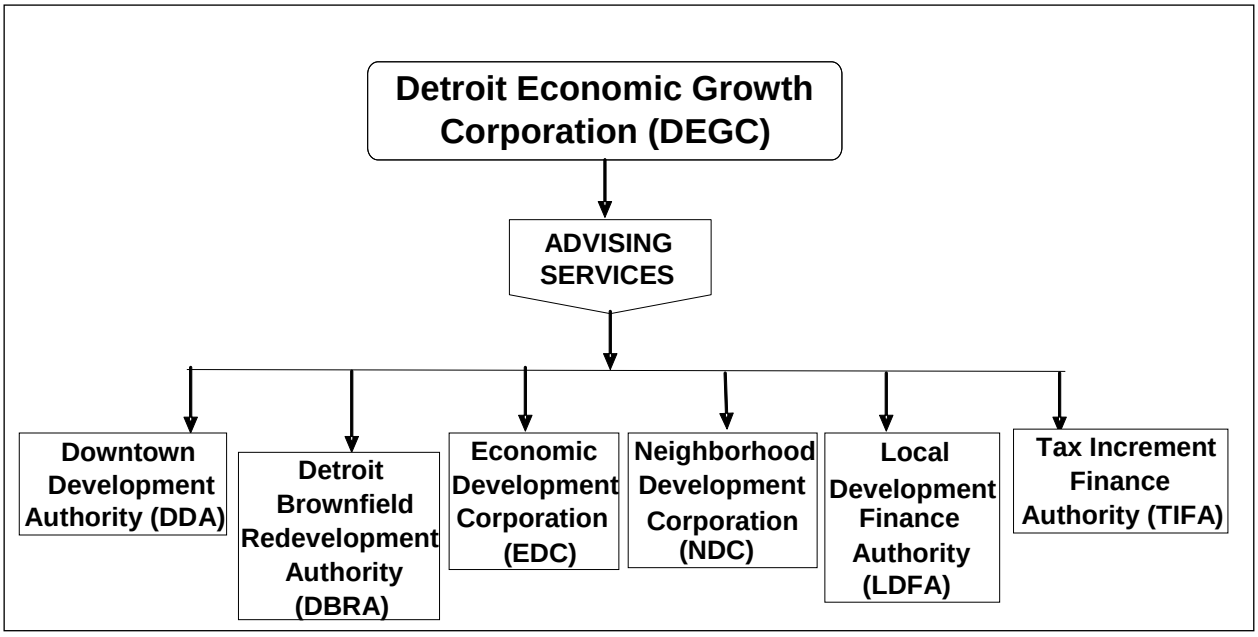

Figure 31. Detroit Economic Growth Corporation (DEGC) Organization Chart

The affiliated organizations have been listed below [*67,68,69,70,71,72*]:

- **Downtown Development Authority (DDA):** The DDA was created in 1976 with the intent on promoting economic growth, focused in the downtown district of the city of Detroit. This area contains approximately two square-miles of land area, and is bounded by: John C. Lodge Freeway (M-10) to the west, Fisher Freeway (I-75) to the north, Chrysler Freeway (I-375) to the east, and the Detroit River to the south.
- **Detroit Brownfield Redevelopment Authority (DBRA):** Provides incentives for the city of Detroit to pursue redevelopment and revitalization efforts in areas in need (e.g., environmentally contaminated, blighted, abandoned, under-utilized). The authority is governed by a nine-member-board of directors.

- **Economic Development Corporation (EDC):** A component unit of both the city of Detroit and the DEGC. Some of the long-term activities involving the EDC include making loans payable to the city of Detroit utilizing U.S. Housing and Urban Development grants (HUD), and designating land parcels for tax benefits and incentives.
- **Neighborhood Development Corporation (NDC):** Established as a subsidiary corporation by the EDC, housing and neighborhood programs within qualified blighted or redevelopment areas can be implemented by the NDC. The NDC can implement a program to acquire property, construct improvements, and rehabilitate or construct houses for immediate sale as long as it is in accordance to a City Council approved project plan.
- **Local Development Finance Authority (LDFA):** A component unit of both the city of Detroit and the DEGC, the LDFA was created in October 1988. The objectives of the authority are as follows: collection of taxes from within tax increment districts to pay debt service used to complete development projects, establishing additional tax increment districts within the city limits (e.g., East Riverfront Conservancy, Jefferson Avenue Chrysler Corporation assembly plant).
- **Tax Incentive Finance Authority (TIFA):** This branch was established in 1982 under PA 450 of 1980. Funding for TIFA comes from tax increments captured as a result of new growth. Spending of funds must be in accordance with a City Council-approved plan.

The city of Detroit has the benefit of a well-defined hierarchy of planning organizations and departments. Throughout the city, there are a number of completed developments that exhibit the full potential of public-private partnerships. For instance, Joe Louis Arena (home of the Detroit Red Wings of the National Hockey League (NHL)) and Cobo Hall were constructed through the use of well-executed PPPs.

Perhaps the most challenging of the barrier to TOD, for the Masonic Temple area, is the lack of demand for development. The world economic crisis has had a devastating effect on the Detroit metropolitan region which is primarily a manufacturing-based economy. Although the total employment for the region is expected to increase by four percent through the year 2020, employment figures in Wayne County and the city of Detroit have been projected to change by 0.4 and -2 percent respectively, for the same duration (based on the 10-year duration from the year 2010 to 2020) [*65*]. These data are listed in Table 14.

Table 14. Projected Employment (2010-2020)

AREA	EMPLOYMENT (x 1,000)			% CHANGE
	2010	2015	2020	
SEMCOG Region	2,586.662	2,638.848	2,690.492	4.0
Wayne County	909.527	908.457	913.495	0.4
City of Detroit	326.620	322.879	320.536	-1.9

(Source: SEMCOG)

As expected, employment figures for the city have a strong correlation with city population. The city of Detroit has been losing significant population for the past six decades. The result of this staggering decline is a city of approximately 800,000 residents distributed across an area of 140 square-miles. Of those 140 square-miles, roughly one-third of the land area is vacant and more than 30,000 structures are empty [*73*]. Factors that further complicate new development, and attracting developers to the city, are related to the affluence level of the potential patrons.

5.3.2. Mechanisms for Effective Implementation at the Masonic Temple Site

There are various mechanisms available to stakeholders pursuing development within the Detroit city limits. As mentioned earlier, there are a number of organizations that operate within the city who are empowered to execute these mechanisms in cooperation with the city.

Institutional mechanisms, such as joint development (JD), have been used for the planning and construction of Cobo Hall, a 700,000 square feet convention center, located in Detroit's CBD. The structure is most notable as the historical home of the North American International Auto Show, held every January. Cobo Hall was opened to the public in 1960, and was constructed in the airspace directly above a portion of the John C. Lodge Freeway (M-10). This project and others that have been supported by the city of Detroit (expansion of Cobo Hall exhibition spaces) suggest that there are no legal objections to development in the airspace over or below public facilities. If this assumption holds true, spaces above or below public facilities may be utilized for more productive uses: commercial, residential, institutional, etc [*74*,*75*].

Mechanisms involving local, state, and Federal organizations and agencies that may be used for the implementation of TOD projects in the city Detroit have been listed in Table 15 and 16 [*76*].

Table 15. Mechanisms: City of Detroit

	JURISDICTION	AGENCY	PROGRAM	APPLICATIONS	FINANCING (TYPE)
1	Federal	FHWA	Pedestrian & Bicycle Safety Program	Research, developing guidelines, tools, safety countermeasures, identifying 'hot' spots	
2		HUD	Sustainable Communities	Regional planning, land use planning, affordable housing, multi-family housing, linking land uses, zoning reform, energy-efficient housing	General fund
3			HOPE VI	Elimination/reclamation of distressed public housing, demolition, rehab, new construction, supportive services for the relocated, green building	Grants (Competitive)
4			Public Housing Program	Operating expenses, repairs, incorporating environmental sustainability, energy & water conservation	Grants (Formula)
5			Housing Choice and Project-Based Vouchers	Provide funding to local public housing agencies for rental subsidies. Allow tenants to relocate closer to work, family, or places of worship	
6			Community Development Block Grants (CDBG)	May be used for low-to-moderate income persons, prevention of slums/blighted area, meets community development needs having urgency.	Grants (Formula)
7			Supportive Housing for the Elderly (Section 202) & Supportive Housing for Persons with Disabilities (Section 811)	Support operating and maintenance costs so that rent prices remain affordable for those with very low incomes	Grants (Competitive)

Table 15. Mechanisms: City of Detroit (cont.)

	JURISDICTION	AGENCY	PROGRAM	APPLICATIONS	FINANCING (TYPE)
8	City of Detroit CBD	DDA	Housing/Office/Retail Development Program	Assistance for the construction, redevelopment, or improvement of real property.	Loans
9			Small Business Loan Transactions Program	Assistance for building owners, tenants, and business owners, with the intent to halt decay of property values and create new employment.	
10		DEGC	Business Development Loan Fund	Foster investment in national or regional recognized chain retail/restaurant ventures.	
11			Real Property Gap Fund	Encourage investment in the rehabilitation of real property by Detroit residents.	
12	City of Detroit		Neighborhood Enterprize Zones (NEZ)	Provides tax incentives for housing developments and improvements.	Tax relief
13			Commercial Rehabilitation Act (PA 210 of 2005)	Encourage the rehabilitation of commercial properties no less than 15 years old by abating taxes on new investments. Particular effort exerted in seeking grocery or produce markets.	
14			Personal Property Tax Abatement Program	Encourage development of the following projects: mining, manufacturing, R&D, wholesale trade, office operations.	
15			Obsolete Property Rehabilitation Program	Encourages rehabilitation and reconstruction in districts that may contain properties that are blighted or functionally obsolete.	
16			Renaissance Zone: Woodward Ave.	Approximately 2 acres of land is eligible for a number of tax incentives: business, income, state education, personal property, real property, utility use.	
17			Creative Corridor Incentive Fund	Intended to develop 125,000 ft^2 of real estate, 400 jobs, new centers of dense commercial activity that may attract creative talent and companies. Project management assistance.	Grants

Table 16. Proposed Land Uses with Available Mechanisms

	LAND USE TYPE	DESCRIPTION	ADDITIONAL INFO	MECHANISMS AVAILABLE
1	Retail/Service/Commercial	Child Care Center		G11, D8, D11, D15
2		Bookstore	e.g., Borders Books & Music, Schuler's Books & Music	G11, D8, D11, D15, D16
3		Casual Dining Restaurant	e.g., Chili's, Applebee's, TGI Friday's, Denny's	G11, D8, D10, D11, D15, D16
4		Grocery or General	e.g., Meijer, Kroger, Target, Wal-Mart	G11, D8, D11, D13, D15, D16
5	Public/Civic/Institutional	Transit Station w/ Shelter	May be integrated into mixed-use structure, located on street-level	G3-G5, G13
6	Residential	Apartment Complex	For Rent, Marketed toward students (WSU, UM, MSU)	G7, G10, G11, D8, D11, D12, D15, D16
7	Public/Civic/Institutional	Traffic calming/Pedestrian facilities	e.g., pedestrian relief island (Woodward Ave.), HAWK pedestrian signals, capacity reduction (Woodward Ave.), "zebra" crosswalk markings	G2, G5, G6, D1

Note: Under the "MECHANISMS AVAILABLE" column, the notations refer to the General Mechanisms table and the Detroit- specific mechanisms table (G: General, D: Detroit). The numbers refer to the row in each table, which point to a specific mechanism.

5.3.3. Mechanisms for Effective Implementation at the Troy-Birmingham Site

The cities of Troy and Birmingham enjoy the state and regional-wide distinction of having robust commercial districts and economies. Such distinction may serve as a proxy for a complex economic growth or planning organization, such as the Detroit DDA and DEGC.

An institutional mechanism was the driving force in the planning and development of the Troy-Birmingham MTC. A consent judgment (mutual agreement between the plaintiff and defendant) combined with intergovernmental collaboration enabled the city of Troy to take ownership and control over a 77-acre parcel of land, located near in the intersection of E. Maple Road and Coolidge Highway. The plaintiff in this case was Grand/Sakwa Properties, Inc., a privately-held land development corporation and the defendant was the city of Troy. The ruling is the result of a dispute between the two parties over zoning regulations for the parcel of land that at one time was zoned as "M-1: Light Industrial by the city of Troy Zoning Ordinance. That definition reflects an earlier period in Troy history when the area was largely undeveloped and the site was utilized as a tractor assembly plant by the Ford Motor Company. Today, much of the 77-acre parcel has undergone complete demolition of the Ford tractor plant, environmental remediation of the land, the eventual construction of the Midtown Square Shopping Center and the Village at Midtown Square residential development. Additionally, the parcel is planned to be re-zoned from "M-1: Light Industrial" to "Mixed-Use" [*77*].

The conditions of the consent judgment, however, required that the remaining portion of the site, (approximately 3.5-acres located the Midtown Square Shopping Center) to be utilized as a transportation center, so that the entire parcel may reflect its new zoning definition [*78*]. At the time of this writing, the cities are anticipating to break ground at the time before the end of this calendar year.

Other mechanisms involving local, state, and federal organizations/agencies that may be used for the implementation of TOD-related projects in the cities of Troy and Birmingham have been listed in Table 17 and 18 [*79,80,81*].

Table 17. Mechanisms: Cities of Troy and Birmingham

JURISDICTION	AGENCY	PROGRAM	APPLICATIONS	FINANCING (TYPE)
Oakland County	Economic Development	Planning & Economic Development Services (PEDS)	Offers community assistance, planning, market research data, aerial imagery, and financial assistance for businesses.	Various
City of Birmingham	Planning Division	Special Land Use Permits (SLUP)	Required for the following: schools, community buildings, churches, publicly-owned buildings, gasoline stations, drive-in facilities, child care centers, beer/wine sales, automatic laundries, trailer camps, bus stations, funeral homes, outdoor storage and parking facilities.	
City of Troy	City Council	Real Estate & Economic Development Department	Assistance in obtaining Federal/State/Local funding, site location, tax incentives, and relocation for businesses.	Various
		Local Development Financing Authority (LDFA)	Offers assistance to local developments so that unemployment is prevented, and additional growth is promoted.	Bonds, permits, tax relief, operations revenue

Table 18. Proposed Land Uses with Available Mechanisms

	LAND USE TYPE	DESCRIPTION	ADDITIONAL INFO	MECHANISMS AVAILABLE
1	Retail/Service/Commercial	Bookstore	e.g., Borders Books & Music, Schuler's Books & Music	G11, T1, T3, T4
2		Child Care Center		G11, T1-T4
3	Public/Civic/Institutional	Common spaces (Troy)	e.g., pedestrian plaza, small park, landscaping, sidewalks/pathways	G2, G5, G6
4		Traffic Calming/Pedestrian Facilities (Both cities)	e.g., pedestrian crossing signals & crosswalks, curb cuts, pedestrian lighting, wayfinding facilities	G2, G5, G6, T2
5	Residential	Apartment complex (Birmingham)	e.g., Affordable senior living community, affordable rental units	G7-G11, T1

Note: Under the "MECHANISMS AVAILABLE" column, the notations refer to the General Mechanisms table and the Troy/Birmingham-specific mechanisms table (G: General, T: Troy/Birmingham). The numbers refer to the row in each table, which point to a specific mechanism.

6. CONCLUSIONS

The term transit-oriented development (TOD) is being used increasingly in transit literature, particularly in studies related to planning and design of urban rail-transit. TOD relates to the integration of diverse (but desirable) land uses with transit, both temporally and spatially, and is designed to increase transit ridership and to promote desirable land uses surrounding the station areas. Over the last decade, there has been increased interest in North American cities, to construct light-rail transit (LRT) systems to improve mobility. LRT stations appear to be ideal sites for TOD programs, primarily because of compatibility in their scale of operation. Currently, there are a number of transit initiatives in the Detroit metropolitan region that, if implemented, may significantly change the transportation characteristics in the southeast Michigan area. A number of studies are currently underway with the intent of exploring the feasibility of constructing an LRT system along Woodward Avenue, one of the most dominant travel corridors in Metropolitan Detroit.

The purpose of this study, conducted jointly at Wayne State University (WSU) and the University of Detroit Mercy (UDM), is to develop TOD programs on two selected stations along the planned LRT route in Metropolitan Detroit (Chapter 1). Reducing the cost of transportation and congestion on our highways, and creating opportunities for economic development, are major challenges in metro Detroit at this time. TOD programs can contribute to these goals by reducing the public's dependence on automobile travel and revitalizing the local economy. A LRT system would present great opportunities to the community to address these critical needs. This study identifies two transit stations along the Woodward Avenue corridor, proposes TOD packages for these sites, and identifies planning, economic, and institutional mechanisms for their effective implementation. The focus of this study is to integrate TOD with the planning and design of selected stations in the Detroit area, with the intent to maximize economic growth potential and to improve the quality of life of the citizens of the local communities and the users of the LRT facility.

The specific conclusions of this study are as follows:

- Four rail stations in the Detroit metropolitan area were initially selected following a preliminary network-level analysis that included two stations in the city of Detroit and two in two different suburban communities based upon land use, transportations, and other factors.
- The network-level analysis culminated in the selection of two stations for further TOD analysis. The two stations selected for TOD analysis are the Masonic Temple site along Woodward Avenue in the city of Detroit, and the Amtrak rail station in the cities of Troy and Birmingham. Pedestrian friendliness (either current or potential) was one of the major factors considered, along with the availability of vacant land, and the proximity to major transportation corridor(s) in selecting the station site.

- Detailed project-level analyses were conducted on the two selected transit stations that are marked by both significant similarities and contrasts. The developments proposed at the two stations encompass a variety of land use including multi-family residential, retail, service-oriented, and other use within the area of influence of the station.
- A set of mechanisms (both general and station-specific) also is presented in recognition of the probability that the implementation of any new program, encompassing transportation-land use interface such as TOD, is likely to be hindered by different institutional barriers. A "mechanism" in this case can be looked upon as a strategy or a group of strategies (planning, economic, financial, etc.) that can be deployed through proper intergovernmental cooperation to implement the proposed development. First, a set of general mechanisms is presented that may be applied to transportation projects in general and that may require interface with land use planning and economic development. This discussion is followed with station-specific mechanisms that attempt to relate the proposed development with strategies that may be deployed to expedite their effective implementation.

7. ACKNOWLEDGEMENTS

The project team wishes to extend its gratitude to the following groups/organizations for their guidance in developing this study:

- City of Birmingham, MI
- City of Troy, MI
- Hamilton Anderson Associates (HAA)
- M1-Rail
- Eton Square Apartments and Townhomes
- Birmingham-Bloomfield Chamber of Commerce
- Troy Chamber of Commerce

The following individuals provided significant assistance and insight towards the report:

- Mr. Korey A. Hall, Regional Manager for the Honorable Debbie Stabenow, U.S. Senator for the State of Michigan
- Mr. R. Brent Savidant, Planning Department, City of Troy
- Dr. Robin M. Boyle, Chair and Professor of Urban Studies and Planning, Wayne State University
- Dr. Shawn McElmurry, Civil & Environmental Engineering, Wayne State University
- Dr. Sabyasachee Mishra, National Center for Smart Growth Research & Education, University of Maryland
- Ms. Cynthia Fondriest, President, Strategic Transportation Initiatives, Alexandria, VA
- Mr. Ronald Flies, Director of Project Management, DEGC (ret.)
- Mr. Malik Goodwin, Vice-President of Project Management, DEGC
- Ms. Victoria Corley, Woodward Place at Brush Park, Crosswinds Communities
- Ms. Michelle Hodges, Troy Chamber of Commerce

8. REFERENCES

1. <http://en.wilkipedia.org/wiki/Transit-oriented_development>.
2. <http://www.ggw.org/rrte/didyouknow/61 cities.htm>.
3. "Realizing the Potential. Expanding Housing Opportunities Near Transit". The Center for Transit Oriented Development. Oakland, CA, April 2007.
4. Arrington, G. B., and Cervero, R. "TCRP Report 128: Effects of TOD on Housing, Parking, and Travel". Transportation Research Board. Washington, D.C.:2008.
5. Hurst, S. "The Economic Case for Light Rail in Detroit; Report Published for Transportation Riders United, Detroit,MI: August 2008.
6. Maurer, T. "Seattle Developer Proposes $121 Million Project in Beaverton". The Oregonian. Beaverton, OR: 1 April 2008. <http://blog.oregonlive.com/breakingnews/2008/04/seattle_developer_proposes_121.htm>.
7. "What is SEMCOG?". SEMCOG. Detroit, MI. Web. 13 June 2010. <http://www.semcog.org/WhatIsSEMCOG.aspx>.
8. SEMCOG. *Improving Transit in Southeast Michigan: A Framework for Action.* Detroit, MI: October 2001.
9. Metropolitan Affairs Coalition: *SpeedLink- A Rapid Transit Option for Greater Detroit* http://www.mac-web.org/Accomplishments/assets/Speedlink/speedlinkfinalreport.pdf
10. *Woodward Corridor Transit Alternatives Study Final Report*; Detroit Transportation Corporation; by IBI Group; May 2000
11. Detroit Department of Transportation (DDOT), Detroit Transit Options for Growth Study (DTOGS). DTOGS Study Results. Detroit, MI: Aug 2008. Web. 10 May 2010 http://www.woodwardlightrail.com/StudyResults.html.
12. M1-RAIL. Detroit, MI. Web. 10 May 2010. < http://www.m-1rail.com/>.
13. "Troy-Birmingham Multi-Modal Transit Center". Revitalizing America's Train Stations, Amtrak. Web. 9 April 2010. <http://www.greatamericanstations.com/station-news/troy-birmingham-multi-modal-transit-center>.
14. City of Birmingham (MI). *Minutes of Meeting: Birmingham City Commission / Planning Board Joint Workshop Session*. Birmingham, MI: 19 October 2009.
15. http://www.reconnectingamerica.org/public/tod
16. http://www.reconnectingamerica.org/public/display_asset/ctod5yearbrochure
17. Belzer, D.; Autler, G. "Transit-Oriented Development: Moving from Rhetoric to Reality". Strategic Economics. June 2002.
18. http://en.wikipedia.org/wiki/Ohlone/Chynoweth%E2%80%93Almaden_%28VTA%29

19. Santa Clara Valley Transportation Authority (VTA). *VTA Transportation Handbook: A Primer for Understanding Transportation in the Silicon Valley*. Chapter 3. San Jose, CA. Web. 30 June 2010.

20. "Transit Oriented Development: Case Study 10". City of Seattle, Washington, Strategic Planning Office. Seattle, WA: 13 Aug 1999.

21. Mathur, S. and Ferrell, C. "Effect of Suburban Transit Oriented Developments on Residential Property Values". Mineta Transportation Institute. MTI Report 08-07. San Jose, CA: June 2009.

22. TriMet. *TriMet Rail System Map*. Portland, OR: 2009. <http://trimet.org/maps/railsystem.htm>.

23. Arrington, G.B. Hencke, J. "TOD and Place Making". Brownfield Renewal. Portland, OR: 2009.

24. Greater Cleveland Regional Transit Authority. "Transit Oriented Development Best Practices". pp. 40-46. Cleveland, OH: Feb 2007.

25. "J.L. Hudson Department Store". Controlled Demolition, Incorporated. Phoenix, MD. Web: 23 June 2010. <http://www.controlled-demolition.com/jl-hudson-department-store>.

26. Byles, J. "Disappeared Detroit". LOST Magazine. Jan 2006.

27. "How it Works". Walk Score. Web Image. 23 June 2010. <http://www.walkscore.com/how-it-works.shtml>.

28. Front Seat: Software for Civic Life. *Walk Score*. Web: 23 June 2010. <http://www.walkscore.com/>.

29. Nolan, J. "Auto Plant Vs. Neighborhood: The Poletown Battle". The Detroit News. Detroit, MI: 27 Jan 2000.

30. County of Wayne v. Edward Hathcock. No. 124070. Michigan Supreme Court. Lansing, MI: 30 July 2004.

31. <http://en.wikipedia.org/wiki/Cadillac_Place>.

32. <http://en.wikipedia.org/wiki/Fisher_Building>.

33. <http://en.wikipedia.org/wiki/Henry_Ford_Hospital>.

34. <http://en.wikipedia.org/wiki/Detroit_Masonic_Temple>.

35. “Crosswinds in the News”. Crossswinds Communities. Novi, MI. Web. 27 June 2010. <http://www.crosswindsus.com/news.html>.

36. “Ford Field Facts and History”. Detroit Lions Inc. Allen Park, MI. Web. 27 June 2010. <http://www.detroitlions.com/ford-field/facts-history.html>.

37. “Comerica Park: Raising the Expectations”. MLB Advanced Media, L.P., Detroit Tigers. Web. 27 June 2010. <http://detroit.tigers.mlb.com/det/ballpark/comericapark.jsp>.

38. “Fortune 500”. CNN Money. Web. 27 June 2010. <http://money.cnn.com/magazines/fortune/fortune500/2009/snapshots/175.html.>.

39. <http://en.wikipedia.org/wiki/The_Henry_Ford>.

40. “About: Fairlane Town Center”. Taubman Centers. Dearborn, MI. Web. 27 June 2010. <http://www.shopfairlane.com/infodesk/index.html>.

41. “Hyatt Regency Dearborn”. Hyatt Corporation. Web. 27 June 2010. <http://www.dearborn.hyatt.com/hyatt/hotels/index.jsp>.

42. <http://www.umd.umich.edu/>

43. <http://www.hfcc.edu/>

44. Detroit Regional Mass Transit (DRMT) and TranSystems. *Comprehensive Regional Transit Service Plan: Final Report 1*. Regional Transit Coordinating Council (RTCC), SEMCOG. Detroit, MI: 21 November 2008.

45. City of Troy (MI). *Meeting Minutes with City of Troy Planning Department Director, R. Brent Savidant*. Troy, MI: 8 October 2009.

46. "Theatre Information: Birmingham 8". Uptown Entertainment. Birmingham, MI. Web. 2 July 2010. <http://www.uptownentertainment.com/theatre_information.htm>.

47. "Detroit, Michigan - Zoning". Municode.com. Accessed: Nov 2009. <http://library.municode.com/index.aspx?clientId=10650&stateId=22&stateName=Michigan>.

48. City of Detroit (MI) Planning and Development Department. *Detroit Zoning Ordinance*. P. 261. Detroit, MI: 1 Nov 2008. http://www.detroitmi.gov/Portals/0/docs/legislative/cpc/Ch%2061%20Aug%2021,%202009.pdf

49. "Woodward Place at Brush Park". Projects Database. Model D Media. Detroit, MI. Web. 3 July 2010. <http://www.modeldmedia.com/developmentprojects/woodward.aspx>.

50. "Village of Brush Park Manor, Paradise Valley". Presbyterian Villages of Michigan. Web. 3 July 2010. <http://www.pvm.org/>.

51. "Crystal Lofts". Residences. Detroit, MI. Web. 3 July 2010. <http://www.crystallofts.com/residences.html>.

52. "The Ellington Lofts". Projects Database. Model D Media. Detroit, MI. Web. 3 July 2010 <http://www.modeldmedia.com/developmentprojects/ellington.aspx>.

53. <http://en.wikipedia.org/wiki/St._John%27s_Episcopal_Church_%28Detroit,_Michigan%29>.

54. Google Inc. *Google EARTH 5 Application*. 2010

55. SEMCOG. *Data and Maps: Traffic Counts, Woodward Avenue in Detroit*. Detroit, MI: 9 Sept 2008.

56. http://www.enhancements.org/download/trb/1636-016.PDF.

57. Arrington, G. B., and Cervero, R. “TCRP Report 128: Effects of TOD on Housing, Parking, and Travel”. Transportation Research Board. Washington, D.C.:2008.

58. "Geographical Information System Online". City of Troy (MI). Troy, MI. Updated: 19 April 2010. Web. <http://gis.troymi.gov/ArcGIS/Maps/Zoning.html>.

59. City of Birmingham (MI). *Map Library: Zoning Map*. Birmingham, MI. Updated: 14 July 2008. <http://www.ci.birmingham.mi.us/index.aspx?page=1176>.

60. City of Troy (MI) Chamber of Commerce. *Facebook Page*. Troy, MI: 2010. <http://www.facebook.com/troychamber#!/troychamber?v=wall>.

61. "About Us". Birmingham-Bloomfield Chamber of Commerce (BBOC). Birmingham, MI. Web: 21 June 2010. <http://www.bbcc.com/about/>.

62. "The District Lofts: 2051 Villa Rd.". Michigan State Housing Development Authority (MSHDA), Michigan Housing Locator. Lansing, MI: 20 Jan 2009. Web. <http://www.michiganhousinglocator.rentlinx.com/Property.aspx?PropertyID=40285>.

63. Lee, A. "Downtown Homes Enjoy Rebirth in Birmingham". The Detroit News. Detroit, MI: 18 Nov 2004.

64. Eton Square Apartments & Townhomes (Ms. Tina). Telephone Interview. 9 July 2010.

65. SEMCOG. *Data By Community, Community Profiles: Southeast Michigan*. Detroit, MI: 6 Aug 2010.

66. U.S. Department of Transportation (USDOT), Department of Housing and Urban Development (HUD), Environmental Protection Agency (EPA). *Leveraging the Partnership: DOT, HUD, and EPA Programs for Sustainable Communities*. Washington, D.C.: April 2010.

67. "About Us". Detroit Economic Growth Corporation (DEGC). Detroit, MI. Web: 11 June 2010. < http://www.degc.org/about.aspx>.

68. American Athiests Inc. et. al. v. City of Detroit Downtown Development Authority. United States Court of Appeals, Sixth Circuit. Detroit, MI: 5 March 2009.

69. "Detroit Brownfield Redevelopment Authority: Revitalizing Detroit Through Brownfield Redevelopment". DEGC. Detroit, MI. Web: 18 June 2010.

70. "Financial Statements". George Johnson & Company, Economic Development Corporation (EDC) for the City of Detroit. Detroit, MI: 20 June 2006, 2007.

71. http://www.degc.org/how-degc-works.aspx

72. "Financial Statements". George Johnson & Company, City of Detroit Local Development Finance Authority. Detroit, MI: 30 June 2008, 2009.

73. American Institute of Architects (AIA). *Leaner, Greener Detroit*. p.3. Sustainable Design Assessment Team. Detroit, MI: 1 Nov 2008.

74. Khasnabis, S. et al. "Applicability of Joint Development Tools in Detroit". Journal of the Urban Planning and Development Division, Proceedings of the American Society of Engineers (ASCE). Vol. 106, No. UP1. Nov 1980.

75. Wisely, J. "Cobo Scales Back Expansion Plan". Detroit Free Press. Detroit, MI: 1 July 2010.

76. DEGC. *Development Incentives Brochure*. Detroit, MI: Feb 2010.

77. Grand/Sakwa Properties, Inc. v. City of Troy, MI. No. 00115121. Oakland County, Circuit Court. Pontiac, MI: 2 Jun 2000.

78. Oparka, T. "Transit Center Gets on Track". C & G Newspapers. Warren, MI: 27 Jan 2010.

79. City of Troy (MI). *TROY, Michigan: An Economic Resource Guide*. Troy, MI: 2008.

80. "Real Estate and Economic Development: Partnerships". City of Troy (MI). Troy, MI. Web. 15 July 2010. <http://troymi.gov/EconomicDevelopment/Partnerships.asp>.

81. "Special Land Use Permits". City of Birmingham (MI), Planning Division. Birmingham, MI. Web. 15 July 2010. <http://www.ci.birmingham.mi.us/index.aspx?page=668>

9. LIST OF ACRONYMS

AATA	Ann Arbor Transportation Authority
ADA	Americans with Disabilities Act
ADT	Average daily traffic
ARRA	American Recovery and Reinvestment Act of 2009
BBCC	Birmingham-Bloomfield Chamber of Commerce
BRT	Bus rapid transit
BWATC	Blue Water Area Transportation Commission
CBD	Central business district
CN	Canadian National Railway
CRT	Commuter rail transit
CTOD	Center for Transit-Oriented Development
DDA	Downtown Development Authority
DDOT	Detroit Department of Transportation
DEGC	Detroit Economic Growth Corporation
DMC	Detroit Medical Center
DOE	Department of Energy
DRC	Detroit Regional Chamber
DTC	Detroit Transportation Corporation
DTW	Detroit Metropolitan Wayne County Airport
EPA	Environmental Protection Agency
FHWA	Federal Highway Administration
FTA	Federal Transit Administration
HUD	Department of Housing and Urban Development
ITE	Institute of Transportation Engineers
JD	Joint development
LET	Lake Erie Transit
LRT	Light rail transit
LRTV	LRT vehicles
MAX	Portland's Metropolitan Area Express
MDOT	Michigan Department of Transportation

MLB	Major League Baseball
MSU	Michigan State University
MTC	Multi-modal transit center
MTI	Mineta Transportation Institute
NFL	National Football League
NHL	National Historical Landmarks
NRHP	National Register of Historic Places
PD	Planned Development District
PHV	Peak-hour volume
PPP	Public private partnership
ROW	Right of way
RRT	Rapid rail transit
SEMCOG	Southeast Michigan Council of Governments
SEMTA	Southeast Michigan Transportation Authority
SMART	Suburban Mobility Authority for Regional Transportation
TCOC	Troy Chamber of Commerce
TCRP	Transit Cooperative Research Program
TIF	Tax increment financing
TOD	Transit oriented development
TriMet	Tri-County Metropolitan Transportation District of Oregon
UDM	University of Detroit Mercy
UM	University of Michigan
VPD	Vehicles per day
VPH	Vehicles per hour
VTA	Santa Clara Valley Transportation Authority
WSU	Wayne State University